DISSERTATION

RHODIUM(III)-CATALYZED AMIDE-DIRECTED C-H ACTIVATION AND [4+2] CYCLOADDITION FOR MODULAR ASSEMBLY OF NITROGEN HETEROCYCLES

Submitted by

Natthawat Semakul

Department of Chemistry

In partial fulfillment of the requirements

For the Degree of Doctor of Philosophy

Colorado State University

Fort Collins, Colorado

Summer 2017

Doctoral committee:

Advisor: Tomislav Rovis

Alan Kennan
Yian Shi
Martin McCullagh
Matt Kipper

ABSTRACT

RHODIUM(III)-CATALYZED AMIDE-DIRECTED C-H ACTIVATION AND [4+2] CYCLOADDITION FOR MODULAR ASSEMBLY OF NITROGEN HETEROCYCLES

This dissertation describes the ligand and reaction developments by amide-directed rhodium(III)-catalyzed C(sp^2)-H bond activation followed by amidoannulation with alkenes to form nitrogen-containing heterocycles. Chapter 1 details the ligand development for stereoselective synthesis of [4.1.0] dihydroisoquinolones through benzamidation of cyclopropenes mediated by Rh(III) catalysis. Quantum chemical calculations revealed the important role of heptamethylindenyl (Ind*) ligand and *O*-substituted ester of benzhydroxamate for achieving high diastereoselectivity in cyclopropene insertion. Efforts toward stereoselective synthesis of [4.1.0] dihydroisoquinolones have been also studied by streptavidin-based artificial metalloenzyme.

Chapter 2 presents the stereoselective synthesis of [4.2.0] dihydroisoquinolones via the benzamidation of cyclobutenes. The transformation proved to have a broad substrate scope and functional group tolerance that generates the cyclobutane-fused azacycles with excellent diastereoselectivity. The artificial metalloenzymes can render this reaction asymmetric furnishing the dihydroisoquinolone products in moderate enantioselectivity.

Chapter 3 communicates Rh(III)-catalyzed C-H activation and [4+2] annulation reaction of *N*-pivaloyloxy acrylamides with alkenes for an efficient synthesis of α,β-unsaturated-δ-lactams. This process offers a platform for the rapid assembly of a diverse set of δ-lactams from simple and abundant precursors. These lactams could serve as useful building blocks to access substituted piperidines.

ACKNOWLEDGEMENTS

First of all, I would like to express my sincere gratitude to Professor Tom Rovis for his excellent supervision and guidance during my graduate study. It is the greatest honor to join his group and having Tom as an advisor. Tom always encourages and inspires students to work on the important problems. I am indebted Professor Thomas Ward (Basel) for providing streptavidin mutants and Professor Robert Paton, Dr. Kelvin Jackson (Oxford) for DFT calculations. In addition, I also thank Professors Yian Shi, Alan Kennan, Martin McCullagh and, Matt Kipper for serving as committees.

I am thankful to past and present members of the Rovis group. They are great colleagues and good friends. I learned many things from excellent people, and this situation facilitates me to think more deeply about science. I enjoy times we spent together inside and outside the lab. Moreover, I am grateful to Todd for initial results of an enantioselective [4.1.0] dihydroisoquinolone. I am thankful to Tiffany, Fedor and Rh(III) team for generously providing $[Cp^xRhCl_2]_2$ precatalysts. I am indebted to many group members (Tim, Todd, Tyler, Oz, Claire, Matt, Tiffany, Darrin, Mike, Jack, and Scott) for proofreading my writing and this dissertation. In addition, I thank classmates and all of my friends for their supportive.

I must thank the Royal Thai Government (DPST graduate scholarship) for a financial support over the years. Last but not least, I would like to thank my family members, especially my mother Piranan Semakul, for her constant supportive. This dissertation is dedicated to my late father, Somnuek Semakul.

TABLE OF CONTENTS

CHAPTER 1

Development of Stereoselective Cyclopropene Benzamidation via Rh(III)-Catalyzed C-H Activation[1]

1.1 Introduction

1.1.1 Background

In recent years, transition metal-catalyzed C–H bond activation has attracted attention for streamlining organic synthesis by increasing step and atom economy.[2] Since C–H bonds are abundant in organic molecules, the transformation of specific C–H bond to a desired functional group is challenging. Traditionally, a C–H bond is converted to a carbon-halogen bond. The well-known cross-coupling reactions can then be used to transform the C-X bond providing the desired functional group (Figure 1a).[3] An ideal strategy would directly transform a C–H bond to the functional group in a single step (Figure 1b). A significant challenge in achieving this goal is controlling the chemo-, regio- and enantio- selectivity of the C–H activation as well as overcoming issues of reactivity and functional group tolerance. A strategy frequently employed to control chemoselectivity is the use of a directing group. Use of a coordinating functional

---

[1] The portion of this work was published, see: Semakul, N.; Jackson, K. E.; Paton, R. S.; Rovis, T. *Chem. Sci.* **2017**, *8*, 1015-1020.

[2] Reviews, see: (a) Daugulis, O.; Do, H. Q.; Shabashov, D. *Acc. Chem. Res.* **2009**, *42*, 1074-1086. (b) Colby, D. A.; Bergman, R. G.; Ellman, J. A. *Chem. Rev.* **2010**, *110*, 624-655. (c) Lyons, T. W.; Sanford, M. S. *Chem. Rev.* **2010,** *110,* 1147-1169. (d) McMurray, L.; O'Hara, F.; Gaunt, M. J. *Chem. Soc. Rev.* **2011,** *40*, 1885-1898. (e) Yeung, C. S.; Dong, V. M. *Chem. Rev.* **2011,** *111*, 1215-1292. (f) Ackermann, L. *Chem. Rev.* **2011**, *111*, 1315-1345. (g) Yamaguchi, J.; Yamaguchi, A. D.; Itami, K. *Angew. Chem. Int. Ed.* **2012**, *51*, 8960-9009. (h) Arockiam, P. B.; Bruneau, C.; Dixneuf, P. H. *Chem. Rev.* **2012**, *112*, 5879-5918 (i) Satoh, T.; Miura, M. *Chem. Eur. J.* **2010**, *16*, 11212-11222.

[3] (a) Seechurn, C.; Kitching, M. O.; Colacot, T. J.; Snieckus, V. *Angew. Chem. Int. Ed.* **2012,** *51*, 5062-5085. (b) Meijere, A. d.; Diederich, F. *Metal-Catalyzed Cross-Coupling Reactions*. Wiley-VCH: 2004; Vol. 2.

group in the organic molecule can serve as a ligand for metal catalyst and direct the C–H activation and functionalization in a highly selective fashion (Figure 1c). Numerous directing groups have been reported for such transformations including carboxylic acids, amides, alcohols, amines, ketones, aldehydes, imines, oximes, and pyridines to overcome the selectivity issues. However, the removal of such directing groups are required after the desired transformation was achieved.

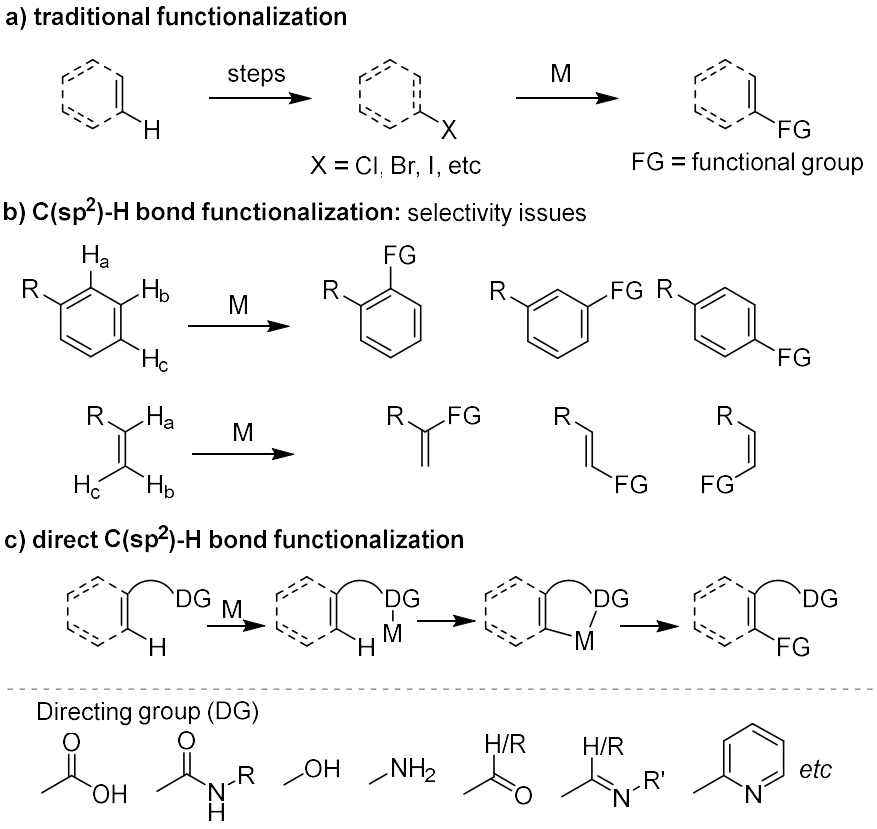

Figure 1.1

The Miura and Satoh laboratory reported the seminal work in which rhodium/copper catalyst system efficiently mediates a coupling between benzoic acids and internal alkynes to afford isocoumarins (Scheme 1.1, eq 1).[4] In this way, the heteroatom directing group also

[4] Ueura, K.; Satoh, T.; Miura, M. *Org. Lett.* **2007,** *9*, 1407-1409.

incorporates and providing synthetically useful heterocycles. The reaction is understood to proceed by the coordination of benzoate ligand to Rh(III) and *ortho* C-H activation to form a five-membered rhodacycle intermediate. Subsequent alkyne coordination, migratory insertion, and reductive elimination generate isocoumarin product and Rh(I) species. The copper cocatalyst then oxidizes Rh(I) to complete a catalytic turnover. The same group also illustrated the C-H activation/C-N bond formation by using phenylazoles with alkynes to produce the imidazoisoquinoline products (eq 2).[5] Concurrently, Fagnou group reported that the C-H activation of anilides with alkynes to deliver indoles (eq 3).[6] In the same year, Jones also studied the Rh(III)-mediated stoichiometric transformation by using pyridine or imine as directing groups to couple with alkynes affording quinolinium salts (eq 4).[7] Along these lines, these works demonstrated that the heteroatom-directed and metal-catalyzed (or mediated) C-H activation, C-C/C-heteroatoms bond formation is an efficient tool to synthesize heterocycles from simple and readily available precursors without substrate preactivations.

[5] Umeda, N.; Tsurugi, H.; Satoh, T.; Miura, M. *Angew. Chem. Int. Ed.* **2008,** *47*, 4019-4022.

[6] Stuart, D. R.; Bertrand-Laperle, M.; Burgess, K. M. N.; Fagnou, K. *J. Am. Chem. Soc.* **2008,** *130*, 16474-16475.

[7] Li, L.; Brennessel, W. W.; Jones, W. D. *J. Am. Chem. Soc.* **2008,** *130*, 12414-12419.

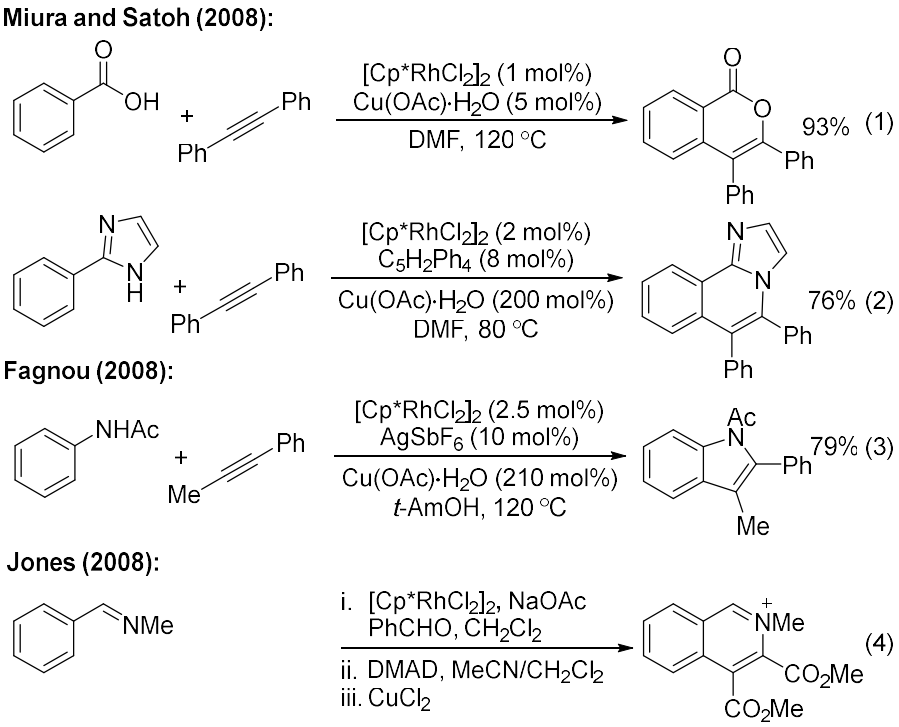

Scheme 1.1

The Rovis lab has long been interested in N-heterocycle synthesis.[8] The amide is a common functional group in organic chemistry. Hence, this directing group can serve as the nitrogen source for the synthesis of *N*-heterocycles via C–H/N–H bond cleavages and C–C/C–N bond formation.[9] Our group and others utilized the amide as a directing group for Rh(III)-catalyzed [4+2] formal cycloaddition of benzamides with alkynes to generate isoquinolones (Scheme 1.2 eqs 5 and 6).[10] However, a stoichiometric oxidant is needed to achieve a catalyst turnover (eq 2). Unfortunately, superstoichiometric amounts of oxidant and its waste limits the

[8] Reviews, see: (a) Johnson, J. B.; Rovis, T. *Acc. Chem. Res.* **2008,** *41*, 327-338. (b) Perreault, S.; Rovis, T. *Chem. Soc. Rev.* **2009,** *38*, 3149-3159.

[9] (a) Zhu, C.; Wang, R.; Falck, J. R. *Chem. Asian J.* **2012,** *7*, 1502-1514. (b) Gulías, M.; Mascareñas, J. L. *Angew. Chem. Int. Ed.* **2016**, *55*, 11000-11019.

[10] (a) Mochida, S.; Umeda, N.; Hirano, K.; Satoh, T.; Miura, M. *Chem. Lett.* **2010,** *39*, 744-746. (b) Hyster, T. K.; Rovis, T. *J. Am. Chem. Soc.* **2010,** *132*, 10565-10569. (b) Song, G. Y.; Chen, D.; Pan, C. L.; Crabtree, R. H.; Li, X. W. *J. Org. Chem.* **2010,** *75*, 7487-7490.

substrate scope and gives undesired side products. Fagnou[11] and Glorius[12] independently investigated Rh(III)-catalyzed annulation of *O*-substituted benzhydroxamic acids with alkene coupling partners. They observed two distinct mechanisms from different directing groups. While -C(O)NHOMe was employed, an olefinated product was observed (eq 7). The transformation delivers dihydroisoquinolone when -C(O)NHOPiv was used as the internal oxidant (eq 8). The application of directing groups that contain an internal oxidant provides mild reaction conditions that do not require metallic oxidants while expanding the variety of components tolerated as a coupling partner.

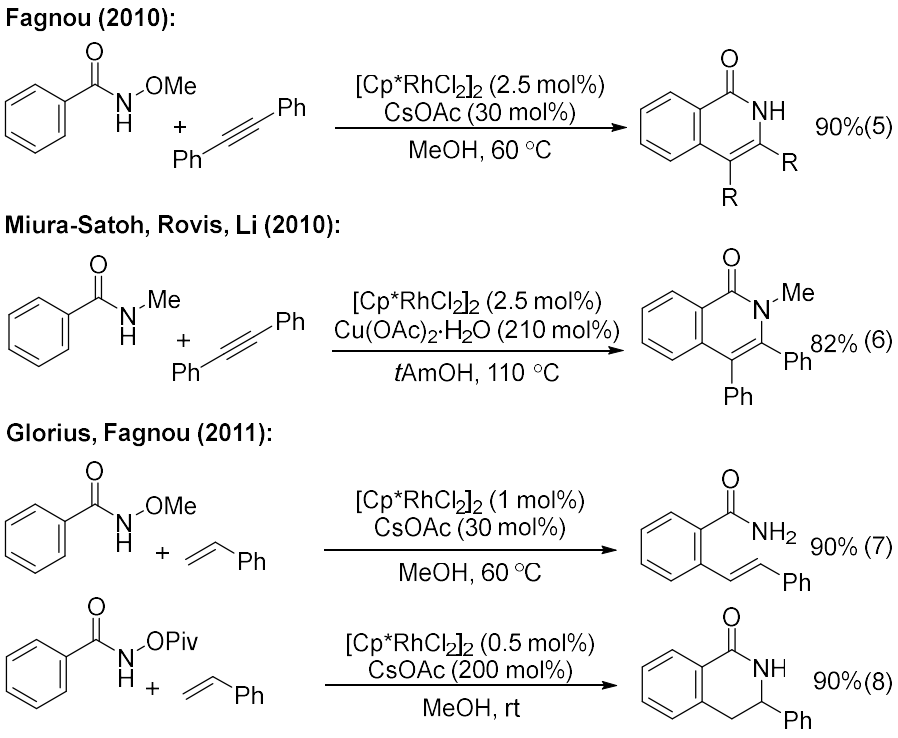

Scheme 1.2

[11] (a) Guimond, N.; Gouliaras, C.; Fagnou, K. *J. Am. Chem. Soc.* **2010,** *132*, 6908. (b) Guimond, N.; Gorelsky, S. I.; Fagnou, K. *J. Am. Chem. Soc.* **2011,** *133*, 6449-6457.

[12] Rakshit, S.; Grohmann, C.; Besset, T.; Glorius, F. *J. Am. Chem. Soc.* **2011,** *133*, 2350-2353.

Proposed reaction mechanism for this transformation is outlined in Figure 1.2. The amide functional group directs *ortho* C–H bond activation to afford rhodacycle **I** *via* concerted metallation-deprotonation (CMD) mechanism. **TSI** shows the transition state for CMD mechanism in which acetate on rhodium(III) deprotonates a C–H bond and rhodium(III) inserts to the C–H bond simultaneously. Consequently, the oxidation state of Rh(III) does not change during this process. Rhodacycle **I** can then undergo alkene or alkyne coordination followed by migratory insertion to afford rhodacycle **II**. Upon reductive elimination of **II** to form dihydroisoquinolone, reductive cleavage of the N–O bond can oxidize Rh(I) to Rh(III) completing a catalyst turnover. In contrast, β-hydride elimination may occur when -C(O)NHOMe was used as a directing group.

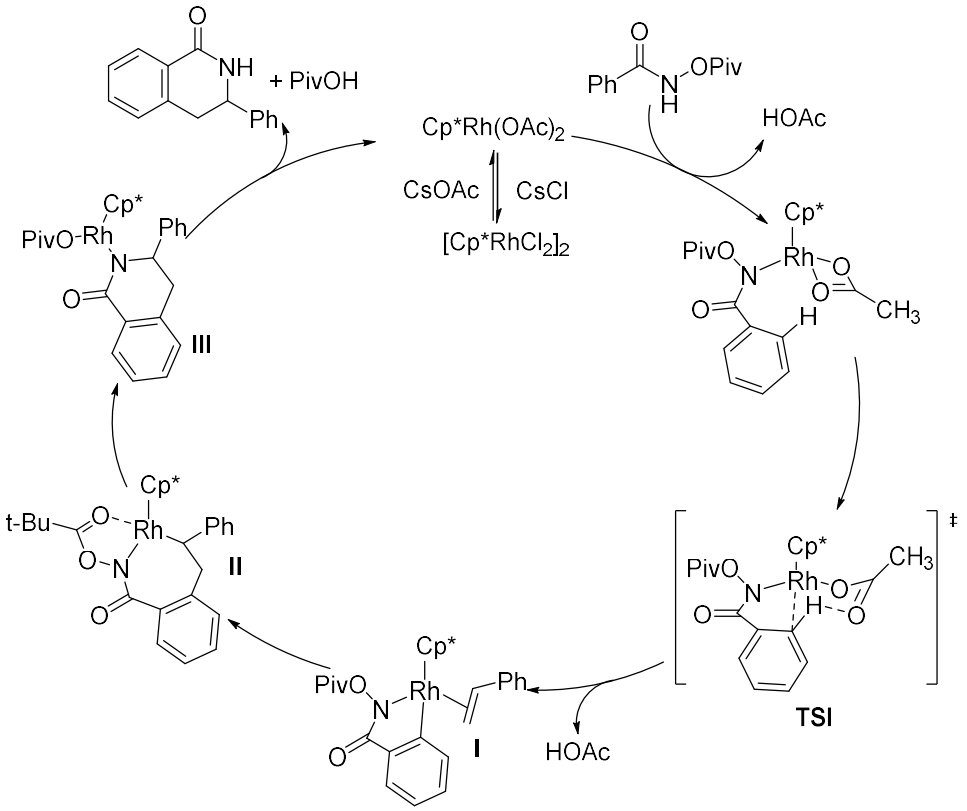

Figure 1.2

Rhodium(III) is a particularly effective catalyst in performing the annulation of aromatic and vinylic C-H bond bearing an amide directing group. Several coupling partners, for example, alkynes, carbon monoxide, alkenes (including cyclopropenes), and donor-acceptor diazo compound have been shown to incorporate to yield *N*-heterocycles *via* C–H activation. The recent development of rhodium(III) catalyzed C–H activation to access *N*-heterocycles by our group is summarized in Figure 1.3.[13] In some case, the reaction generates stereocenter(s) in which the chiral catalyst potentially render the reaction asymmetric.

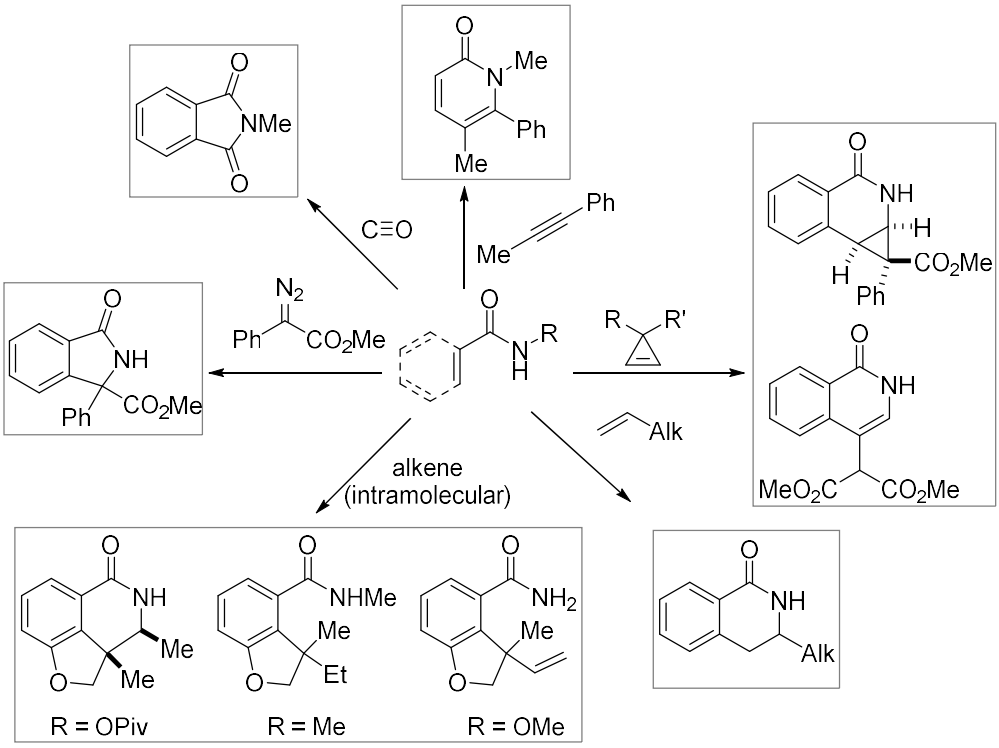

Figure 1.3 Examples of heterocyclic structures accessed using Rh(III) catalyzed C-H activation annulations in the Rovis group

[13] The use of amide as a direct group, see: (a) Hyster, T. K.; Rovis, T. *Chem. Sci.* **2011,** *2*, 1606-1610. (b) Du, Y.; Hyster, T. K.; Rovis, T. *Chem. Comm.* **2011,** *47*, 12074-12076. (c) Hyster, T. K.; Ruhl, K. E.; Rovis, T. *J. Am. Chem. Soc.* **2013,** *135*, 5364-5367. (d) Davis, T. A.; Hyster, T. K.; Rovis, T. *Angew. Chem. Int. Ed.* **2013,** *52*, 14181-14185. (e) Hyster, T. K.; Dalton, D. M.; Rovis, T. *Chem. Sci.* **2015,** *6*, 254-258. Review, see: Zhu, R. Y.; Farmer, M. E.; Chen, Y. Q.; Yu, J. Q., *Angew. Chem. Int. Ed.* **2016**, *55*, 10578-10599.

The ability to render rhodium(III)-catalyzed C–H activation reaction asymmetric is an ongoing challenge in the field. Figure 1.4 depicts the structure of Cp*Rh(III) three-legged piano-stool complex (or half-sandwich complex). Indeed, the introduction of exogenous chiral ligand is non-productive since three coordinating sites are required for ligand attachment (two X-type ligands and one L-type ligand) during a catalytic cycle. The engineering of chiral ligand-metal complexes has been demonstrated by Cramer,[14] You,[15] Antonchick, and Waldmann[16] to render the reaction asymmetric. However, several limitations for example, multistep synthesis, structural variability and electronic properties of those chiral Cp ligands, remain unsolved.

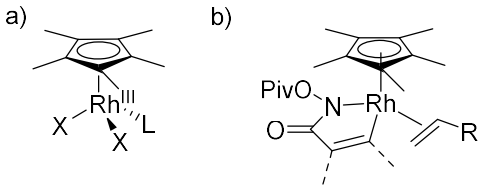

Figure 1.4 a) Cp*Rh(III) piano-stool complex b) the requirement of three coordinating sites during the catalytic cycles

An alternative approach to rendering an asymmetric transformation is to anchor the catalyst to a supramolecular scaffold. An enzyme catalysis is a powerful tool since nature can use proteins to create molecules in a highly asymmetric fashion. The marriage of transition metal catalysis with an enzyme or a so-called "artificial metalloenzyme" will provide useful tools for organic synthesis.[17] In addition, biology tools such as site-directed mutagenesis and directed evolution can tailor the amino acid residues in the enzyme pocket to achieve higher reactivity

---

[14] For review, see: (a) Ye, B. H.; Cramer, N. *Acc. Chem. Res.* **2015,** *48*, 1308-1318. (b) Newton, C. G.; Kossler, D.; Cramer, N. *J. Am. Chem. Soc.* **2016,** *138*, 3935-3941.

[15] Zheng, J.; Cui, W. J.; Zheng, C.; You, S. L., *J. Am. Chem. Soc.* **2016,** *138*, 5242-5245.

[16] Jia, Z. J.; Merten, C.; Gontla, R.; Daniliuc, C. G.; Antonchick, A. P.; Waldmann, H., *Angew. Chem. Int. Ed.* **2017,** *56*, 2429-2434.

[17] Heinisch, T.; Ward, T. R., *Acc. Chem. Res.* **2016,** *49*, 1711-1721.

and selectivity. In this vein, Rovis, Ward and coworkers explored an artificial metalloenzyme based on biotinylated rhodium(III) ligated streptavidin as a tool for asymmetric C–H activation. The introduction of a biotin-tethered pentamethylcyclopentadienyl (Cp*) ligand to the streptavidin (SAV) resulted in a high concentration of the metal in the enzyme. In this way, the biotinylated $[RhCp^*Cl_2]_2$ complex was anchored to streptavidin and catalyzed the coupling of *O*-pivaloylbenzhydroxamic acid **1a** with alkene **2a** to furnish the dihydroisoquinolone **3aa**.[18] With the best mutant S112Y-K121E, dihydroisoquinolone **3aa** could be accessed in high yield, high regioselectivity, and good enantioselectivity (eq 9). An engineered streptavidin with a carboxylate amino acid residue allows for greater rate of carboxylate-assisted C–H bond cleavage which is the turnover-limiting step and accelerating the reaction.

Rovis and Ward (2012)

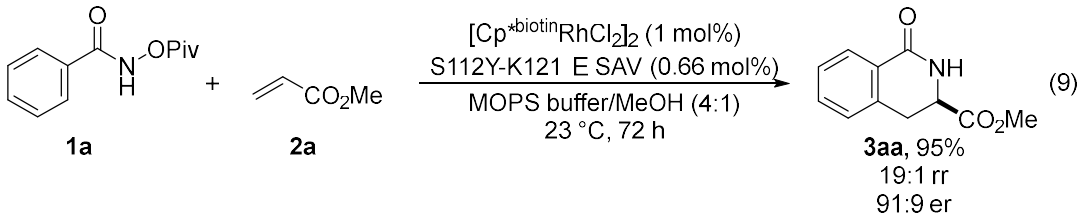

1a **2a** **3aa**, 95%
19:1 rr
91:9 er

Hyster and Rovis also found that *O*-pivaloyl benzhydroxamic acid **1a** could be coupled to 3,3-disubstituted cyclopropene **4a**, generating [4.1.0] dihydroisoquinolone **5aa** in 95% yield (1.4:1 dr, Table 1.1, entry 1).[19] However, the low diastereoselectivity is thought to result from a lack of facial selectivity during cyclopropene migratory insertion. Hyster also explored this reaction using SAV-based artificial metalloenzymes. In this study, the N118K-K121E SAV mutant provided the [4.1.0] dihydroisoquinolone product (**5aa**) in 80% yield (1.4:1 dr, 89:11 er,

[18] Hyster, T. K.; Knorr, L.; Ward, T. R.; Rovis, T. *Science* **2012,** *338*, 500-503.

[19] Hyster, T. K.; Rovis, T. *Synlett* **2013,** *24*, 1842-1844.

entry 2).[20] Additionally, the S112Y-K121E mutant gave **5aa** in 60% yield (1.4:1 dr, 83:17 er, entry 3). Ongoing efforts are directed towards developing a stereoselective coupling between *O*-pivaloyl benzhydroxamic acids with cyclopropenes.

Table 1.1

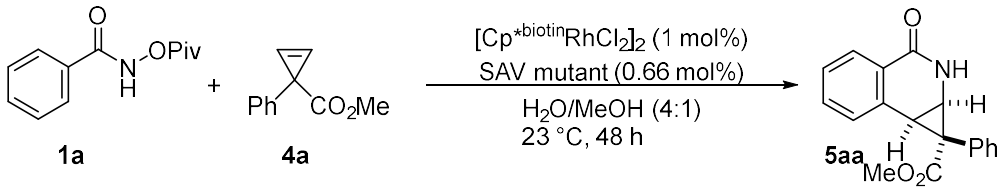

1a **4a** **5aa**

entry	SAV mutant	yield (%)	dr	er
1	-	80	1.4:1	50:50
2	N118K-K121E SAV	80	1.4:1	89:11
3	S112Y-K121E SAV	60	1.4:1	83:17

1.1.2 Ligand Development in Rh(III) Catalysis

Rh(III)-catalyzed C-H bond functionalization strategies have emerged as a powerful synthetic tool.[21] The methodology allows for the functionalization of simple organic molecules and expedient synthesis of *N*-heterocycles from readily available precursors. Cyclopropenes constitute a class of building blocks with a special reactivity due to their high ring strain energy (54 kcal/mol). In this context, a handful of reactions utilizing transition metals has been developed for the stereoselective functionalization of cyclopropenes.[22] Under the aegis of Rh(III)

---

[20] Hyster, T. K. (2013) Ligand and reaction development in the rhodium(III)-catalyzed C-H activation-mediated synthesis of N-heterocycles (Doctoral dissertation).

[21] For the review of Rh(III)-catalyzed C-H activation, see: (a) Colby, D. A.; Bergman, R. G.; Ellman, J. A., *Chem. Rev.* **2010,** *110*, 624-655. (b) Satoh, T.; Miura, M. *Chem. Eur. J.* **2010,** *16*, 11212-11222. (c) Patureau, F. W.; Wencel-Delord, J.; Glorius, F. *Aldrichimica Acta* **2012,** *45,* 31. (d) Song, G. Y.; Wang, F.; Li, X. W. *Chem. Soc. Rev.* **2012,** *41*, 3651-3678. (e) Zhu, C.; Wang, R.; Falck, J. R. *Chem. Asian. J.* **2012,** *7*, 1502-1514 (f) Song, G. Y.; Li, X. W. *Acc. Chem. Res.* **2015,** *48*, 1007-1020.

[22] For the review for the functionalization of cyclopropene, see: Rubin, M.; Rubina, M.; Gevorgyan, V. *Chem. Rev.* **2007,** *107*, 3117-3179. Selected examples: (a) Rubina, M.; Rubin, M.; Gevorgyan, V. *J. Am. Chem. Soc.* **2002,** *124*,

catalysis, Wang and coworkers have shown that cyclopropenes **7** participate in a Rh(III) catalyzed reaction with *N*-phenoxyacetamide **6** to give 2*H*-chromenes **8** (eq 2).[23]

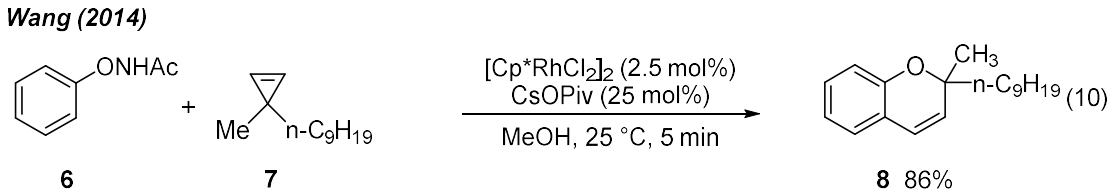

6 **7** **8** 86%

Our group reported the Rh(III)-mediated coupling of *O*-pivaloyl benzhydroxamate **1a** with 3,3-diester substituted cyclopropene **4b** to afford 4-substituted isoquinolone **9** after ring opening of the three-membered ring (Scheme 1.3, eq 11). During this study, when using the less activated methyl 1-phenylcycloprop-2-ene-1-carboxylate **4a** as a substrate, the Cp*Rh(III) catalyst gives the [4.1.0] bicyclic product **5aa** in low diastereoselectivity (Scheme 1.3, 1.4:1 dr, eq 12). We believe the lack of diastereoselectivity stems from the poor facial selectivity during coordination of the cyclopropene and the migratory insertion step of cyclopropene unit. We reasoned that creating anisotropy around the cyclopentadienyl ligand of the rhodium metal center could solve this selectivity issue.

11566-11567. (b) Rubina, M.; Rubin, M.; Gevorgyan, V. *J. Am. Chem. Soc.* **2003,** *125*, 7198-7199. (c) Rubina, M.; Rubin, M.; Gevorgyan, V. *J. Am. Chem. Soc.* **2004,** *126*, 3688-3689. (d) Phan, D. H. T.; Kou, K. G. M.; Dong, V. M. *J. Am. Chem. Soc.* **2010,** *132*, 16354-16355. (e) Tian, B.; Liu, Q.; Tong, X. F.; Tian, P.; Lin, G. Q. *Org. Chem. Front.* **2014,** *1*, 1116-1122. (f) Parra, A.; Amenos, L.; Guisan-Ceinos, M.; Lopez, A.; Ruano, J. L. G.; Tortosa, M. *J. Am. Chem. Soc.* **2014,** *136*, 15833-15836. (g) Muller, D. S.; Marek, I. *J. Am. Chem. Soc.* **2015,** *137*, 15414-15417.

[23] Zhang, H.; Wang, K.; Wang, B.; Yi, H.; Hu, F. D.; Li, C. K.; Zhang, Y.; Wang, J. B. *Angew. Chem. Int. Ed.* **2014,** *53*, 13234-13238.

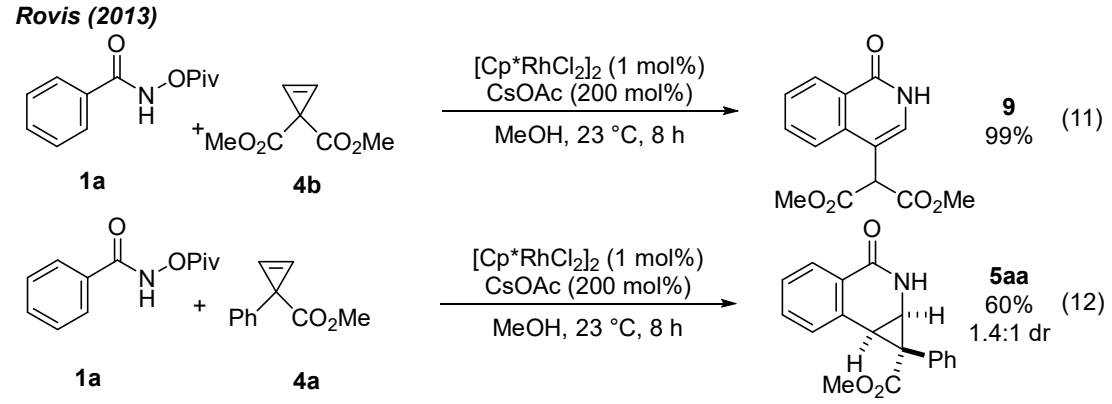

Scheme 1.3

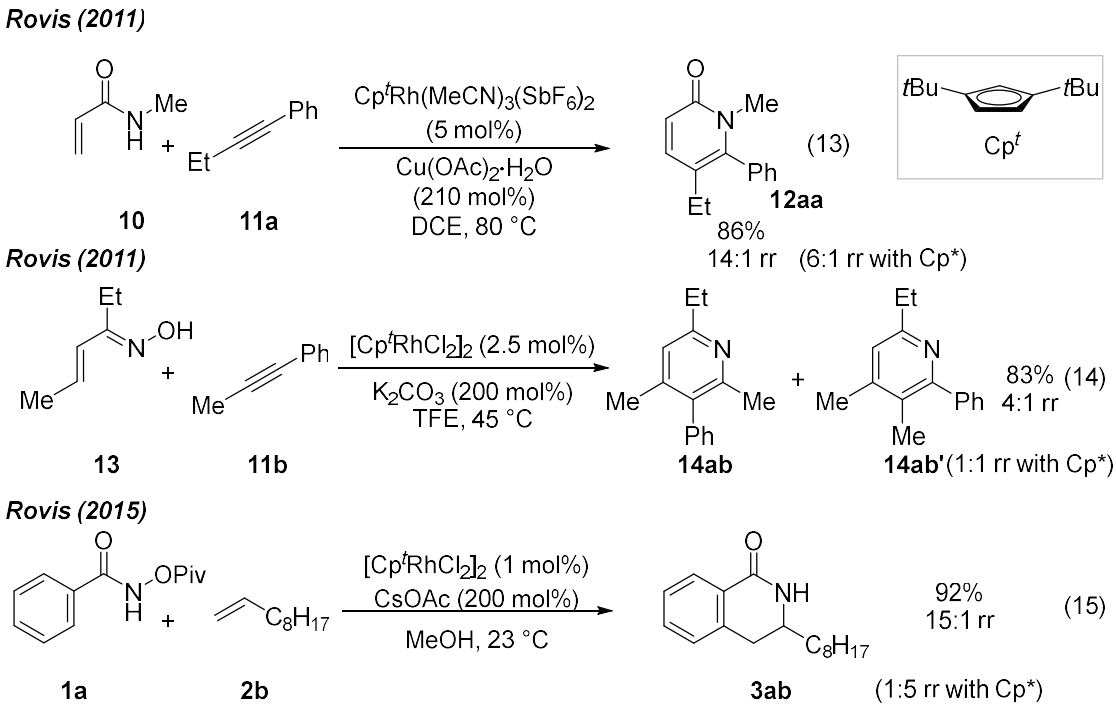

Scheme 1.4

Our group[24] and others[25] have developed several Rh(III)-catalyzed transformations where the nature of the Cp ligand drastically impacts the reactivity and selectivity of the reaction. For

[24] Electron deficient Cp*^{CF3}, see: (a) Neely, J. M.; Rovis, T. *J. Am. Chem. Soc.* **2014,** *136*, 2735-2738. (b) Romanov-Michailidis, F.; Sedillo, K. F.; Neely, J. M.; Rovis, T. *J. Am. Chem. Soc.* **2015,** *137*, 8892-8895. Cp*^{bisCF3Ar}, see: (c) Davis, T. A.; Wang, C. Q.; Rovis, T. *Synlett* **2015,** *26*, 1520-1524.

example, the sterically bulky di-*tert*-butylcyclopentadienyl (Cp^t) ligand[26] has been shown to improve the regiochemistry of alkyne (**11a** and **11b**) and alkene (**12b**) insertion events in the synthesis of pyridones (**12aa**, eq 13), pyridines (**14ab** and **14ab'**, eq 14) and dihydroisoquinolones (**3ab**, eq 15).

Recently, our group disclosed a cyclopropanation reaction with the coupling of *N*-enoxyphthalimides **15** and electron-deficient alkenes (**2c** and **2d**). Monoisopropylcyclopentadienyl (Cp^{iPr}) ligand[27] outperforms the more common Cp* ligand, furnishing the *trans*-cyclopropane (**16ac**) in high diastereoselectivity (eq 11). Alternatively, a divergent carboamination path was identified when using a hindered *tert*-buyltetramethylcyclopentadienyl ($Cp^{*t\text{-}Bu}$) ligand delivering the acyclic adduct (**16ad**) with high chemoselectivity (eq 12).[28]

---

[25] (a) Shibata, Y.; Tanaka, K. *Angew. Chem. Int. Ed.* **2011,** *50*, 10917-10921. (b) Fukui, M.; Hoshino, Y.; Satoh, T.; Miura, M.; Tanaka, K. *Adv. Synth. Catal.* **2014,** *356*, 1638-1644. (c) Hoshino, Y.; Shibata, Y.; Tanaka, K. *Adv. Synth. Catal.* **2014,** *356*, 1577-1585.

[26] (a) Hyster, T. K.; Rovis, T. *Chem. Sci.* **2011,** *2*, 1606-1610. (b) Hyster, T. K.; Rovis, T. *Chem. Commun.* **2011,** *47*, 11846-11848. (c) Hyster, T. K.; Dalton, D. M.; Rovis, T. *Chem. Sci.* **2015,** *6*, 254-258.

[27] Piou, T.; Rovis, T. *J. Am. Chem. Soc.* **2014,** *136*, 11292–11295.

[28] Piou, T.; Rovis, T. *Nature* **2015,** *527*, 86-90.

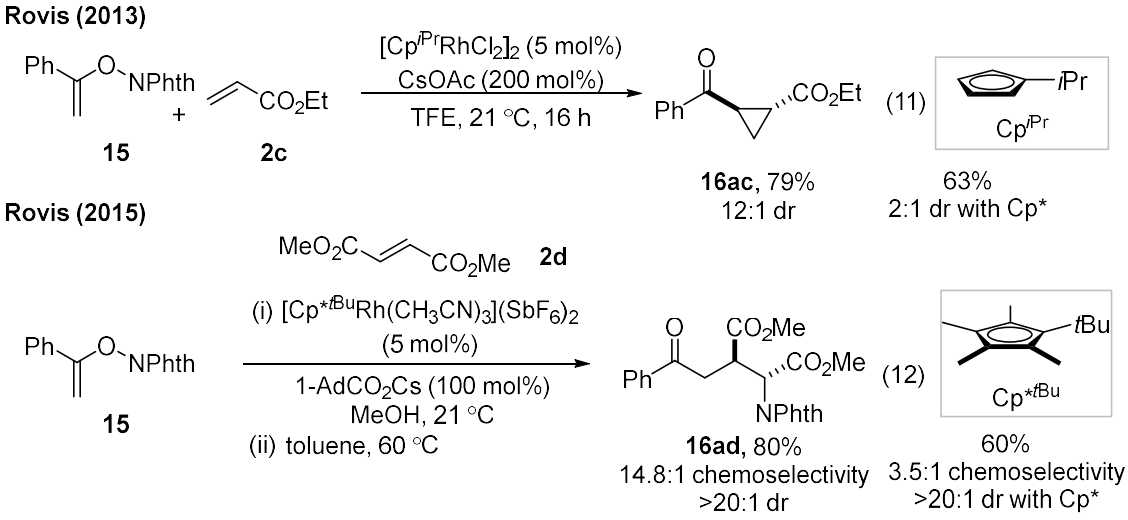

Scheme 1.5

Motivated by these results, we believed ligand design could provide a solution to the inherent selectivity issues encountered for the coupling of benzamide **1** and 3,3-disubstituted cyclopropenes **4** (eq 13).

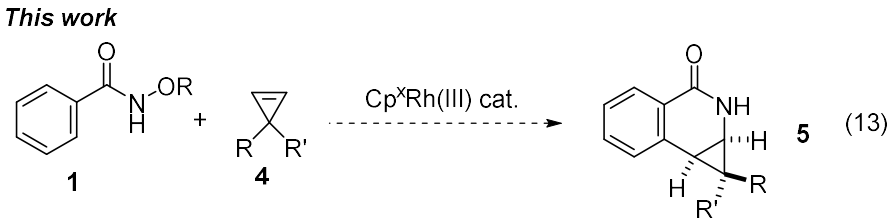

1.2 Results and Discussion

1.2.1 Efforts Towards Stereoselective Benzamidation of Cyclopropenes

Initially, the project goal was to identify the SAV mutant needed to improve the diastereoselectivity and enantioselectivity of this transformation. Several streptavidin mutants, provided by Professor Thomas Ward (University of Basel), were screened under optimal conditions. Our main goal was to find a SAV mutant that would lead to increased diastereoselection. Coupling between *O*-pivaloyl benzhydroxamic acid **1a** and cyclopropene **4a** were used as the model system. A variety of SAV mutants at the S112 position were examined as

summarized in Table 1.2. We found that the S112F SAV mutant gave the desired product in 36% yield and 1.4:1 dr (entry 1). However, other mutants at the S112 position did not provide the corresponding product (entries 2-8). Utilizing the methyl acrylate as the coupling partner in the presence of metalloenzyme gave the same results as previously reported, confirming the integrity of the SAV mutant.

Table 1.2

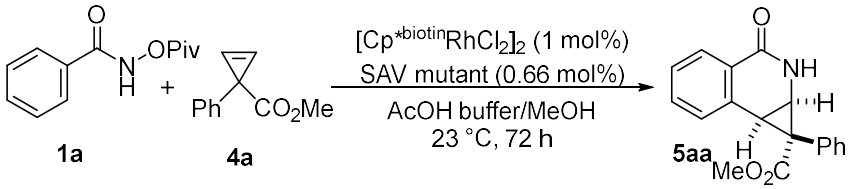

1a 4a 5aa

entry	Mutant	yield	dr	er (major)	er (minor)
1	S112F	36	1.7:1	80:20	78:22
2	S112Y	<5	-	-	-
3	S112A	0	-	-	-
4	S112K	<5	-	-	-
5	S112R	<5	-	-	-
6	S112C	0	-	-	-
7	S112H	0	-	-	-
8	S112M	0	-	-	-

reaction conditions: **1** (10 μmol), **4** (11 μmol), AcOH buffer (pH 5.7) as a solvent
yield and diastereoselectivity (dr) were obtained from ^{1}H-NMR or chiral HPLC.
enantioselectivity (er) was determined by chiral HPLC.

Next, mutations at the K121 position were examined (Table 1.3). We found that the desired product **5aa** was afforded in modest yields when K121A, K121E, and K121F SAV mutants were employed (44-69% yield, entries 1-3). The K121N SAV mutant provided the product in low yield (entry 4). No reactivity was obtained from the K121C, K121H, and K121M SAV mutants (entries 5-7). This is likely due to the coordinating ability of the cysteine,

methionine, and histidine residues to the Rh(III) active site. Double mutants such as N118K/K121D SAV gave the desired product **5aa** in 39% yield (91:9 and 92:8 er) despite low level of diastereoselection (entry 8). Higher reactivity was obtained when S112Y/K121E SAV was employed (entry 9). Overall, no notable improvements in diastereoselection were observed with these mutants.

Table 1.3

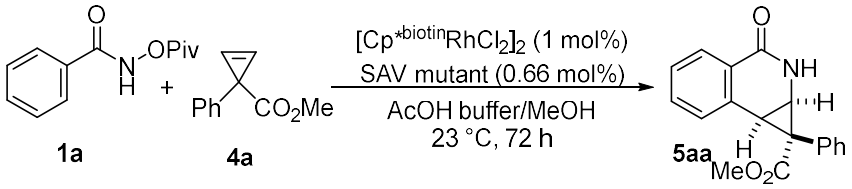

1a **4a** **5aa**

entry	Mutant	yield	dr	er (major)	er (minor)
1	K121A	69	1.9:1	70:30	67:33
2	K121E	66	1.6:1	81:19	85:15
3	K121F	44	1.3:1	86:14	79:21
4	K121N	28	1.5:1	75:25	78:22
5	K121C	<5	-	-	-
6	K121H	0	-	-	-
7	K121M	0	-	-	-
8[a]	N118K/K121D	39	1.7:1	91:9	92:8
9[a]	S112Y/K121E	84	1.6:1	89:11	89:11

reaction conditions: **1** (10 μmol), **4** (11 μmol), AcOH buffer (pH 5.7) as a solvent
[a] H_2O as a solvent.
yield and diastereoselectivity (dr) were obtained from ^{1}H-NMR or chiral HPLC.
enantioselectivity (er) was determined by chiral HPLC.

We hypothesized that steric bulk of substituents on cyclopropene may assist in differentiating facial selectivity during cyclopropene insertion. To test this hypothesis, cyclopropenes **4c-4e** were prepared (Table 1.4). To our delight, we observed that increasing steric on the ester moeity (**4c** and **4d**) substantially improves the diastereoselectivity of

cyclopropene insertion with $[Cp^*RhCl_2]_2$ (ranging from 2:1 to >10:1 dr). However, cyclopropene **4c** gave the product **5ac** with the same level of diastereoselectivity when the S112Y-K121E SAV mutant was employed as the catalyst (entry 1, 1.5:1 dr). Cyclopropene **4d** was found to be ineffective under the metalloenzyme conditions, presumably due to the steric and solubility factors and the ability of the substrate to enter into the catalytic pocket (entry 2). However, cyclopropene **4e** delivered the product with good diastereoselectivity, albeit low enantioselection (entry 3).

Table 1.4

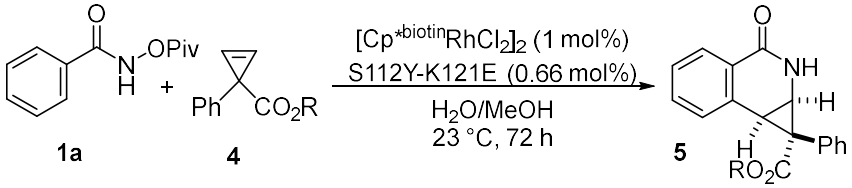

entry	cyclopropene	product	yield (%)	dr	er
1	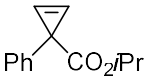 **4c**	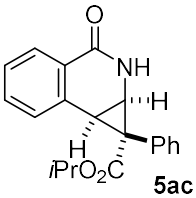 **5ac**	85[a]	2.1:1	50:50
			47[b]	1.5:1	86:14
2	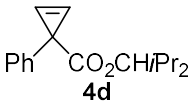 **4d**	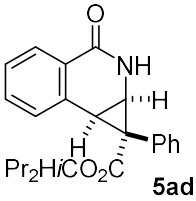 **5ad**	89[a]	>10:1	-
			0[b]	-	-
3	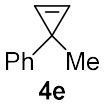 **4e**	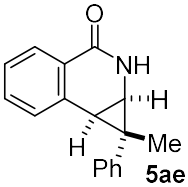 **5ae**	90[a]	7.7:1	50:50
			86[b]	>10:1	66:34

[a] without SAV mutant.
[b] with SAV: **1** (10 μmol), **4** (11 μmol).
yield and dr were obtained from ^{1}H-NMR or chiral HPLC.
er (major and minor diastereomers) was determined by chiral HPLC.

We also found that the *O*-acyloxy substituent of the benzhydroxamate precursor slightly influences the diastereoselectivity of cyclopropene insertion (Table 1.5). Benzhydroxamate ester precursors **1b** and **1c** were found to improve the diastereoselectivity up to 5:1 dr of the product **5aa** by using $[Cp^*RhCl_2]_2$ precatalyst. However, *O*-Boc substrate **1b** was hydrolyzed under metalloenzyme conditions to give a benzhydroxamic acid (entry 1). Substrate **1c**, which has steric properties analogous to O-Boc, was examined. Precursor **1c** delivered the corresponding product (**5**) in good yield (1.6:1 dr) and slightly improved enantioselectivity (93:7 er) under metalloenzyme conditions (entry 2).

Table 1.5 [a,b]

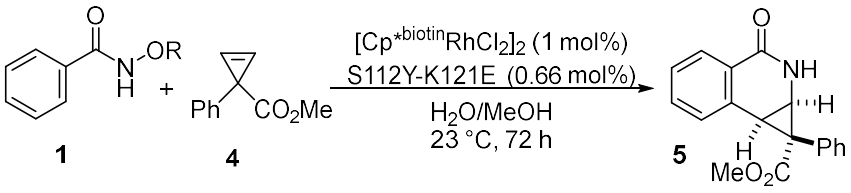

1 **4** **5**

entry	R	product	yield (%)	dr	er
1	CO_2tBu or Boc **1b**	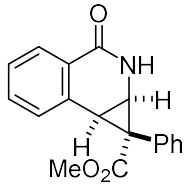	quant[a]	4.4:1	-
			0[b]	-	-
2	$COCH_2tBu$ **1c**	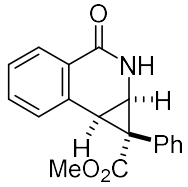	85[a]	4.6:1	-
			87[b]	1.6:1	93:7

[a] without SAV mutant.
[b] asymmetric reaction: **1** (10 μmol), **4** (11 μmol).
yield and dr were obtained from ^{1}H-NMR or chiral HPLC.
er (major and minor diastereomers) was determined by chiral HPLC.

Although promising levels of enantioselection were observed, we did not see an improvement of diastereoselectivity under metalloenzyme conditions. We questioned whether

steric and electronic modulations of cyclopentadienyl ligands on rhodium(III) might have a beneficial effect on the diastereoselectivity of cyclopropene insertion.

1.2.2 Ligand Development for Diastereoselective Benzanulation of Cyclopropene

We began our investigation by employing *O*-pivaloyl benzhydroxamate ester **1a** and cyclopropene **4e** as model substrates for the optimization of the catalytic process (Table 1.6). $[Cp^*RhCl_2]_2$ provides the desired product in a moderate yield and diastereoselectivity (entry 1, 5.8:1 dr). The relative stereochemistry of the major diastereoisomer of **5ae** was confirmed by NOESY. By modulating the steric and electronic properties of the Cp ligand, we have shown that the diastereoselectivity of the reaction is considerably affected. Sterically hindered di-*tert*-butylcyclopentadienyl (Cp^t) and the electron-poor trifluoromethyl tetramethylcyclopentadienyl (Cp^{*CF3}) ligands give only modest diastereoselectivity (entries 2, 3). The monoisopropylcyclopentadienyl ligand (Cp^{iPr}) gave the desired product in a good yield albeit with no diastereocontrol (entry 4). 3,5-(Bistrifluoromethyl)aryltetramethylcyclopentadienyl ($Cp^{*bisCF3Ar}$) provides the desired product in good yield with slightly improved diastereoselectivity (7.0:1 dr, entry 5). Good level of diastereocontrol (8.8:1 dr) is achieved when *tert*-butyl tetramethylcyclopentadienyl (Cp^{*tBu}) ligand was employed (entry 6). Gratifyingly, heptamethylindenyl ligand[29] (Ind*) provides high reactivity and diastereoselectivity with 90% yield and 15.2:1 dr (entry 7). To demonstrate the scalability of the transformation, the reaction was performed on 2 mmol scale of substrate **1a**, which gives the expected product with comparable yield and selectivity. The catalyst loading can be lowered to 0.5 mol% $[Ind^*RhCl_2]_2$ without affecting the reactivity.

---

[29] Kakkar, A. K.; Stringer, G.; Taylor, N. J.; Marder, T. B. *Can. J. Chem.* **1995,** *73*, 981-988.

We then examined the nature of the directing group. It was found that using *O*-Boc benzhydroxamate ester **1b** as a substrate gave excellent diastereoselectivity (>20:1 dr) but with slightly lower yield (Scheme 1.6, eq 14), presumably due to a competitive Lossen rearrangement under the basic conditions (Scheme 1.6).[30]

Table 1.6 Ligand Optimization[a,b,c]

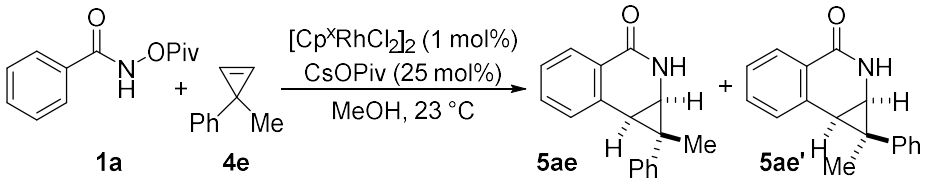

1a **4e** **5ae** **5ae'**

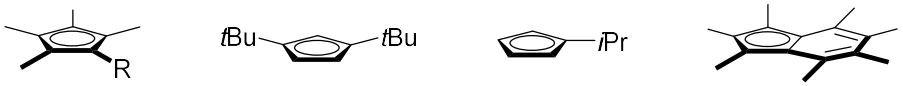

Cp*: R = Me
Cp*^{CF3}: R = CF_3
Cp*^{tBu}: R = *t*Bu
Cp*^{bisCF3Ar}: R = 3,5-*bis*CF_3Ar

Cp^t Cp^{iPr} Ind*

entry	Cp^X	yield[b]	dr[b]
1	Cp*	63	5.8:1
2	Cp^t	82	5.0:1
3	Cp^{*CF3}	75	5.3:1
4	Cp^{iPr}	73	1.1:1
5	Cp^{*bisCF3Ar}	80	7.0:1
6	Cp^{*tBu}	64	8.8:1
7	Ind*	90[c]	15.2:1

[a] Reaction conditions: **1a** (0.1 mmol), **4e** (0.11 mmol), Rh catalyst (1 mol %), CsOPiv (0.25 mol%) in MeOH (0.1 M) at 23 °C for 18 h.
[b] The yield and diastereoselectivity were measured from the ^{1}H-NMR analysis of the unpurified reaction mixture using 1,3,5-trimethoxybenzene as an internal standard.
[c] Isolated yield.

[30] Webb, N. J.; Marsden, S. P.; Raw, S. A. *Org. Lett.* **2014,** *16*, 4718-4721.

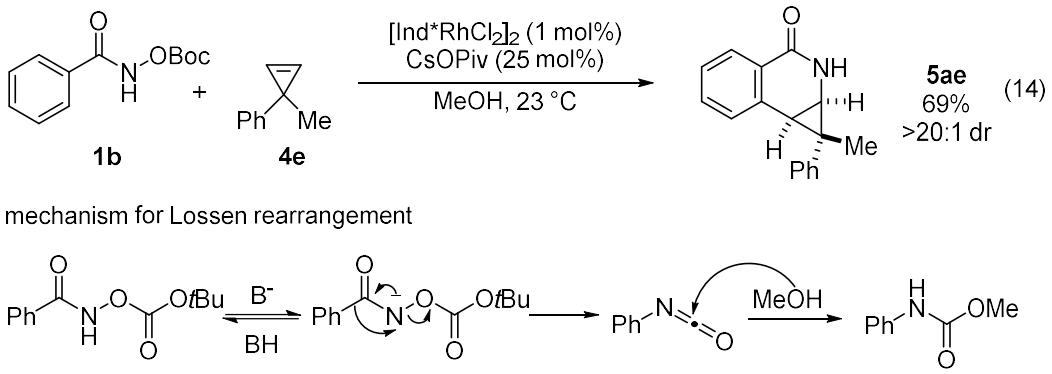

Scheme 1.6

1.2.3 Substrate Scope

Both benzamide directing groups, *O*-Piv (condition A) and *O*-Boc (condition B), were used for studying the scope of the transformation (Table 1.7). Substituents at the *para* position of the benzamide are tolerated in the reaction (**1d-1h**). The *O*-Piv directing group with an electron rich *para*-methoxy substituent (OMe) gave excellent diastereoselectivity (>20:1 dr, product **5ee**) compared to electron deficient substituents (~10:1 dr, products **5fe**, **5ge** and **5he**). The electron-rich benzamide derived from gallic acid furnishes the desired product with good yield and excellent diastereoselectivity (>20:1 dr, product **5je**). The *O*-Boc directing group gives the products in good to excellent diastereoselectivity (**5de-5ge**). Of interest are halogen substituents at the *para* positions (Cl and Br) which provide a functional group handle for further chemical modification. The *ortho*-methyl arylbenzhydroxamate substrate retards the transformation presumably due to steric hindrance. Substituents at the *meta* position on the arylhydroxamates can potentially deliver two regioisomeric products arising from the selectivity of C-H activation. *Meta*-trifluoromethyl arylhydroxamate exclusively provides the 6-substituted product (**5je**) in good yield and diastereoselectivity. Tetrahydronaphthalene-derived arylhydroxamate underwent the transformation with good regioselective at the less hindered position (8.6:1 ratio) to give the desired product (**5ke**) in good yield and high diastereoselectivity. However, *meta*-methyl

arylhydroxamate gave ~3.6:1 regioisomeric ratio of C-H activation in good yield and diastereoselectivity (**5le**). *meta*-Methoxy arylhydroxamate provided 1:1 mixture of regioisomeric products (**5me** and **5me'**) in good diastereocontrol, presumably a consequence of a combination of steric effects and kinetic acidity issues. In addition, X-ray structure of **5me** unambiguously confirmed the relative stereochemistry of *trans*-diastereomer.

Table 1.7 Benzamide Scope[a,b,c]

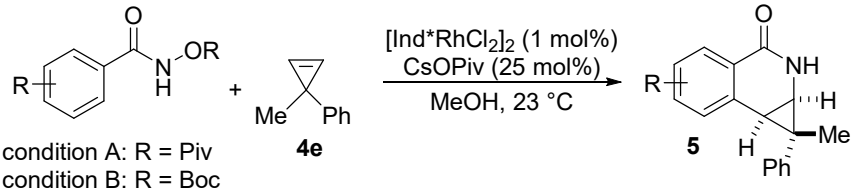

condition A: R = Piv
condition B: R = Boc

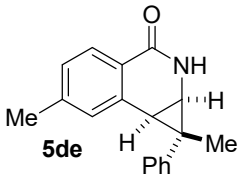

A 90% (>20:1 dr)
B 68% (>20:1 dr)

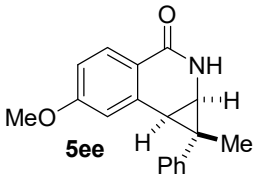

A 89% (>20:1 dr)
B 64% (>20:1 dr)

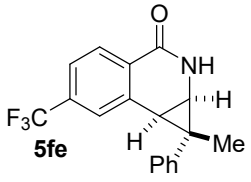

A 77% (10.2:1 dr)
B 67% (17:1 dr)

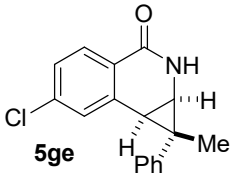

A 73% (8.5:1 dr)
B 63% (>20:1 dr)

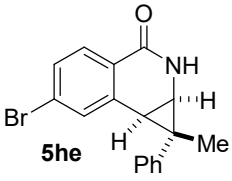

A 83% (11.2:1 dr)

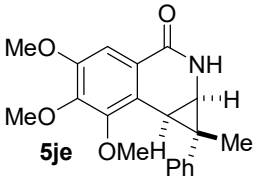

A 62% (>20:1 dr)

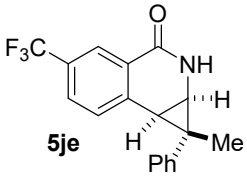

A 85%
single regioisomer
(19:1 dr)

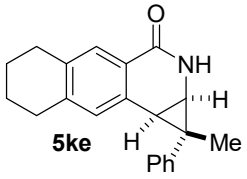

A 86%
8.2:1 rr
(15.3:1 dr)

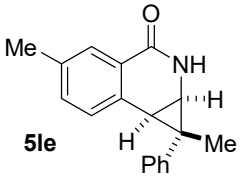

A 92%
3.6:1 rr
(>20:1 dr)

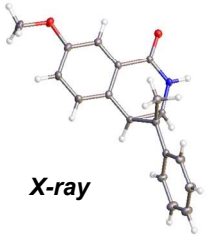

X-ray

≡

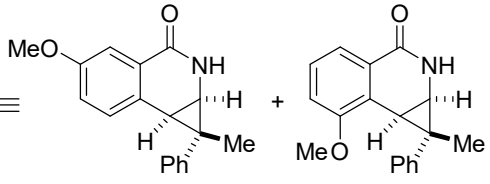

A 86%
1:1 rr
(>20:1 dr)

[a] Conditions: OPiv for condition A or OBoc for condition B (0.1 mmol), **4e** (0.11 mmol), Rh catalyst (1 mol %), CsOPiv (25 mol%) in MeOH (0.1 M) at 23 °C for 18 h.

[b] Isolated yield of the major diastereomer after silica gel column chromatography.

[c] Diastereoselectivity was measured by ^{1}H-NMR spectra of the unpurified material.

Variations of the cyclopropene coupling partner were explored for the transformation using the *O*-Boc benzhydroxamate **1b** (Table 1.8). Cyclopropenes bearing substituents at the para position gave the desired products in moderate yields and excellent diastereoselectivity regardless of the electronic nature of substituents (**5bf**, **5bg** and **5bh**). Cyclopropene with a *meta*-methoxy group **4i** undergoes the transformation with slightly lower diastereoselectivity relative to the *para*-methoxy group (**4g**). A naphthalene-substituted cyclopropene **4j** and a spiro-tetralin containing substrate **4k** each furnish the desired products **5bj** and **5bk** in good yield and excellent diastereoselectivity. In our previous studies, we found that methyl 1-phenylcycloprop-2-ene-1-carboxylate **4a** reacts with benzamide **1a** and gives the desired product **5aa** with low diastereoselectivity (1.4:1 dr) using $[Cp^*RhCl_2]_2$ as the precatalyst. With the $[Ind^*RhCl_2]_2$ ligand, we were pleased to find that cyclopropene **4a** affords the dihydroisoquinolone **5aa** with improved diastereoselectivity (8.7:1 dr). The relative stereochemistry of the major diastereomer of **5aa** was confirmed by NOESY. The observed major diastereomer can be rationalized by the size of the substituents on the cyclopropane ring. Thus, the phenyl group is larger than the carboxylate ester (A-values for Ph- and $-CO_2Me$ are 3.0 and 1.3, respectively) leading to higher diastereoselectivity observed in these reactions. The amidoarylation with benzyl substituted cyclopropene **4l** affords the desired product **5bl** in good yield but with lower diastereoselectivity. This observation can be explained by the steric differences of phenyl vs benzyl groups (A-values for Ph and Bn are 3.0 and 1.75, respectively). 2,3,3-Trisubstituted cyclopropenes did not participate in the Rh(III)-catalyzed coupling with benzamides.

Table 1.8 Cyclopropene Scope[a,b,c]

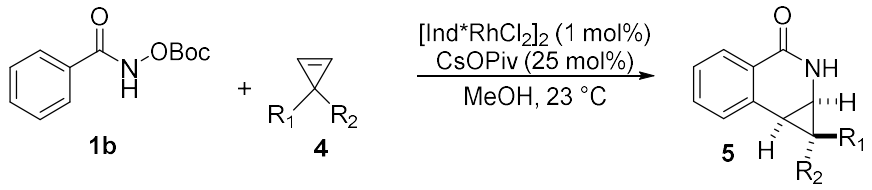

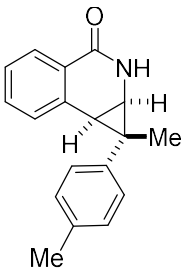

5bf, 58%
>20:1 dr

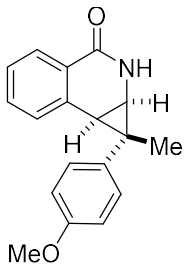

5bg, 67%
>20:1 dr

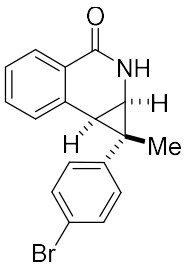

5bh, 52%
>20:1 dr

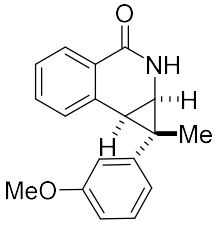

5bi, 58%
13.5:1 dr

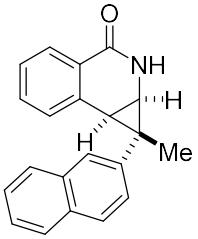

5bj, 75%
>20:1 dr

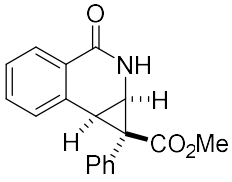

5aa = 5ba, 75%
8.7:1 dr

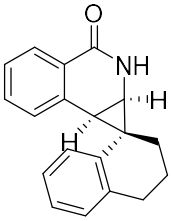

5bk, 72%
>20:1 dr

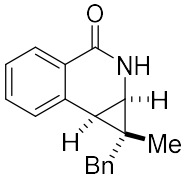

5bl, 64%
2.3:1 dr

[a] Conditions: **1b** (0.1 mmol), **4** (0.11 mmol), Rh catalyst (1 mol %), CsOPiv (25 mol%) in MeOH (0.1 M) at 23 °C for 18 h.
[b] Isolated yield of the major diastereomer after silica gel column chromatography.
[c] Diastereoselectivity was measured by ^{1}H-NMR spectra of the unpurified material.

1.2.4 Mechanistic Studies

We then investigated the mechanism of the transformation (Scheme 1.7). The reversibility of C-H activation was first examined. Trace deuterium incorporation (<5%) was observed when the reaction was run in CD_3OD, suggesting the C-H activation is largely irreversible (eq 15). The competitive reaction between *p*-bromobenzamide (**1h**) and unsubstituted benzamide (**1a**) was conducted to probe the electronic preference of reaction (eq 16). The product formation favors an electron deficient substrate in a 3:1 ratio. Kinetic isotope studies revealed KIE values of 6.7 and 5.7 for the parallel and competition experiments, respectively (eq 17). These studies together suggest that the C-H activation occurs *via* concerted metallation-deprotonation (CMD) mechanism and is the rate-determining step, as seen in several previous examples of C-H activation with Rh(III). To determine if epimerization of the product occurs under the reaction conditions, we independently prepared product **5ae** (1:1 dr) and resubjected it to the reaction conditions of benzamide **1f'** and cyclopropene **4e**. After full conversion to **5fe** (70% yield, 17:1 dr), we did not observe any change of the dr of **5ae**, indicating the products are not epimerized under the reaction conditions (eq 18).

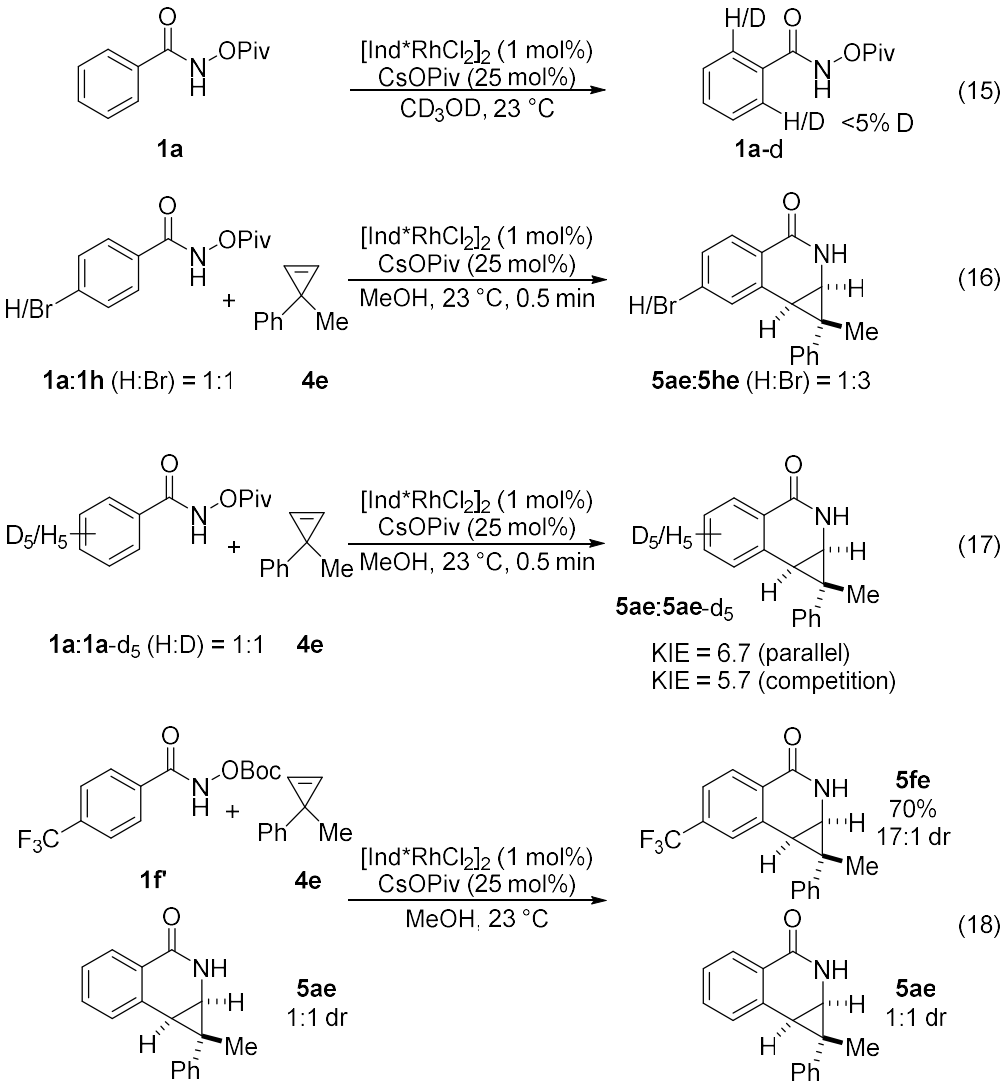

Scheme 1.7 Mechanistic experiments

Based on literature precedent[31] and our mechanistic studies, the mechanism of the transformation is proposed in Figure 1.5. The Ind*Rh(OPiv)$_2$ species is generated *in situ* by an anion exchange of [Ind*RhCl$_2$]$_2$ and CsOPiv. The amide directed C-H activation occurs *via* a CMD mechanism to give the five-membered rhodacycle intermediate **I**, which then coordinates

[31] Concerted metallation deprotonation (CMD) mechanism in Rh(III) catalyzed C-H activation, see: (a) Lapointe, D.; Fagnou, K. *Chem. Lett.* **2010,** *39*, 1119-1126. Computational, see: (d) Guo, W.; Xia, Y. Z. *J. Org. Chem.* **2015,** *80*, 8113-8121.

the cyclopropene giving intermediate **II**. Migratory insertion of cyclopropene gives intermediate **III**. Reductive elimination (C-N bond formation) occurs to generate a Rh(I) species. The saturated coordination of acyl directing group to Rh(III) of intermediate **III** is important for the reductive elimination step since *O*-methyl benzhydroxamate is not reactive for the transformation. Finally, the Rh(I) is oxidized by insertion into the N-O bond to regenerate the active Rh(III) catalyst species and liberate the dihydroisoquinolone product. The Rh(V)-nitrenoid intermediate, after the migration of O-Boc to Rh, was invoked from several computational studies. Finally, reductive elimination (C-N bond formation) occurs to generate Rh(III) species and liberate the dihydroisoquinolone product.

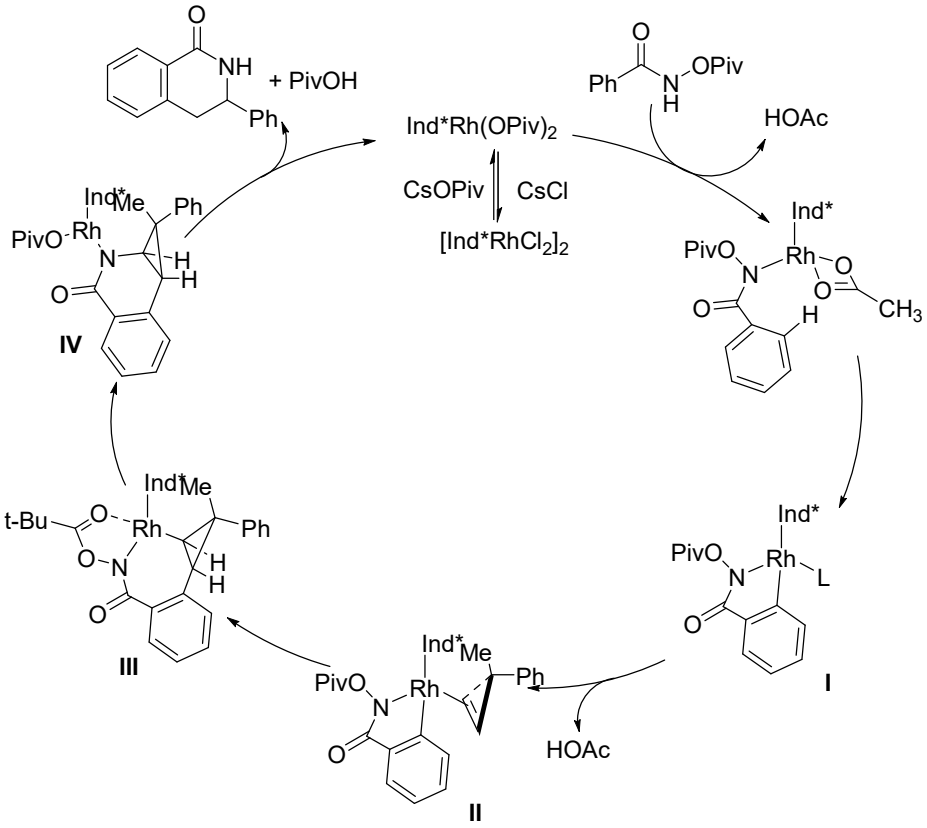

Figure 1.5 Proposed reaction mechanism

We performed density functional theory (DFT) calculations in collaboration with Kelvin Jackson and Professor Robert Paton (University of Oxford) to understand diastereoselectivity and the effect of the Ind* ligand for this transformation.[32] We hypothesized that the diastereoselectivity arises from the facial selectivity during the coordination and migratory insertion of the cyclopropene. The calculations indicate that the migratory insertion step is largely irreversible step, hence this step determines the diastereoselectivity of the transformation. The coordination and the insertion step of the cyclopropene can occur through four possible transition states *i.e. trans-endo, trans-exo, cis-endo* and *cis-exo* TSs as depicted in Figure 1.6. It should be noted that *trans-* and *cis-* nomenclature was adopted from the *trans-* and *cis-* products that observed experimentally. In addition, two conformers exist in which the cyclopropene oriented towards (*endo*) or away (*exo*) from the benzamide moiety. The observed *trans*-product agrees with the calculation in which *trans-exo* TS is the most favorable. In this transition state, the methyl group oriented towards the Ind* ligand. However, *trans-endo* is less favorable due to the H---H clash (2.16Å) about the incipient C-C bond. In contrast, the *cis*-diastereomer results from the unfavorable steric interaction resulting by the phenyl group pointed towards the Ind* ligand (*cis-exo* TS) or towards the benzamide and directing group (*cis-endo* TS). These calculations also confirmed the synergistic steric interactions involving the Ind* ligand and directing group on the facial selectivity.

[32] See full details about calculations in ref. 1.

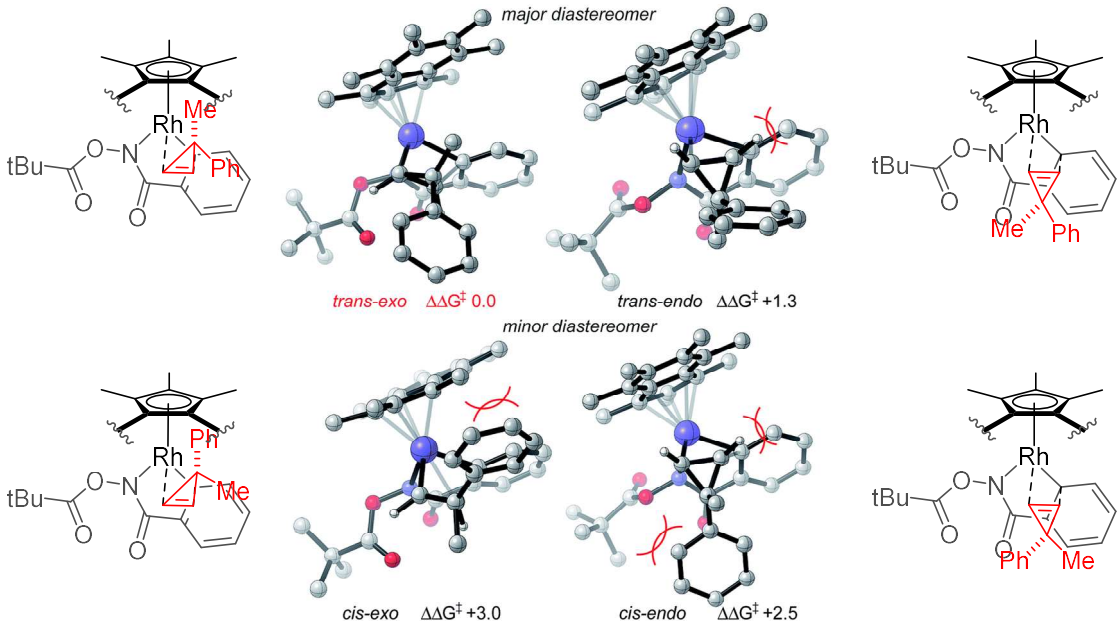

Figure 1.6 Stereochemical model for diastereoselectivity. Gibbs energies in kcal/mol.

1.2.5 Derivatizations of Product

The prevalence of nitrogen-containing heterocycles in pharmaceuticals led us to investigate the derivatization of the dihydroisoquinolones bearing [4.1.0] bicycles.[33] For example, the chloro- and *O*-triflate substituted dihydroisoquinolines (**17** and **18**), which are versatile functional group handles for further cross-coupling reactions could be easily prepared from the dihydroisoquinolone products in good yields, allowing for easy incorporation of these bicycles into pharmaceuticals or bio-active molecules.

[33] Examples of [4.1.0] dihydroisoquinolone moeity in bioactive molecules and its synthesis, see: (a) Cromarty, A.; Haque, K. E.; Proctor, G. R., J. *J. Chem. Soc.* **1971,** 3536–3540. (b) Lantos, I.; Bhattacharjee, D.; Eggleston, D. S. *J. Org. Chem.* **1986,** *51*, 4147-4150. (c) Perchonock, C. D.; Lantos, I.; Finkelstein, J. A.; Holden, K. G. *J. Org. Chem.* **1980,** *45*, 1950-1953. (d) Pedroni, J.; Saget, T.; Donets, P. A.; Cramer, N. *Chem. Sci.* **2015**, *6*, 5164-5171.

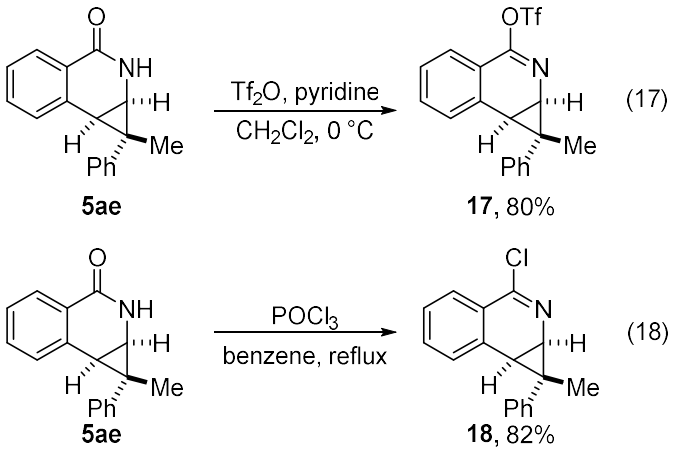

Scheme 1.7 Derivatization of Product

1.3 Conclusion

In summary, we have developed a heptamethylindenyl (Ind*) ligand that enables high diastereoselectivity for cyclopropene insertion in the Rh(III)-catalyzed synthesis of cyclopropa[c]dihydroisoquinolone. The steric interaction of the ligand on rhodium and the ester substitution of O-substituted benzhydroxamate work cooperatively to improve the diastereoselectivity of cyclopropene insertion.[34] Mechanistically, the C–H activation proceeds via a concerted metallation-deprotonation pathway and is the turnover-limiting step. This methodology is useful for the rapid synthesis of nitrogen-containing heterocycles with a [4.1.0] motif and their derivatives.

[34] Our group studied the correlation of selectivity to Cp ligand properties. This studies reveal the ability of Ind* ligand to accommodate the slippage, thus improves the diastereoselectivity, see: Piou, T.; Romanov-Michailidis, F.; Romanova-Michaelides, M.; Jackson, K. E.; Semakul, N.; Taggart, T. D.; Newell, B. S.; Rithner, C. D.; Paton, R. S.; Rovis, T., *J. Am. Chem. Soc.* **2017,** *139*, 1296-1310.

CHAPTER 2

Development of Stereoselective [4.2.0] Dihydroisoquinolones Synthesis via Rh(III)-Catalyzed C-H Activation and [4+2] Annulation with Cyclobutenes

2.1 Introduction

Since cyclobutane frameworks are occasionally found in natural products and bioactive molecules (Figure 2.1), the synthesis of these motifs has become the topic of some interest.[35] Specifically, these motifs have been utilized in the drug discovery and development, partly due to the structural rigidity and the defined spatial arrangement and of the cyclobutane ring.[36] In addition, nitrogen heterocycles such as isoquinolones and pyridones are of particular interest due to their prevalence in natural products and drug-like molecules. Targeting new synthetic methods towards these cyclobutane-fused nitrogen heterocycles would be potentially useful.

[35] Recent comprehensive reviews in the synthesis of cyclobutane, see: (a) Xu, Y.; Conner, M. L.; Brown, M. K. *Angew. Chem. Int. Ed.* **2015,** *54*, 11918-11928. (b) Poplata, S.; Troster, A.; Zou, Y. Q.; Bach, T. *Chem. Rev.* **2016,** *116*, 9748-9815.

[36] (a) Blakemore, D. C.; Bryans, J. S.; Carnell, P.; Carr, C. L.; Chessum, N. E. A.; Field, M. J.; Kinsella, N.; Osborne, S. A.; Warren, A. N.; Williams, S. C. *Bioorg. Med. Chem. Lett.* **2010,** *20*, 461-464. (b) Marson, C. M. *Chem. Soc. Rev.* **2011,** *40*, 5514-5533.

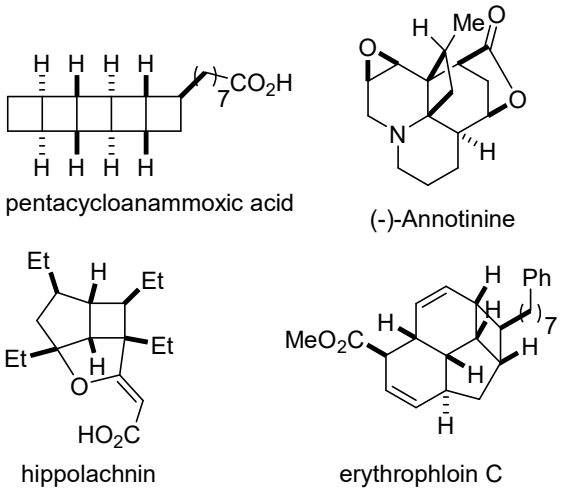

Figure 2.1

In this regard, Yudin and coworkers investigated the [3,3]-sigmatropic rearrangement of *N*-vinyl-β-lactams **1** to generate eight-membered lactams **2** (eq 1).[37] During this study, the formation of a fused [4.2.0] aminocyclobutane-containing δ-lactam was observed as a byproduct, which is thought to proceed through a 6π-electrocyclization of the eight-membered lactam **3** (Scheme 2.1). After extensive optimization, the latter product could be obtained by using CuI and Cs_2CO_3 as additives under microwave heating. However, harsh reaction conditions limited functional group tolerance.

[37] (a) Cheung, L. L. W.; Yudin, A. K. *Org. Lett.* **2009,** *11*, 1281-1284. (b) Cheung, L. L. W.; Yudin, A. K. *Chem. Eur. J.* **2010,** *16*, 4100-4109.

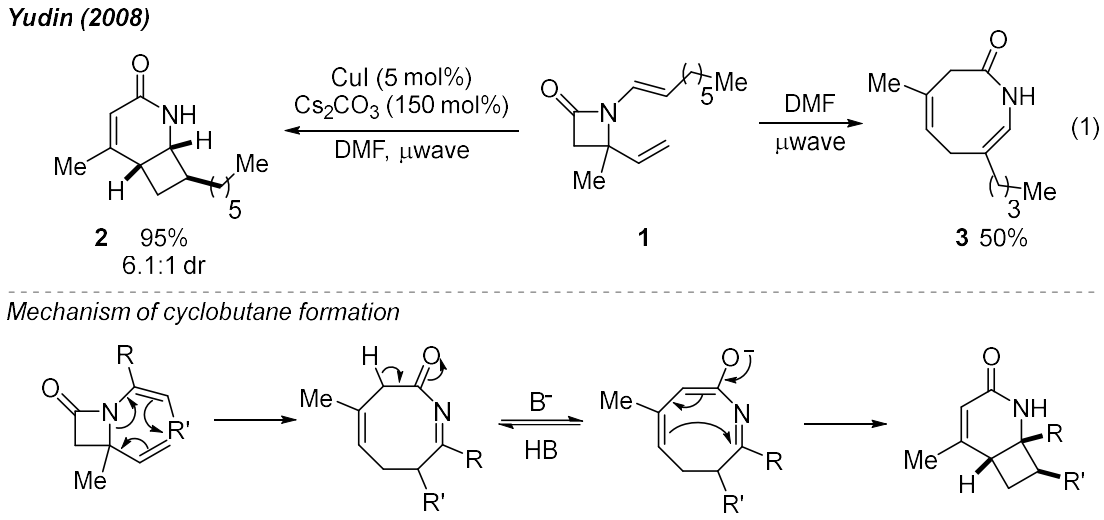

Scheme 2.1

Bach and coworkers have demonstrated the enantioselective synthesis of [4.2.0] dihydroisoquinolones (eq 2).[38] They employed a chiral hydrogen-bonding template **T** to render the intermolecular [2+2] photocycloaddition of isoquinolones (**4**) and alkenes (**5**) enantioselective to generate enantioenriched fused [4.2.0] dihydrosioquinolones (**6**). However, the superstoichiometric amount of the chiral template (2.5 equiv.) and alkene (10 equiv.) are required to attain good reactivity and selectivity.

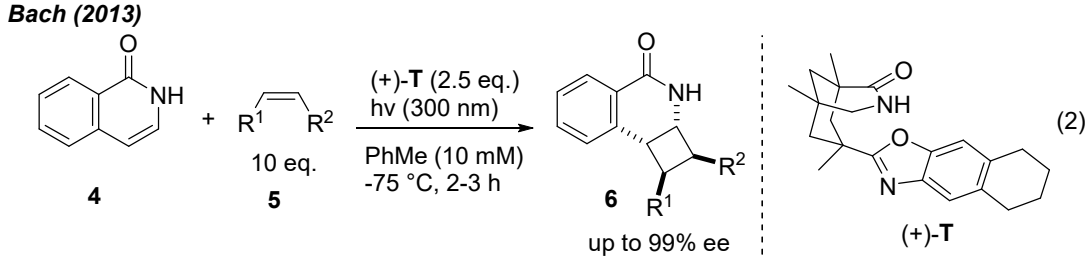

[38] (a) Coote, S. C.; Bach, T. *J. Am. Chem. Soc.* **2013,** *135*, 14948-14951. (b) Coote, S. C.; Pothig, A.; Bach, T. *Chem. Eur. J.* **2015,** *21*, 6906-6912. For intramolecular [2+2] photocycloaddition, see: Austin, K. A. B.; Herdtweck, E.; Bach, T. *Angew. Chem. Int. Ed.* **2011,** *50*, 8416-8419.

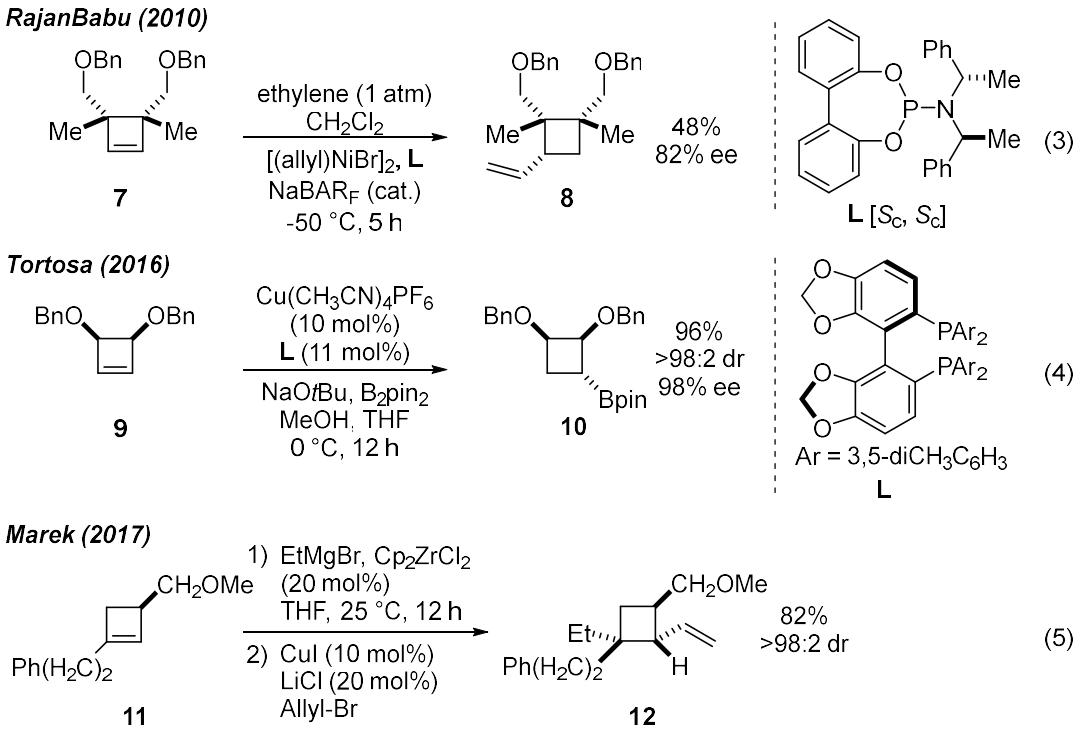

Scheme 2.2

Cyclobutenes have been utilized as monomers in polymer chemistry due to their high strain energy (30.6 kcal/mol).[39] These molecules can be accessible in a few steps from cheap starting materials. In contrast, the use of cyclobutenes to access functionalized cyclobutanes has been underexplored.[40] Only a few groups have demonstrated that cyclobutenes can be used to provide decorated cyclobutanes (Scheme 2.2). In this vein, RajanBabu found that cyclobutene **7** is an effective substrate for the nickel-catalyzed hydrovinylation to generate vinylated cyclobutane **8** in moderate yield (eq 3).[41] Tortosa and coworkers demonstrated an elegant enantioselective and diastereoselective copper-catalyzed hydroboration of cyclobutene **9** to

[39] Recent review of cyclobutenes in polymer chemistry, see: Le, D.; Morandi, G.; Legoupy, S.; Pascual, S.; Montembault, V.; Fontaine, L. *Eur. Polym. J.* **2013,** *49*, 972-983.

[40] Asymmetric synthesis of cyclobutene and its utilities, see: Misale, A.; Niyomchon, S.; Maulide, N. *Acc. Chem. Res.* **2016,** *49*, 2444-2458.

[41] Liu, W.; RajanBabu, T. V. *J. Org. Chem.* **2010,** *75*, 7636-7643.

furnish chiral cyclobutylboronate **10** (eq 4).[42] More recently, Marek and coworkers developed a highly regio- and diastereoselective zirconocene-catalyzed carbomagnesiation of cyclobutene **11** to afford cyclobutylmagnesium intermediate. This intermediate is configurationally stable for transmetallation to a metal catalyst. Thus, this process allows subsequent functionalization to generate polysubstituted cyclobutanes **12** (eq 3).[43]

Strained alkenes such as cyclopropene are effective coupling partners with *O*-pivaloyl benzhydroxamates to generate [4.1.0] dihydroisoquinolones (Chapter 1).[44] Expanding on this, we felt that Rh(III)-catalyzed C-H activation of *O*-pivaloyl benzhydroxamate and *N*-pivaloyloxy acrylamide precursor (**13**) with cyclobutene (**14**) would provide an efficient route for accessing [4.2.0] dihydroisoquinolones and dihydropyridones (**15**) (eq 6). In addition, an enantioselective variant could be developed by using a streptavidin-based metalloenzyme.

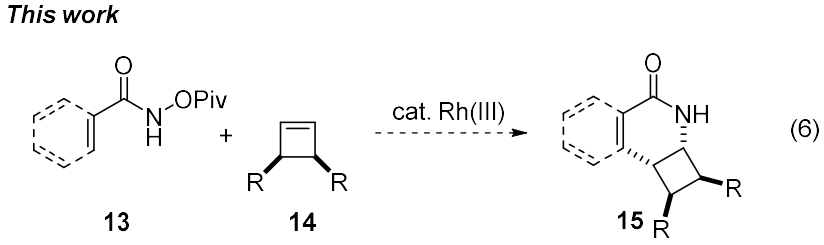

2.2 Results and Discussion

2.2.1 Substrate Scope

We began our study by examining the Rh(III)-catalyzed coupling of *O*-pivaloyl benzhydroxamate **13a** with cyclobutene **14a** in the presence of $[Cp^*RhCl_2]_2$ (1 mol%), CsOPiv (0.25 mol%) in MeOH. To our delight, cyclobutene **14a** underwent the [4+2] annulation and delivered [4.2.0] dihydroisoquinolone **15aa** in an excellent yield and diastereoselectivity (>20:1

[42] Guisan-Ceinos, M.; Parra, A.; Martin-Heras, V.; Tortosa, M. *Angew. Chem. Int. Ed.* **2016,** *55*, 6969-6972.

[43] Roy, S. R.; Eijsberg, H.; Bruffaerts, J.; Marek, I. *Chem. Sci.* **2017,** *8*, 334-339.

[44] (a) Hyster, T. K.; Rovis, T. *Synlett* **2013,** *24*, 1842-1844. (b) Semakul, N.; Jackson, K. E.; Paton, R. S.; Rovis, T. *Chem. Sci.* **2017,** *8*, 1015-1020.

dr). This transformation was applied to a broad scope of *O*-pivaloyl arylhydroxamate substrates (Table 2.1). *para*-Substituents with electron donating group and electron withdrawing group (-OMe (**13b**), -Cl (**13c**), -Br (**13d**), and -CF_3 (**13e**)) fare well in the transformation providing good yields of products (**15ba-15ea**). Of note, the halogen functional groups (**15ca** and **15da**) are a handle for further cross coupling reactions. The relative *trans* diastereomer of the product **15ea** was confirmed by X-ray single crystal structure analysis.

Table 2.1 *O*-Pivaloyl Arylhydroxamate Scope

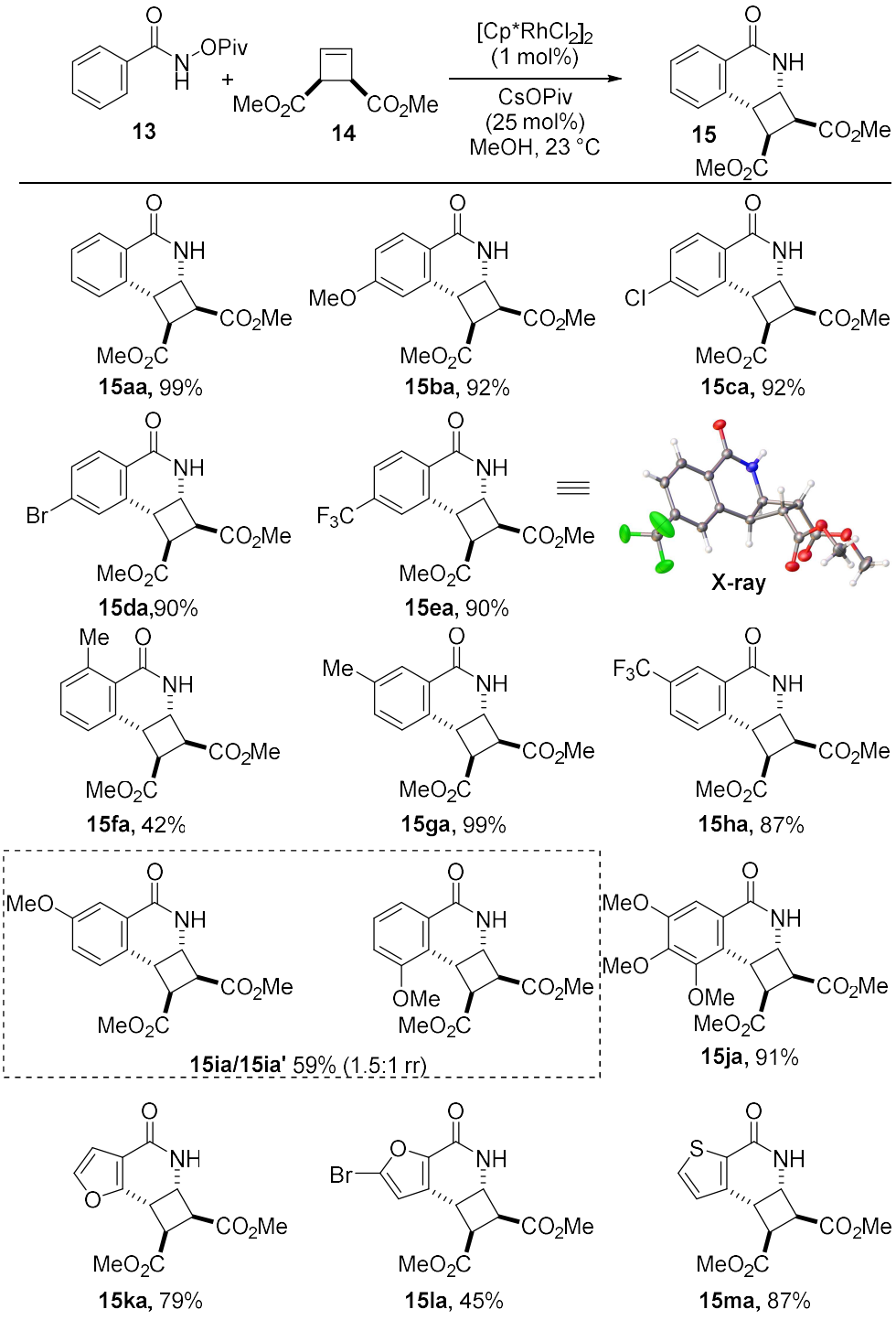

Reaction condition: **13** (0.1 mmol), **14** (0.11 mmol), $[Cp^*RhCl_2]_2$ (1 mol%), CsOPiv (25 mol%) in MeOH (0.1 M) at 23 °C for 18 h. Isolated yield was reported.

The reaction is robust since *ortho*-substituent (**13f**) was also capable of furnishing the product **15fa** in 42% yield. *meta*-Methyl and trifluoromethyl substituted benzamides (**13g** and **13h**) gave the dihydroisoquinolone products **15ga** and **15gh** in good yield. These products arise from the C-H activation at the less sterically hindered position. However, the mixture of regioisomeric products (**15ia:15ia'** *ca.* 1.5:1 ratio) was obtained when *meta*-methoxy substrate **13i** was used. This result may be explained by a combination of steric effects and kinetic acidity issues. Benzamide derived from gallic acid derivative **13j** also provides the corresponding product **15ja** in good yield. In addition, we were pleased to find that *O*-pivaloyl heteroarylhydroxamate substrates such as furan (**13k** and **13l**) and thiophene (**13m**) were capable substrates furnishing the corresponding products (**15ka-15ma**) in yields ranging from 45-87%. However, pyridine derivatives such as *N*-pivaloyloxy nicotinamide and *N*-pivaloyloxy isonicotinamide were found to be inactive, presumably due to the coordinative inhibition of pyridine moiety to Rh(III) catalyst. Attempts to heating the reaction (up to 60 °C) led to the decomposition of the cyclobutene **14** to diene product via [2+2]-cycloreversion (Scheme 2.3).[45]

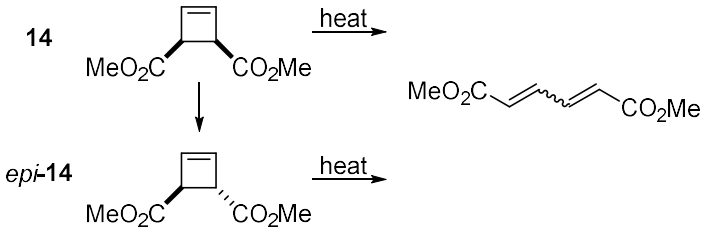

Scheme 2.3

[45] Binns, F.; Hayes, R.; Ingham, S.; Saengchantara, S. T.; Turner, R. W.; Wallace, T. W. *Tetrahedron* **1992,** *48*, 515-530.

The substrate scope regarding 3,4-disubstituted cyclobutenes was then investigated (Table 2.2). Tolerance of unprotected alcohols was demonstrated by the good reactivity of cyclobutene **14b**, providing the product **15ab** in good yield. Protected alcohols derived from cyclobutene **14b** (*i.e.* methyl ether **14c**, benzyl ether **14d**, acetyl **14e** and silyl protected alcohols **1f**) furnished the corresponding products **15ac-15ag** in 86-99% yields. Finally, cyclobutene **14g** provided the product **15ag** in 95% yield.

Table 2.2 Cyclobutene Scope

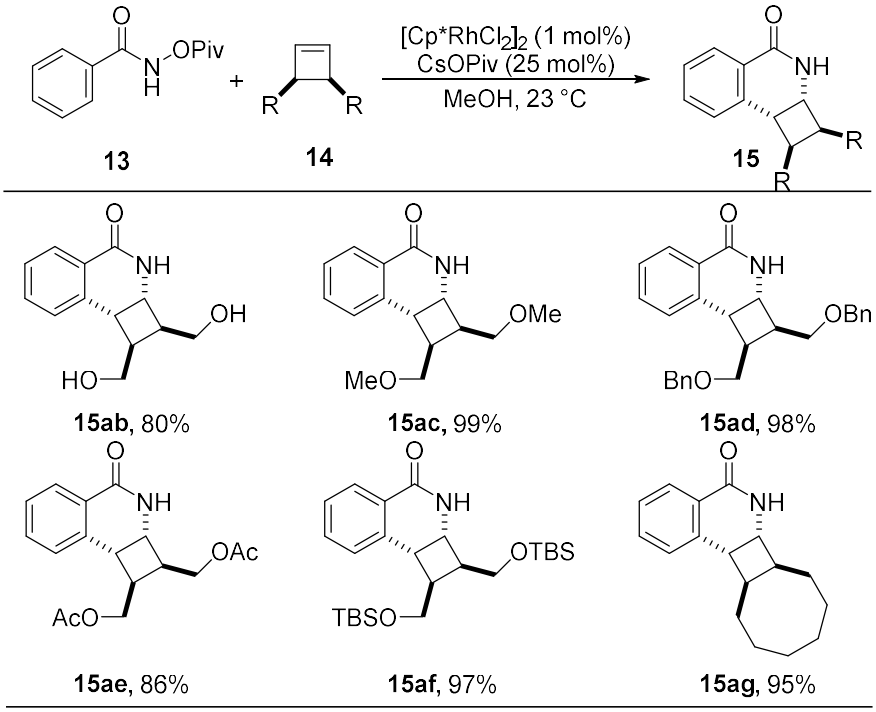

Reaction condition: **13** (0.1 mmol), **14** (0.11 mmol). Isolated yield was reported.

We also found that *N*-pivaloyloxy acrylamides and cyclobutenes react to give [4.2.0] dihydropyridone products in excellent diastereoselectivity (Table 2.3). The preliminary scope demonstrates that the α-substituted substrates (alkyl **16a-b** and aryl **16c**) react to give corresponding dihydropyridone products **17aa-17ca** in moderate to good yields (49-86%). This example demonstrates that Rh(III)-catalyzed C-H activation can be used as an efficient tool for synthesizing cyclobutane-fused *N*-heterocycles which are difficult to access by other means.

Table 2.3 *N*-Pivaloyloxy Acrylamide Scope

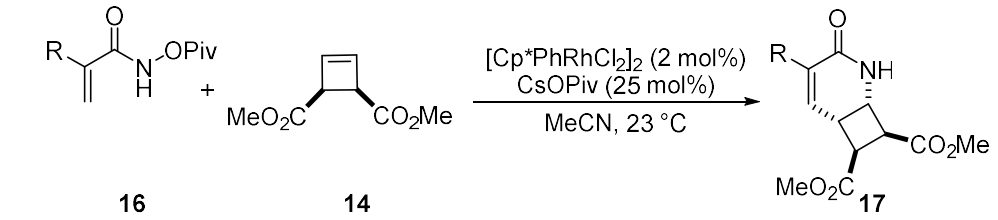

16 **14** **17**

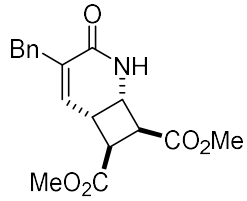

17aa, 49%

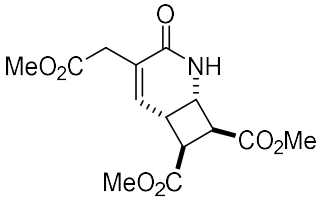

17ba, 77%

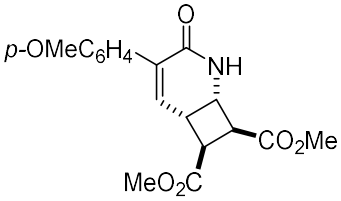

17ca, 86%

Reaction condition: **16** (0.1 mmol), **14** (0.11 mmol). Isolated yield was reported.

It should be noted that the observed *trans*-derived product agrees with the explanation that benzamidation preferentially occurs at the less sterically hindered alkene face. The high diastereoselectivity of *trans* product is thought to proceed through *trans-exo* or *trans-endo* transition states as the stereochemical model was proposed in Figure 2.2.

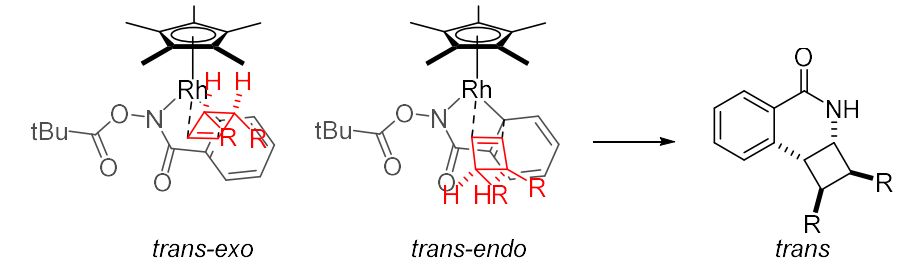

Figure 2.2 Proposed stereochemical model for the observed diastereoselectivity

2.2.2 Efforts Towards Enantioselective Benzamidation of Cyclobutenes

We were interested in developing an asymmetric transformation by using a streptavidin-based metalloenzyme technology (Table 2.3).[46] When the *O*-pivaloyl benzhydroxamate **13** and cyclobutene **14a** were subjected to the optimal conditions for the metalloenzyme, we found the dihydroisoquinolone product **15aa** formation in <5% yield. We inspected the crude reaction mixture by ^{1}H-NMR spectroscopy. However, we did not see cyclobutene **14a**. Instead, we detected the full conversion of cyclobutene **14a** to cyclobutene epimer ***epi*-14a**. We speculate that the formation of thermodynamically stable cyclobutene epimer ***epi*-14a** occurs via the base-mediated epimerization. In addition, the cyclobutene ***epi*-14a** was found to be an ineffective substrate in the transformation. To circumvent the problem, we used a cyclobutene that cannot epimerize to study the reaction. Gratifyingly, cyclobutene **14b** with unprotected alcohols undergoes the benzamidation and provides the product **15ab** in 70% yield and 72:28 *er*. Cyclobutene with diacetyl groups **14e** also furnished the products in an excellent yield and the same level of enantioselectivity. Cyclobutene with dimethoxy groups **14c** also reacts to give the product **15ac** in good yield with a slightly increased enantioselectivity (80:20 *er*). However, cyclobutene with dibenzyl broups **14d** was found to be inactive, probably due to its inherent lipophilicity or the sterically hindered dibenzyl groups that limited entrance into the active site of the metalloenzyme.

[46] Hyster, T. K.; Knorr, L.; Ward, T. R.; Rovis, T. *Science* **2012,** *338*, 500-503.

Table 2.3 Enantioselective Benzamidation Scope[a]

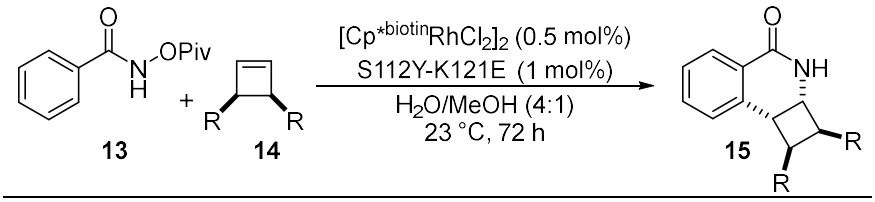

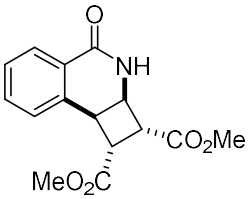

15aa, <5%

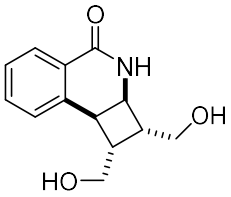

15ab,70%
72:28 er

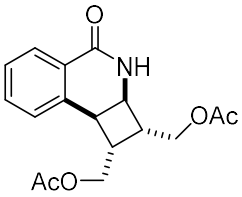

15ae, 99%
72:28 er

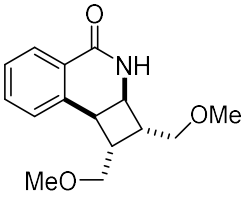

15ac, 82%
80:20 er

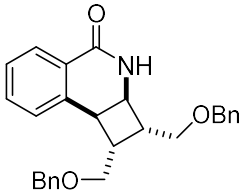

15ad, 0%

[a] reaction conditions: **13** (10 μmol), **14** (11 μmol). See Appendix for more details.
yield was obtained from ^{1}H-NMR or chiral HPLC.
er was determined by chiral HPLC.

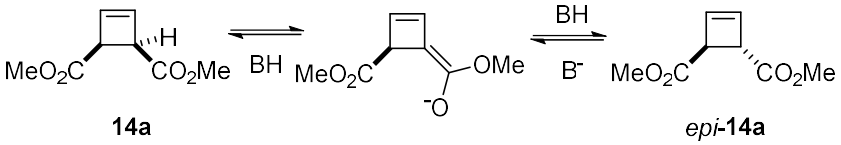

14a *epi*-**14a**

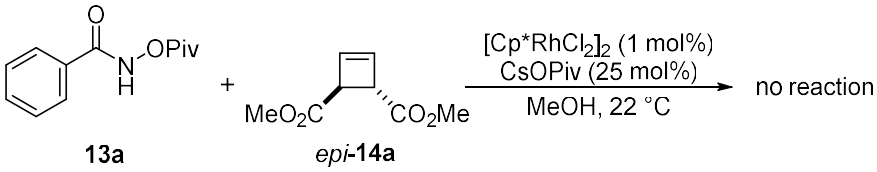

Scheme 2.4

2.3 Conclusion

In summary, we have successfully developed an efficient route to access [4.2.0] nitrogen heterocycles via Rh(III)-catalyzed C-H activation of benzamide and acrylamide substrates followed by the [4+2] annulation with cyclobutenes. The transformation appears to be highly diastereoselective with a good degree of functional group tolerant. Furthermore, an asymmetric variant was preliminarily investigated using a streptavidin-based metalloenzyme to provide the enantioenriched dihydroisoquinolone products in up to 80:20 *er*.

CHAPTER 3

Rh(III)-Catalyzed Coupling of *N*-Pivaloyloxy Acrylamides with Alkenes via C-H Activation: Direct Modular Assembly of Piperidones

3.1 Introduction

3.1.1 The Importance of Nitrogen Heterocycles

The α,β-unsaturated-δ-lactam (or piperidone) motif is present in an array of complex molecules and serves as a key intermediate towards accessing other alkaloids including piperidine (Figure 3.1).[47] Of interest is that among 640 FDA approved small molecule drugs that containing *N*-heterocycle, piperidine is the most common *N*-heterocycles, outcompeting even the ubiquitous pyridine.[48] In addition, recent studies found that the degree of saturation (complexity) as well as the presence of stereocenters correlate with the success rate of drug discovery.[49]

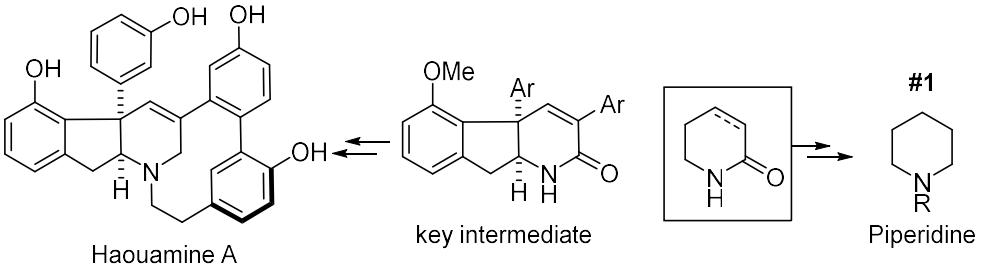

Figure 3.1

[47] (a) Huang, C.-G.; Chang, B.-R.; Chang, N.-C. *Tetrahedron Lett.* **2002,** *43*, 2721–2723. (b) Baran, P. S.; Burns, N. Z. *J. Am. Chem. Soc.* **2006,** *128*, 3908-3909. (c) Amat, M.; Pérez, M.; Minaglia, A. T.; Bosch, J. *J. Org. Chem.* **2008**, *73*, 6920–6923. (d) Hanessian, S.; Riber, L.; Marin, J. *Synlett* **2009**, *1*, 71-74. (e) Albrecht, D.; Vogt, F.; Bach, T. *Chem. Eur. J.* **2010**, *16*, 4284–4296.

[48] Vitaku, E.; Smith, D. T.; Njardarson, J. T. *J. Med. Chem.* **2014**, *57*, 10257-10274. For a comprehensive review on piperidine synthesis, see: Nebe, M.M.; Opatz, T. *Adv. Heterocycl. Chem.* **2017**, 122, 191-244.

[49] Lovering, F.; Bikker, J.; Humblet, C. *J. Med. Chem.* **2009,** *52*, 6752-6756.

Because of aforementioned reasons, extensive efforts targeting α,β-unsaturated-δ-lactams have been demonstrated (Figure 3.2).[50] Among intramolecular cyclizations that involve nucleophilic attack by the nitrogen atom, one of the synthetic strategies for α,β-unsaturated-δ-lactam formation is C-C double bond construction. This avenue has been exploited by ring closing metatheses,[51] McMurry couplings,[52] and aldol condensations.[53] Nevertheless, there are still limitations associated with the availability of these precursors, the harsh reaction conditions, and elevated temperatures. Two-component approaches such as cycloadditions or annulations are inherently more attractive. Recently, organocatalytic [4+2] cycloaddition approaches have been devised, as exemplified by transformations with *N*-heterocyclic carbene,[54] cinchona alkaloid, [55] and chiral phosphoric acid catalysis. [56] However, these strategies are limited to specific classes of precursors as well as practicality issues. To address these drawbacks, a new and efficient methodology that enables access to α,β-unsaturated-δ-lactams from simple precursors would prove useful and open many avenues to the field.

[50] Weintraub, P. M.; Sabol, J. S.; Kane, J. A.; Borcherding, D. R. *Tetrahedron* **2003,** *59,* 2953-2989.

[51] (a) Huwe, C. M.; Kiehl, O. C.; Blechert, S. *Synlett* **1996**, *1*, 65-66. (b) Fiorelli; C.; Savoia, D. *J. Org. Chem.* **2007**, *72*, 6022-6028. (c) Hietanen, A.; Saloranta, T.; Rosenberg, S.; Laitinen, E.; Leino, R.; Kanerva, L. T. *Eur. J. Org. Chem.* **2010,** 909-919. (d) Cogswell, T. J.; Donald, C. S.; Long, D.-L.; Marquez, R. *Org. Biomol. Chem.* **2015**, *13*, 717–728. (e) Han, S.-J.; Stoltz, B. M. *Tetrahedron Lett.* **2016**, *57*, 2233-2235.

[52] Momoi, Y.; Okuyama, K.; Toya, H.; Sugimoto, K.; Okano, K.; Tokuyama, H. *Angew. Chem. Int. Ed.* **2014**, *53*, 13215.

[53] Jeong, J.; Weinreb, S. M. *Org. Lett.* **2006,** *8*, 2309-2312.

[54] Xu, J.; Jin, Z.; Chi, Y. R. *Org. Lett.* **2013**, *15,* 5028-5031.

[55] Jia, W. Q.; Chen, X.-Y.; Sun, L.-H.; Ye, S. *Org. Biomol. Chem*. **2014**, *12*, 2167-2171.

[56] Weilbeer, C.; Sickert, M.; Naumov, S.; Schneider, C. *Chem. Eur. J.* **2017**, *23*, 513-518.

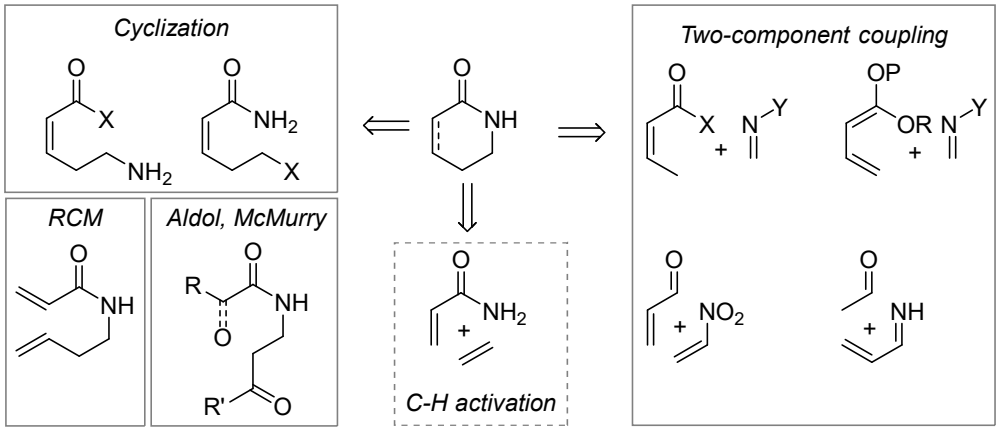

Figure 3.2

In this context, the C-H activation and annulation approach would provide direct access to α,β-unsaturated-δ-lactams from acrylamide and alkene precursors. This strategy is attractive because of easily accessible acrylamides and the abundance of alkenes. Daugulis developed a cobalt-catalyzed aminoquinoline-directed C-H activation of acrylamides and styrene to provide δ-lactams (Scheme 3.1).[57] Nonetheless, an extra step is required for the removal of a directing group to reveal free lactams. Despite progress in this area, a practical synthesis of piperidones from simple starting materials has not been developed.

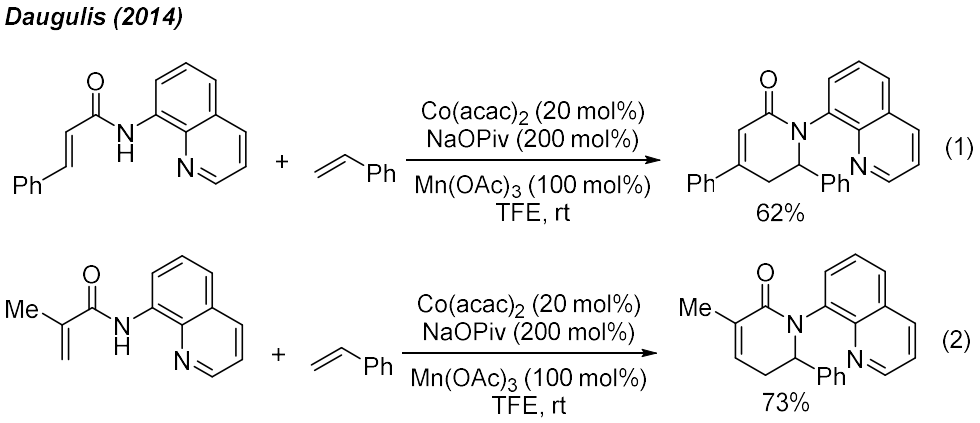

Scheme 3.1

[57] Grigorjeva, L.; Daugulis, O. *Org. Lett.* **2014,** *16*, 4684-4687.

3.1.2 Rh(III)-catalyzed C-H Activation in Nitrogen Heterocycles Syntheses

Rh(III)-catalyzed C-H activation annulation has been used to synthesize several *N*-heterocycles and has become an important tool in synthesis.[58] Seminal work by Fagnou,[59] Miura, Satoh,[60] Rovis[61] and Li[62] have demonstrated the directed C-H activation of benzamides with alkynes to deliver isoquinolones (Scheme 3.2, eqs 3 and 4). Furthermore, Glorius,[63] and Fagnou[64] have developed the *N*-acyloxy hydroxamate directing group, which allows for alkene insertion and subsequent N-O bond cleavage/C-N bond formation to deliver dihydroisoquinolone (eq 5). In addition, this process generates a stereocenter for which the catalytic asymmetric variants were developed by Rovis and Ward[65] as well as Cramer.[66]

---

[58] For selected reviews, see: (a) Colby, D. A.; Bergman, R. G.; Ellman, J. A. *Chem. Rev*. **2010**, *110*, 624-655. (b) Satoh, T.; Miura, M. *Chem. Eur. J.* **2010**, *16*, 11212-11222. (c) Patureau, F. W.; Wencel-Delord, J.; Glorius, F. *Aldrichimica Acta* **2012**, *45*, 31-41. (d) Song, G. Y.; Wang, F.; Li, X. W. *Chem. Soc. Rev.* **2012**, *41*, 3651-3678. (e) Song, G. Y.; Li, X. W. *Acc. Chem. Res.* **2015**, *48*, 1007-1020. (f) Zhu, C.; Wang, R.; Falck, J. R. *Chem. Asian. J.* **2012**, *7*, 1502-1514. (g) Gensch, T.; Hopkinson, M. N.; Glorius, F.; Wencel-Delord, J. *Chem. Soc. Rev.,* **2016**, *45*, 2900. (h) Gulías, M.; Mascareñas, J. L. *Angew. Chem. Int. Ed.* **2016**, *55*, 11000-11019.

[59] Guimond, N.; Gouliaras, C.; Fagnou, K. *J. Am. Chem. Soc.* **2010,** *132*, 6908-6909.

[60] Mochida, S.; Umeda, N.; Hirano, K.; Satoh, T.; Miura, M. *Chem. Lett.* **2010**, 39, 744-746.

[61] Song, G.; Chen, D.; Pan, C. L.; Crabtree, R. H.; Li, X. *J. Org. Chem.* **2010**, 75, 7487-7490.

[62] Hyster, T. K.; Rovis, T. *J. Am. Chem. Soc.* **2010**, *132*, 10565-10569.

[63] Rakshit, S.; Grohmann, C.; Besset, T.; Glorius, F. *J. Am. Chem. Soc.* **2011,** *133*, 2350-2353.

[64] Guimond, N.; Gorelsky S. I.; Fagnou, K. *J. Am. Chem. Soc.* **2011,** *133*, 6449-6457.

[65] Hyster, T. K.; Knorr, L.; Ward, T. R.; Rovis, T. *Science* **2012,** *338*, 500-503.

[66] Ye, B. H.; Cramer, N. *Science* **2012,** *338*, 504-506.

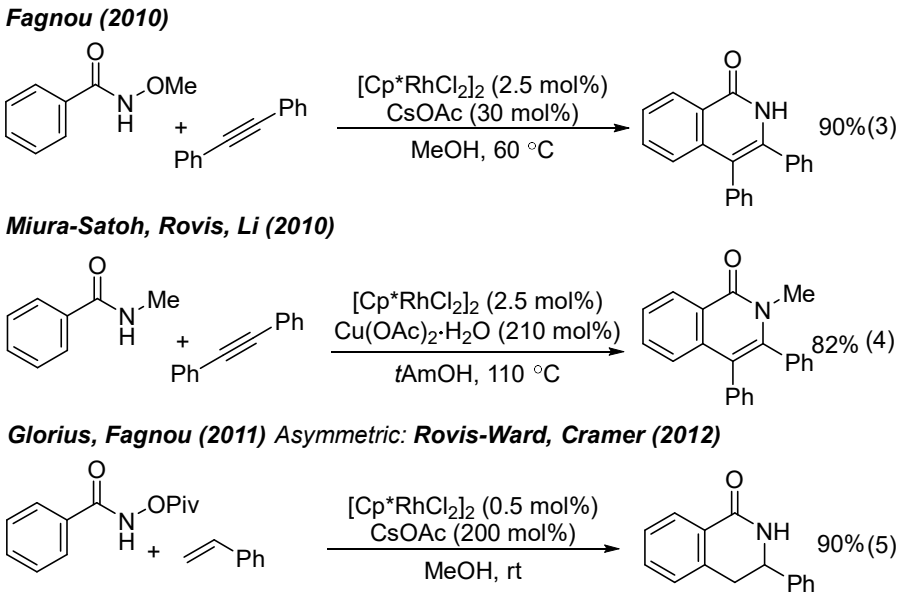

Scheme 3.2

The above strategies effectively deliver bicyclic nitrogen heterocycles, with a disproportionate emphasis on aromatic structures. Vinylic C-H activation of acrylamides with alkenes would provide access to valuable monocyclic heterocycles with a stereocenter. Several examples regarding to vinylic C-H bond activation of acrylamides are documented. Specifically, Li,[67] and Rovis[68] have reported the directed C-H activation annulation between acrylamides with alkynes to access pyridones (Scheme 3.3, eq 6).[69] However, transformations between acrylamide derivatives with alkenes only proceed through β-elimination pathways to generate β-functionalization products (eqs 7-12).[70] Inspired by the use of the *N*-acyloxy directing group that

[67] Su, Y.; Zhao, M. A.; Han, K. L.; Song, G. Y.; Li, X. W. *Org. Lett.* **2010,** *12*, 5462-5465.

[68] Hyster, T. K.; Rovis, T. *Chem. Sci.* **2011,** *2*, 1606-1610.

[69] Intramolecular annulation with alkyne, see: (a) Xu, X.; Liu, Y.; Park, C. M. *Angew. Chem. Int. Ed.* **2012**, *51*, 9372–9376. (b) Quinones, N.; Seoane, A.; Garcia-Fandino, R. Mascarenas, J. L.; Gulias, M. *Chem. Sci.,* **2013**, *4*, 2874–2879.

[70] (a) Besset, T.; Kuhl, N.; Patureau, F. W.; Glorius, F. *Chem. Eur. J.* **2011**, 17, 7167-7171. (b) Zhang, J.; Loh, T. P. *Chem. Commun.*, **2012**, *48*, 11232. (c) Zhang, S.-S.; Wu, J.-Q.; Lao, Y.-X.; Liu, X.-G.; Liu, Y.; Lv, W.-X.; Tan, D.-H.; Zeng, Y.-F.; Wang, H. *Org. Lett.* **2014**, *16*, 6412−6415. (d) Wu, J.-Q.; Qiu, Z.-P.; Zhang, S.-S.; Liu, J.-G.;

prevents β-hydride elimination and promotes C-N bond formation, Rh(III)-catalyzed C-H activation of *N*-pivaloyloxy acrylamides with alkene coupling partners was seen as an attractive strategy as this would generate unprotected α,β-unsaturated-δ-lactams (eq 13). However, this particular approach has proven challenging as no examples of this transformation have been reported to date. The challenges that are inherent with *N*-pivaloyloxy acrylamides may be attributed to the reactivity of acrylamide as a good Michael acceptor and their decomposition under the reaction conditions relative to their more stable *N*-alkyl and *N*-methoxy counterparts. Herein, we disclose an intermolecular Rh(III)-catalyzed redox-neutral [4+2] annulation between *N*-pivaloyloxy α-substituted acrylamides and simple alkene coupling partners to generate synthetically useful α,β-unsaturated-δ-lactams.

Lao,Y.-X.; Gu, L.-Q.; Huang, Z.-S.; Li, J.; Wang, H. *Chem. Commun.*, **2015**, *51*, 77-80. (e) Zhang, S.-S.; Wu, J.-Q.; Liu, X.; Wang, H. *ACS Catal.* **2015**, *5*, 210−214. (f) Yu, C.; Li, F. Zhang, J.; Zhong, G. *Chem. Commun.*, **2017**, *53*, 533-536.

Li, Rovis (2011)

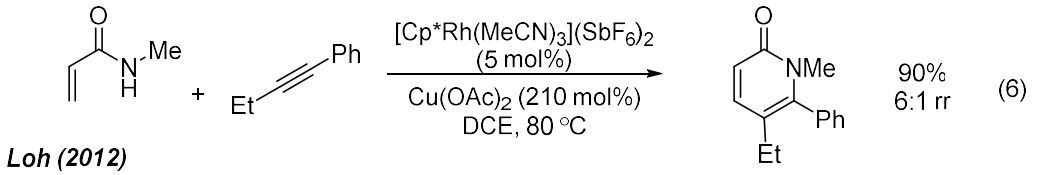

(6)

Loh (2012)

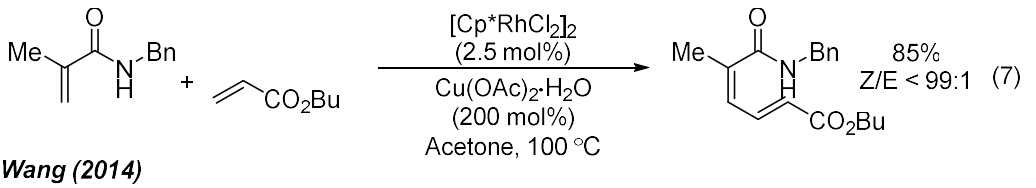

(7)

Wang (2014)

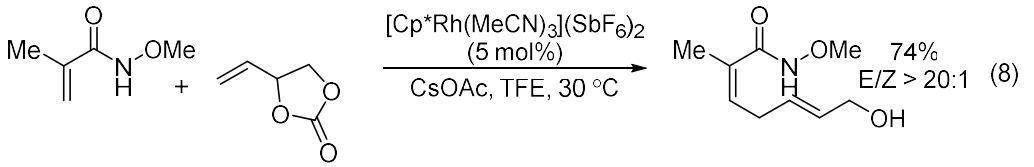

(8)

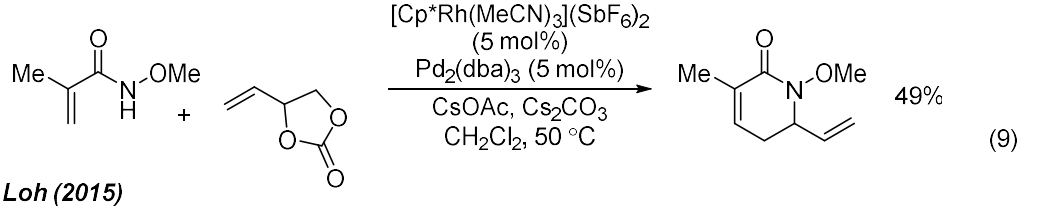

(9)

Loh (2015)

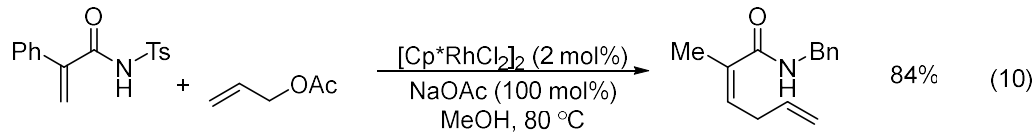

(10)

Wang (2015)

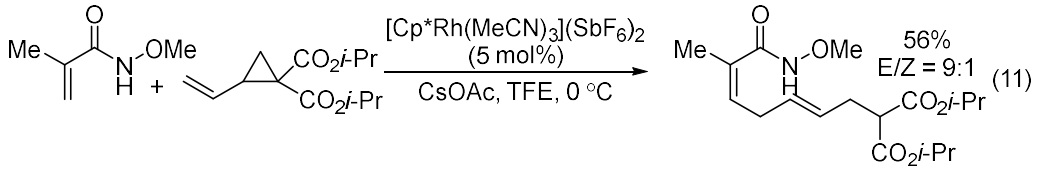

(11)

Zhang, Zhong (2017)

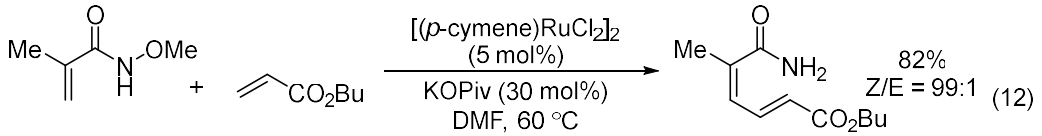

(12)

This work:

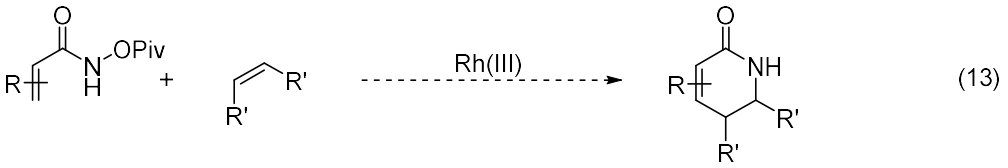

(13)

Scheme 3.3

3.2 Results and Discussion

3.2.1 Reaction Discovery

Thanks to the cyclopropene's reactivity, the Rh(III)-catalyzed [4+2] annulation of *N*-pivaloyloxy acrylamide **1** with cyclopropene **2** provided the dihydropyridone product **3** in 30% yield (2:1 dr, eq 14).

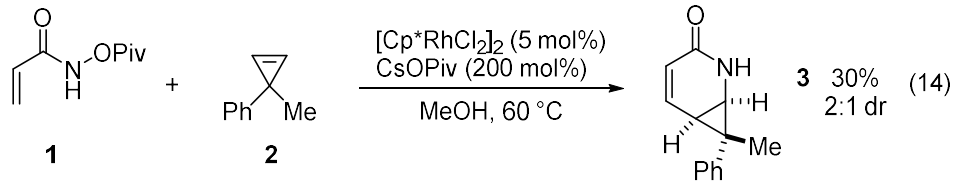

The reaction conditions were optimized using high-throughput experimentations (HTE) with different bases (CsOAc, CsOPiv) and solvents (MeOH, EtOH, tAmylOH, DCE, dioxane, MeCN, TFE, HFIP). The product formation was analyzed by LC/MS with multiple injections in a single experimental run (MISER). The optimal condition, $[Cp^*RhCl_2]_2$ (2 mol%), CsOPiv (0.25 equiv), MeCN (0.2 M) at 60 °C, gave a product in 37 % yield (Table 3.1, entry 1). Increasing the concentration to 0.3 M gave the similar yield (entry 2). Other precatalysts such as $Cp^*Rh(OAc)_2$ and $[Cp^*Rh(MeCN)_3](SbF_6)_2$ are also effective (entry 3, 4). To prevent the decomposition of *N*-pivaloyloxy acrylamide, the reaction was conducted at room temperature, which revealed the product with slightly improved yield (entry 5, 6). The use of excess amount of *N*-pivaloyloxy acrylamide (2 equiv.) provided 49% yield of product (entry 7).

Table 3.1 Reaction Condition Optimizations[a,c]

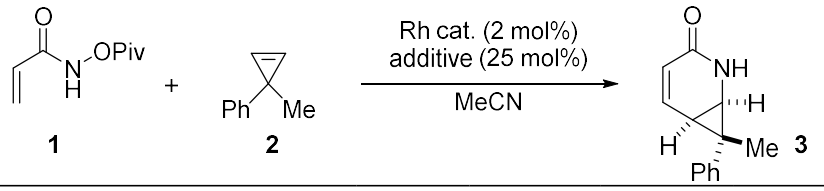

entry	precatalyst	additive	conc. (M)	temp (°C)	yield[a]
1	$[Cp^*RhCl_2]_2$	CsOPiv	0.2	60	36
2	$[Cp^*RhCl_2]_2$	CsOPiv	0.3	60	36
3	$Cp^*Rh(OAc)_2$	-	0.3	60	33
4	$[Cp^*Rh(MeCN)_3](SbF_6)_2$	CsOPiv	0.3	60	36
5	$[Cp^*Rh(MeCN)_3](SbF_6)_2$	CsOPiv	0.3	23	39
6	$[Cp^*RhCl_2]_2$	CsOPiv	0.3	23	39
7[b]	$[Cp^*Rh(MeCN)_3](SbF_6)_2$	CsOPiv	0.3	23	49

Reaction conditions: *N*-pivaloyloxy acrylamide (0.10 mmol), cyclopropene (0.11 mmol).
[a] NMR yield and diastereoselectivity were determined by ^{1}H-NMR using 1,3,5-trimethoxybenzene as an internal standard. The 2:1 dr was obtained in all cases.
[b] *N*-pivaloyloxy acrylamide (0.20 mmol), cyclopropene (0.11 mmol) were used.

Previous works in the field demonstrated that the reactivity and selectivity of Rh(III)-catalyzed reaction could be improved using the ligand development (cf. Chapter 1). Again, the similar approach should solve the reactivity and diastereoselectivity problems in this case. The representative library of Cp ligands was examined and the results are summarized in Table 3.2. We observed the reactivity of the transformation is affected by the steric and electronic properties of Cp ligand. The electron-deficient Cp ligands ($Cp^{*bisCF3Ar}$, Cp^{*C6H5}, and Cp^{*CF3}) are less reactive and gave little or no yield. We also found that heptamethylindenyl (Ind*), 1,3-di-tert-butylcyclopentadienyl (Cp^t), and 1,3-dimethyl-2,4,5-triphenylcyclopentadienyl (Cp^{Ph3Me2}) ligands were unsuccessful in this transformation. Among the Cp precatalysts investigated in the study, Cp^{*Ph}, Cp^{*chex}, Cp^{*iPr}, Cp^{*tBu}, $Cp^{*1,3\text{-}diPh}$, $Cp^{*p\text{-}OMeAr}$, Cp^{*Bn} and Cp^{*Ar} are the most effective ligands which provide the corresponding product in 46-70% yield. Other ligands *i.e.*

$Cp^{Me,tBu\text{-}Cy}$, $Cp^{*1,2\text{-}diPh}$, $Cp^{Me,chex\text{-}Cy}$ and Cp^{TM} delivered the product in low yields (27-39%). Disappointingly, the diastereoselectivity did not improve by tuning steric or electronic properties of the Cp ligands.

Table 3.2 Cp Ligand Optimizations [a,b]

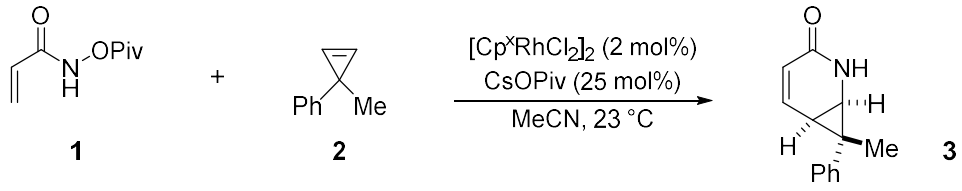

1 2 3

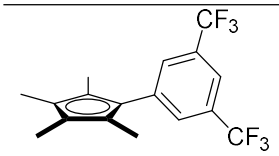

$Cp^{*bis\text{CF3Ar}}$ 22% 2:1 dr

Cp^{*C6F5} 7% n.d.

Cp^{*CF3} 0%

Ind* 0%

Cp^{t} <5% n.d.

$Cp^{*1,3,5\text{-triPh}}$ <5% n.d.

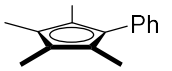

Cp^{*Ph} 69% 2:1 dr

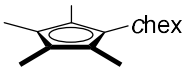

Cp^{*chex} 64% 2:1 dr

Cp^{*iPr} 60% 2:1 dr

Cp^{*tBu} 59% 2:1 dr

$Cp^{*1,3\text{-diPh}}$ 56% 2:1 dr

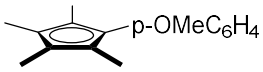

$Cp^{*p\text{-OMeAr}}$ 52% 2:1 dr

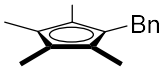

Cp^{*Bn} 51% 2:1 dr

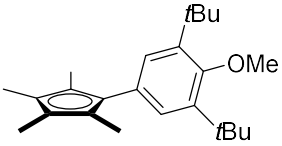

Cp^{*Ar} 46% 2:1 dr

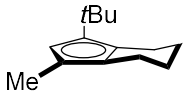

$Cp^{Me,tBu\text{-}Cy}$ 39% 2:1 dr

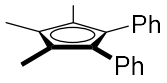

$Cp^{*1,2\text{-diPh}}$ 31% 2:1 dr

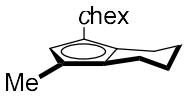

$Cp^{Me,chex\text{-}Cy}$ 28% 2:1 dr

Cp^{TM} 27% 2:1 dr

[a] Reaction conditions: N-pivaloyloxy acrylamide (0.10 mmol), cyclopropene (0.11 mmol), MeCN (0.3 M) at 23 °C for 24 h.

[b] NMR yield and diastereoselectivity were determined by ^{1}H-NMR using 1,3,5-trimethoxybenzene as an internal standard.

After obtaining the optimal condition for reactivity, a preliminary scope of substituted *N*-pivaloyloxy acrylamides was studied (Table 3.3). α-substituted *N*-pivaloyloxy acrylamides (**1b** and **1c**) performed well, generating the products **3ba** and **3ca** in moderate to good yields. Cyclohexenyl carboxamide **1d** delivered the product **3da** with excellent diastereocontrol. The steric properties of the substrate **1d** may render the diastereoselectivity similar to the aryl counterpart. However, other α,β-substituted *N*-pivaloyloxy acrylamides (**1e** and **1f**) only gave trace product. β-Substituted *N*-pivaloyloxy acrylamides (**1g**, **1h**, and **1i**) are unreactive substrates in this transformation.

Table 3.3 Preliminary Substrate Scope

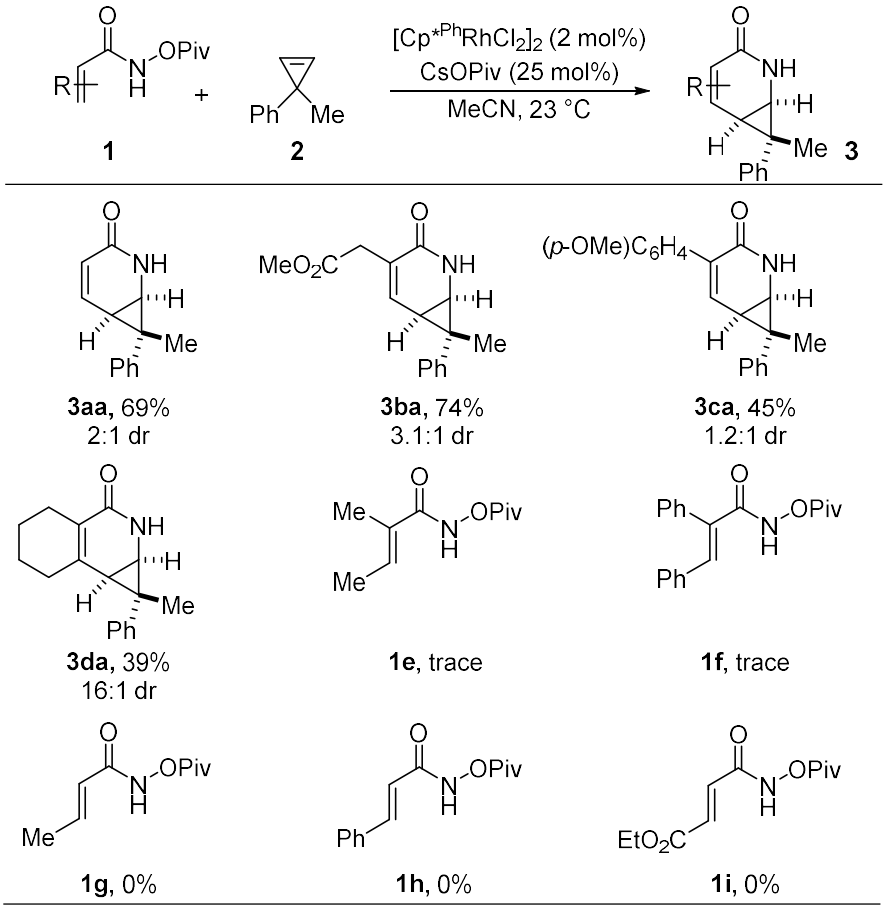

[a] Reaction conditions: N-pivaloyloxy acrylamide (0.1 mmol), cyclopropene (0.11 mmol)
[b] NMR yield

Next, we explored less strained cycloalkenes and acyclic olefin partners using optimal conditions (Table 3.4). We chose *N*-pivaloyloxy α-benzylacrylamide **4** as a model substrate. We were pleased to see that norbornadiene (**5a**), norbornene (**5b**), and cyclopentene (**5c**) reacted under the optimal condition generating the δ-lactam products in low yield (19-28% yield). However, cyclohexene (**5d**) is unreactive. Acyclic alkenes were also investigated (entries 5-10). Styrene (**5e**), ethyl acrylate (**5f**), dimethyl fumarate (**5g**) and dimethyl maleate (**5h**) were not reactive coupling partners, however, we were excited to see that aliphatic alkenes (*i.e.* allyl benzene (**5i**) and 1-heptene (**5j**)) underwent the transformation and provided the products **6ai** and **6aj** in low yields with *ca.* 2:1 regioisomeric ratio. We noticed the reactant decomposed under the reaction conditions during these studies. However, attempts at isolation and identification of the side products were unsuccessful.

We next prepared acrylamide precursor **4a** which contains *para*-bromo group to aid in the characterization of byproducts (eq 15). After subjecting **4a** to the optimal conditions, **4a** partially decomposed to methyl benzyl ketone **7** and N-O bond cleavage product **8**. Methyl benzyl ketone **7** may be produced through the base-mediated Lossen rearrangement/hydrolysis. The formation of byproduct **8** may be argued by the formation of Rh(I) species via the oxidation of dihydropyridone **6** to form the corresponding pyridone as detected by UPLC/MS. Then, Rh(I) oxidizes N-O bond to generate amide **8**.

Table 3.4 Investigations of cycloalkenes and acyclic alkenes[a,b]

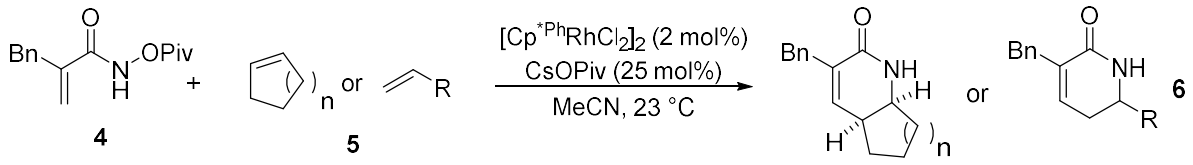

entry	alkene	product	yield	entry	alkene	product	yield
1	 **5a**	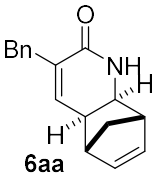 **6aa**	25 >20:1 dr	6	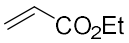 **5f**	-	0
2	 **5b**	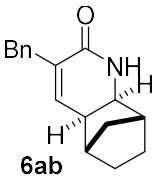 **6ab**	19 >20:1 dr	7	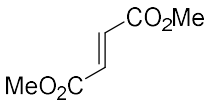 **5g**	-	0
3	 **5c**	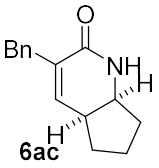 **6ac**	28 >20:1 dr	8	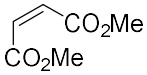 **5h**	-	0
4	 **5d**	-	0	9	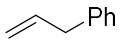 **5i**	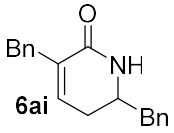 **6ai**	20 2:1 rr
5	 **5e**	-	0	10	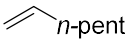 **5j**	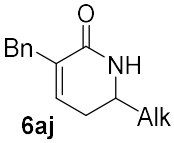 **6aj**	20 2:1 rr

[a] Reaction conditions: *N*-pivaloyloxy acrylamide **4** (0.1 mmol), alkene **5** (0.11 mmol)
[b] isolated yield

Ar = *p*-BrC_6H_4

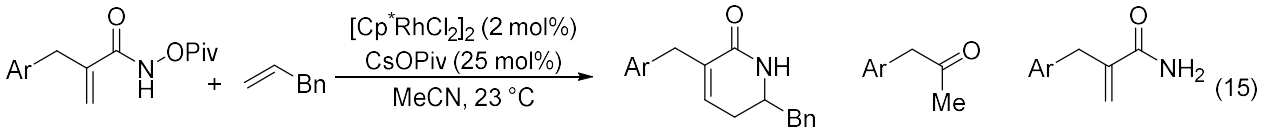

(15)

3.2.2 Reaction Optimization

Table 3.5 Optimization of Reaction Conditions[a]

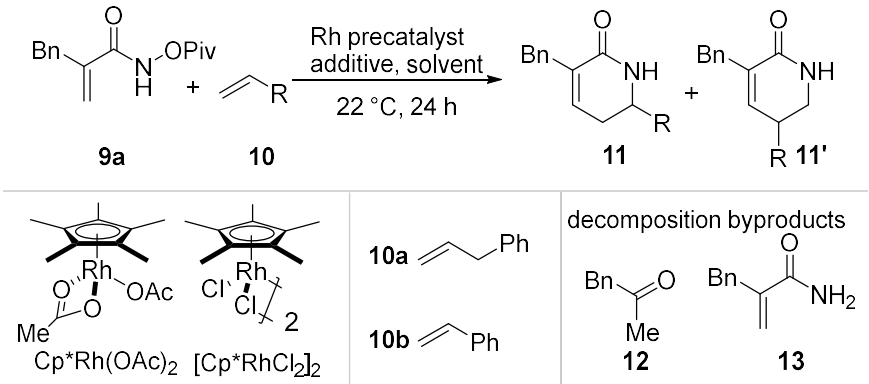

entry	alkene	precatalyst	additive	solvent	yield[b]	rr[c]
1	**10a**	$Cp^*Rh(OAc)_2$	-	MeCN	17	1:2
2	**10a**	$Cp^*Rh(OAc)_2$	-	HFIP	44	1:2
3	**10a**	$Cp^*Rh(OAc)_2$	-	TFE	84	1:2
4	**10a**	$[Cp^*RhCl_2]_2$	CsOAc	TFE	85	1:2
5	**10b**	$[Cp^*RhCl_2]_2$	CsOAc	TFE	88 (85)	>10:1
6[d]	**10b**	$[Cp^*RhCl_2]_2$	CsOAc	TFE	83	>10:1
7[e]	**10b**	$[Cp^*RhCl_2]_2$	CsOAc	TFE	60	>10:1
8[f]	**10b**	$[Cp^*RhCl_2]_2$	CsOAc	TFE	52	>10:1

[a] **9a** (0.10 mmol), alkene (0.11 mmol), 5 mol% Rh, 25% additive in a solvent (0.3 M).
[b] yield was determined by ^{1}H-NMR using phenyltrimethylbenzene as an internal standard and the isolated yield was given in parenthesis.
[c] The regioisomeric ratio (rr) was obtained by ^{1}H-NMR.
[d] 4 mol% Rh. [e] 2 mol% Rh. [f] 1 mol% Rh.

We reoptimized the reaction conditions by using $Cp^*Rh(OAc)_2$ as the precatalyst to avoid any excess base that may result in the decomposition of **1a**. Under this reaction condition, **9a** reacts with **10a** to provide **11aa** in low yield (Table 3.5, entry 1). However, we also observed decomposition of reactant **9a** to byproducts **12** and **13**. In addition, we surmised that solvent acidity may alleviate the starting material decomposition. The yield was substantially improved

when the hexafluoroisopropanol (HFIP, pK_a = 9.3) was employed as the solvent (entry 2). We were pleased to find that trifluoroethanol (TFE, pK_a = 12.5) was the optimal solvent as dihydropyridones were furnished in high yield (entry 3). Additionally, less decomposition byproducts were observed. The use of $Cp^*Rh(OAc)_2$ as a precatalyst proved problematic due to its inherent hygroscopicity and practicality when extending to other Cp^x ligands. Fortunately, $[Cp^*RhCl_2]_2$/CsOAc combination also works comparatively well (entry 4). Next, styrene **10b** was found to be an amenable coupling partner, providing the corresponding product **11ab** in good yield and regioselectivity (entry 5). The optimal catalyst loading remained at 2.5 mol% $[Cp^*RhCl_2]_2$, as lowering the catalyst loading resulted in incomplete conversion after 24 h (entries 6-8). It should be noted that the process is practical and operationally simple, as it is not sensitive to air or moisture.

3.2.3 Substrate Scope

Having optimized the reaction conditions, we next explored the *N*-pivaloyloxy acrylamides scope using styrene **10b** as the coupling partner (Table 3.6). An array of α-alkyl substituted acrylamides (**9a-9d**) engaged in reactivity, providing the corresponding δ-lactams in good to high yields (**11ab-11db**). More specifically, *N*-pivaloyloxy α-benzyl (**9a**) and α-(*para*-bromo)-benzyl acrylamides (**9b**) underwent the annulation to deliver **11ab** and **11bb** in high yields. *N*-pivaloyloxy methacrylate (**9c**) also proved fruitful as the desired annulation product **11cb** was afforded in good yield. *N*-pivaloyloxy acrylamide **9d**, derived from the itaconic acid, provided the product **11db** in 94% yield. Next, *N*-pivaloyloxy α-arylacrylamides (**9e-9j**) were found to be reactive, providing the products (**11eb-11jb**) in moderate to high yield. Substituents at *para*- (**9e-9h**), *meta*- (**9i**), and *ortho*- (**9j**) positions were well tolerated. Bromoarene derived products (**11bb** and **11hb**) are of considerable interest as the halogen provides a handle for cross-

coupling reactions. Interestingly, *N*-pivaloyloxy α-ethoxyacrylamide (**9k**) was also competent as the corresponding product (**11kb**) was acquired in 58% yield. α,β-disubstituted *N*-pivaloyloxy acrylamides (**9l** and **9m**) gave only trace amount of product according to UPLC/MS analysis. *N*-pivaloyloxy acrylamide (**9n**) and β-substituted acrylamides (**9o** and **9p**) did not react under the optimal conditions.

Table 3.6 Acrylamide Scope[a]

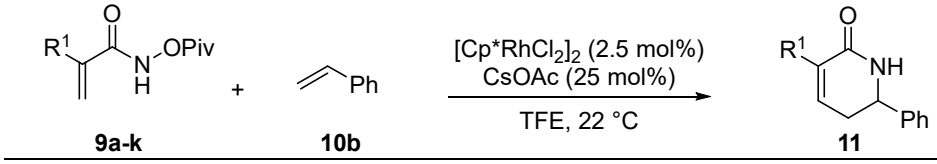

9a-k **10b** **11**

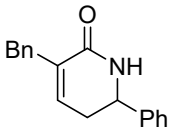

11ab, 85%

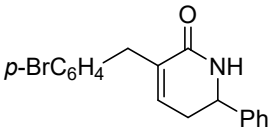

11bb, 90%

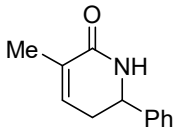

11cb, 78%

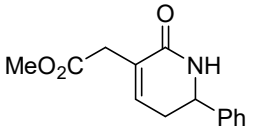

11db, 94%

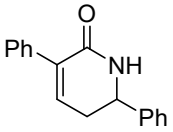

11eb, 55%

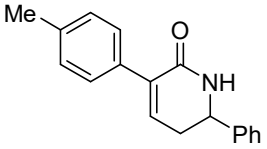

11fb, 80%

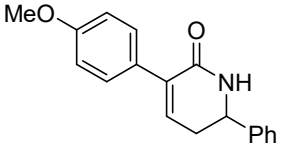

11gb, 84%

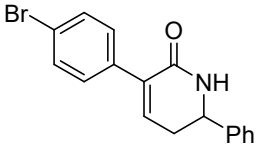

11hb, 60%

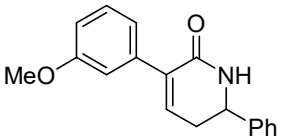

11ib, 81%

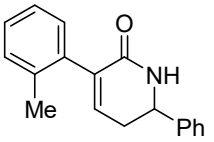

11jb, 77%

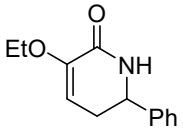

11kb, 58%

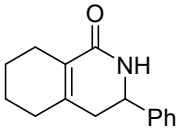

11lb, trace

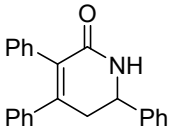

11mb, trace

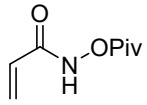

9n

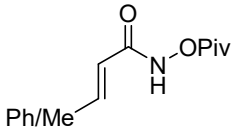

9o and **9p**

[a] Reaction conditions: 9 (0.10 mmol), 10 (0.11 mmol), $[Cp^*RhCl_2]_2$ (2.5 mol%), CsOAc (25 mol%) in TFE (0.3 M) for 24-48 h. The isolated yield was reported.

A styrene scope was next investigated with substrate **1a** as the coupling partner (Table 3.6). Good regioselectivity could be obtained in all cases, partly due to the electronic bias of styrene substrates. First, *para*-substituted styrene derivatives (**10c-10h**) were examined. The electronic nature of the substituents influenced product yield. More specifically, electron-donating groups at the *para*-position (**10c** and **10d)** provided higher yields compared to electron-withdrawing substituents (**10e** and **10h**). *Meta*-substituted styrenes (**10i-10n**) were also tolerated as the corresponding δ-lactams (**11ai-11an**) were furnished in modest to good yields (35-88%). 3-Vinylbenzaldehyde (**10n**) was compatible as **11an** was provided in 30% yield. This example demonstrates that the transformation can tolerate an unprotected carboxaldehyde functional group. 2-Vinylnapthalene (**10o**) also reacted to provide **11ao** in good yield. Most *ortho*-substituted styrenes proved fruitless. These substrates may be too sterically cumbersome to promote the reactivity. However, less sterically hindered 2-fluorostyrene (**10p**) furnished the product **11ap** in moderate yield. Electron-deficient pentafluorostyrene **10q** was a capable coupling partner as **11aq** was provided in a moderate yield. 4-Vinylpyridine was an ineffective substrate, likely due to the inhibitory coordination of pyridine on Rh(III). It should also be noted that electron-deficient ethyl acrylate was unsuccessful for the transformation.

Table 3.7 Vinyl Arene Scope [a,b]

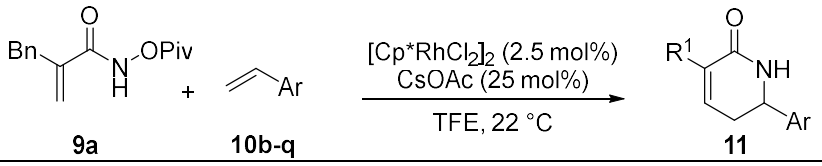

9a **10b-q** **11**

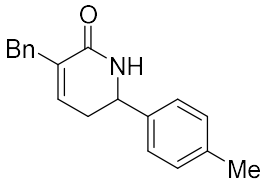

11ac, 92%

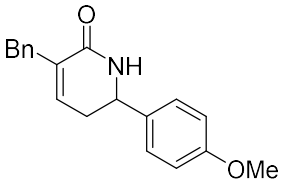

11ad, 89% (83%[b])

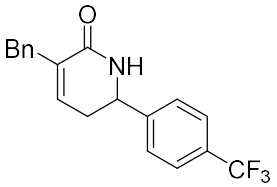

11ae, 78%

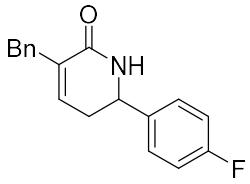

11af, 70%

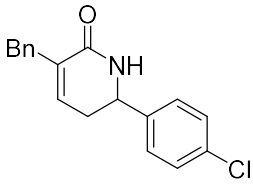

11ag, 71%

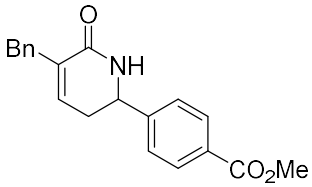

11ah, 57%

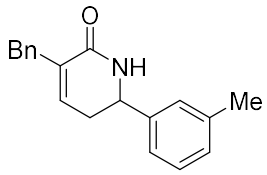

11ai, 84%

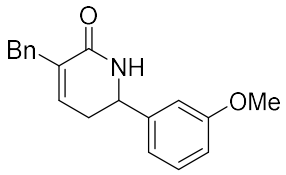

11aj, 88%

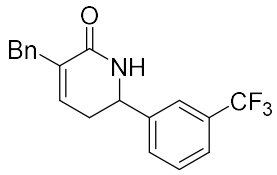

11ak, 44%

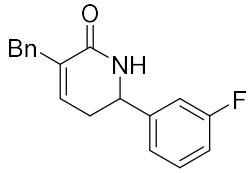

11al, 71%

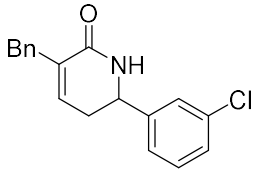

11am, 58%

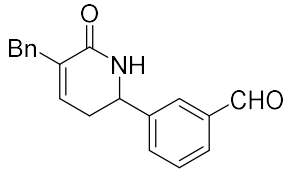

11an, 35%

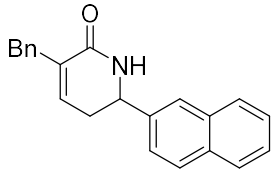

11ao, 70%

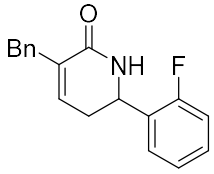

11ap, 60%

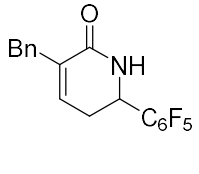

11aq, 50%

[a] Reaction conditions: 9 (0.10 mmol), 10 (0.11 mmol), $[Cp^*RhCl_2]_2$ (2.5 mol%), CsOAc (25 mol%) in TFE (0.3 M) for 24-48 h. The isolated yield was reported.

[b] The reaction was performed in 1 mmol scale.

Interestingly, this reaction showed generality for a variety of cyclic alkenes that efficiently generate fused-δ-lactams (Table 3.8). Strained cyclic alkenes such as norbornadiene (**12a**) and norbornene (**12b**) engaged under optimal conditions providing fused-bicyclic structures (**13aa** and **13ab**) in high yield. Less strained cyclic alkenes such as cyclopentene (**12c**) and indene (**12d**) were also competent substrates as they delivered useful fused-δ-lactams (**13ac** and **13ad**) in good yields. Furthermore, 1,3-cyclohexadiene (**12e**) reacted to give a fused-lactam product **13ae** in good yield. However, the less strained cyclohexene coupling partner (**12f**) provided only trace product **13af**. Dihydronaphthalene (**12g**) was also a competent substrate and afforded product **13ag** in 63% yield. Cyclooctene (**12h**) also reacted to give 75% yield of product **13ah**.

Table 3.8 Cyclic Alkene Scope[a,b]

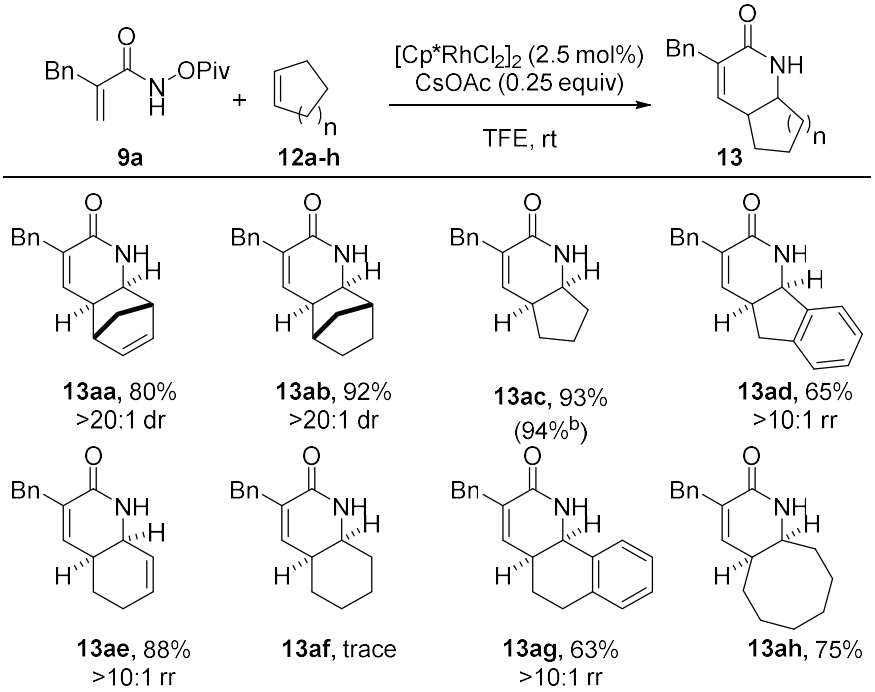

[a] Reaction conditions: **9** (0.10 mmol), **12** (0.11 mmol), $[Cp^*RhCl_2]_2$ (2.5 mol%), CsOAc (25 mol%) in TFE (0.3 M) for 24-48 h. The isolated yield was reported.
[b] The reaction was performed in 1 mmol scale.

So far, unactivated alkenes have proven to be challenging substrates in the selective functionalization due to the lack of the electronic bias relative to styrenes (Table 3.9).[71] These alkenes, in theory, should produce a regioisomeric mixture of 5- and 6-substituted α,β-unsaturated-δ-lactams. Vinyl cyclohexane **10r** gave predominantly the 6-substituted product **11ar** when subjected to optimized reaction conditions. To our surprise, vinyl cyclopentane **10s** gave the 5-substitued product **11as'** as the major regioisomer under optimal conditions. The steric bulk of the di-1,3-di-*tert*-butylcyclopentadienyl ligand (Cp^t)[72] improved the regioselectivity of product **11as'** to >10:1 rr. Allylbenzene (**10a**) gave 5-substituted product **11aa'** as a major regioisomer (2:1 rr). Again, the Cp^t ligand improved the regioisomeric ratio substantially to >10:1 rr favoring **11aa'**. Other aliphatic alkenes such as 4-phenyl-1-butene (**10t**) and 1-heptene (**11u**) gave the corresponding products (**11at'** and **11au'**) in sufficient yields. Bromo- (**10v**), ester- (**10w**) functional groups were tolerated as the corresponding annulation products (**11av'** and **11aw'**) were afforded in moderate yields. These results demonstrate a dichotomy of alkene insertion to access regioisomeric products from different alkenes. However, the reason for this anomaly of regioselectivity is unclear at this moment.

[71] Selected examples: (a) Tsai, A. S.; Brasse, M.; Bergman, R. G. Ellman, J. A. *Org. Lett.*, **2011**, *13*, 540–542. (b) Neely, J. M.; Rovis, T. *J. Am. Chem. Soc.*, **2013**, *135*, 66−69. (b) Takahama, Y.; Shibata, Y.; Tanaka, K. *Chem. Eur. J.*, **2015**, *21*, 9053-9056.

[72] (a) Hyster, T. K.; Rovis, T. *Chem. Sci.*, **2011**, *2*, 1606-1610. (b) Hyster, T. K.; Dalton, D. M.; Rovis, T. *Chem. Sci.*, **2015**, *6*, 254-258.

Table 3.9 Unactivated Alkene Scope [a]

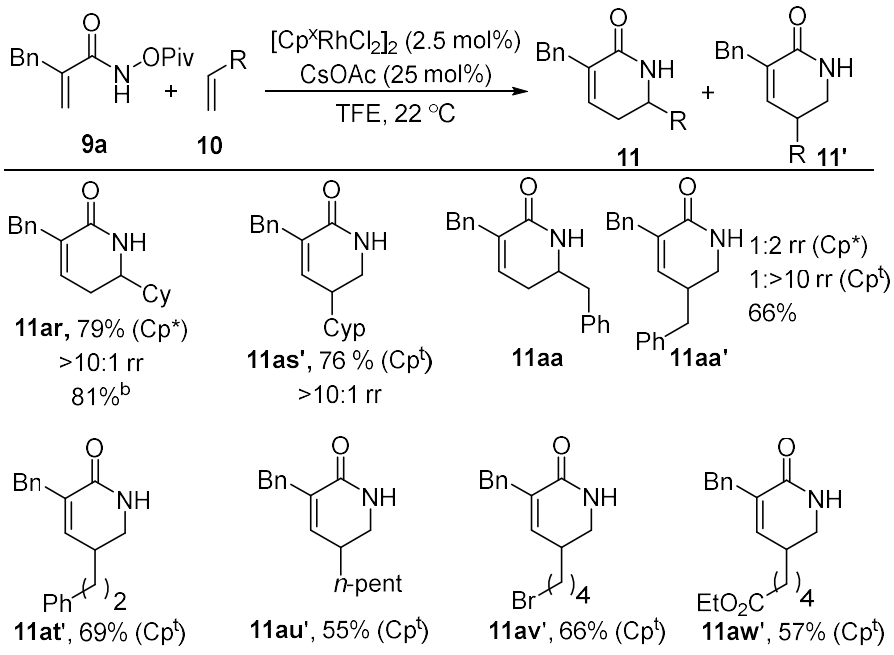

[a] Reaction conditions: **9** (0.10 mmol), **10** (0.11 mmol), $[Cp^*RhCl_2]_2$ or $[Cp^tRhCl_2]_2$ (2.5 mol%), CsOAc (25 mol%) in TFE (0.3 M) for 24-48 h. Isolated yield of a major product was given. Regioselectivity determined by ^{1}H-NMR of the crude material.

3.2.4 Mechanistic Studies

During the investigation of the scope, *N*-pivaloyloxy acrylamide **9n** and ethyl acrylate **10x** were found to be incompetent substrates under the optimal condition. We speculate that they might be a good ligand on rhodium. Control experiments employing *N*-pivaloyloxy acrylamide **9a** and ethyl acrylate **10a** as additives under the optimal condition (using **9n** and **10x**) completely shut down the reaction, no annulation products **11aa** and **11aa'** were observed in both cases (Table 3.10). These results indicate that an inhibitory effect of the *N*-pivaloyloxy acrylamide **9n** and ethyl acrylate **10x** in this reaction.

Table 3.10

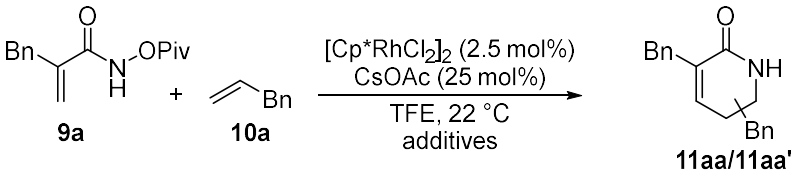

entry	additives	11aa/11aa' yield
1	-	85
2	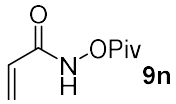 9n	0
3	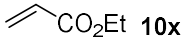 10x	0

An isotope experiment was performed to investigate the reaction mechanism (Scheme 3.4). The reversibility of the C-H activation was determined by running the reaction in the absence of any alkene coupling partner in TFE-d_1. After 1 h, 65% deuterium incorporation at the C-H bond *cis* to amide was observed, as determined by ^{1}H-NMR (eq 16). Additionally, an experiment with styrene **10b** was conducted using TFE-d_1. After 1 h (ca. 60% conversion), 51% deuterium incorporation to **9a**-d at the C-H bond *cis* to the amide was observed. The KIE value (P_H/P_D) of 2.3 was calculated (eq 17). However, the reversibility of C-H activation may be taken into account for KIE value. The results together suggest that the C-H activation is fast, reversible, and may not be involved in the turnover-limiting step. Finally, *N*-methoxy α-benzyl acrylamide **9q** did not give any product, implying that the *N*-pivaloyloxy group is essential for this reaction (eq 19).

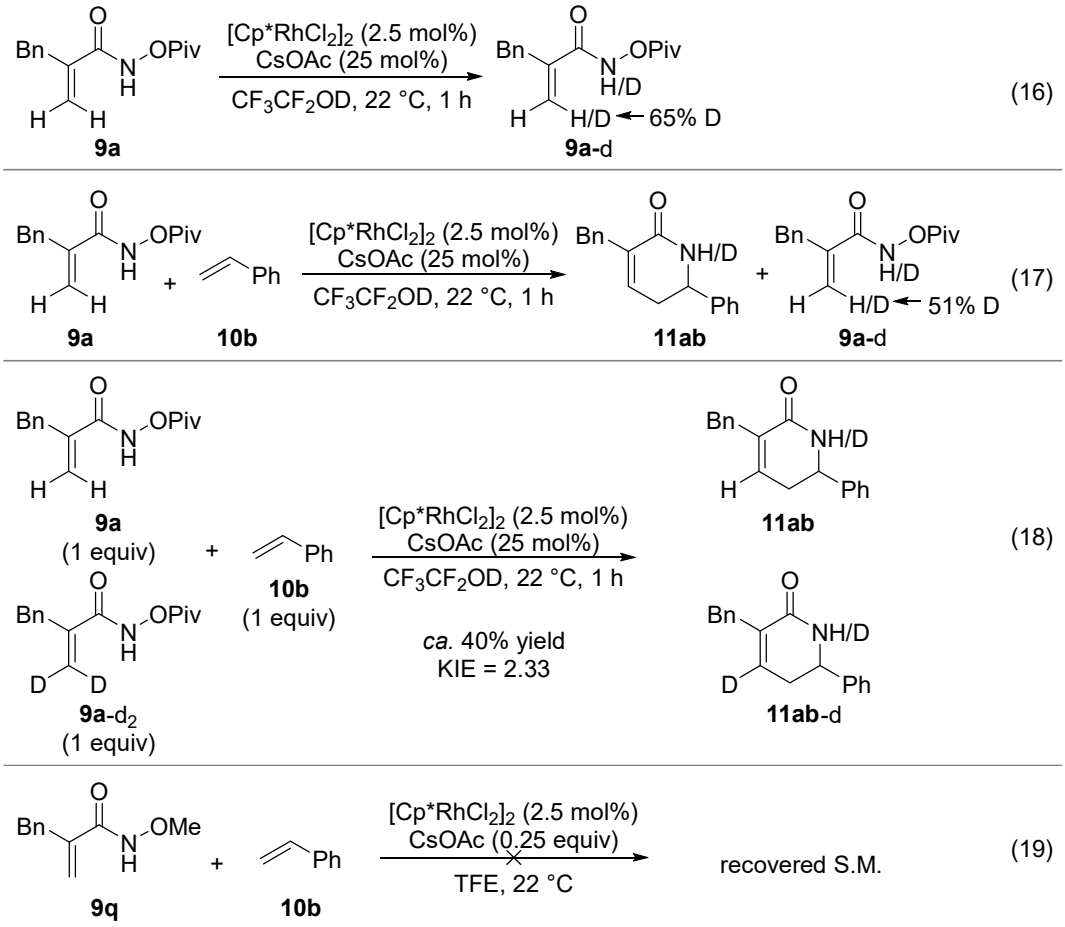

Scheme 3.4 Mechanistic experiments

With these preliminary mechanistic results, a plausible catalytic cycle for this reaction is proposed in Figure 3.3. Initially, coordination of the amide to rhodium by deprotonation of the N-H bond by acetate base generates intermediate **I**. This brings the rhodium in proximity to the vinylic C-H bond. The *reversible* C-H activation occurs, presumably via the concerted-metallation deprotonation (CMD) mechanism, providing five-membered rhodacycle **II**. Subsequent alkene coordination and *irreversible* migratory insertion give seven-membered rhodacycle **IV**. *N*-Acyloxy coordination to Rh(III) precludes the β-hydride elimination. Instead, N-O bond cleavage occurs via the transient Rh(V) nitrenoid intermediate **V**.[73] Finally, reductive

[73] Xu, L.; Zhu, Q.; Huang, G.; Cheng, B.; Xia, Y. *J. Org. Chem.*, **2012**, *77*, 3017–3024.

elimination and C-N bond formation regenerates Rh(III) to close the catalytic cycle. An alternative mechanism involving C-N bond formation to generate Rh(I) intermediate **V'** and N-O bond cleavage to restore Rh(III) can be invoked as well.[8b]

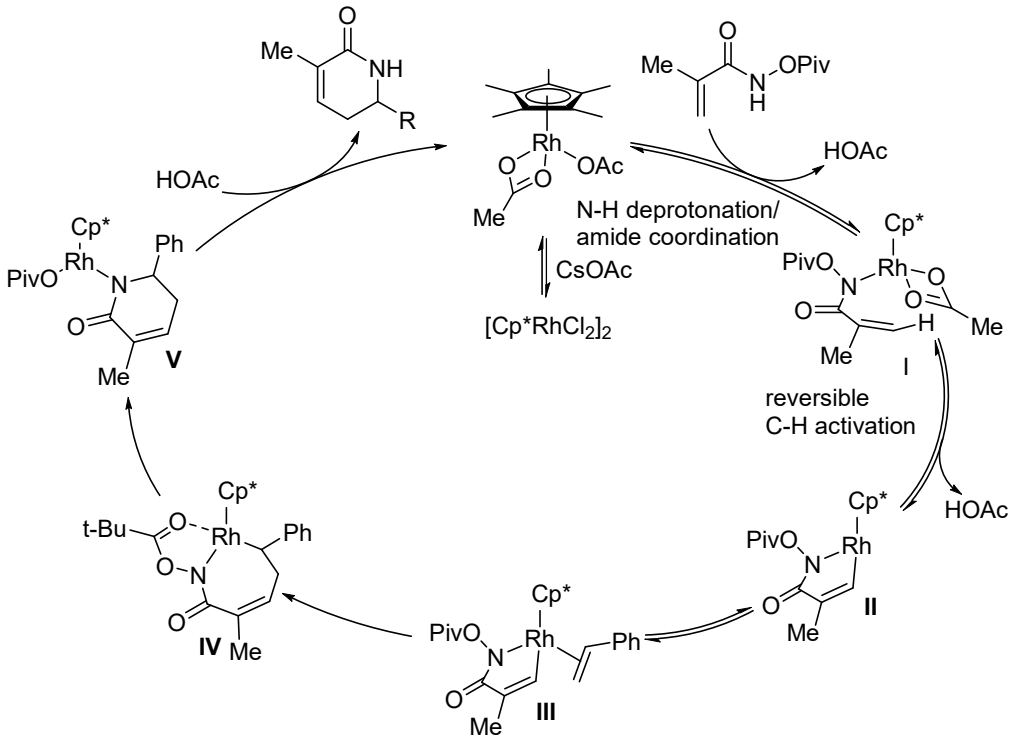

Figure 3.3 Proposed reaction mechanism

3.2.5 Product Derivatization

The derivatization of these δ-lactams highlights their synthetic utility to access other nitrogen heterocycles (Scheme 3.4). The Pd/C-catalyzed hydrogenation of C-C double bond of **11ad** and **13ad** afforded piperidones **14ad** and **14ac** in good diastereoselectivity. In addition, the piperidine derivatives would be accessed by the reduction of the corresponding δ-lactams.

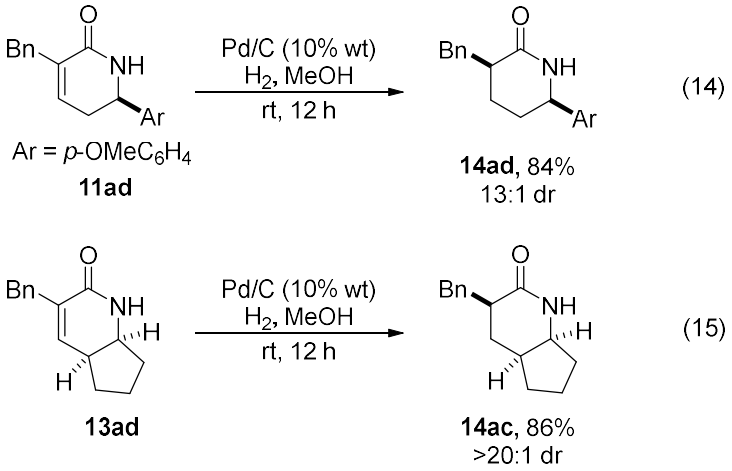

Scheme 3.4

3.3 Conclusions

In summary, we have developed an intermolecular Rh(III)-catalyzed C-H activation reaction for the synthesis of α,β-unsaturated-δ-lactams from *N*-pivaloyloxy α-substituted acrylamides and alkenes. Preliminary mechanistic studies suggest that the reaction proceeds through the reversible C-H activation, irreversible alkene migratory insertion, and N-O bond cleavage/C-N bond formation pathways. We believe that this transformation should not only provide applications for expedient access of α,β-unsaturated-δ-lactams and related alkaloids from simple manipulations, but also serve as a starting point for the development of regioselective and enantioselective variants.

APPENDIX 1

Development of Stereoselective Cyclopropene Benzamidation via Rh(III)-Catalyzed C-H Activation[74]

1. General methods

Unless otherwise noted, reactions were performed in flame-dried glassware and carried out under an atmosphere of nitrogen with magnetic stirring. Tetrahydrofuran (THF), diethyl ether (Et_2O), and dichloromethane (DCM) were degassed with argon and passed through two columns of neutral alumina. Toluene was degassed with argon and passed through one column of neutral alumina and one column of Q5 reagent. Flash column chromatography was performed on SiliCycle Inc.® silica gel 60 (230-400 mesh). Thin Layer chromatography was performed on SiliCycle Inc.® 0.25 mm silica gel 60-F plates. Visualization was accomplished with UV light (254 nm), $KMnO_4$, or CAM. ^{1}H-NMR and ^{13}C-NMR spectra were recorded on a Varian 400 MHz spectrometers or a Bruker Avance III 500 (500 MHz) at ambient temperature. ^{1}H-NMR data are reported as the following: chemical shift in parts per million (δ, ppm) from chloroform ($CHCl_3$) taken as 7.26 ppm, integration, multiplicity (s=singlet, d=doublet, t=triplet, q=quartet, m=multiplet, dd=doublet of doublets) and coupling constant (J in Hz unit). ^{13}C-NMR is reported as the following: chemical shifts are reported in ppm from $CDCl_3$ taken as 77.0 ppm. Several spectra contain a probe-shielding artifact that consistently appeared on all spectra taken at that instrument over a period of months. Mass spectra were obtained on an Agilent Technologies 6130 Quadrupole Mass Spec (LRMS, ESI+APCI). Infrared spectra (IR) were obtained on Bruker Tensor 27 FT-IR spectrometer.

2. Preparation of starting materials and rhodium precatalysts

O-pivaloyl arylhydroxamates,[75] *O*-Boc arylhydroxamates[76] and 3,3-disubstituted cyclopropenes[77-78] were prepared by previously reported procedure. *Catalyst Synthesis:* $[Cp^*RhCl_2]_2$[79], $[Cp^{*t\text{-}Bu}RhCl_2]_2$[80],

[74] Adapted from: Semakul, N.; Jackson, K. E.; Paton, R. P.; Rovis, T. *Chem. Sci.* **2017,** *8*, 1015-1020.

[75] (a) Guimond, N,; Gorelsky, S. I.; Fagnou, K. *J. Am. Chem. Soc.* **2011**, *133*, 6449-6457. (b) Wang, H.; Glorius, F. *Angew. Chem. Int. Ed.* **2012**, *51*, 7318-7322. (c) Hyster, T. K.; Ruhl, K. E.; Rovis, T. *J. Am. Chem. Soc.* **2013**, *135*, 5364-5367.

[76] (a) Guimond, N,; Gorelsky, S. I.; Fagnou, K. *J. Am. Chem. Soc.* **2011**, *133*, 6449-6457. (b) Ye, B.; Cramer, N. *Science* **2012,** *338,* 504-506.

[77] Rubin, M.; Gevorgyan, V. *Synthesis* **2004**, 796-800.

[78] Phan, D. H. T.; Kou, K. G. M.; Dong, V. M. *J. Am. Chem. Soc.* **2010**, *132*, 16354-16355.

[79] Fujita, K.; Takahashi, Y.; Owaki, M.; Yamamoto, K.; Yamaguchi, R. *Org. Lett.* **2004**, *6*, 2785-2788.

[80] Piou, T.; Rovis, T. *Nature* **2015,** *527,* 86-90.

$[Cp^{*CF3}RhCl_2]_2$[81], $[Cp^{*bisCF3Ar}RhCl_2]_2$[82] and $[Cp^{iPr}RhCl_2]_2$[83] were synthesized by reported procedures. $[Cp^{t}RhCl_2]_2$ was purchased from Sigma-Aldrich (RNI00147).

Synthesis of heptamethylindenyl rhodium chloride dimer $[Ind^*RhCl_2]_2$

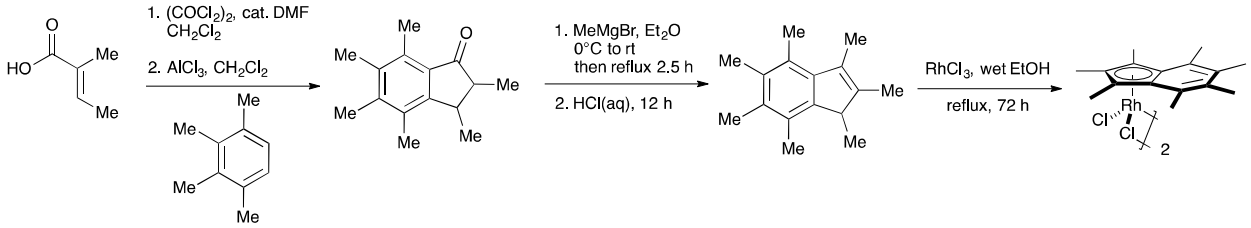

To a flame-dried round bottom flask charged with a stir bar, 2,3,4,5,6,7-hexamethylindan-1-one[84] (700 mg, 3.23 mmol, 1 equiv.), Et_2O (11 mL, 0.3 M) were added and cooled to 0°C. 3 M MeMgBr (2.16 mL, 6.47 mmol, 2 equiv.) was added to the solution dropwise. The reaction was mixture was warmed to room temperature and refluxed for 2.5 h. At 0°C, H_2O was added to the reaction mixture following by conc HCl and stirred at room temperature for 12 h. The reaction was extracted with Et_2O (×3 times), washed with satd $NaHCO_3$, H_2O, brine, dried over $MgSO_4$, filtered and solvent was evaporated under reduced pressure. The crude product was purified by column chromatography using 5% Et_2O/hexane as an eluent to afford heptamethylindene (Ind^*H)[85] (334 mg, 48% yield). The characterizations were agreed with the previously report. **^{1}H-NMR** ($CDCl_3$, 400 MHz) δ 3.28 (m, 1H), 2.61 (s, 3H), 2.42 (s, 3H), 2.35 (s, 9H), 2.05 (s, 3H), 1.33 (d, J = 4 Hz, 3H). **^{13}C-NMR** ($CDCl_3$, 100 MHz) δ 144.9, 142.9, 140.9, 133.8, 132.0, 130.8, 128.4, 126.5, 46.4, 16.7, 16.4, 16.2, 16.1, 16.0, 15.3, 12.3.

Heptamethylindene (Ind^*H) (1.26 equiv., 1.2 mmol, 260 mg) was dissolved in EtOH (0.063 M, 15 mL) and a few drops of water. $RhCl_3·H_2O$ (1 equiv., 0.95 mmol, 250 mg) was added to the reaction mixture which was subsequently refluxed for 72 h. The mixture was cooled to room temperature and the solvent was evaporated to dryness. The crude product was washed several times with hexane to remove excess ligand. The crude solid was redissolved in CH_2Cl_2 and filtered through Celite. The filtrate was concentrated which give $[Ind^*RhCl_2]_2$ complex as a red-brown solid (60 mg, 48% yield). The characterizations were agreed with the previously report[86]. **^{1}H-NMR** ($CDCl_3$, 400 MHz) δ 2.54 (s, 6H),

---

[81] Gassman, P. G.; Mickelson, J. W.; Sowa, J. R. *J. Am. Chem. Soc.* **1992**, *114*, 6942-6944.

[82] Davis, T. A.; Wang, C. Q.; Rovis, T. *Synlett* **2015,** *26*, 1520-1524.

[83] Piou, T.; Rovis, T. *J. Am. Chem. Soc.* **2014,** *136,* 11292-11295.

[84] Arnold, T. A.-Q.; Buffet, J.-C.; Turner, Z. R.; O'Hare, D. *J. Organomet. Chem.* **2015,** *792*, 55-56.

[85] O'Hare, D.; Green, J. C.; Marder, T.; Collins, S.; Stringer, G.; Kakkar, A. K.; Kaltsoyannis, N.; Kuhn, A.; Lewis, R.; Mehnert, C.; Scott, P.; Kurmoo, M.; Pugh, S. *Organometallics* **1992,** *11*, 48-55.

[86] Kakkar, A. K.; Stringer, G.; Taylor, N. J.; Marder, T. B. *Can. J. Chem.* **1995,** *73,* 981-988.

2.07 (s, 6H), 1.97 (s, 6H), 1.59 (s, 3H). **^{13}C-NMR** ($CDCl_3$, 126 MHz) δ 143.7, 130.4, 102.6, 95.2 (d), 81.0(d), 18.5, 17.8, 13.4, 10.3. **IR** (neat, cm^{-1}) 2922.6, 2852.3.

3. General procedures for Rh(III)-catalyzed amidoarylation O-substituted arylhydroxamate with cyclopropene

Without any precaution of air and moisture, *O*-substituted arylhydroxamate (0.1 mmol, 1 eq), $[ind^*RhCl_2]_2$ (0.001 mmol, 1 mol%), CsOPiv (0.025 mmol, 0.25 equiv) and MeOH (1 mL, 0.1 M) were weighed into a dram vial charged with a stir bar. The mixture was stirred for 30 seconds and cyclopropene (0.11 mmol, 1.1 equiv) was then added. The reaction was stirred at room temperature for 16 h until the starting material was consumed (monitoring by TLC). The reaction was quenched with saturated $NaHCO_3$ and extracted 3 times with EtOAc. The organic layer was washed with brine, dried over $MgSO_4$, filtered, and solvent was evaporated to obtain crude product. The crude product was purified by column chromatography using 1/3 to 2/1 EtOAc/hexane to obtain the desired product.

Condition A: using *O*-pivaloyl arylhydroxamate

Condition B: using *O*-Boc arylhydroxamate

4. Product characterizations

(1*S*,1a*R*,7b*R*)-1-methyl-1-phenyl-1,1a,2,7b-tetrahydro-3*H*-cyclopropa[*c*]isoquinolin-3-one

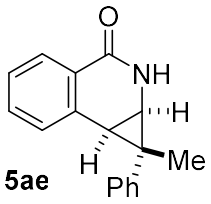

5ae

General procedure B, *O*-Boc arylhydroxamate (0.1 mmol, 23.7 mg) reacted with cyclopropene (0.11 mmol, 14.3 mg) gives the desired dihydroisoquinolone (>20:1 dr of the crude reaction mixture). The major diastereomer was obtained after purification by column chromatography using 1/3 to 2/1 EtOAc/hexane as a white solid (17.9 mg, 68% yield).

^{1}H-NMR ($CDCl_3$, 400 MHz): δ 8.20 (d, *J* = 8.0 Hz, 1H), 7.51 (t, *J* = 8.0 Hz, 1H), 7.44-7.32 (m, 6H), 7.28-7.24 (m, 1H), 6.99 (br. s, NH), 3.49 (dd, *J* = 8.0, 4.0 Hz, 1H), 2.72 (d, *J* = 8.0 Hz, 1H), 1.13 (s, 3H)

^{13}C- NMR ($CDCl_3$, 100 MHz): δ 164.1, 144.8, 136.4, 132.5, 129.5, 128.7, 128.2, 126.95, 126.86, 126.78, 126.5, 40.7, 26.7, 24.9, 13.1

IR (neat, cm^{-1}) 3174, 2923, 1658, 1599

LRMS m/z (ESI+APCI) calcd for $C_{17}H_{15}NO$ [M+H]: 250.1; Found: 250.1

(1*S*,1a*R*,7b*R*)-1,6-dimethyl-1-phenyl-1,1a,2,7b-tetrahydro-3*H*-cyclopropa[*c*]isoquinolin-3-one

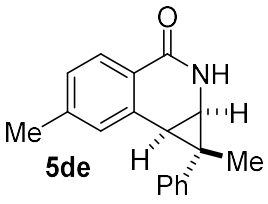

5de

General procedure A, *O*-Piv arylhydroxamate (0.1 mmol, 23.5 mg) reacted with cyclopropene (0.11 mmol, 14.3 mg) gives the desired dihydroisoquinolone (>20:1 dr of the crude reaction mixture). The major diastereomer was obtained after purification by column chromatography using 1/3 to 2/1 EtOAc/hexane as an off-white solid (21.0 mg, 90 % yield).

General procedure B, *O*-Boc arylhydroxamate (0.1 mmol, 25.1 mg) reacted with cyclopropene (0.11 mmol, 14.3 mg) gives the desired dihydroisoquinolone (>20:1 dr of the crude reaction mixture). The major diastereomer was obtained after purification by column chromatography using 1/3 to 2/1 EtOAc/hexane as a white solid (17.9 mg, 68% yield).

^{1}H-NMR ($CDCl_3$, 400 MHz): δ 8.05 (d, *J* = 8.0 Hz, 1H), 7.39-7.32 (m, 4H), 7.28-2.22 (m, 2H), 7.17 (d, *J* = 8.0 Hz, 1H), 6.89 (br. s, 1H), 3.47 (dd, *J* = 8.0, 4.0 Hz, 1H), 2.67 (d, *J* = 8.0 Hz, 1H), 2.41 (s, 3H), 1.13 (s, 3H)

^{13}C- NMR ($CDCl_3$, 100 MHz): δ 164.3, 144.9, 143.1, 136.3, 130.0, 128.7, 128.2, 127.9, 126.8, 126.4, 124.3, 40.7, 26.7, 25.0, 21.6, 13.2

IR (neat, cm^{-1}) 3176, 3024, 2919, 1575, 1614

LRMS m/z (ESI+APCI) calcd for $C_{18}H_{17}NO$ [M+H]: 264.1; Found: 264.2

(1*S*,1a*R*,7b*R*)-6-methoxy-1-methyl-1-phenyl-1,1a,2,7b-tetrahydro-3*H*-cyclopropa[*c*]isoquinolin-3-one

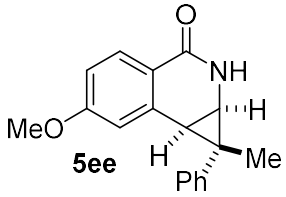

5ee

General procedure A, *O*-Piv arylhydroxamate **1e** (0.1 mmol, 25.1 mg) reacted with cyclopropene **2c** (0.11 mmol, 14.3 mg) gives the desired dihydroisoquinolone (>20:1 dr of the crude reaction mixture). The major diastereomer was obtained after purification by column chromatography using 1/3 to 2/1 EtOAc/hexane as an off-white solid (24.9 mg, 89 % yield).

General procedure B, using *O*-Boc arylhydroxamate **1e'** (0.1 mmol, 26.7 mg) gives the desired dihydroisoquinolone (>20:1 dr of the crude reaction mixture). The major diastereomer was obtained after purification by column chromatography using 1/3 to 2/1 EtOAc/hexane as an off-white solid (17.9 mg, 64% yield).

^{1}H-NMR ($CDCl_3$, 400 MHz): δ 8.13 (d, *J* = 8.0 Hz, 1H), 7.39-7.31 (m, 4H), 7.27-7.23 (m, 1H), 6.89-6.83 (m, 2H), 6.83 (br. s, 1H), 3.88 (s, 3H), 3.47 (dd, *J* = 8.0, 4.0 Hz, 1H), 2.67 (d, *J* = 8 Hz), 1.15 (s, 3H)

^{13}C- NMR ($CDCl_3$, 100 MHz): δ 164.1, 162.8, 144.9, 138.5, 130.4, 128.7, 126.7, 126.4, 119.9, 114.0, 112.9, 55.4, 41.0, 27.0, 25.2, 13.1

IR (neat, cm^{-1}) 3189, 3024, 2927, 1445, 1603, 1445, 1266

LRMS m/z (ESI+APCI) calcd for $C_{18}H_{17}NO_2$ [M+H]: 280.1; Found: 280.1

(1*S*,1a*R*,7b*R*)-1-methyl-1-phenyl-6-(trifluoromethyl)-1,1a,2,7b-tetrahydro-3*H*-cyclopropa[*c*]isoquinolin-3-one

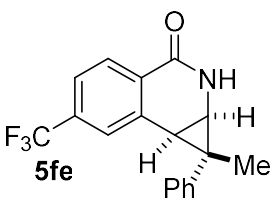

5fe

General procedure A, *O*-Piv arylhydroxamate (0.1 mmol, 28.9 mg) reacted with cyclopropene (0.11 mmol, 14.3 mg) gives the desired dihydroisoquinolone (10.2:1 dr of the crude reaction mixture). The major diastereomer was obtained

after purification by column chromatography using 1/3 to 2/1 EtOAc/hexane as an off-white solid (25.1 mg, 77 % yield).

General procedure B, using *O*-Boc arylhydroxamate (0.1 mmol, 30.0 mg) gives the desired dihydroisoquinolone (17:1 dr of the crude reaction mixture). The major diastereomer was obtained after purification by column chromatography using 1/3 to 2/1 EtOAc/hexane as an off-white solid (21.2 mg, 67% yield).

^{1}H-NMR ($CDCl_3$, 400 MHz): δ 8.32 (d, J = 8.0 Hz, 1H), 7.70 (s, 1H), 7.62 (d, *J* = 8.0 Hz, 1H), 7.41-7.35 (m, 5H), 7.30-7.27 (m, 1H), 3.56 (dd, *J* = 8.0, 4.0 Hz, 1H), 2.76 (d, *J* = 8.0 Hz, 1H), 1.14 (s, 3H)

^{13}C- NMR ($CDCl_3$, 100 MHz): δ 163.1, 144.1, 140.4, 130.1, 129.4 (q), 128.8, 128.8 (q), 127.5, 126.9, 126.8, 126.3 (q), 125.4 (q), 40.8, 26.4, 25.9, 13.2

^{19}F-NMR ($CDCl_3$, 386 MHz): δ -63.1

IR (neat, cm^{-1}) 3200, 1560, 1311, 1168, 1127

LRMS m/z (ESI+APCI) calcd for $C_{18}H_{14}F_3NO$ [M+H]: 318.1; Found: 318.1

(1*S*,1a*R*,7b*R*)-6-chloro-1-methyl-1-phenyl-1,1a,2,7b-tetrahydro-3*H*-cyclopropa[*c*]isoquinolin-3-one

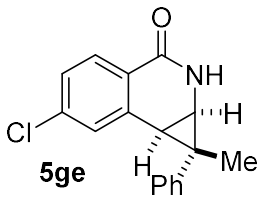

5ge

General procedure A, *O*-Piv arylhydroxamate (0.1 mmol, 25.6 mg) reacted with cyclopropene (0.11 mmol, 14.3 mg) gives the desired dihydroisoquinolone (8.5:1 dr of the crude reaction mixture). The major diastereomer was obtained after purification by column chromatography using 1/3 to 2/1 EtOAc/hexane as an off-white solid (20.8 mg, 73 % yield).

General procedure B, using *O*-Boc arylhydroxamate (0.1 mmol, 27.2 mg) gives the desired dihydroisoquinolone (>20:1 dr of the crude reaction mixture). The major diastereomer was obtained after purification by column chromatography using 1/3 to 2/1 EtOAc/hexane as an off-white solid (17.6 mg, 63% yield).

^{1}H-NMR ($CDCl_3$, 400 MHz): δ 8.11 (d, *J* = 8.0 Hz), 7.41-7.23 (m, 7H), 6.79 (br. s, 1H), 3.48 (dd, *J* = 8.0, 4.0 Hz, 1H), 2.64 (d, *J* = 8 Hz, 1H), 1.11 (s, 3H)

^{13}C- NMR ($CDCl_3$, 100 MHz): δ 163.2, 144.3, 138.7, 138.2, 129.9, 129.3, 128.8, 127.4, 126.9, 126.7, 125.4, 40.7, 26.2, 25.7, 13.3

IR (neat, cm^{-1}) 3173, 2921, 1490, 1596

LRMS m/z (ESI+APCI) calcd for $C_{17}H_{14}ClNO$ [M+H]: 284.1; Found: 284.1

(1*S*,1a*R*,7b*R*)-6-bromo-1-methyl-1-phenyl-1,1a,2,7b-tetrahydro-3*H*-cyclopropa[*c*]isoquinolin-3-one

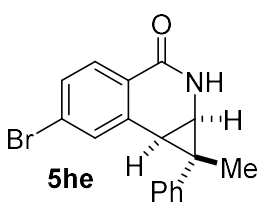

5he

General procedure A, *O*-Piv arylhydroxamate (0.1 mmol, 30.0 mg) reacted with cyclopropene (0.11 mmol, 14.3 mg) gives the desired dihydroisoquinolone (11.2:1 dr of the crude reaction mixture). The major diastereomer was obtained

after purification by column chromatography using 1/3 to 2/1 EtOAc/hexane as an off-white solid (27.3 mg, 83 % yield).

^{1}H-NMR ($CDCl_3$, 400 MHz): δ 8.05 (d, *J* = 8.0 Hz, 1H), 7.60 (s, 1H), 7.50 (d, *J* = 8.0 Hz, 1H), 7.40-7.30 (m, 4H), 7.27 (t, *J* = 8.0 Hz, 1H), 6.82 (br. s, 1H), 3.50 (dd, *J* = 8.0, 4.0 Hz, 1H), 2.66 (d, *J* = 8.0 Hz, 1H), 1.14 (s, 3H)

^{13}C- NMR ($CDCl_3$, 100 MHz): δ 163.4, 144.3, 138.4, 132.2, 130.4, 130.0, 128.8, 127.3, 126.9, 126.7, 125.8, 40.7, 26.2, 25.7, 13.3

IR (neat, cm^{-1}) 2924, 1668, 1591, 1469, 1444, 1371, 765, 700

LRMS m/z (ESI+APCI) calcd for $C_{17}H_{14}BrNO$ [M+H]: 328.0; Found: 328.0, 330.0

(1*S*,1a*R*,7b*S*)-5,6,7-trimethoxy-1-methyl-1-phenyl-1,1a,2,7b-tetrahydro-3*H*-cyclopropa[*c*]isoquinolin-3-one

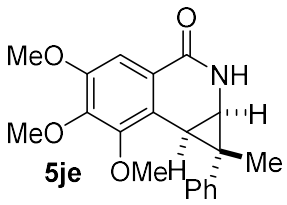

General procedure A, *O*-Piv arylhydroxamate (0.1 mmol, 31.1 mg) reacted with cyclopropene (0.11 mmol, 14.3 mg) gives the desired dihydroisoquinolone (>20:1 dr of the crude reaction mixture). The major diastereomer was obtained after purification by column chromatography using 1/3 to 2/1 EtOAc/hexane as an off-white solid (20.5 mg, 62 % yield).

^{1}H-NMR ($CDCl_3$, 400 MHz): δ 7.55 (s, 1H), 7.42-7.34 (m, 4H), 7.26-7.23 (m, 1H), 6.87 (br. s, 1H), 3.97 (s, 3H), 3.93 (s, 3H), 3.91 (s, 3H), 3.39 (dd, *J* = 8.0, 4.0 Hz, 1H), 2.87 (d, *J* = 8.0 Hz, 1H), 1.13 (s, 3H)

^{13}C- NMR ($CDCl_3$, 100 MHz): δ 163.7, 152.3, 151.9, 145.9, 144.9, 128.7, 127.1, 126.5, 123.7, 122.3, 106.7, 61.1, 61.0, 56.1, 40.6, 23.9, 21.2, 13.6

IR (neat, cm^{-1}) 3200, 2937, 1575, 1597, 1576, 1479, 1113

LRMS m/z (ESI+APCI) calcd for $C_{20}H_{21}NO_4$ [M+H]: 340.2; Found: 340.2

(1*S*,1a*R*,7b*R*)-1-methyl-1-phenyl-5-(trifluoromethyl)-1,1a,2,7b-tetrahydro-3*H*-cyclopropa[*c*]isoquinolin-3-one

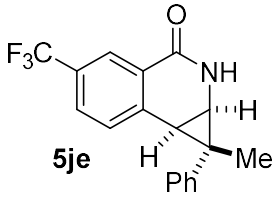

General procedure A, *O*-Piv arylhydroxamate (0.1 mmol, 28.5 mg) reacted with cyclopropene (0.11 mmol, 14.3 mg) gives the desired dihydroisoquinolone (single regioselectivity, >20:1 dr of the crude reaction mixture). The major diastereomer was obtained after purification by column chromatography using 1/3 to 2/1 EtOAc/hexane as an off-white solid (28.3 mg, 85 % yield).

^{1}H-NMR ($CDCl_3$, 400 MHz): δ 8.50 (s, 1H), 7.80 (br. s, NH), 7.75 (d, *J* = 8 Hz, 1H), 7.57 (d, *J* = 8 Hz, 1H), 7.42-7.33 (m, 4H), 7.29 (d, *J* = 8 Hz, 1H), 3.58 (dd, *J* = 8.0, 4.0 Hz, 1H), 2.75 (d, *J* = 8.0 Hz), 1.14 (*s*, 3H)

^{13}C- NMR ($CDCl_3$, 100 MHz): δ 163.1, 144.1, 140.4, 130.1, 129.4 (q), 128.8, 128.8 (q), 127.5 (q), 126.9 (q), 126.8, 125.4, 123.8, 40.8, 26.4, 25.9, 13.2.

^{19}F-NMR ($CDCl_3$, 386 MHz): δ -61.8

IR (neat, cm^{-1}) 3193, 3060, 2928, 1669, 1617, 1502, 1167, 1125

LRMS m/z (ESI+APCI) calcd for $C_{18}H_{14}F_3NO$ [M+H]: 318.1; Found: 318.1

(1*S*,1a*R*,9b*R*)-1-methyl-1-phenyl-1,1a,2,5,6,7,8,9b-octahydro-3*H*-benzo[*g*]cyclopropa[*c*]isoquinolin-3-one

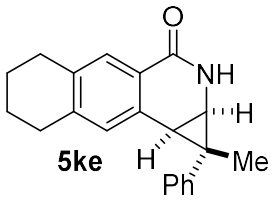

A 86%
8.2:1 rr
(15.3:1 dr)

General procedure A, *O*-Piv arylhydroxamate (0.1 mmol, 27.5 mg) reacted with cyclopropene (0.11 mmol, 14.3 mg) gives the desired dihydroisoquinolone (8.5:1 regioselectivity, >20:1 dr of the crude reaction mixture). The mixture of product (8.5:1 regioselectivity, >20:1 dr) was obtained after purification by column chromatography using 1/3 to 2/1 EtOAc/hexane as an off-white solid (28.6 mg, 94 % yield).

^{1}H-NMR ($CDCl_3$, 400 MHz): δ 7.90 (s, 1H), 7.38-7.32 (m, 4H), 7.25-7.22 (m, 1H), 7.11 (s, 1H), 3.45 (dd, *J* = 8.0, 4.0 Hz, 1H), 2.81 (m, 4H), 2.64 (d, *J* = 8.0 Hz, 1H), 1.82 (m, 4H), 1.13 (s, 3H)

^{13}C- NMR ($CDCl_3$, 100 MHz): δ 164.7, 145.1, 142.4, 136.2, 133.1, 129.9, 128.7, 128.6, 126.8, 126.7, 126.3, 40.7, 29.5, 29.0, 26.5, 24.6, 23.0, 22.9, 13.1

IR (neat, cm^{-1}) 3190, 2926, 1660, 1613, 1445, 909, 731

LRMS m/z (ESI+APCI) calcd for $C_{21}H_{21}NO$ [M+H]: 303.2; Found: 303.2

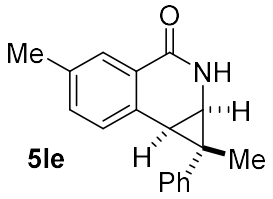

General procedure A, *O*-Piv arylhydroxamate (0.1 mmol, 23.5 mg) reacted with cyclopropene (0.11 mmol, 14.3 mg) gives the desired dihydroisoquinolone (3:1 regioselectivity, >20:1 dr of the crude reaction mixture). The mixture of products (3:1 regioselectiviy, >20:1 dr) was obtained after purification by column chromatography using 1/3 to 2/1 EtOAc/hexane as an off-white solid (25.5 mg, 92 % yield).

^{1}H-NMR ($CDCl_3$, 400 MHz): (See spectra)

^{13}C- NMR ($CDCl_3$, 100 MHz): (See spectra)

IR (neat, cm^{-1}) 3196, 3025, 2923, 1665, 1613, 1500

LRMS m/z (ESI+APCI) calcd for $C_{18}H_{17}NO$ [M+H]: 264.1; Found: 264.1

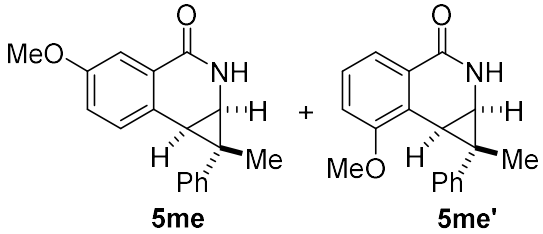

General procedure A, *O*-Piv arylhydroxamate (0.1 mmol, 25.1 mg) reacted with cyclopropene (0.11 mmol, 14.3 mg) gives the desired dihydroisoquinolone (1:1 regioselectivity, >20:1 dr of the crude reaction mixture). The mixture of product was obtained after purification by

column chromatography using 1/3 to 2/1 EtOAc/hexane as an off-white solid (25.1 mg, 86 % yield).

^{1}H-NMR ($CDCl_3$, 400 MHz): (See spectra)

^{13}C- NMR ($CDCl_3$, 100 MHz): (See spectra)

IR (neat, cm^{-1}) 3187, 2932, 1668, 1581, 1494, 1263, 1057, 1032, 752

LRMS m/z (ESI+APCI) calcd for $C_{18}H_{17}NO_2$ [M+H]: 280.1; Found: 280.1

(1*S*,1a*R*,7b*R*)-1-methyl-1-(*p*-tolyl)-1,1a,2,7b-tetrahydro-3*H*-cyclopropa[*c*]isoquinolin-3-one

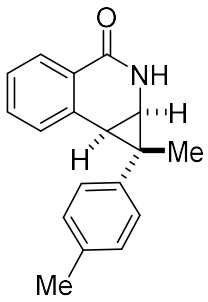

5bf

General procedure B, *O*-Boc arylhydroxamate (0.1 mmol, 23.7 mg) reacted with cyclopropene (0.11 mmol, 15.9 mg) gives the desired dihydroisoquinolone (>20:1 dr of the crude reaction mixture). The major diastereomer was obtained after purification by column chromatography using 1/3 to 2/1 EtOAc/hexane as an off-white solid (15.3 mg, 58 % yield).

^{1}H-NMR ($CDCl_3$, 400 MHz): δ 8.19 (d, *J* = 8.0 Hz, 1H), 7.50 (t, *J* = 8.0 Hz, 1H), 7.42 (d, *J* = 8.0 Hz, 1H), 7.36 (t, *J* = 8.0 Hz, 1H), 7.24-7.15 (m, 4H), 6.91 (br. s, 1H), 3.45 (dd, *J* = 8.0, 4.0 Hz, 1H), 2.68 (d, *J* = 8.0 Hz, 1H), 2.35 (s, 3H), 1.11 (s, 3H)

^{13}C- NMR ($CDCl_3$, 100 MHz): δ 164.1, 141.8, 136.5, 136.2, 132.4, 129.44, 129.39, 128.2, 126.87, 126.85, 126.7, 40.6, 26.6, 24.7, 21.0, 13.2

IR (neat, cm^{-1}) 3188, 3028, 2919, 1662, 1597, 1479, 1341, 777

LRMS m/z (ESI+APCI) calcd for $C_{18}H_{17}NO$ [M+H]: 264.1; Found: 264.2

(1*S*,1a*R*,7b*R*)-1-(4-methoxyphenyl)-1-methyl-1,1a,2,7b-tetrahydro-3*H*-cyclopropa[*c*]isoquinolin-3-one

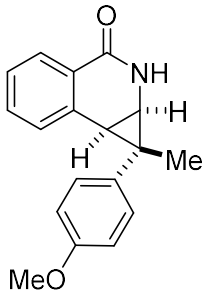

5bg

General procedure B, *O*-Boc arylhydroxamate **1d** (0.1 mmol, 23.7 mg) reacted with cyclopropene **2e** (0.11 mmol, 17.6 mg) gives the desired dihydroisoquinolone (>20:1 dr of the crude reaction mixture). The major diastereomer was obtained after purification by column chromatography using 1/3 to 2/1 EtOAc/hexane as an off-white solid (18.7 mg, 67 % yield).

^{1}H-NMR ($CDCl_3$, 400 MHz): δ 8.19 (d, J = 8 Hz, 1H), 7.50 (t, J = 8 Hz, 1H), 7.42 (d, J = 8 Hz, 1H), 7.36 (t, J = 8 Hz, 1H), 7.27 (d, J = 8 Hz, 2H), 7.11 (brs, 1H), 6.90 (d, J = 8 Hz, 2H), 3.81 (s, 3H), 3.44 (dd, J = 4, 8 Hz, 1H), 2.65 (d, J = 8 Hz, 1H), 1.09 (s, 3H)

^{13}C- NMR ($CDCl_3$, 100 MHz): δ 164.2, 158.2, 137.0, 136.6, 132.4, 129.4, 128.1, 128.1, 126.8, 114.1, 55.3, 40.5, 26.4, 24.5, 13.6

IR (neat, cm^{-1}) 3196, 3039, 2929, 2830, 1662, 1513, 1240, 1178, 1030, 777, 737

LRMS m/z (ESI+APCI) calcd for $C_{18}H_{17}NO_2$ [M+H]: 280.1; Found: 280.1

(1*S*,1a*R*,7b*R*)-1-(4-bromophenyl)-1-methyl-1,1a,2,7b-tetrahydro-3*H*-cyclopropa[*c*]isoquinolin-3-one

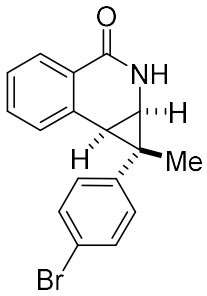

5bh

General procedure B, *O*-Boc arylhydroxamate (0.1 mmol, 23.7 mg) reacted with cyclopropene (0.11 mmol, 23.0 mg) gives the desired dihydroisoquinolone (>20:1 dr of the crude reaction mixture). The major diastereomer was obtained after purification by column chromatography using 1/3 to 2/1 EtOAc/hexane as an off-white solid (17.1 mg, 52 % yield).

^{1}H-NMR ($CDCl_3$, 400 MHz): δ 8.19 (d, *J* = 8.0 Hz, 1H), 7.51 (t, *J* = 8.0 Hz, 1H), 7.48 (d, *J* = 8.0 Hz, 2H), 7.42-7.34 (m, 2H), 7.20 (d, *J* = 8.0 Hz, 2H), 7.10 (br. s, 1H), 6.90 (d, *J* = 8.0 Hz, 2H), 3.46 (dd, *J* = 8.0, 4.0 Hz, 1H), 2.67 (d, *J* = 8.0 Hz, 1H), 1.10 (s, 3H)

^{13}C- NMR ($CDCl_3$, 100 MHz): 164.0, 143.9, 136.0, 132.5, 131.8, 129.4, 128.6, 128.2, 127.1, 126.8, 120.3, 40.6, 26.7, 24.6, 13.0

IR (neat, cm^{-1}) 3171, 3028, 2921, 1662, 1490, 1437

LRMS m/z (ESI+APCI) calcd for $C_{17}H_{14}BrNO$ [M+H]: 328.0, 330.0; Found: 328.0, 330.1

(1*S*,1a*R*,7b*R*)-1-(3-methoxyphenyl)-1-methyl-1,1a,2,7b-tetrahydro-3*H*-cyclopropa[*c*]isoquinolin-3-one

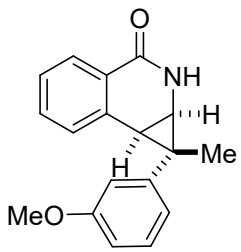

5bi

General procedure B, *O*-Boc arylhydroxamate (0.1 mmol, 23.7 mg) reacted with cyclopropene (0.11 mmol, 17.6 mg) gives the desired dihydroisoquinolone (13.5:1 dr of the crude reaction mixture). The major diastereomer was obtained after purification by column chromatography using 1/3 to 2/1 EtOAc/hexane as an off-white solid (16.2 mg, 58 % yield).

^{1}H-NMR ($CDCl_3$, 400 MHz): δ 8.20 (d, *J* = 8.0 Hz, 1H), 7.50 (t, *J* = 8.0 Hz, 1H), 7.41 (d, *J* = 8.0 Hz, 1H), 7.36 (t, *J* = 8.0 Hz, 1H), 7.30 (t, *J* = 8.0 Hz, 1H), 6.92 (d, *J* = 8.0 Hz, 1H), 6.88 (s, 1H), 6.80 (d, *J* = 8.0 Hz, 1H), 3.84 (s, 3H), 3.45 (dd, *J* = 8.0, 4.0 Hz, 1H), 2.71 (d, *J* = 8.0 Hz, 1H), 1.12 (s, 3H)

^{13}C- NMR ($CDCl_3$, 100 MHz): δ 164.1, 159.9, 146.5, 136.3, 132.5, 129.7, 129.5, 128.2, 126.95, 126.89, 119.0, 113.2, 111.2, 55.3, 40.8, 26.8, 24.9, 13.0

IR (neat, cm^{-1}) 2952, 1633, 1560, 1482, 1341, 1291, 1039, 773, 699

LRMS m/z (ESI+APCI) calcd for $C_{18}H_{17}NO_2$ [M+H]: 280.1; Found: 280.1

(1*S*,1a*R*,7b*R*)-1-methyl-1-(naphthalen-2-yl)-1,1a,2,7b-tetrahydro-3*H*-cyclopropa[*c*]isoquinolin-3-one

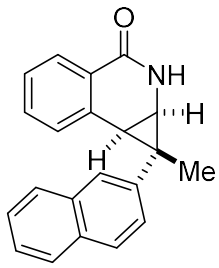

5bj

General procedure B, *O*-Boc arylhydroxamate (0.1 mmol, 23.7 mg) reacted with cyclopropene (0.11 mmol, 19.8 mg) gives the desired dihydroisoquinolone (>20:1 dr of the crude reaction mixture). The major diastereomer was obtained after purification by column chromatography using 1/3 to 2/1 EtOAc/hexane as an off-white solid (23.3 mg, 78% yield).

^{1}H-NMR ($CDCl_3$, 400 MHz): δ 8.23 (d, J = 8 Hz), 7.87-7.79 (m, 4H), 7.55-7.45 (m, 5H), 7.39 (t, J = 8 Hz, 1H), 6.99 (brs, 1H), 3.61 (dd, J = 4, 8 Hz, 1H), 2.82 (d, J = 8 Hz, 1H), 1.22 (s, 3H)

^{13}C- NMR ($CDCl_3$, 100 MHz): δ 164.1, 142.1, 136.4, 133.4, 132.5, 132.1, 129.5, 128.6, 128.2, 127.6, 127.0, 126.9, 126.4, 125.8, 125.38, 125.36, 40.5, 26.5, 25.4, 13.4

IR (neat, cm^{-1}) 3185, 3042, 2924, 1665, 1600, 777

LRMS m/z (ESI+APCI) calcd for $C_{21}H_{17}NO$ [M+H]: 300.1; Found: 300.2

methyl (1*R*,1a*R*,7b*R*)-3-oxo-1-phenyl-1a,2,3,7b-tetrahydro-1*H*-cyclopropa[*c*]isoquinoline-1-carboxylate

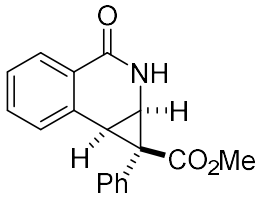

5aa = 5ba

General procedure B, *O*-Boc arylhydroxamate (0.1 mmol, 23.7 mg) reacted with cyclopropene (0.11 mmol, 19.2 mg) gives the desired dihydroisoquinolone (8:1 dr of the crude reaction mixture). The major diastereomer (>10:1 dr purity) was obtained after purification by column chromatography using 1/3 to 2/1 EtOAc/hexane as an off-white solid (22.0 mg, 75% yield).

^{1}H-NMR ($CDCl_3$, 400 MHz): δ 8.19 (d, *J* = 8 Hz, 1 Hz), 7.56-7.50 (m, 2H), 7.48-7.30 (m, 5H), 3.48 (dd, *J* = 8.0, 4.0 Hz), 3.36 (s, 3H), 3.11 (d, *J* = 8.0 Hz, 1H)

^{13}C- NMR ($CDCl_3$, 100 MHz): δ 167.5, 163.8, 138.0, 134.2, 133.4, 132.5, 129.2, 129.1, 128.8, 127.9, 127.7, 127.0, 52.2, 41.7, 35.6, 28.2

IR (neat, cm^{-1}) 3057, 2950, 1726, 1670, 1445, 909, 731

LRMS m/z (ESI+APCI) calcd for $C_{18}H_{15}NO_3$ [M+H]: 293.1; Found: 293.1

(1*S*,1a*R*,7b*R*)-1a,3',4',7b-tetrahydro-2'*H*-spiro[cyclopropa[*c*]isoquinoline-1,1'-naphthalen]-3(2*H*)-one

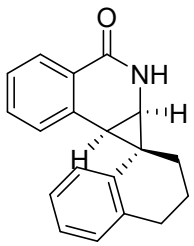

5bk

General procedure B, *O*-Boc arylhydroxamate (0.1 mmol, 23.7 mg) reacted with cyclopropene (0.11 mmol, 17.2 mg) gives the desired dihydroisoquinolone (>20:1 dr of the crude reaction mixture). The major diastereomer was obtained after purification by column chromatography using 1/3 to 2/1 EtOAc/hexane as an off-white solid (19.8 mg, 72% yield).

^{1}H-NMR ($CDCl_3$, 400 MHz): δ 8.18 (d, *J* = 8.0 Hz, 1H), 7.47 (t, *J* = 8.0 Hz, 1H), 7.36 (t, *J* = 8.0 Hz, 1H), 7.32 (d, *J* = 8.0 Hz, 1H), 7.24-7.12 (m, 3H), 6.79 (br. s, NH), 6.68 (d, *J* = 8.0 Hz), 3.50 (dd, *J* = 8.0, 4.0 Hz), 2.83 (t, *J* = 8.0 Hz, 2H), 2.78 (d, *J* = 8.0 Hz, 1H), 1.75-1.55 (m, 2H), 1.35-1.26 (m, 2H)

^{13}C- NMR ($CDCl_3$, 100 MHz): δ 164.0, 139.1, 137.9, 136.0, 132.5, 129.5, 129.0, 128.1, 127.04, 127.00, 126.6, 125.3, 119.6, 43.7, 30.7, 30.2, 22.9, 21.6, 21.3

IR (neat, cm^{-1}) 2920, 1657, 1598, 1479, 1344, 751

LRMS m/z (ESI+APCI) calcd for $C_{19}H_{17}NO$ [M+H]: 275.1; Found: 276.1

(1*R*,1a*R*,7b*R*)-1-benzyl-1-methyl-1,1a,2,7b-tetrahydro-3*H*-cyclopropa[*c*]isoquinolin-3-one

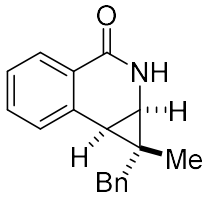

General procedure B, *O*-Boc arylhydroxamate (0.1 mmol, 23.7 mg) reacted with cyclopropene **2j** (0.11 mmol, 15.9 mg) gives the desired dihydroisoquinolone (2.3:1 dr of the crude reaction mixture). The mixture of product was obtained after purification by column chromatography using 1/3 to 2/1 EtOAc/hexane as an off-white solid (16.8 mg, 64% yield).

^{1}H-NMR ($CDCl_3$, 400 MHz): (See spectra)

^{13}C- NMR ($CDCl_3$, 100 MHz): (See spectra)

LRMS m/z (ESI+APCI) calcd for $C_{18}H_{17}NO$ [M+H]: 264.1; Found: 264.1

5. Mechanistic studies

C-H activation reversibility

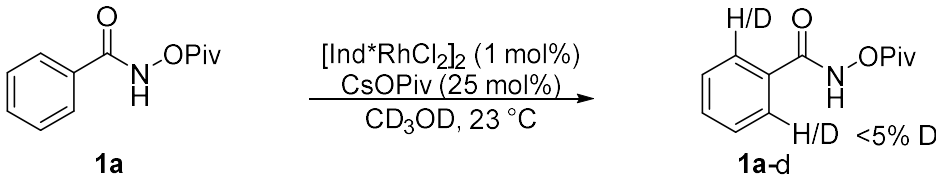

1a **1a**-d

A 1-dram vial was charged with a stir bar, *O*-pivaloyl benzhydroxamate (0.1 mmol, 1 equiv., 22.1 mg), $[Ind^*RhCl_2]_2$ (0.001 mmol, 1 mol%, 0.7 mg) and CsOPiv (0.025 mmol, 0.25 equiv., 5.9 mg) were weighed. The mixture was dissolved in CD_3OD (0.1 M, 1 mL) and stirred for 1 min. The mixture was

determined the deuterium incorporation by ^{1}H-NMR spectroscopy using 1,3,5-trimethoxybenzene as an internal standard.

Electronic preference of the reaction

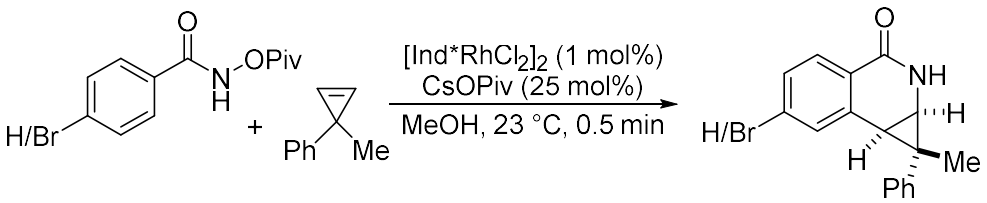

1a:**1h** (H:Br) = 1:1 **4e** **5ae**:**5he** (H:Br) = 1:3

A 1-dram vial charged with a stir bar, *O*-pivaloyl benzhydroxamate (0.05 mmol, 0.5 equiv., 11.1 mg), *O*-pivaloyl p-bromo benzhydroxamate (0.05 mmol, 0.5 equiv., 15.0 mg), $[Ind^*RhCl_2]_2$ (0.001 mmol, 1 mol%, 0.7 mg) and CsOPiv (0.025 mmol, 0.25 equiv., 5.9 mg) were weighed. The mixture was dissolved in CH_3OH and stirred for 30 sec at 0°C. Then, cyclopropene (0.1 mmol, 0.5 equiv., 5.9 mg) was added and stirred for 30 sec at 0°C. The reaction was quenched using satd. $NaHCO_3$ and extracted 3 times with EtOAc. The combined organic layers were washed with brine, dried over $MgSO_4$, filtered and solvent was evaporated. The crude mixture was characterized by ^{1}H-NMR spectroscopy using 1,3,5-trimethoxybenzene as an internal standard.

Kinetic isotope study

D_5-benzoic acid was prepared according to the reported procedure.[87] Then, *O*-pivaloyl D_5-benzhydroxamate was prepared.

O-pivaloyl D_5-benzhydroxamate (0.1 mmol, 0.1 equiv., 22.6 mg), cyclopropene (0.11 mmol, 0.11 equiv., 14.3 mg), $[Ind^*RhCl_2]_2$ (0.001 mmol, 1 mol%, 0.7 mg) and CsOPiv (0.025 mmol, 0.25 equiv., 5.9 mg) were weighed in a dram vial. The reaction mixture was stirred at room temperature for 16 h. The major diastereomer was obtained after purification by column chromatography using 1/3 to 2/1 EtOAc/hexane as an off-white solid (82% yield, >20:1 dr).

^{1}H-NMR ($CDCl_3$, 400 MHz): δ 7.37-7.31 (m, 4H), 7.23 (t, *J* = 8.0 Hz, 1H), 3.45 (dd, *J* = 8.0, 4.0 Hz, 1H), 2.70 (d, *J* = 8.0 Hz), 1.11 (s, 3H)

LRMS m/z (ESI+APCI) calcd for $C_{17}H_{11}D_4NO$ [M+H]: 254.1; Found: 254.1

[87] Chioung, H. A.; Pham, Q.-N.; Daugulis, O. *J. Am. Chem. Soc.*, **2007**, *129*, 9879-9884.

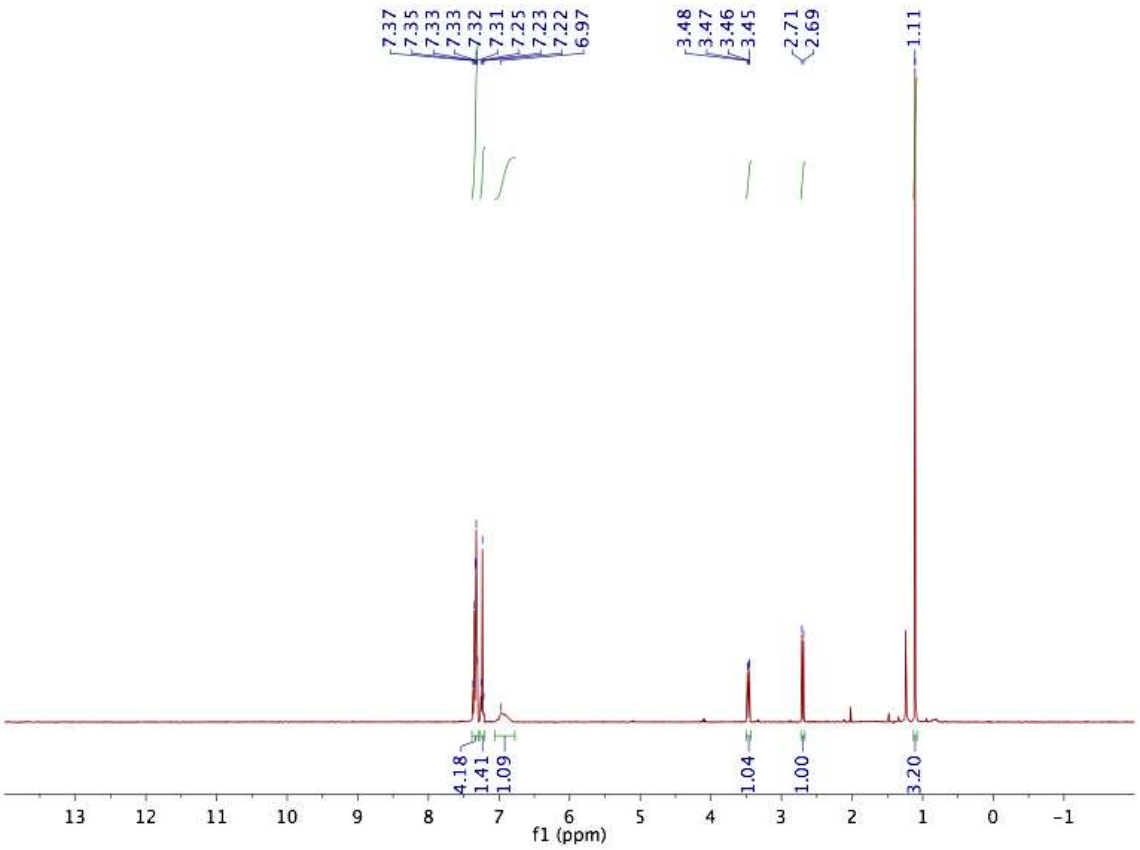

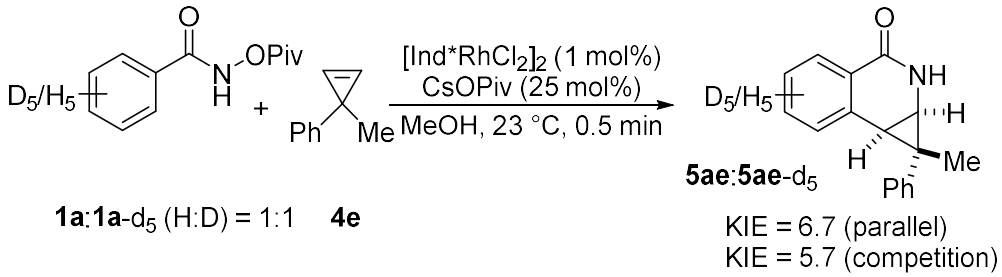

1a:**1a**-d_5 (H:D) = 1:1 **4e**

5ae:**5ae**-d_5

KIE = 6.7 (parallel)
KIE = 5.7 (competition)

Parallel experiment: Two 1-dram vials were charged with a stir bar, proteo- and deutero- benzamide substrate (0.1 mmol, 1 equiv), $[Ind^*RhCl_2]_2$ (1 mol%) and CsOPiv (0.25 equiv) were weighed. The mixture was dissolved in CD_3OD (0.1 M, 1 mL) and stirred for 30 sec at 0°C. Then, cyclopropene (0.1 mmol, 0.5 equiv., 5.9 mg) was added and stirred for 30 sec. The reaction was quenched using satd. $NaHCO_3$ and extracted 3 times with EtOAc. The combined organic layers were washed with brine, dried over $MgSO_4$, filtered and solvent was evaporated. The crude mixture was characterized by ^{1}H-NMR spectroscopy using 1,3,5-trimethoxybenzene as an internal standard.

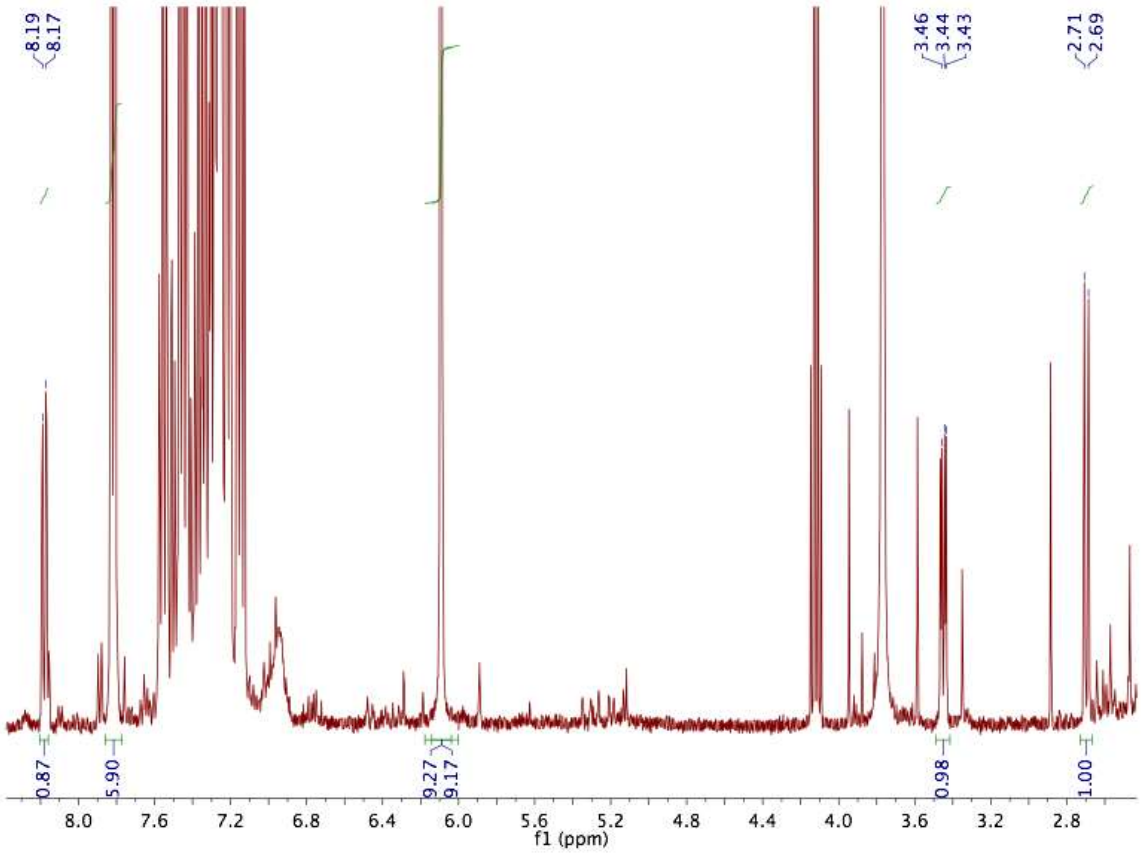

Competition experiment: A 1-dram vial were charged with a stir bar, proteo- and deutero- benzamide substrate (0.05 mmol, 0.5 equiv), $[Ind^*RhCl_2]_2$ (0.001 mmol, 1 mol%, 0.7 mg) and CsOPiv (0.025, 0.25 equiv., 5.9 mg) were weighed. The mixture was dissolved in CD_3OD (0.1 M, 1 mL) and stirred for 30 sec at 0°C. Then, cyclopropene (0.1 mmol, 0.5 equiv., 5.9 mg) was added and stirred for 30 sec. The reaction was quenched using satd. $NaHCO_3$ and extracted 3 times with EtOAc. The combined organic layers were washed with brine, dried over $MgSO_4$, filtered and solvent was evaporated. The crude mixture was characterized by ^{1}H-NMR spectroscopy using 1,3,5-trimethoxybenzene as an internal standard.

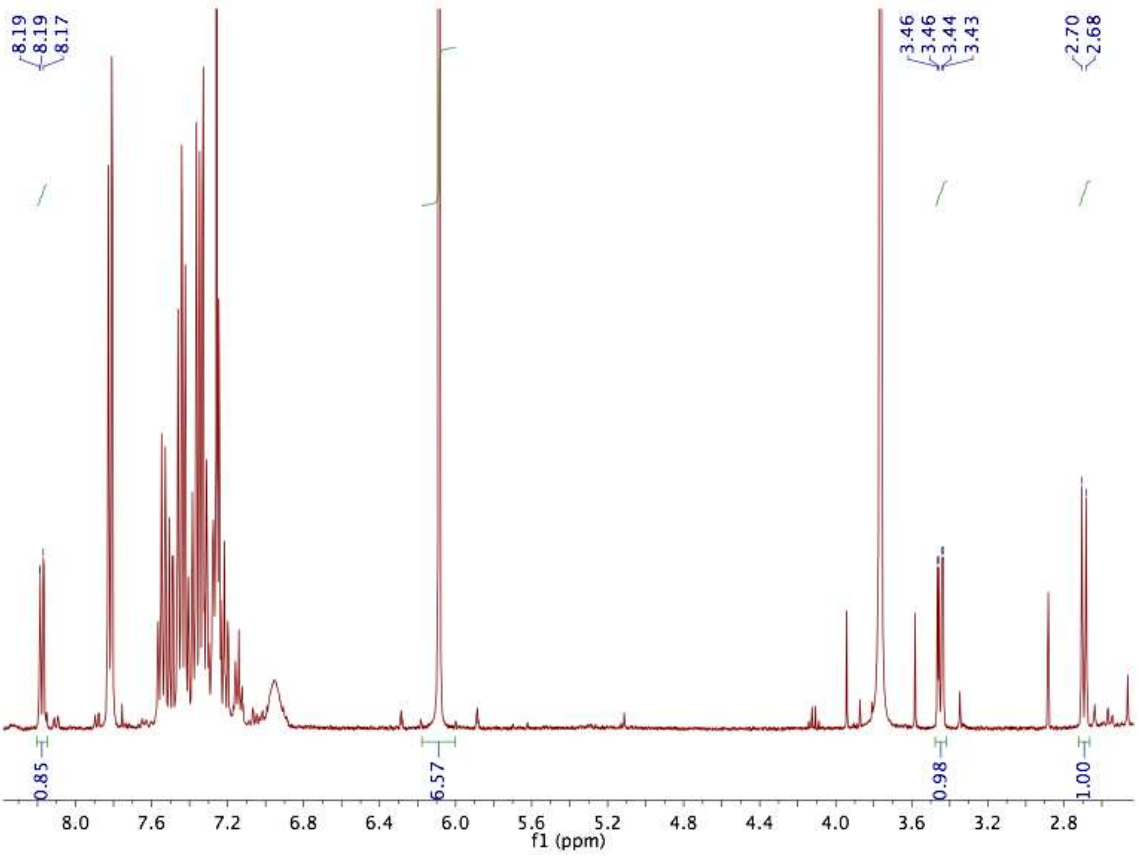

Epimerization study

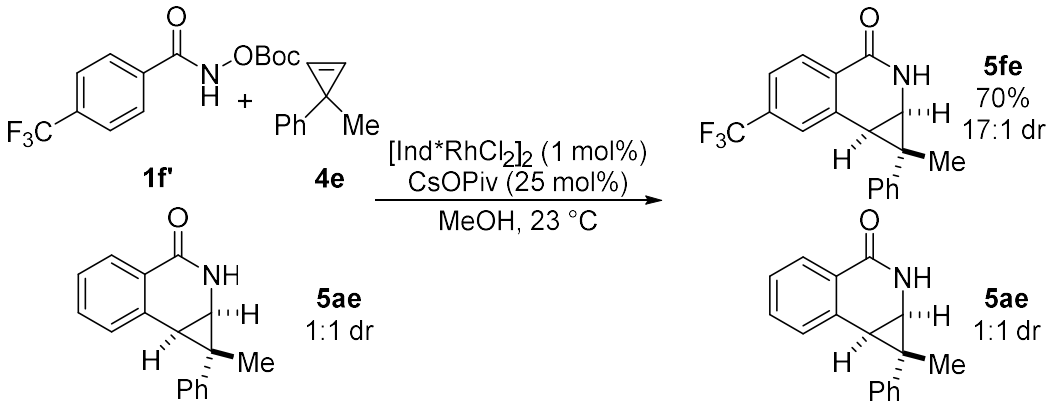

A diastereomeric mixture of dihydroisoquinolone **5ae** (1:1 dr), substrate **1f'** (0.1 mmol, 1 equiv., 30.2 mg), [ind*$RhCl_2$]$_2$ (0.001, 1 mol%, 0.8 mg) CsOPiv (0.025 mmol, 0.25 equiv., 5.9 mg) were weighed in a dram vial charged with a stir bar. MeOH (1mL, 0.1 M) was added and the mixture was stirred for 30 seconds and cyclopropene **4e** (0.11 mmol, 14.9 μL, 1.1 equiv to **1e**) was then added. The reaction was stirred at room temperature for 16 hours and the starting material **1f'** was monitored by TLC. The reaction was quenched using satd. $NaHCO_3$ and extracted 3 times with EtOAc. The combined organic layers were

washed with brine, dried over $MgSO_4$, filtered and the solvent was evaporated. The crude mixture was characterized by ^{1}H-NMR spectroscopy using 1,3,5-trimethoxybenzene as an internal standard.

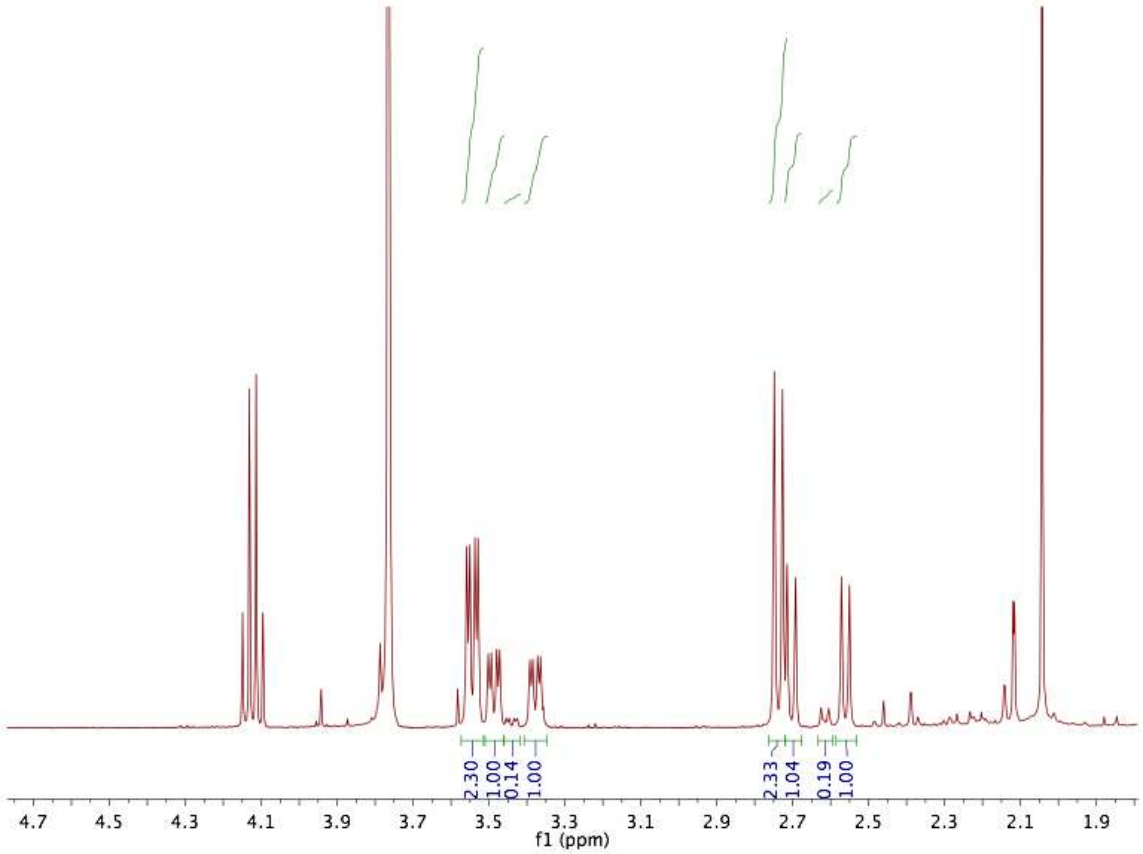

6. Derivatizations of dihydroisoquinolone products

(1*S*,1a*R*,7b*R*)-3-chloro-1-methyl-1-phenyl-1a,7b-dihydro-1*H*-cyclopropa[*c*]isoquinoline

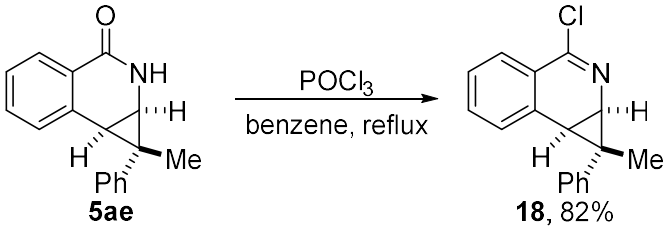

5ae **18**, 82%

To a flamed dried round-bottom flask equipped with a stir bar and reflux condenser, dihydroisoquinolone (0.39 mmol, 97 mg), dry benzene and $POCl_3$ were added. The reaction mixture was refluxed for 6 h. After the completion, the reaction mixture was evaporated under reduced pressure at 60°C and treated with 5% Et_3N/Et_2O at -30°C. After stirring for 10 minutes, the crude was passed through alumina column chromatography using 1:1 Et_2O/hexane as an eluent to give a crude imidoyl chloride as a white solid (85 mg, 82% yield).

^{1}H-NMR ($CDCl_3$, 400 MHz): δ 7.99 (d, *J* = 8.0 Hz, 1H), 7.55-7.45 (m, 4H), 7.42-7.36 (m, 3H), 7.28 (t, *J* = 8.0 Hz, 1H), 4.08 (d, *J* = 8.0 Hz, 1H), 2.75 (d, *J* = 8.0 Hz, 1H), 0.93 (s, 3H)

^{13}C- NMR ($CDCl_3$, 100 MHz): δ 151.9, 145.3, 136.2, 132.5, 129.2, 128.8, 127.9, 127.8, 127.0, 126.8, 125.0, 50.7, 31.4, 22.2, 13.4

IR (neat, cm^{-1}) 3024, 1614, 1599, 1567, 1218

LRMS m/z (ESI+APCI) calcd for $C_{17}H_{14}ClN$ [M+H]: 268.1; Found: 268.1

(1*S*,1a*R*,7b*R*)-1-methyl-1-phenyl-1a,7b-dihydro-1*H*-cyclopropa[*c*]isoquinolin-3-yl trifluoromethanesulfonate

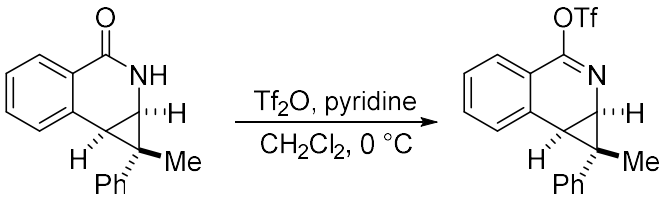

5ae **17**, 80%

To a flamed-dried round equipped with a stir bar, dihydroisoquinolone (0.5 mmol, 125 mg) in CH_2Cl_2 (5 mL) was added. The reaction mixture was cooled at -0°C. Then, Tf_2O (0.77 mmol, 0.13 mL) and pyridine (0.765 mmol, 61 μL) was slowly added to the reaction mixture which was then stirred at the same temperature for 10 mins. The reaction was diluted with CH_2Cl_2 and washed with satd. $NaHCO_3$. The combined organic extracts were dried over $MgSO_4$ and concentrated to give a crude product. The crude was purified by alumina column chromatography using EtOAc as an eluent to give the desired product as a purple solid (152 mg, 80% yield).

^{1}H-NMR ($CDCl_3$, 400 MHz): δ 8.19 (d, *J* = 8.0 Hz, 1H), 7.66 (t, *J* = 8.0 Hz, 1H), 7.53 (t, *J* = 8 Hz, 3H), 7.47-7.38 (m, 3H), 7.30 (t, *J* = 8.0 Hz, 1H), 4.05 (d, *J* = 8.0 Hz, 1H), 2.86 (d, *J* = 8.0 Hz, 1H), 1.23 (s, 3H)

^{13}C- NMR ($CDCl_3$, 100 MHz): δ 161.7, 143.4, 136.1, 134.8, 129.8, 129.7, 129.0, 128.0, 127.9, 127.5, 125.4, 121.2 (q), 44.7, 29.2, 25.9, 15.5

^{19}F- NMR ($CDCl_3$, 381 MHz): 72.3

IR (neat, cm^{-1}) 3061, 1078, 1603, 1492, 1466, 1291, 1093, 792, 720, 688

LRMS m/z (ESI+APCI) calcd for $C_{18}H_{14}F_3NO_3S$ [M+H]: 382.1; Found: 382.1

7. X-ray Structure

CCDC 1472771

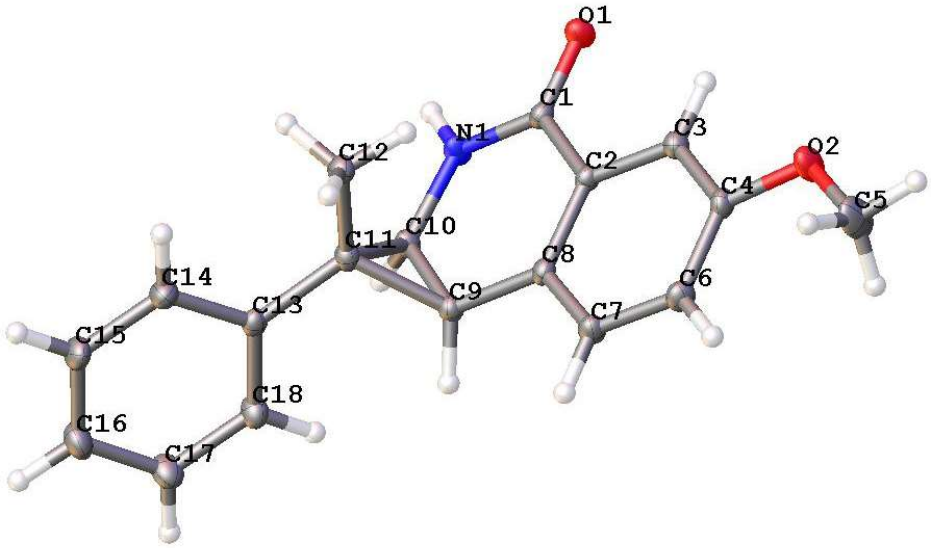

Table 1 Crystal data and structure refinement.

Identification code	Rovis227-1
Empirical formula	$C_{18}H_{17}NO_2$
Formula weight	279.32
Temperature/K	99.77
Crystal system	monoclinic
Space group	$P2_1/n$
a/Å	8.5035(2)
b/Å	7.1303(2)
c/Å	23.6793(6)
α/°	90
β/°	95.7420(12)
γ/°	90
Volume/Å^3	1428.53(6)
Z	4
ρ_{calc}g/cm^3	1.299
μ/mm^{-1}	0.085
F(000)	592.0
Crystal size/mm^3	0.25 × 0.124 × 0.107
Radiation	MoKα (λ = 0.71073)

2Θ range for data collection/°	5.97 to 66.776
Index ranges	$-13 \leq h \leq 12$, $-7 \leq k \leq 10$, $-36 \leq l \leq 36$
Reflections collected	30307
Independent reflections	5464 [R_{int} = 0.0926, R_{sigma} = 0.0945]
Data/restraints/parameters	5464/0/192
Goodness-of-fit on F^2	1.033
Final R indexes [I>=2σ (I)]	R_1 = 0.0685, wR_2 = 0.1558
Final R indexes [all data]	R_1 = 0.1350, wR_2 = 0.1811
Largest diff. peak/hole / e Å^{-3}	0.54/-0.29

Table 2 Fractional Atomic Coordinates ($\times 10^4$) and Equivalent Isotropic Displacement Parameters (Å$^2 \times 10^3$). U_{eq} is defined as 1/3 of of the trace of the orthogonalised U_{IJ} tensor.

Atom	***x***	***y***	***z***	**U(eq)**
O1	6707.2(13)	3443.8(17)	54.8(5)	18.0(3)
O2	9731.6(14)	-2398.8(19)	511.4(6)	23.2(3)
N3	4408.4(16)	3146(2)	448.1(6)	15.5(3)
C4	7791.1(18)	-66(2)	452.3(7)	15.0(3)
C5	6334.4(18)	637(2)	575.3(6)	13.0(3)
C6	5347.7(18)	-415(2)	898.4(6)	13.7(3)
C7	3777.6(18)	313(2)	1014.8(6)	13.6(3)
C8	3308.6(18)	2188(2)	768.8(7)	14.4(3)
C9	5837.4(18)	2508(2)	341.3(7)	13.5(3)
C10	8283.4(19)	-1830(2)	653.3(7)	15.8(3)
C11	3616.3(18)	2012(2)	1415.3(7)	14.6(3)
C12	2168.9(18)	2069(2)	1732.1(7)	14.2(3)
C13	7307.4(19)	-2900(3)	968.6(7)	17.5(3)
C14	5853.7(19)	-2186(2)	1085.9(7)	16.7(3)
C15	5107.6(19)	2856(3)	1709.6(7)	17.1(3)
C16	765.3(19)	1151(3)	1531.6(7)	18.4(4)
C17	2171(2)	3097(3)	2237.5(8)	19.7(4)
C18	-578(2)	1240(3)	1825.7(8)	23.0(4)
C19	-552(2)	2286(3)	2321.1(8)	24.0(4)
C20	826(2)	3196(3)	2525.4(8)	23.1(4)
C21	10328(2)	-4149(3)	736.9(10)	31.4(5)

Table 3 Anisotropic Displacement Parameters ($Å^2×10^3$). The Anisotropic displacement factor exponent takes the form: $-2\pi^2[h^2a^{*2}U_{11}+2hka^*b^*U_{12}+\ldots]$.

Atom	U_{11}	U_{22}	U_{33}	U_{23}	U_{13}	U_{12}
O1	18.0(6)	14.9(6)	21.8(6)	4.6(5)	5.8(5)	2.3(5)
O2	19.8(6)	20.0(7)	31.6(7)	5.7(5)	10.4(5)	7.9(5)
N3	17.4(6)	12.7(7)	16.8(7)	6.0(5)	4.3(5)	4.8(5)
C4	14.7(7)	14.6(8)	16.0(7)	-1.0(6)	2.9(6)	0.7(6)
C5	15.9(7)	10.4(8)	12.8(7)	0.5(6)	1.5(6)	1.2(6)
C6	15.9(7)	12.2(8)	13.1(7)	-2.1(6)	2.0(6)	1.0(6)
C7	14.0(7)	13.2(8)	13.8(7)	0.3(6)	2.4(6)	1.0(6)
C8	14.7(7)	14.4(8)	14.3(7)	2.5(6)	3.5(5)	2.7(6)
C9	16.1(7)	10.8(8)	13.6(7)	-0.8(6)	1.8(6)	1.1(6)
C10	14.7(7)	15.7(9)	17.2(8)	-2.0(6)	2.8(6)	3.3(6)
C11	16.3(7)	14.5(8)	13.3(7)	0.7(6)	2.9(6)	1.9(6)
C12	16.9(7)	11.9(8)	14.1(7)	0.6(6)	2.7(6)	2.1(6)
C13	19.9(8)	13.8(8)	19.1(8)	2.6(7)	3.0(6)	3.2(7)
C14	19.1(7)	14.1(8)	17.5(8)	2.2(6)	5.0(6)	1.6(6)
C15	17.1(7)	17.8(9)	16.5(8)	-2.5(7)	2.9(6)	-0.7(7)
C16	18.0(8)	22.7(10)	14.7(8)	-2.7(7)	1.9(6)	1.2(7)
C17	19.7(8)	18.4(9)	21.5(8)	-4.2(7)	4.5(6)	-2.4(7)
C18	16.5(8)	29.6(11)	23.1(9)	-3.8(8)	2.4(7)	-0.6(7)
C19	20.8(8)	29.1(11)	23.4(9)	-2.4(8)	8.5(7)	1.6(8)
C20	26.5(9)	23.8(10)	20.4(9)	-7.9(7)	8.9(7)	-2.8(7)
C21	24.9(9)	26.1(11)	45.0(12)	8.2(10)	12.8(8)	14.1(8)

Table 4 Bond Lengths

Atom	Atom	Length/Å
O1	C9	1.2461(19)
O2	C10	1.3700(19)
O2	C21	1.430(2)
N3	C8	1.435(2)
N3	C9	1.345(2)
C7	C11	1.553(2)
C8	C11	1.532(2)
C10	C13	1.398(2)
C11	C12	1.505(2)
C11	C15	1.510(2)

C4	C5	1.394(2)	C12	C16	1.402(2)
C4	C10	1.394(2)	C12	C17	1.403(2)
C5	C6	1.407(2)	C13	C14	1.390(2)
C5	C9	1.489(2)	C16	C18	1.397(2)
C6	C7	1.484(2)	C17	C20	1.391(2)
C6	C14	1.392(2)	C18	C19	1.388(3)
C7	C8	1.497(2)	C19	C20	1.384(3)

Table 5 Bond Angles

Atom	**Atom**	**Atom**	**Angle/°**	**Atom**	**Atom**	**Atom**	**Angle/°**
C10	O2	C21	117.45(13)	O2	C10	C13	124.44(15)
C9	N3	C8	125.98(14)	C4	C10	C13	120.07(14)
C10	C4	C5	119.75(15)	C8	C11	C7	58.03(10)
C4	C5	C6	120.82(15)	C12	C11	C7	116.89(14)
C4	C5	C9	118.01(14)	C12	C11	C8	115.43(13)
C6	C5	C9	121.15(14)	C12	C11	C15	116.76(14)
C5	C6	C7	120.72(15)	C15	C11	C7	118.13(13)
C14	C6	C5	118.35(14)	C15	C11	C8	118.68(14)
C14	C6	C7	120.88(14)	C16	C12	C11	121.99(15)
C6	C7	C8	116.74(13)	C16	C12	C17	117.46(15)
C6	C7	C11	121.50(14)	C17	C12	C11	120.53(15)
C8	C7	C11	60.29(11)	C14	C13	C10	119.60(16)
N3	C8	C7	117.95(13)	C13	C14	C6	121.41(15)
N3	C8	C11	120.84(14)	C18	C16	C12	121.38(16)
C7	C8	C11	61.67(11)	C20	C17	C12	120.91(16)
O1	C9	N3	121.19(15)	C19	C18	C16	120.08(17)
O1	C9	C5	121.36(14)	C20	C19	C18	119.22(16)
N3	C9	C5	117.45(14)	C19	C20	C17	120.94(17)
O2	C10	C4	115.48(14)				

Table 6 Hydrogen Atom Coordinates (Å×10^4) and Isotropic Displacement Parameters (Å^2×10^3)

Atom	*x*	*y*	*z*	U(eq)
H3	4122	4252	309	19
H4	8446	653	232	18
H7	2913	-640	1006	16
H8	2172	2310	618	17
H13	7635	-4109	1102	21
H14	5192	-2922	1299	20
H15A	5395	2196	2068	26
H15B	4930	4186	1787	26
H15C	5966	2735	1465	26
H16	726	455	1189	22
H17	3104	3734	2385	24
H18	-1509	584	1687	28
H19	-1470	2376	2518	29
H20	854	3899	2867	28
H21A	11371	-4387	609	47
H21B	9603	-5160	604	47
H21C	10420	-4100	1153	47

Experimental

Single crystals of $C_{18}H_{17}NO_2$ were obtained by the vapor diffusion method using CH_3Cl and pentane. A suitable crystal was selected and collected on a Bruker APEX-II CCD diffractometer. The crystal was kept at 99.77 K during data collection. Using Olex2[88], the structure was solved with the XS[89] structure solution program using Direct Methods and refined with the XL[90] refinement package using Least Squares minimisation.

Crystal structure determination

Crystal Data for $C_{18}H_{17}NO_2$ (M =279.32 g/mol): monoclinic, space group $P2_1/n$ (no. 14), a = 8.5035(2) Å, b = 7.1303(2) Å, c = 23.6793(6) Å, β = 95.7420(12)°, V = 1428.53(6) Å^3, Z = 4, T = 99.77 K, μ(MoKα) = 0.085 mm^{-1}, *Dcalc* = 1.299 g/cm^3, 30307 reflections measured (5.97° ≤ 2Θ ≤ 66.776°), 5464 unique (R_{int} = 0.0926, R_{sigma} = 0.0945) which were used in all calculations. The final R_1

[88] Dolomanov, O.V., Bourhis, L.J., Gildea, R.J, Howard, J.A.K. & Puschmann, H. *J. Appl. Cryst.* **2009**, *42*, 339

[89] Sheldrick, G.M. *Acta Cryst.* **2008**, *A64*, 112

[90] Sheldrick, G.M. *Acta Cryst.* **2008**, *A64*, 112

was 0.0685 ($I > 2\sigma(I)$) and wR_2 was 0.1811 (all data).

8. NMR Spectra

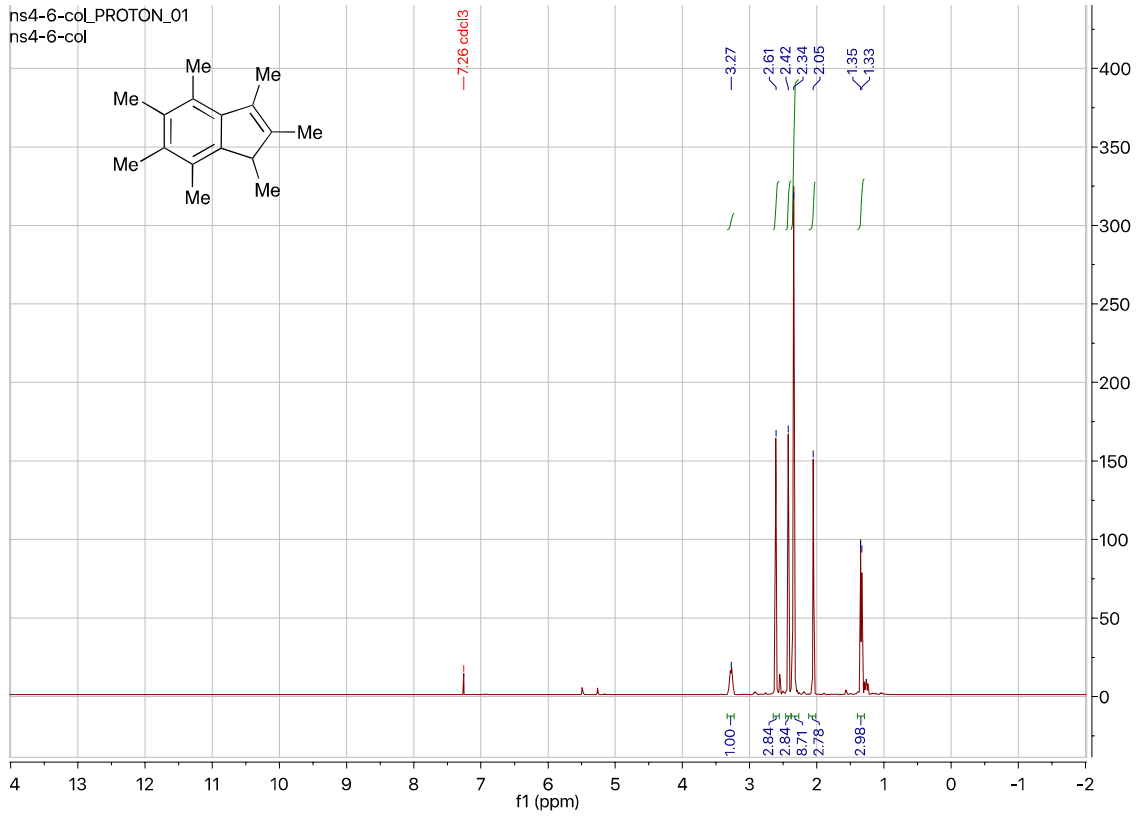
ns4-6-col_PROTON_01
ns4-6-col
Me
Me
Me
Me
Me
Me
7.26 cdcl3
3.27
2.61
2.42
2.34
2.05
1.35
1.33
1.00
2.84
2.84
8.71
2.78
2.98
f1 (ppm)

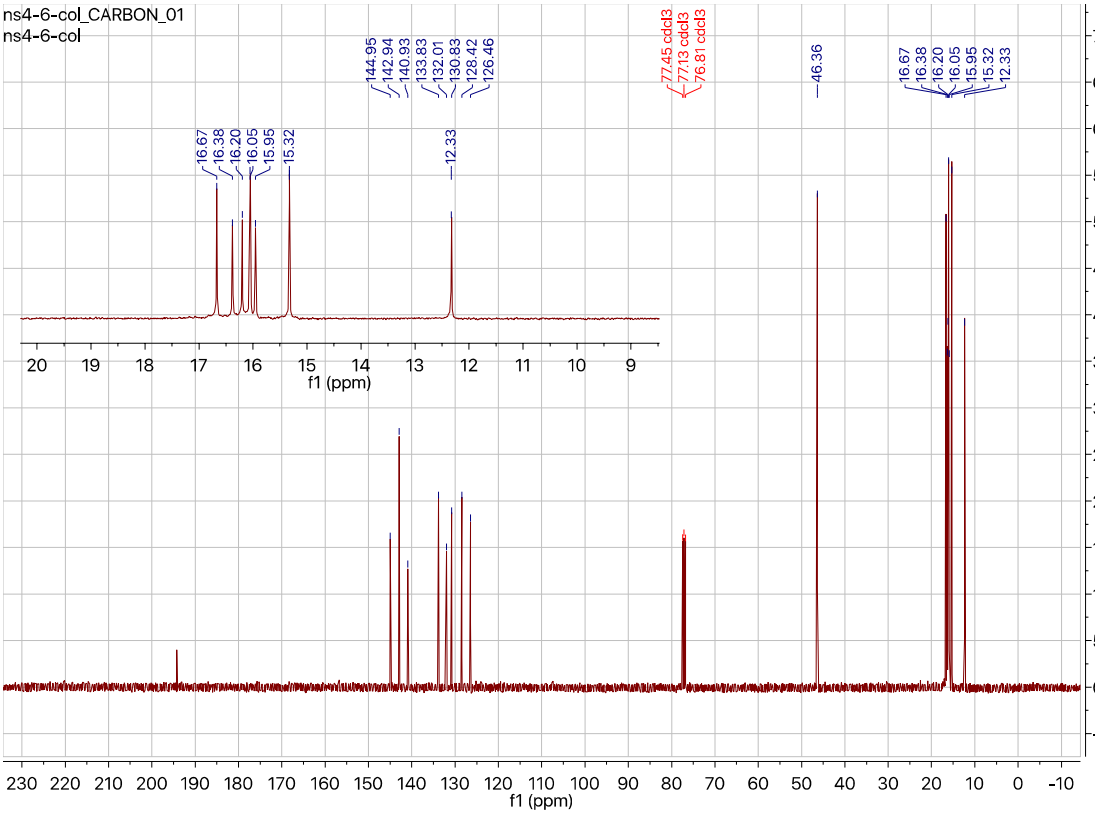
ns4-6-col_CARBON_01
ns4-6-col
144.95
142.94
140.93
133.83
132.01
130.83
128.42
126.46
77.45 cdcl3
77.13 cdcl3
76.81 cdcl3
46.36
16.67
16.38
16.20
16.05
15.95
15.32
12.33
f1 (ppm)

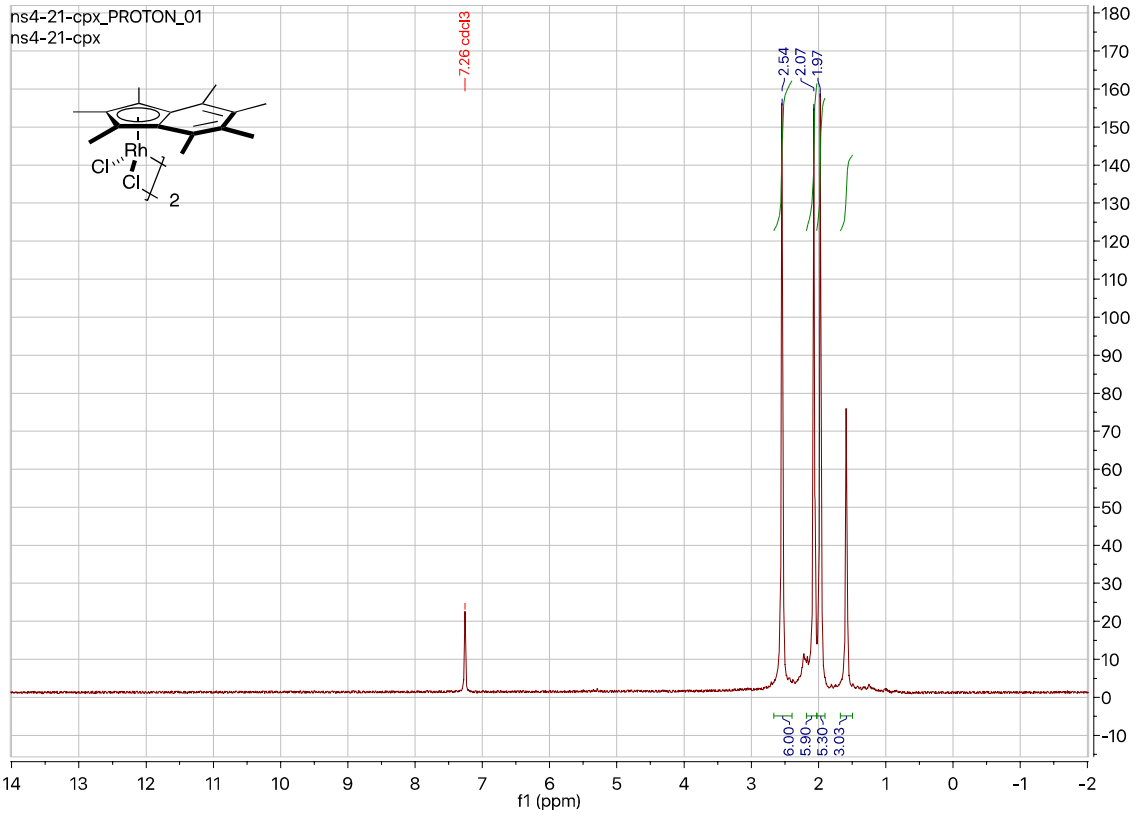
ns4-21-cpx_PROTON_01
ns4-21-cpx
7.26 cdcl3
2.54
2.07
1.97
6.00
5.90
5.30
3.03
Rh
Cl
Cl
2
f1 (ppm)

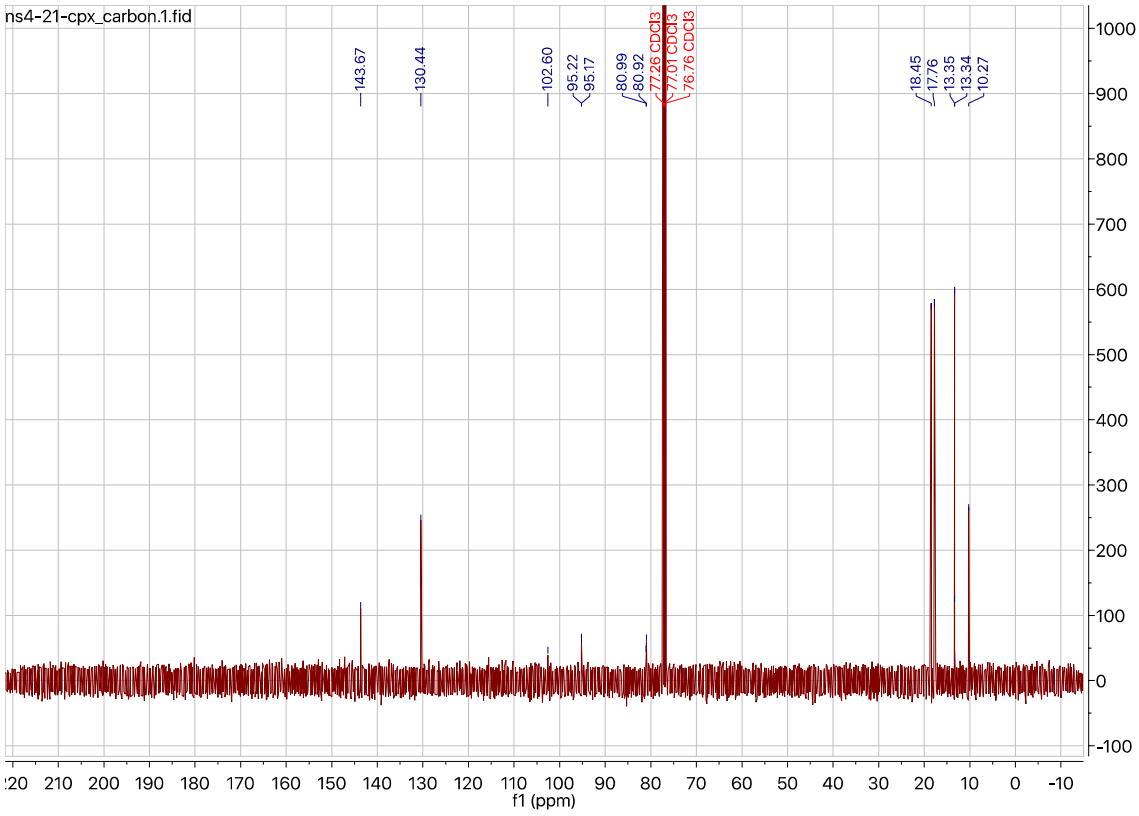
ns4-21-cpx_carbon.1.fid
143.67
130.44
102.60
95.22
95.17
80.99
80.92
77.26 CDCl3
77.01 CDCl3
76.76 CDCl3
18.45
17.76
13.35
13.34
10.27
f1 (ppm)

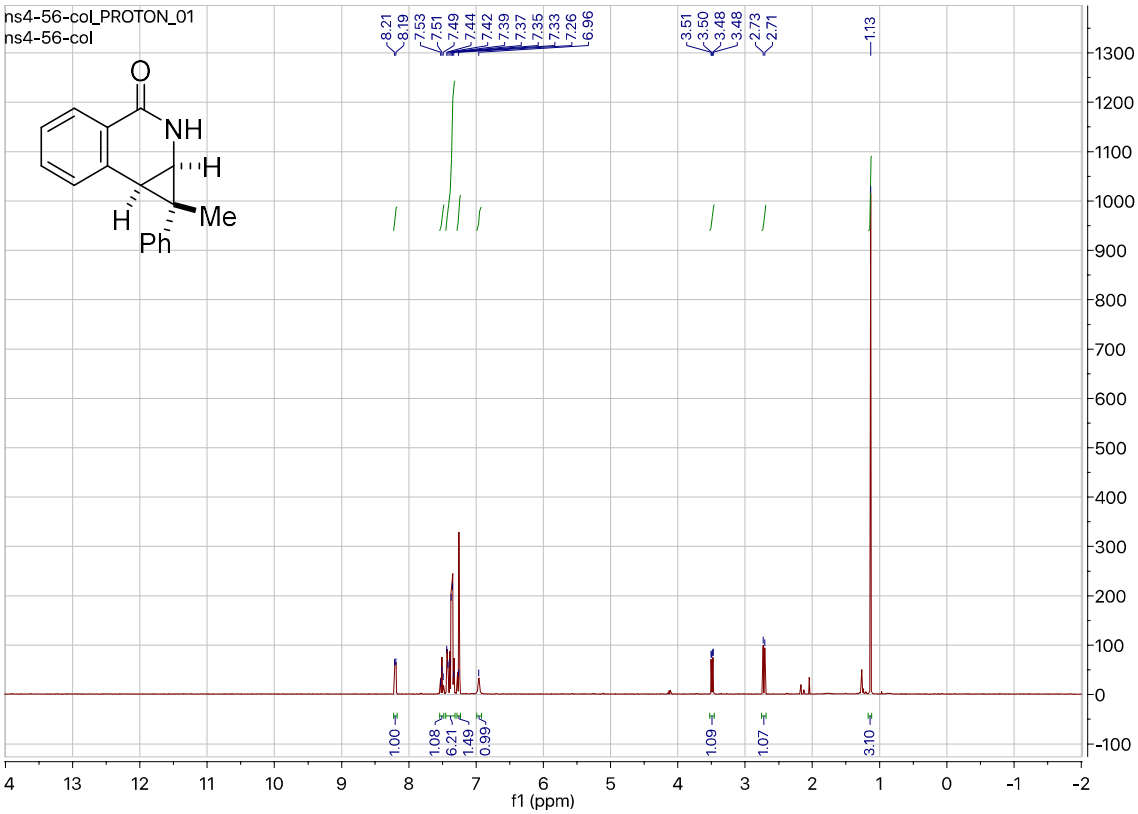
ns4-56-col_PROTON_01
ns4-56-col
O
NH
H
H
Me
Ph
8.21
8.19
7.53
7.51
7.49
7.44
7.42
7.39
7.37
7.35
7.33
7.26
6.96
3.51
3.50
3.48
3.48
2.73
2.71
1.13
1.00
1.08
6.21
1.49
0.99
1.09
1.07
3.10
f1 (ppm)

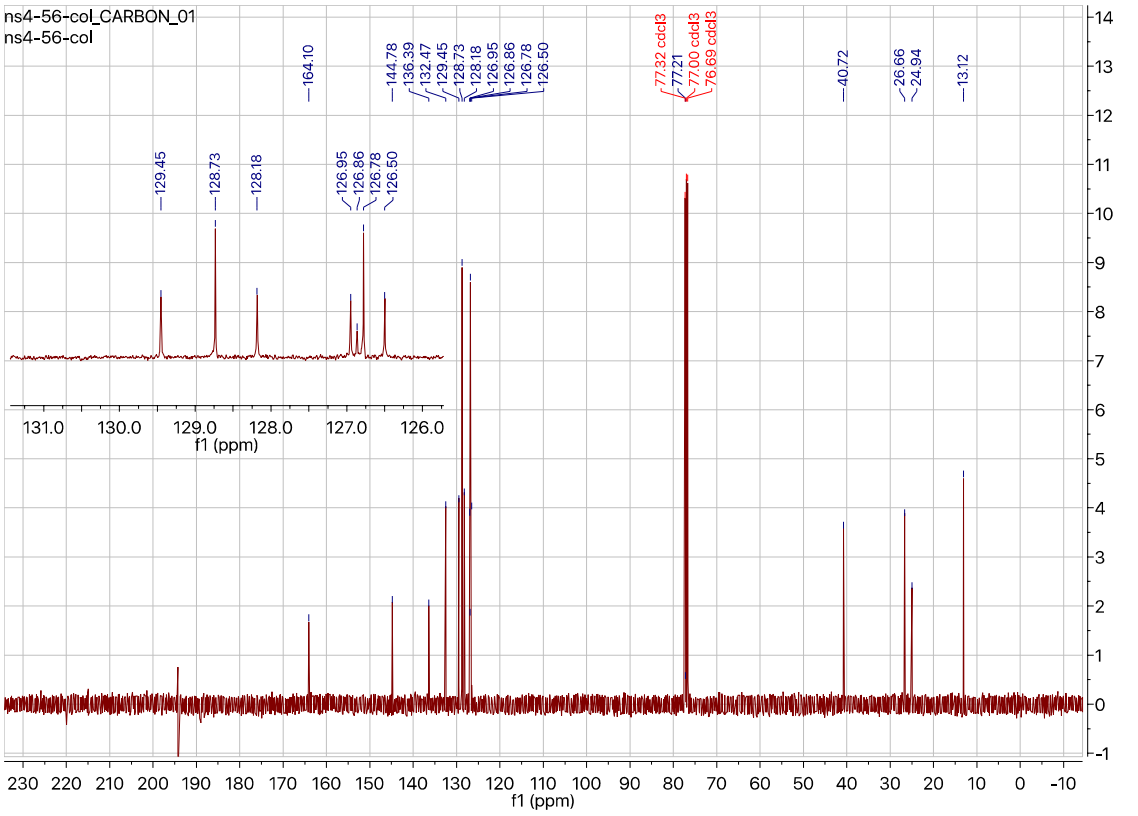
ns4-56-col_CARBON_01
ns4-56-col
164.10
144.78
136.39
132.47
129.45
128.73
128.18
126.95
126.86
126.78
126.50
77.32 cdcl3
77.21
77.00 cdcl3
76.69 cdcl3
40.72
26.66
24.94
13.12
129.45
128.73
128.18
126.95
126.86
126.78
126.50
f1 (ppm)
f1 (ppm)

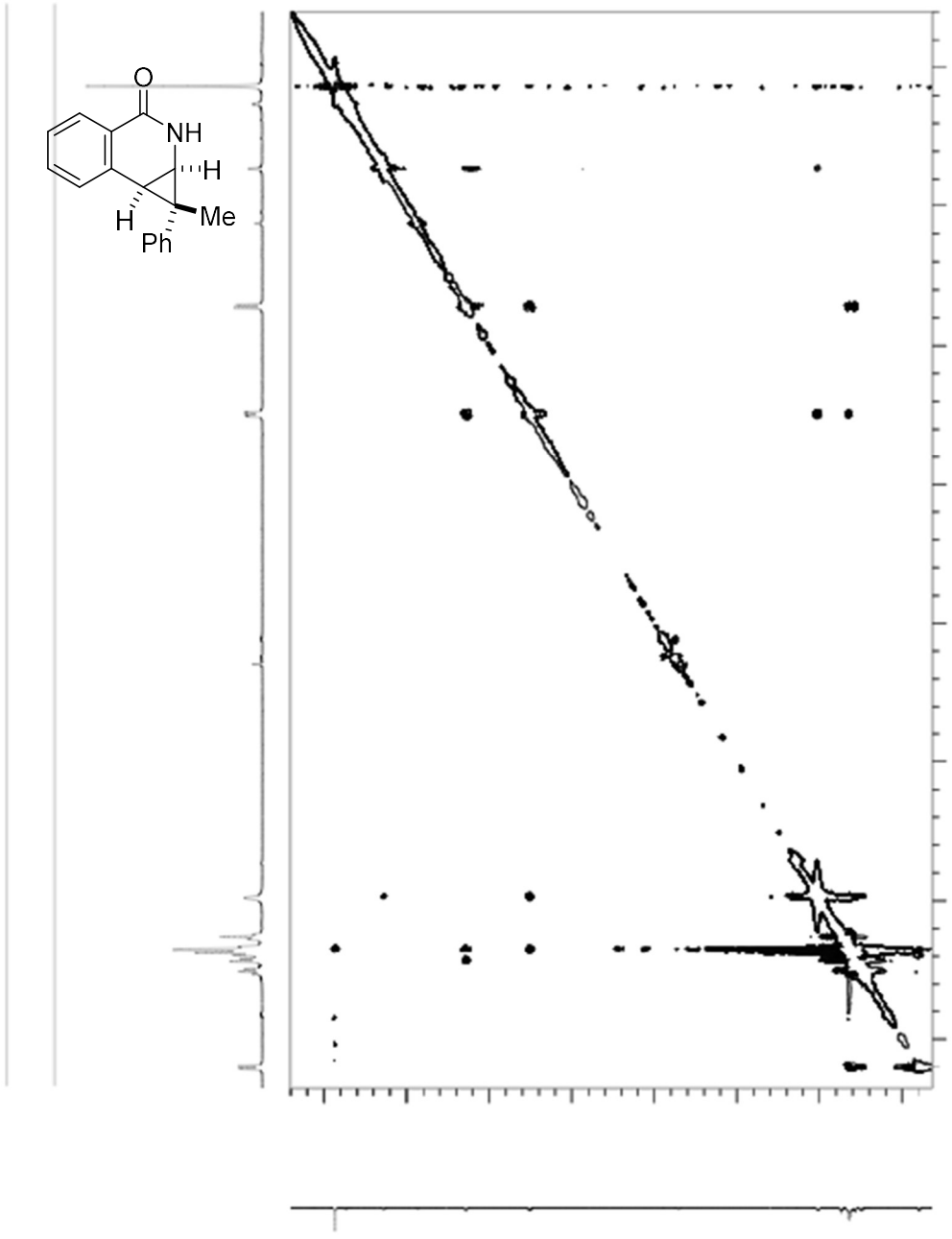
O
NH
H
H
Me
Ph

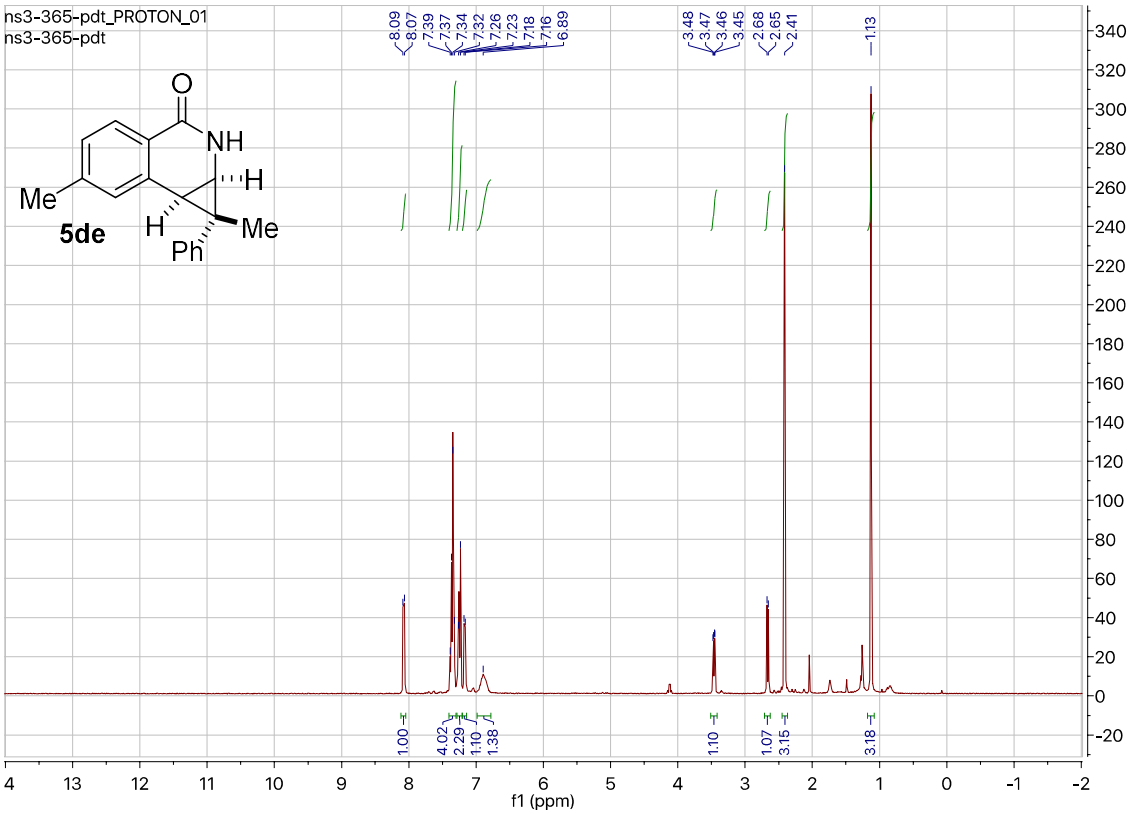
ns3-365-pdt_PROTON_01
ns3-365-pdt
O
NH
H
Me
H
Me
Ph
5de
8.09
8.07
7.39
7.37
7.34
7.32
7.26
7.23
7.18
7.16
6.89
3.48
3.47
3.46
3.45
2.68
2.65
2.41
1.13
1.00
4.02
2.29
1.10
1.38
1.10
1.07
3.15
3.18
f1 (ppm)

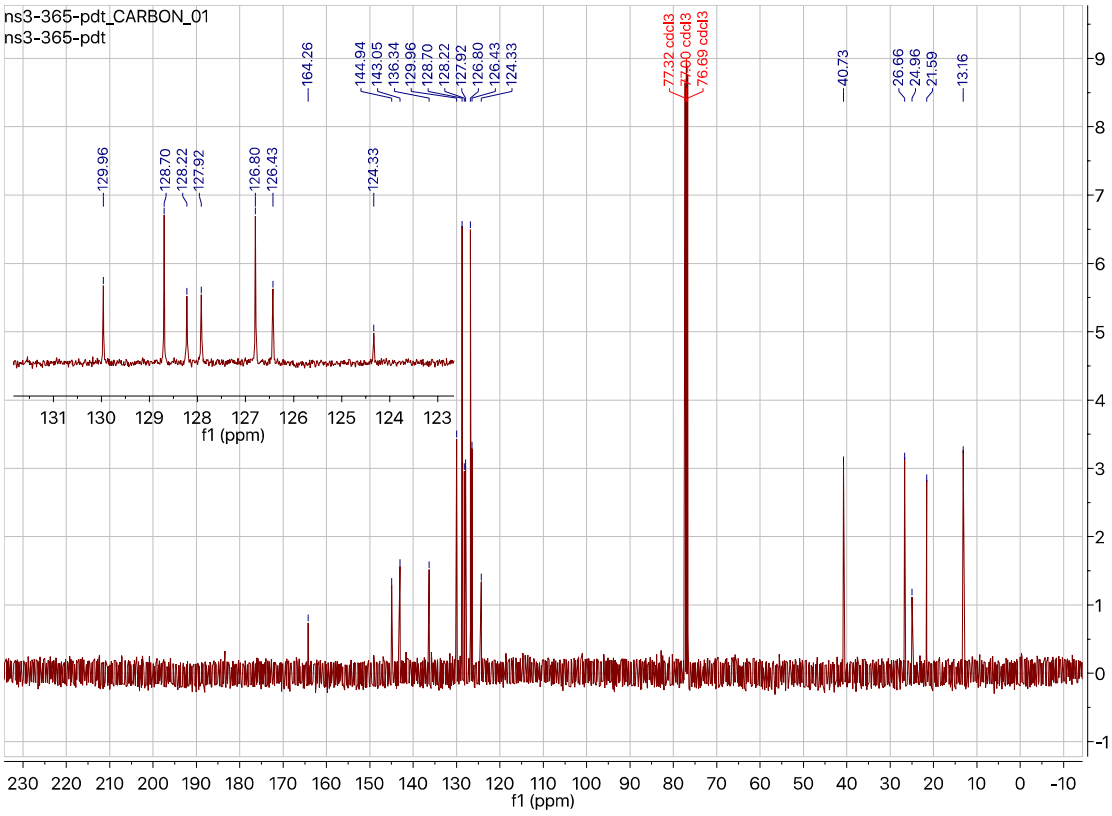
ns3-365-pdt_CARBON_01
ns3-365-pdt
164.26
144.94
143.05
136.34
129.96
128.70
128.22
127.92
126.80
126.43
124.33
77.32 cdcl3
77.00 cdcl3
76.69 cdcl3
40.73
26.66
24.96
21.59
13.16
f1 (ppm)

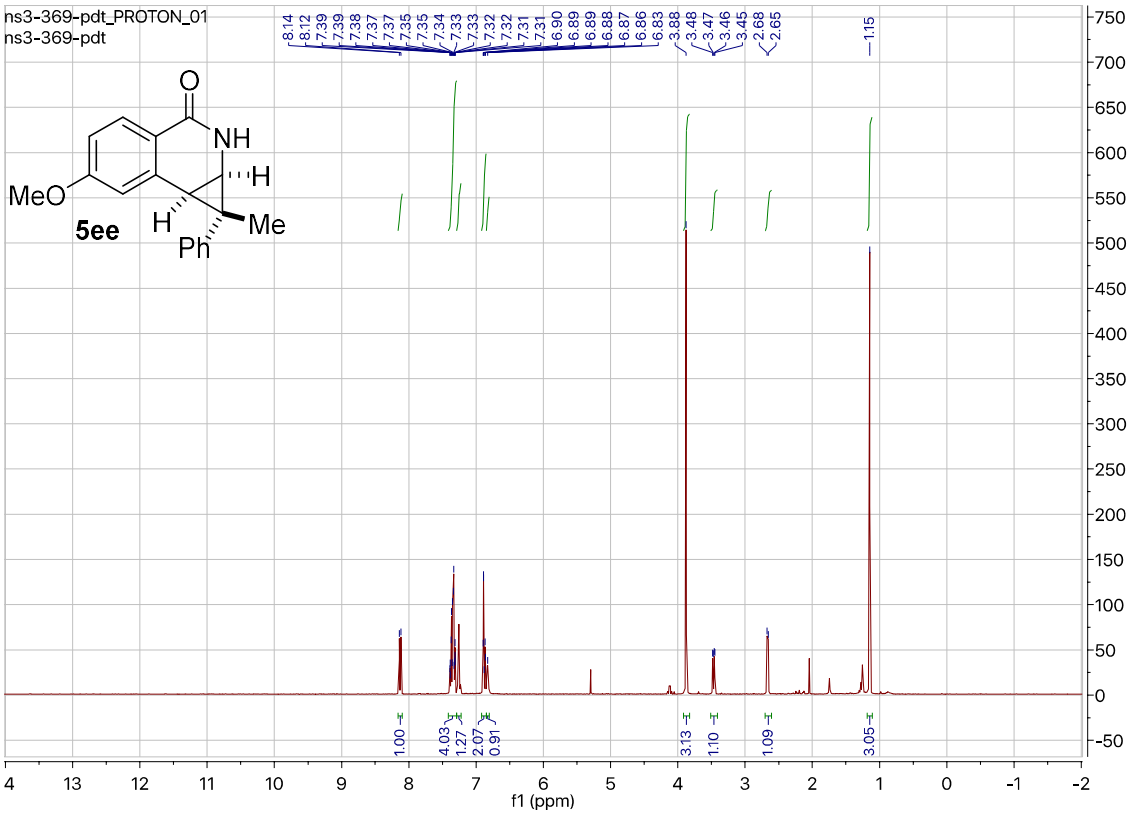
ns3-369-pdt_PROTON_01
ns3-369-pdt
O
NH
H
MeO
H
Me
Ph
5ee
8.14
8.12
7.39
7.39
7.38
7.37
7.37
7.35
7.35
7.34
7.33
7.33
7.32
7.32
7.31
7.31
6.90
6.89
6.89
6.88
6.87
6.86
6.83
3.88
3.48
3.47
3.46
3.45
2.68
2.65
1.15
1.00
4.03
1.27
2.07
0.91
3.13
1.10
1.09
3.05
f1 (ppm)

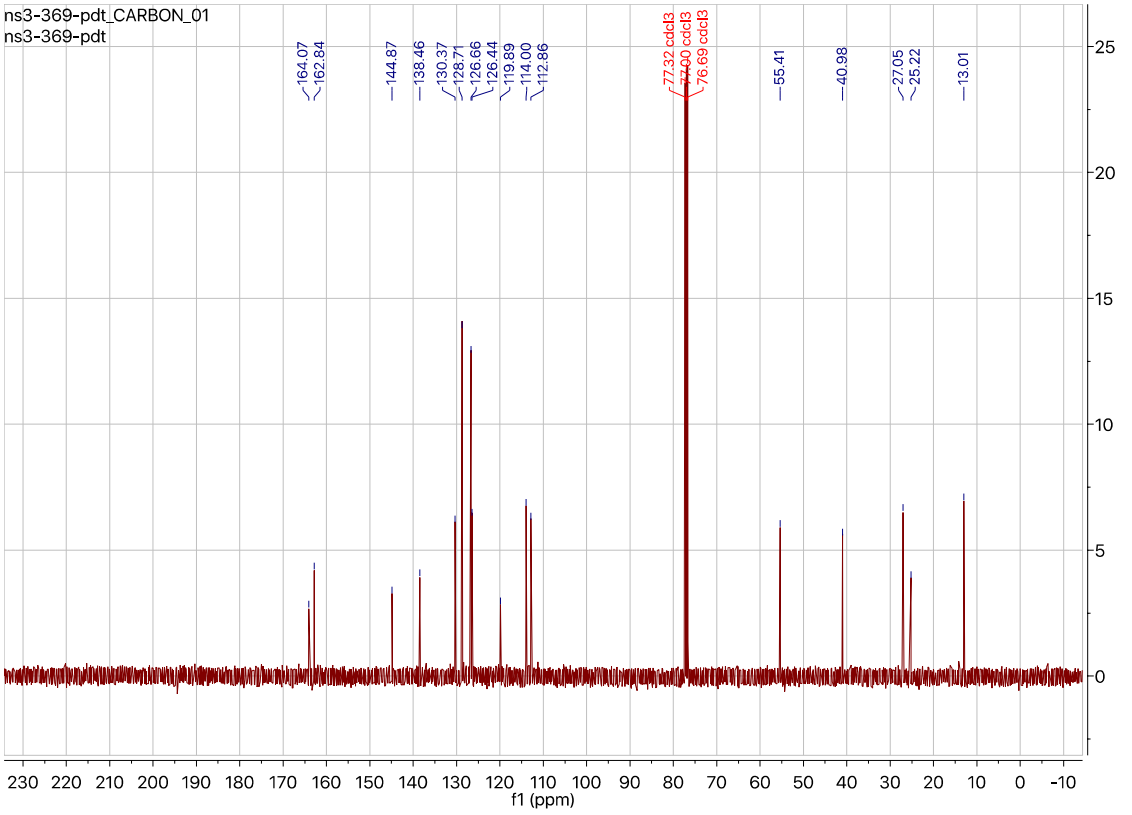
ns3-369-pdt_CARBON_01
ns3-369-pdt
164.07
162.84
144.87
138.46
130.37
128.71
126.66
126.44
119.89
114.00
112.86
77.32 cdcl3
77.00 cdcl3
76.69 cdcl3
55.41
40.98
27.05
25.22
13.01
f1 (ppm)

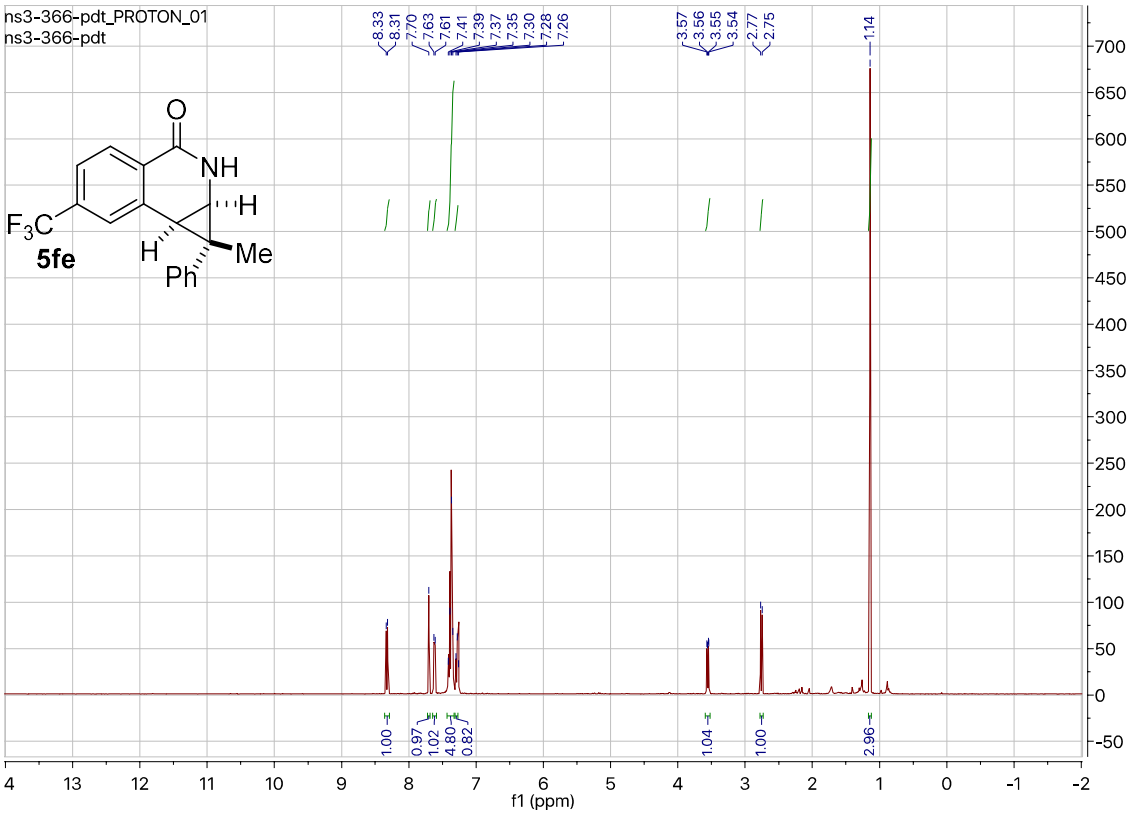
ns3-366-pdt_PROTON_01
ns3-366-pdt
O
NH
H
F3C
H
Me
Ph
5fe
8.33
8.31
7.70
7.63
7.61
7.41
7.39
7.37
7.35
7.30
7.28
7.26
3.57
3.56
3.55
3.54
2.77
2.75
1.14
1.00
0.97
1.02
4.80
0.82
1.04
1.00
2.96
f1 (ppm)

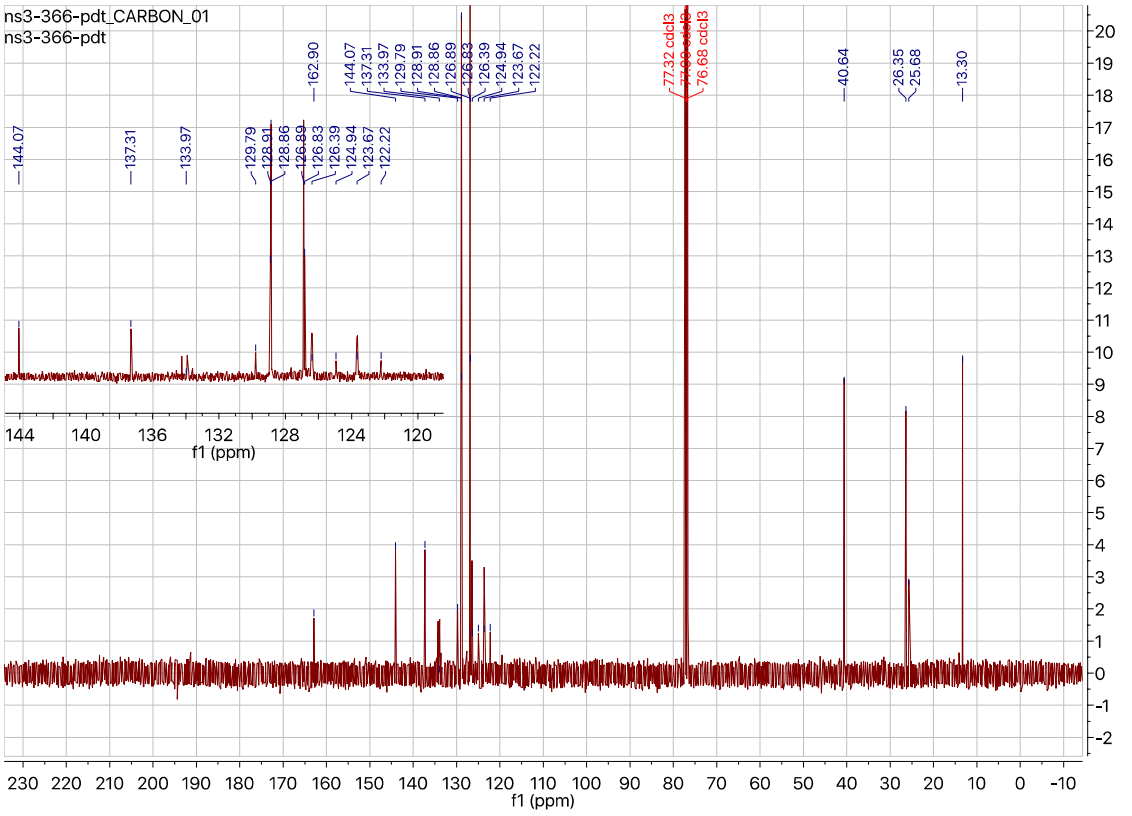
ns3-366-pdt_CARBON_01
ns3-366-pdt
162.90
144.07
137.31
133.97
129.79
128.91
128.86
126.89
126.83
126.39
124.94
123.67
122.22
77.32 cdcl3
76.68 cdcl3
40.64
26.35
25.68
13.30
f1 (ppm)

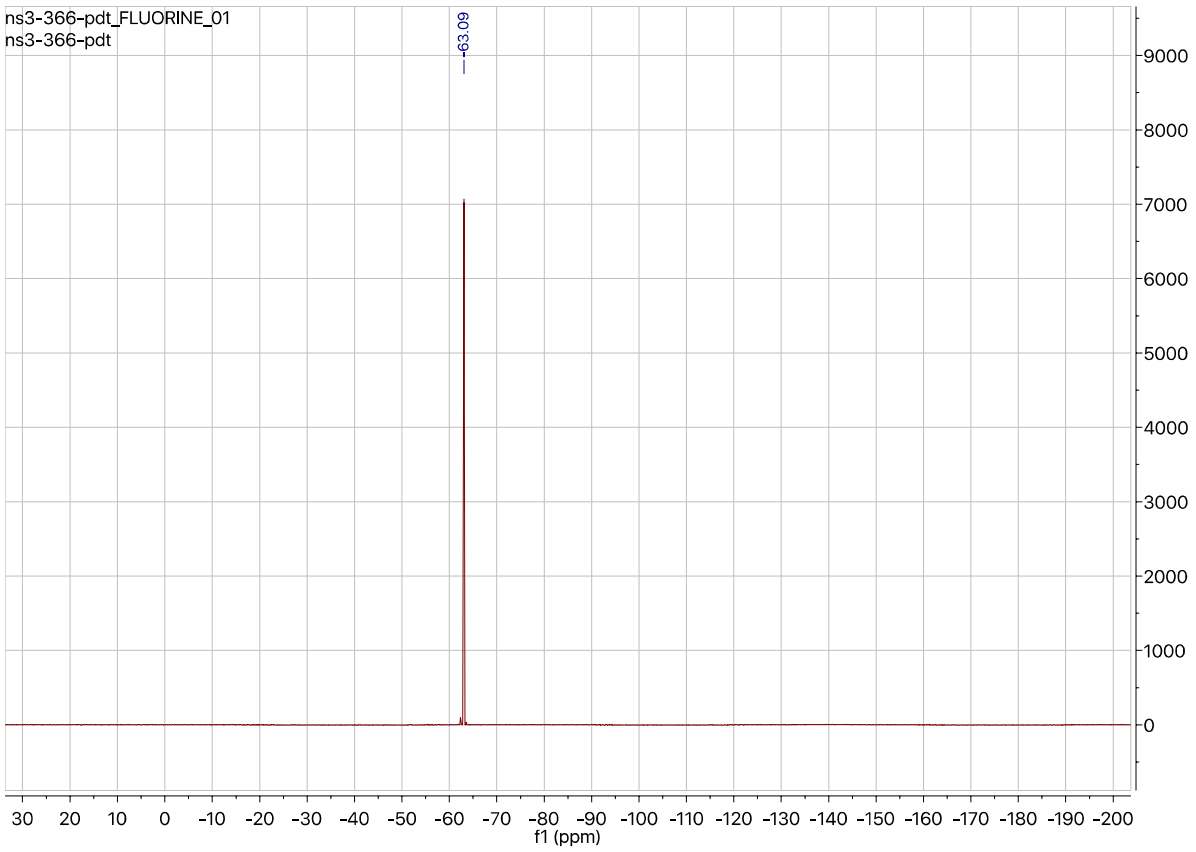
ns3-366-pdt_FLUORINE_01
ns3-366-pdt
-63.09
9000
8000
7000
6000
5000
4000
3000
2000
1000
0
30 20 10 0 -10 -20 -30 -40 -50 -60 -70 -80 -90 -100 -110 -120 -130 -140 -150 -160 -170 -180 -190 -200
f1 (ppm)

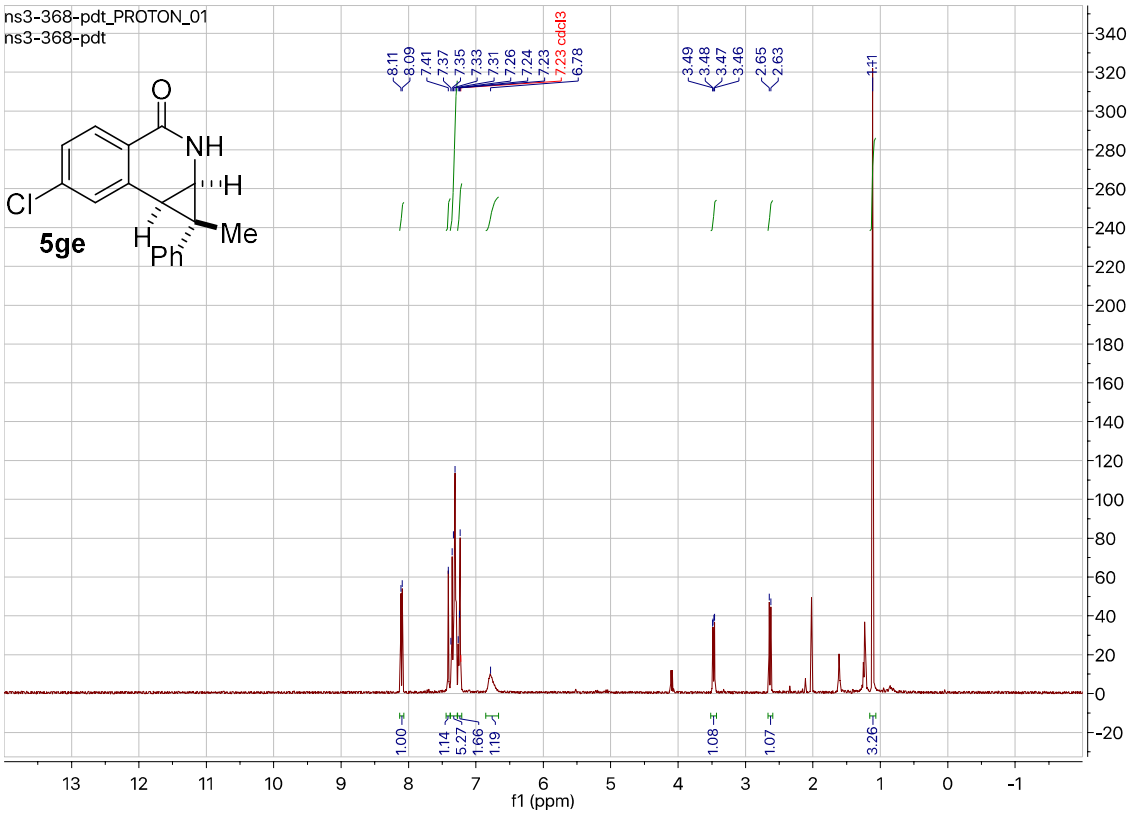
ns3-368-pdt_PROTON_01
ns3-368-pdt
O
NH
H
Cl
H
Ph
Me
5ge
8.11
8.09
7.41
7.37
7.35
7.33
7.31
7.26
7.24
7.23
7.23 cdcl3
6.78
3.49
3.48
3.47
3.46
2.65
2.63
1.11
1.00
1.14
5.27
1.66
1.19
1.08
1.07
3.26
f1 (ppm)

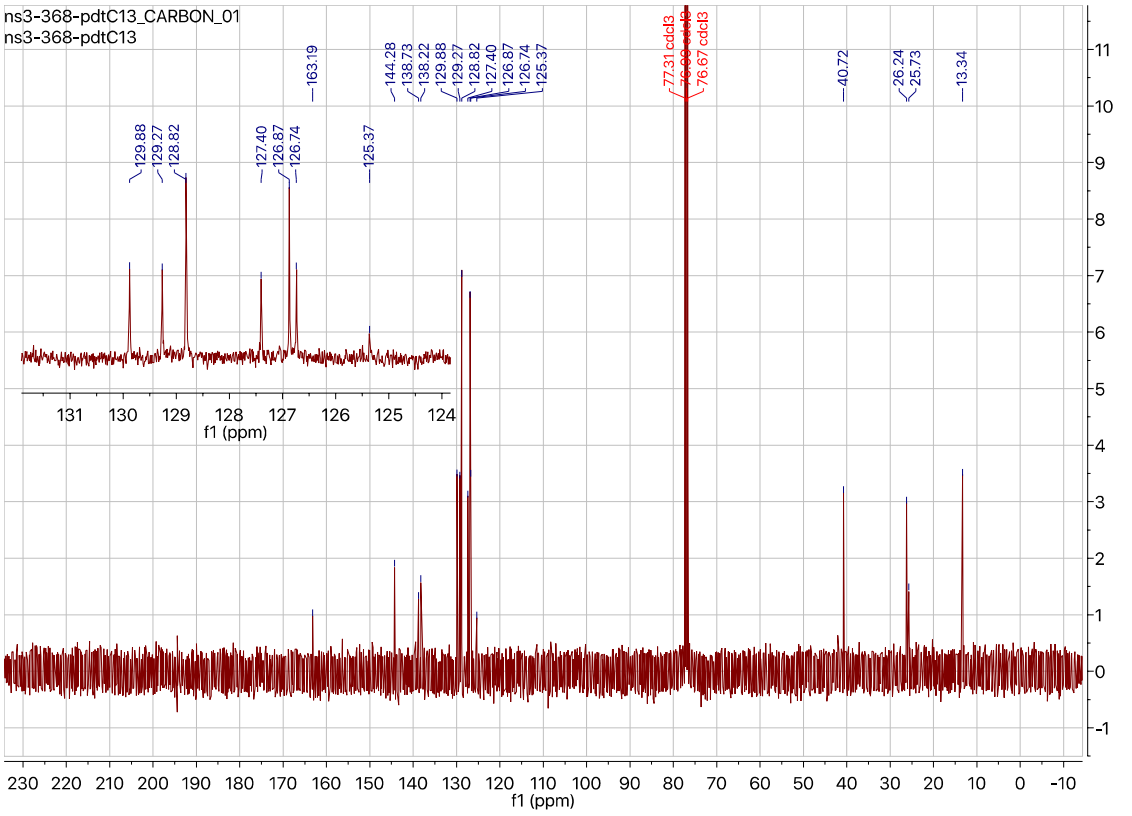
ns3-368-pdtC13_CARBON_01
ns3-368-pdtC13
163.19
144.28
138.73
138.22
129.88
129.27
128.82
127.40
126.87
126.74
125.37
77.31 cdcl3
76.67 cdcl3
40.72
26.24
25.73
13.34
f1 (ppm)

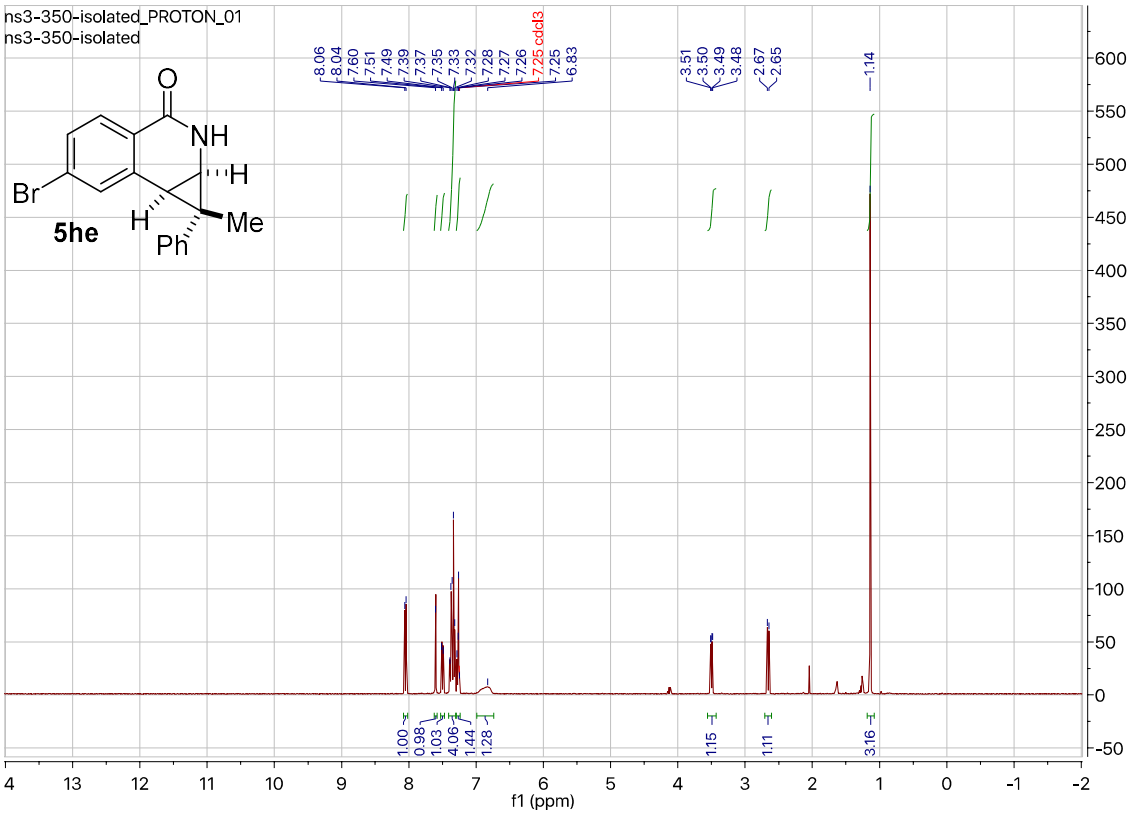
ns3-350-isolated_PROTON_01
ns3-350-isolated
O
NH
H
Br
H
Me
Ph
5he
8.06
8.04
7.60
7.51
7.49
7.39
7.37
7.35
7.33
7.32
7.28
7.27
7.26
7.25 cdcl3
7.25
6.83
3.51
3.50
3.49
3.48
2.67
2.65
1.14
1.00
0.98
1.03
4.06
1.44
1.28
1.15
1.11
3.16
f1 (ppm)

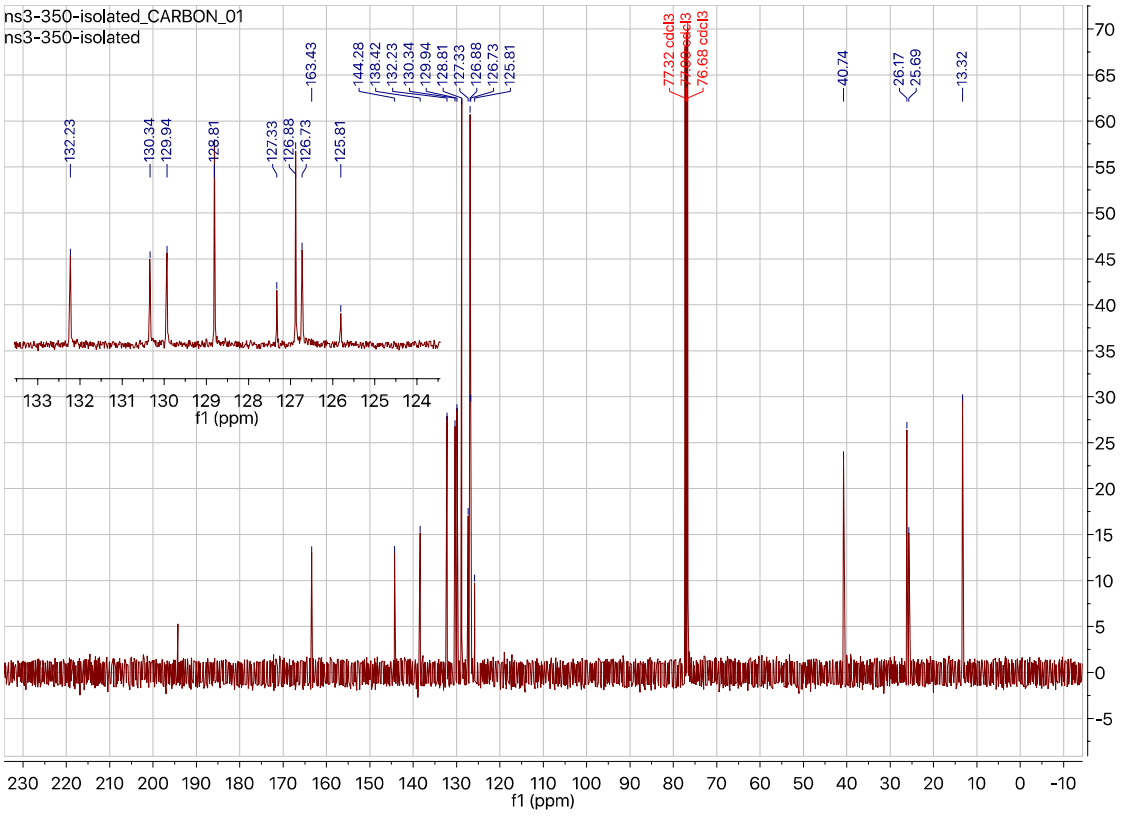
ns3-350-isolated_CARBON_01
ns3-350-isolated
163.43
144.28
138.42
132.23
130.34
129.94
128.81
127.33
126.88
126.73
125.81
77.32 cdcl3
77.00 cdcl3
76.68 cdcl3
40.74
26.17
25.69
13.32
132.23
130.34
129.94
128.81
127.33
126.88
126.73
125.81
f1 (ppm)

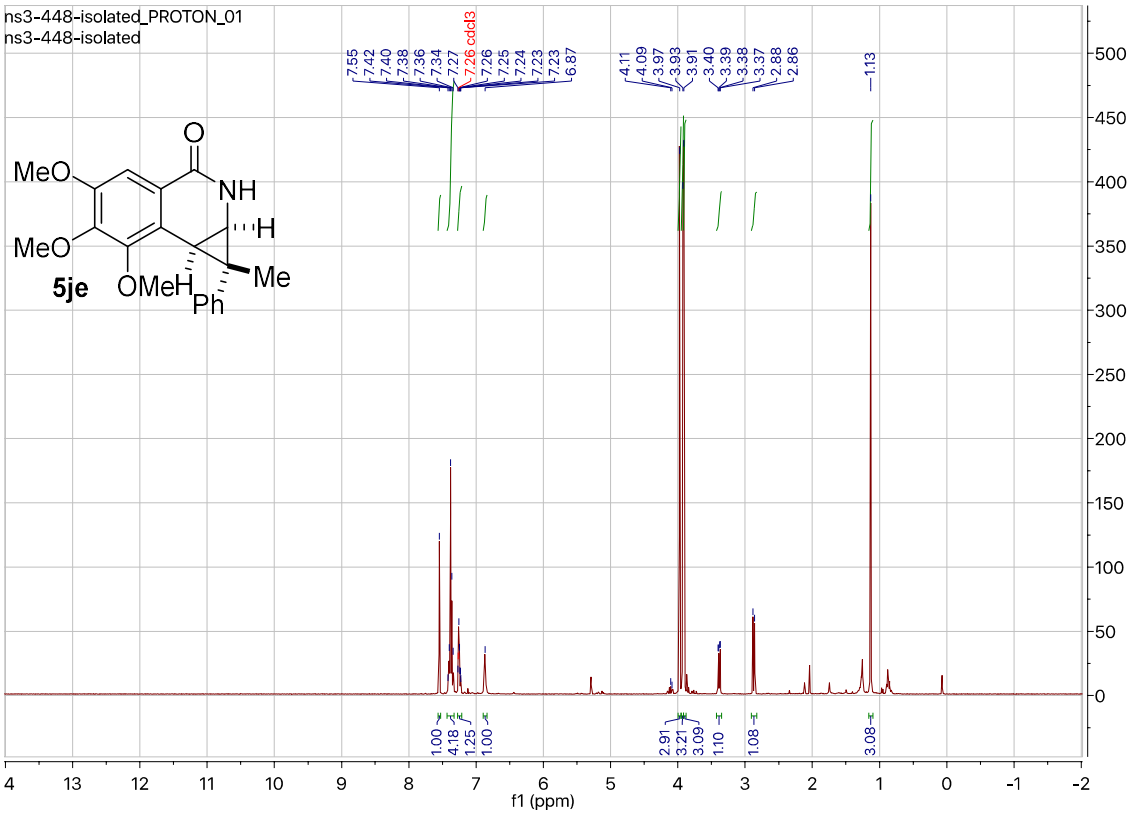
ns3-448-isolated_PROTON_01
ns3-448-isolated
MeO
MeO
O
NH
H
Me
OMe
H
Ph
5je
7.55
7.42
7.40
7.38
7.36
7.34
7.27
7.26 cdcl3
7.26
7.25
7.24
7.23
7.23
6.87
4.11
4.09
3.97
3.93
3.91
3.40
3.39
3.38
3.37
2.88
2.86
1.13
1.00
4.18
1.25
1.00
2.91
3.21
3.09
1.10
1.08
3.08
f1 (ppm)

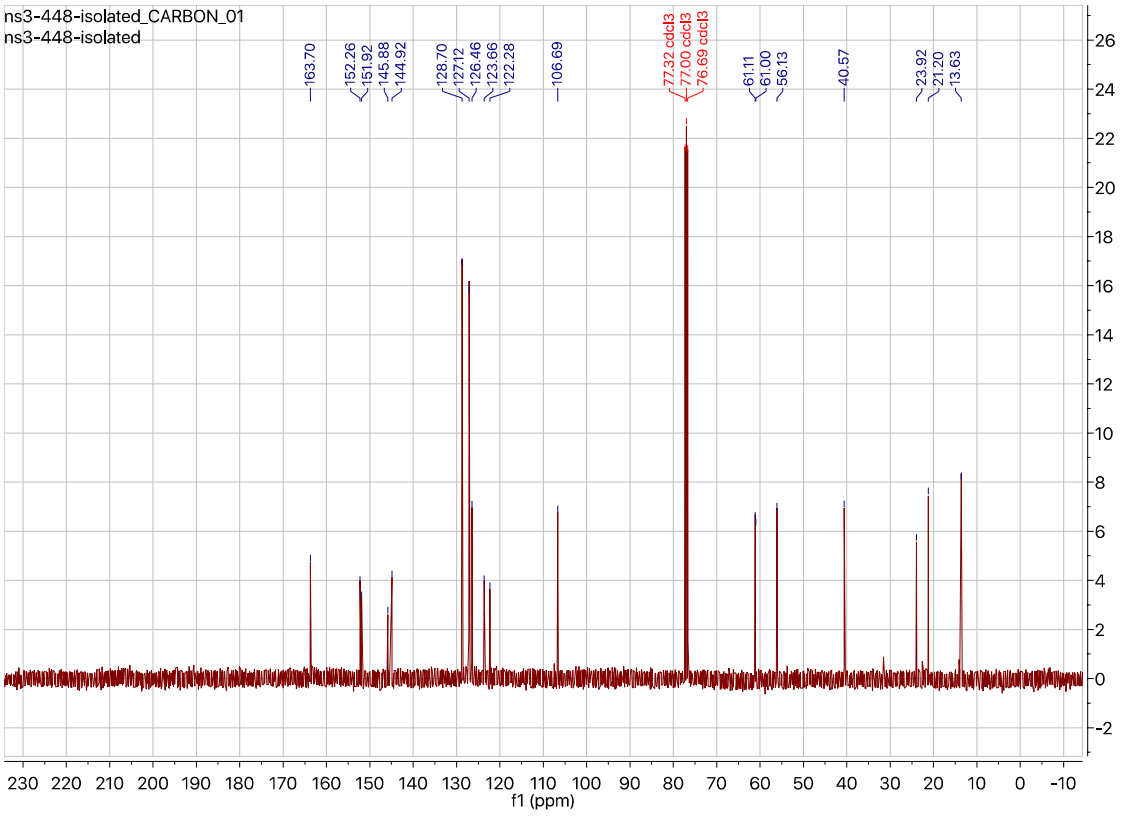
ns3-448-isolated_CARBON_01
ns3-448-isolated
163.70
152.26
151.92
145.88
144.92
128.70
127.12
126.46
123.66
122.28
106.69
77.32 cdcl3
77.00 cdcl3
76.69 cdcl3
61.11
61.00
56.13
40.57
23.92
21.20
13.63
f1 (ppm)

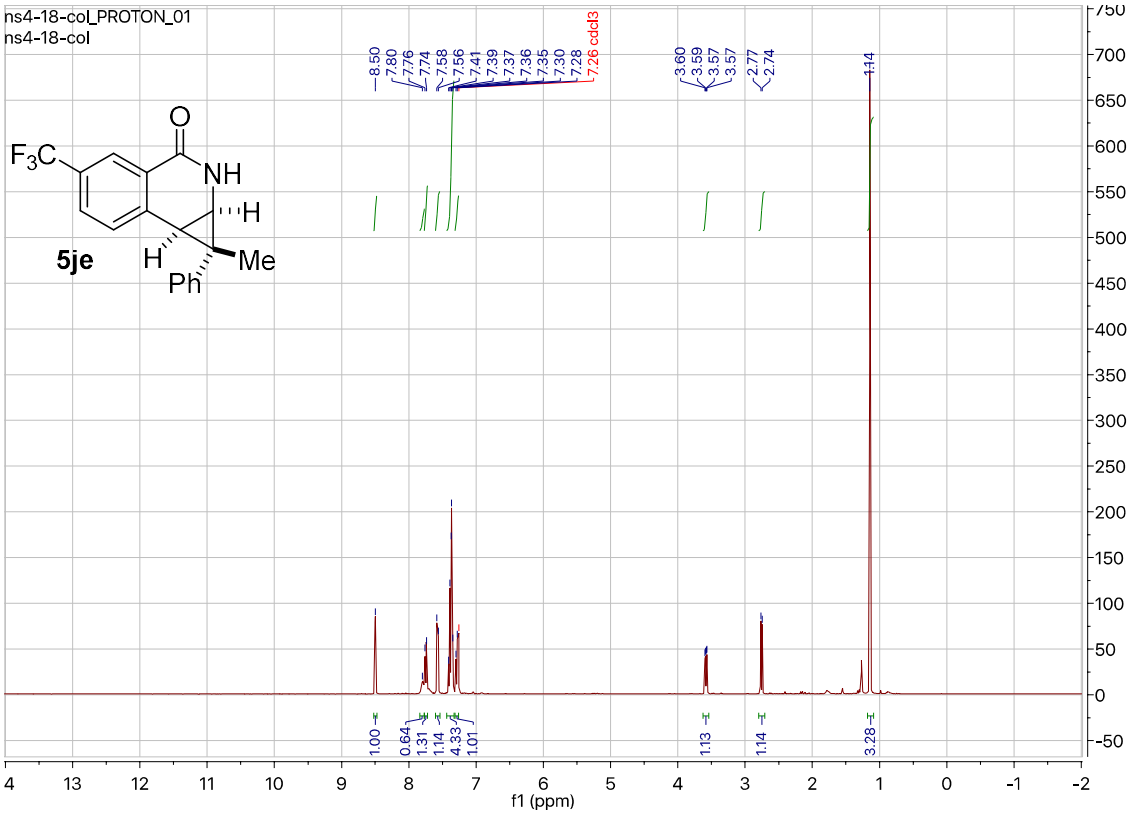
ns4-18-col_PROTON_01
ns4-18-col
5je
f1 (ppm)

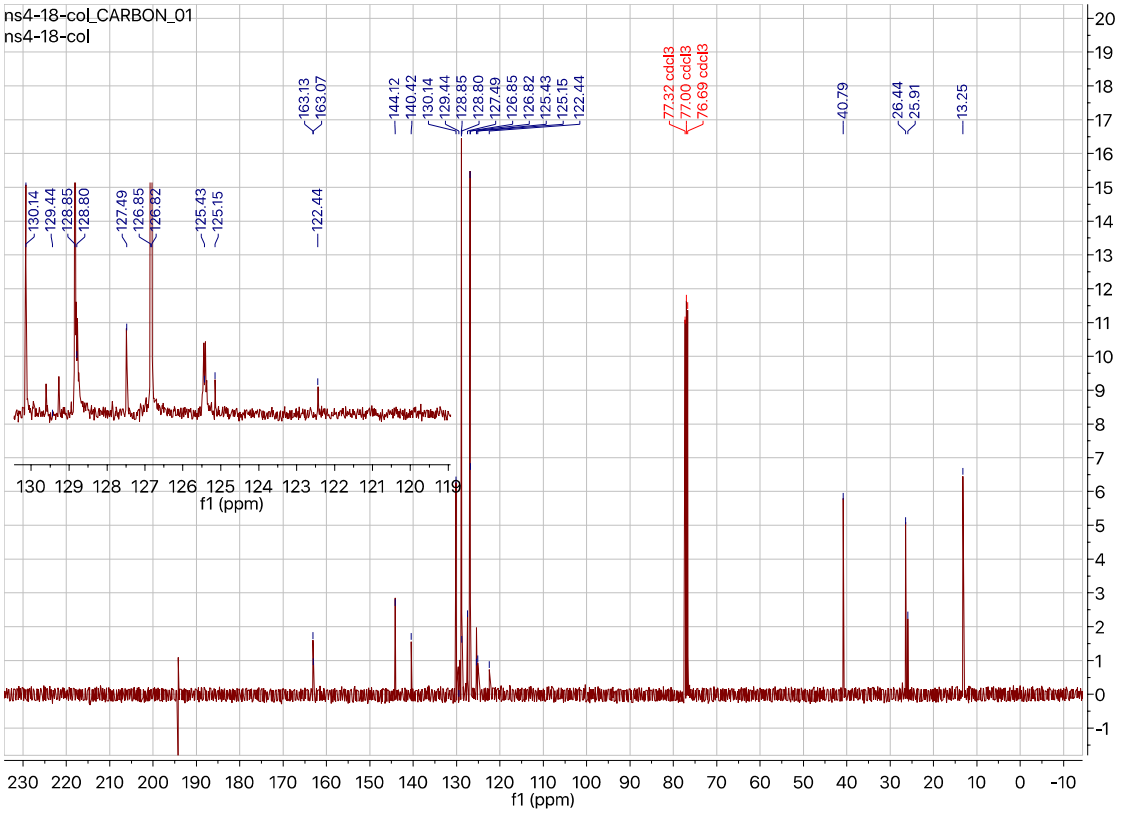
ns4-18-col_CARBON_01
ns4-18-col
f1 (ppm)

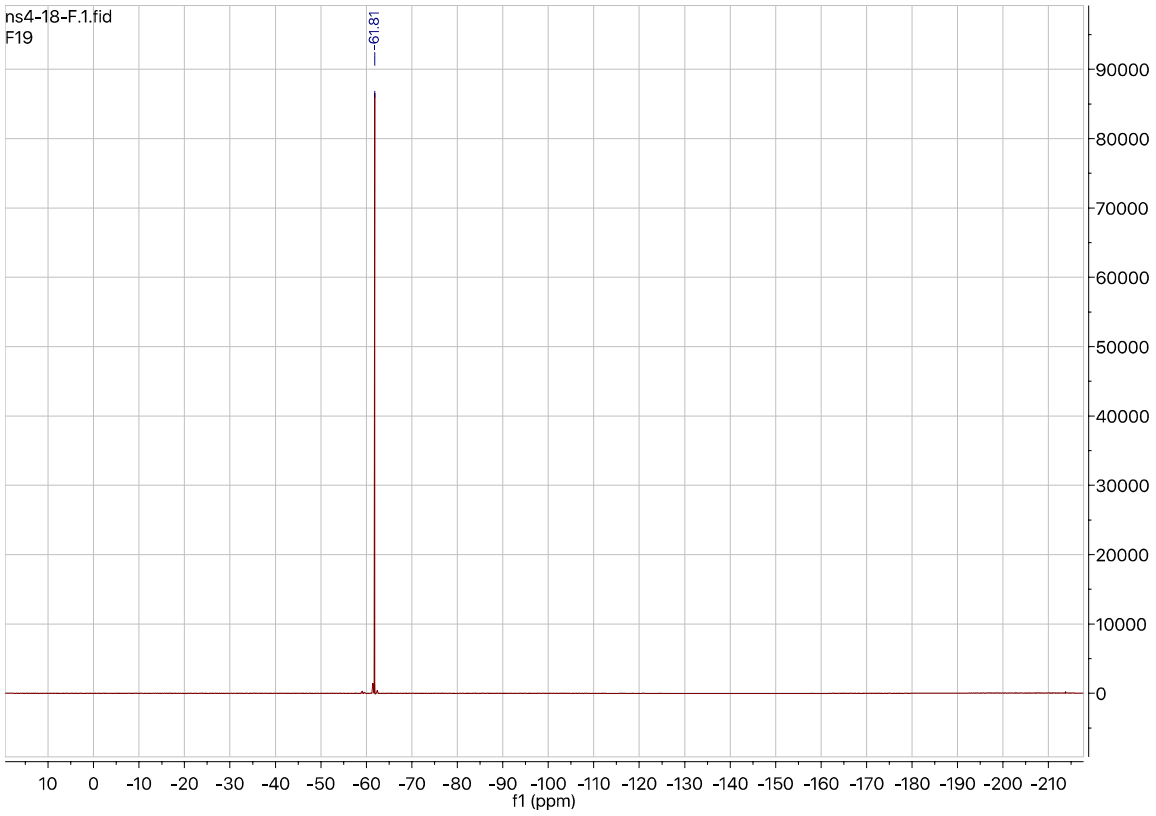
ns4-18-F.1.fid
F19
-61.81
90000
80000
70000
60000
50000
40000
30000
20000
10000
0
10 0 -10 -20 -30 -40 -50 -60 -70 -80 -90 -100 -110 -120 -130 -140 -150 -160 -170 -180 -190 -200 -210
f1 (ppm)

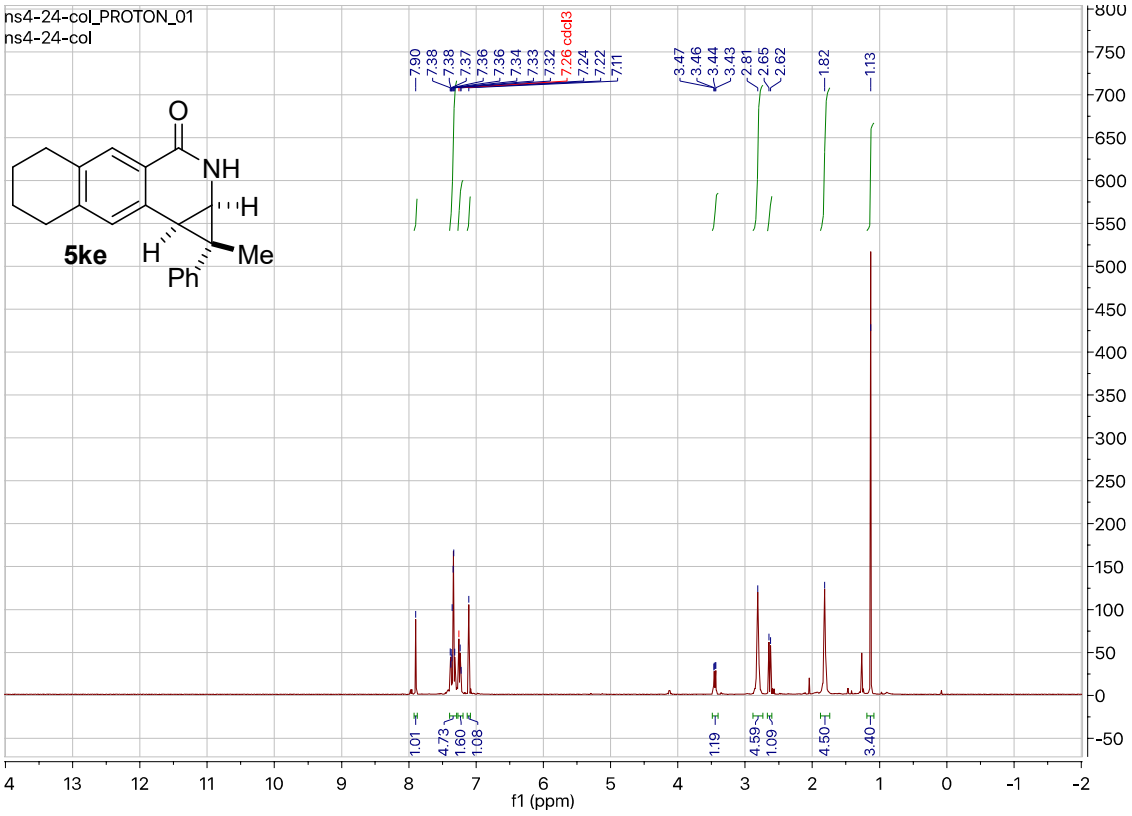
ns4-24-col_PROTON_01
ns4-24-col
O
NH
H
H
Me
Ph
5ke
7.90
7.38
7.38
7.37
7.36
7.36
7.34
7.33
7.32
7.26 cdcl3
7.24
7.22
7.11
3.47
3.46
3.44
3.43
2.81
2.65
2.62
1.82
1.13
1.01
4.73
1.60
1.08
1.19
4.59
1.09
4.50
3.40
f1 (ppm)

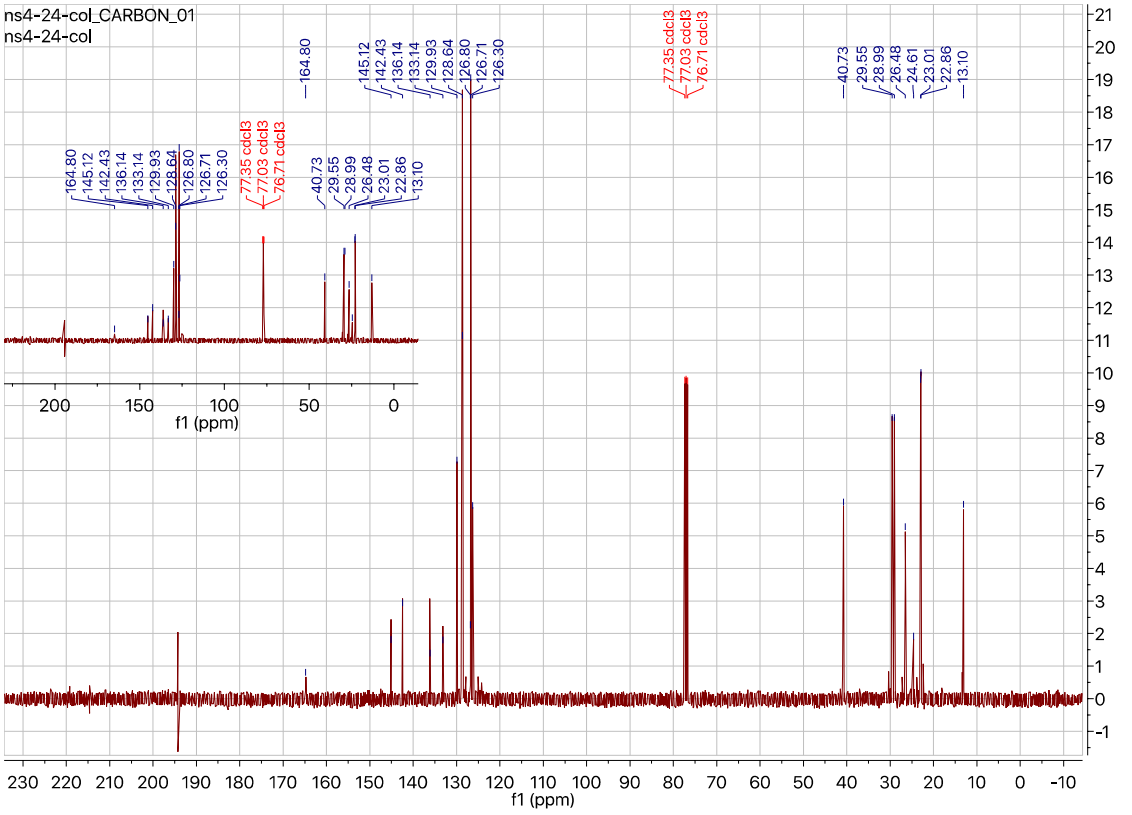
ns4-24-col_CARBON_01
ns4-24-col
164.80
145.12
142.43
136.14
133.14
129.93
128.64
126.80
126.71
126.30
77.35 cdcl3
77.03 cdcl3
76.71 cdcl3
40.73
29.55
28.99
26.48
24.61
23.01
22.86
13.10
f1 (ppm)

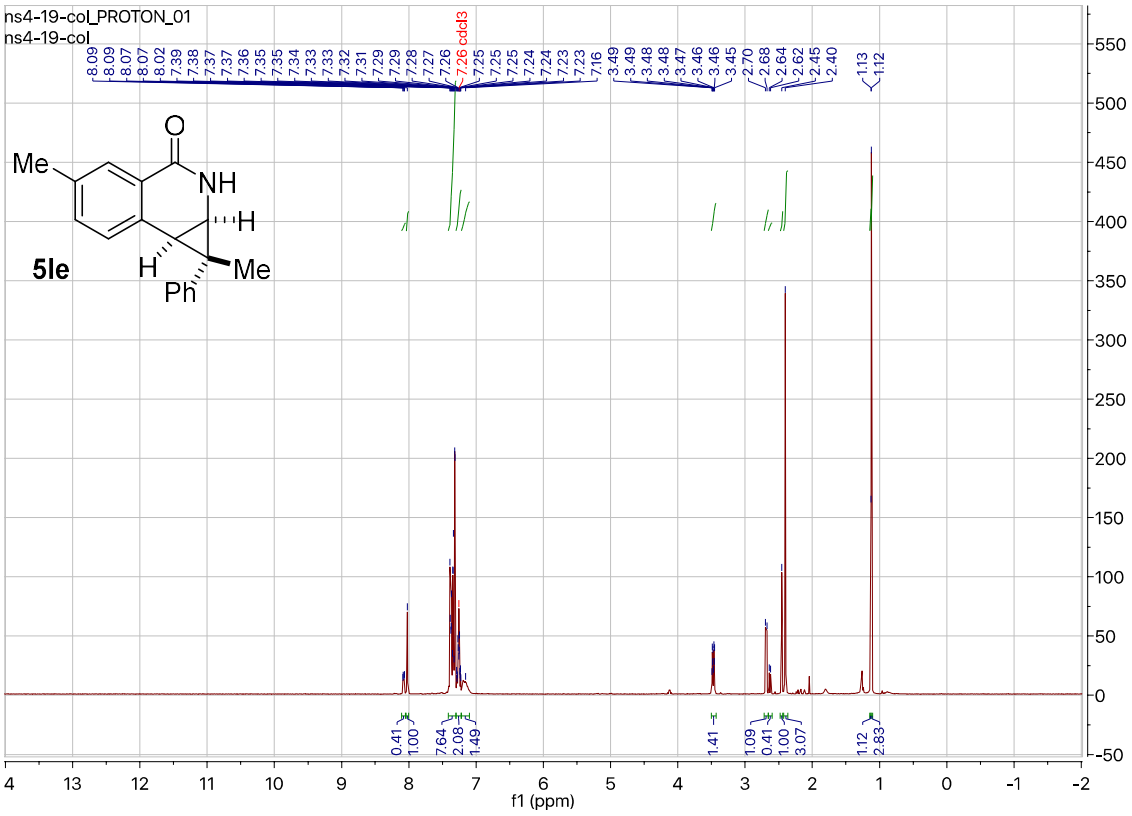
ns4-19-col_PROTON_01
ns4-19-col
O
Me
NH
H
H
Me
Ph
5le
f1 (ppm)

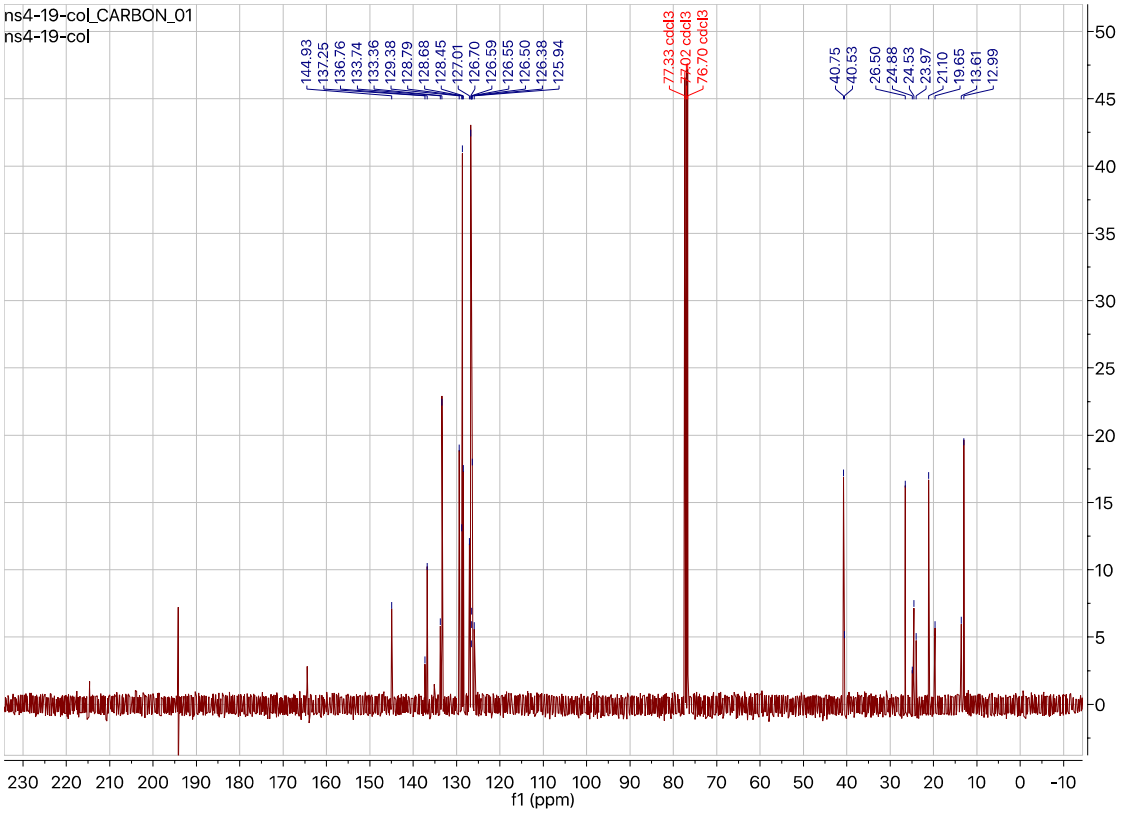
ns4-19-col_CARBON_01
ns4-19-col
f1 (ppm)

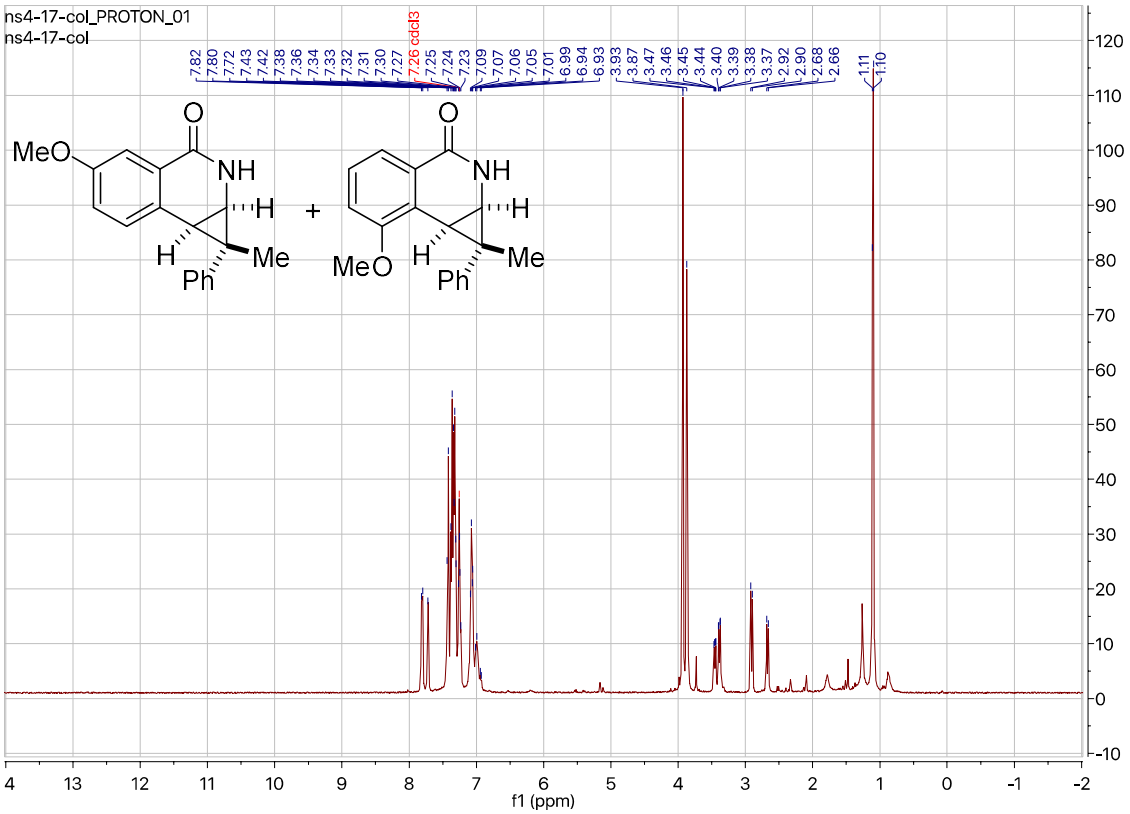
ns4-17-col_PROTON_01
ns4-17-col
MeO
NH
H
Me
Ph
+
MeO
NH
H
Me
Ph
f1 (ppm)

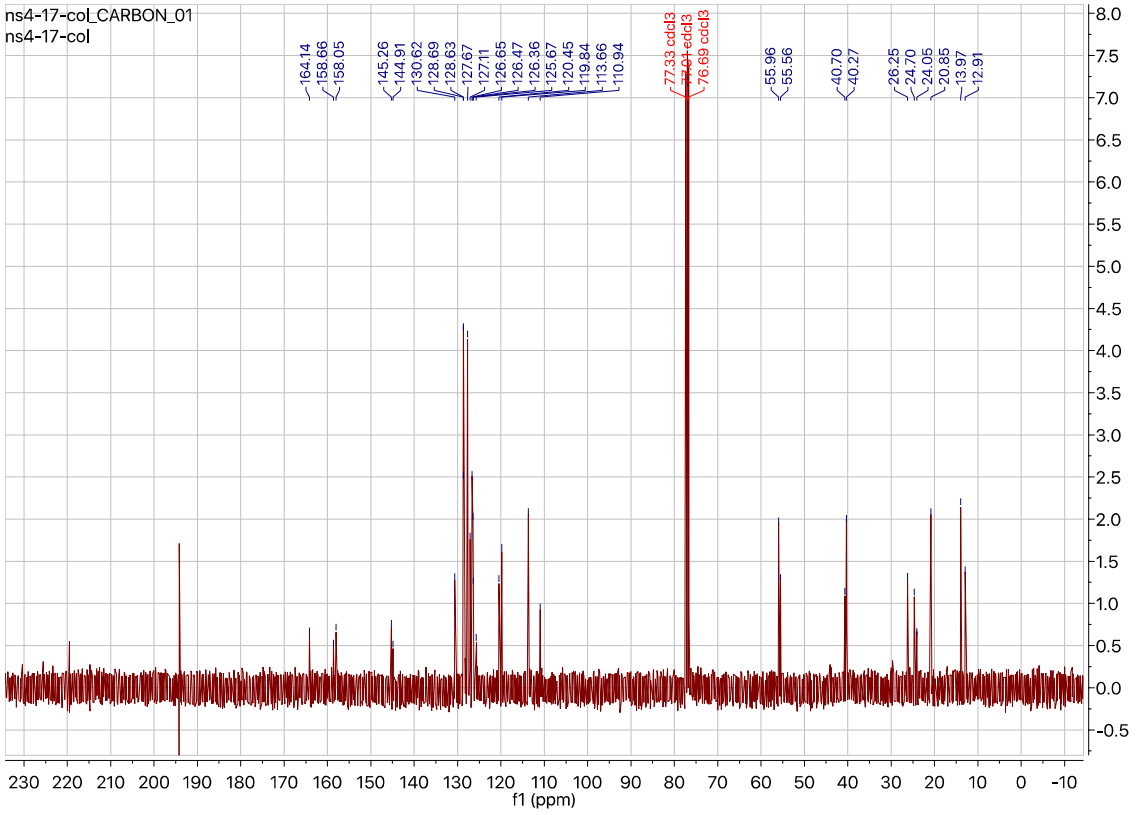
ns4-17-col_CARBON_01
ns4-17-col
f1 (ppm)

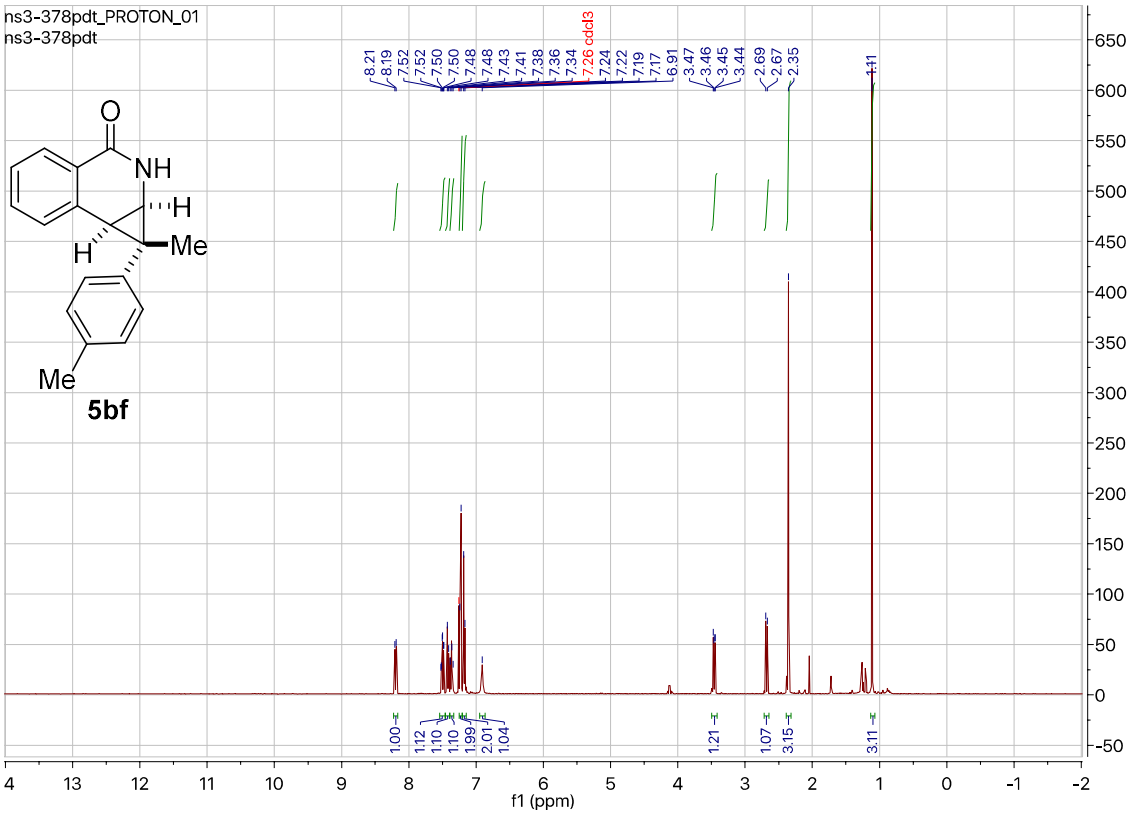
ns3-378pdt_PROTON_01
ns3-378pdt
O
NH
H
H
Me
Me
5bf
f1 (ppm)

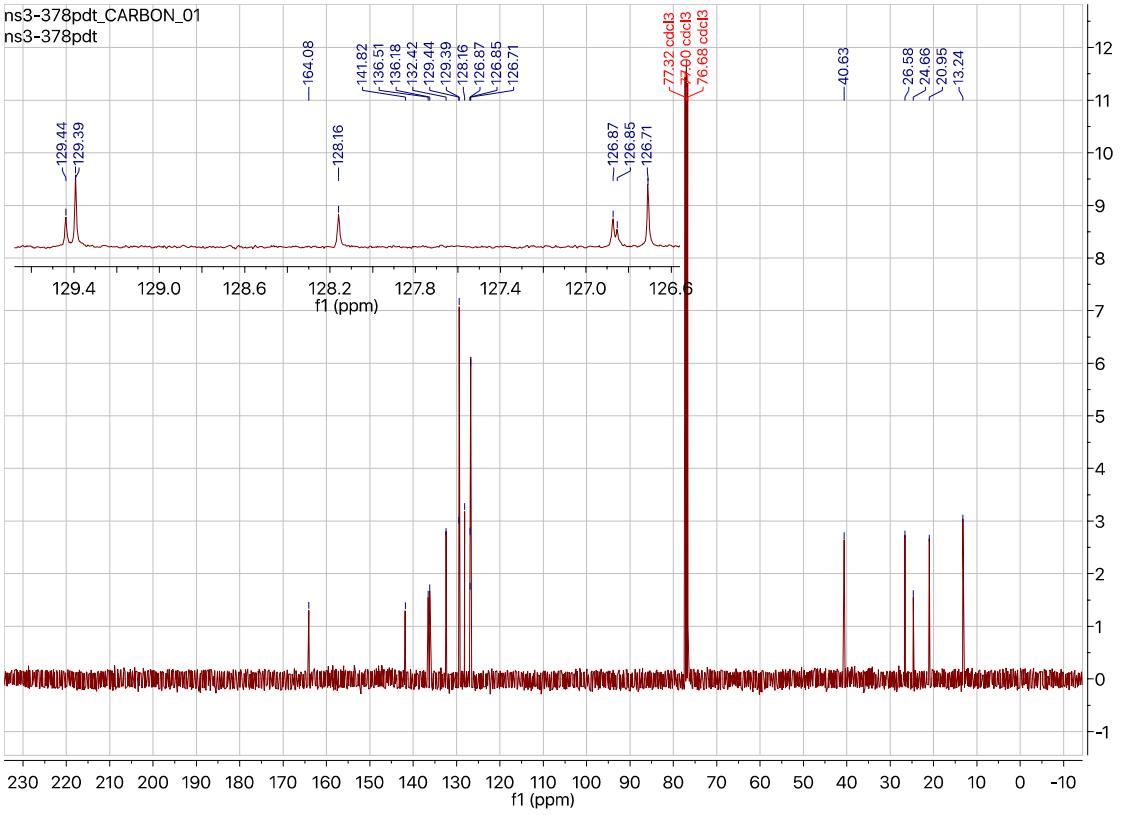
ns3-378pdt_CARBON_01
ns3-378pdt
f1 (ppm)

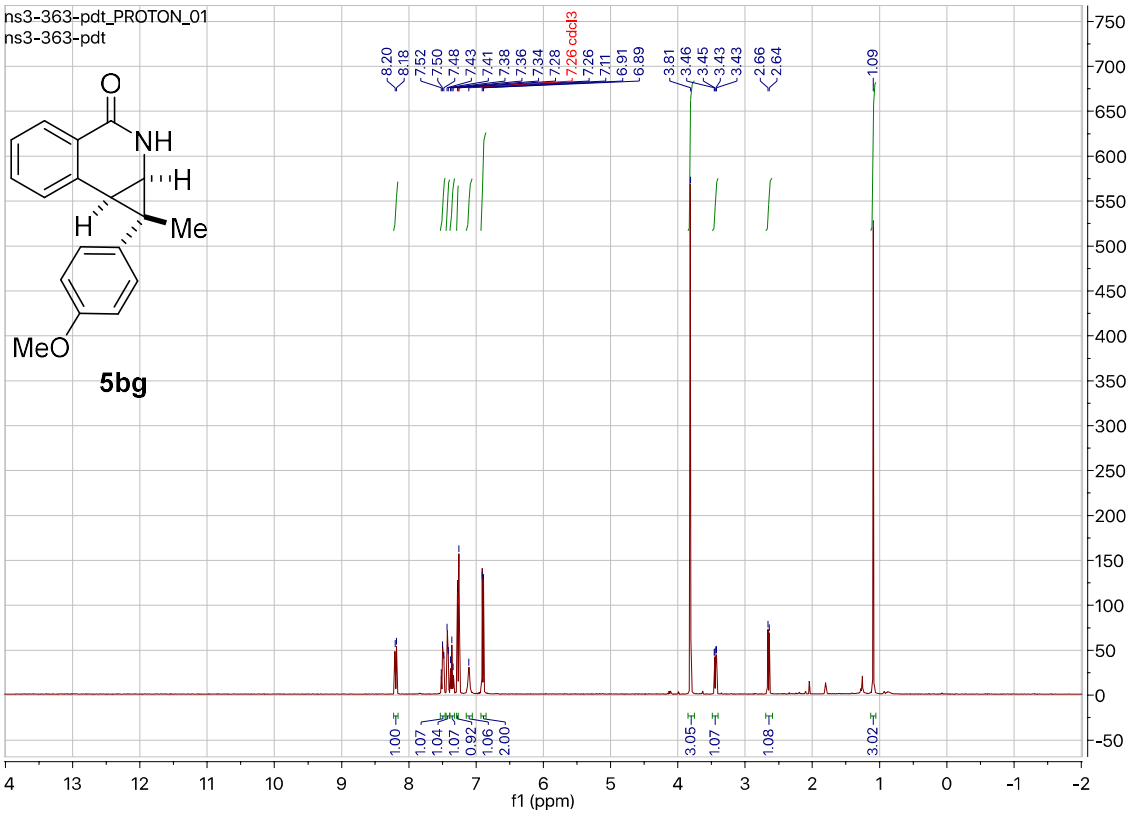
ns3-363-pdt_PROTON_01
ns3-363-pdt
O
NH
H
H
Me
MeO
5bg
8.20
8.18
7.52
7.50
7.48
7.43
7.41
7.38
7.36
7.34
7.28
7.26 cdcl3
7.26
7.11
6.91
6.89
3.81
3.46
3.45
3.43
3.43
2.66
2.64
1.09
1.00
1.07
1.04
1.07
0.92
1.06
2.00
3.05
1.07
1.08
3.02
f1 (ppm)

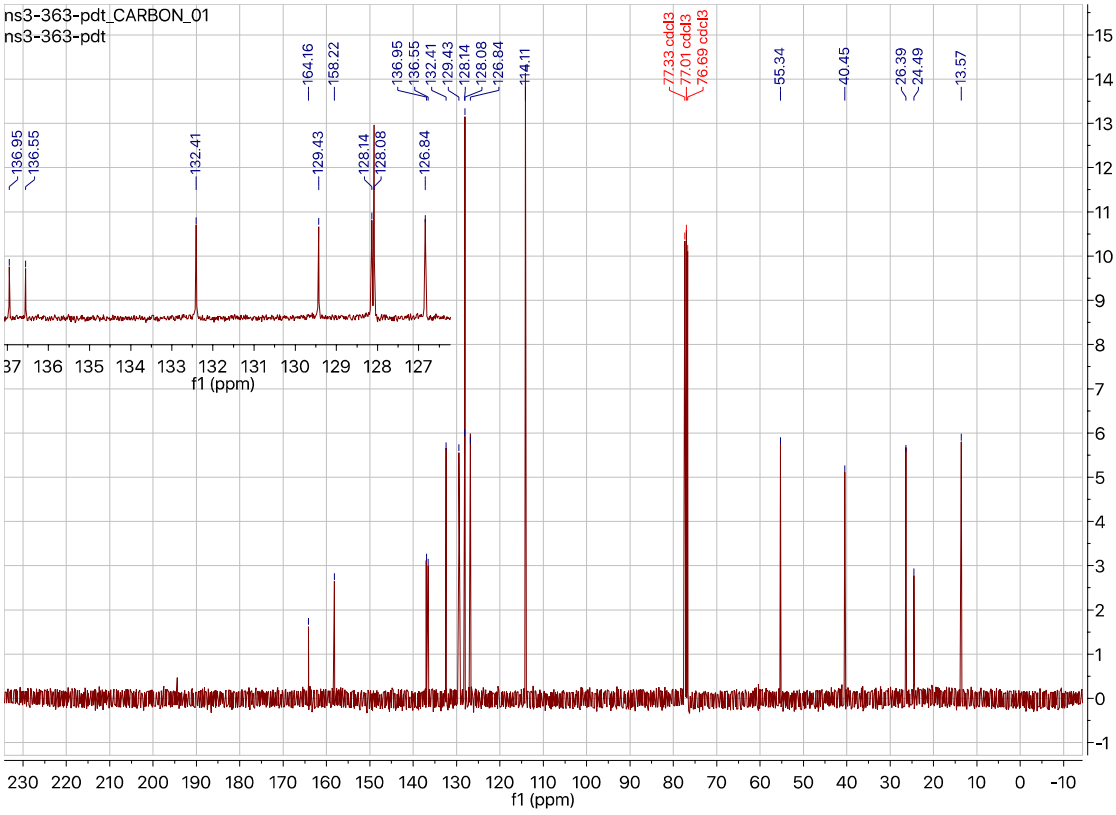
ns3-363-pdt_CARBON_01
ns3-363-pdt
164.16
158.22
136.95
136.55
132.41
129.43
128.14
128.08
126.84
114.11
77.33 cdcl3
77.01 cdcl3
76.69 cdcl3
55.34
40.45
26.39
24.49
13.57
f1 (ppm)

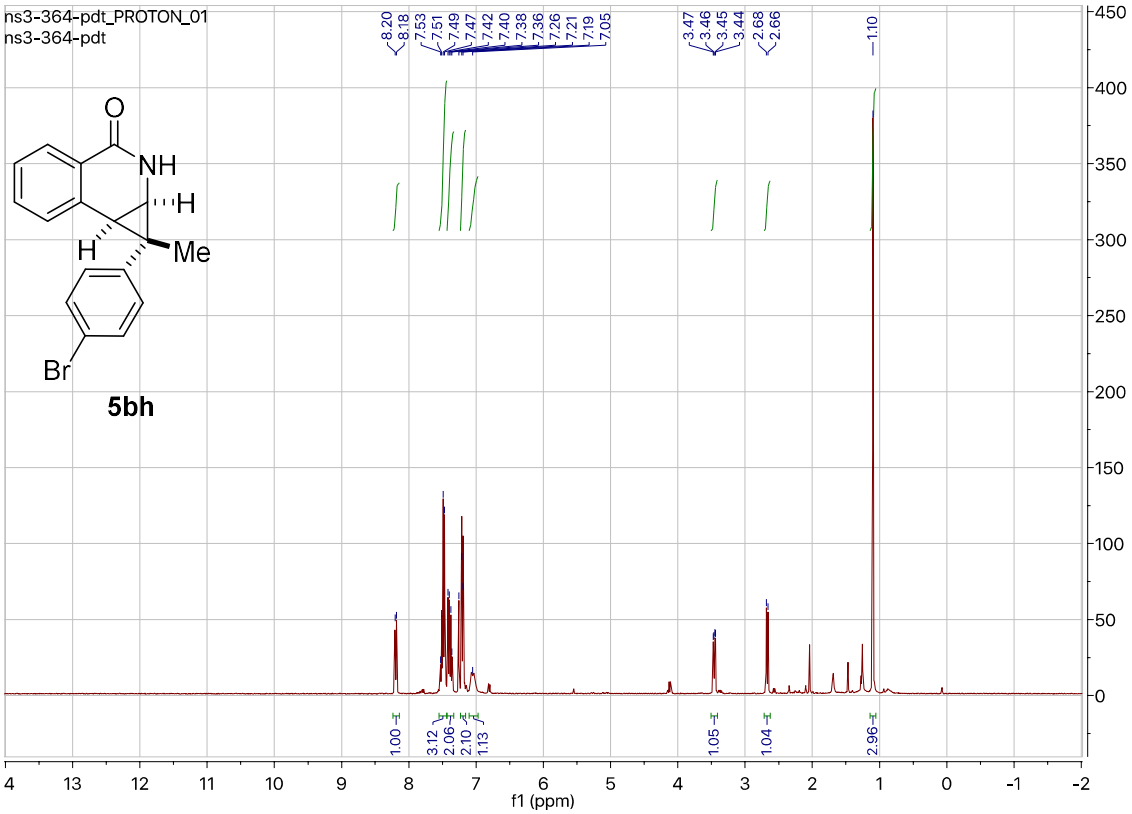
ns3-364-pdt_PROTON_01
ns3-364-pdt
O
NH
H
H
Me
Br
5bh
8.20
8.18
7.53
7.51
7.49
7.47
7.42
7.40
7.38
7.36
7.26
7.21
7.19
7.05
3.47
3.46
3.45
3.44
2.68
2.66
1.10
1.00
3.12
2.06
2.10
1.13
1.05
1.04
2.96
f1 (ppm)

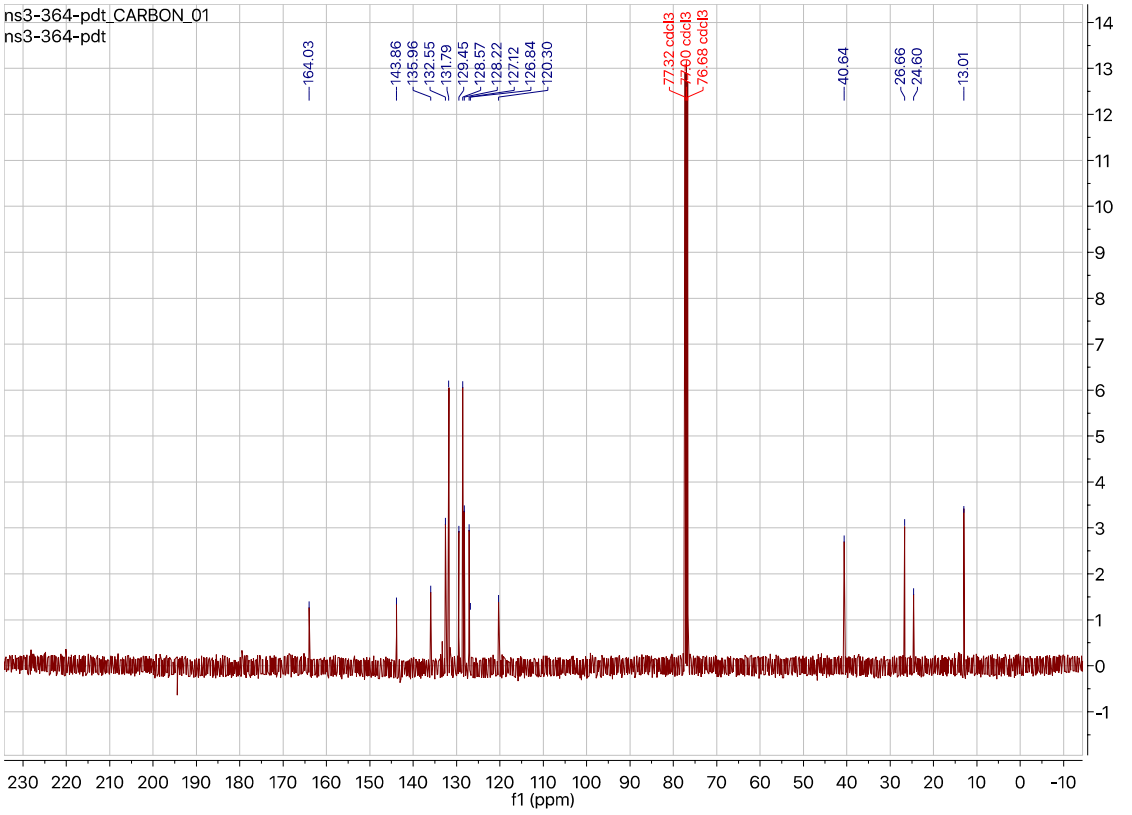
ns3-364-pdt_CARBON_01
ns3-364-pdt
164.03
143.86
135.96
132.55
131.79
129.45
128.57
128.22
127.12
126.84
120.30
77.32 cdcl3
77.00 cdcl3
76.68 cdcl3
40.64
26.66
24.60
13.01
f1 (ppm)

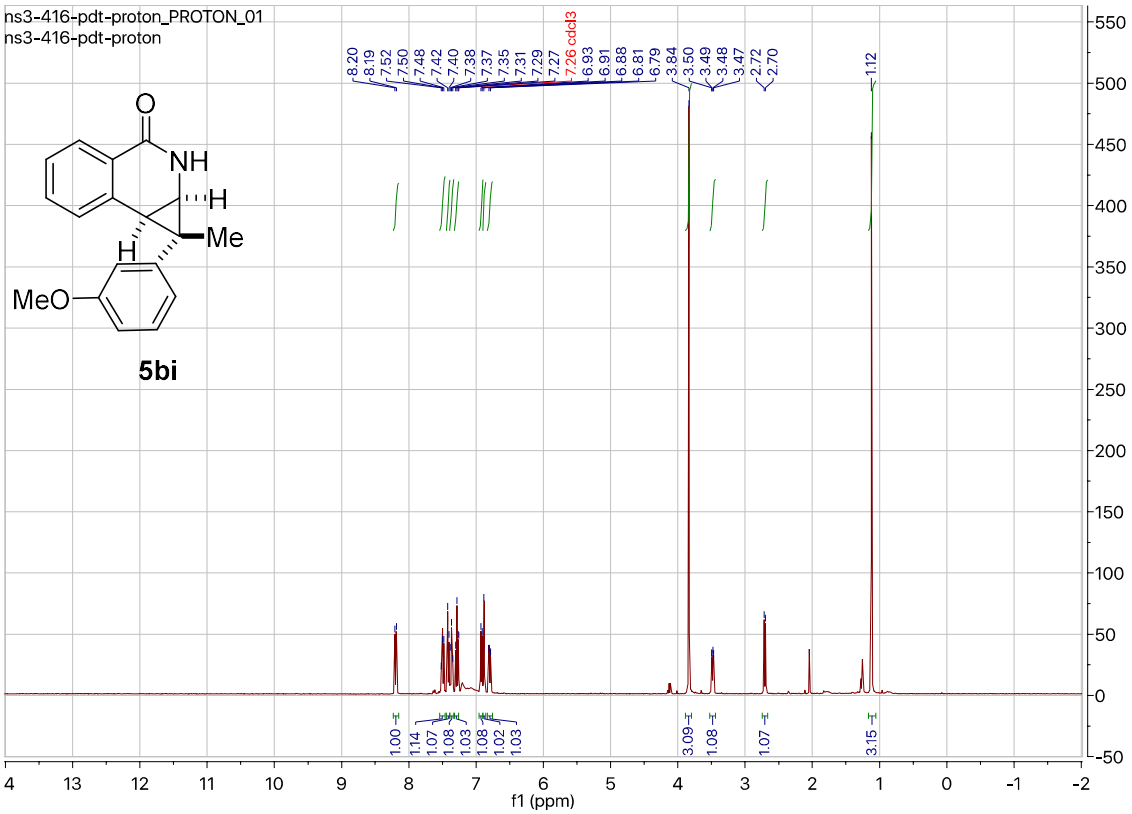
ns3-416-pdt-proton_PROTON_01
ns3-416-pdt-proton
O
NH
H
Me
H
MeO
5bi
8.20
8.19
7.52
7.50
7.48
7.42
7.40
7.38
7.37
7.35
7.31
7.29
7.27
7.26 cdcl3
6.93
6.91
6.88
6.81
6.79
3.84
3.50
3.49
3.48
3.47
2.72
2.70
1.12
1.00
1.14
1.07
1.08
1.03
1.08
1.02
1.03
3.09
1.08
1.07
3.15
f1 (ppm)

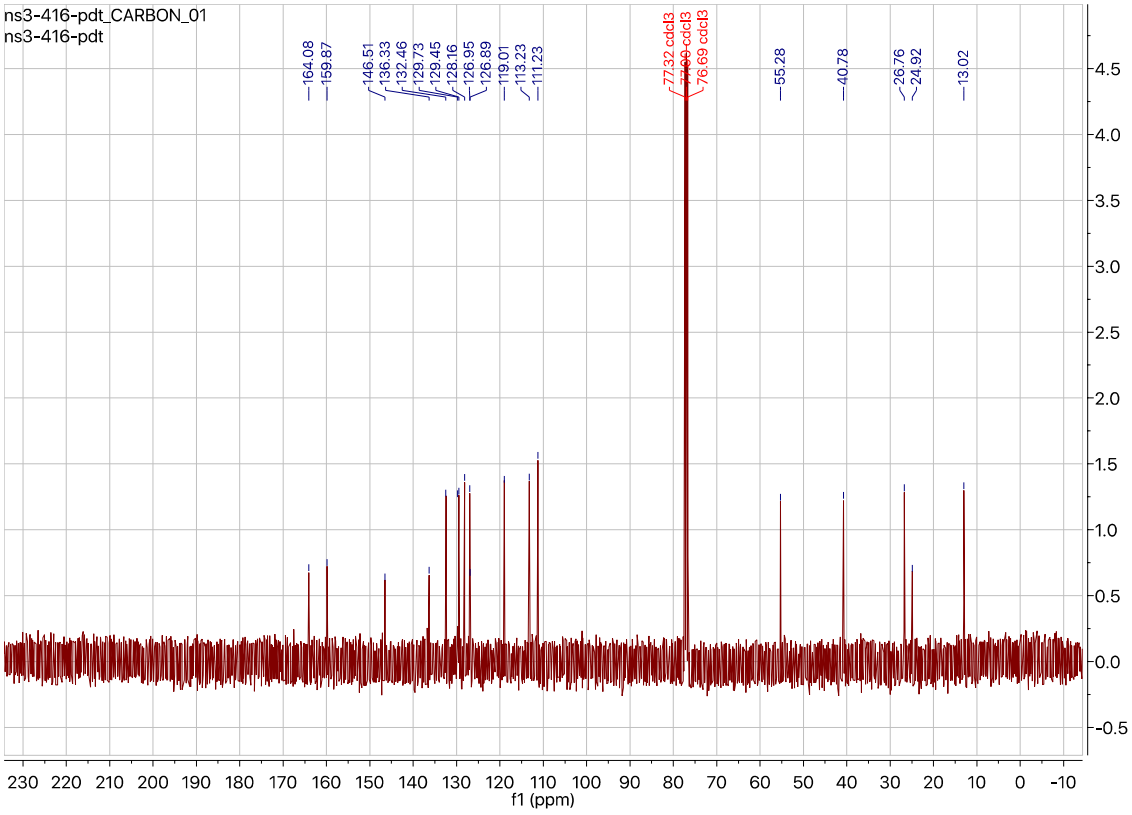
ns3-416-pdt_CARBON_01
ns3-416-pdt
164.08
159.87
146.51
136.33
132.46
129.73
129.45
128.16
126.95
126.89
119.01
113.23
111.23
77.32 cdcl3
77.00 cdcl3
76.69 cdcl3
55.28
40.78
26.76
24.92
13.02
f1 (ppm)

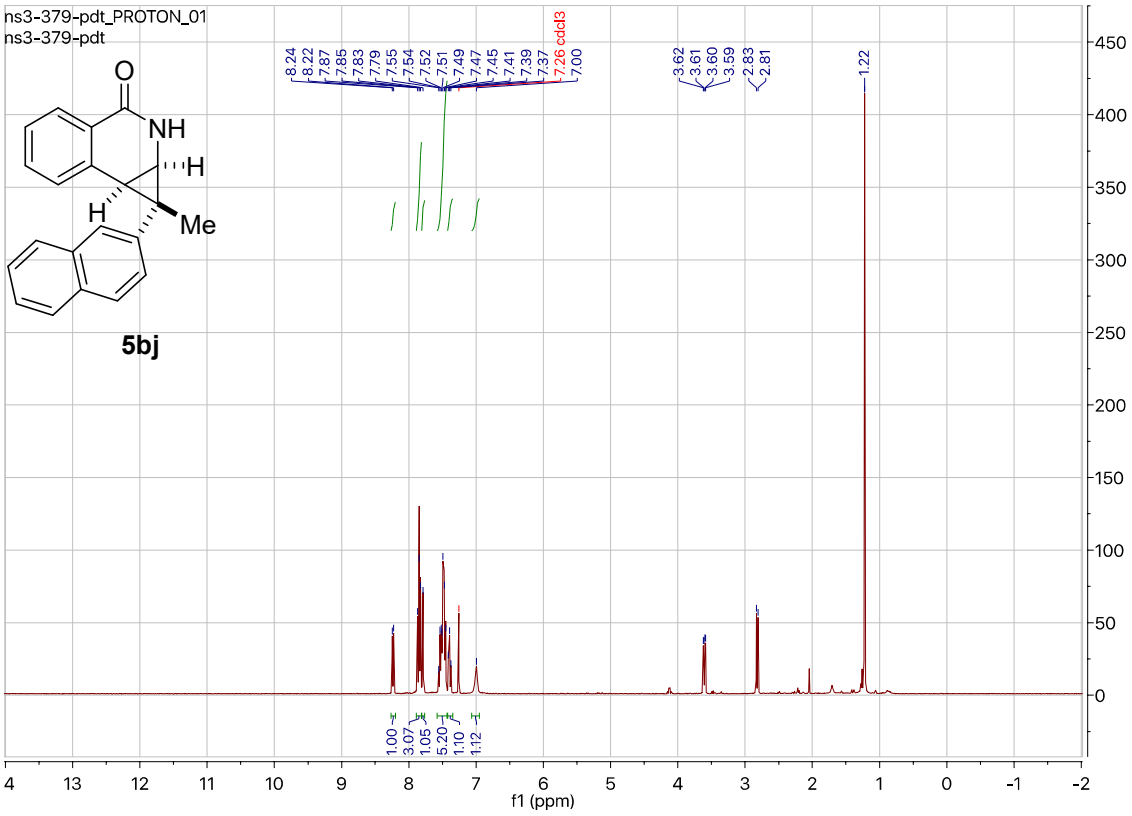
ns3-379-pdt_PROTON_01
ns3-379-pdt
O
NH
H
H
Me
5bj
8.24
8.22
7.87
7.85
7.83
7.79
7.55
7.54
7.52
7.51
7.49
7.47
7.45
7.41
7.39
7.37
7.26 cdcl3
7.00
3.62
3.61
3.60
3.59
2.83
2.81
1.22
1.00
3.07
1.05
5.20
1.10
1.12
f1 (ppm)

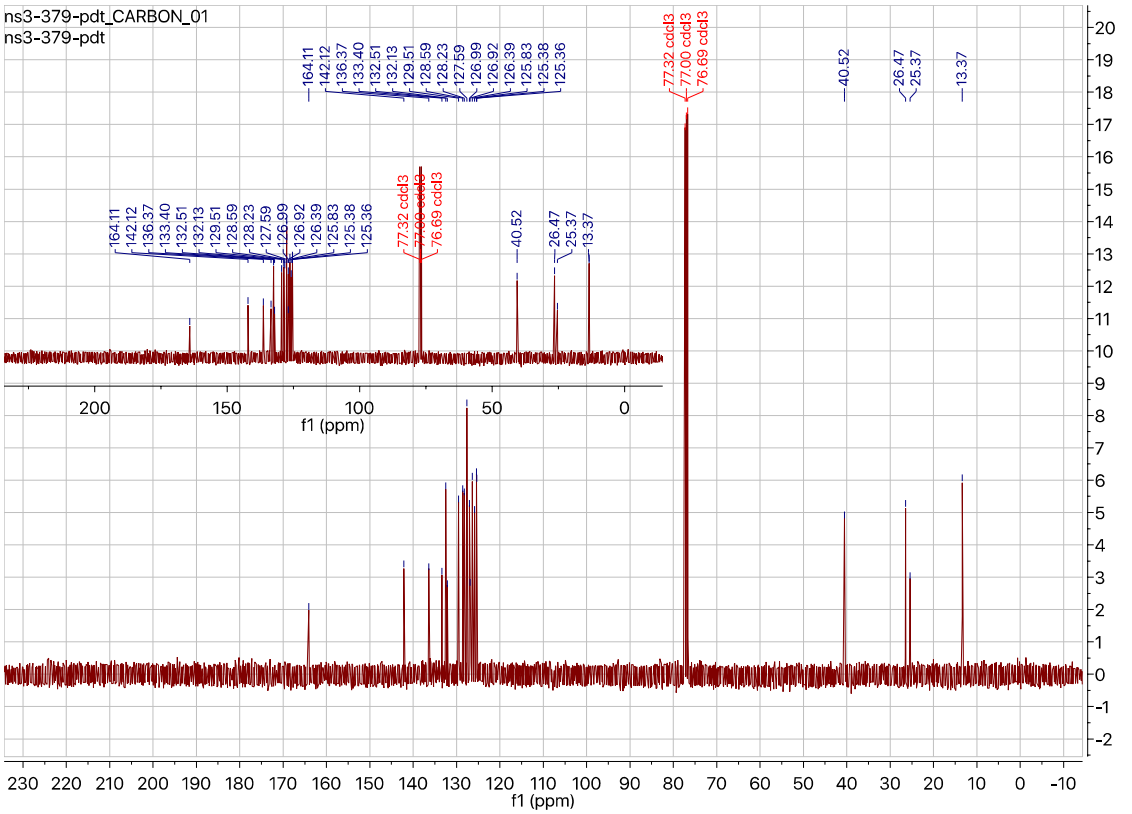
ns3-379-pdt_CARBON_01
ns3-379-pdt
164.11
142.12
136.37
133.40
132.51
132.13
129.51
128.59
128.23
127.59
126.99
126.92
126.39
125.83
125.38
125.36
77.32 cdcl3
77.00 cdcl3
76.69 cdcl3
40.52
26.47
25.37
13.37
f1 (ppm)

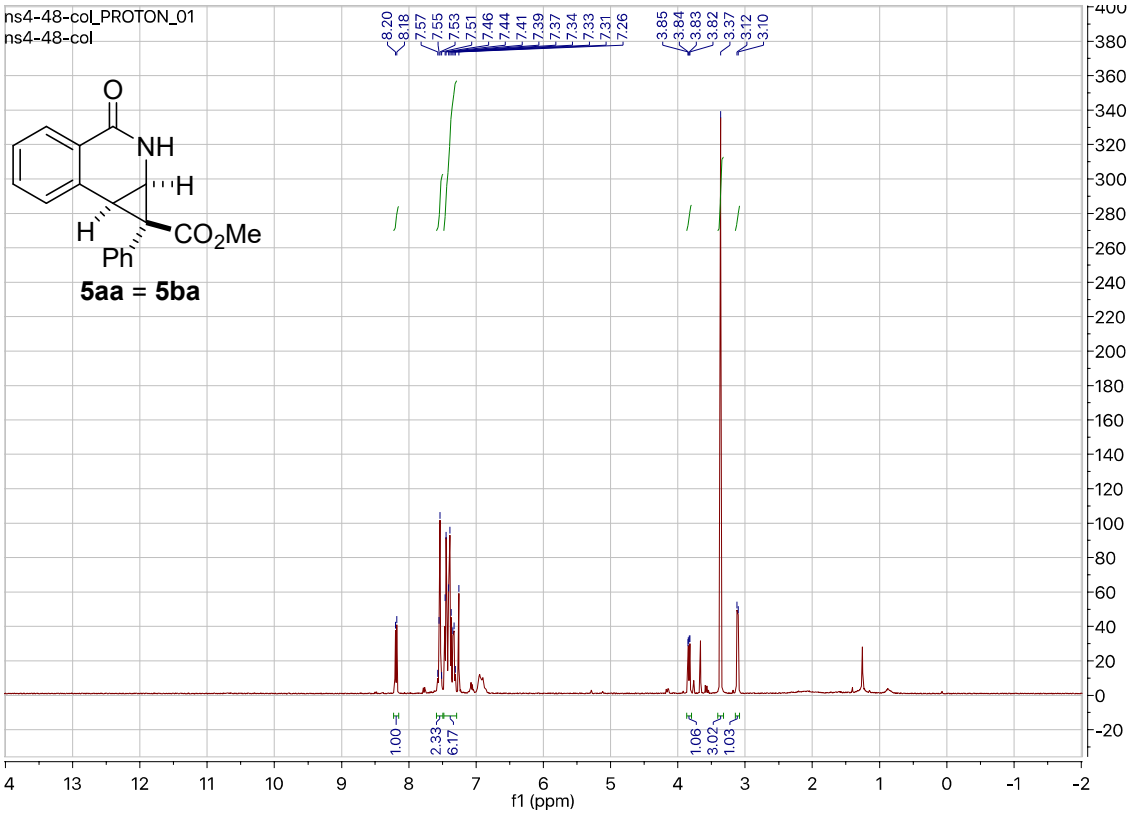
ns4-48-col_PROTON_01
ns4-48-col
O
NH
H
H
CO2Me
Ph
5aa = 5ba
8.20
8.18
7.57
7.55
7.53
7.51
7.46
7.44
7.41
7.39
7.37
7.34
7.33
7.31
7.26
3.85
3.84
3.83
3.82
3.37
3.12
3.10
1.00
2.33
6.17
1.06
3.02
1.03
f1 (ppm)

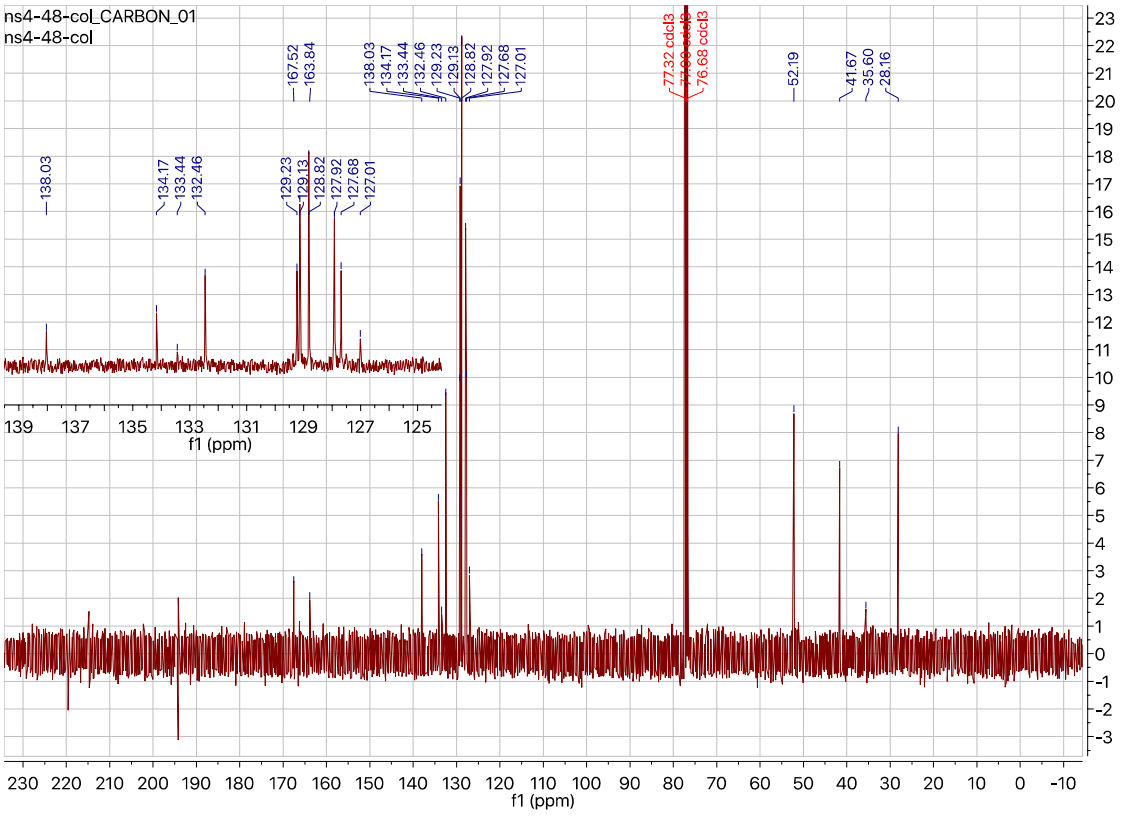
ns4-48-col_CARBON_01
ns4-48-col
167.52
163.84
138.03
134.17
133.44
132.46
129.23
129.13
128.82
127.92
127.68
127.01
77.32 cdcl3
76.68 cdcl3
52.19
41.67
35.60
28.16
f1 (ppm)

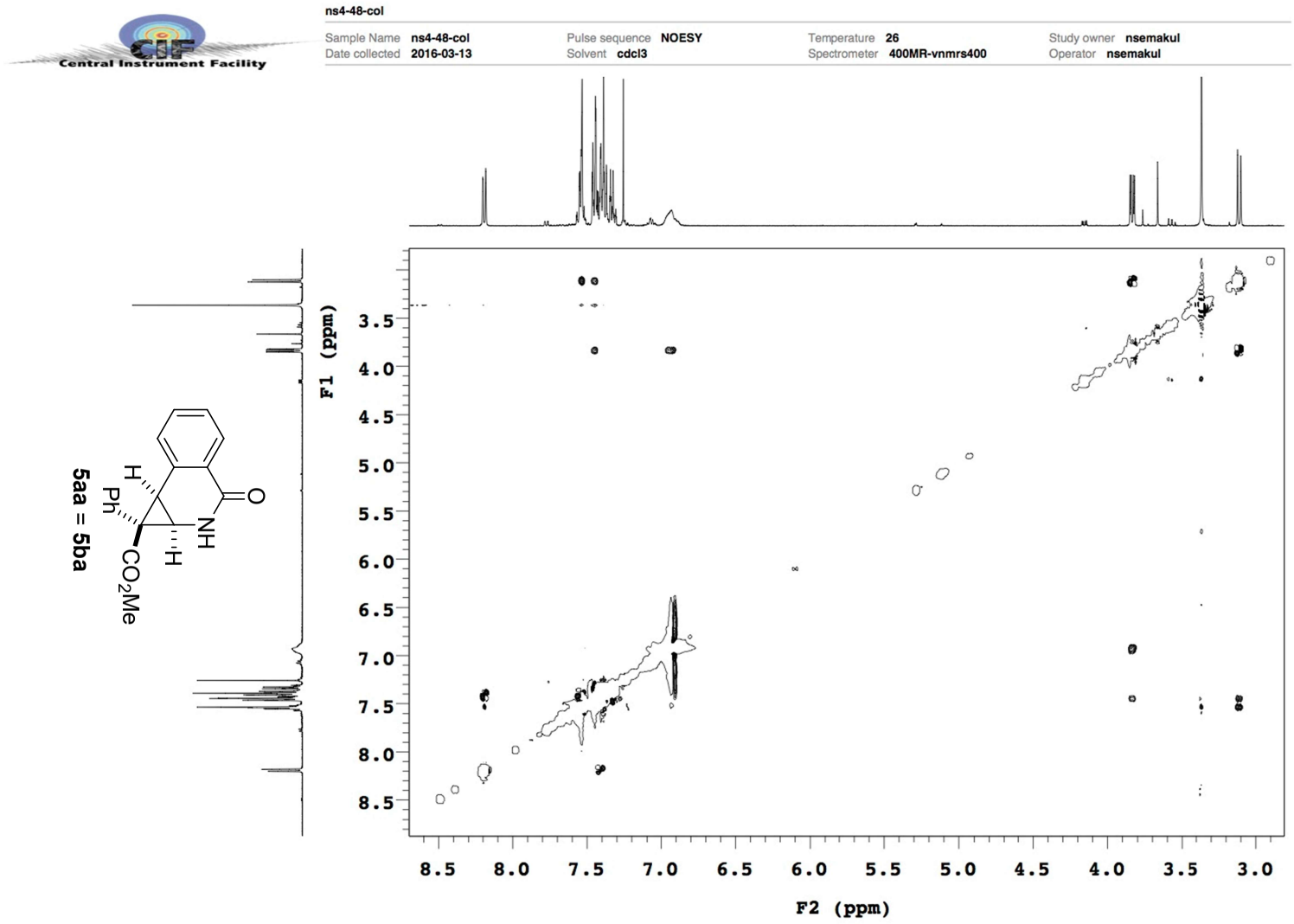
Central Instrument Facility
ns4-48-col
Sample Name ns4-48-col
Date collected 2016-03-13
Pulse sequence NOESY
Solvent cdcl3
Temperature 26
Spectrometer 400MR-vnmrs400
Study owner nsemakul
Operator nsemakul
F1 (ppm)
F2 (ppm)
3.5
4.0
4.5
5.0
5.5
6.0
6.5
7.0
7.5
8.0
8.5
3.0
H
Ph
CO2Me
H
NH
O
5aa = 5ba
Data file /home/_data/walkup/nsemakul/ns4-48-col_20160313_01/ns4-48-col_NOESY_01
Plot date 2016-03-14

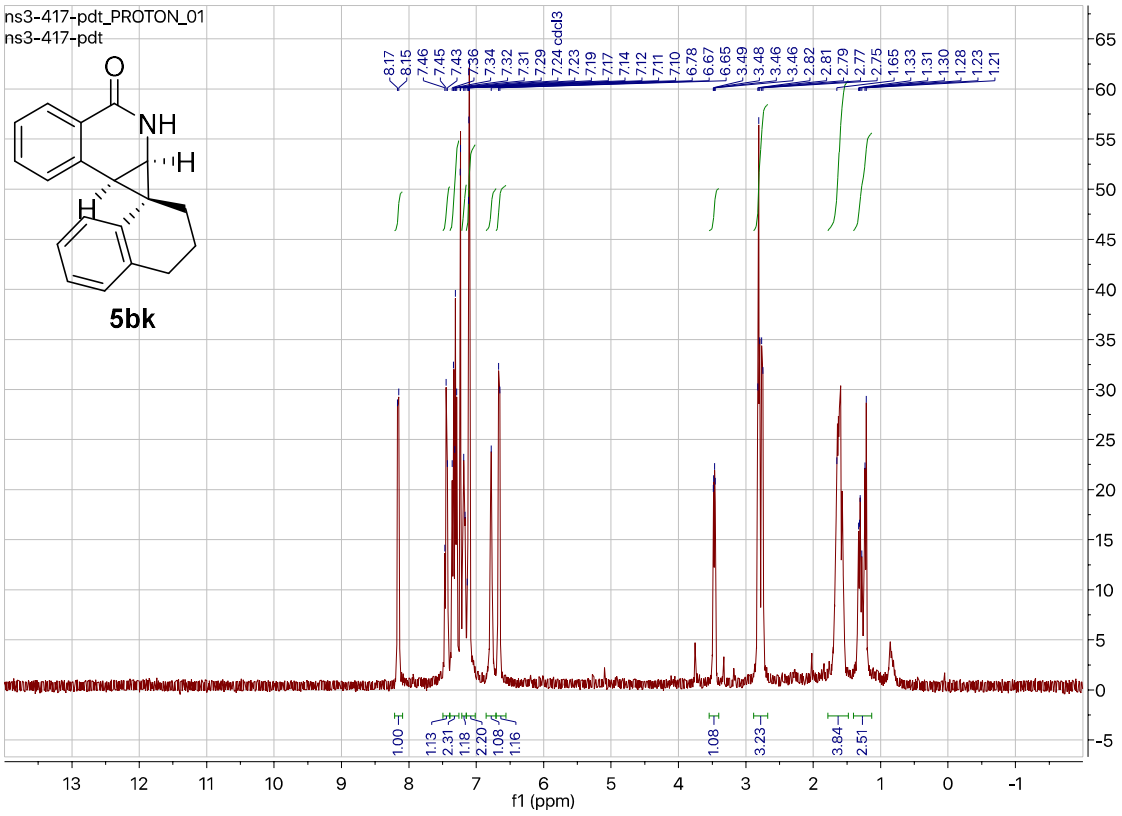
ns3-417-pdt_PROTON_01
ns3-417-pdt
O
NH
H
H
5bk
8.17
8.15
7.46
7.45
7.43
7.36
7.34
7.32
7.31
7.29
7.24 cdcl3
7.23
7.19
7.17
7.14
7.12
7.11
7.10
6.78
6.67
6.65
3.49
3.48
3.46
3.46
2.82
2.81
2.79
2.77
2.75
1.65
1.33
1.31
1.30
1.28
1.23
1.21
1.00
1.13
2.31
1.18
2.20
1.08
1.16
1.08
3.23
3.84
2.51
f1 (ppm)

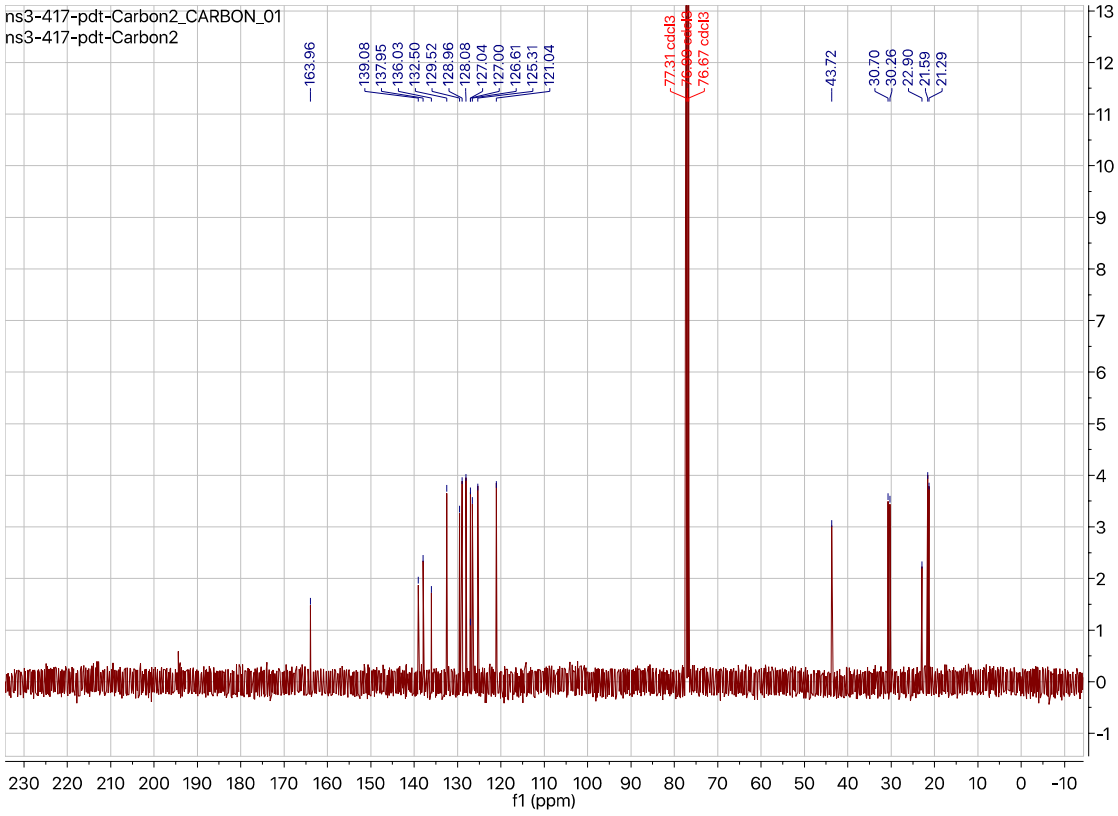
ns3-417-pdt-Carbon2_CARBON_01
ns3-417-pdt-Carbon2
163.96
139.08
137.95
136.03
132.50
129.52
128.96
128.08
127.04
127.00
126.61
125.31
121.04
77.31 cdcl3
76.67 cdcl3
43.72
30.70
30.26
22.90
21.59
21.29
f1 (ppm)

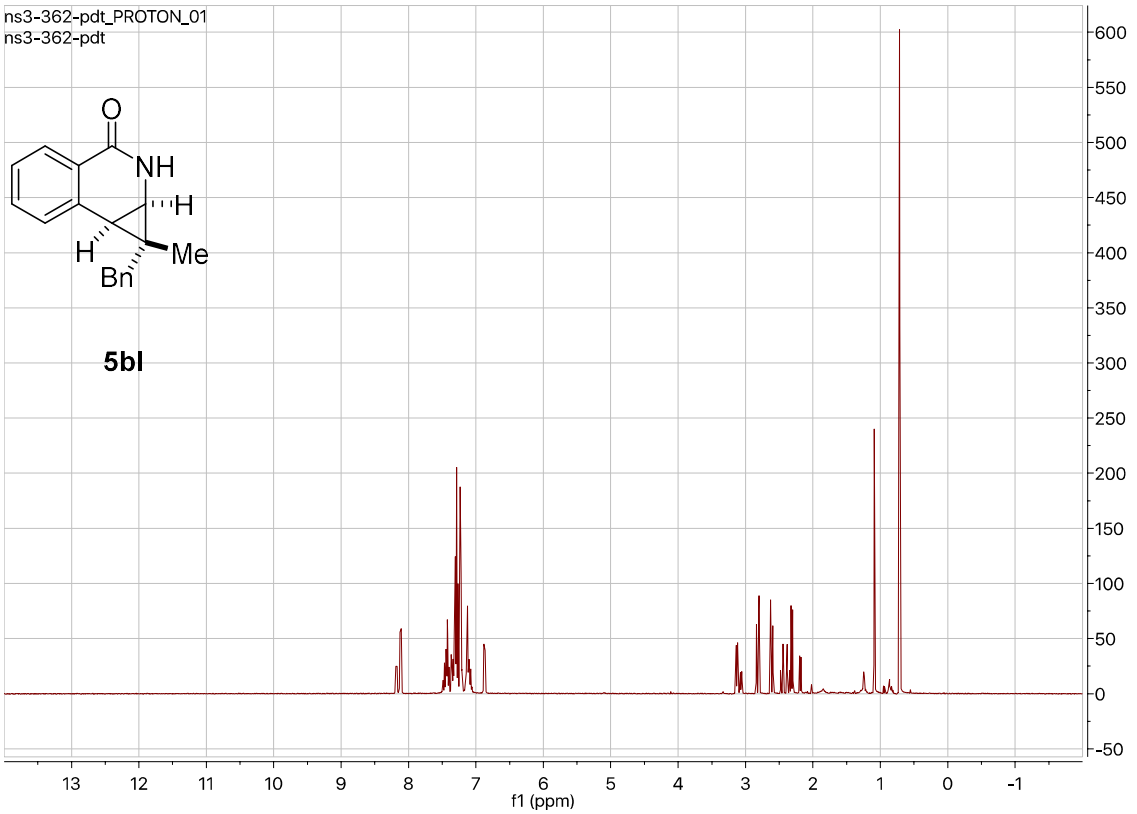
ns3-362-pdt_PROTON_01
ns3-362-pdt
O
NH
H
H
Me
Bn
5bl
f1 (ppm)

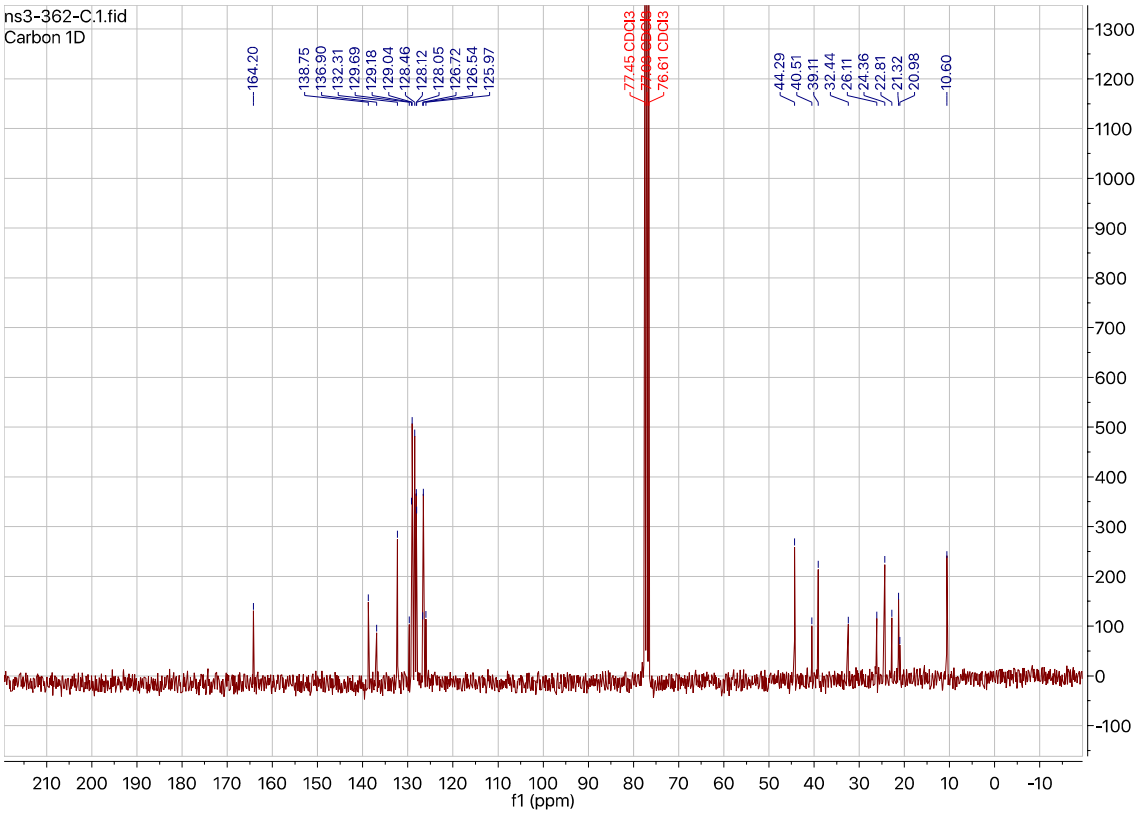
ns3-362-C.1.fid
Carbon 1D
164.20
138.75
136.90
132.31
129.69
129.18
129.04
128.46
128.12
128.05
126.72
126.54
125.97
77.45 CDCl3
76.61 CDCl3
44.29
40.51
39.11
32.44
26.11
24.36
22.81
21.32
20.98
10.60
f1 (ppm)

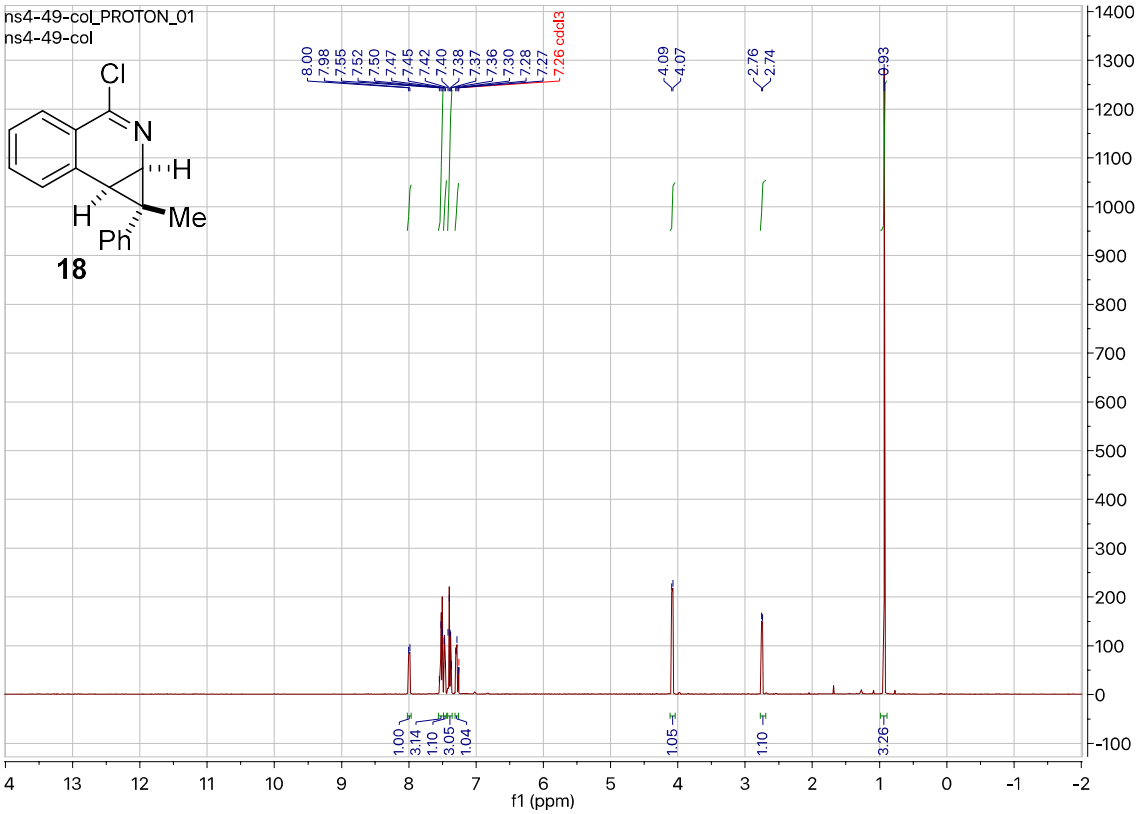
ns4-49-col_PROTON_01
ns4-49-col
Cl
N
H
H
Me
Ph
18
8.00
7.98
7.55
7.52
7.50
7.47
7.45
7.42
7.40
7.38
7.37
7.36
7.30
7.28
7.27
7.26 cdcl3
4.09
4.07
2.76
2.74
9.93
1.00
3.14
1.10
3.05
1.04
1.05
1.10
3.26
f1 (ppm)

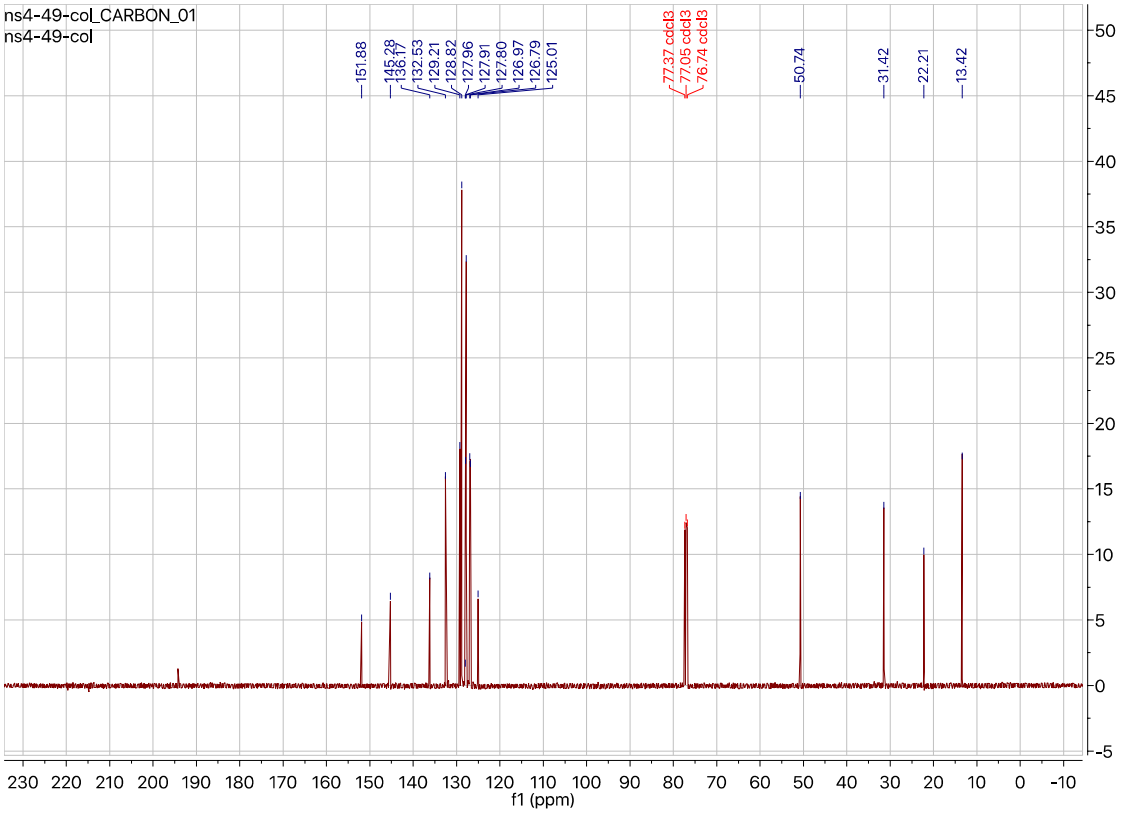
ns4-49-col_CARBON_01
ns4-49-col
151.88
145.28
138.17
132.53
129.21
128.82
127.96
127.91
127.80
126.97
126.79
125.01
77.37 cdcl3
77.05 cdcl3
76.74 cdcl3
50.74
31.42
22.21
13.42
f1 (ppm)

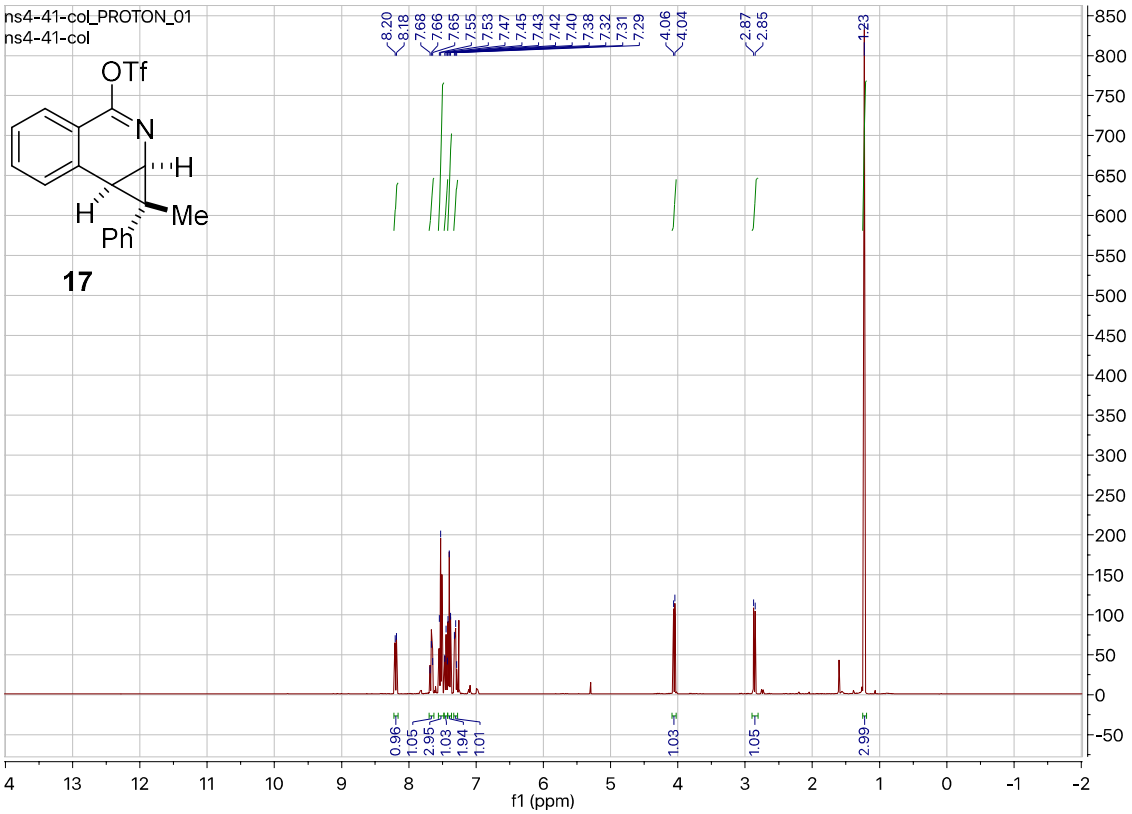
ns4-41-col_PROTON_01
ns4-41-col
OTf
N
H
H
Me
Ph
17
8.20
8.18
7.68
7.66
7.65
7.55
7.53
7.47
7.45
7.43
7.42
7.40
7.38
7.32
7.31
7.29
4.06
4.04
2.87
2.85
1.23
0.96
1.05
2.95
1.03
1.94
1.01
1.03
1.05
2.99
f1 (ppm)

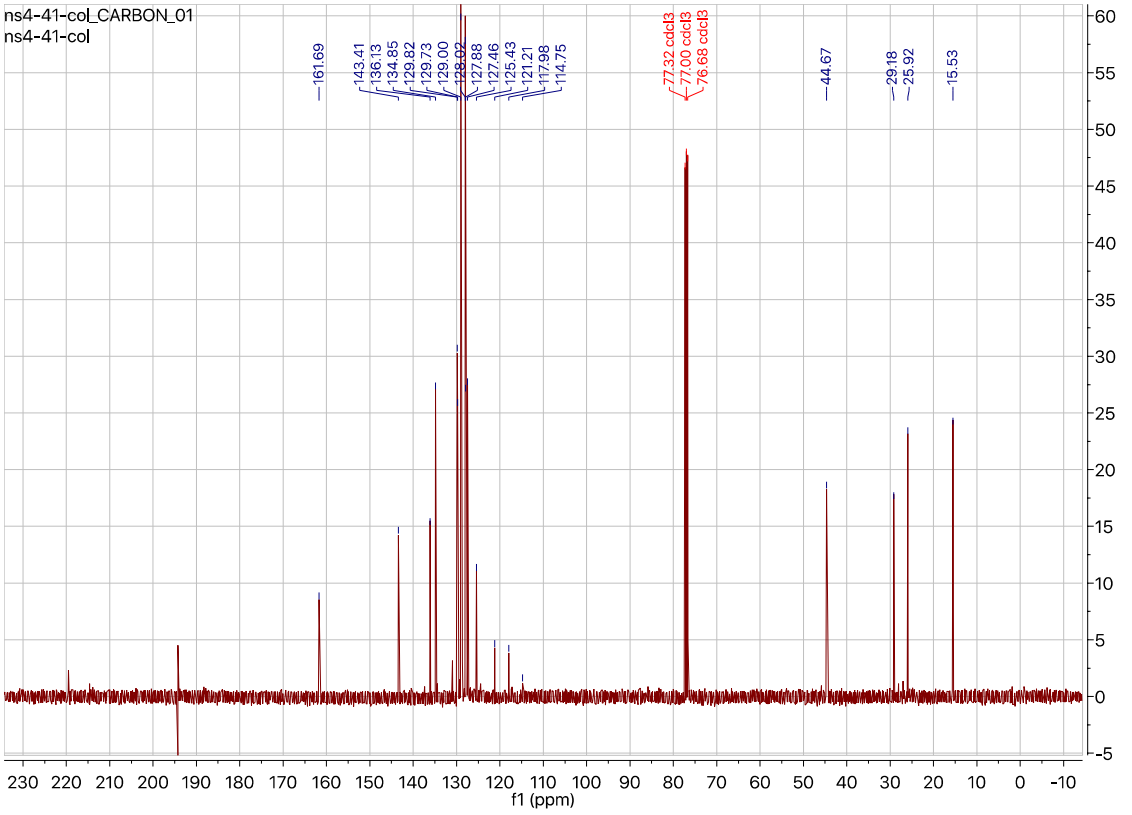
ns4-41-col_CARBON_01
ns4-41-col
161.69
143.41
136.13
134.85
129.82
129.73
129.00
128.02
127.88
127.46
125.43
121.21
117.98
114.75
77.32 cdcl3
77.00 cdcl3
76.68 cdcl3
44.67
29.18
25.92
15.53
f1 (ppm)

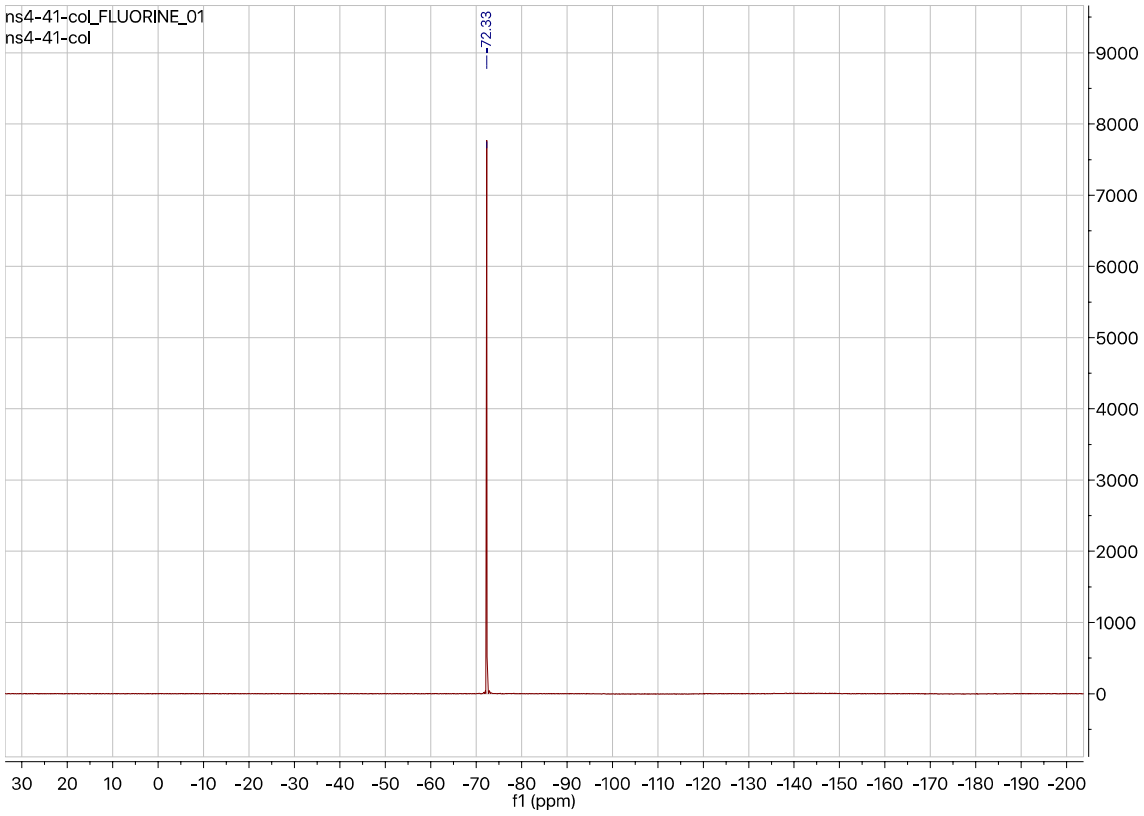
ns4-41-col_FLUORINE_01
ns4-41-col
-72.33
9000
8000
7000
6000
5000
4000
3000
2000
1000
0
30 20 10 0 -10 -20 -30 -40 -50 -60 -70 -80 -90 -100 -110 -120 -130 -140 -150 -160 -170 -180 -190 -200
f1 (ppm)

APPENDIX 2

Development of Stereoselective [4.2.0] Dihydroisoquinolones Synthesis via Rh(III)-Catalyzed C-H Activation and [4+2] Annulation with Cyclobutenes

1. General Methods

When necessary, organic solvents were dried and/or distilled prior to use under argon. Air and moisture sensitive reactions were carried out in oven or flame-dried glassware. Column chromatography was performed on Silicycle® SilicaFlash® P60 (230-400 mesh) silica gel. Thin layer chromatography was performed on Silicycle® 250μm silica gel 60A plates. Visualization was accomplished with UV light (254 nm) or potassium permanganate. ^{1}H, ^{19}F, and ^{13}C NMR spectra were collected at ambient temperature in $CDCl_3$ on a Varian 400 MHz or a Bruker 300 or 500 MHz spectrometers. Chemical shifts are reported as parts per million (δ, ppm) and are referenced to the residual solvent peaks of the deuterated solvents employed. Coupling constants (J) are reported in Hz. Coupling uses the following abbreviations: s = singlet, d = doublet, t = triplet, q = quartet, and m = multiplet. Mass spectra were obtained on an Agilent Technologies 6130 Quadropole Mass Spec (LRMS) or ACQUITY Waters UPLC/mass spectrometer equipped with electrospray ionization. Infrared (IR) spectra were recorded with neat samples on a Bruker Tensor 27 FT-IR or Perkin Elmer Paragon 1000 FT-IR spectrometer.

2. General procedures for Rh(III)-catalyzed reaction

Without any precaution of air and moisture, *O*-pivaloyl arylhydroxamic acid (0.1 mmol, 1 equiv), $[Cp^*RhCl_2]_2$ (0.001 mmol, 1 mol%), CsOPiv (0.025 mmol, 0.25 equiv), cyclobutene (0.11 mmol, 1.1 equiv), and MeOH (1 mL, 0.1 M) were charged into a dram vial with a stir bar. The reaction was stirred at room temperature until the starting material was consumed (monitoring by TLC). The reaction was quenched with saturated $NaHCO_3$ and extracted 3 times with EtOAc. The organic layer was washed with brine, dried over $MgSO_4$, filtered, and solvent was evaporated to obtain crude product. The crude product was purified by column chromatography using 25% to 75% EtOAc/hexane/1% Et_3N to obtain the corresponding product.

3. Preparations of Starting Materials

O-pivaloyl arylhydroxamates[91] were prepared by previously reported procedures.

Cyclobutenes were prepared by previously reported procedures.

[91] (a) Guimond, N,; Gorelsky, S. I.; Fagnou, K. *J. Am. Chem. Soc.* **2011,** *133*, 6449-6457. (b) Wang, H.; Glorius, F. *Angew. Chem. Int. Ed.* **2012**, *51*, 7318-7322. (c) Hyster, T. K.; Ruhl, K. E.; Rovis, T. *J. Am. Chem. Soc.* **2013**, *135*, 5364-5367.

4. Characterizations of New Compounds

dimethyl (1S,2S,2aS,8bR)-4-oxo-1,2,2a,3,4,8b-hexahydrocyclobuta[c]isoquinoline-1,2-dicarboxylate

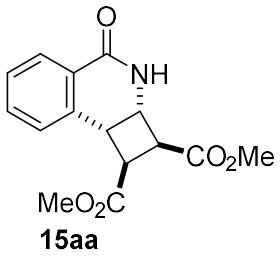

15aa

Off-white solid (28.8 mg, 99% yield)

^{1}H NMR (400 MHz, $CDCl_3$) δ 8.16 (d, *J* = 7.9 Hz, 1H), 7.52 (t, *J* = 7.5 Hz, 1H), 7.37 (t, *J* = 7.6 Hz, 1H), 7.27 (d, *J* = 7.9 Hz, 1H), 6.72 (s, NH), 4.70 (ddd, *J* = 9.3, 7.0, 4.1, 1H), 4.07 (dd, *J* = 9.2, 4.1 Hz, 1H), 3.76 (s, 3H), 3.70 (s, 3H), 3.56 (ddt, *J* = 9.1, 6.8, 1.0 Hz, 1H), 3.44 – 3.33 (m, 1H).

^{13}C NMR (101 MHz, $CDCl_3$) δ 172.35, 171.12, 163.62, 138.35, 133.16, 128.39, 127.85, 127.69, 126.61, 52.43, 52.17, 49.31, 49.17, 47.12, 36.53.

LRMS (ESI) m/z calcd for $C_{15}H_{15}NO_5$ $[M+H]^+$: 290.1, found: 290.1.

dimethyl (1S,2S,2aS,8bR)-7-methoxy-4-oxo-1,2,2a,3,4,8b-hexahydrocyclobuta[c]isoquinoline-1,2-dicarboxylate

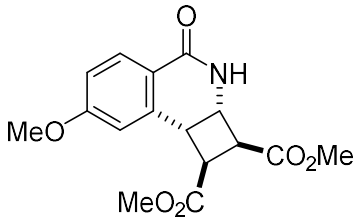

15ba

Off-white solid (29.3 mg, 92% yield)

^{1}H NMR (400 MHz, $CDCl_3$) δ 8.09 (d, *J* = 8.8 Hz, 1H), 6.87 (dd, *J* = 8.8, 2.5 Hz, 1H), 6.71 (d, *J* = 2.5 Hz, 1H), 6.55 (s, NH), 4.66 (dddt, *J* = 7.9, 6.1, 4.1, 1.0 Hz, 1H), 4.10 – 3.98 (m, 1H), 3.84 (s, 3H), 3.75 (s, 3H), 3.69 (s, 3H), 3.55 (ddd, *J* = 9.8, 6.9, 1.1 Hz, 1H), 3.39 (ddd, *J* = 9.8, 4.2, 1.0 Hz, 1H).

^{13}C NMR (101 MHz, $CDCl_3$) δ 172.33, 171.13, 163.62, 163.32, 140.45, 130.62, 119.45, 113.62, 112.30, 55.50, 52.42, 52.15, 49.32, 49.23, 47.02, 36.86.

LRMS (ESI) m/z calcd for $C_{16}H_{17}NO_6$ $[M+H]^+$: 320.1, found: 320.1.

dimethyl (1S,2S,2aS,8bR)-7-chloro-4-oxo-1,2,2a,3,4,8b-hexahydrocyclobuta[c]isoquinoline-1,2-dicarboxylate

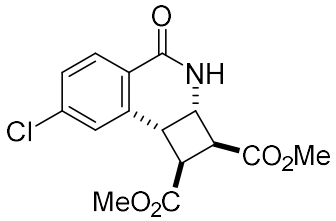

15ca

Off-white solid (29.3 mg, 92% yield)

^{1}H NMR (400 MHz, $CDCl_3$) δ 8.10 (d, *J* = 8.4, Hz, 1H), 7.35 (d, *J* = 8.4 Hz, 1H), 7.27 (s, 1H), 6.70 (s, NH), 4.68 (dddt, *J* = 8.9, 6.8, 4.1, 0.9 Hz, 1H), 4.05 (ddd, *J* = 9.4, 4.4, 1.0 Hz, 1H), 3.77 (s, 3H), 3.70 (s, 3H), 3.55 (ddd, *J* = 9.8, 6.8, 1.1 Hz, 1H), 3.41 (ddd, *J* = 9.8, 4.3, 1.1 Hz, 1H).

^{13}C NMR (101 MHz, $CDCl_3$) δ 216.93, 172.01, 170.88, 162.79, 162.77, 140.02, 139.36, 130.15, 128.22, 127.78, 125.10, 52.54, 52.25, 49.34, 49.19, 46.88, 36.36.

LRMS (ESI) m/z calcd for $C_{15}H_{14}ClNO_5$ $[M+H]^+$: 324.1, found: 324.1.

dimethyl (1S,2S,2aS,8bR)-7-bromo-4-oxo-1,2,2a,3,4,8b-hexahydrocyclobuta[c]isoquinoline-1,2-dicarboxylate

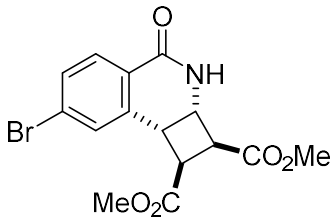

15da

Off-white solide (36.8 mg, 90% yield)

^{1}H NMR (400 MHz, $CDCl_3$) δ 8.03 (d, *J* = 8.4 Hz, 1H), 7.51 (d, *J* = 8.4 Hz, 1H), 7.43 (s, 1H), 6.59 (s, NH), 4.69 (dddt, *J* = 9.1, 6.4, 4.1, 1.0 Hz, 1H), 4.11 – 4.00 (m, 1H), 3.78 (s, 3H), 3.71 (s, 1H), 3.55 (ddd, *J* = 9.8, 6.9, 1.1 Hz, 1H), 3.41 (ddd, *J* = 9.8, 4.2, 1.1 Hz, 1H).

^{13}C NMR (101 MHz, $CDCl_3$) δ 172.00, 170.85, 162.85, 140.15, 131.20, 130.78, 130.23, 127.97, 125.51, 52.55, 52.26, 49.35, 49.19, 46.88, 36.27.

LRMS (ESI) m/z calcd for $C_{15}H_{14}BrNO_5$ $[M+H]^+$: 368.0, 370.0, found: 368.0, 370.0.

dimethyl (1S,2S,2aS,8bR)-4-oxo-7-(trifluoromethyl)-1,2,2a,3,4,8b-hexahydrocyclobuta[c]isoquinoline-1,2-dicarboxylate

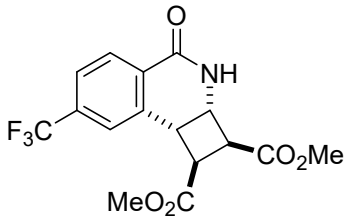

15ea

Off-white solid (32.0 mg, 90% yield)

^{1}H NMR (400 MHz, $CDCl_3$) δ 8.30 (d, *J* = 8.1, 1H), 7.64 (d, *J* = 8.2 Hz, 1H), 7.54 – 7.50 (s, 1H), 6.90 (d, *J* = 4.0 Hz, NH), 4.73 (dddd, *J* = 9.2, 6.8, 4.0, 1.1 Hz, 1H), 4.14 (dd, *J* = 9.2, 4.4 Hz, 1H), 3.79 (s, 3H), 3.72 (s, 3H), 3.56 (ddd, *J* = 9.8, 6.7, 1.1 Hz, 1H), 3.44 (ddd, *J* = 9.8, 4.4, 1.0 Hz, 1H).

^{13}C NMR (101 MHz, $CDCl_3$) δ 171.89, 170.79, 162.29, 139.06, 134.59 (q), 129.62, 129.24, 124.96 (m), 124.52 (m), 123.38 (q), 52.58, 52.30, 49.42, 49.04, 46.91, 36.32.

^{19}F NMR (376 MHz, $CDCl_3$) δ -63.18.

LRMS (ESI) m/z calcd for $C_{16}H_{14}F_3NO_5$ $[M+H]^+$: 358.1, found: 358.1.

dimethyl (1S,2S,2aS,8bR)-5-methyl-4-oxo-1,2,2a,3,4,8b-hexahydrocyclobuta[c]isoquinoline-1,2-dicarboxylate

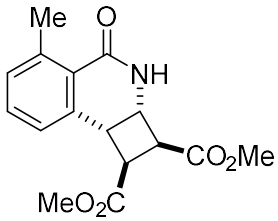

15fa

^{1}H NMR (400 MHz, $CDCl_3$) δ 7.37 (t, *J* = 7.6 Hz, 1H), 7.17 (d, *J* = 7.5 Hz, 1H), 7.13 (d, *J* = 7.6 Hz, 1H), 6.18 (s, NH), 4.64 – 4.51 (m, 1H), 4.08 (dd, *J* = 9.2, 4.5 Hz, 1H), 3.76 (s, 3H), 3.71 (s, 3H), 3.52 (ddd, *J* = 9.6, 6.4, 1.1 Hz, 1H), 3.39 (ddd, *J* = 9.7, 4.5, 1.0 Hz, 1H), 2.74 (s, 3H).

^{13}C NMR (101 MHz, cdcl$_3$) δ 172.39, 171.20, 164.72, 142.17, 139.81, 132.28, 131.80, 126.19, 124.56, 52.37, 52.15, 49.07, 48.86, 47.41, 37.24, 23.59.

LRMS (ESI) m/z calcd for $C_{16}H_{17}NO_5$ $[M+H]^+$: 304.1, found: 304.1.

dimethyl (1S,2S,2aS,8bR)-6-methyl-4-oxo-1,2,2a,3,4,8b-hexahydrocyclobuta[c]isoquinoline-1,2-dicarboxylate

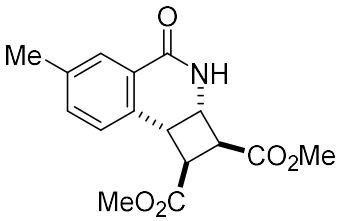

15ga

Off-white solid (30.5 mg, 99% yield)

^{1}H NMR (400 MHz, $CDCl_3$) δ 7.98 (s, 1H), 7.33 (d, *J* = 9.7 Hz, 1H), 7.16 (d, *J* = 8.0 Hz, 1H), 6.56 (s, NH), 4.74 – 4.60 (m, 1H), 4.02 (dd, *J* = 9.4, 3.9 Hz, 1H), 3.76 (s, 3H), 3.69 (s, 3H), 3.54 (ddd, *J* = 9.8, 7.1, 1.2 Hz, 1H), 3.36 (ddd, *J* = 9.7, 3.9, 1.1 Hz, 1H), 2.38 (s, 3H).

^{13}C NMR (101 MHz, $CDCl_3$) δ 172.44, 171.17, 163.81, 137.61, 135.38, 134.02, 128.63, 127.80, 126.35, 52.40, 52.14, 49.26, 49.21, 47.18, 36.37, 21.08.

LRMS (ESI) m/z calcd for $C_{16}H_{17}NO_5$ $[M+H]^+$: 304.1, found: 304.1.

dimethyl (1S,2S,2aS,8bR)-4-oxo-6-(trifluoromethyl)-1,2,2a,3,4,8b-hexahydrocyclobuta[c]isoquinoline-1,2-dicarboxylate

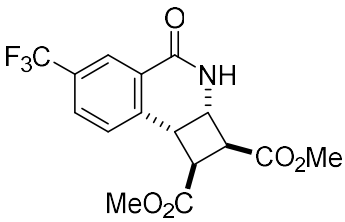

15ha

Off-white solid (31 mg, 87% yield)

^{1}H NMR (400 MHz, $CDCl_3$) δ 8.46 (s, 1H), 7.77 (d, *J* = 8.1 Hz, 1H), 7.44 (d, *J* = 8.1 Hz, 1H), 6.87 (s, NH), 4.72 (dddd, *J* = 9.2, 6.7, 4.0, 1.1 Hz, 1H), 4.20 – 4.10 (m, 1H), 3.78 (s, 3H), 3.72 (s, 3H), 3.56 (ddd, *J* = 9.8, 6.6, 1.1 Hz, 1H), 3.43 (ddd, *J* = 9.8, 4.5, 1.1 Hz, 1H).

^{13}C NMR (101 MHz, $CDCl_3$) δ 171.88, 170.79, 162.26, 141.96, 130.37 (q, *J* = 33.3 Hz), 129.52 (q, *J* = 3.6 Hz), 128.67, 127.30, 125.70 (q, *J* = 4.0 Hz), 123.54 (q, *J* = 272.2 Hz), 52.57, 52.31, 49.44, 49.06, 46.89, 36.33.

^{19}F NMR (376 MHz, $CDCl_3$) δ -62.90.

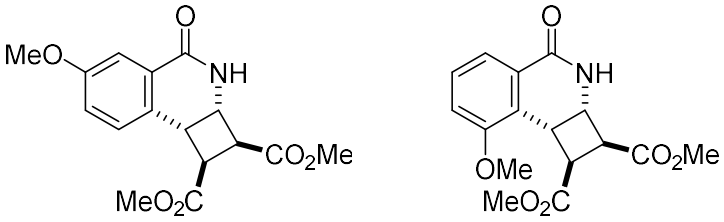

15ia/15ia'

LRMS (ESI) m/z calcd for $C_{16}H_{14}F_3NO_5$ $[M+H]^+$: 358.1, found: 358.1

Off-white solid (18.8 mg, 59% yield) *ca.* 1.5:1 regioisomeric ratio

^{1}H NMR (400 MHz, $CDCl_3$) see ^{1}H NMR spectra

^{13}C NMR (101 MHz, $CDCl_3$) δ 172.99, 172.45, 171.20, 171.18, 163.55, 163.49, 159.07, 156.56, 130.41, 129.16, 128.35, 127.70, 127.66, 126.64, 121.20, 120.18, 114.05, 111.03, 55.69, 55.60, 52.40, 52.32, 52.15, 52.07, 49.23, 49.21, 48.86, 47.21, 45.79, 36.18, 33.55.

LRMS (ESI) m/z calcd for $C_{16}H_{17}NO_6$ $[M+H]^+$: 320.1, found: 320.1

dimethyl (1S,2S)-6,7,8-trimethoxy-4-oxo-1,2,2a,3,4,8b-hexahydrocyclobuta[c]isoquinoline-1,2-dicarboxylate

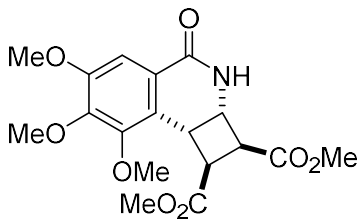

15ja

Off-white solid (34.5 mg, 91% yield)

^{1}H NMR (400 MHz, $CDCl_3$) δ 7.48 (s, 1H), 6.42 (s, NH), 4.76 (dddt, *J* = 9.1, 8.3, 4.6, 0.9 Hz, 1H), 3.99 – 3.85 (m, 10H), 3.77 (s, 3H), 3.67 (s, 3H), 3.55 (ddd, *J* = 9.6, 8.3, 1.2 Hz, 1H), 3.26 (ddd, *J* = 10.1, 3.0, 1.0 Hz, 1H).

^{13}C NMR (101 MHz, $CDCl_3$) δ 172.88, 171.21, 163.24, 153.25, 150.50, 145.66, 124.79, 122.09, 106.28, 60.82, 60.61, 56.15, 52.36, 52.06, 49.04, 48.96, 46.46, 33.59.

LRMS (ESI) m/z calcd for $C_{18}H_{21}NO_8$ $[M+H]^+$: 380.1, found: 380.2

dimethyl (5aS,6S,7S,7aS)-4-oxo-4,5,5a,6,7,7a-hexahydrocyclobuta[b]furo[2,3-d]pyridine-6,7-dicarboxylate

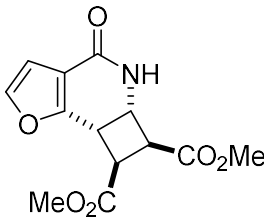

15ka

Off-white solid (22.0 mg, 79% yield)

^{1}H NMR (400 MHz, $CDCl_3$) δ 7.43 (d, *J* = 2.0 Hz, 1H), 6.76 (d, *J* = 2.0 Hz, 1H), 6.12 (s, NH), 4.87 (dddd, *J* = 9.6, 8.9, 4.8, 1.1 Hz, 1H), 4.04 – 3.95 (m, 1H), 3.76 (s, 3H), 3.69 (m, 4H), 3.46 (ddd, *J* = 9.9, 2.3, 1.0 Hz, 1H).

^{13}C NMR (101 MHz, $CDCl_3$) δ 171.91, 170.73, 162.88, 156.74, 144.11, 115.51, 108.03, 52.61, 52.20, 50.56, 49.34, 43.10, 34.80.

LRMS (ESI) m/z calcd for $C_{13}H_{13}NO_6$ $[M+H]^+$: 280.1, found: 280.1.

dimethyl (5aS,6S,7S,7aR)-2-bromo-4-oxo-4,5,5a,6,7,7a-hexahydrocyclobuta[b]furo[3,2-d]pyridine-6,7-dicarboxylate

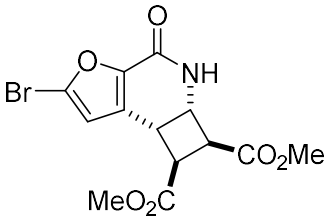

15la

Off-white solid (16.3 mg, 45% yield)

^{1}H NMR (400 MHz, $CDCl_3$) δ 6.42 (s, 1H), 6.05 (s, NH), 4.78 (tdd, *J* = 8.9, 4.8, 1.1 Hz, 1H), 3.89 (ddd, *J* = 9.1, 2.6, 1.3 Hz, 1H), 3.82 – 3.73 (m, 4H), 3.70 (s, 3H), 3.32 (ddd, *J* = 9.9, 2.6, 1.1 Hz, 1H).

^{13}C NMR (101 MHz, $CDCl_3$) δ 172.00, 170.73, 155.69, 143.36, 131.58, 129.69, 111.95, 52.60, 52.25, 51.09, 49.03, 45.13, 34.62.

LRMS (ESI) m/z calcd for $C_{13}H_{12}BrNO_6$ $[M+H]^+$: 358.0, 360.0 found: 358.0, 360.0.

dimethyl (5aS,6S,7S,7aR)-4-oxo-4,5,5a,6,7,7a-hexahydrocyclobuta[b]thieno[3,2-d]pyridine-6,7-dicarboxylate

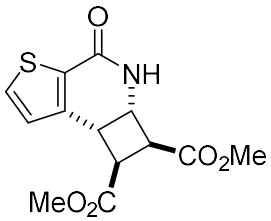

15ma

Off-white solid (25.6 mg, 87% yield)

^{1}H NMR (400 MHz, $CDCl_3$) δ 7.59 (d, *J* = 5.0 Hz, 1H), 6.98 (d, *J* = 5.1 Hz, 1H), 6.38 (s, NH), 4.82 (dddd, *J* = 9.3, 8.3, 4.5, 1.0 Hz, 1H), 3.97 (ddd, *J* = 9.3, 2.8, 1.2 Hz, 1H), 3.76 (s, 3H), 3.73 – 3.65 (m, 4H), 3.32 (ddd, *J* = 9.9, 2.9, 1.0 Hz, 1H).

^{13}C NMR (101 MHz, $CDCl_3$) δ 172.30, 171.01, 160.67, 143.59, 132.97, 130.95, 126.74, 52.50, 52.15, 51.09, 49.09, 45.84, 36.12.

LRMS (ESI) m/z calcd for C13H13NO5S $[M+H]^+$: 296.1 found: 296.1.

5. X-ray Structure

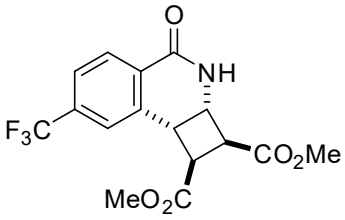

15ea

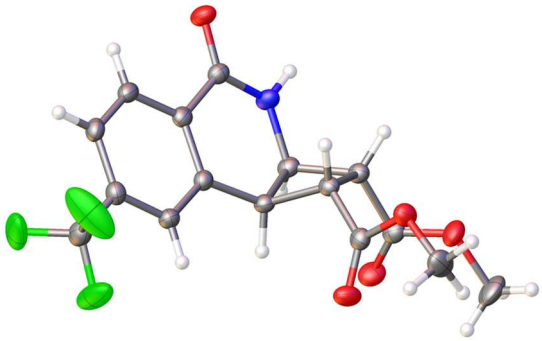

Computing details: Program(s) used to refine structure: *SHELXL2014*/7 (Sheldrick, 2014); molecular graphics: Olex2 (Dolomanov *et al.*, 2009); software used to prepare material for publication: Olex2 (Dolomanov *et al.*, 2009).

Crystal data

$C_{16}H_{14}F_3NO_5$	V = 1539.33 (7) Å^3
M_r = 357.28	Z = 4
Monoclinic, $P2_1/c$	F(000) = 736
a = 13.9171 (4) Å	D_x = 1.542 Mg m^{-3}
b = 8.4431 (2) Å	Mo *K*a radiation, l = 0.71073 Å
c = 13.1482 (4) Å	m = 0.14 mm^{-1}
b = 94.892 (3)°	T = 140 K

Data collection

10791 measured reflections	q_{max} = 26.4°, q_{min} = 3.3°
3139 independent reflections	h = -17⩽15
2717 reflections with $I > 2s(I)$	k = -10⩽10

R_{int} = 0.029	l = -16→16

Refinement

Refinement on F^2	58 restraints
Least-squares matrix: full	Hydrogen site location: mixed
$R[F^2 > 2s(F^2)]$ = 0.044	H atoms treated by a mixture of independent and constrained refinement
$wR(F^2)$ = 0.103	$w = 1/[s^2(F_o^2) + (0.0376P)^2 + 0.9964P]$ where $P = (F_o^2 + 2F_c^2)/3$
S = 1.01	$(D/s)_{max}$ = 0.004
3139 reflections	$D\rho_{max}$ = 0.24 e Å^{-3}
263 parameters	$D\rho_{min}$ = -0.34 e Å^{-3}

Special details

Geometry. All esds (except the esd in the dihedral angle between two l.s. planes) are estimated using the full covariance matrix. The cell esds are taken into account individually in the estimation of esds in distances, angles and torsion angles; correlations between esds in cell parameters are only used when they are defined by crystal symmetry. An approximate (isotropic) treatment of cell esds is used for estimating esds involving l.s. planes.

Fractional atomic coordinates and isotropic or equivalent isotropic displacement parameters (Å^2)

	x	*y*	*z*	U_{iso}*/U_{eq}	Occ. (<1)
N1	0.07832 (10)	0.84066 (17)	0.45335 (10)	0.0232 (3)	
H1	0.0543 (15)	0.938 (3)	0.4379 (15)	0.037 (6)*	
C2	0.04648 (11)	0.77335 (19)	0.53671 (12)	0.0214 (3)	
O3	-0.01448 (9)	0.83843 (14)	0.58590 (9)	0.0295 (3)	
C4	0.08745 (11)	0.61582 (19)	0.56979 (12)	0.0201 (3)	
C5	0.04998 (12)	0.53810 (19)	0.65090 (12)	0.0225 (3)	
H5	-0.0030	0.5829	0.6818	0.027*	
C6	0.08915 (12)	0.3958 (2)	0.68711 (12)	0.0238 (4)	
H6	0.0647	0.3446	0.7439	0.029*	
C7	0.16490 (12)	0.32893 (19)	0.63898 (13)	0.0240 (4)	
C8	0.20716 (14)	0.1751 (2)	0.67837 (14)	0.0321 (4)	
F9	0.14043 (12)	0.06734 (18)	0.69384 (19)	0.0584 (6)	0.876 (4)
F10	0.2574 (2)	0.1918 (2)	0.76757 (17)	0.0881 (10)	0.876 (4)
F11	0.26380 (17)	0.1061 (2)	0.61550 (16)	0.0681 (8)	0.876 (4)

F9B	0.1743 (10)	0.1237 (17)	0.7567 (10)	0.059 (4)	0.124 (4)
F10B	0.3012 (6)	0.1870 (13)	0.6930 (11)	0.049 (3)	0.124 (4)
F11B	0.1955 (13)	0.0674 (14)	0.6095 (11)	0.073 (4)	0.124 (4)
C12	0.20147 (12)	0.40372 (19)	0.55634 (12)	0.0230 (4)	
H12	0.2519	0.3555	0.5230	0.028*	
C13	0.16424 (11)	0.54922 (19)	0.52237 (12)	0.0197 (3)	
C14	0.20753 (11)	0.64058 (19)	0.44055 (12)	0.0198 (3)	
H14	0.2318	0.5670	0.3889	0.024*	
C15	0.14648 (11)	0.77373 (19)	0.38716 (12)	0.0210 (3)	
H15	0.1174	0.7456	0.3173	0.025*	
C16	0.23835 (12)	0.87736 (19)	0.38790 (12)	0.0211 (3)	
H16	0.2289	0.9890	0.4104	0.025*	
C17	0.28992 (12)	0.86320 (19)	0.29211 (12)	0.0225 (3)	
O18	0.26835 (9)	0.77748 (15)	0.22116 (9)	0.0311 (3)	
O19	0.36832 (9)	0.95671 (15)	0.29989 (9)	0.0321 (3)	
C20	0.43194 (15)	0.9444 (3)	0.21848 (15)	0.0433 (5)	
H20A	0.4483	0.8330	0.2083	0.065*	
H20B	0.4910	1.0048	0.2368	0.065*	
H20C	0.3995	0.9871	0.1553	0.065*	
C21	0.28569 (11)	0.76587 (18)	0.47463 (12)	0.0198 (3)	
H21	0.2760	0.8086	0.5439	0.024*	
C22	0.38933 (12)	0.71896 (19)	0.46671 (12)	0.0216 (3)	
O23	0.41443 (9)	0.61002 (15)	0.41611 (10)	0.0315 (3)	
O24	0.45003 (8)	0.81568 (14)	0.52093 (9)	0.0274 (3)	
C25	0.55146 (12)	0.7847 (2)	0.51169 (16)	0.0362 (5)	
H25A	0.5670	0.6766	0.5346	0.054*	
H25B	0.5906	0.8602	0.5540	0.054*	
H25C	0.5652	0.7965	0.4402	0.054*	

Atomic displacement parameters (Å²)

	U^{11}	U^{22}	U^{33}	U^{12}	U^{13}	U^{23}
N1	0.0229 (7)	0.0234 (7)	0.0238 (7)	0.0065 (6)	0.0053 (6)	0.0039 (6)
C2	0.0191 (8)	0.0243 (8)	0.0209 (8)	0.0001 (7)	0.0027 (6)	-0.0010 (6)
O3	0.0304 (7)	0.0282 (6)	0.0318 (6)	0.0077 (5)	0.0140 (5)	0.0033 (5)
C4	0.0202 (8)	0.0209 (8)	0.0192 (7)	-0.0022 (6)	0.0012 (6)	-0.0021 (6)

C5	0.0216 (8)	0.0239 (8)	0.0227 (8)	-0.0024 (7)	0.0055 (7)	-0.0038 (7)
C6	0.0262 (8)	0.0239 (8)	0.0219 (8)	-0.0056 (7)	0.0056 (7)	0.0012 (7)
C7	0.0250 (8)	0.0210 (8)	0.0262 (8)	-0.0025 (7)	0.0026 (7)	0.0011 (7)
C8	0.0344 (10)	0.0272 (9)	0.0363 (10)	0.0020 (8)	0.0113 (8)	0.0068 (8)
F9	0.0483 (10)	0.0251 (8)	0.1048 (17)	0.0000 (7)	0.0247 (10)	0.0228 (9)
F10	0.134 (2)	0.0387 (9)	0.0795 (15)	0.0130 (11)	-0.0630 (16)	0.0088 (9)
F11	0.0830 (16)	0.0425 (10)	0.0877 (14)	0.0354 (10)	0.0585 (13)	0.0312 (10)
F9B	0.066 (8)	0.056 (8)	0.059 (6)	0.022 (6)	0.033 (6)	0.032 (6)
F10B	0.036 (4)	0.039 (6)	0.071 (8)	0.012 (3)	0.007 (4)	0.037 (5)
F11B	0.095 (9)	0.041 (6)	0.082 (6)	0.021 (6)	-0.001 (6)	-0.015 (5)
C12	0.0226 (8)	0.0214 (8)	0.0258 (8)	0.0005 (7)	0.0067 (7)	-0.0009 (7)
C13	0.0200 (8)	0.0205 (8)	0.0189 (7)	-0.0024 (6)	0.0024 (6)	-0.0011 (6)
C14	0.0209 (8)	0.0203 (8)	0.0186 (7)	0.0016 (6)	0.0043 (6)	-0.0010 (6)
C15	0.0225 (8)	0.0240 (8)	0.0170 (7)	0.0015 (7)	0.0037 (6)	0.0010 (6)
C16	0.0245 (8)	0.0202 (8)	0.0188 (8)	0.0024 (7)	0.0042 (6)	0.0018 (6)
C17	0.0251 (8)	0.0230 (8)	0.0196 (8)	0.0034 (7)	0.0033 (7)	0.0045 (7)
O18	0.0338 (7)	0.0386 (7)	0.0211 (6)	-0.0004 (6)	0.0042 (5)	-0.0035 (5)
O19	0.0342 (7)	0.0364 (7)	0.0276 (6)	-0.0089 (6)	0.0127 (6)	-0.0005 (5)
C20	0.0405 (11)	0.0587 (14)	0.0335 (10)	-0.0104 (10)	0.0199 (9)	0.0017 (10)
C21	0.0236 (8)	0.0197 (8)	0.0163 (7)	0.0008 (6)	0.0035 (6)	0.0008 (6)
C22	0.0241 (8)	0.0218 (8)	0.0190 (7)	-0.0005 (7)	0.0028 (6)	0.0035 (6)
O23	0.0259 (6)	0.0319 (7)	0.0370 (7)	0.0037 (5)	0.0055 (5)	-0.0106 (6)
O24	0.0213 (6)	0.0260 (6)	0.0350 (7)	-0.0013 (5)	0.0020 (5)	-0.0041 (5)
C25	0.0194 (8)	0.0346 (10)	0.0545 (12)	-0.0011 (8)	0.0020 (8)	-0.0052 (9)

Geometric parameters (Å, º)

N1—H1	0.90 (2)	C14—H14	1.0000
N1—C2	1.343 (2)	C14—C15	1.542 (2)
N1—C15	1.455 (2)	C14—C21	1.556 (2)
C2—O3	1.2383 (19)	C15—H15	1.0000
C2—C4	1.497 (2)	C15—C16	1.549 (2)
C4—C5	1.391 (2)	C16—H16	1.0000
C4—C13	1.400 (2)	C16—C17	1.507 (2)
C5—H5	0.9500	C16—C21	1.579 (2)
C5—C6	1.387 (2)	C17—O18	1.199 (2)

C6—H6	0.9500	C17—O19	1.344 (2)
C6—C7	1.395 (2)	O19—C20	1.450 (2)
C7—C8	1.500 (2)	C20—H20A	0.9800
C7—C12	1.390 (2)	C20—H20B	0.9800
C8—F9	1.328 (2)	C20—H20C	0.9800
C8—F10	1.321 (3)	C21—H21	1.0000
C8—F11	1.325 (2)	C21—C22	1.508 (2)
C8—F9B	1.241 (9)	C22—O23	1.204 (2)
C8—F10B	1.311 (9)	C22—O24	1.336 (2)
C8—F11B	1.283 (11)	O24—C25	1.451 (2)
C12—H12	0.9500	C25—H25A	0.9800
C12—C13	1.392 (2)	C25—H25B	0.9800
C13—C14	1.492 (2)	C25—H25C	0.9800
C2—N1—H1	115.3 (13)	C15—C14—C21	88.85 (12)
C2—N1—C15	126.95 (14)	C21—C14—H14	110.4
C15—N1—H1	117.8 (13)	N1—C15—C14	111.90 (12)
N1—C2—C4	117.97 (14)	N1—C15—H15	114.1
O3—C2—N1	121.80 (15)	N1—C15—C16	110.90 (13)
O3—C2—C4	120.23 (14)	C14—C15—H15	114.1
C5—C4—C2	118.91 (14)	C14—C15—C16	89.23 (12)
C5—C4—C13	120.15 (15)	C16—C15—H15	114.1
C13—C4—C2	120.91 (14)	C15—C16—H16	113.9
C4—C5—H5	119.7	C15—C16—C21	87.77 (11)
C6—C5—C4	120.65 (15)	C17—C16—C15	113.70 (13)
C6—C5—H5	119.7	C17—C16—H16	113.9
C5—C6—H6	120.5	C17—C16—C21	110.93 (13)
C5—C6—C7	119.04 (15)	C21—C16—H16	113.9
C7—C6—H6	120.5	O18—C17—C16	126.37 (15)
C6—C7—C8	118.91 (15)	O18—C17—O19	124.19 (15)
C12—C7—C6	120.80 (15)	O19—C17—C16	109.36 (14)
C12—C7—C8	120.29 (15)	C17—O19—C20	116.41 (14)
F9—C8—C7	112.79 (16)	O19—C20—H20A	109.5
F10—C8—C7	112.12 (16)	O19—C20—H20B	109.5

F10—C8—F9	105.14 (19)	O19—C20—H20C	109.5
F10—C8—F11	107.6 (2)	H20A—C20—H20B	109.5
F11—C8—C7	113.70 (15)	H20A—C20—H20C	109.5
F11—C8—F9	104.79 (18)	H20B—C20—H20C	109.5
F9B—C8—C7	115.4 (5)	C14—C21—C16	87.65 (11)
F9B—C8—F10B	109.8 (8)	C14—C21—H21	111.2
F9B—C8—F11B	107.7 (10)	C16—C21—H21	111.2
F10B—C8—C7	110.0 (4)	C22—C21—C14	116.81 (13)
F11B—C8—C7	110.4 (6)	C22—C21—C16	116.71 (12)
F11B—C8—F10B	102.8 (9)	C22—C21—H21	111.2
C7—C12—H12	120.0	O23—C22—C21	124.26 (15)
C7—C12—C13	120.04 (15)	O23—C22—O24	124.16 (15)
C13—C12—H12	120.0	O24—C22—C21	111.56 (13)
C4—C13—C14	118.94 (14)	C22—O24—C25	114.86 (13)
C12—C13—C4	119.27 (14)	O24—C25—H25A	109.5
C12—C13—C14	121.70 (14)	O24—C25—H25B	109.5
C13—C14—H14	110.4	O24—C25—H25C	109.5
C13—C14—C15	117.68 (13)	H25A—C25—H25B	109.5
C13—C14—C21	117.35 (13)	H25A—C25—H25C	109.5
C15—C14—H14	110.4	H25B—C25—H25C	109.5

N1—C2—C4—C5	-174.88 (15)	C12—C7—C8—F11B	-62.6 (10)
N1—C2—C4—C13	7.1 (2)	C12—C13—C14—C15	163.16 (15)
N1—C15—C16—C17	-153.98 (13)	C12—C13—C14—C21	-92.61 (19)
N1—C15—C16—C21	94.09 (13)	C13—C4—C5—C6	1.3 (2)
C2—N1—C15—C14	-20.0 (2)	C13—C14—C15—N1	27.7 (2)
C2—N1—C15—C16	-117.89 (17)	C13—C14—C15—C16	139.96 (14)
C2—C4—C5—C6	-176.77 (15)	C13—C14—C21—C16	-139.88 (14)
C2—C4—C13—C12	178.95 (14)	C13—C14—C21—C22	101.22 (16)
C2—C4—C13—C14	2.3 (2)	C14—C15—C16—C17	92.81 (14)
O3—C2—C4—C5	5.5 (2)	C14—C15—C16—C21	-19.12 (11)
O3—C2—C4—C13	-172.51 (15)	C14—C21—C22—O23	17.4 (2)
C4—C5—C6—C7	-2.0 (2)	C14—C21—C22—O24	-164.05 (13)
C4—C13—C14—C15	-20.3 (2)	C15—N1—C2—O3	-177.39 (16)

C4—C13—C14—C21	83.94 (19)	C15—N1—C2—C4	3.0 (2)
C5—C4—C13—C12	1.0 (2)	C15—C14—C21—C16	-19.03 (11)
C5—C4—C13—C14	-175.68 (14)	C15—C14—C21—C22	-137.93 (13)
C5—C6—C7—C8	179.95 (16)	C15—C16—C17—O18	-3.1 (2)
C5—C6—C7—C12	0.5 (2)	C15—C16—C17—O19	-179.91 (13)
C6—C7—C8—F9	47.5 (3)	C15—C16—C21—C14	18.96 (11)
C6—C7—C8—F10	-70.9 (3)	C15—C16—C21—C22	137.94 (14)
C6—C7—C8—F11	166.7 (2)	C16—C17—O19—C20	173.68 (15)
C6—C7—C8—F9B	-4.5 (10)	C16—C21—C22—O23	-84.3 (2)
C6—C7—C8—F10B	-129.3 (7)	C16—C21—C22—O24	94.26 (16)
C6—C7—C8—F11B	117.9 (10)	C17—C16—C21—C14	-95.61 (14)
C6—C7—C12—C13	1.7 (2)	C17—C16—C21—C22	23.38 (19)
C7—C12—C13—C4	-2.4 (2)	O18—C17—O19—C20	-3.2 (2)
C7—C12—C13—C14	174.10 (15)	C21—C14—C15—N1	-92.88 (14)
C8—C7—C12—C13	-177.73 (16)	C21—C14—C15—C16	19.40 (11)
C12—C7—C8—F9	-133.0 (2)	C21—C16—C17—O18	93.9 (2)
C12—C7—C8—F10	108.5 (2)	C21—C16—C17—O19	-82.88 (16)
C12—C7—C8—F11	-13.9 (3)	C21—C22—O24—C25	-176.05 (14)
C12—C7—C8—F9B	175.0 (10)	O23—C22—O24—C25	2.5 (2)
C12—C7—C8—F10B	50.1 (8)		

Hydrogen-bond geometry (Å, º)

D—H···*A*	*D*—H	H···*A*	*D*···*A*	*D*—H···*A*
N1—H1···O3^{i}	0.90 (2)	1.98 (2)	2.8842 (18)	173.4 (19)

Symmetry code: (i) -*x*, -*y*+2, -*z*+1.

Document origin: *publCIF* [Westrip, S. P. (2010). *J. Apply. Cryst.*, **43**, 920-925.

6. NMR Spectra

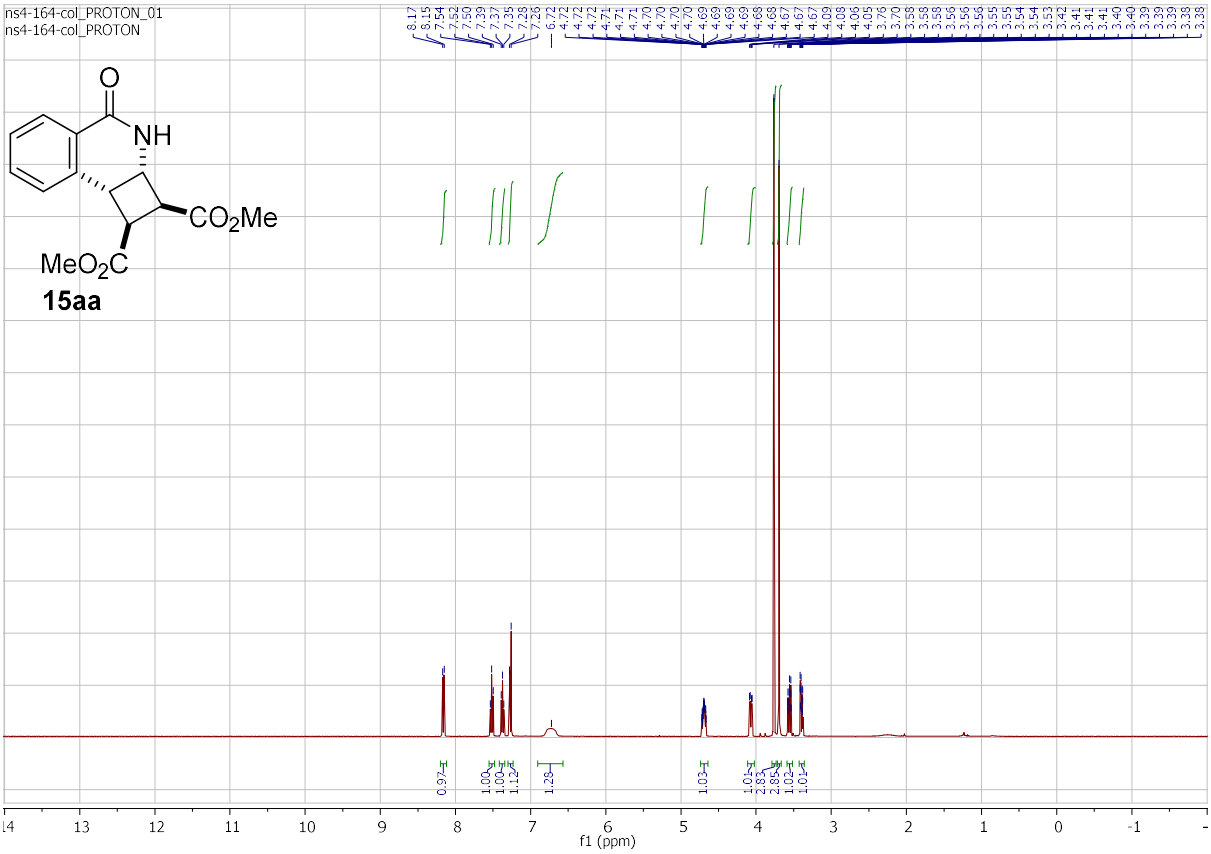
ns4-164-col_PROTON_01
ns4-164-col_PROTON
O
NH
CO2Me
MeO2C
15aa
f1 (ppm)

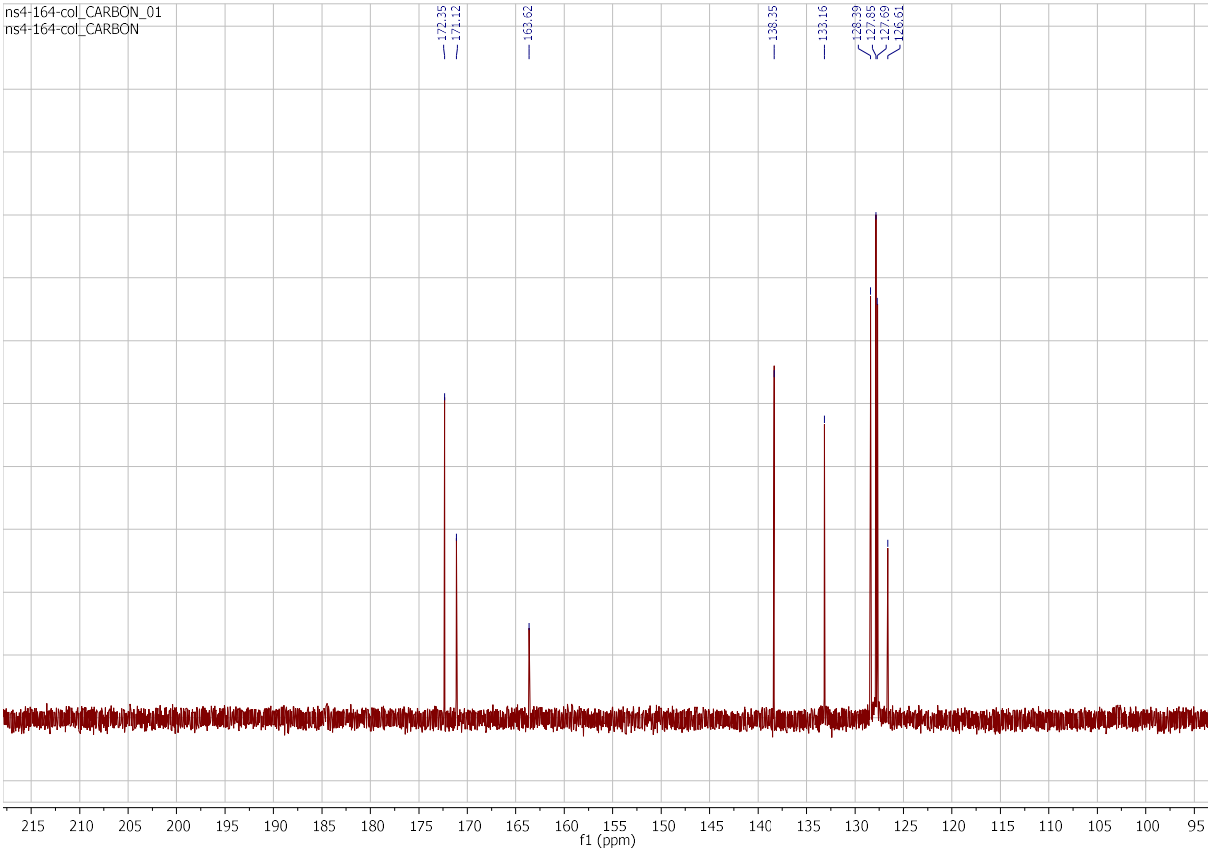
ns4-164-col_CARBON_01
ns4-164-col_CARBON
172.35
171.12
163.62
138.35
133.16
128.39
127.85
127.69
126.61
f1 (ppm)

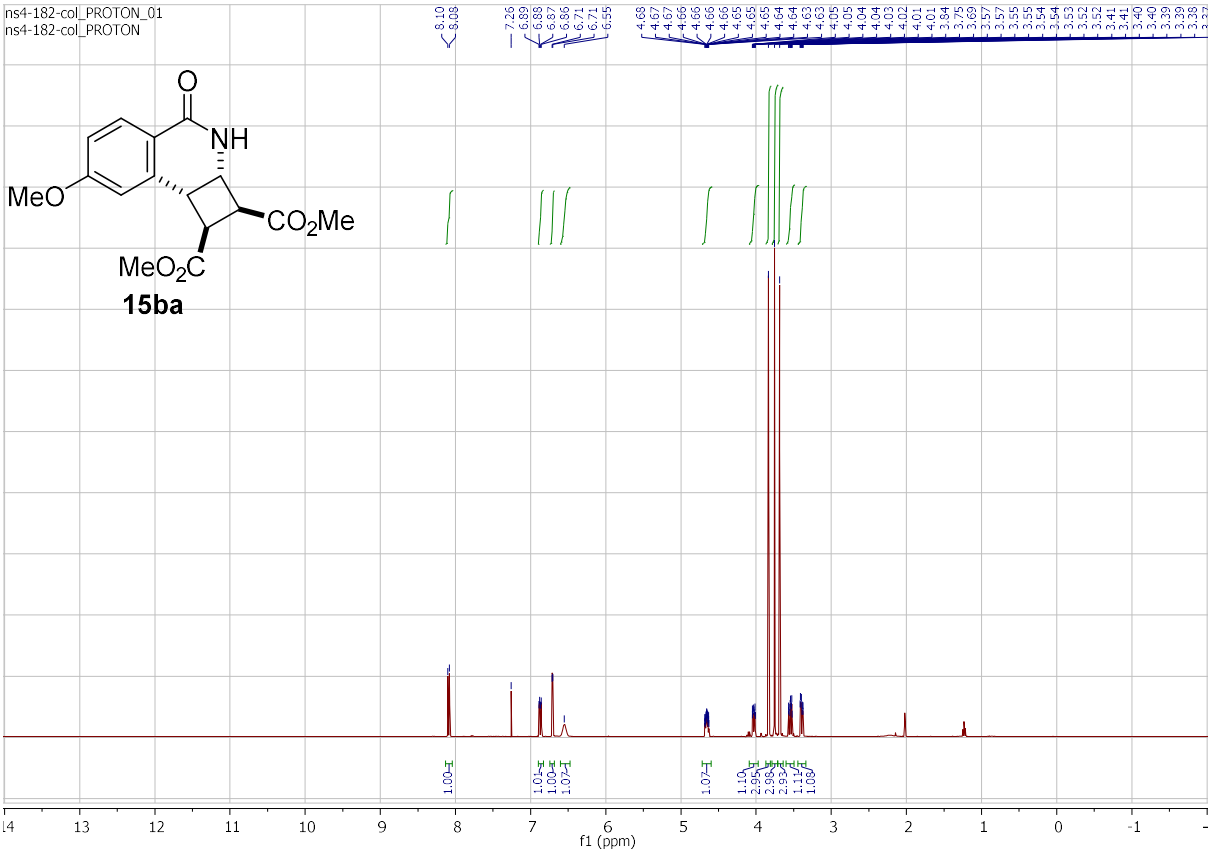
ns4-182-col_PROTON_01
ns4-182-col_PROTON
O
NH
MeO
CO2Me
MeO2C
15ba
f1 (ppm)

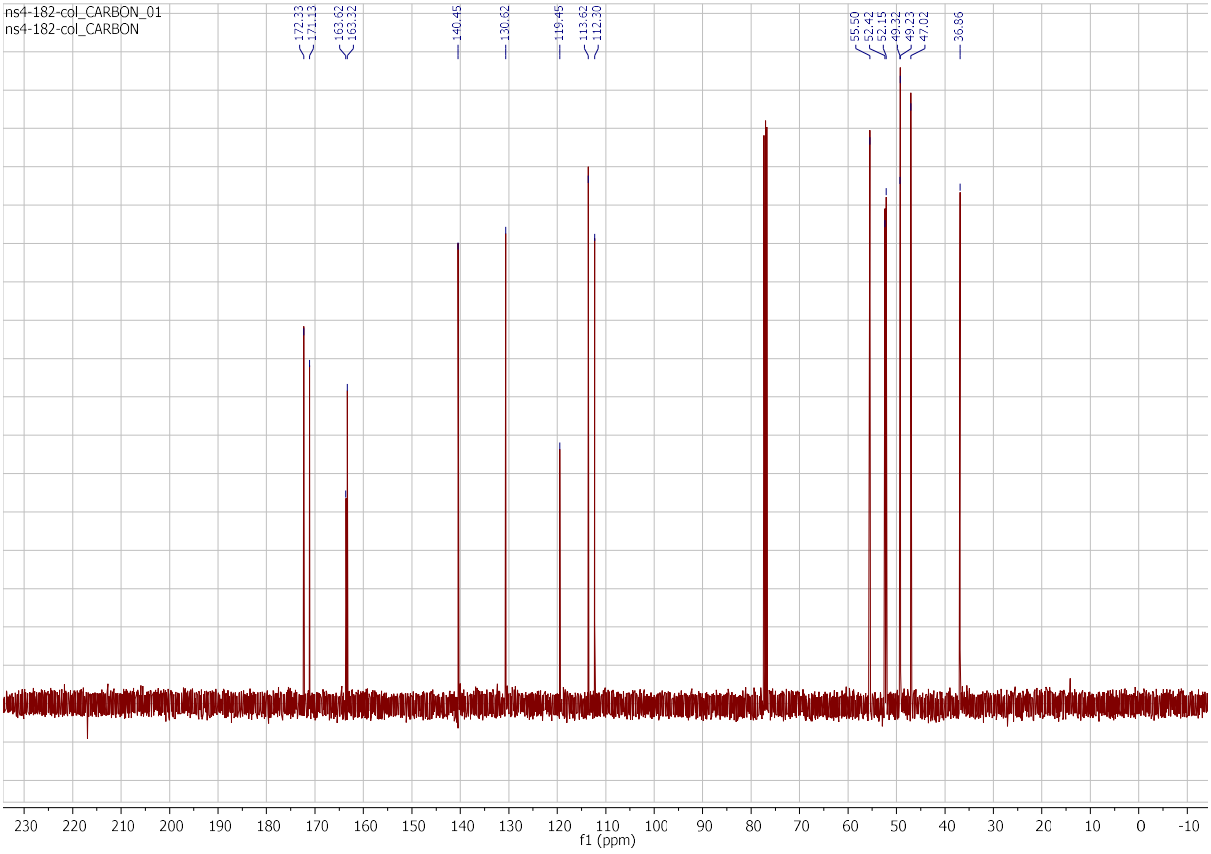
ns4-182-col_CARBON_01
ns4-182-col_CARBON
f1 (ppm)

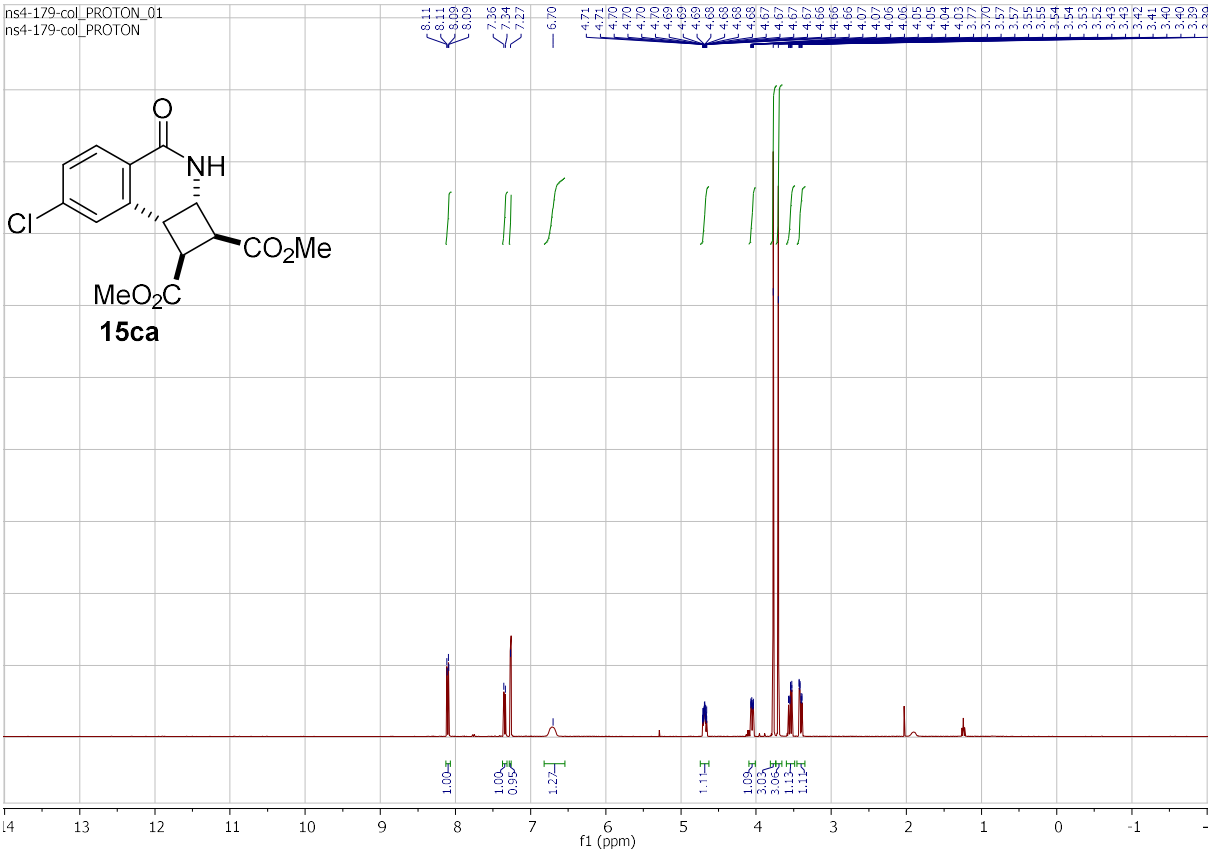
ns4-179-col_PROTON_01
ns4-179-col_PROTON
O
NH
Cl
CO2Me
MeO2C
15ca
f1 (ppm)

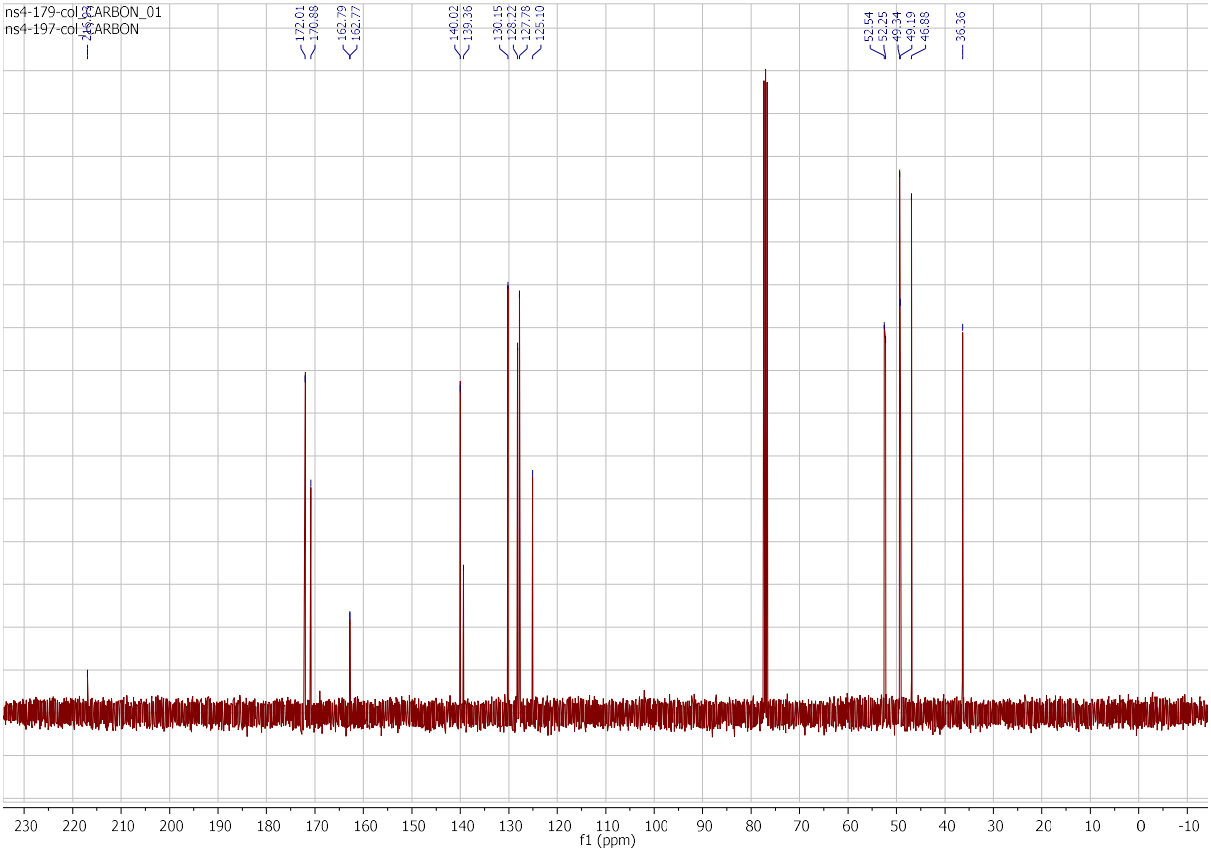
ns4-179-col_CARBON_01
ns4-197-col_CARBON
f1 (ppm)

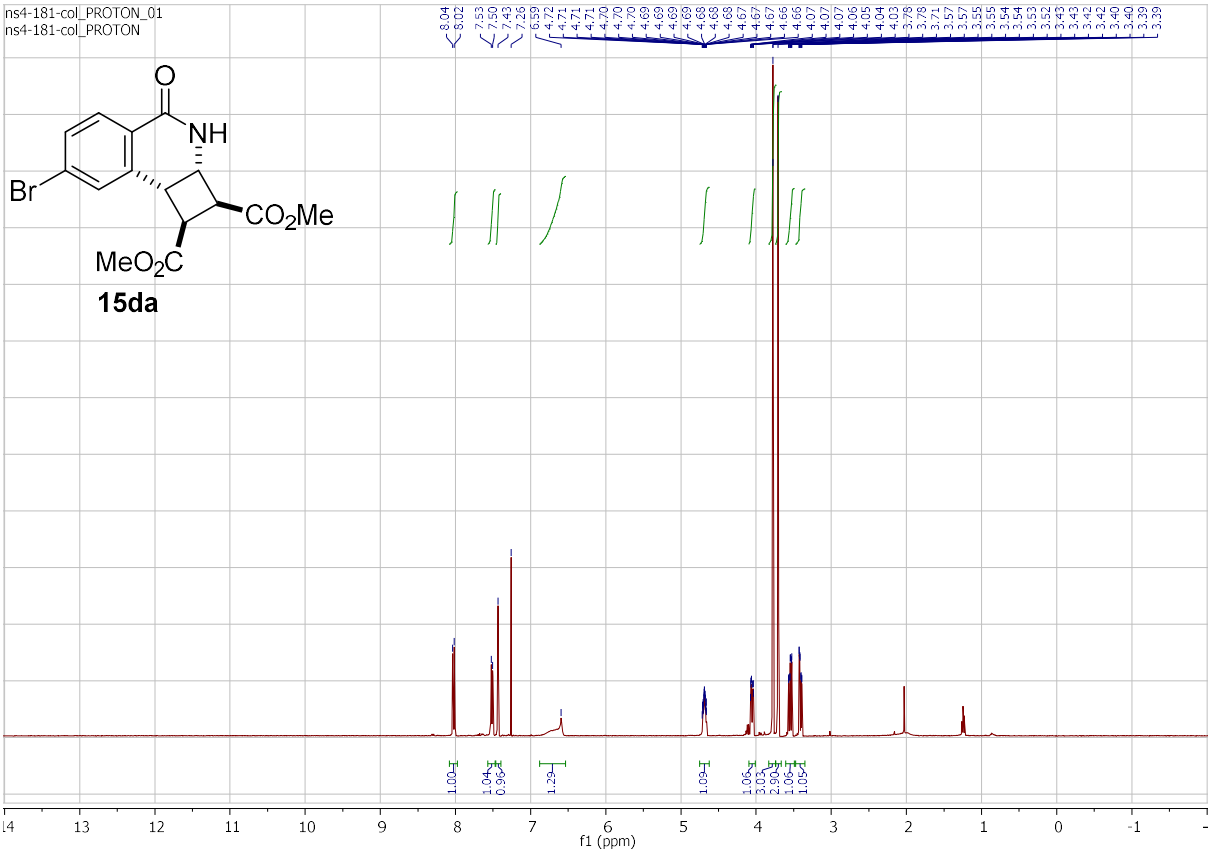
ns4-181-col_PROTON_01
ns4-181-col_PROTON
O
NH
Br
CO2Me
MeO2C
15da
f1 (ppm)

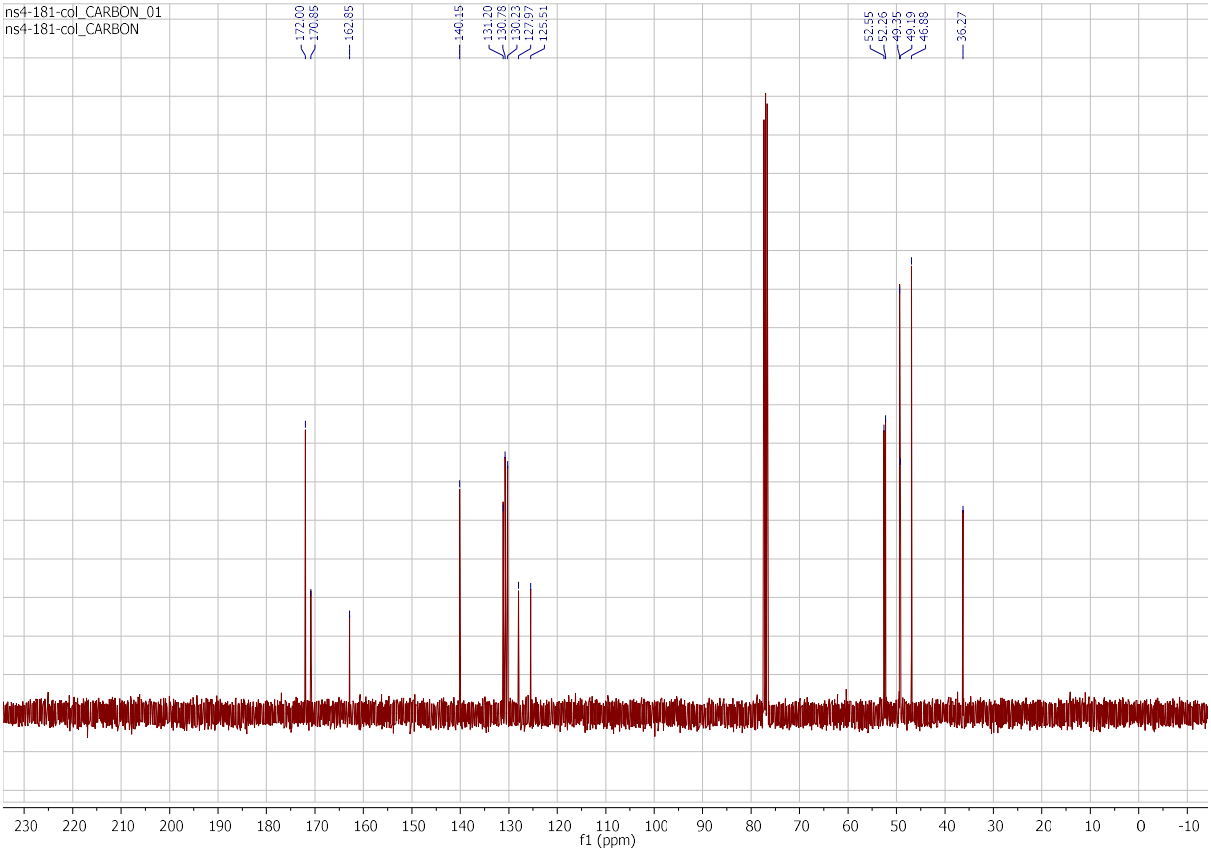
ns4-181-col_CARBON_01
ns4-181-col_CARBON
f1 (ppm)

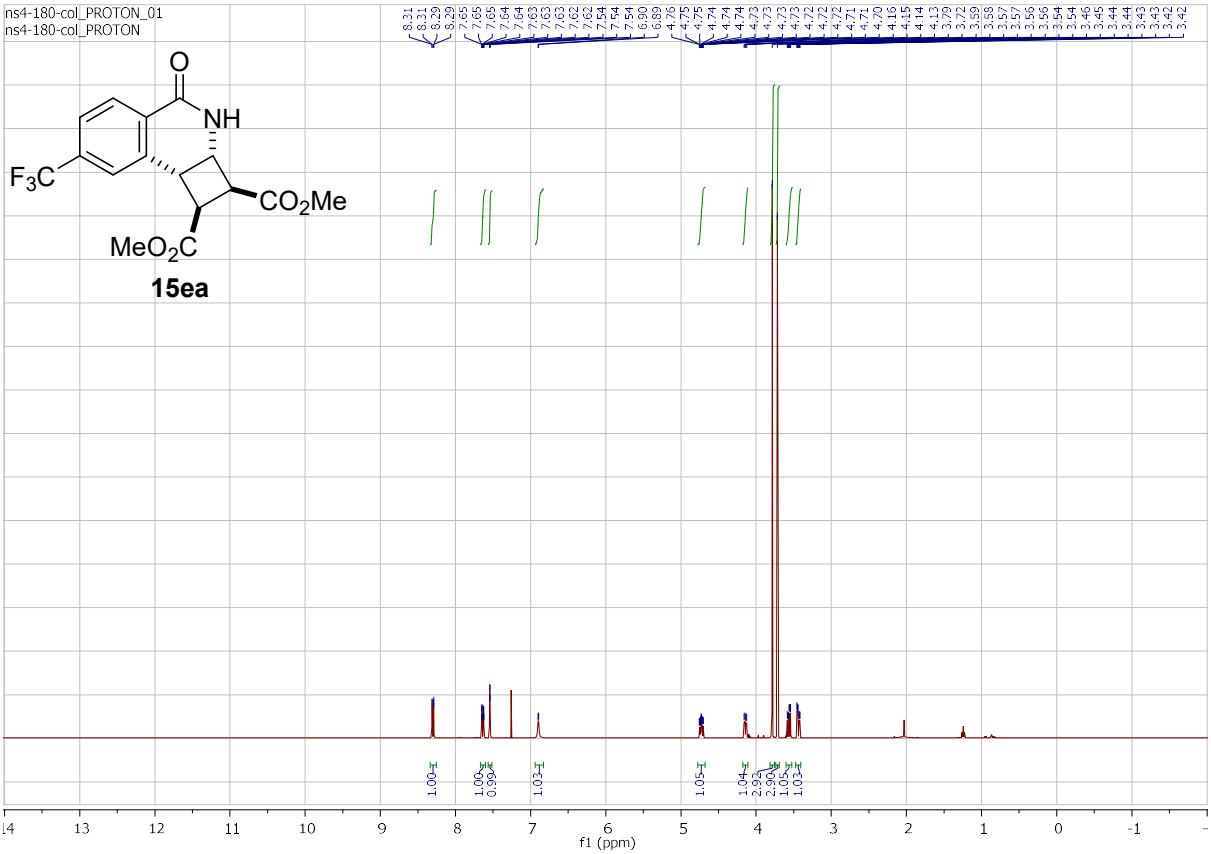
ns4-180-col_PROTON_01
ns4-180-col_PROTON
O
NH
F3C
CO2Me
MeO2C
15ea
f1 (ppm)

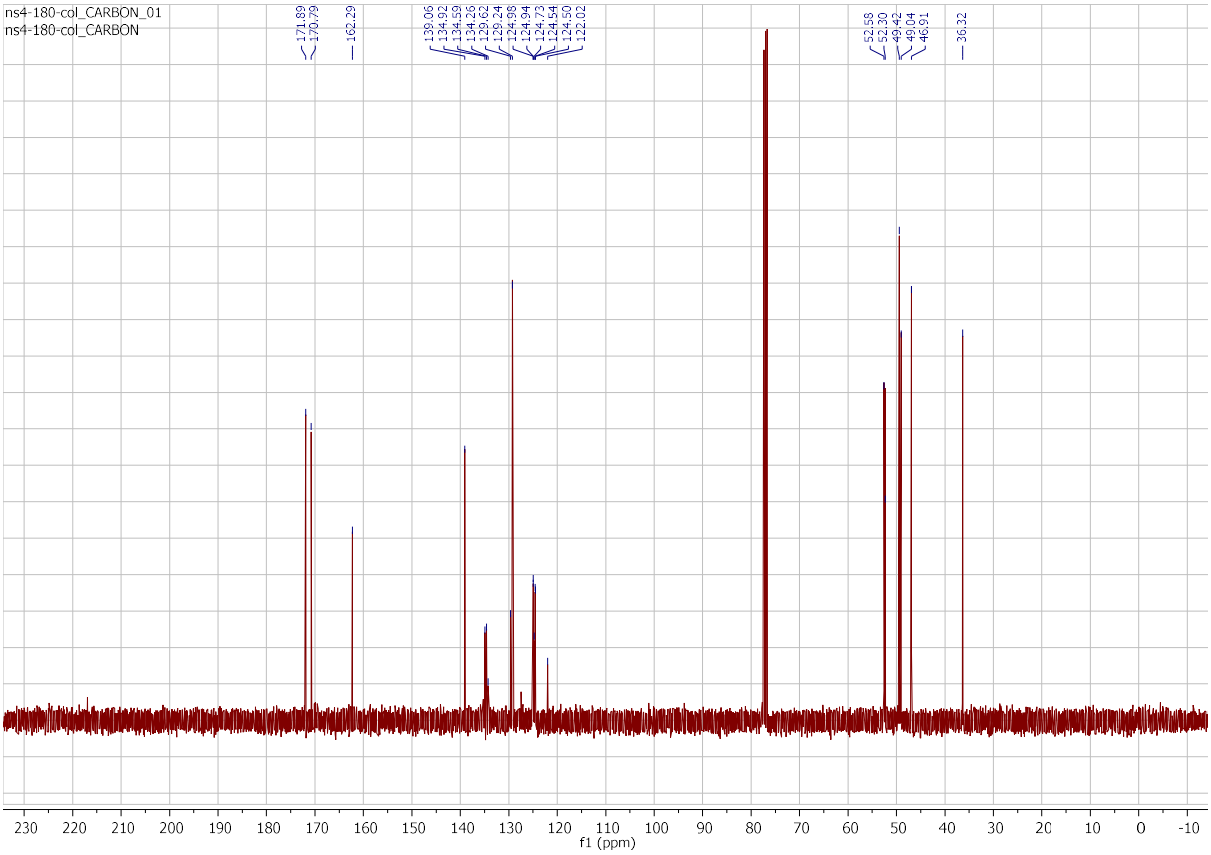
ns4-180-col_CARBON_01
ns4-180-col_CARBON
f1 (ppm)

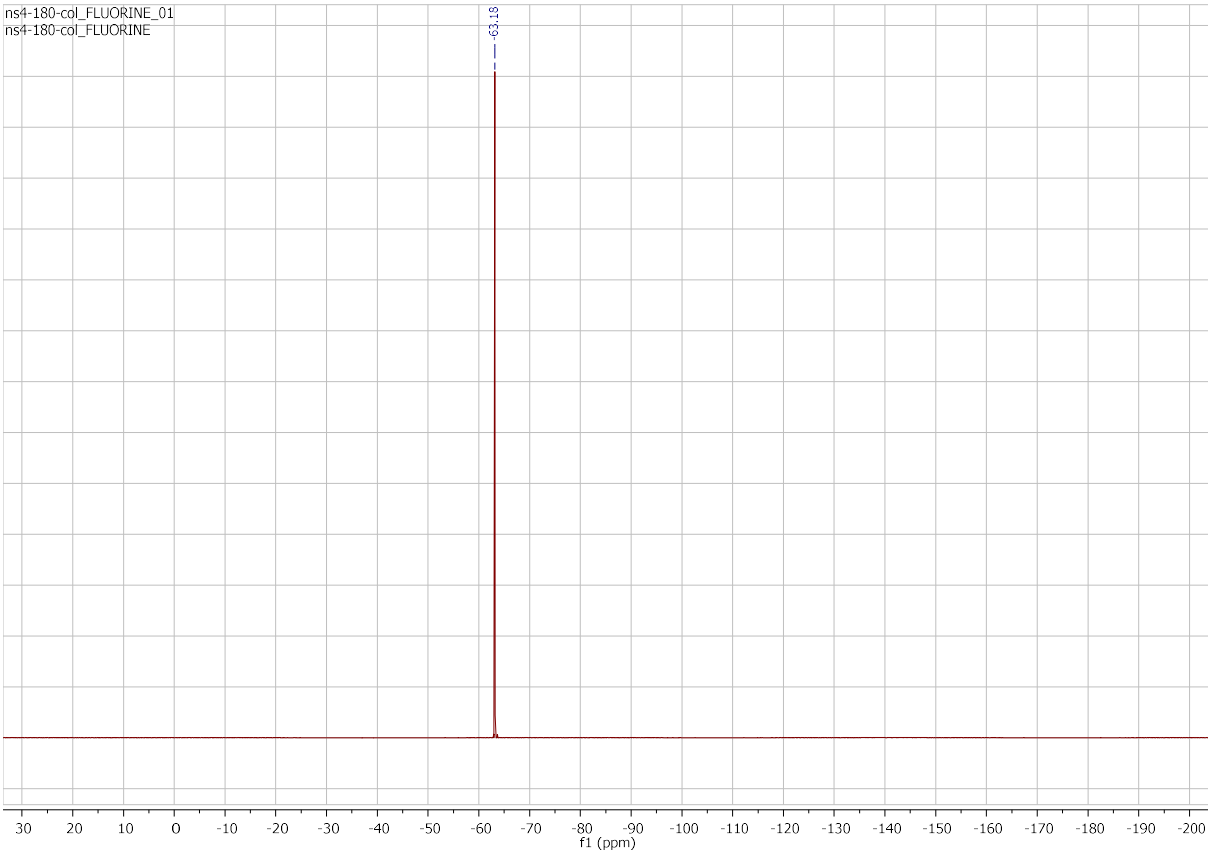
ns4-180-col_FLUORINE_01
ns4-180-col_FLUORINE
-63.18
30 20 10 0 -10 -20 -30 -40 -50 -60 -70 -80 -90 -100 -110 -120 -130 -140 -150 -160 -170 -180 -190 -200
f1 (ppm)

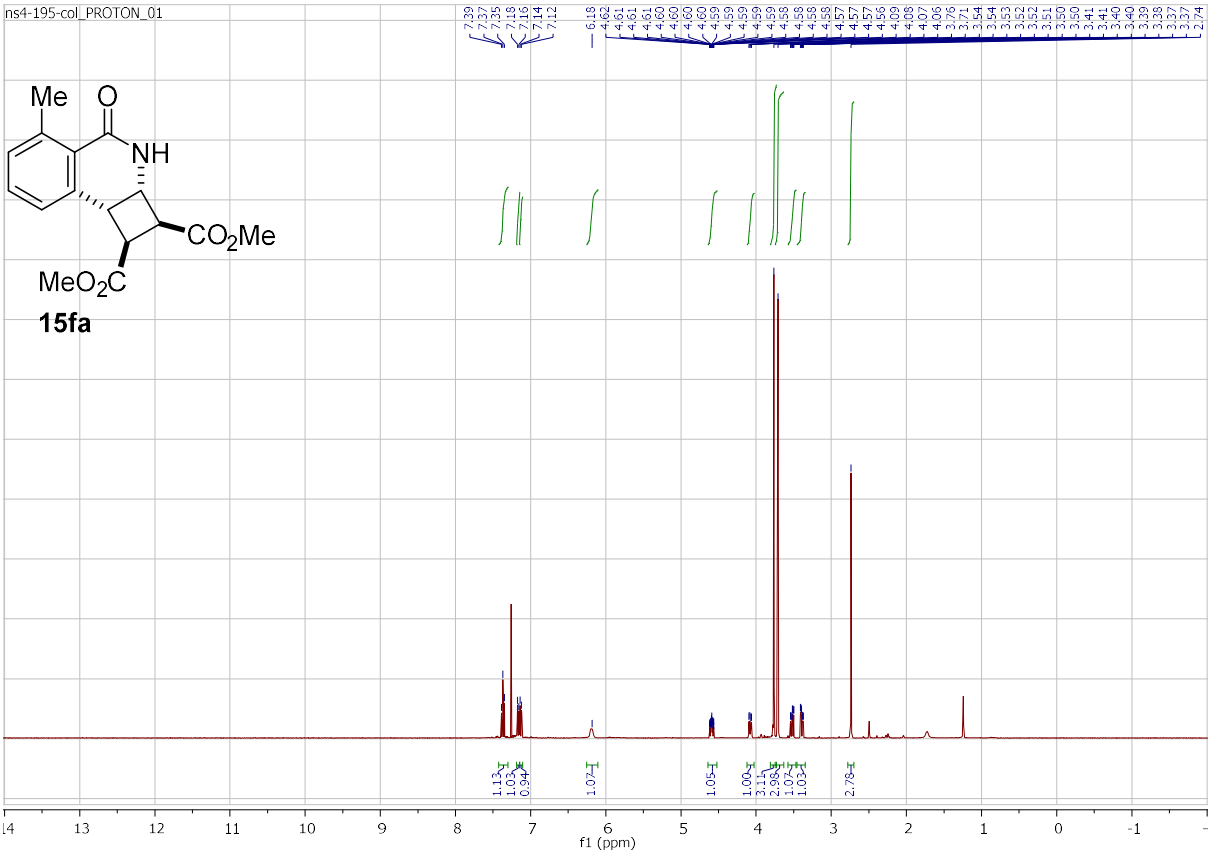
ns4-195-col_PROTON_01
Me
O
NH
CO2Me
MeO2C
15fa
f1 (ppm)

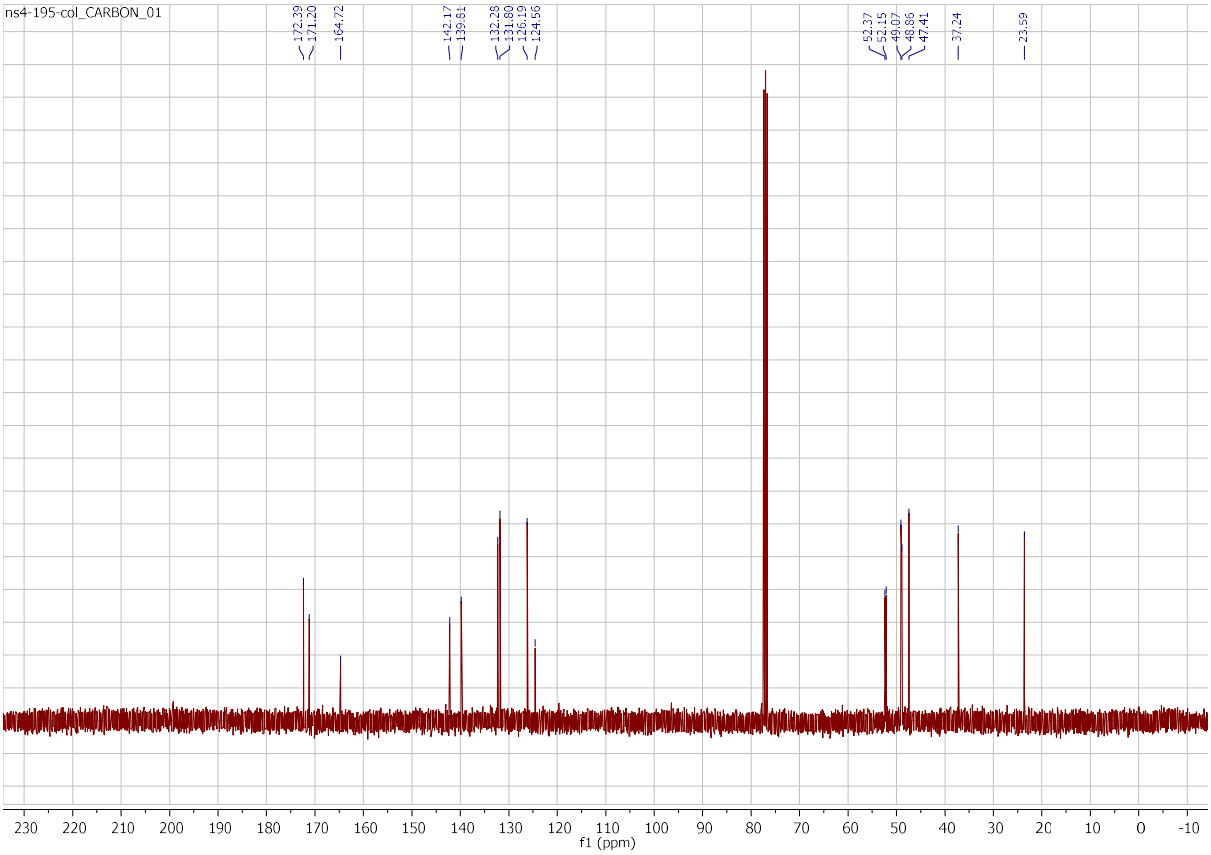
ns4-195-col_CARBON_01
f1 (ppm)

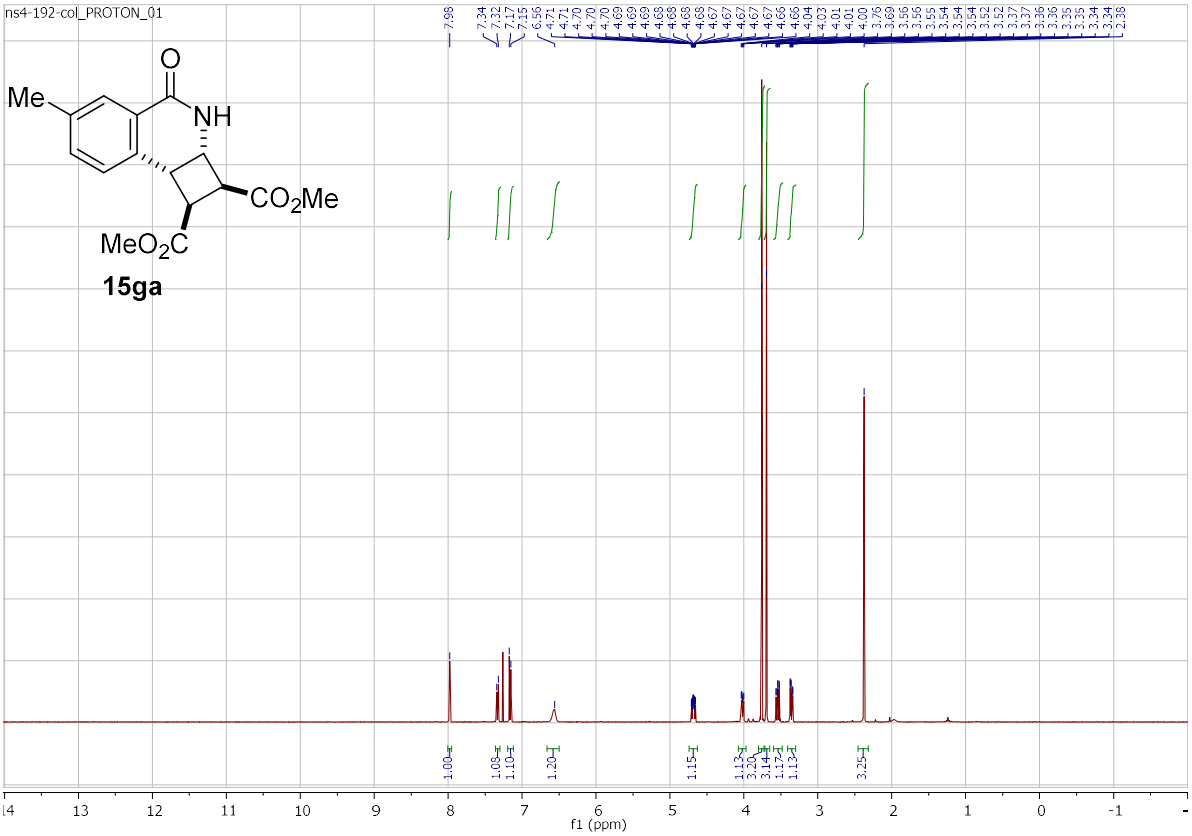
ns4-192-col_PROTON_01
Me
O
NH
CO2Me
MeO2C
15ga
f1 (ppm)

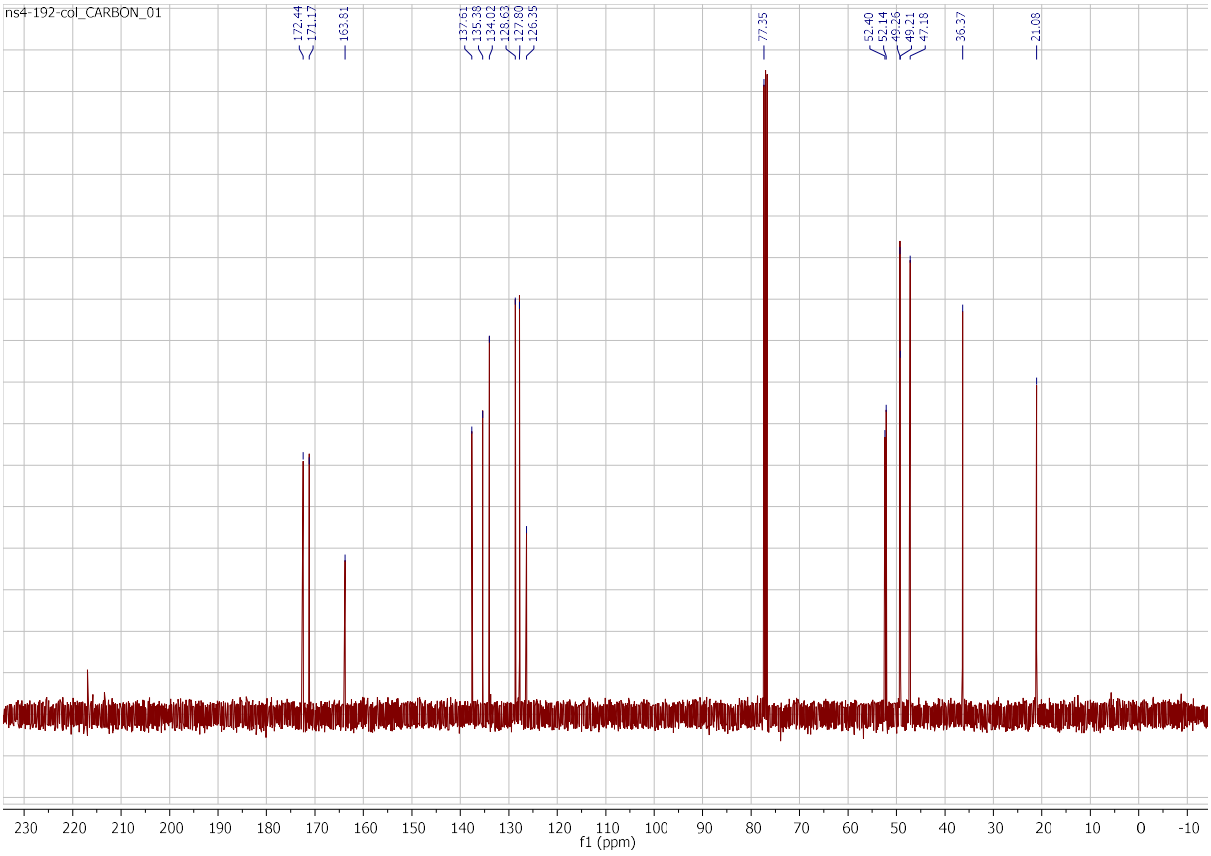
ns4-192-col_CARBON_01
f1 (ppm)

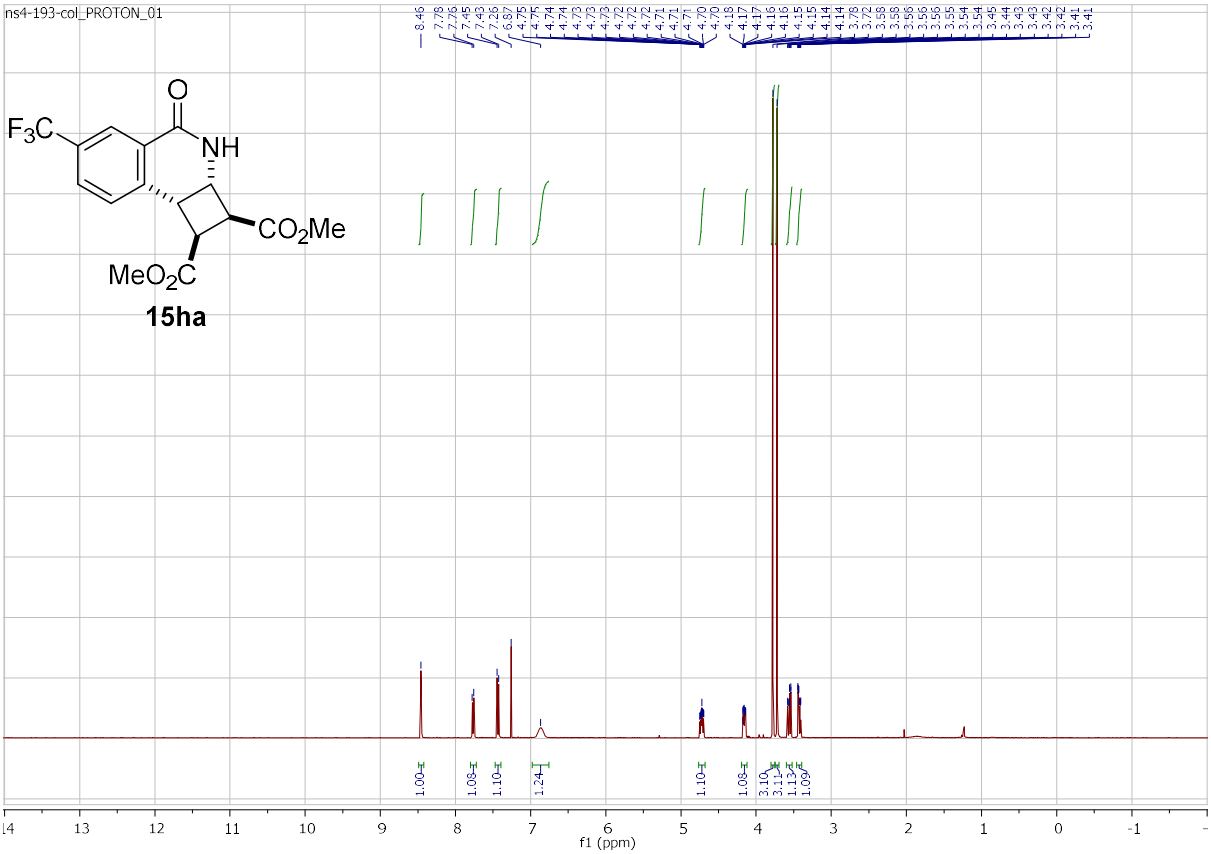
ns4-193-col_PROTON_01
F3C
O
NH
CO2Me
MeO2C
15ha
f1 (ppm)

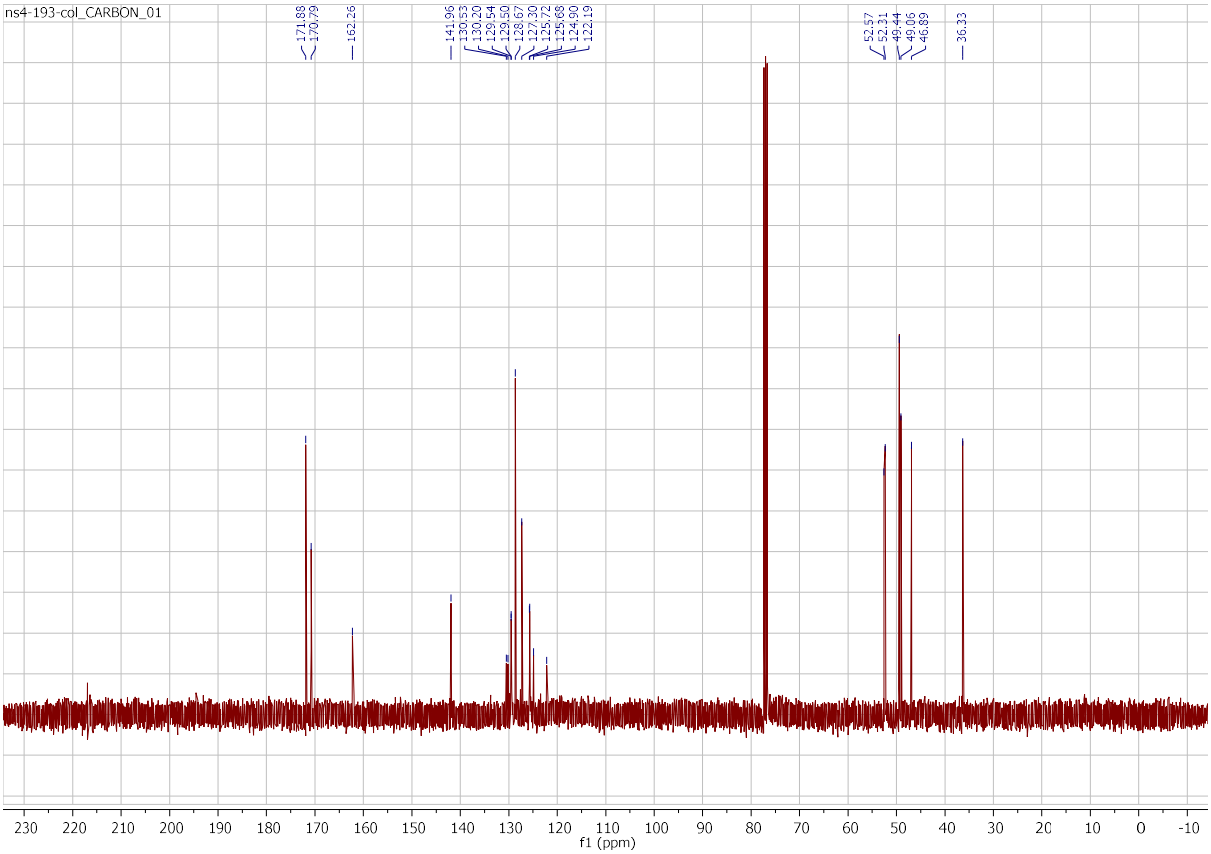
ns4-193-col_CARBON_01
f1 (ppm)

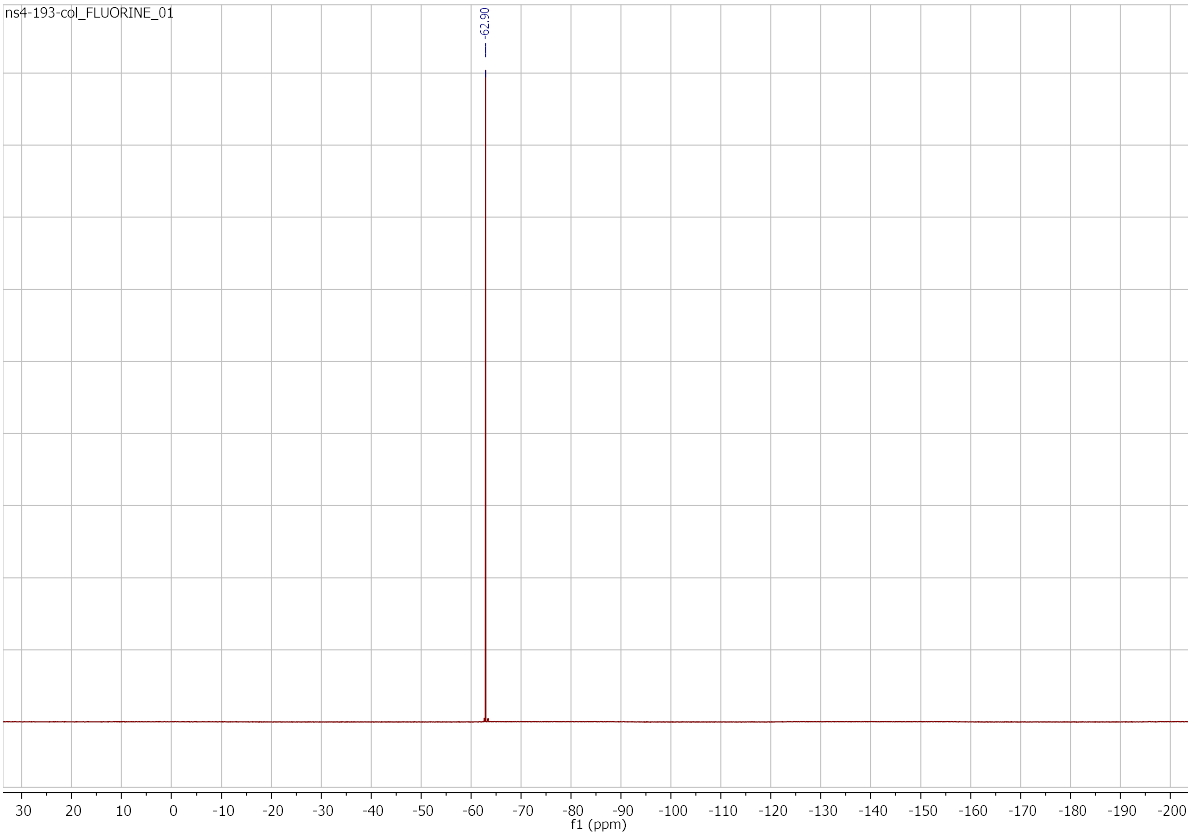
ns4-193-col_FLUORINE_01
-62.90
30 20 10 0 -10 -20 -30 -40 -50 -60 -70 -80 -90 -100 -110 -120 -130 -140 -150 -160 -170 -180 -190 -200
f1 (ppm)

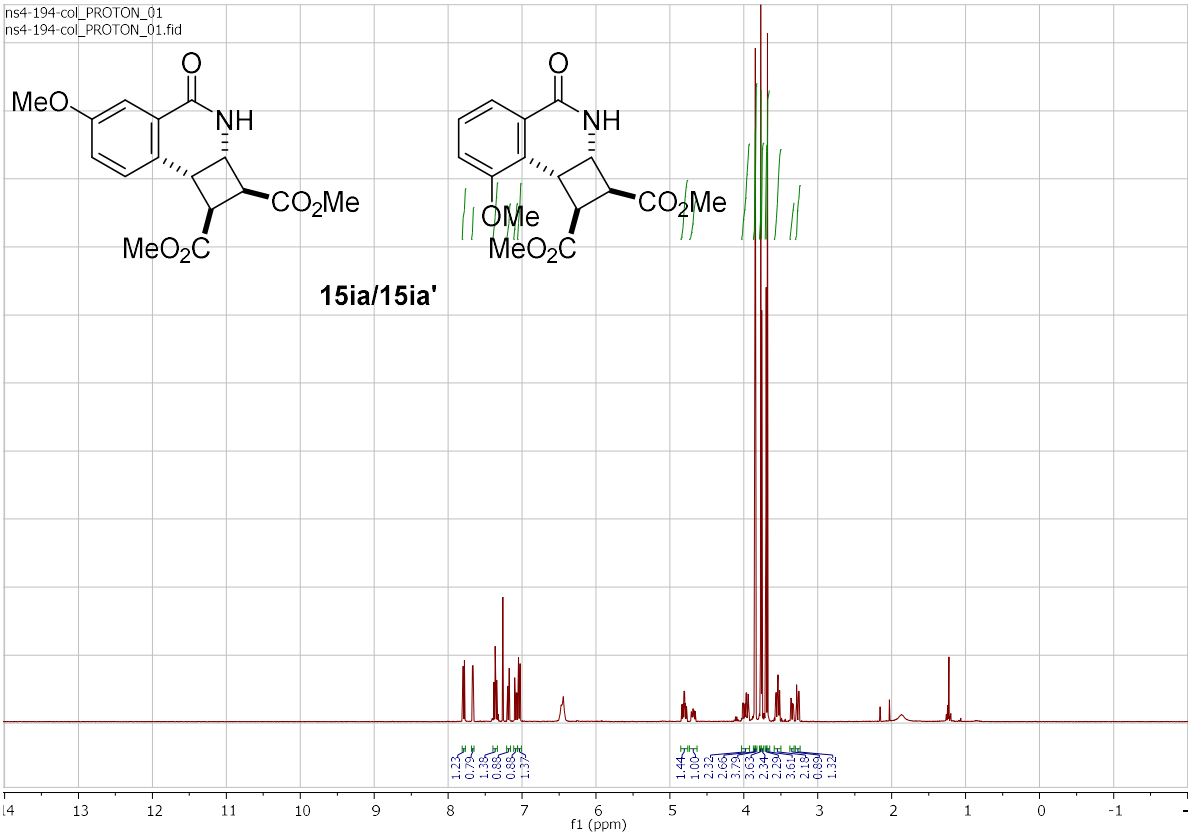
ns4-194-col_PROTON_01
ns4-194-col_PROTON_01.fid
MeO
O
NH
CO2Me
MeO2C
OMe
15ia/15ia'
f1 (ppm)

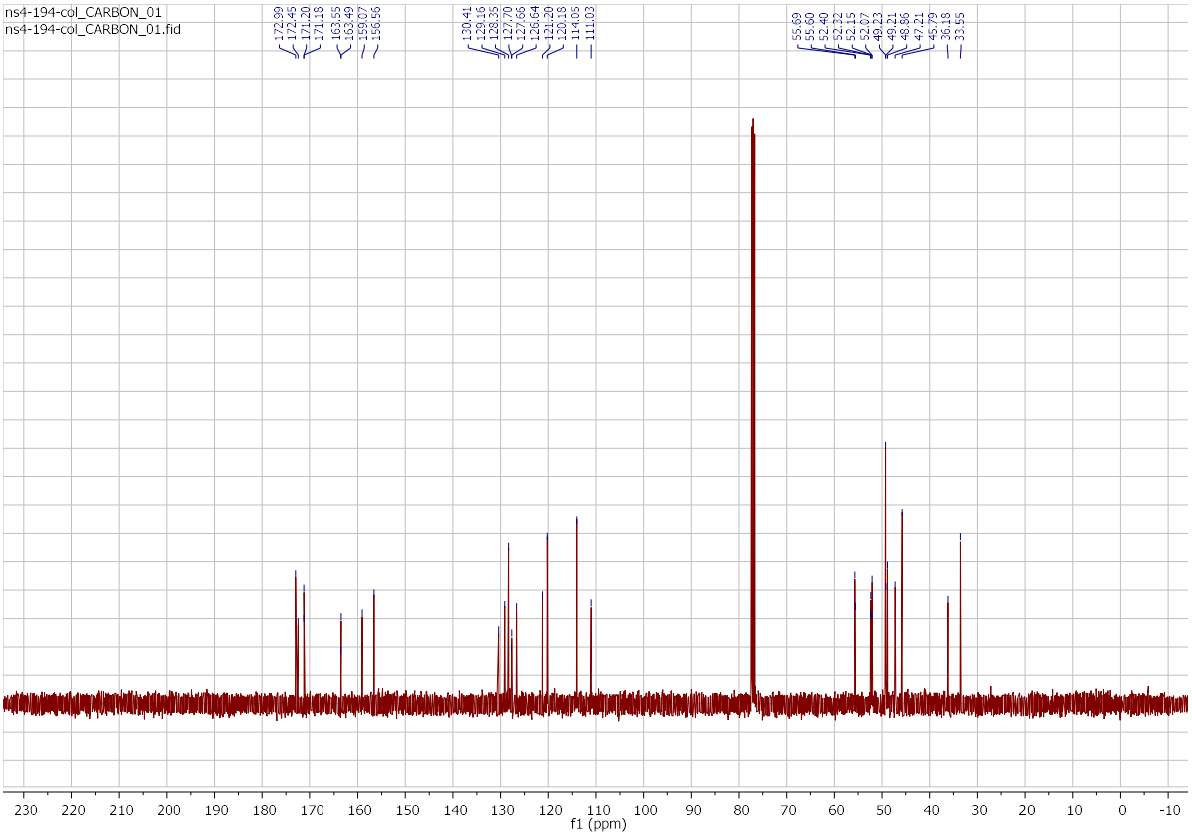
ns4-194-col_CARBON_01
ns4-194-col_CARBON_01.fid
f1 (ppm)

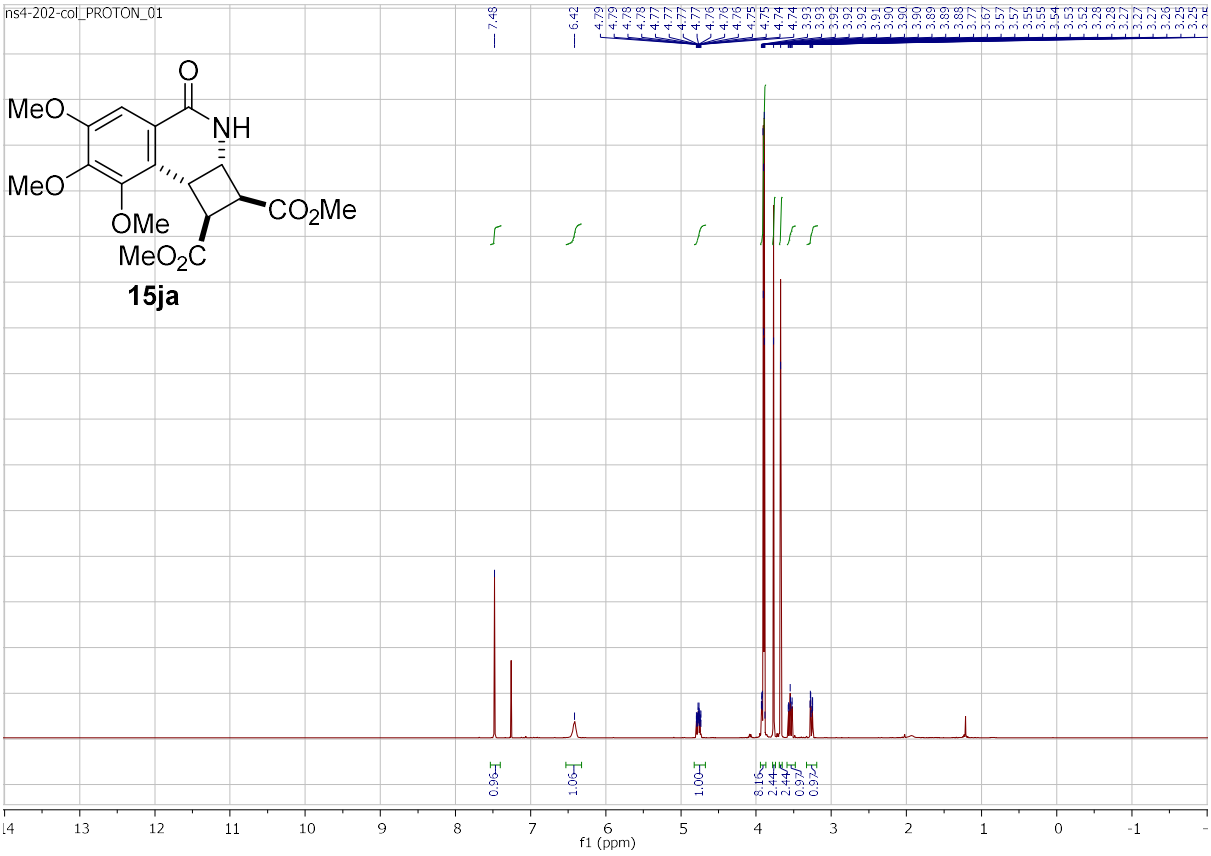
ns4-202-col_PROTON_01
MeO
MeO
OMe
MeO2C
O
NH
CO2Me
15ja
f1 (ppm)

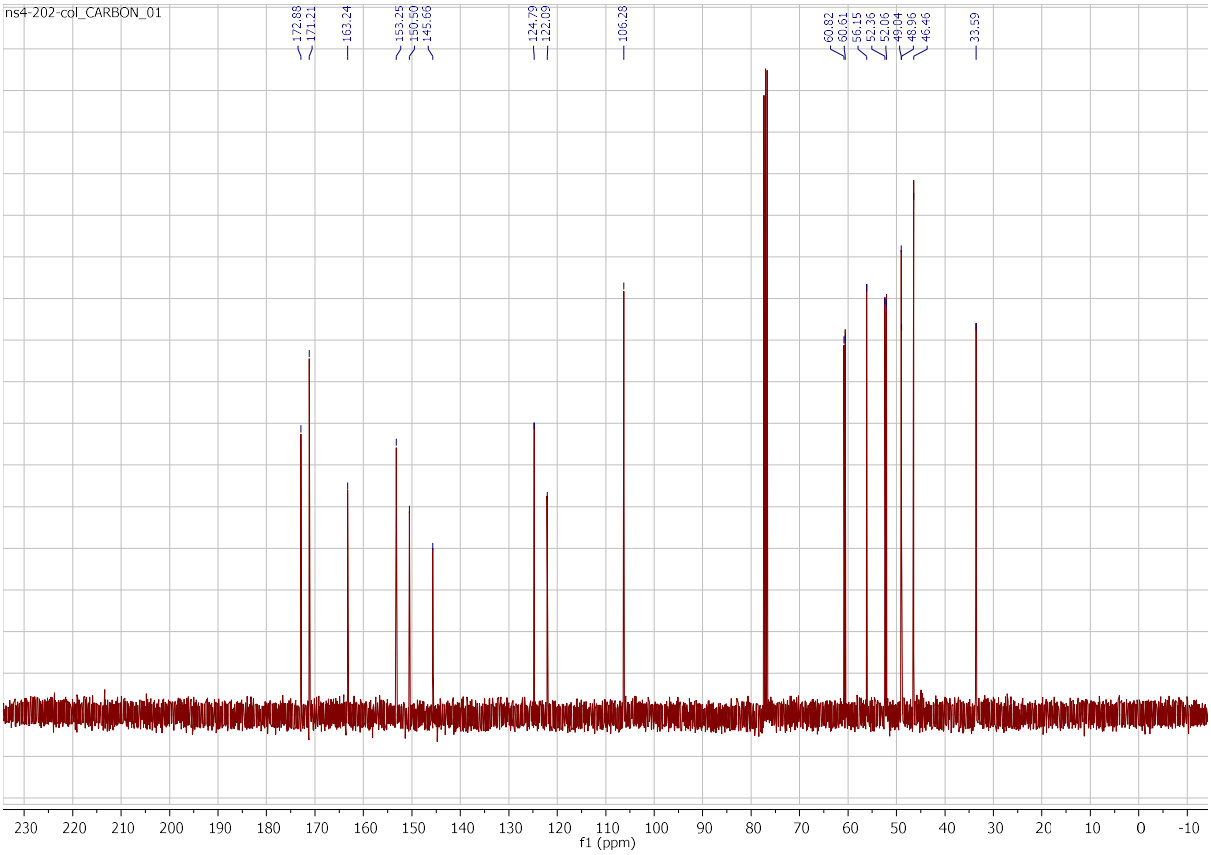
ns4-202-col_CARBON_01
f1 (ppm)

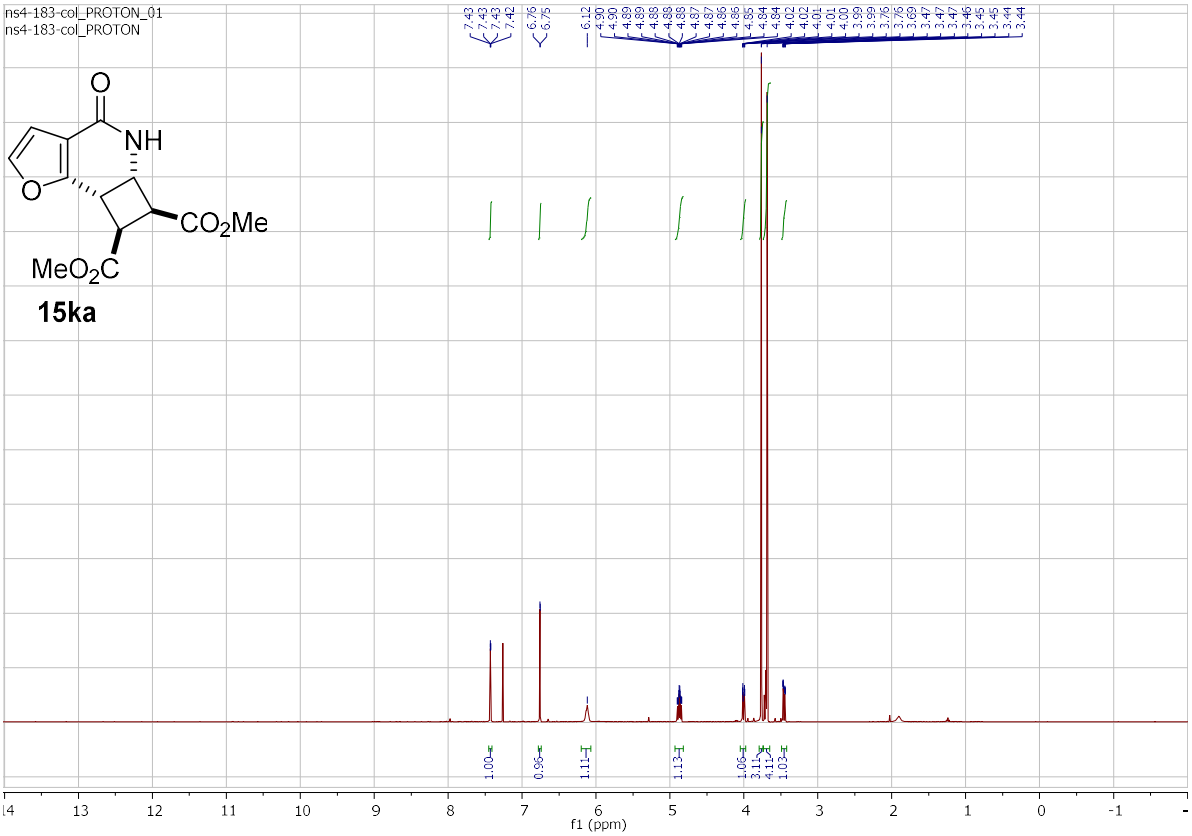
ns4-183-col_PROTON_01
ns4-183-col_PROTON
O
NH
O
CO2Me
MeO2C
15ka
f1 (ppm)

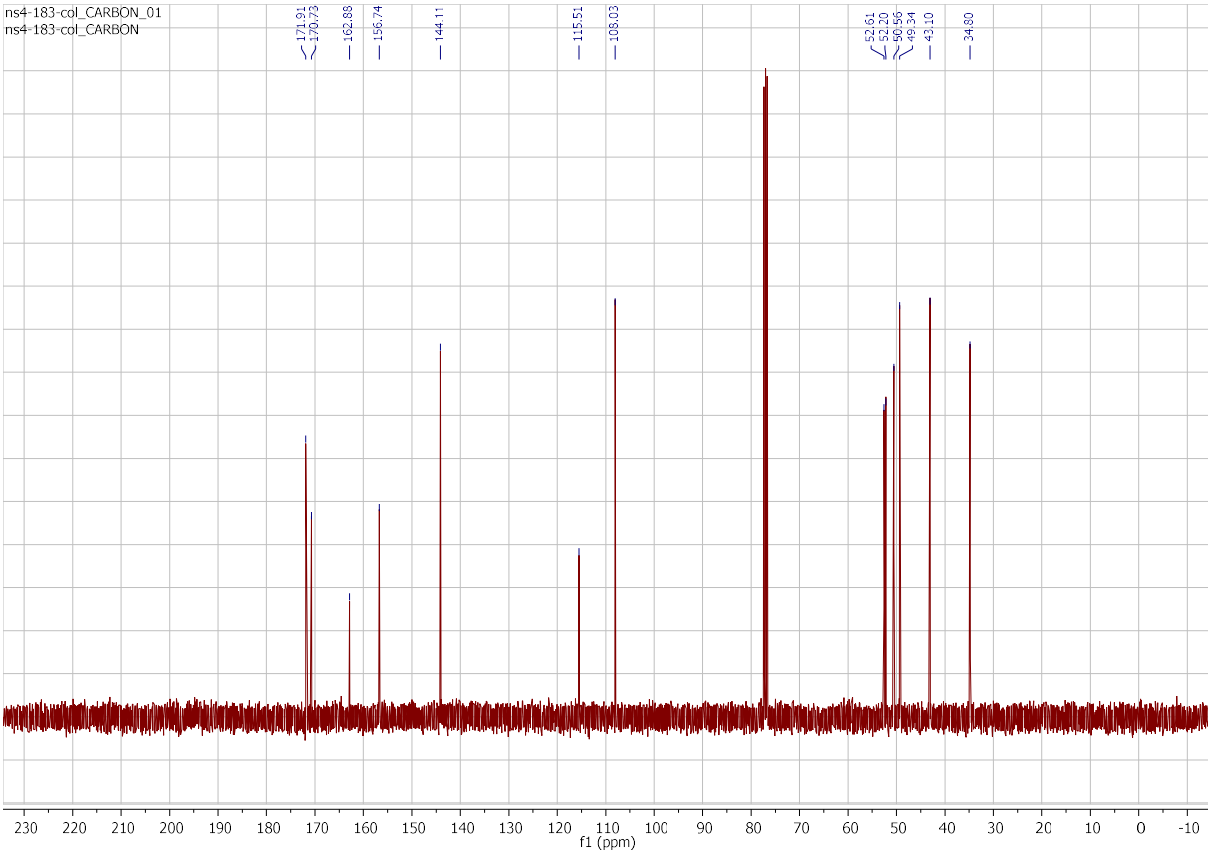
ns4-183-col_CARBON_01
ns4-183-col_CARBON
f1 (ppm)

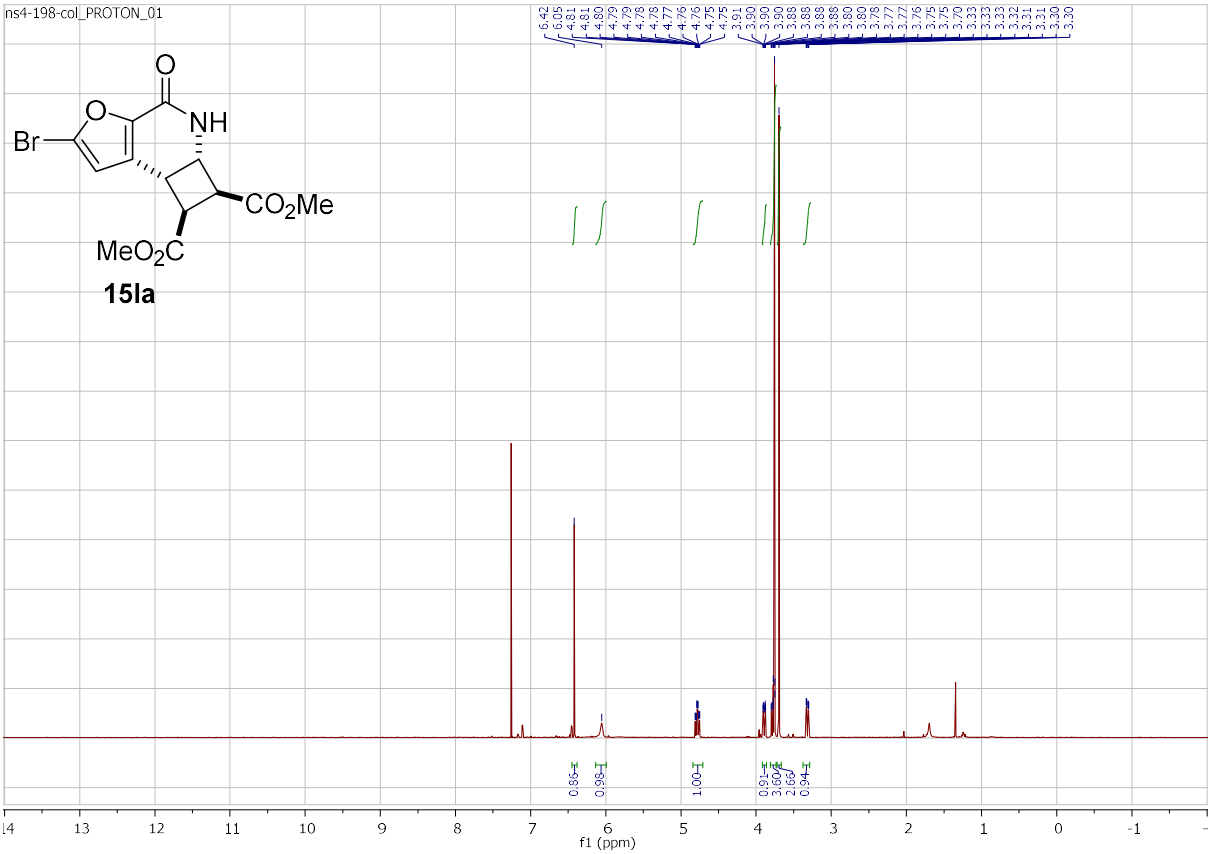
ns4-198-col_PROTON_01
O
O
NH
Br
CO2Me
MeO2C
15la
f1 (ppm)

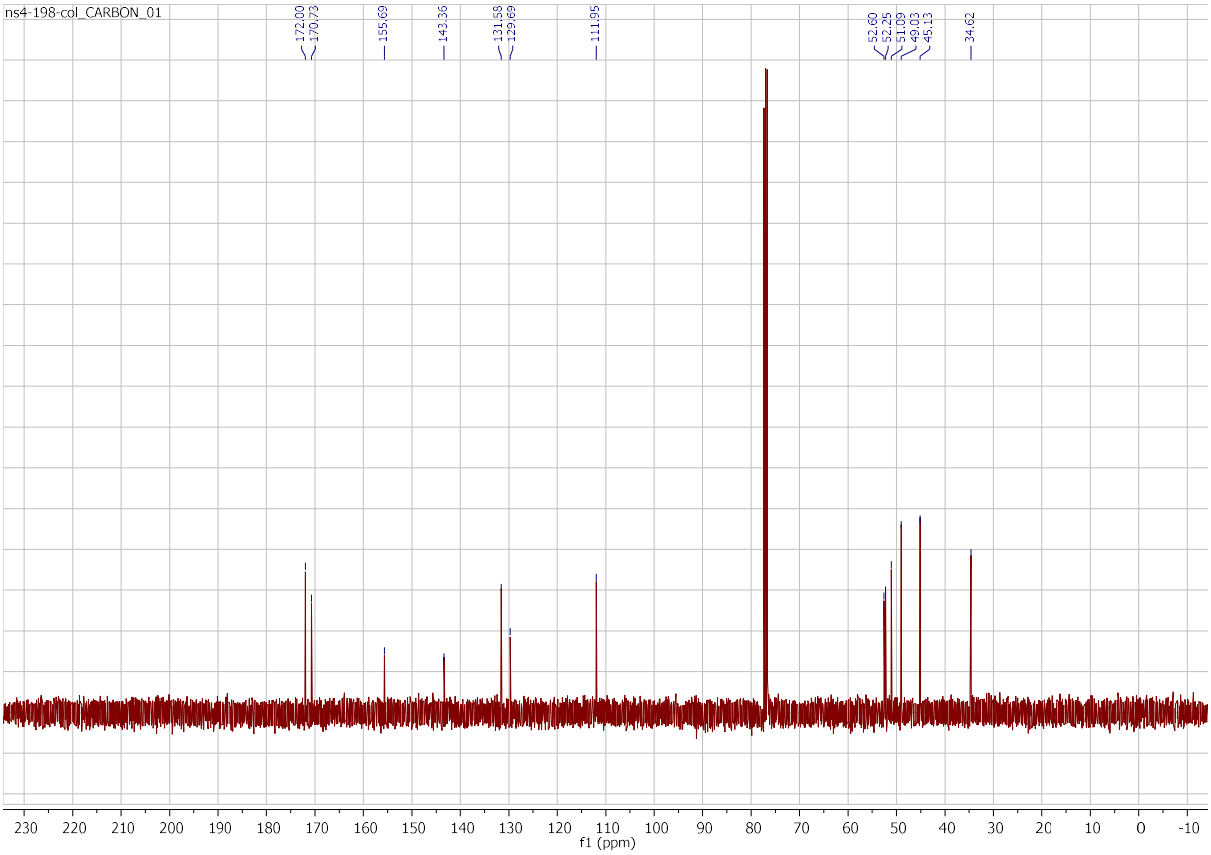
ns4-198-col_CARBON_01
172.00
170.73
155.69
143.36
131.58
129.69
111.95
52.60
52.25
51.09
49.03
45.13
34.62
f1 (ppm)

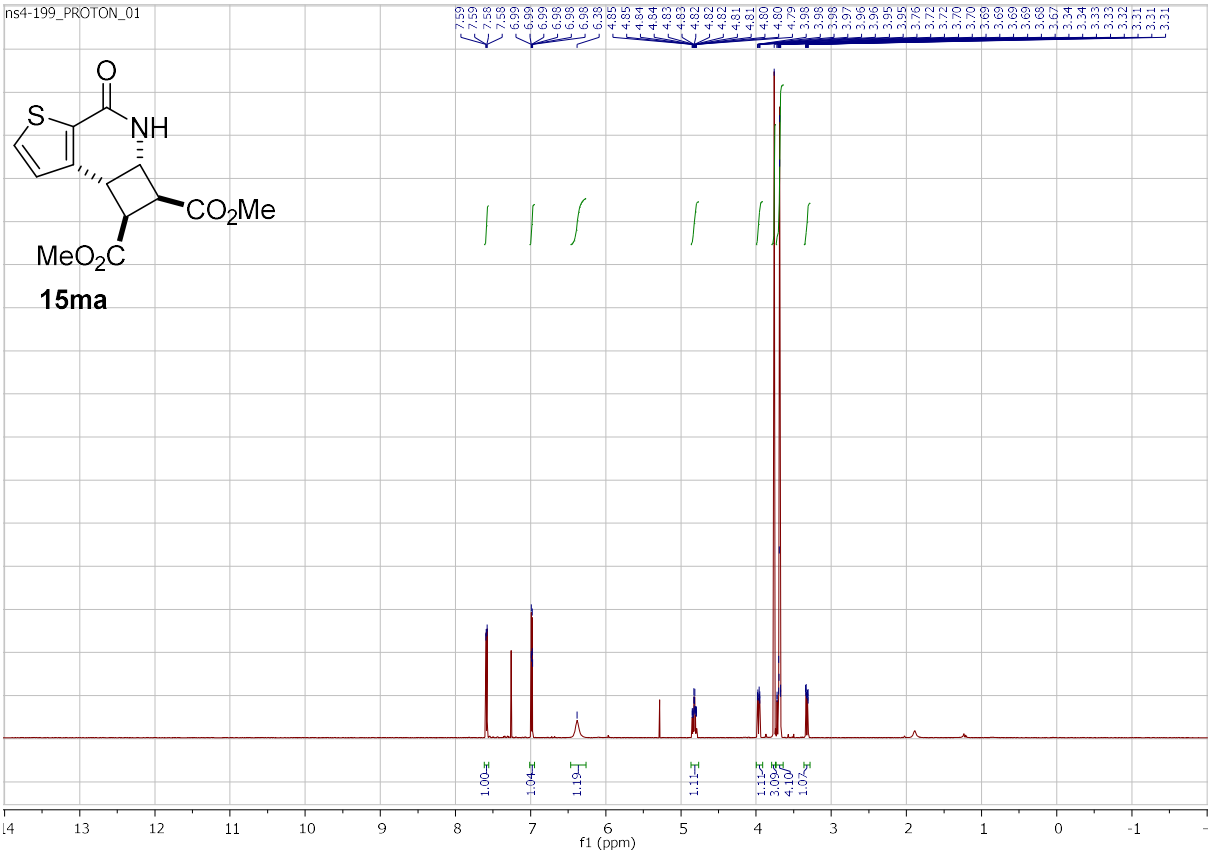
ns4-199_PROTON_01
O
S
NH
CO2Me
MeO2C
15ma
f1 (ppm)

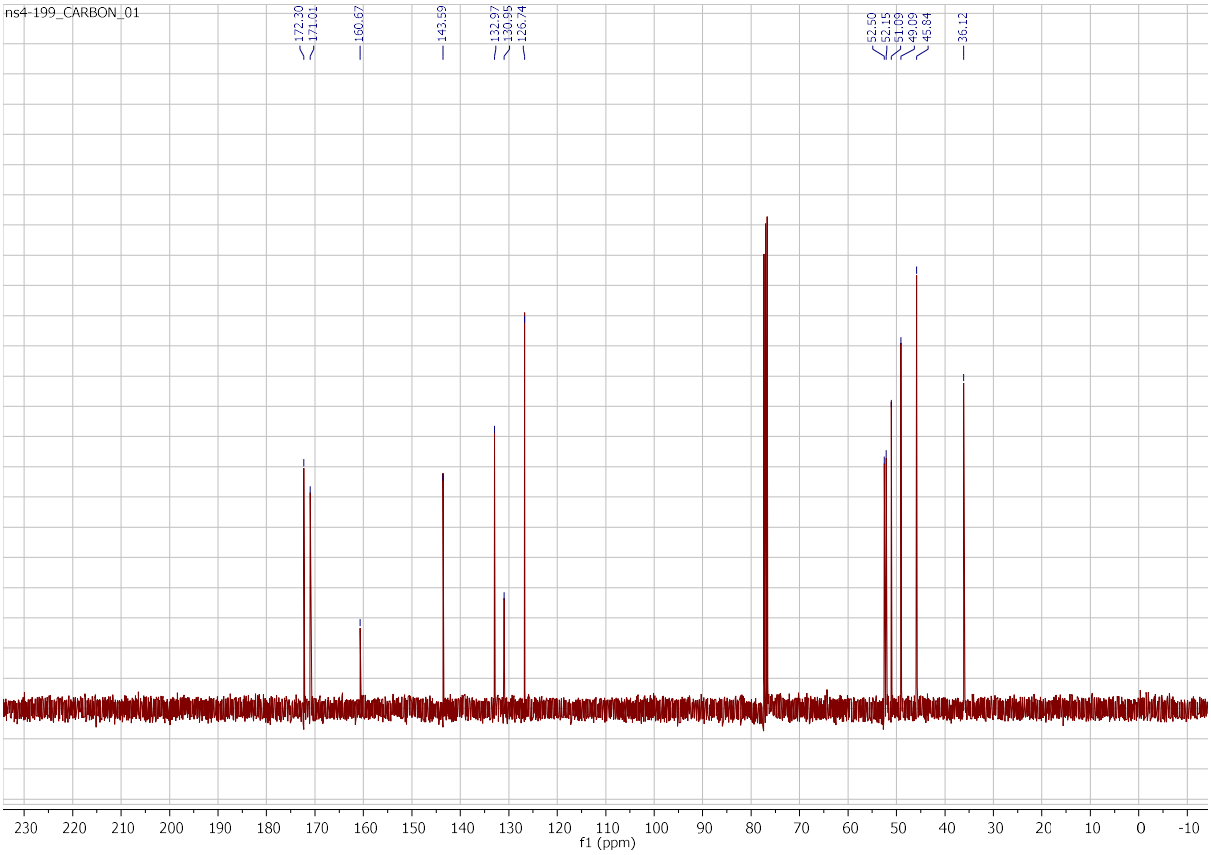
ns4-199_CARBON_01
f1 (ppm)

APPENDIX 3

Rh(III)-Catalyzed Coupling of *N*-Pivaloyloxy Acrylamides with Alkenes via C-H Activation:

Direct Modular Assembly of Piperidones

1. General methods

Unless otherwise noted, reactions were performed in flame-dried or oven-dried glassware and carried out under an atmosphere of nitrogen with magnetic stirring. Dichloromethane (DCM) were degassed with argon and passed through two columns of neutral alumina. Flash column chromatography was performed on SiliCycle Inc.® silica gel 60 (230-400 mesh). Thin Layer chromatography was performed on SiliCycle Inc.® 0.25 mm silica gel 60-F plates. Visualization was accomplished with UV light (254 nm) or $KMnO_4$ staining.

^{1}H-NMR and ^{13}C-NMR spectra were recorded on Bruker 300, 400 or 500 MHz spectrometers at ambient temperature. ^{1}H-NMR data are reported as the following: chemical shift in parts per million (δ, ppm) from chloroform ($CDCl_3$) taken as 7.26 ppm, integration, multiplicity (s=singlet, d=doublet, t=triplet, q=quartet, m=multiplet, dd=doublet of doublets) and coupling constant (*J* in Hz unit). ^{13}C-NMR is reported as the following: chemical shifts are reported in ppm from $CDCl_3$ taken as 77.0 ppm. Low-resolution mass spectra (LSMS) were obtained on ACQUITY Waters UPLC/mass spectrometer equipped with electrospray ionization. Infrared spectra (IR) were recored on a Perkin Elmer Paragon 1000 FT-IR spectrometer.

2. Preparation of starting materials

2-substituted acrylic acids[92] (for **9a** and **9b**), partial esterification of itaconic acid[93] (for **9d**), 2-aryl acrylic acids[94] (**9e-9j**) and 2-ethoxy acrylic acid[95] for (**9k**) were prepared according to the procedure. All alkenes in this study were purchased from commercial sources and used without further purification.

***N*-pivaloyloxy α-substituted acrylamides**

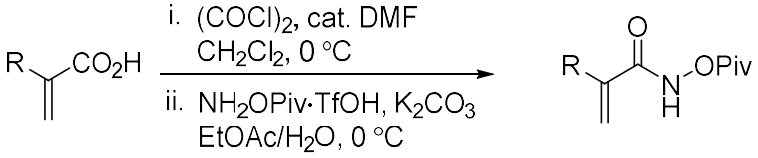

[92] Lai, Y; Sun, L; Sit, M. K.; Wang, Y.; Dai, W.-M. *Tetrahedron* **2016**, *72*, 664-673.

[93] Gowda, R. R.; Chen, E. Y.-X. *Org. Chem. Front.*, **2014**, *1*, 230-234.

[94] Felpin, F. X.; Miqueu, K.; Sotiropoulos, J. M.; Fouquet, E.; Ibarguren, O.; Laudien, J. *Chem. Eur. J.* **2010**, *16*, 5191-5204.

[95] Gloegaard, C.; Berg, T. C. US Patent Application Publication 2008/0242889 A1

i. To a solution of 2-substituted acrylic acid (1 equiv) in dry CH_2Cl_2 (0.17 M) at 0°C (ice bath) under N_2 was added dropwise oxalyl chloride (1.1 equiv) and a few drops of DMF. The reaction was then stirred at 0 °C to room temperature (typically 2-3 h). The volatile was removed under reduced pressure to give a crude acid chloride.

ii. To the solution of $NH_2OPiv{\cdot}TfOH$ (1.1 equiv), K_2CO_3 (2.0 equiv) and EtOAc/H_2O (2/1 by v/v, 0.1M) at 0 °C (ice bath), the crude acid chloride was added dropwise (while a small amount of EtOAc can be used as a solvent). The mixture was stirred at the same temperature for 1 h (prolong the reaction time led to the decomposition of the *N*-pivaloyloxy acrylamide). Upon the completion (monitored by TLC), a saturated $NaHCO_3$ was added. The aqueous layer was extracted with EtOAc (×3), washed with brine, dried with $MgSO_4$, filtered. The solvent was removed under reduced pressure to give a crude N-(pivaloyloxy) α-substituted acrylamide, which was purified by a flash column chromatography (5% to 25% EtOAc/hexane).

2-benzyl-N-(pivaloyloxy)acrylamide

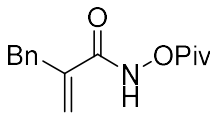

9a

^{1}H NMR (500 MHz, $CDCl_3$) δ 8.97 (s, NH), 7.35 (t, *J* = 7.4 Hz, 2H), 7.26 (m, 2H), 5.96 (s, 1H), 5.39 (t, *J* = 1.3 Hz, 1H), 3.69 (s, 2H), 1.33 (s, 9H).

^{13}C NMR (126 MHz, $CDCl_3$) δ 176.73, 166.93, 141.07, 137.47, 129.00, 128.75, 126.82, 122.52, 38.39, 38.10, 26.99.

IR (neat, cm^{-1}) 3217, 2981, 1780, 1668, 1080.

LRMS (ESI) m/z calcd for $C_{15}H_{19}NO_3$ $[M+H]^+$: 262.1, found: 262.2.

2-(4-bromobenzyl)-N-(pivaloyloxy)acrylamide

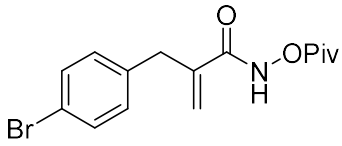

9b

^{1}H NMR (500 MHz, $CDCl_3$) δ 9.03 (s, NH), 7.45 (d, *J* = 8.4 Hz, 2H), 7.11 (d, *J* = 8.4 Hz, 2H), 5.91 (s, 1H), 5.39 (t, *J* = 1.4 Hz, 1H), 3.63 (s, 2H), 1.33 (s, 9H).

^{13}C NMR (126 MHz, $CDCl_3$) δ 176.77, 166.75, 140.84, 136.60, 131.78, 130.74, 122.28, 120.69, 38.39, 37.57, 26.98.

IR (neat, cm^{-1}) 3221, 29675, 1779, 1668, 1624, 1487, 1073, 1032, 1012.

LRMS (ESI) m/z calcd for $C_{15}H_{18}BrNO_3$ $[M+H]^+$: 340.1, 342.1, found: 340.0, 342.0.

N-(pivaloyloxy)methacrylamide

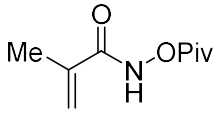

9c

^{1}H NMR (500 MHz, $CDCl_3$) δ 9.22 (s, NH), 5.84 (s, 1H), 5.50 – 5.47 (m, 1H), 1.99 (t, *J* = 1.3 Hz, 3H), 1.34 (s, 9H).

^{13}C NMR (126 MHz, $CDCl_3$) δ 176.90, 167.26, 136.91, 121.97, 38.39, 26.98, 18.29

IR (neat, cm^{-1}) 3225, 2977, 1782, 1671, 1629, 1481, 1055, 1033, 1015.

LRMS (ESI) m/z calcd for $C_9H_{15}NO_3$ $[M+H]^+$: 186.1, found: 186.2.

methyl 3-((pivaloyloxy)carbamoyl)but-3-enoate

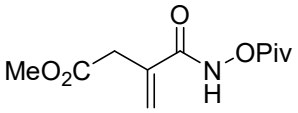

9d

^{1}H NMR (500 MHz, $CDCl_3$) δ 9.77 (s, NH), 6.07 (s, 1H), 5.63 (s, 1H), 3.74 (s, 3H), 3.42 (s, 2H), 1.34 (s, 9H).

^{13}C NMR (126 MHz, $CDCl_3$) δ 176.49, 171.40, 166.39, 134.56, 125.32, 52.48, 38.39, 37.77, 27.02.

IR (neat, cm^{-1}) 2972, 1741, 1055, 1033, 1013.

LRMS (ESI) m/z calcd for $C_{11}H_{17}NO_5$ $[M+H]^+$, $[M+Na]^+$: 244.1, found: 244.1, 266.1.

2-phenyl-N-(pivaloyloxy)acrylamide

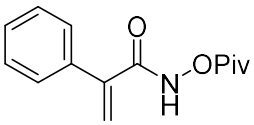

9e

^{1}H NMR (500 MHz, $CDCl_3$) δ 9.18 (s, NH), 7.47 (m, 2H), 7.38 (m, 3H), 6.11 (s, 1H), 5.75 (s, 1H), 1.33 (s, 9H).

^{13}C NMR (126 MHz, $CDCl_3$) δ 176.61, 166.00, 141.59, 135.62, 128.87, 128.77, 127.77, 123.06, 38.36, 27.00.

IR (neat, cm^{-1}) 3205, 2975, 1779, 1668, 1480, 1077, 1031, 701.

LRMS (ESI) m/z calcd for $C_{14}H_{17}NO_3$ $[M+H]^+$: 248.1, found: 248.1.

N-(pivaloyloxy)-2-(p-tolyl)acrylamide

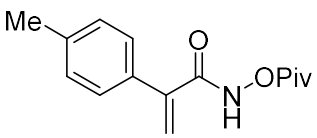

9f

^{1}H NMR (500 MHz, $CDCl_3$) δ 9.32 (s, 1H), 7.33 (d, J = 7.9 Hz, 2H), 7.15 (d, J = 7.6 Hz, 2H), 5.99 (s, 1H), 5.67 (s, 1H), 2.35 (s, 3H), 1.31 (s, 9H).

^{13}C NMR (126 MHz, $CDCl_3$) δ 176.41, 166.31, 141.43, 138.71, 132.74, 129.38, 127.59, 121.94, 38.30, 26.99, 21.20.

IR (neat, cm^{-1}) 3195, 2975, 1781, 1667, 1612, 1077, 826.

LRMS (ESI) m/z calcd for $C_{15}H_{19}NO_3$ $[M+H]^+$: 262.1, found: 262.1.

2-(4-methoxyphenyl)-N-(pivaloyloxy)acrylamide

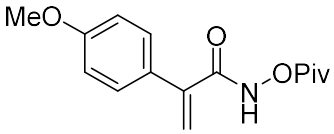

9g

^{1}H NMR (500 MHz, $CDCl_3$) δ 9.23 (s, NH), 7.38 (d, J = 8.7 Hz, 2H), 6.88 (d, J = 8.6 Hz, 2H), 5.97 (s, 1H), 5.66 (s, 1H), 3.79 (s, 3H), 1.32 (s, 9H).

^{13}C NMR (126 MHz, $CDCl_3$) δ 176.60, 166.48, 160.04, 141.04, 129.00, 127.96, 121.19, 114.11, 55.29, 38.34, 26.99.

IR (neat, cm^{-1}) 3229, 2973, 1780, 1670, 1608, 1513, 1252, 1181, 1076, 1033, 837.

LRMS (ESI) m/z calcd for $C_{15}H_{19}NO_4$ $[M+H]^+$, $[M+Na]^+$: 278.1, found: 278.1.

2-(4-bromophenyl)-N-(pivaloyloxy)acrylamide

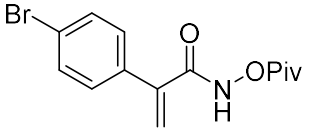

9h

^{1}H NMR (500 MHz, $CDCl_3$) δ 9.05 (s, NH), 7.51 (d, J = 8.4 Hz, 2H), 7.35 (d, J = 8.5 Hz, 2H), 6.09 (s, 1H), 5.78 (s, 1H), 1.34 (s, 9H).

^{13}C NMR (126 MHz, $CDCl_3$) δ 176.65, 165.79, 140.66, 134.39, 131.93, 129.33, 123.24, 123.10, 38.38, 26.99.

IR (neat, cm^{-1}) 3200, 2975, 1781, 1670, 1489, 1074, 1033, 1011, 833.

LRMS (ESI) m/z calcd for $C_{14}H_{16}BrNO_3$ $[M+H]^+$: 326.0, found: 326.0, 328.0.

2-(3-methoxyphenyl)-N-(pivaloyloxy)acrylamide

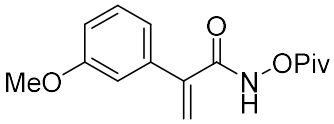

9i

^{1}H NMR (500 MHz, $CDCl_3$) δ 9.30 (s, NH), 7.25 (t, *J* = 7.9 Hz, 1H), 7.01 (d, *J* = 7.6 Hz, 1H), 6.98 (s, 1H), 6.86 (d, *J* = 8.2 Hz, 1H), 6.06 (s, 1H), 5.71 (s, 1H), 3.77 (s, 3H), 1.30 (s, 9H).

^{13}C NMR (126 MHz, $CDCl_3$) δ 176.42, 171.28, 159.65, 141.45, 136.96, 129.77, 120.10, 114.59, 113.14, 55.23, 38.30, 26.96.

IR (neat, cm^{-1}) 3203, 2974, 1779, 1670, 1600, 1579, 1484, 1462, 1247, 1034, 1075.

LRMS (ESI) m/z calcd for $C_{15}H_{19}NO_4$ $[M+H]^+$: 278.1, found: 278.1.

N-(pivaloyloxy)-2-(o-tolyl)acrylamide

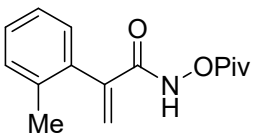

9j

^{1}H NMR (500 MHz, $CDCl_3$) δ 8.91 (s, NH), 7.53 – 6.95 (m, 4H), 6.45 (s, 1H), 5.52 (s, 1H), 2.29 (s, 3H), 1.26 (s, 9H).

^{13}C NMR (126 MHz, $CDCl_3$) δ 176.23, 171.06, 140.80, 136.74, 135.57, 130.44, 129.73, 128.89, 126.61, 126.13, 53.47, 38.22, 26.91.

IR (neat, cm^{-1}) 3207, 2974, 1780, 1671, 1480, 1459, 1074, 1033, 768, 729.

LRMS (ESI) m/z calcd for $C_{15}H_{19}NO_3$ $[M+H]^+$: 262.1, found: 262.1.

2-ethoxy-N-(pivaloyloxy)acrylamide

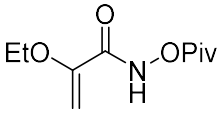

9k

^{1}H NMR (500 MHz, $CDCl_3$) δ 9.70 (s, 1H), 5.36 (s, 59H), 4.49 (s, 1H), 3.84 (q, *J* = 6.8 Hz, 3H), 1.35 (t, *J* = 7.0 Hz, 5H), 1.31 (s, 9H).

^{13}C NMR (126 MHz, $CDCl_3$) δ 176.18, 160.01, 151.78, 91.76, 64.25, 38.35, 26.95, 14.18.

IR (neat, cm^{-1}) 3245, 2979, 2937, 1782, 1693, 1628, 1479, 1300, 1059, 1081.

LRMS (ESI) m/z calcd for $C_{10}H_{17}NO_4$ $[M+H]^+$: 216.1, found: 216.2.

3. General procedures for dihydropyridone synthesis

Without any precaution of air and moisture, substituted *N*-(pivaloyloxy) acrylamide (0.1 mmol, 1 eq), $[Cp^*RhCl_2]_2$ (0.0025 mmol, 2.5 mol%), CsOAc (0.025 mmol, 0.25 equiv) and alkenes (0.11 mmol, 1.1 equiv) were charged into a dram vial charged with a stir bar. Trifluoroethanol (TFE) (0.33 mL, 0.3 M) was added and the mixture was stirred at room temperature until the starting material was consumed (monitoring by TLC). The reaction was quenched with saturated $NaHCO_3$ and extracted 3 times with EtOAc. The organic layer was washed with brine, dried over $MgSO_4$, filtered, and solvent was evaporated to obtain crude product. The crude product was purified by column chromatography using gradient 10% to 50% EtOAc/hexane containing 1% Et_3N as an eluent to obtain the product.

4. Product characterizations

3-benzyl-6-phenyl-5,6-dihydropyridin-2(1H)-one

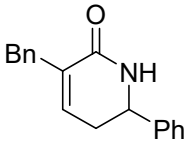

11ab

Off-white solid (22.2 mg, 85% yield).

^{1}H NMR (500 MHz, $CDCl_3$) δ 7.40-7.23 (m, 10H), 6.16 (ddt, *J* = 5.1, 3.4, 1.6 Hz, 1H), 5.71 (s, NH), 4.71 (dd, *J* = 10.4, 6.7 Hz, 1H), 3.69 (s, 2H), 2.53 (m, 2H).

^{13}C NMR (126 MHz, $CDCl_3$) δ 166.96, 141.20, 139.29, 135.01, 134.99, 129.35, 128.91, 128.42, 128.27, 126.45, 126.21, 55.91, 36.06, 33.41.

IR (neat, cm^{-1}) 3206, 3061, 3027, 2917, 1673, 1630, 1494, 1453, 1424, 1290, 698.

LRMS (ESI) m/z calcd for $C_{18}H_{17}NO$ $[M+H]^+$: 265.1, found: 265.1.

The regiochemistry based on COSY.

3-(4-bromobenzyl)-6-phenyl-5,6-dihydropyridin-2(1*H*)-one

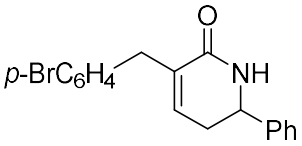

11bb

Off-white solid (30.9 mg, 90% yield).

^{1}H NMR (500 MHz, $CDCl_3$) δ 7.41 (d, *J* = 8.3 Hz, 2H), 7.37-7.30 (m, 5H), 7.11 (d, *J* = 8.3 Hz, 2H), 6.18 (m, 1H), 5.76 (s, NH), 4.67 (dd, *J* = 10.8, 6.2 Hz, 1H), 3.60 (s, 2H), 2.57-2.46 (m, 1H).

^{13}C NMR ($CDCl_3$, 126 MHz) δ 166.69, 141.06, 138.40, 135.24, 134.54, 131.46, 131.03, 128.92, 128.30, 126.42, 120.08, 55.81, 35.66, 33.35.

IR (neat, cm^{-1}) 3202, 3061, 2919, 1674, 1631, 1425, 1454, 1486, 1289, 1070, 1011, 699.

LRMS (ESI) m/z calcd for $C_{18}H_{16}BrNO$ $[M+H]^+$: 342.0, 344.0, found: 342.0, 344.0.

3-methyl-6-phenyl-5,6-dihydropyridin-2(1*H*)-one

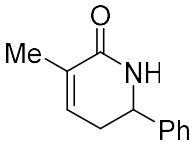

11cb

Off-white solid (13.1 mg, 70% yield).

^{1}H NMR (500 MHz, $CDCl_3$) δ 7.39-7.26 (m, 5H), 6.34 (m, 1H), 5.66 (s, NH), 4.70 (dd, *J* = 10.5, 6.7 Hz, 1H), 2.50 (m, 2H), 1.93 (s, 3H).

^{13}C NMR ($CDCl_3$, 126 MHz) δ 167.73, 141.35, 134.27, 130.92, 128.90, 128.23, 126.39, 56.21, 33.37, 16.61. IR (neat, cm^{-1}) 3214, 3063, 2923, 2886, 1676, 1633, 699.

LRMS (ESI) m/z calcd for $C_{12}H_{13}NO$ $[M+H]^+$: 188.1, found: 188.2.

methyl 2-(2-oxo-6-phenyl-1,2,5,6-tetrahydropyridin-3-yl)acetate

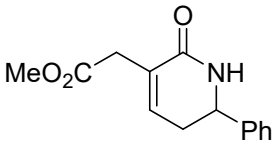

11db

Off-white solid (18.4 mg, 75% yield).

^{1}H NMR (500 MHz, $CDCl_3$) δ 7.40-7.31 (m, 5H), 6.49 (m, 1H), 5.69 (s, NH), 4.77 (dd, *J* = 10.8, 6.2 Hz, 1H), 3.71 (s, 3H), 3.41 (d, *J* = 16.5 Hz, 1H), 3.28 (d, *J* = 16.5 Hz, 1H), 2.65-2.53 (m, 2H).

^{13}C NMR ($CDCl_3$, 126 MHz) δ 171.71, 166.16, 141.02, 137.39, 128.95, 128.71, 128.35, 126.46, 55.89, 52.02, 35.61, 33.36.

IR (neat, cm^{-1}) 3207, 3062, 2950, 1737, 1680, 1636.

LRMS (ESI) m/z calcd for $C_{14}H_{15}NO_3$ $[M+H]^+$, $[M+Na]^+$: 246.1, 268.1, found: 246.2, 268.1.

3,6-diphenyl-5,6-dihydropyridin-2(1*H*)-one

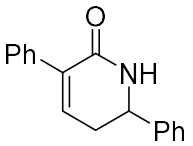

11eb

Off-white solid (13.3 mg, 55% yield).

^{1}H NMR (500 MHz, $CDCl_3$) δ 7.49 (d, *J* = 6.9 Hz, 2H), 7.41-7.31 (m, 8H), 6.71 (dd, *J* = 5.5, 3.5 Hz, 1H), 5.86 (s, NH), 4.83 (dd, *J* = 11.4, 5.5 Hz, 1H), 2.78-2.66 (m, 2H).

^{13}C NMR ($CDCl_3$, 126 MHz) δ 166.08, 141.00, 136.62, 136.27, 135.71, 129.00, 128.59, 128.39, 128.06, 127.81, 126.47, 55.84, 33.72.

IR (neat, cm^{-1}) 3218, 3059, 2932, 1669, 1616, 697.

LRMS (ESI) m/z calcd for $C_{17}H_{15}NO$ $[M+H]^+$, $[M+Na]^+$: 250.1, found: 250.2, 272.1.

6-phenyl-3-(*p*-tolyl)-5,6-dihydropyridin-2(1*H*)-one

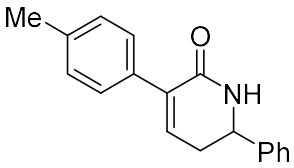

11fb

Off-white solid (21.1 mg, 80% yield).

^{1}H NMR (500 MHz, $CDCl_3$) δ 7.41-7.35 (s, 7H), 7.18 (d, *J* = 7.9 Hz, 2H), 6.67 (dd, *J* = 5.5, 3.5 Hz, 1H), 5.88 (s, NH), 4.81 (dd, *J* = 11.3, 5.5 Hz, 1H), 2.78–2.58 (m, 2H), 2.36 (s, 3H).

^{13}C NMR ($CDCl_3$, 126 MHz) δ 166.23, 141.10, 137.58, 135.90, 135.56, 133.41, 128.98, 128.78, 128.46, 128.34, 126.48, 55.83, 33.70, 21.22.

IR (neat, cm^{-1}) 3182, 3056, 2921, 1665, 1511, 823, 699.

LRMS (ESI) m/z calcd for $C_{18}H_{17}NO$ $[M+H]^+$, $[M+Na]^+$: 264.1, 286.1, found: 264.2, 286.1.

3-(4-methoxyphenyl)-6-phenyl-5,6-dihydropyridin-2(1*H*)-one

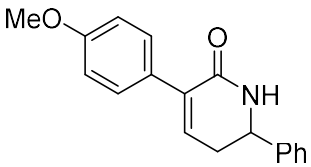

11gb

Off-white solid (16.5 mg, 59% yield).

^{1}H NMR (500 MHz, $CDCl_3$) δ 7.43 (d, *J* = 8.8 Hz, 2H), 7.41-7.34 (m, 5H), 6.90 (d, *J* = 8.8 Hz, 2H), 6.64 (dd, *J* = 5.4, 3.6 Hz, 1H), 5.82 (s, NH), 4.81 (dd, *J* = 10.3, 6.7 Hz, 1H), 3.82 (s, 3H), 2.98 – 2.54 (m, 2H).

^{13}C NMR ($CDCl_3$, 126 MHz) δ 166.30, 159.36, 141.08, 135.30, 135.06, 129.75, 128.98, 128.79, 128.36, 126.47, 113.54, 55.87, 55.31, 33.71.

IR (neat, cm^{-1}) 3198, 3059, 2933, 2836, 1665, 1607, 1510, 1244, 830.

LRMS (ESI) m/z calcd for $C_{18}H_{17}NO_2$ $[M+H]^+$, $[M+Na]^+$: 280.1, found: 280.2, 302.1.

3-(4-bromophenyl)-6-phenyl-5,6-dihydropyridin-2(1*H*)-one

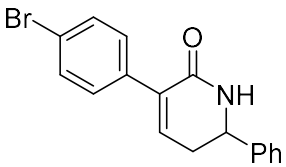

11hb

Off-white solid (19.6 mg, 60% yield).

^{1}H NMR (500 MHz, $CDCl_3$) δ 7.48 (d, *J* = 8.5 Hz, 2H), 7.40 (m, 4H), 7.35 (s, 1H), 7.36 (d, *J* = 8.5 Hz, 2H), 6.71 (dd, *J* = 5.6, 3.4 Hz, 1H), 5.91 (s, NH), 4.82 (dd, *J* = 11.1, 5.8 Hz, 1H), 2.98–2.46 (m,2H).

^{13}C NMR ($CDCl_3$, 126 MHz) δ 165.70, 140.80, 137.00, 135.12, 134.68, 131.18, 130.26, 129.04, 128.46, 126.44, 122.07, 55.76, 33.68.

IR (neat, cm^{-1}) 3202, 3060, 2924, 1666, 1614, 1487, 824.

LRMS (ESI) m/z calcd for $C_{17}H_{14}BrNO$ $[M+H]^+$: 327.0, 330.0, found: 328.0, 330.0.

3-(3-methoxyphenyl)-6-phenyl-5,6-dihydropyridin-2(1*H*)-one

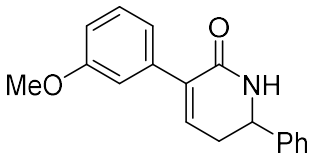

11ib

Off-white solid (22.7 mg, 81% yield).

^{1}H NMR (500 MHz, $CDCl_3$) 7.47 – 7.31 (m, 5H), 7.28 (d, *J* = 8.2 Hz, 1H), 7.12 – 7.02 (m, 2H), 6.92 – 6.84 (m, 1H), 6.70 (dd, *J* = 5.5, 3.5 Hz, 1H), 5.89 (s, NH), 4.84 – 4.78 (m, 1H), 3.82 (s, 3H), 2.77-2.65 (m, 2H).

^{13}C NMR ($CDCl_3$, 126 MHz) δ 165.98, 159.25, 140.99, 137.65, 136.79, 135.56, 129.03, 129.00, 128.38, 126.47, 121.08, 114.25, 113.60, 55.78, 55.27, 33.69.

IR (neat, cm^{-1}) 3211, 3061, 2938, 1669, 1270, 697.

LRMS (ESI) m/z calcd for $C_{18}H_{17}NO_2$ $[M+H]^+$, $[M+Na]^+$: 280.1, 302.1, found: 280.1, 302.1.

6-phenyl-3-(o-tolyl)-5,6-dihydropyridin-2(1H)-one

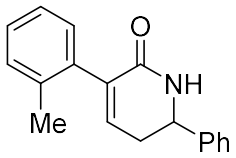

11jb

Off-white solid (26.3 mg, 77% yield).

^{1}H NMR (500 MHz, $CDCl_3$) δ 7.56 – 7.07 (m, 9H), 6.56 (dd, *J* = 5.0, 3.7 Hz, 1H), 5.90 (s, NH), 4.90 (dd, *J* = 10.1, 6.7 Hz, 1H), 2.79 – 2.69 (m, 2H), 2.31 (s, 3H).

^{13}C NMR ($CDCl_3$, 126 MHz) δ 165.89, 141.07, 137.73, 136.78, 136.61, 136.53, 129.92, 129.78, 129.00, 128.37, 128.05, 126.46, 125.63, 56.01, 33.59, 20.21.

IR (neat, cm^{-1}) 3206, 3061, 2924, 1669, 1622, 727.

LRMS (ESI) m/z calcd for $C_{18}H_{17}NO$ $[M+H]^+$, $[M+Na]^+$: 264.1, 286.1, found: 264.2, 286.1.

3-ethoxy-6-phenyl-5,6-dihydropyridin-2(1H)-one

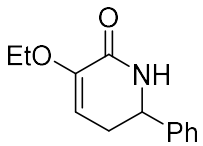

11kb

(13.0 mg, 58% yield)

^{1}H NMR (500 MHz, $CDCl_3$) δ 7.51 – 7.30 (m, 5H), 5.81 (s, NH), 5.42 – 5.38 (m, 1H), 4.72 (dd, *J* = 10.2, 6.9 Hz, 1H), 3.84 (q, *J* = 7.1 Hz, 2H), 2.66 – 2.55 (m, 2H), 1.44 (t, *J* = 7.0 Hz, 3H).

^{13}C NMR ($CDCl_3$, 126 MHz) δ 163.48, 146.86, 140.86, 128.92, 128.78, 128.32, 126.34, 104.53, 63.57, 56.00, 31.92, 14.34.

IR (neat, cm^{-1}) 3228, 2979, 2932, 1682, 1633, 1224, 700.

LRMS (ESI) m/z calcd for $C_{13}H_{15}NO_2$ $[M+H]^+$: 218.1, 240.1, found: 218.1, 240.1.

3-benzyl-6-(p-tolyl)-5,6-dihydropyridin-2(1H)-one

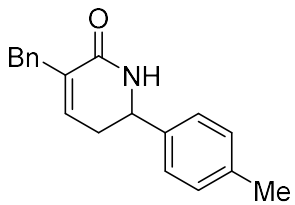

11ac

Off-white solid (25.4 mg, 92% yield).

^{1}H NMR (500 MHz, $CDCl_3$) δ 7.34 (t, *J* = 5.0 Hz, 2H), 7.28 (m, 3H), 7.24 (d, *J* = 10.0 Hz, 2H), 7.19 (d, *J* = 10.0 Hz, 2H), 6.16 (t, *J* = 10.0 Hz, 1H), 5.76 (s, NH), 4.67 (t, *J* = 10.0 Hz, 1H), 3.69 (s, 2H), 2.49 (m, 2H), 2.38 (s, 3H).

^{13}C NMR ($CDCl_3$, 126 MHz) δ 167.04, 139.33, 138.21, 138.05, 135.12,

134.96, 129.55, 129.36, 128.42, 126.37, 126.20, 55.64, 36.05, 33.46, 21.11.

IR (neat, cm^{-1}) 3205, 3059, 3026, 2920, 1673, 1630, 699.

LRMS (ESI) m/z calcd for $C_{19}H_{19}NO$ $[M+H]^+$, $[M+Na]^+$: 278.1, 300.1, found: 278.2, 300.1.

3-benzyl-6-(4-methoxyphenyl)-5,6-dihydropyridin-2(1*H*)-one

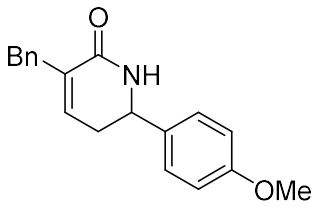

11ad

Off-white solid (26.0 mg, 89% yield).

1 mmol scale - 244.2, 83% yield

^{1}H NMR (500 MHz, $CDCl_3$) δ 7.33 (t, *J* = 15.0 Hz, 2H), 7.27 (d, *J* = 15.0 Hz, 2H), 7.28-7.23 (m, 3H), 6.90 (d, *J* = 15.0 Hz, 2H), 6.16 (t, *J* = 5.0 Hz, 1H), 5.71 (s, NH), 4.65 (t, *J* = 10.0 Hz, 1H), 3.83 (s, 3H), 3.69 (s, 2H), 2.50-2.47 (m, 1H).

^{13}C NMR ($CDCl_3$, 126 MHz) δ 167.02, 159.50, 139.33, 135.16, 134.95, 133.18, 129.34, 128.41, 127.67, 126.19, 114.22, 55.38, 55.34, 36.05, 33.50.

IR (neat, cm^{-1}) 3207, 3060, 3027, 2932, 2836, 1672, 1629, 1512, 1247, 1032, 826, 700.

LRMS (ESI) m/z calcd for $C_{19}H_{19}NO_2$ $[M+H]^+$, $[M+Na]^+$: 294.1, 316.1, found: 294.1, 316.1.

3-benzyl-6-(4-(trifluoromethyl)phenyl)-5,6-dihydropyridin-2(1*H*)-one

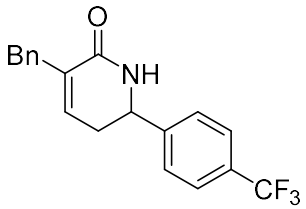

11ae

Off-white solid (15.3 mg, 46% yield).

^{1}H NMR (500 MHz, $CDCl_3$) δ 7.63 (d, *J* = 8.1 Hz, 2H), 7.45 (d, *J* = 8.0 Hz, 2H), 7.32 (m, 2H), 7.25 (m, 3H), 6.16 (m, 1H), 5.93 (s, NH), 4.78 (dd, *J* = 10.7, 5.7 Hz, 1H), 3.68 (s, 2H), 2.84-2.56 (m, 1H), 2.55-2.38 (m, 1H).

^{13}C NMR ($CDCl_3$, 126 MHz) δ 166.87, 145.23, 139.07, 135.23, 134.49, 130.49, 129.28, 128.44, 126.79, 126.29, 125.88, 55.30, 36.07, 33.12.

IR (neat, cm^{-1}) 3212, 3064, 2922, 1675, 1630, 1324, 1164, 1121, 1068, 826, 700.

LRMS (ESI) m/z calcd for $C_{19}H_{16}F_3NO$ $[M+H]^+$: 332.1, found: 332.1.

3-benzyl-6-(4-fluorophenyl)-5,6-dihydropyridin-2(1*H*)-one

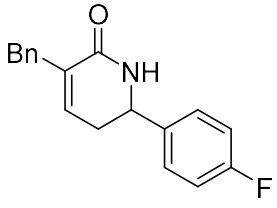

11af

Yellow oil (18.9 mg, 67% yield).

^{1}H NMR (500 MHz, $CDCl_3$) δ 7.32-7.27 (m, 4H), 7.23-7.20 (m, 3H), 7.03 (t, *J* = 8.6 Hz, 1H), 6.13 (m, 1H), 5.77 (s, NH), 4.67 (dd, *J* = 11.0, 5.9 Hz, 1H), 3.65 (s, 2H), 2.54-2.41 (m, 2H).

^{13}C NMR ($CDCl_3$, 126 MHz) δ 166.93, 162.71, 139.21, 136.98, 135.07, 134.82, 129.31, 128.43, 128.15, 126.24, 115.88 115.69, 55.20, 36.05, 33.42.

^{19}F NMR ($CDCl_3$, 282 MHz) δ 112.89.

IR (neat, cm^{-1}) 3207, 3062, 3028, 2922, 1673, 1630, 1510, 1427, 1225, 827, 699.

LRMS (ESI) m/z calcd for $C_{18}H_{16}FNO$ $[M+H]^+$: 281.1, found: 281.1.

3-benzyl-6-(4-chlorophenyl)-5,6-dihydropyridin-2(1*H*)-one

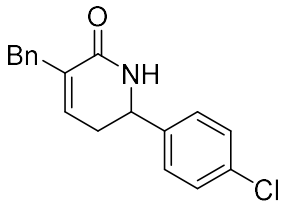

11ag

Off-white solid (21.2 mg, 71% yield).

^{1}H NMR (500 MHz, $CDCl_3$) δ 7.30-7.28 (m, 4H), 7.24-7.19 (m, 5H), 6.10 (m, 1H), 5.88 (s, NH), 4.65 (dd, *J* = 5.0, 10.0 Hz, 1H), 3.62 (s, 2H), 2.53-2.49 (m, 1H), 2.44-2.38 (m, 1H).

^{13}C NMR ($CDCl_3$, 126 MHz) δ 166.94, 139.74, 139.17, 135.12, 134.68, 133.98, 129.31, 129.04, 128.43, 127.82, 126.25, 55.15, 36.06, 33.25.

IR (neat, cm^{-1}) 3207, 3061, 3028, 2921, 1674, 1631, 1492, 1092, 1014, 822, 699.

LRMS (ESI) m/z calcd for $C_{18}H_{16}ClNO$ $[M+H]^+$: 298.1, found: 298.1.

methyl 4-(5-benzyl-6-oxo-1,2,3,6-tetrahydropyridin-2-yl)benzoate

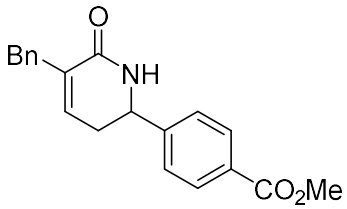

11ah

(18.3 mg, 57% yield)

^{1}H NMR (500 MHz, $CDCl_3$) δ 8.04 (d, *J* = 8.3 Hz, 2H), 7.40 (d, *J* = 8.3 Hz, 2H), 7.37 – 7.29 (m, 2H), 7.24 (m, 3H), 6.15 (ddt, *J* = 5.1, 3.3, 1.6 Hz, 1H), 5.87 (s, NH), 4.77 (dd, *J* = 10.8, 5.7 Hz, 1H) 3.94 (s, 3H), 3.67 (s, 2H), 2.60 (dtd, *J* = 17.5, 5.5, 1.4 Hz, 1H), 2.49 (dddd, *J* = 16.3, 13.3, 5.2, 2.4 Hz, 1H).

^{13}C NMR ($CDCl_3$, 126 MHz) δ 166.84, 166.55, 146.24, 139.11, 135.17, 134.56, 130.19, 130.09, 129.30, 128.43, 126.41, 126.26, 55.48, 52.22, 36.06, 33.10.

IR (neat, cm^{-1}) 3211, 3028, 2950, 1720, 1675, 1631, 1280, 1111, 701.

LRMS (ESI) m/z calcd for $C_{20}H_{19}NO_3$ $[M+H]^+$: 322.1, found 322.1.

3-benzyl-6-(*m*-tolyl)-5,6-dihydropyridin-2(1*H*)-one

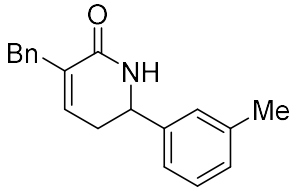

11ai

Off-white solid (23.3 mg, 84% yield).

^{1}H NMR (500 MHz, $CDCl_3$) δ 7.33 (t, *J* =7.4 Hz, 2H), 7.28-7.23 (m, 4H), 7.16-7.13 (m, 3H), 6.16 (m, 1H), 5.68 (s, NH), 4.67 (m, 1H), 3.70 (s, 2H), 2.52 (m, 2H), 2.37 (s, 3H).

^{13}C NMR ($CDCl_3$, 126 MHz) δ 166.93, 141.20, 139.33, 138.67, 135.05, 134.94, 129.33, 128.97, 128.79, 128.42, 127.12, 126.20, 123.50, 55.85, 36.07, 33.42, 21.44.

IR (neat, cm^{-1}) 3207, 3060, 3027, 1673, 1630, 1423, 1289, 780, 700.

LRMS (ESI) m/z calcd for $C_{19}H_{19}NO$ $[M+H]^+$, $[M+Na]^+$: 278.2, 300.2, found: 278.2, 300.1.

3-benzyl-6-(3-methoxyphenyl)-5,6-dihydropyridin-2(1*H*)-one

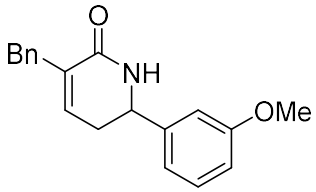

11aj

Off-white solid (25.8 mg, 88% yield).

^{1}H NMR (500 MHz, $CDCl_3$) δ 7.34-7.23 (m, 6H), 6.93-6.87 (m, 3H), 6.16 (m, 1H), 5.76 (m, NH), 4.68 (dd, *J* = 10.3, 7.0 Hz, 1H), 3.81 (s, 3H), 3.68 (s, 2H), 2.52 (m, 2H).

^{13}C NMR ($CDCl_3$, 126 MHz) δ 166.96, 159.98, 142.84, 139.29, 135.08, 134.95, 129.98, 129.34, 128.43, 126.21, 118.67, 113.69, 111.96, 55.87, 55.28, 36.05, 33.38.

IR (neat, cm^{-1}) 3209, 3027, 2935, 1674, 1630, 1454, 1262, 1048, 699.

LRMS (ESI) m/z calcd for $C_{19}H_{19}NO_2$ $[M+H]^+$: 294.1, Found: 294.2.

3-benzyl-6-(3-(trifluoromethyl)phenyl)-5,6-dihydropyridin-2(1*H*)-one

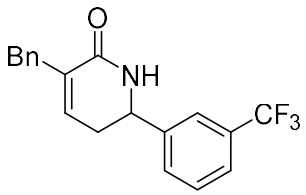

11ak

Off-white solid (14.5 mg, 44% yield).

^{1}H NMR (500 MHz, $CDCl_3$) δ 7.62 (s, 1H), 7.61 (d, *J* = 10.0 Hz, 1H), 7.54-7.48 (m, 2H), 7.36-7.31 (m, 2H), 7.26-7.23 (m, 3H), 6.17 (m, 1H), 5.90 (s, NH), 4.79 (dd, *J* = 5.0, 10.0 Hz, 1H), 3.69 (s, 2H), 2.64-2.59 (m, 1H), 2.54-2.47 (m, 1H).

^{13}C NMR ($CDCl_3$, 126 MHz) δ 166.90, 142.31, 139.07, 135.20, 134.58, 131.46, 131.20, 130.94, 129.80, 129.46, 129.28, 128.46, 126.28, 125.11, 123.27, 55.43, 36.02, 33.21.

^{19}F NMR ($CDCl_3$, 282 MHz) δ -61.82.

IR (neat, cm^{-1}) 2939, 1676, 1631, 1328, 700.

LRMS (ESI) m/z calcd for $C_{19}H_{16}F_3NO$ $[M+H]^+$: 332.1, found: 332.1.

3-benzyl-6-(3-fluorophenyl)-5,6-dihydropyridin-2(1*H*)-one

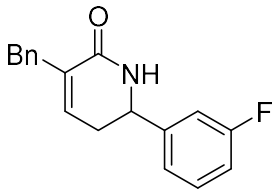

11al

Yellow oil (19.9 mg, 71% yield).

^{1}H NMR (500 MHz, $CDCl_3$) δ 7.34-7.29 (m, 3H), 7.23-7.20 (m, 3H), 7.09 (d, *J* = 7.8, Hz, 1H), 7.06-6.97 (m, 2H), 6.13 (m, 1H), 5.80 (s, NH), 4.68 (dd, *J* = 11.0, 5.7 Hz, 1H), 3.65 (s, 2H), 2.58-2.52 (m, 1H), 2.49-2.42 (m, 1H).

^{13}C NMR ($CDCl_3$, 126 MHz) δ 166.85, 163.94, 161.98, 143.87, 143.82, 139.14, 135.09, 134.68, 130.54, 130.48, 129.31, 128.44, 126.25, 122.04, 122.01, 115.25, 115.08, 113.58, 113.40, 55.33, 36.04, 33.18.

IR (neat, cm^{-1}) 3208, 3062, 3028, 2920, 1674, 1631, 784, 699.

LRMS (ESI) m/z calcd for $C_{18}H_{16}FNO$ $[M+H]^+$: 282.1, found: 282.1.

3-benzyl-6-(3-chlorophenyl)-5,6-dihydropyridin-2(1*H*)-one

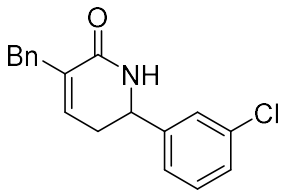

11am

Off-white solid (17.4 mg, 58% yield).

^{1}H NMR (500 MHz, $CDCl_3$) δ 7.33-7.28 (m, 5H), 7.23-7.18 (m, 4H), 6.13 (m, 1H), 5.82 (s, NH), 4.67 (dd, *J* = 5.0, 10.0 Hz, 1H), 3.55 (s, 2H), 2.58-2.53 (m, 1H), 2.49-2.43 (m, 1H).

^{13}C NMR ($CDCl_3$, 126 MHz) δ 166.84, 143.33, 139.13, 135.11, 134.78, 134.64, 130.20, 129.29, 128.45, 128.41, 126.69, 126.25, 124.57, 55.29, 36.04, 33.16.

IR (neat, cm^{-1}) 3204, 2897, 1674, 1630, 1422, 696.

LRMS (ESI) m/z calcd for $C_{18}H_{16}ClNO$ $[M+H]^+$: 298.1, found: 298.1.

3-(5-benzyl-6-oxo-1,2,3,6-tetrahydropyridin-2-yl)benzaldehyde

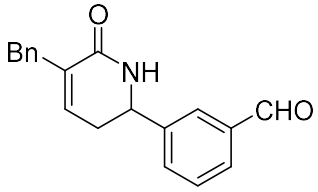

11an

Off-white solid (10.2 mg, 35% yield).

^{1}H NMR (500 MHz, $CDCl_3$) δ 9.99 (s, CHO), 7.85 (d, *J* = 10.0 Hz, 1H), 7.84 (s, 1H), 7.61 (d, *J* = 10.0 Hz, 1H), 7.55 (t, *J* = 5.0 Hz, 1H), 7.33-7.30 (m, 2H), 7.25-7.23 (m, 3H), 6.17 (m, 1H), 5.91 (s, NH), 4.82 (dd, *J* = 5.0, 10.0 Hz, 1H), 3.71 (d, *J* = 15.0 Hz, 1H), 3.66 (d, *J* = 15.0 Hz, 1H).

^{13}C NMR ($CDCl_3$, 126 MHz) δ 191.79, 166.82, 142.55, 139.12, 136.89, 135.26, 134.45, 132.33, 129.67, 129.58, 129.29, 128.45, 127.48, 126.28, 55.26, 36.09, 33.13.

IR (neat, cm^{-1}) 3211, 3060, 3027, 2918, 1696, 1673, 1629, 698.

LRMS (ESI) m/z calcd for $C_{19}H_{17}NO_2$ $[M+H]^+$: 292.1, found: 292.1.

3-benzyl-6-(naphthalen-2-yl)-5,6-dihydropyridin-2(1*H*)-one

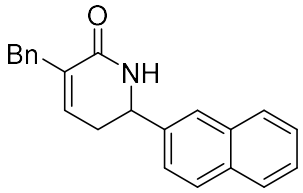

11ao

Off-white solid (16.8 mg, 60% yield).

^{1}H NMR (500 MHz, $CDCl_3$) δ 7.88-7.77 (m, 4H), 7.55-7.47 (m, 3H), 7.35-7.24 (m, 5H), 6.19 (m, 1H), 5.91 (s, NH), 4.58 (dd, *J* = 5.0, 10.0 Hz), 3.72 (s, 2H), 2.63 (m, 2H).

^{13}C NMR ($CDCl_3$, 126 MHz) δ 166.99, 139.30, 138.51, 135.03, 134.93, 133.23, 133.11, 129.34, 128.84, 128.45, 127.96, 127.71, 126.55, 126.34, 126.23, 125.40, 124.16, 55.87, 36.14, 33.26.

IR (neat, cm^{-1}) 3209, 3057, 3027, 2919, 1672, 1629, 1424, 747, 699.

LRMS (ESI) m/z calcd for $C_{22}H_{19}NO$ $[M+H]^+$: 314.2, found: 314.1.

3-benzyl-6-(2-fluorophenyl)-5,6-dihydropyridin-2(1H)-one

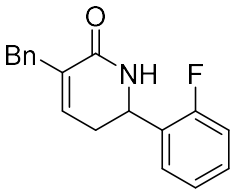

11ap

(16.8 mg, 60% yield)

^{1}H NMR (500 MHz, $CDCl_3$) δ 7.40 – 7.27 (m, 4H), 7.25 (d, *J* = 7.5 Hz, 3H), 7.14 (t, *J* = 7.6 Hz, 1H), 7.11 – 7.03 (m, 1H), 6.15 (ddt, *J* = 5.2, 3.4, 1.5 Hz, 1H), 5.66 (s, NH), 5.08 (ddd, *J* = 9.7, 5.9, 1.8 Hz, 1H), 3.71 (d, *J* = 16.6 Hz, 1H), 3.66 (d, *J* = 15.7 Hz, 1H), 2.69 (dt, *J* = 17.7, 5.5 Hz, 1H), 2.51 (dddt, *J* = 17.6, 9.7, 3.9, 2.1 Hz, 1H).

^{13}C NMR ($CDCl_3$, 126 MHz) δ 167.00, 160.92, 158.95, 139.16, 134.96, 134.71, 129.60, 129.53, 129.34, 128.41, 128.29, 128.19, 127.50, 127.47, 126.23, 124.53, 124.50, 115.77, 115.60, 48.69, 48.66, 36.07, 31.35.

^{19}F NMR ($CDCl_3$, 282 MHz) δ -118.24.

IR (neat, cm^{-1}) 3207, 3063, 2922, 1676, 1632, 1491, 757, 700.

LRMS (ESI) m/z calcd for $C_{18}H_{16}FNO$ $[M+H]^+$, $[M+Na]^+$: 281.1, found: 282.1, 304.1.

3-benzyl-6-(6,6,6,6,6-pentafluoro-6λ$_8$-hexa-1,3,5-triyn-1-yl)-5,6-dihydropyridin-2(1*H*)-one

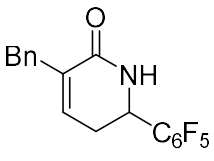

11aq

Yellow oil (17.7 mg, 50% yield).

^{1}H NMR (500 MHz, $CDCl_3$) δ 7.32-7.29 (m, 2H), 7.24-7.20 (m, 3H), 6.42 (s, NH), 6.15 (m, 1H), 5.14 (dd, *J* = 5.0, 10.0 Hz, 1H), 3.62 (q, *J* = 15.0 Hz), 2.76-2.71 (m, 1H), 2.54-2.48 (m, 1H).

^{13}C NMR ($CDCl_3$, 126 MHz) δ 166.53, 138.78, 135.29, 134.53, 129.35, 128.47, 126.33, 46.12, 35.92, 29.54.

^{19}F NMR ($CDCl_3$, 282 MHz) δ -138.86 – -140.68 (m), -151.01 – -153.96 (m), -159.97 (dd, *J* = 20.8, 14.0 Hz). IR (neat, cm^{-1}) 3207, 3065, 2926, 1679, 1633, 1522, 1502, 1000, 958, 700.

LRMS (ESI) m/z calcd for $C_{18}H_{12}F_5NO$ $[M+H]^+$: 353.1, found: 354.1.

(4a*S*,5*S*,8*R*,8a*S*)-3-benzyl-4a,5,6,7,8,8a-hexahydro-5,8-methanoquinolin-2(1*H*)-one

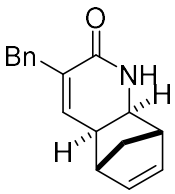

13aa

Off-white solid (20 mg, 80% yield).

^{1}H NMR (500 MHz, $CDCl_3$) δ 7.34 – 7.25 (m, 3H), 7.21 (d, *J* = 7.8 Hz, 2H), 6.19 (dd, *J* = 5.7, 3.0 Hz, 1H), 6.03 (s, NH), 6.01 (dd, *J* = 5.7, 3.0 Hz, 1H), 5.96 (d, *J* = 4.3 Hz, 1H), 3.63 (d, *J* = 15.7 Hz, 1H), 3.57 (d, *J* = 15.7 Hz, 1H), 3.49 (d, *J* = 9.4 Hz, 1H), 2.76 (s, 1H), 2.67 (s, 1H), 2.42-2.40 (m, 1H), 1.71 (d, *J* = 9.2 Hz, 1H), 1.48 (d, *J* = 9.2 Hz, 1H).

^{13}C NMR ($CDCl_3$, 126 MHz) 164.97, 139.63, 138.86, 137.67, 134.55, 131.71, 129.22, 128.35, 126.07, 54.24, 52.35, 48.47, 42.83, 37.86, 36.18.

IR (neat, cm^{-1}) 3204, 3059, 2970, 1681, 1634, 1477, 1453, 1279, 700.

LRMS (ESI) m/z calcd for $C_{17}H_{17}NO$ $[M+H]^+$, $[M+Na]^+$: 252.1, found: 252.2, 274.1.

(4a*S*,5*S*,8*R*,8a*S*)-3-benzyl-4a,5,6,7,8,8a-hexahydro-5,8-methanoquinolin-2(1*H*)-one

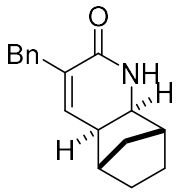

13ab

Off-white solid (23.2 mg, 92% yield).

^{1}H NMR (500 MHz, $CDCl_3$) δ 7.30 (t, *J* = 7.5 Hz, 2H), 7.22 (d, *J* = 7.7 Hz, 3H), 5.87 (d, *J* = 4.3 Hz, 1H), 5.75 (s, NH), 3.72 – 3.50 (m, 3H), 2.64 – 2.39 (m, 1H), 2.12 (s, 1H), 2.06 (s, 1H), 1.74 (m, 2H), 1.57 (m, 2H), 1.39 – 1.14 (m, 2H).

^{13}C NMR ($CDCl_3$, 126 MHz) 164.62, 139.74, 137.51, 130.92, 129.21, 128.32, 126.01, 58.25, 46.43, 43.19, 42.61, 35.93, 32.52, 29.60, 25.66.

IR (neat, cm^{-1}) 3204, 2952, 2872, 1683, 1635, 1453, 1477, 698.

LRMS m/z (ESI+APCI) calcd for $C_{17}H_{19}NO$ $[M+H]^+$: 254.2, found: 254.2.

3-benzyl-1,4a,5,6,7,7a-hexahydro-2*H*-cyclopenta[*b*]pyridin-2-one

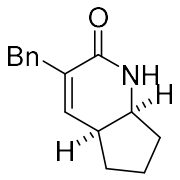

13ac

Off-white solid (20.2 mg, 93% yield).

1 mmol scale - 213 mg, 94% yield

^{1}H NMR (500 MHz, $CDCl_3$) δ 7.38 – 7.29 (m, 2H), 7.28 – 7.15 (m, 3H), 6.10 (dt, *J* = 5.1, 1.5 Hz, 1H), 5.61 (s, NH), 3.97 (dddd, *J* = 7.6, 5.6, 3.6, 1.6 Hz, 1H), 3.65 (d, *J* = 15.8 Hz, 1H), 3.59 (d, *J* = 15.7 Hz, 1H), 2.64 (p, *J* = 7.4 Hz, 1H), 2.12 – 1.88 (m, 2H), 1.88 – 1.45 (m, 4H).

^{13}C NMR ($CDCl_3$, 126 MHz) δ 165.49, 139.61, 139.50, 132.06, 129.26, 128.34, 126.04, 55.34, 38.53, 35.99, 34.93, 32.09, 23.13.

IR (neat, cm^{-1}) 3204, 3027, 2956, 1675, 1629, 1494, 1452, 699.

LRMS (ESI) m/z calcd for $C_{15}H_{17}NO$ $[M+H]^+$: 228.1, found: 228.2.

3-benzyl-1,4a,5,9b-tetrahydro-2*H*-indeno[1,2-*b*]pyridin-2-one

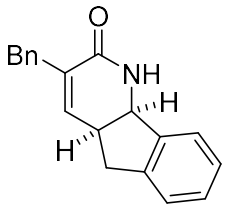

13ad

Off-white solid (17.8 mg, 65% yield).

^{1}H NMR (500 MHz, $CDCl_3$) δ 7.32-7.25 (m, 6H), 7.20 (t, *J* = 5.0 Hz, 1H), 7.20 (d, *J* = 5.0 Hz, 2H), 6.42 (s, NH), 6.07 (d, *J* = 5.0 Hz, 1H), 4.93 (dd, *J* = 5.0, 7.5 Hz, 1H), 3.67 (d, *J* = 15.0 Hz, 1H), 3.56 (d, *J* = 15.0 Hz, 1H), 3.35 (m, 1H), 3.24 (dd, *J* = 5.0, 15.0 Hz, 1H), 2.92 (dd, *J* = 5.0, 15.0 Hz, 1H).

^{13}C NMR ($CDCl_3$, 126 MHz) δ 164.87, 142.60, 141.18, 139.32, 138.93, 133.63, 129.14, 128.33, 127.21, 126.05, 124.77, 123.81, 58.20, 38.91, 38.13, 35.98.

IR (neat, cm^{-1}) 3210, 3026, 2915, 1676, 1629, 1478, 743, 699.

LRMS (ESI) m/z calcd for $C_{19}H_{17}NO$ $[M+H]^+$, $[M+Na]^+$: 276.1, 298.1, found: 276.1, 298.0.

(4aS,8aS)-3-benzyl-4a,5,6,8a-tetrahydroquinolin-2(1H)-one

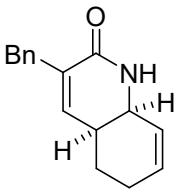

13ae

Off-white solid (21 mg, 88% yield).

^{1}H NMR (500 MHz, $CDCl_3$) δ 7.32 – 7.25 (m, 2H), 7.20 (d, *J* = 7.1 Hz, 3H), 6.06 (d, *J* = 5.1 Hz, 1H), 5.93 (dt, *J* = 8.7, 4.1 Hz, 1H), 5.61 (ddt, *J* = 9.9, 4.3, 2.2 Hz, 2H), 5.58 (s, NH), 4.04 (m, 1H), 3.65 (d, *J* = 15.8 Hz, 1H), 3.57 (d, *J* = 15.8 Hz, 1H), 2.48 – 2.37 (m, 1H), 2.15 – 1.95 (m, 2H), 1.76 – 1.53 (m, 2H).

^{13}C NMR ($CDCl_3$, 126 MHz) δ 165.70, 139.96, 139.46, 133.96, 131.28, 129.25, 128.35, 126.08, 124.98, 76.79, 48.13, 35.98, 34.01, 24.13, 22.69.

IR (neat, cm^{-1}) 3206, 3026, 2923, 1674, 1628, 1429, 1453, 738, 700.

LRMS (ESI) m/z calcd for $C_{16}H_{17}NO$ $[M+H]^+$, $[M+Na]^+$: 240.1, 262.1, found: 240.2, 262.2.

(4a*S*,10b*R*)-3-benzyl-4a,5,6,10b-tetrahydrobenzo[*h*]quinolin-2(1*H*)-one

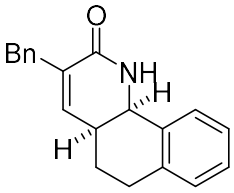

13ag

Off-white solid (18.3 mg, 63% yield).

^{1}H NMR (500 MHz, $CDCl_3$) δ 7.37 – 7.16 (m, 9H), 6.27 (d, *J* = 5.9 Hz, 1H), 5.45 (s, NH), 4.72 (d, *J* = 5.0 Hz, 1H), 3.74 (d, *J* = 15.8 Hz, 1H), 3.62 (d, *J* = 15.8 Hz, 1H), 2.90 (ddd, *J* = 17.0, 5.3, 2.9 Hz, 1H), 2.79 (ddd, *J* = 17.1, 11.8, 5.6 Hz, 1H), 2.57 – 2.47 (m, 1H), 1.92 (dtd, *J* = 13.4, 11.8, 5.2 Hz, 1H), 1.79 (ddt, *J* = 13.3, 5.9, 3.0 Hz, 1H).

^{13}C NMR ($CDCl_3$, 126 MHz) δ 165.54, 139.87, 139.32, 136.54, 134.30, 134.25, 129.48, 129.29, 128.64, 128.42, 128.27, 126.87, 126.17, 51.62, 35.98, 34.83, 28.71, 22.49.

IR (neat, cm^{-1}) 3060, 2925, 1674, 1631, 1494, 1427, 741, 700.

LRMS (ESI) m/z calcd for $C_{20}H_{19}NO$ $[M+H]^+$, $[M+Na]^+$: 290.2, 312.2, found: 290.1, 312.1.

(4a*S*,10a*S*)-3-benzyl-4a,5,6,7,8,9,10,10a-octahydrocycloocta[*b*]pyridin-2(1*H*)-one

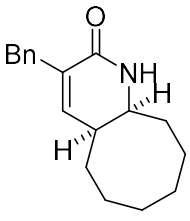

13ah

Off-white solid (20.1 mg, 75% yield).

^{1}H NMR (500 MHz, $CDCl_3$) δ 7.30-7.26 (m, 2H), 7.20-7.18 (m, 3H), 6.09 (d, *J* = 6.2 Hz, 1H), 5.48 (s, NH), 3.67 (dt, *J* = 10.1, 4.5 Hz, 1H), 3.58 (dd, *J* = 42.5, 15.8 Hz, 2H), 2.48-2.44 (m, 1H), 1.84 (m, 2H), 1.70-1.59 (m, 4H), 1.32-1.26 (m, 1H).

^{13}C NMR ($CDCl_3$, 126 MHz) δ 167.01, 142.45, 139.60, 132.14, 129.24, 128.35, 126.04, 54.03, 36.88, 35.72, 29.03, 28.27, 27.12, 25.29, 24.91, 23.50.

IR (neat, cm^{-1}) 3204, 2920, 2852, 1675, 1631, 1452, 1427, 698.

LRMS m/z (ESI+APCI) calcd for $C_{18}H_{23}NO$ $[M+H]^+$, $[M+Na]^+$: 270.2, 292.2, found: 270.2, 292.1.

3-benzyl-6-cyclohexyl-5,6-dihydropyridin-2(1H)-one

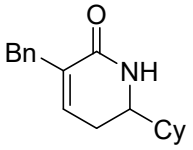

11ar

Off-white solid (21.2 mg, 79% yield) was obtained from $[Cp^*RhCl_2]_2$ precatalyst.

1 mmol scale - 220 mg, 81% yield

^{1}H NMR (500 MHz, $CDCl_3$) δ 7.35 – 7.28 (m, 2H), 7.23 (m, 3H), 6.13 (ddt, *J* = 5.0, 3.3, 1.6 Hz, 1H), 5.64 (s, NH), 3.65 (d, *J* = 15.8 Hz, 1H), 3.60 (d, *J* = 15.8 Hz, 1H), 3.34 (dt, *J* = 11.3, 6.0 Hz, 1H), 2.31 – 2.15 (m, 2H), 1.87 – 1.65 (m, 4H), 1.41 (tdt, *J* = 12.0, 6.4, 3.3 Hz, 1H), 1.31 – 1.10 (m, 4H), 1.00 (qt, *J* = 12.5, 2.9 Hz, 2H).

^{13}C NMR ($CDCl_3$, 126 MHz) δ 167.09, 139.48, 135.78, 134.66, 129.30, 128.35, 126.09, 55.81, 41.76, 35.95, 28.81, 28.71, 27.30, 26.28, 26.04, 26.00.

IR (neat, cm^{-1}) 3205, 3062, 2923, 2852, 1674, 1631, 1450, 1428, 698.

LRMS (ESI) m/z calcd for $C_{18}H_{23}NO$ $[M+H]^+$: 270.2, found: 270.1.

The regiochemsitry based on COSY experiment.

3-benzyl-5-cyclopentyl-5,6-dihydropyridin-2(1H)-one

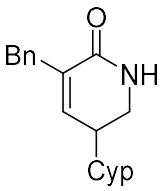

11as'

Off-white solid (16.8 mg, 76% yield) was obtained from $[Cp^tRhCl_2]_2$ precatalyst.

^{1}H NMR (500 MHz, $CDCl_3$) δ 7.34 – 7.28 (m, 2H), 7.23 (dd, *J* = 7.8, 2.9 Hz, 3H), 6.17 (m, 1H), 6.10 (s, NH), 3.66 (d, *J* = 15.7 Hz, 1H), 3.61 (d, *J* = 15.7 Hz, 1H), 3.42 (ddd, *J* = 12.0, 5.8, 3.0 Hz, 1H), 3.21 (ddd, *J* = 11.7, 8.5, 2.3 Hz, 1H), 2.28 – 2.20 (m, 1H), 1.87 (dtd, *J* = 16.5, 9.3, 7.4 Hz, 1H), 1.81 – 1.70 (m, 2H), 1.63 (m, 2H), 1.58 – 1.50 (m, 2H), 1.22 – 1.09 (m, 2H).

^{13}C NMR ($CDCl_3$, 126 MHz) δ 166.89, 140.72, 139.51, 134.09, 129.17, 128.35, 126.08, 44.26, 41.95, 40.03, 36.24, 30.89, 30.20, 25.24, 25.08.

IR (neat, cm^{-1}) 2949, 2866, 1676, 1628, 1477, 1452, 1032, 699.

LRMS m/z (ESI+APCI) calcd for $C_{17}H_{21}NO$ $[M+H]^+$, $[M+Na]^+$: 256.2, found: 256.2, 278.2.

The regiochemsitry based on COSY experiment.

3,6-dibenzyl-5,6-dihydropyridin-2(1H)-one

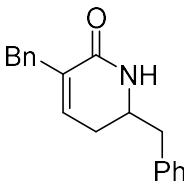

11aa

Off-white solid (7.2 mg, 32% yield)

^{1}H NMR (500 MHz, $CDCl_3$) δ 7.38 – 7.25 (m, 5H), 7.26 – 7.20 (m, 3H), 7.18 (m, 2H), 6.13 (ddt, *J* = 5.9, 3.1, 1.6 Hz, 1H), 5.47 (s, NH), 3.84 – 3.76 (m, 1H), 3.64 (d, *J* = 16.8 Hz, 1H), 3.60 (d, *J* = 15.9 Hz, 1H), 2.89 (dd, *J* = 13.5, 5.5 Hz, 1H), 2.74 (dd, *J* = 13.5, 8.9 Hz, 1H), 2.39 (dtd, *J* = 17.4, 5.4, 1.4 Hz, 1H), 2.25 (ddq, *J* = 16.6, 11.1, 2.6 Hz, 1H).

^{13}C NMR ($CDCl_3$, 126 MHz) δ 166.86, 139.32, 136.55, 135.26, 135.05, 129.29, 129.12, 128.94, 128.39, 127.11, 126.16, 52.21, 41.82, 35.97, 30.41.

IR (neat, cm^{-1}) 3204, 2923, 1675, 1630, 1453, 1032, 701.

LRMS (ESI) m/z calcd for $C_{19}H_{19}NO$ $[M+H]^+$: 278.2, found: 278.2.

3,5-dibenzyl-5,6-dihydropyridin-2(1H)-one

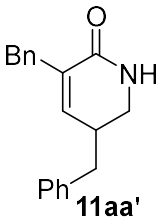

11aa'

Off-white solid (13.4 mg, 48% yield)

^{1}H NMR (500 MHz, $CDCl_3$) δ 7.31 (m, 4H), 7.28 – 7.20 (m, 4H), 7.16 – 7.10 (m, 2H), 6.15 – 6.10 (m, 1H), 5.78 (s, NH), 3.66 (d, *J* = 15.8 Hz, 1H), 3.62 (d, *J* = 15.7 Hz, 1H), 3.34 (ddd, *J* = 12.2, 5.2, 2.1 Hz, 1H), 3.15 (ddd, *J* = 12.2, 6.7, 2.3 Hz, 1H), 2.84 – 2.76 (m, 1H), 2.75 – 2.60 (m, 2H).

^{13}C NMR ($CDCl_3$, 126 MHz) δ 166.60, 140.57, 139.25, 138.67, 134.56, 129.27, 128.92, 128.60, 128.39, 126.55, 126.17, 43.87, 38.03, 36.28, 36.13.

IR (neat, cm^{-1}) 3217, 3061, 3027, 2921, 2851, 1675, 1627, 1477, 1452, 735, 700.

LRMS (ESI) m /z calcd for $C_{19}H_{19}NO$ $[M+H]^+$: 278.2, found: 278.2.

3-benzyl-5-phenethyl-5,6-dihydropyridin-2(1H)-one

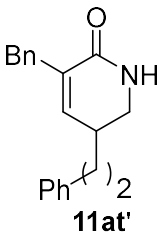

11at'

Off-white solid (20 mg, 69% yield) was obtained from $[Cp^tRhCl_2]_2$ precatalyst.

^{1}H NMR (500 MHz, $CDCl_3$) δ 7.38 – 7.27 (m, 4H), 7.26 – 7.18 (m, 4H), 7.17 – 7.11 (m, 2H), 6.11 (m, 1H), 6.00 (s, NH), 3.64 (s, 2H), 3.47 (ddd, *J* = 12.1, 5.8, 2.9 Hz, 1H), 3.20 (ddd, *J* = 12.1, 7.9, 2.7 Hz, 1H), 2.64 (ddd, *J* = 9.0, 7.1, 2.3 Hz, 2H), 2.45 (m, 1H), 1.96 – 1.66 (m, 2H).

^{13}C NMR ($CDCl_3$, 126 MHz) δ 166.70, 141.24, 140.83, 139.33, 134.37, 129.25, 128.52, 128.41, 128.27, 126.16, 126.12, 44.47, 36.12, 33.80, 33.63, 33.08.

IR (neat, cm^{-1}) 3291, 2923, 2858, 1671, 1623, 1478, 1453, 1030, 747, 699.

LRMS (ESI) m/z calcd for $C_{20}H_{21}NO$ $[M+H]^+$: 292.2, found: 292.1.

3-benzyl-5-pentyl-5,6-dihydropyridin-2(1H)-one

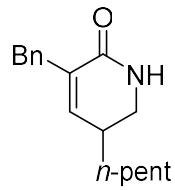

11au'

Off-white solid (14.2 mg, 55% yield) was obtained from $[Cp^tRhCl_2]_2$ precatalyst

^{1}H NMR (500 MHz, $CDCl_3$) δ 7.35 – 7.29 (m, 2H), 7.23 (d, *J* = 7.7 Hz, 3H), 6.10 – 6.08 (m, 1H), 6.02 (s, NH), 3.63 (s, 2H), 3.42 (ddd, *J* = 11.9, 5.8, 2.4 Hz, 1H), 3.14 (ddd, *J* = 12.0, 8.4, 2.0 Hz, 1H), 2.42 (m, 1H), 1.53 – 1.36 (m, 2H), 1.36 – 1.18 (m, 6H), 0.90 (t, *J* = 6.9 Hz, 3H).

^{13}C NMR ($CDCl_3$, 126 MHz) δ 166.85, 141.54, 139.46, 133.89, 129.22, 128.36, 126.09, 44.60, 36.12, 34.47, 31.99, 31.73, 26.56, 22.49, 14.00.

IR (neat, cm^{-1}) 3202, 3062, 2952, 2923, 2854, 1678, 1626, 1483, 744, 701.

LRMS (ESI) m/z calcd for $C_{17}H_{23}NO$ $[M+H]^+$: 258.2, found: 258.2.

The regiochemsitry based on COSY experiment.

3-benzyl-5-(4-bromobutyl)-5,6-dihydropyridin-2(1H)-one

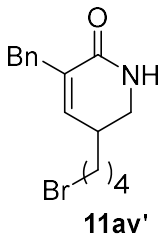

11av'

(21.3 mg, 66% yield) was obtained from $[Cp^tRhCl_2]_2$ precatalyst. **^{1}H NMR** (500 MHz, $CDCl_3$) δ 7.34 – 7.29 (m, 2H), 7.27 – 7.21 (m, 3H), 6.08 (m, 1H), 6.08 (s, NH), 3.63 (s, 2H), 3.45 (ddd, *J* = 12.0, 5.8, 2.8 Hz, 1H), 3.41 (t, *J* = 6.6 Hz, 2H), 3.16 (ddd, *J* = 12.0, 8.1, 2.4 Hz, 1H), 2.43 (ddt, *J* = 7.9, 4.0, 2.1 Hz, 1H), 1.86 (m, 4H), 1.46 (m, 4H).

^{13}C NMR ($CDCl_3$, 126 MHz) δ 166.72, 140.81, 139.30, 134.34, 129.24, 128.41, 126.16, 44.46, 36.11, 34.29, 33.45, 32.48, 31.12, 25.43.

IR (neat, cm^{-1}) 3216, 2931, 2858, 1675, 1627, 1477, 1453, 701.

LRMS m/z (ESI+APCI) calcd for $C_{16}H_{20}BrNO$ $[M+H]^+$: 322.1, 324.1, found: 322.0, 323.9.

ethyl 5-(5-benzyl-6-oxo-1,2,3,6-tetrahydropyridin-3-yl)pentanoate

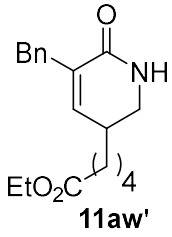

11aw'

(17.2 mg, 55% yield) was obtained from $[Cp^tRhCl_2]_2$ precatalyst. **^{1}H NMR** (500 MHz, $CDCl_3$) δ 7.35 – 7.27 (m, 2H), 7.22 (m, 3H), 6.08 (m, 1H), 5.91 (s, NH), 4.14 (q, *J* = 7.1 Hz, 2H), 3.62 (s, 2H), 3.43 (ddd, *J* = 12.1, 5.9, 2.8 Hz, 1H), 3.14 (ddd, *J* = 12.0, 8.2, 2.3 Hz, 1H), 2.49 – 2.38 (m, 2H), 2.30 (t, *J* = 7.4 Hz, 2H), 1.74 – 1.36 (m, 4H), 1.27 (t, *J* = 7.1 Hz, 3H). **^{13}C NMR** ($CDCl_3$, 126 MHz) δ 173.46, 166.69, 141.06, 139.35, 134.16, 129.22, 128.38, 126.13, 60.30, 44.51, 36.12, 34.28, 34.05, 31.68, 26.39, 24.81, 14.27.

IR (neat, cm^{-1}) 3220, 2931, 2860, 1731, 1676, 1628, 1477, 1266, 1183, 733, 701.

LRMS (ESI) m/z calcd for $C_{19}H_{25}NO_3$ $[M+H]^+$: 315.2, found: 316.1.

5. Control Experiments and Mechanistic Studies

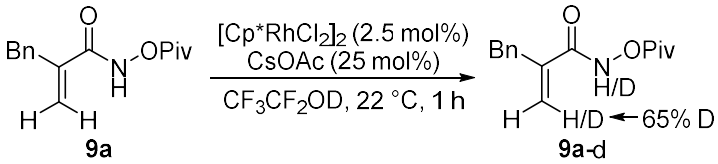

The reversibility of the C-H activation was determined by running the reaction in the absence of styrene in TFE-d_1. After 1 h, 65% deuterium incorporation at the C-H bond *cis* to amide was observed, as determined by ^{1}H-NMR.

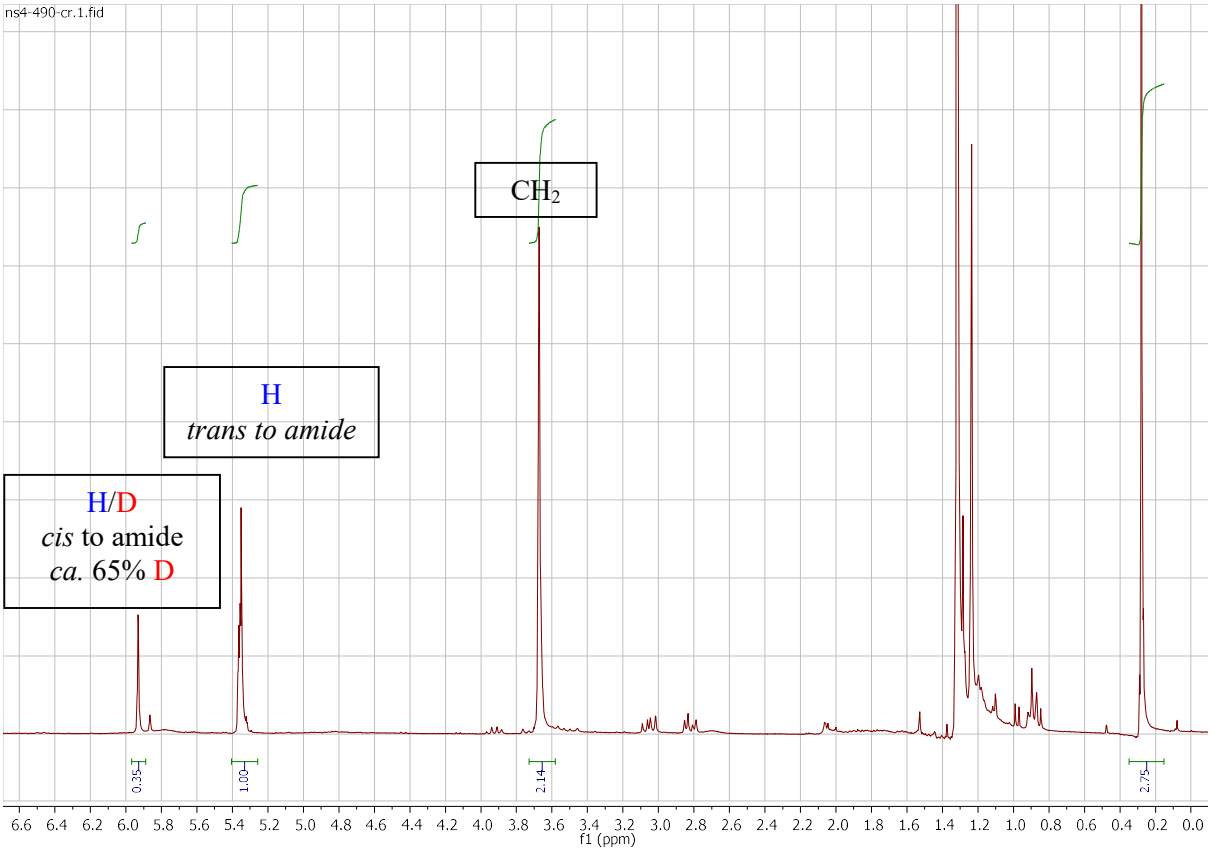

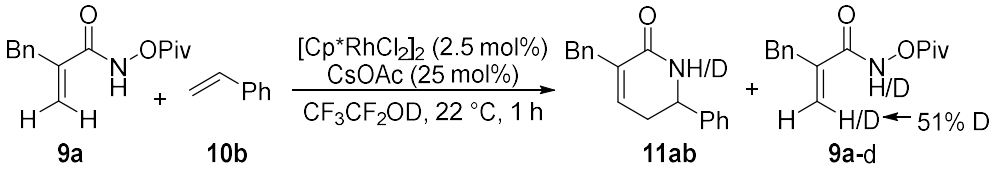

Additionally, an experiment with styrene was conducted using TFE-d_1. After 1 h (ca. 60% conversion), 51% deuterium incorporation to **1a**-d at the C-H bond *cis* to the amide was observed. These results together suggest that the C-H activation is fast and reversible step.

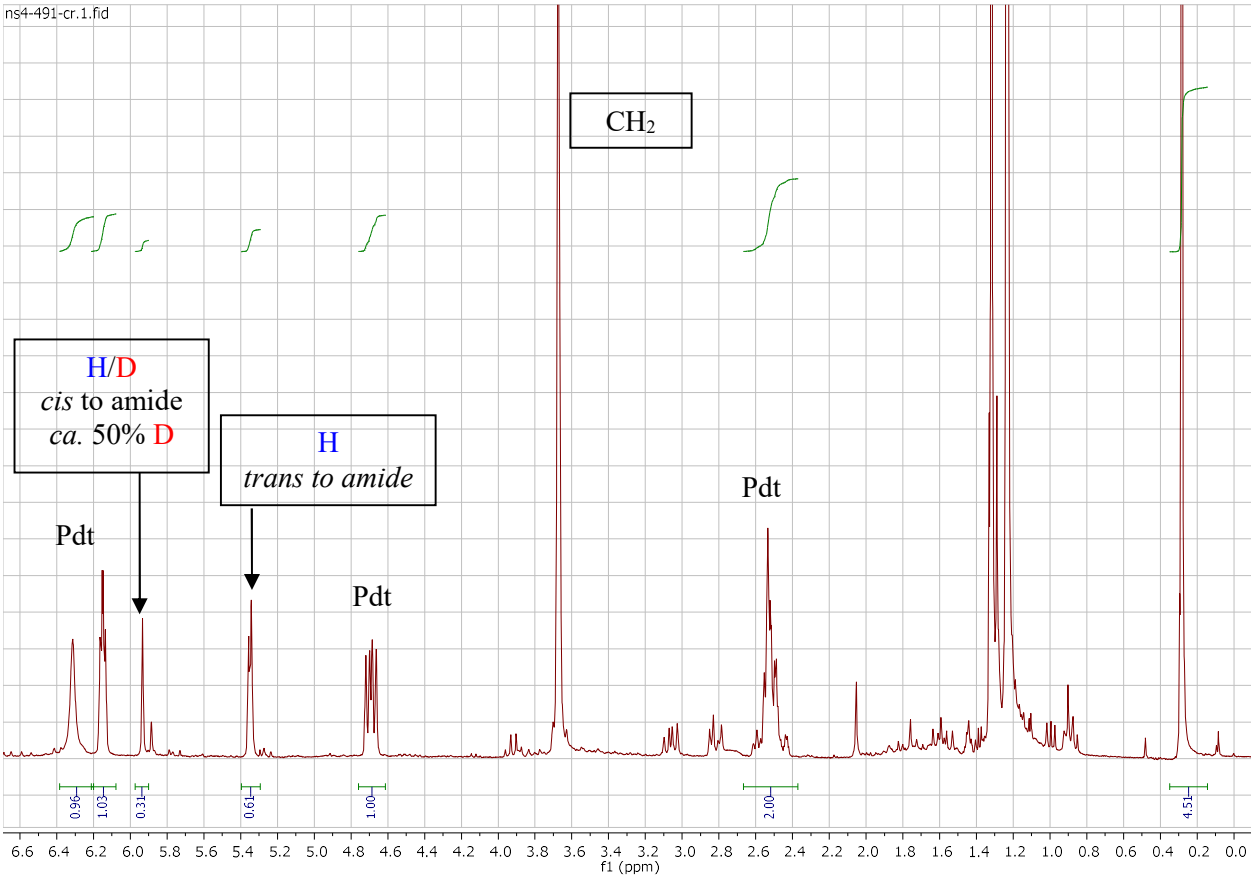

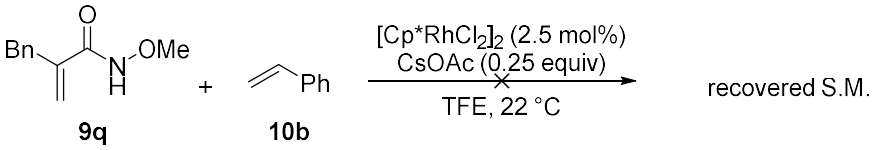

N-methoxy α-benzyl acrylamide did not give any product, implies that the *N*-pivaloyloxy group is essential for this reaction.

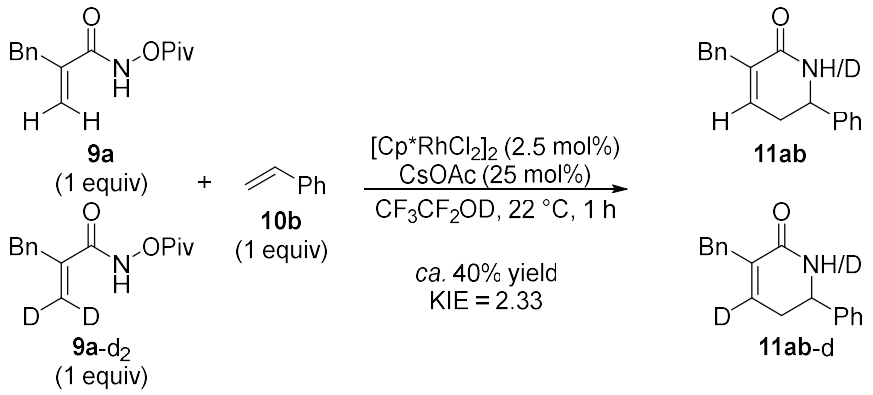

9a (13.1 mg, 0.05 mmol, 1 eq), **9a-**d_2 (13.2 mg, 0.05 mmol, 1 eq), $[Cp^*RhCl_2]_2$ (1.5 mg, 0.0025 mmol, 2.5 mol%), CsOAc (4.8 mg, 0.025 mmol, 0.25 equiv) and styrene (12.6 μL, 0.11 mmol, 1.1 equiv) were charged into a dram vial charged with a stir bar. Trifluoroethanol-d_1 (TFE-d_1) (0.33 mL, 0.3 M) was added and the mixture was stirred at room temperature for 1 h. The reaction was quenched with saturated $NaHCO_3$ and extracted 3 times with EtOAc. The organic layer was washed with brine, dried over $MgSO_4$, filtered, and solvent was evaporated to obtain crude product. The crude was analyzed by ^{1}H-NMR spectrometer. The KIE value (P_H/P_D) of 2.3 was calculated by integrating the H_a of the product **11ab** (0.70) and H_c of products **11ab** (0.70) and **11ab**-d (0.30). However the reversibility of C-H activation may be taken to account for KIE.

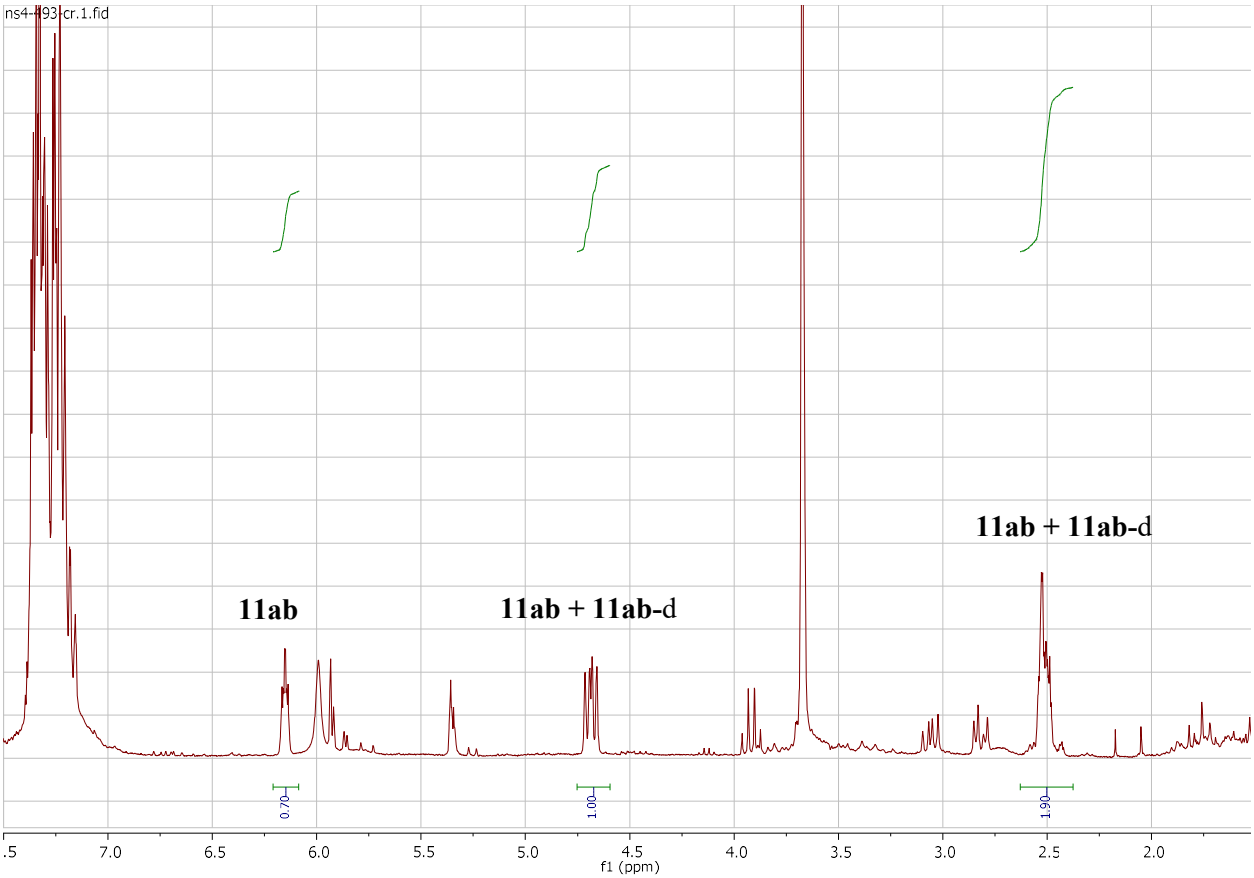

6. Product derivatizations

General procedure for the hydrogenation: Pd/C (10% wt) was weighed to the N_2-filled round bottom flask containing the α,β-unsaturated-δ-lactams (0.1 mmol). This was evacuated and refilled with N_2 (×3), following by adding MeOH (0.1 M). Then, the suspension was stirred under H_2 (balloon) until completion as indicated by TLC. The resulting solution was filtered through a plug of celite and washed with EtOAc. The desired saturated lactams was obtained after the volatiles were removed under reduced pressure.

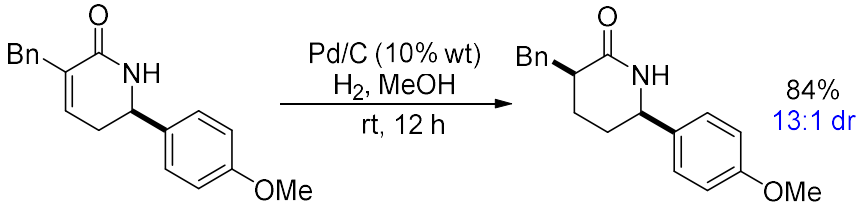

(3S,6R)-3-benzyl-6-(4-methoxyphenyl)piperidin-2-one

Off-white solid (24.5 mg, 84% yield, 13:1 dr)

^{1}H NMR (500 MHz, $CDCl_3$) δ 7.38 – 7.29 (m, 2H), 7.27 – 7.21 (m, 3H), 7.05 (d, *J* = 8.6 Hz, 2H), 6.85 (d, *J* = 8.7 Hz, 2H), 5.98 (s, NH), 4.62 – 4.50 (m, 1H), 3.82 (s, 3H), 3.32 (dd, *J* = 13.5, 4.0 Hz, 1H), 2.93

(dd, *J* = 13.5, 9.7 Hz, 1H), 2.78 – 2.63 (m, 1H), 1.99 (dddd, *J* = 13.4, 8.4, 5.1, 3.3 Hz, 1H), 1.80 – 1.70 (m, 1H), 1.71 – 1.52 (m, 2H).

^{13}C NMR ($CDCl_3$, 126 MHz) δ 174.35, 159.07, 139.45, 134.53, 129.52, 128.42, 127.18, 126.33, 114.02, 56.46, 55.32, 42.34, 37.56, 29.39, 21.80.

IR (neat, cm^{-1}) 3204, 2934, 1622, 1511, 1454, 1247.

LRMS (ESI) m/z calcd for $C_{19}H_{21}NO_2$ $[M+H]^+$, $[M+Na]^+$: 295.2, found: 296.1, 318.1.

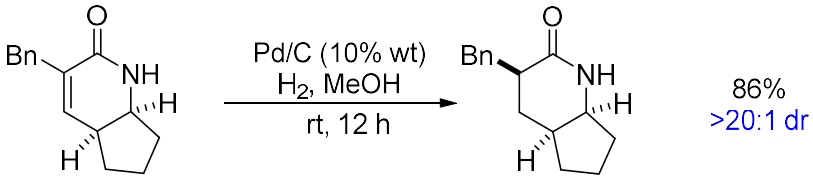

(3S,4aS,7aS)-3-benzyloctahydro-2H-cyclopenta[b]pyridin-2-one

Off-white solid (19.7 mg, 86% yield, >20:1 dr)

^{1}H NMR (500 MHz, $CDCl_3$) δ 7.31 (m, 2H), 7.22 (m, 3H), 6.16 (s, NH), 3.70 (qd, *J* = 7.5, 1.9 Hz, 1H), 3.52 (dd, *J* = 13.8, 3.8 Hz, 1H), 2.52 (dd, *J* = 13.8, 10.2 Hz, 1H), 2.39 (ddt, *J* = 14.2, 10.1, 4.2 Hz, 1H), 2.21 (dtdd, *J* = 12.2, 8.0, 5.8, 4.3 Hz, 1H), 2.01 – 1.90 (m, 1H), 1.85 (dtd, *J* = 13.3, 7.9, 5.6 Hz, 1H), 1.75 (tdd, *J* = 10.2, 7.6, 4.6 Hz, 2H), 1.53 (tdd, *J* = 10.6, 7.6, 5.2 Hz, 2H), 1.41 – 1.33 (m, 1H), 1.25 (q, *J* = 12.6 Hz, 1H).

^{13}C NMR ($CDCl_3$, 126 MHz) δ 175.18, 140.38, 129.24, 128.32, 126.03, 55.29, 42.28, 36.51, 36.26, 34.32, 31.55, 30.80, 22.95.

IR (neat, cm^{-1}) 3203, 2943, 1662, 1453, 701.

LRMS (ESI) m/z calcd for $C_{15}H_{19}NO$ $[M+H]^+$, $[M+Na]^+$: 229.2, found: 230.2, 252.2.

7. NMR Spectra

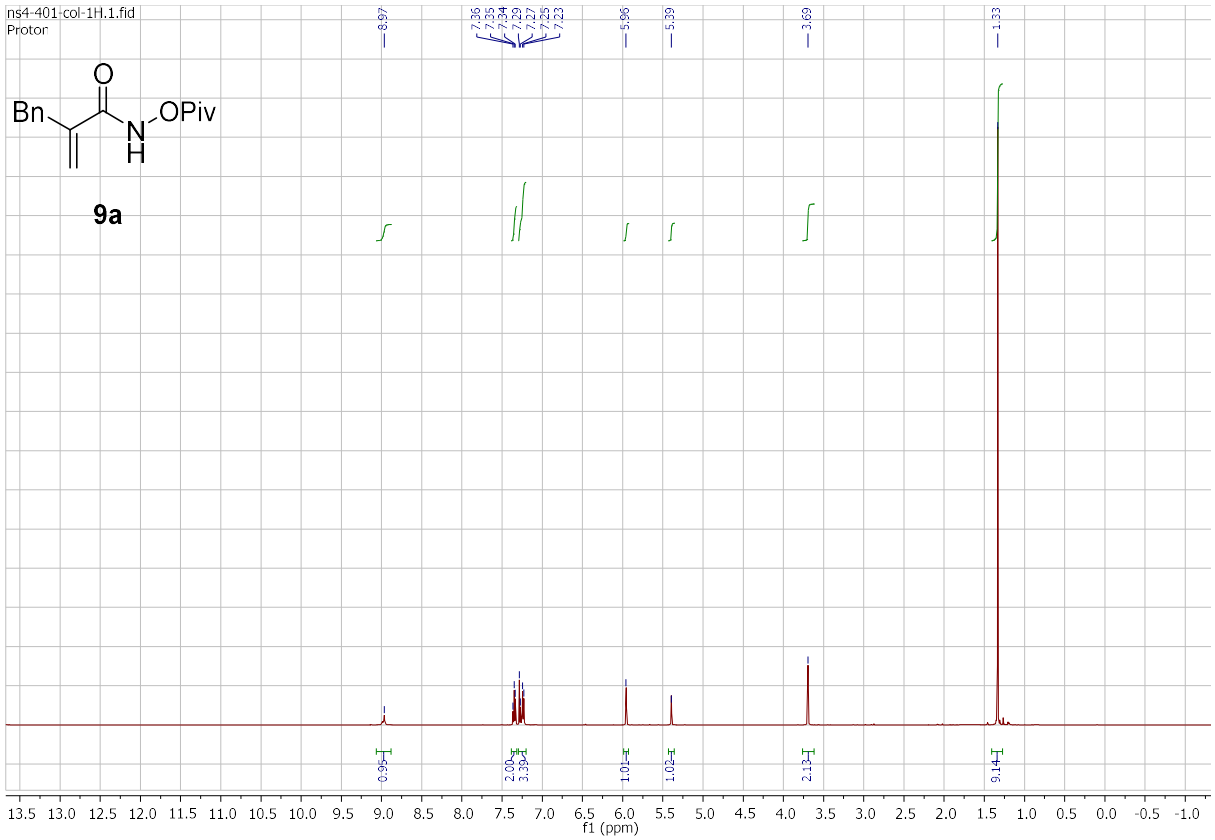
ns4-401-col-1H.1.fid
Protor
Bn
O
N
H
OPiv
9a
8.97
7.36
7.35
7.34
7.29
7.27
7.25
7.23
5.96
5.39
3.69
1.33
0.96
2.00
3.39
1.01
1.02
2.13
9.14
f1 (ppm)

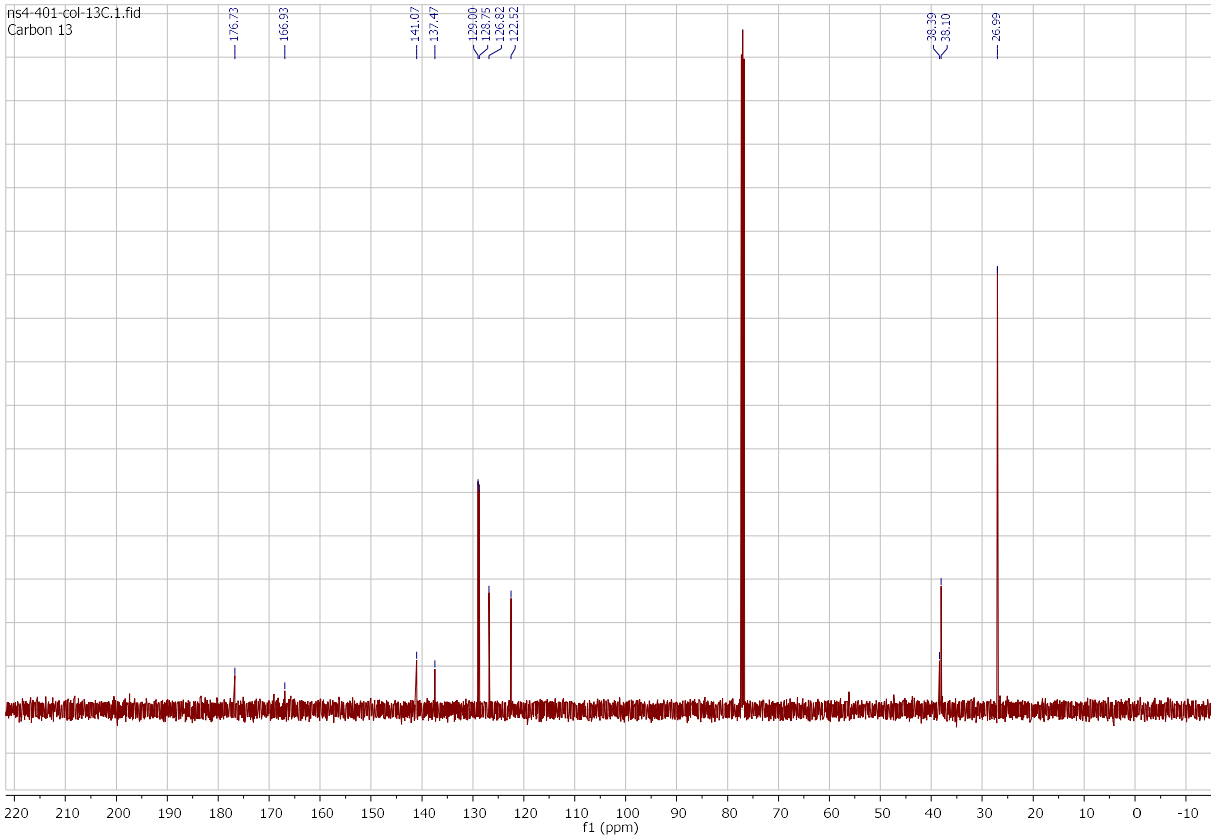
ns4-401-col-13C.1.fid
Carbon 13
176.73
166.93
141.07
137.47
129.00
128.75
126.82
122.52
38.39
38.10
26.99
f1 (ppm)

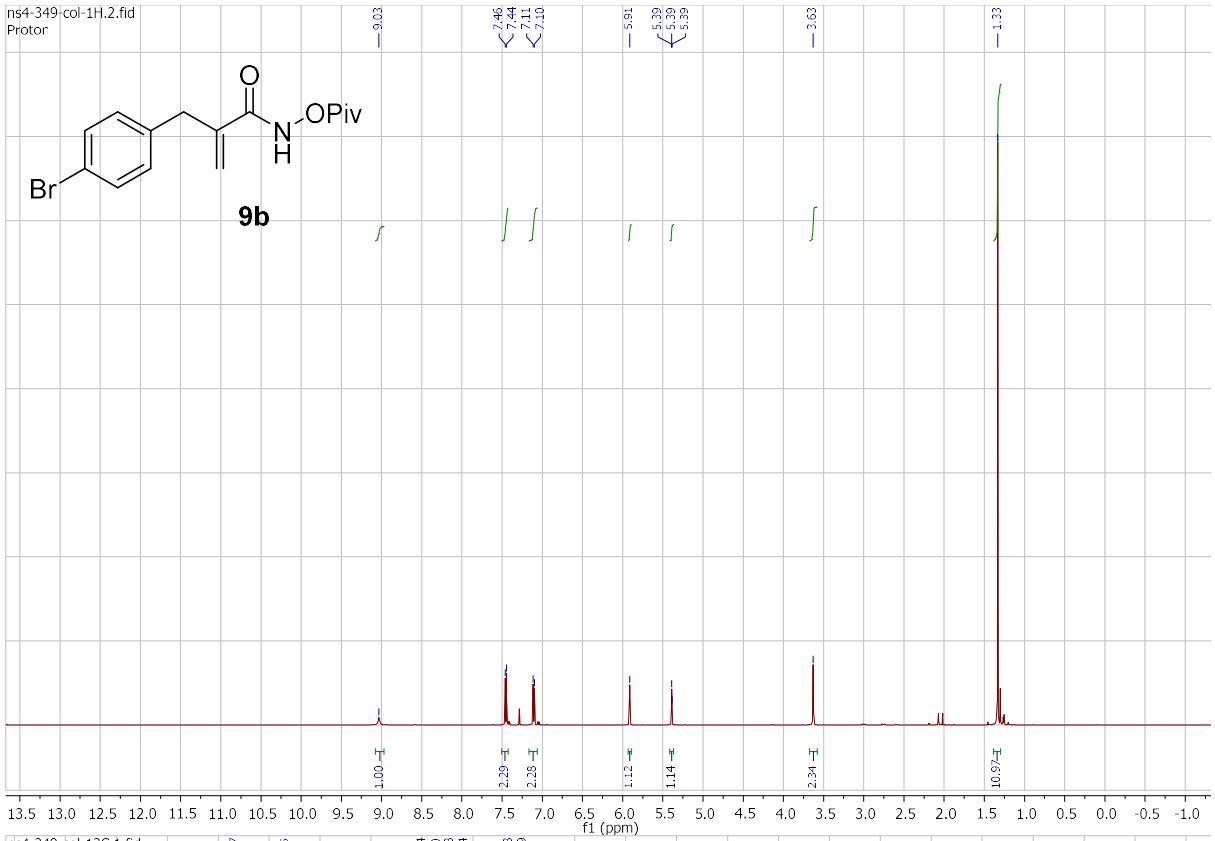
ns4-349-col-1H.2.fid
Protor
9.03
7.46
7.44
7.11
7.10
5.91
5.39
5.39
5.39
3.63
1.33
O
N
H
OPiv
Br
9b
1.00
2.29
2.28
1.12
1.14
2.34
10.97
f1 (ppm)

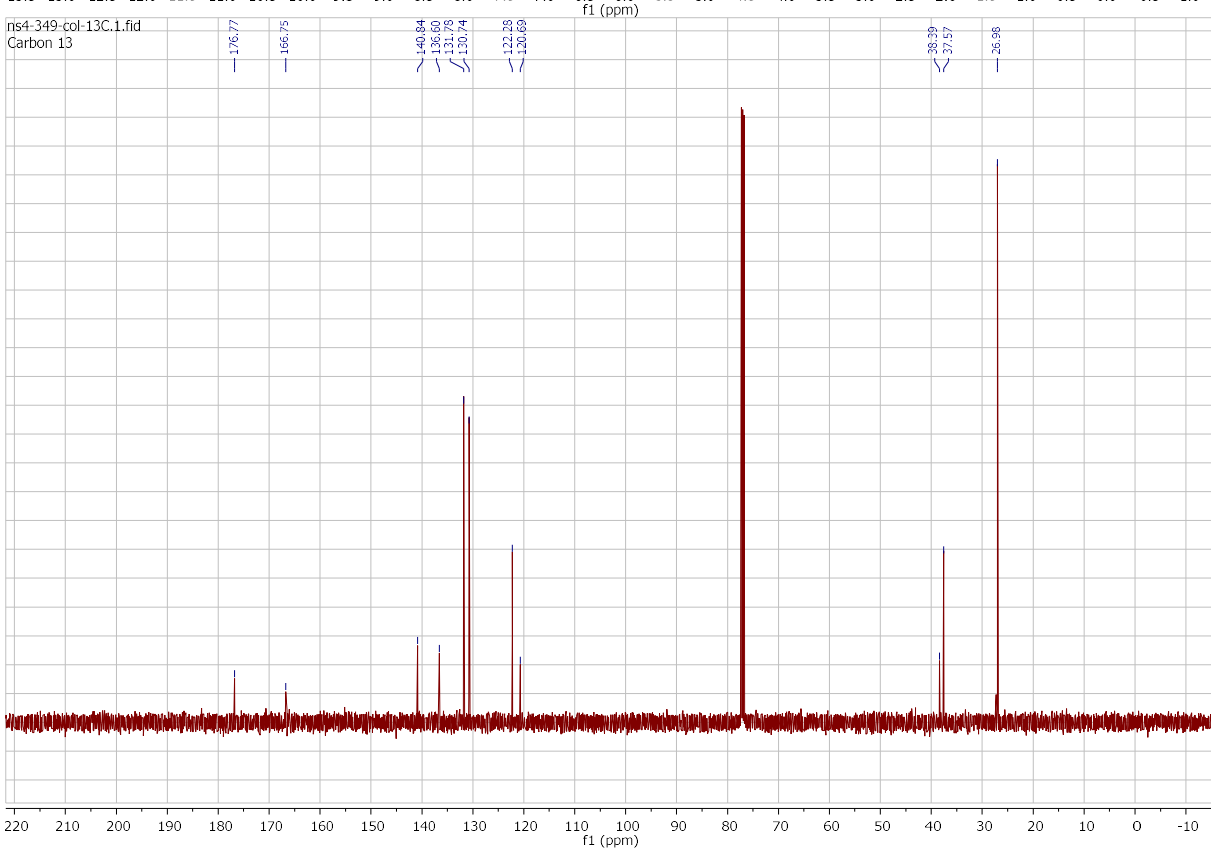
ns4-349-col-13C.1.fid
Carbon 13
176.77
166.75
140.84
136.60
131.78
130.74
122.28
120.69
38.39
37.57
26.98
f1 (ppm)

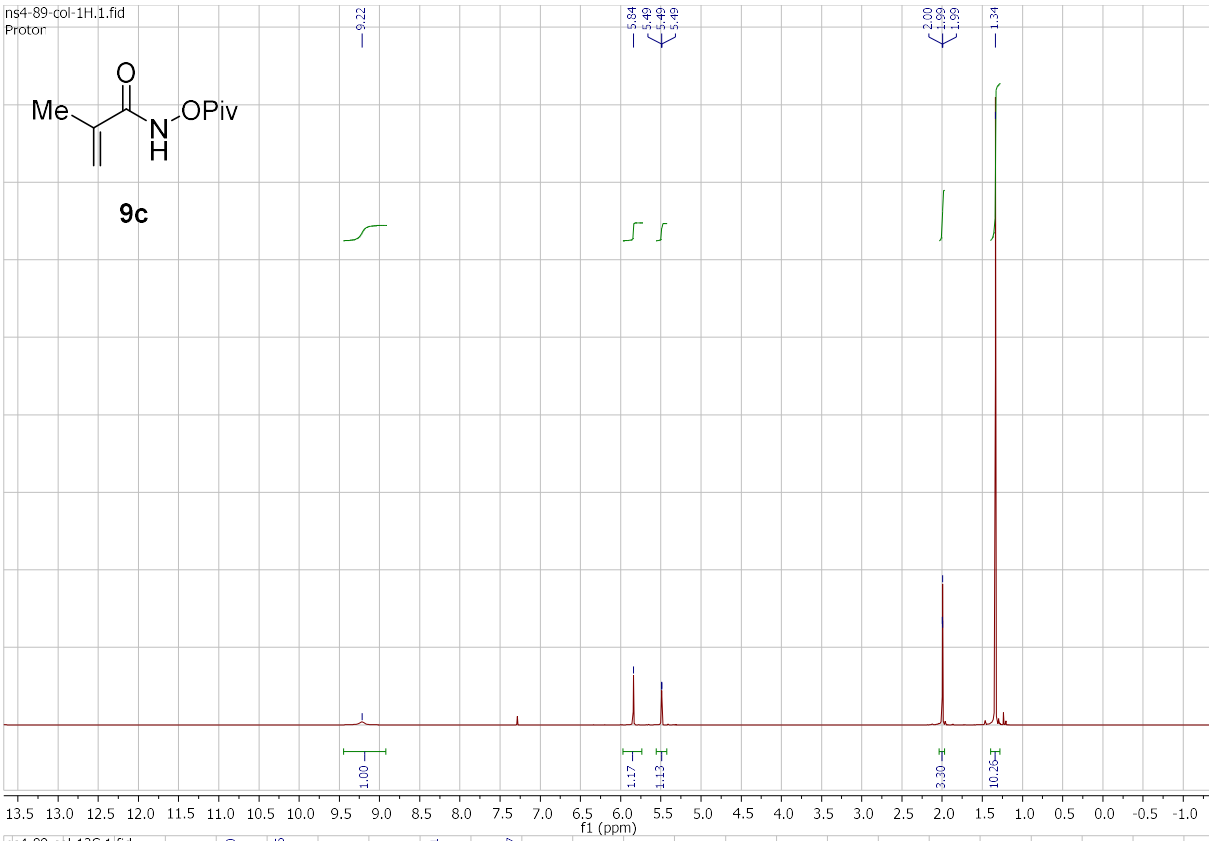
ns4-89-col-1H.1.fid
Proton
Me
O
N
H
OPiv
9c
9.22
5.84
5.49
5.49
5.49
2.00
1.99
1.99
1.34
1.00
1.17
1.13
3.30
10.26
f1 (ppm)

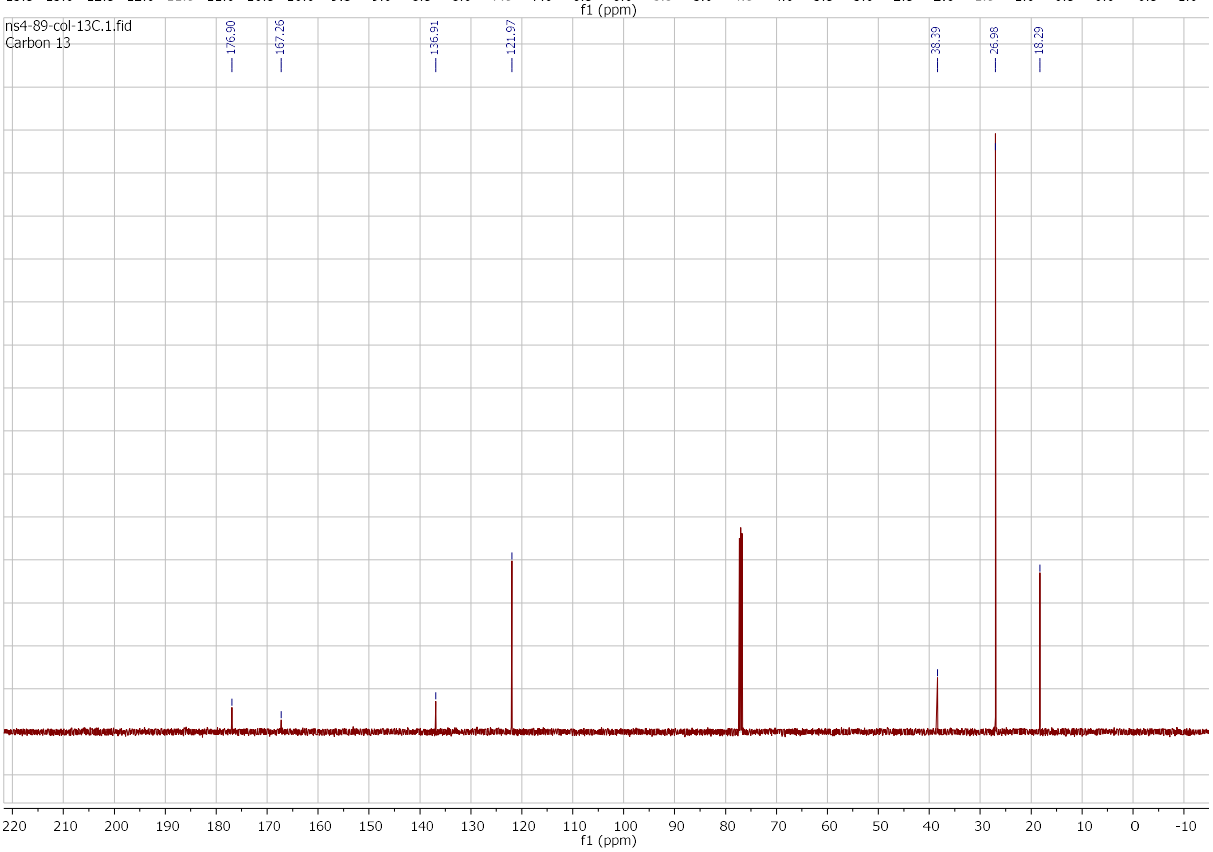
ns4-89-col-13C.1.fid
Carbon 13
176.90
167.26
136.91
121.97
38.39
26.98
18.29
f1 (ppm)

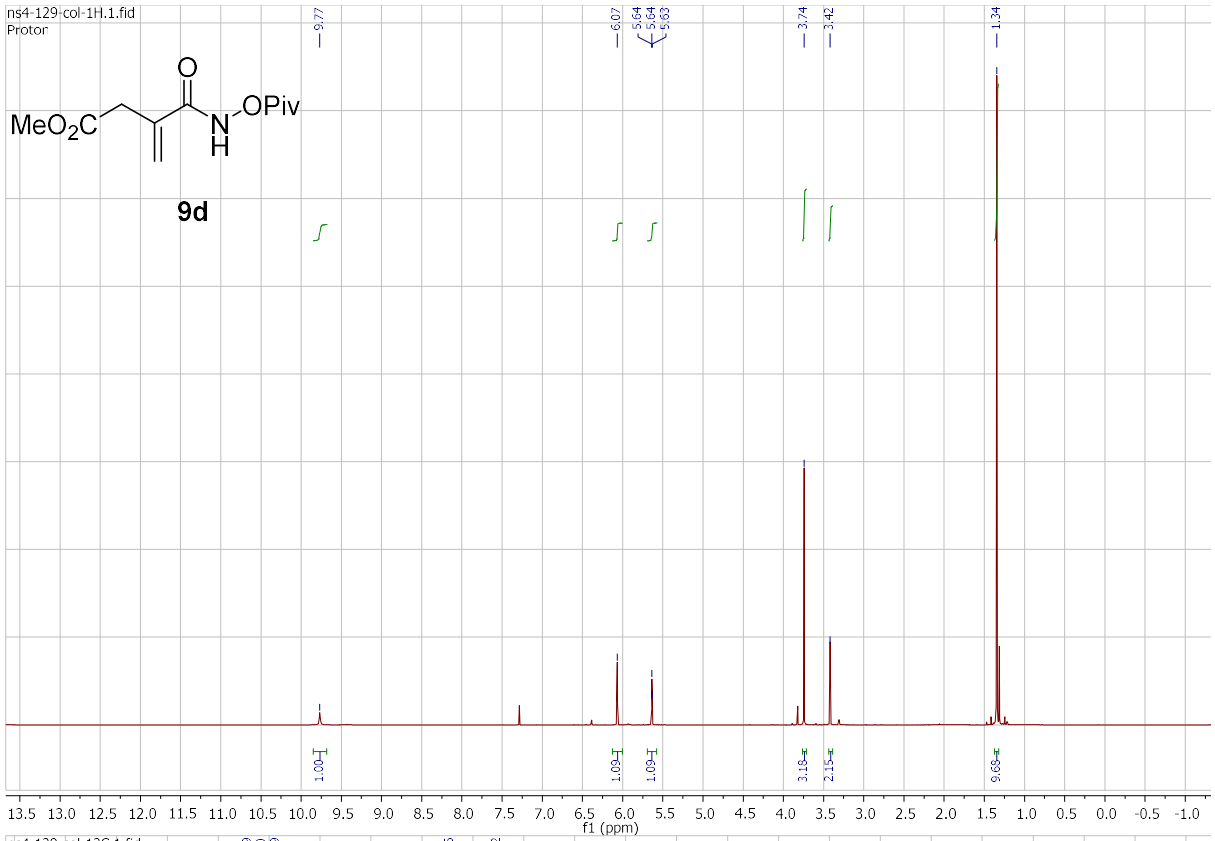
ns4-129-col-1H.1.fid
Protor
MeO2C
O
N
H
OPiv
9d
9.77
6.07
5.64
5.64
5.63
3.74
3.42
1.34
1.00
1.09
1.09
3.18
2.15
9.68
f1 (ppm)

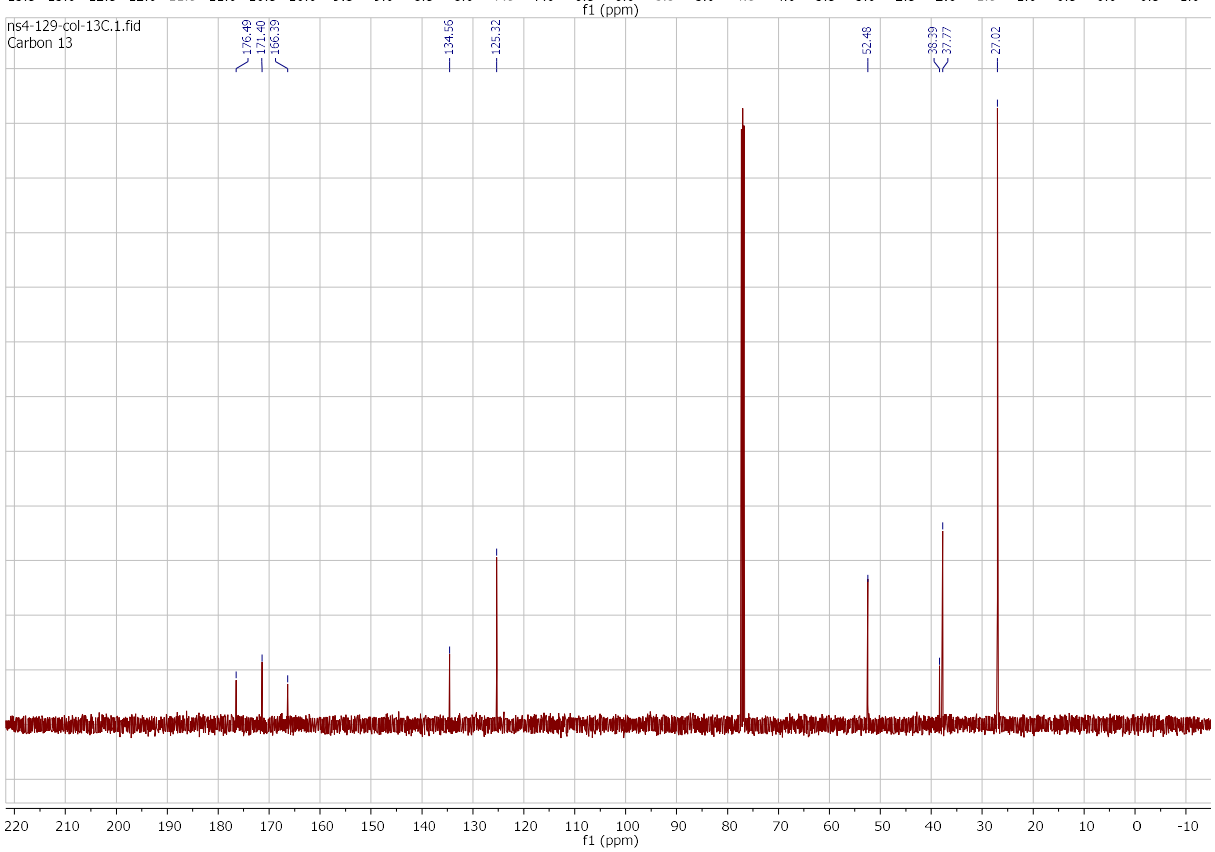
ns4-129-col-13C.1.fid
Carbon 13
176.49
171.40
166.39
134.56
125.32
52.48
38.39
37.77
27.02
f1 (ppm)

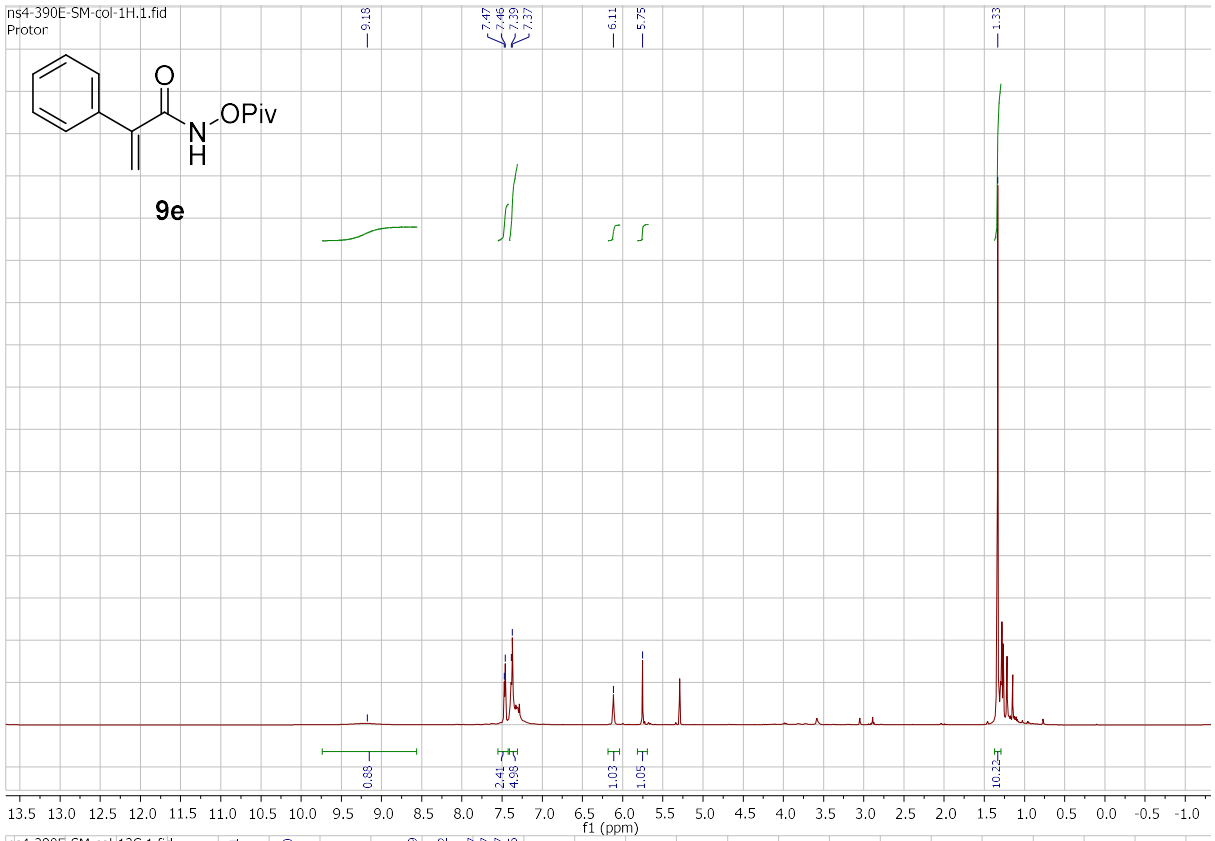
ns4-390E-SM-col-1H.1.fid
Proton
O
N
H
OPiv
9e
9.18
7.47
7.46
7.39
7.37
6.11
5.75
1.33
0.88
2.41
4.98
1.03
1.05
10.23
f1 (ppm)

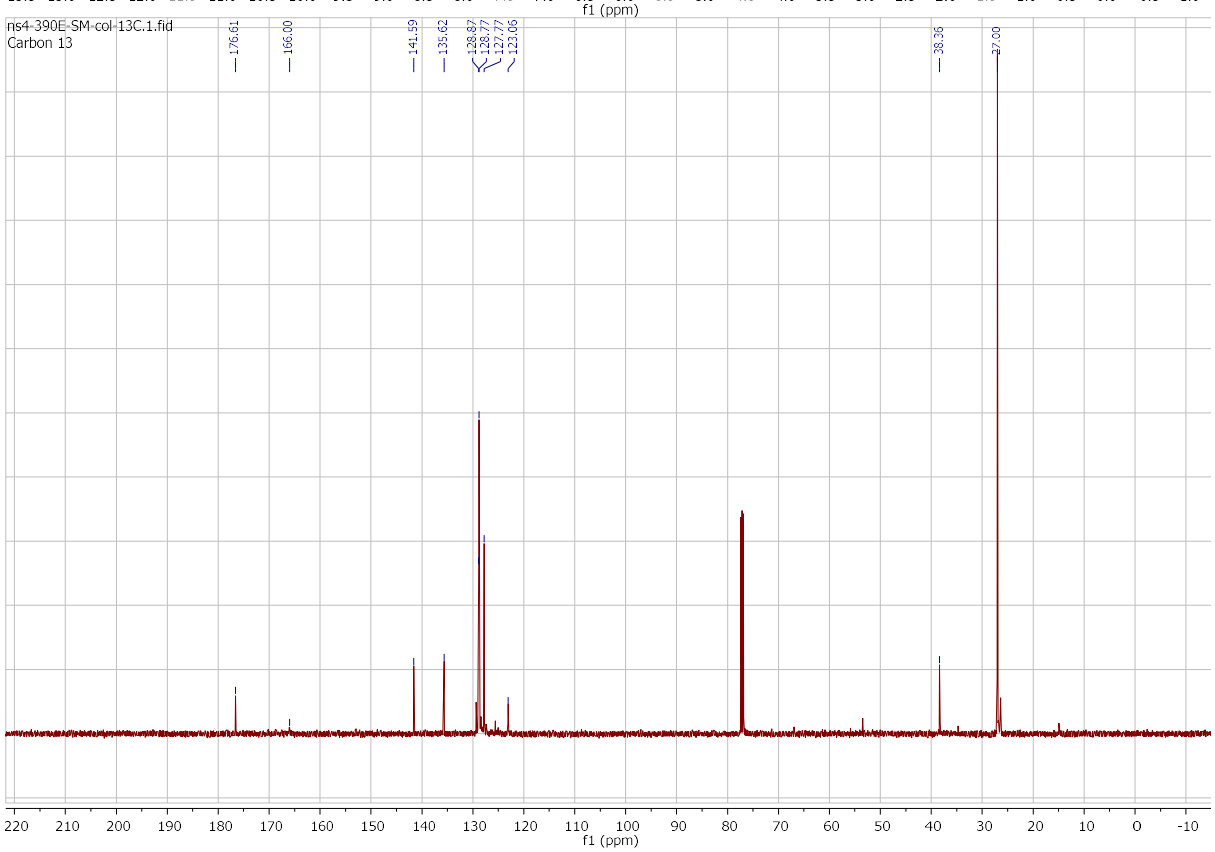
ns4-390E-SM-col-13C.1.fid
Carbon 13
176.61
166.00
141.59
135.62
128.87
128.77
127.77
123.06
38.36
27.00
f1 (ppm)

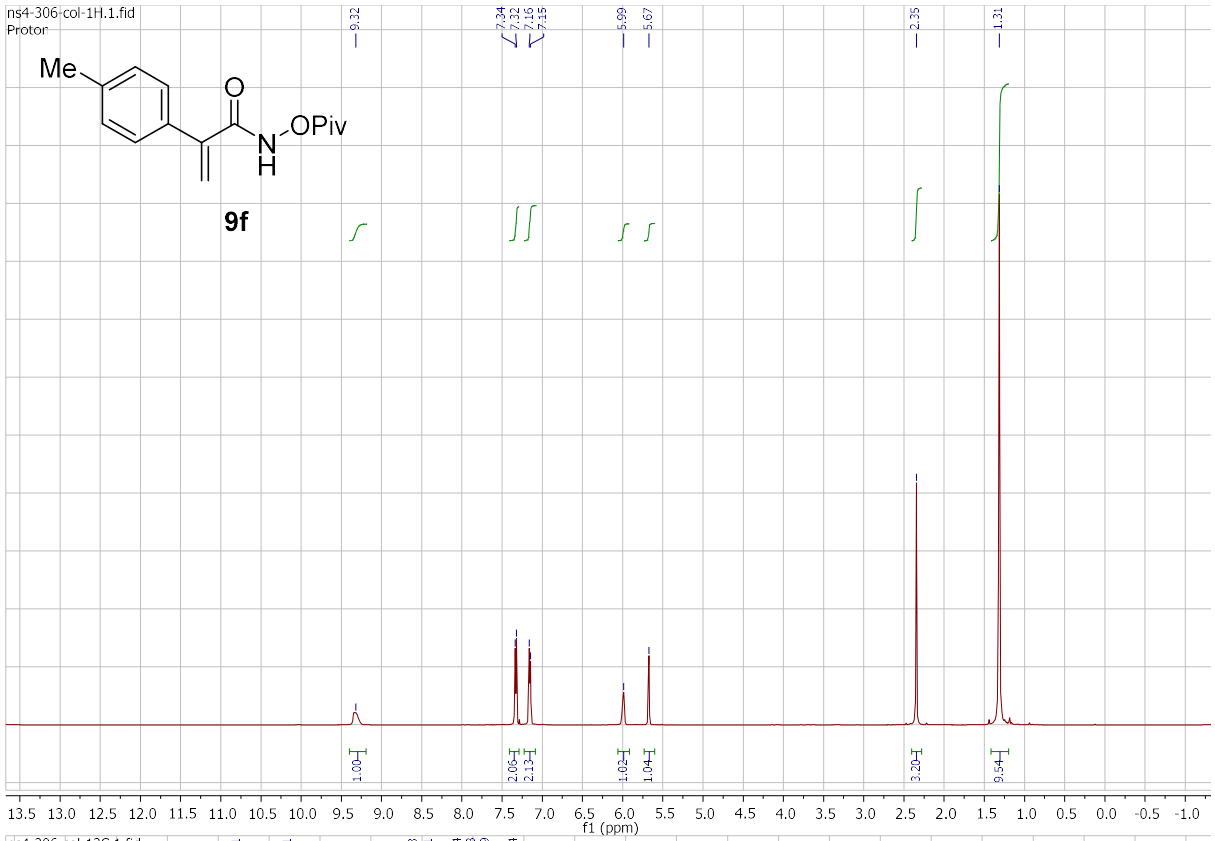
ns4-306-col-1H.1.fid
Proton
Me
O
N
H
OPiv
9f
9.32
7.34
7.32
7.16
7.15
5.99
5.67
2.35
1.31
1.00
2.06
2.13
1.02
1.04
3.20
9.54
f1 (ppm)

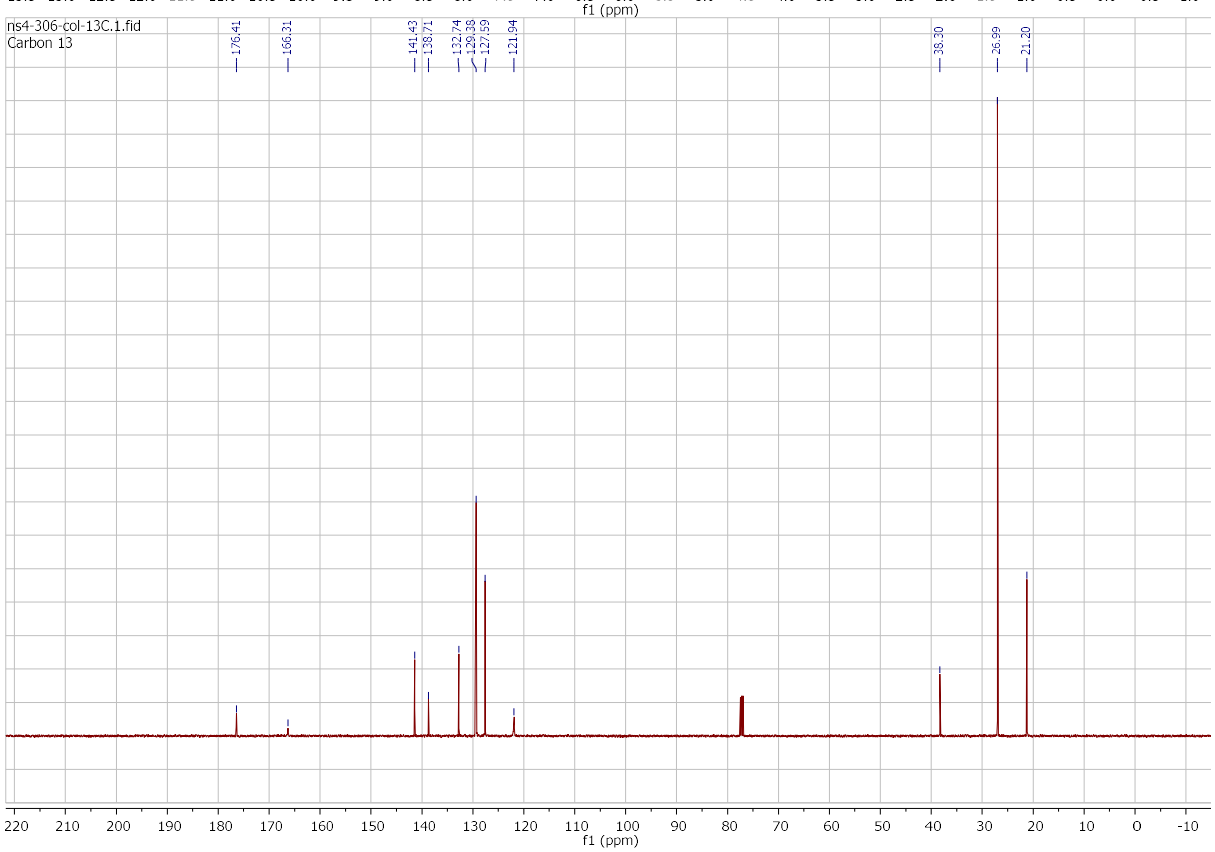
ns4-306-col-13C.1.fid
Carbon 13
176.41
166.31
141.43
138.71
132.74
129.38
127.59
121.94
38.30
26.99
21.20
f1 (ppm)

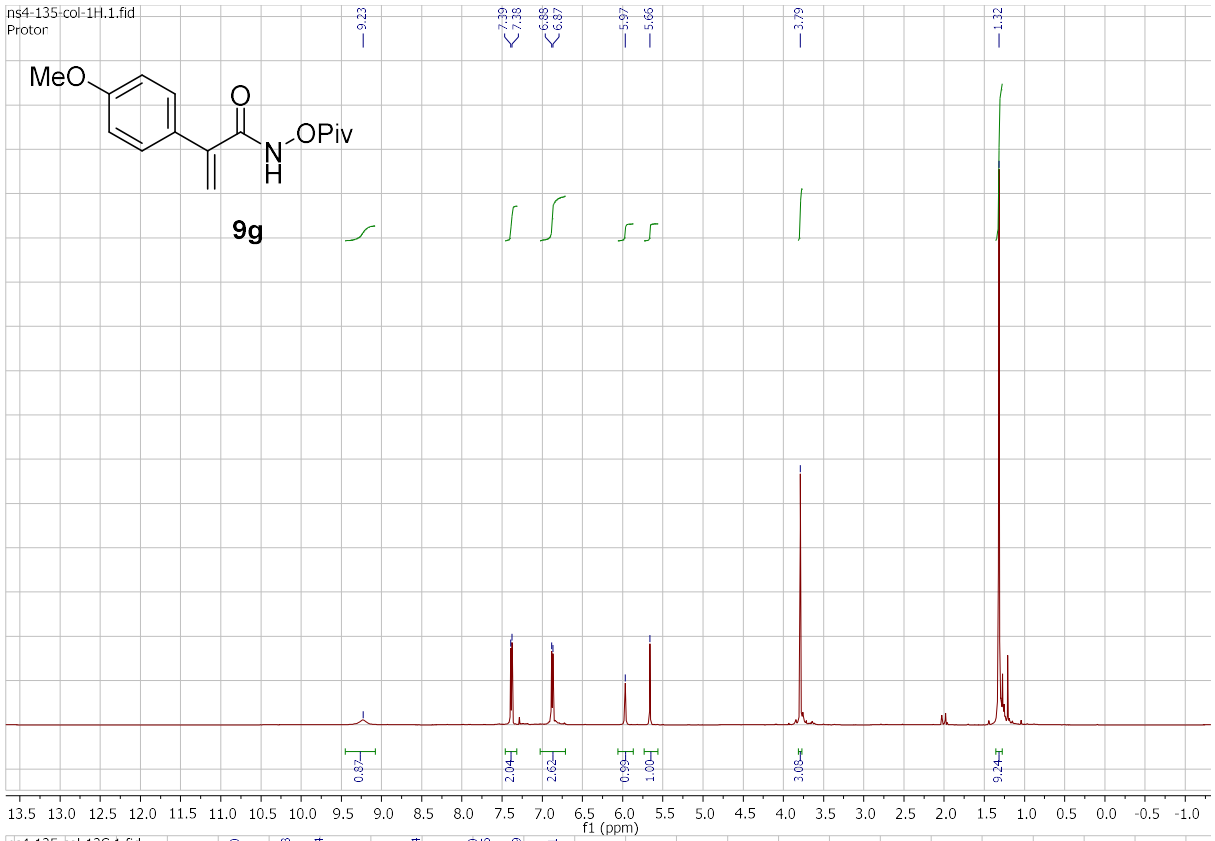
ns4-135-col-1H.1.fid
Proton
MeO
O
N
H
OPiv
9g
9.23
7.39
7.38
6.88
6.87
5.97
5.66
3.79
1.32
0.87
2.04
2.62
0.99
1.00
3.08
9.24
f1 (ppm)

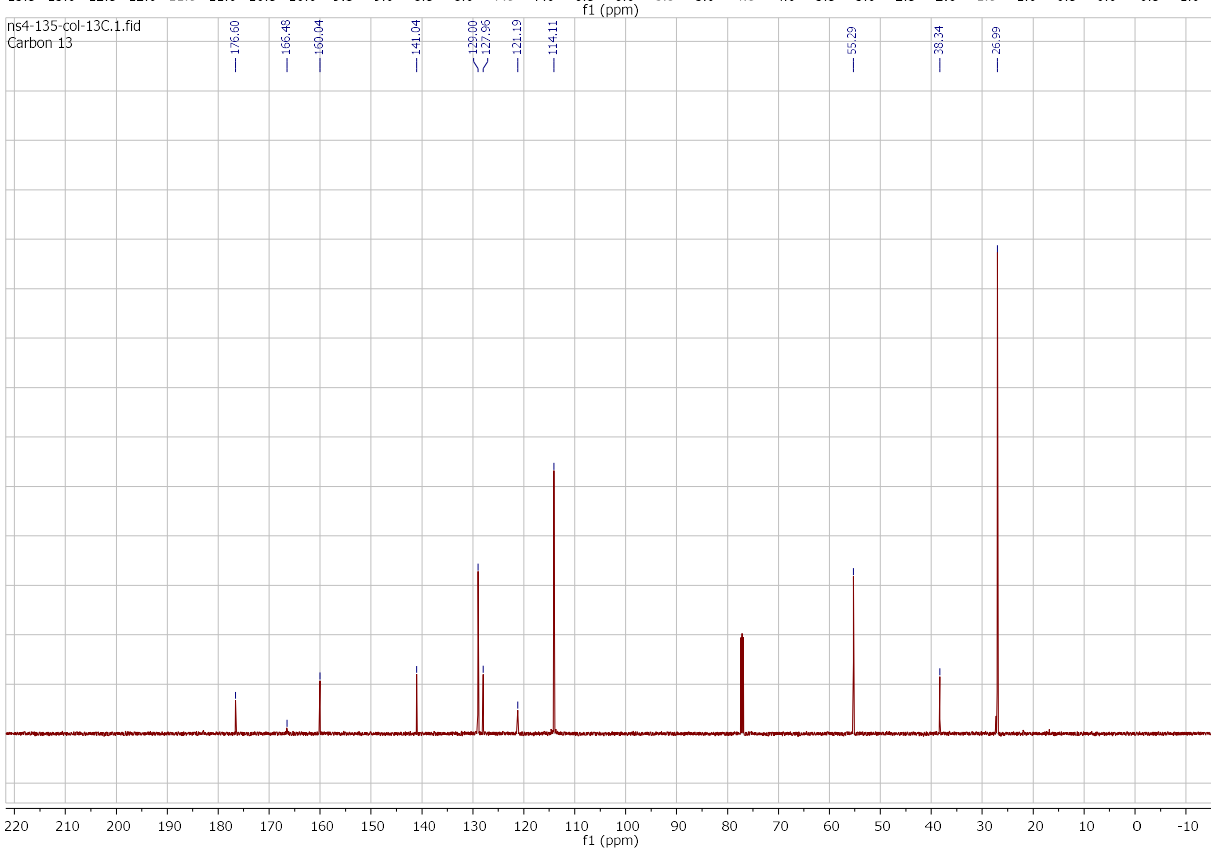
ns4-135-col-13C.1.fid
Carbon 13
176.60
166.48
160.04
141.04
129.00
127.96
121.19
114.11
55.29
38.34
26.99
f1 (ppm)

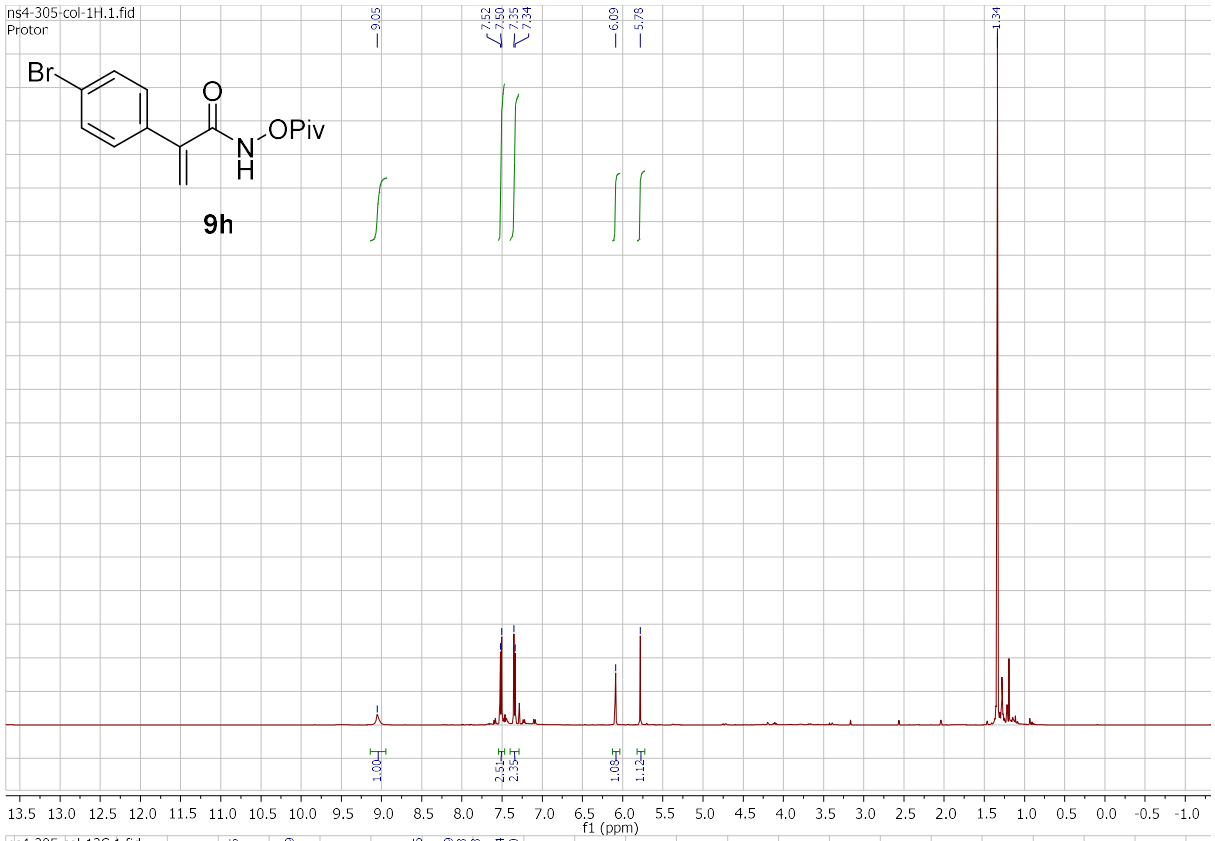
ns4-305-col-1H.1.fid
Protor
Br
O
N
H
OPiv
9h
9.05
7.52
7.50
7.35
7.34
6.09
5.78
1.34
1.00
2.54
2.35
1.09
1.13
f1 (ppm)

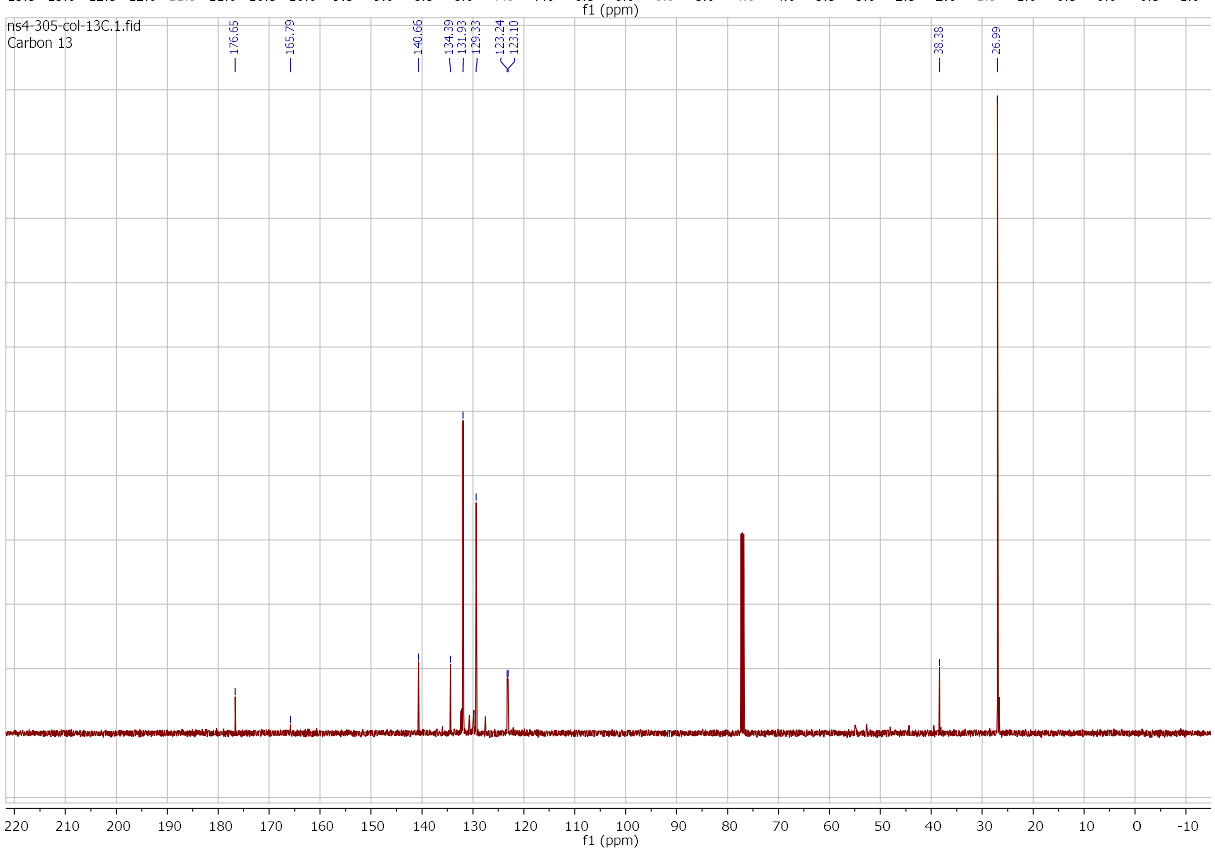
ns4-305-col-13C.1.fid
Carbon 13
176.65
165.79
140.66
134.39
131.93
129.33
123.24
123.10
38.38
26.99
f1 (ppm)

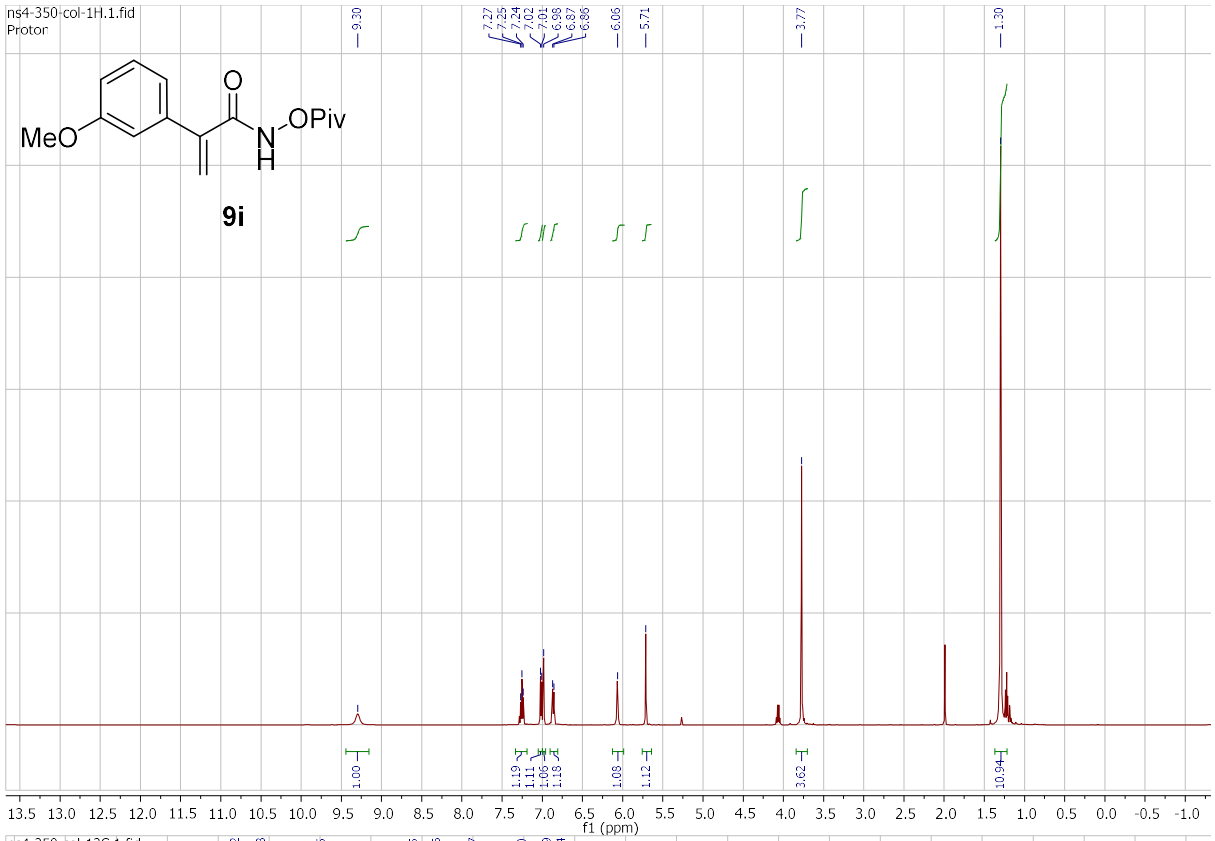
ns4-350-col-1H.1.fid
Proton
MeO
O
N
H
OPiv
9i
9.30
7.27
7.25
7.24
7.02
7.01
6.98
6.87
6.86
6.06
5.71
3.77
1.30
1.00
1.19
1.11
1.06
1.19
1.08
1.12
3.62
10.94
f1 (ppm)

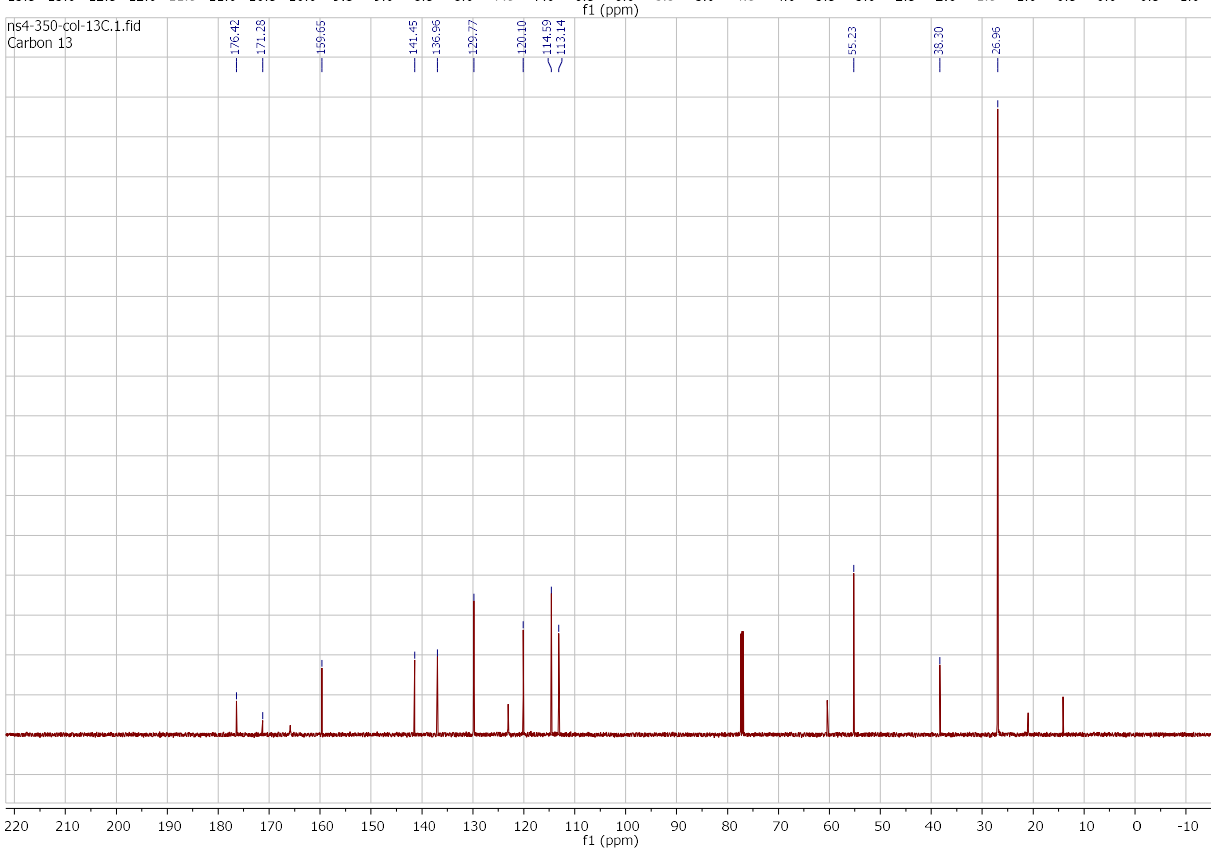
ns4-350-col-13C.1.fid
Carbon 13
176.42
171.28
159.65
141.45
136.96
129.77
120.10
114.59
113.14
55.23
38.30
26.96
f1 (ppm)

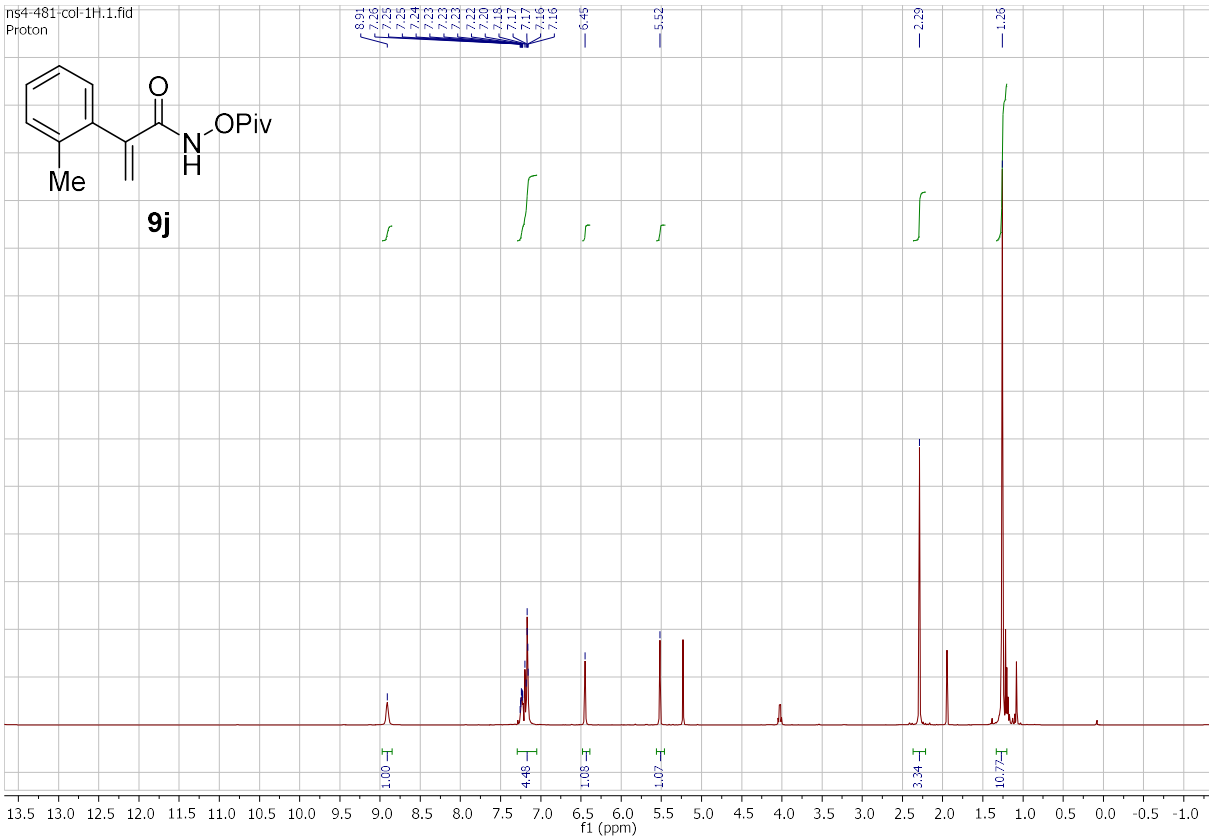
ns4-481-col-1H.1.fid
Proton
O
N
H
OPiv
Me
9j
f1 (ppm)

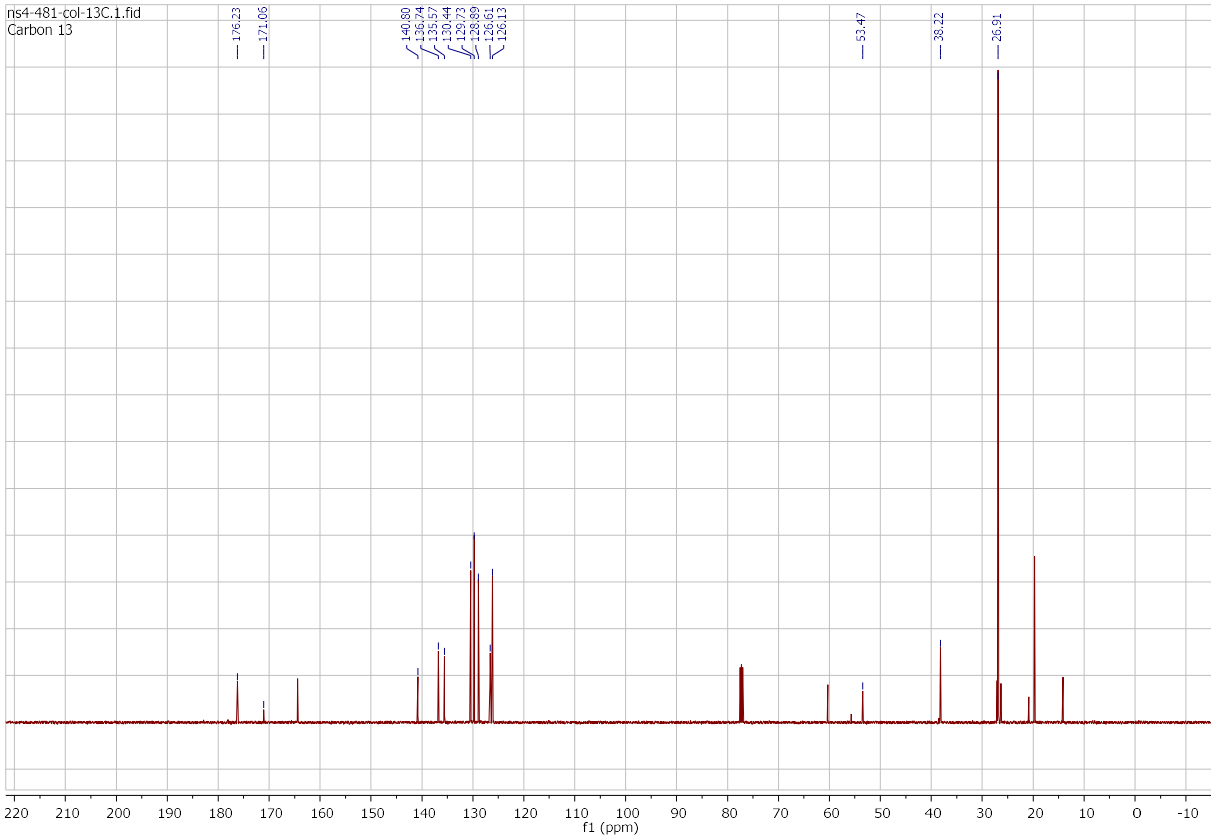
ns4-481-col-13C.1.fid
Carbon 13
f1 (ppm)

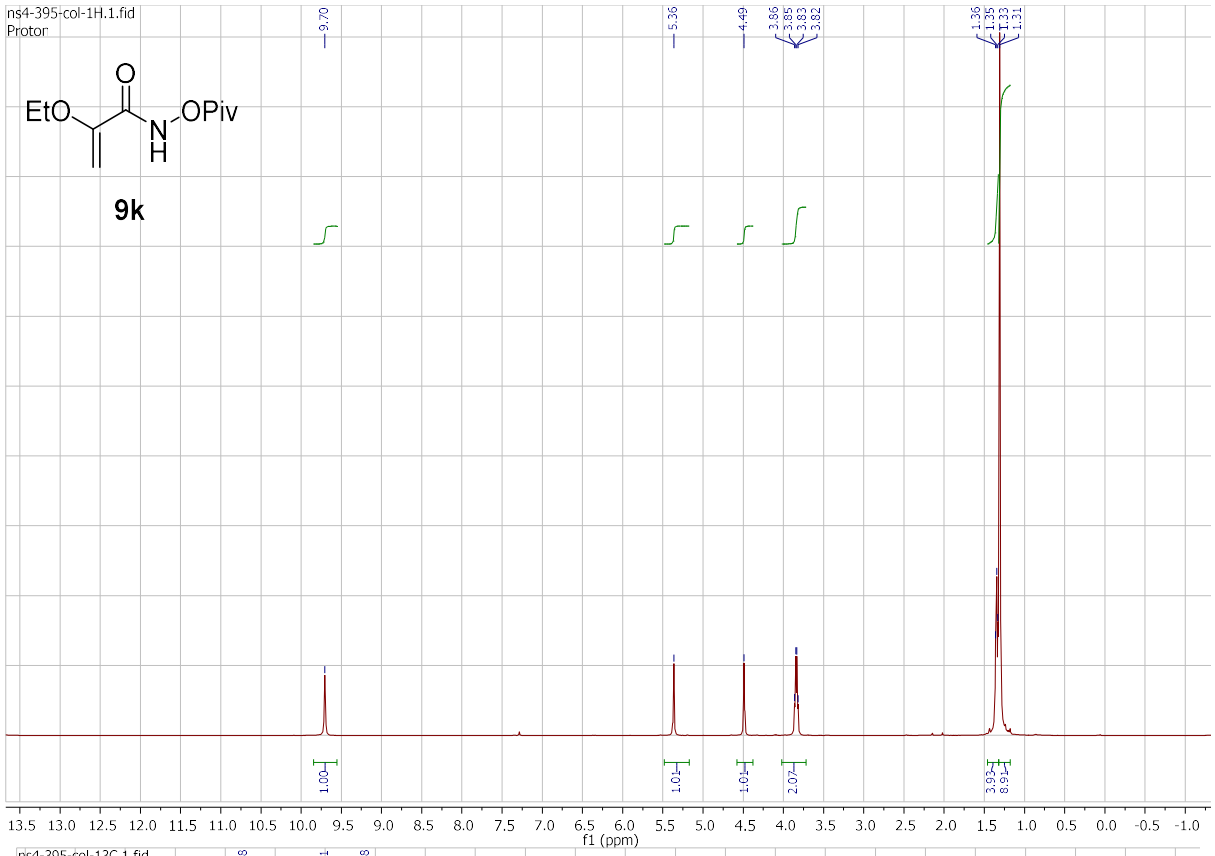
ns4-395-col-1H.1.fid
Protor
EtO
O
N
H
OPiv
9k
9.70
5.36
4.49
3.86
3.85
3.83
3.82
1.36
1.35
1.33
1.31
1.00
1.01
1.01
2.07
3.93
8.91
f1 (ppm)

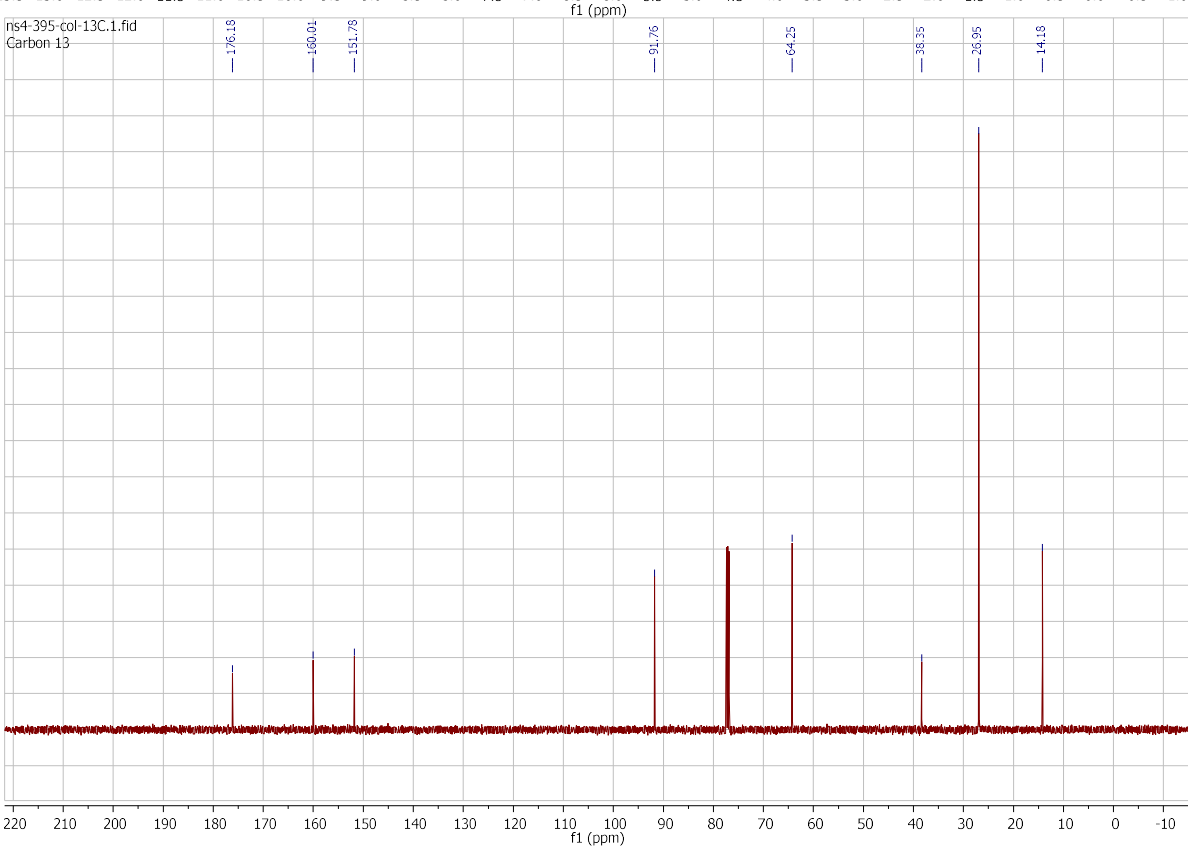
ns4-395-col-13C.1.fid
Carbon 13
176.18
160.01
151.78
91.76
64.25
36.35
26.95
14.18
f1 (ppm)

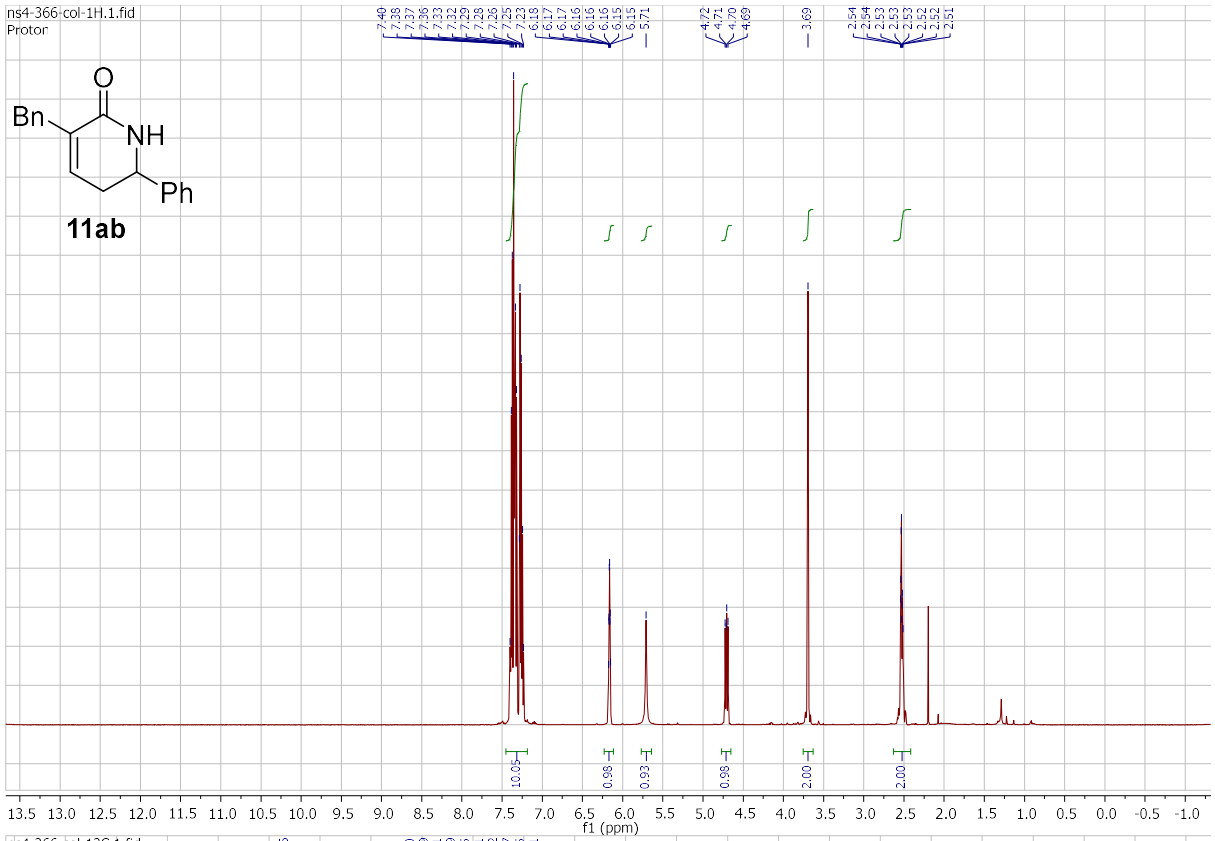
ns4-366-col-1H.1.fid
Protor
Bn
NH
Ph
11ab
f1 (ppm)

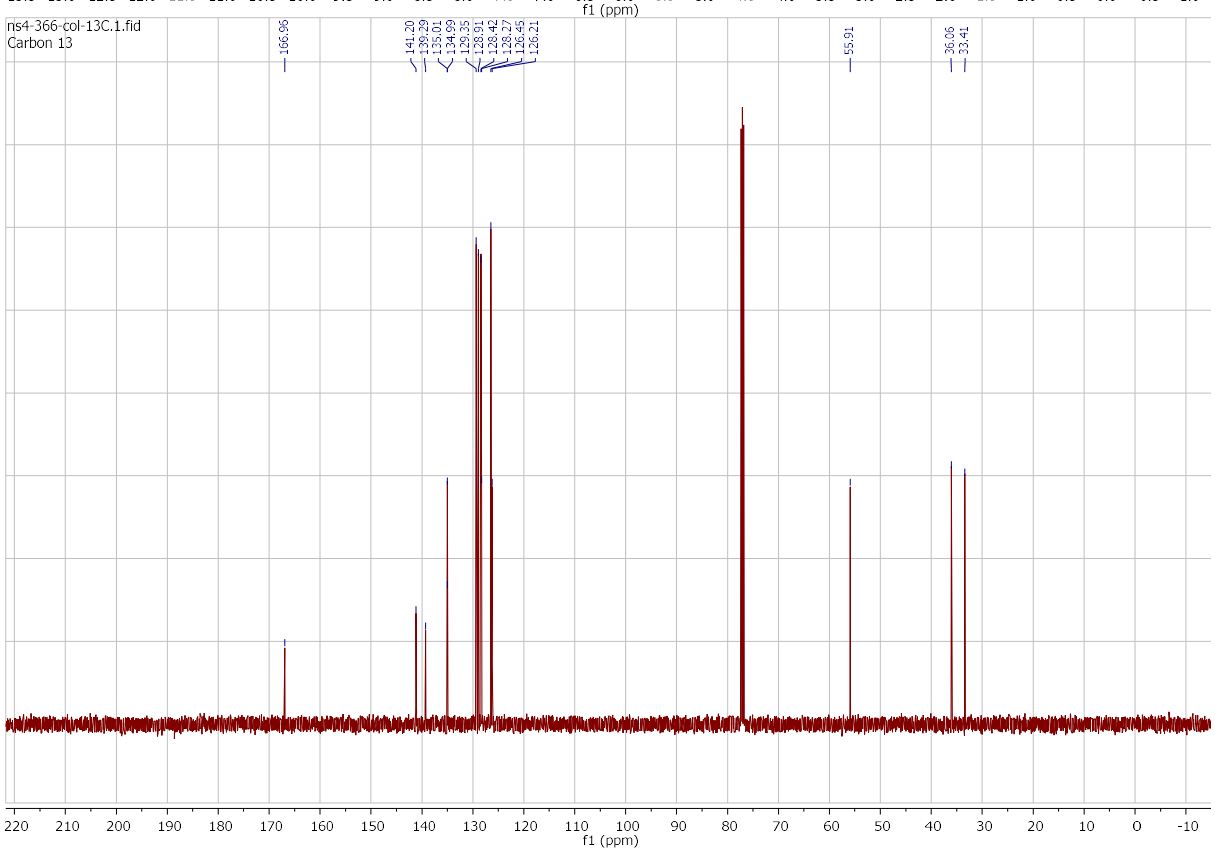
ns4-366-col-13C.1.fid
Carbon 13
f1 (ppm)

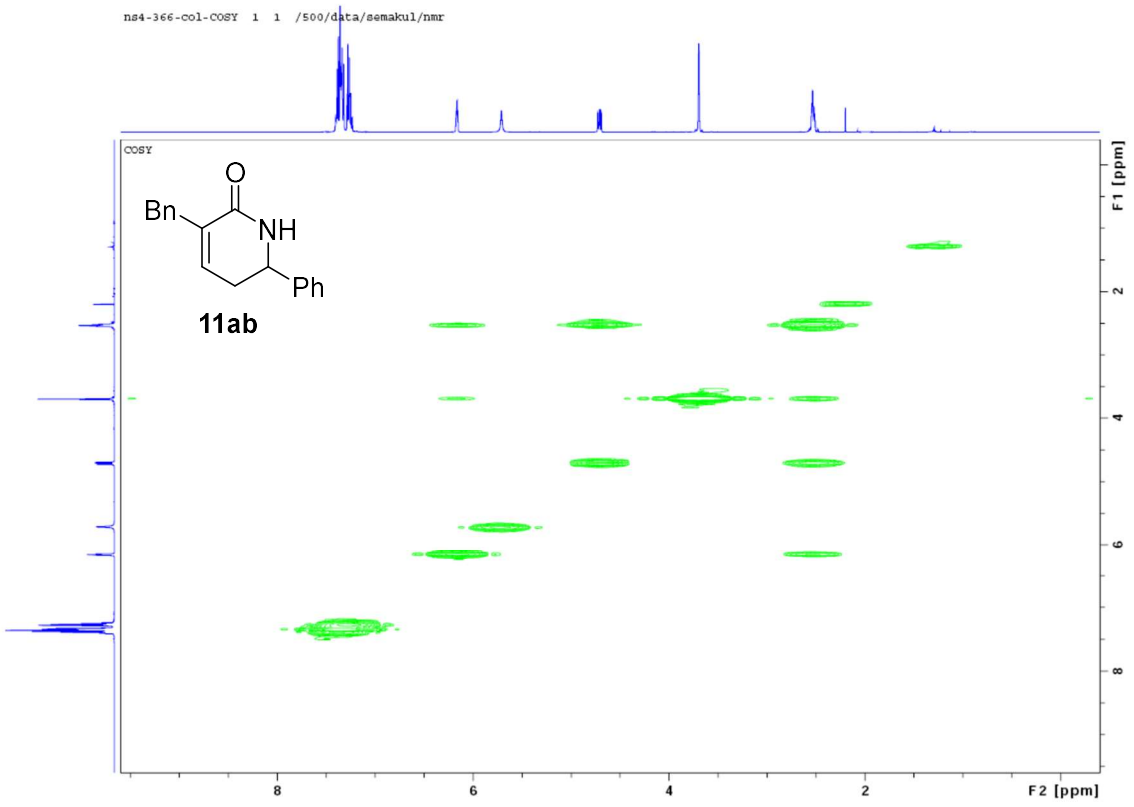
ns4-366-col-COSY 1 1 /500/data/semakul/nmr
COSY
O
Bn
NH
Ph
11ab
F1 [ppm]
F2 [ppm]
2
4
6
8

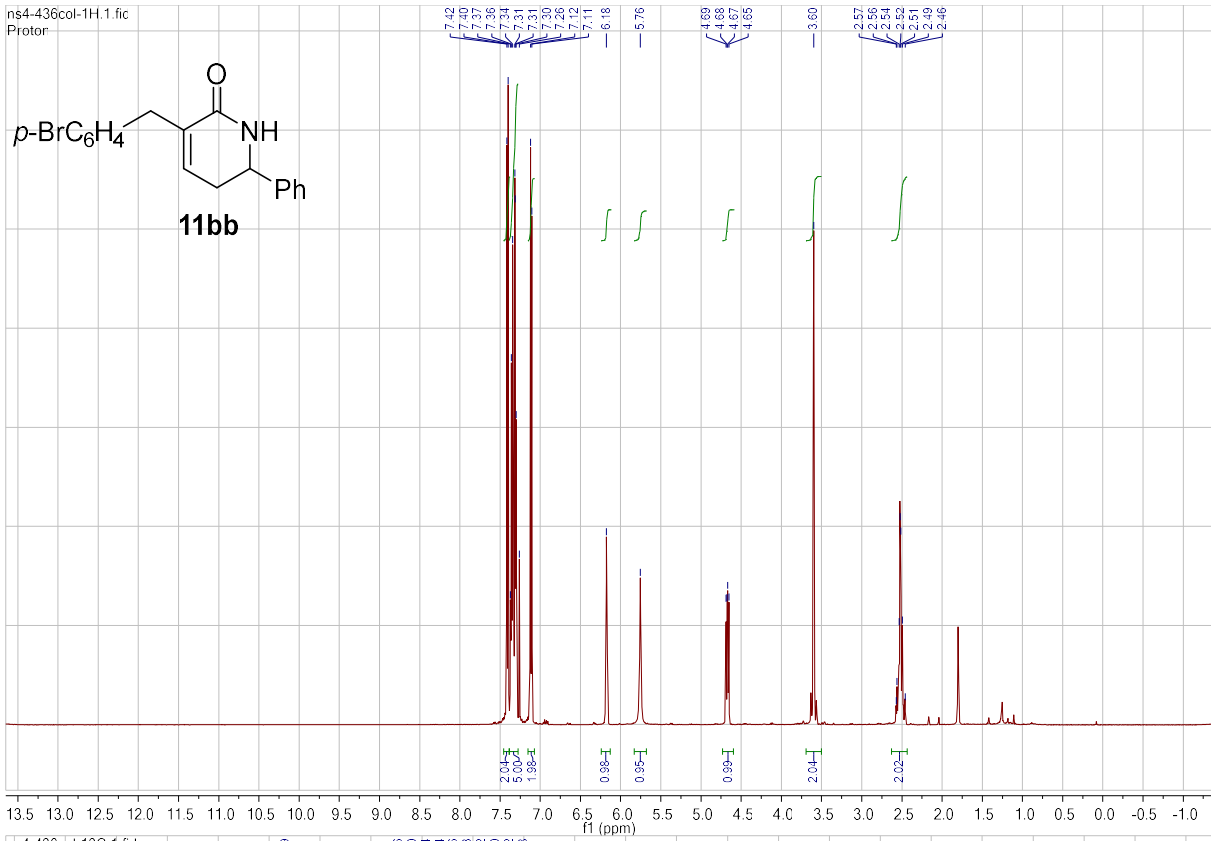
ns4-436col-1H.1.fic
Protor
O
NH
Ph
p-BrC6H4
11bb
7.42
7.40
7.37
7.36
7.34
7.31
7.31
7.30
7.26
7.12
7.11
6.18
5.76
4.69
4.68
4.67
4.65
3.60
2.57
2.56
2.54
2.52
2.51
2.49
2.46
2.04
5.00
1.98
0.98
0.96
0.99
2.04
2.02
f1 (ppm)

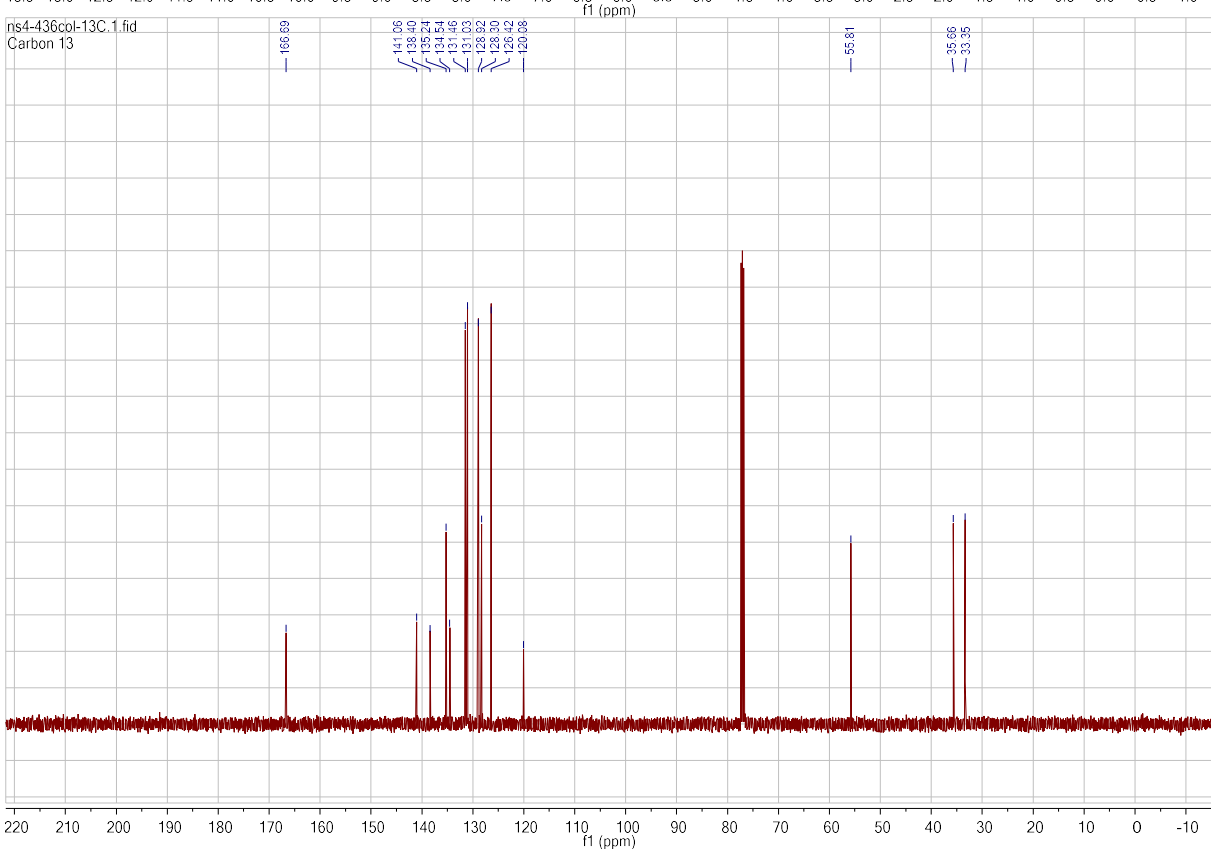
ns4-436col-13C.1.fid
Carbon 13
166.89
141.06
138.40
135.24
134.54
131.46
131.03
128.92
128.30
126.42
120.08
55.81
35.66
33.35
f1 (ppm)

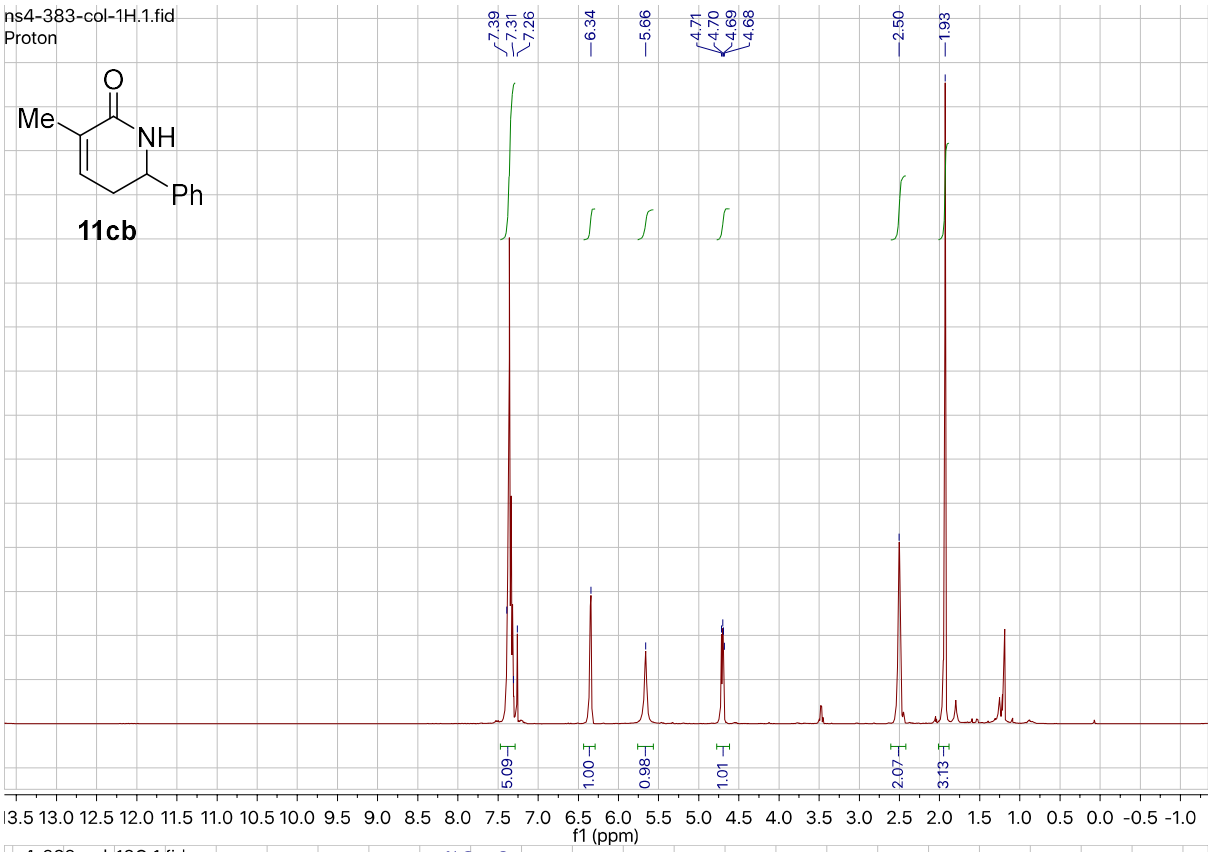
ns4-383-col-1H.1.fid
Proton
Me
NH
Ph
11cb
7.39
7.31
7.26
6.34
5.66
4.71
4.70
4.69
4.68
2.50
1.93
5.09
1.00
0.98
1.01
2.07
3.13
f1 (ppm)

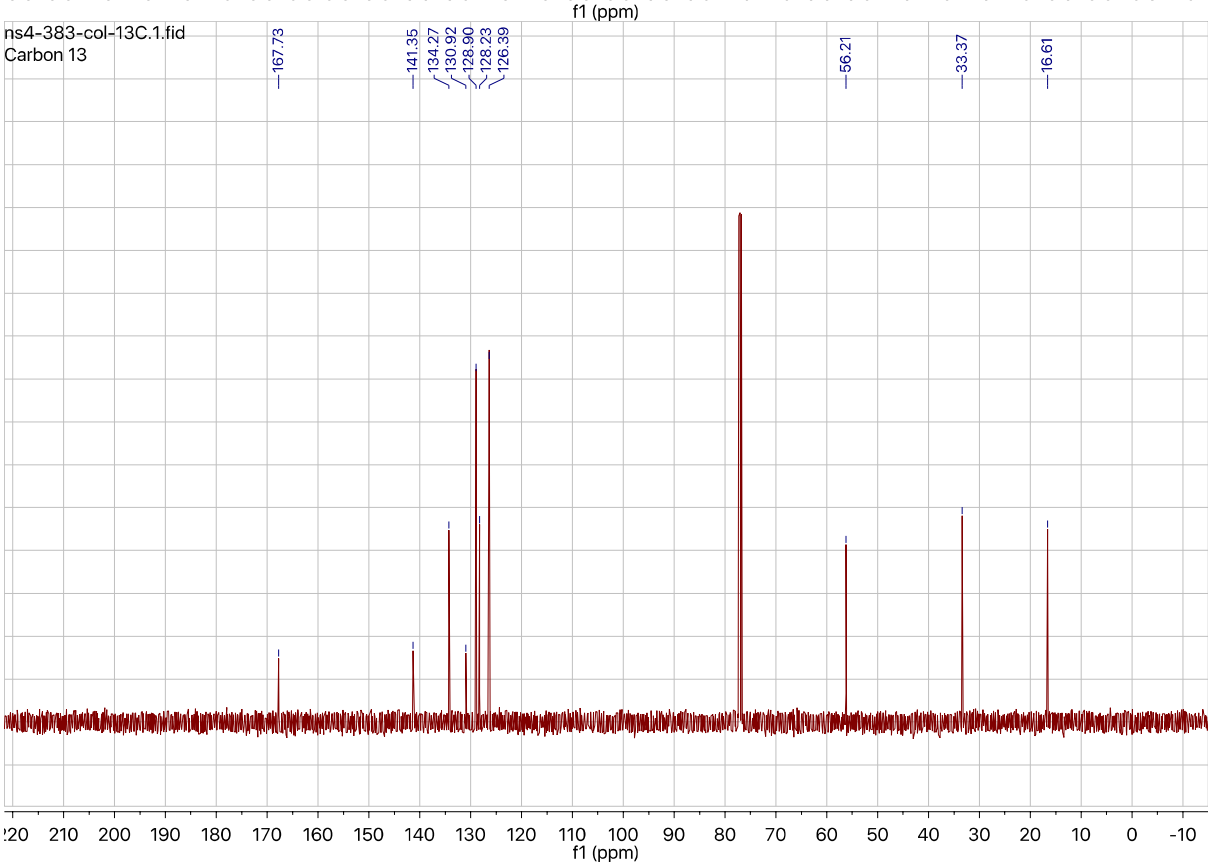
ns4-383-col-13C.1.fid
Carbon 13
167.73
141.35
134.27
130.92
128.90
128.23
126.39
56.21
33.37
16.61
f1 (ppm)

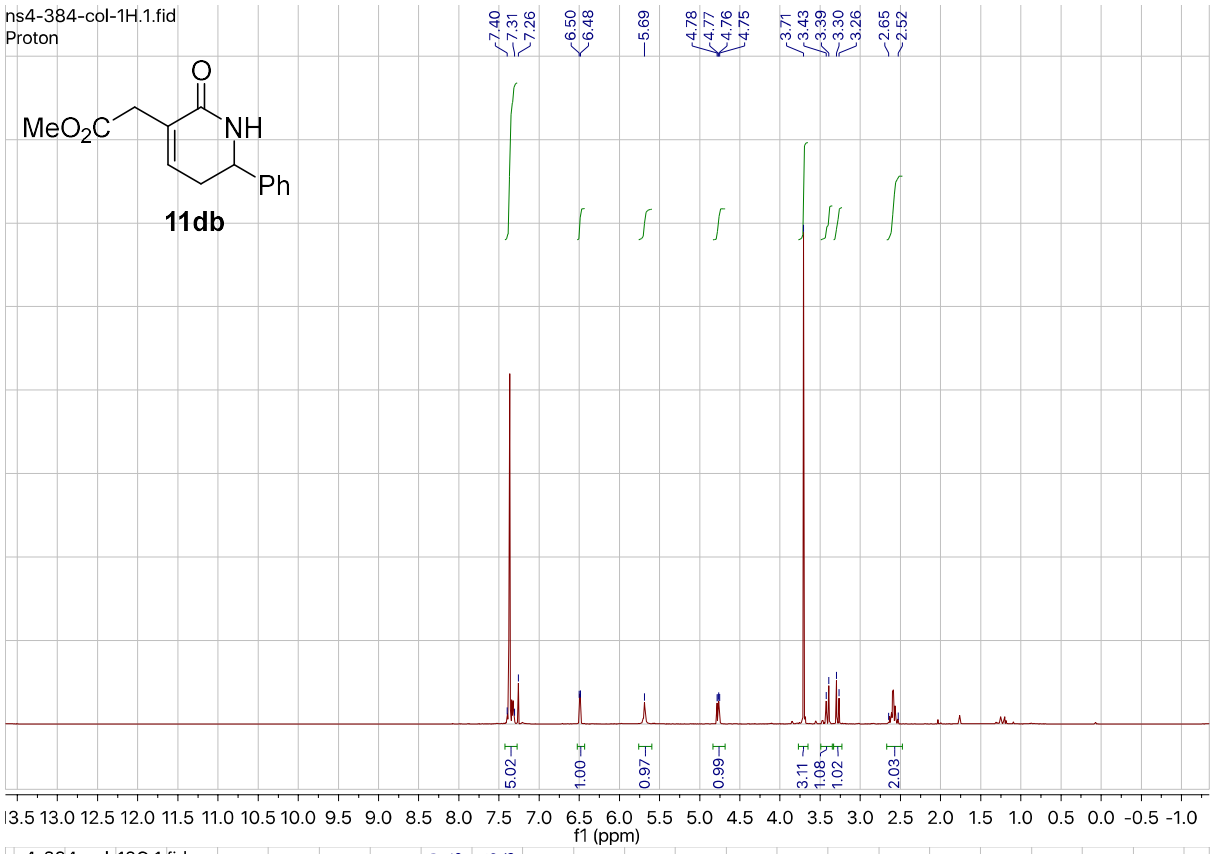
ns4-384-col-1H.1.fid
Proton
MeO2C
NH
Ph
11db
7.40
7.31
7.26
6.50
6.48
5.69
4.78
4.77
4.76
4.75
3.71
3.43
3.39
3.30
3.26
2.65
2.52
5.02
1.00
0.97
0.99
3.11
1.08
1.02
2.03
f1 (ppm)

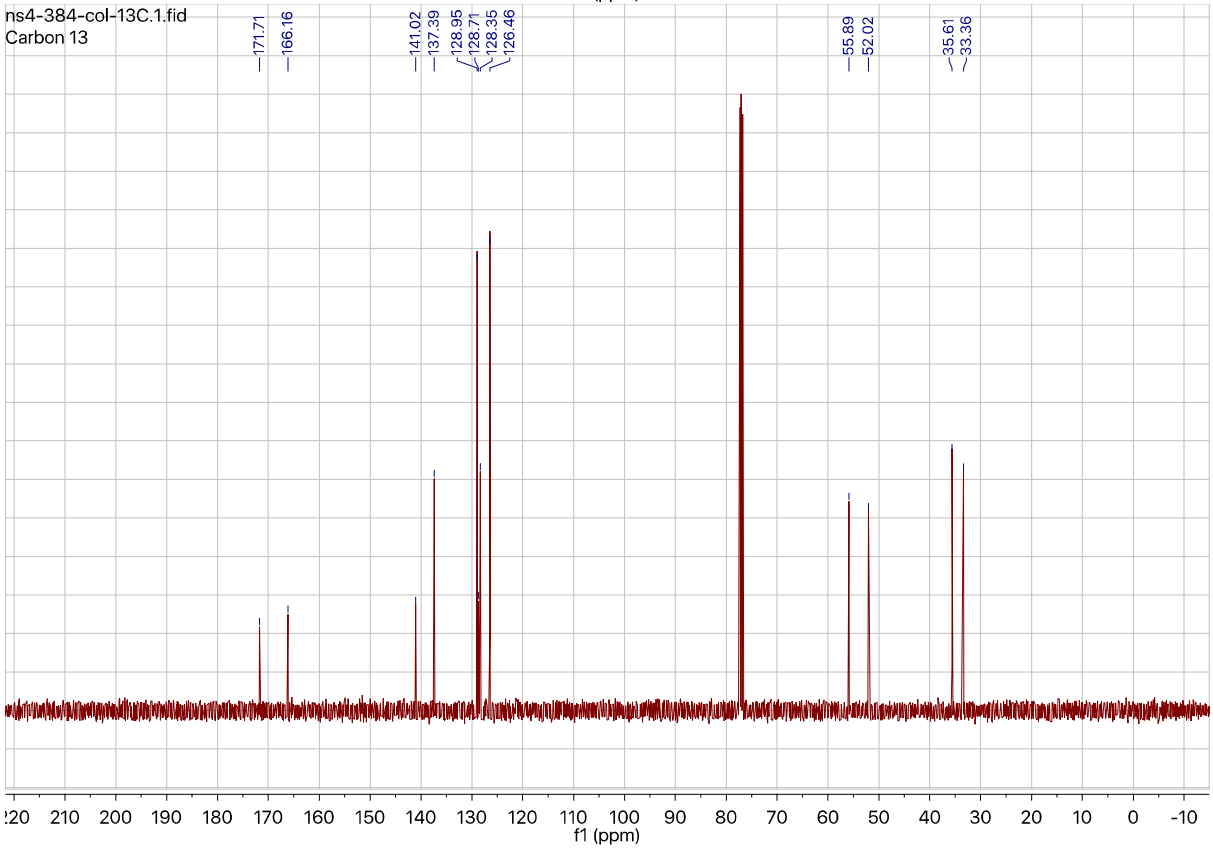
ns4-384-col-13C.1.fid
Carbon 13
171.71
166.16
141.02
137.39
128.95
128.71
128.35
126.46
55.89
52.02
35.61
33.36
f1 (ppm)

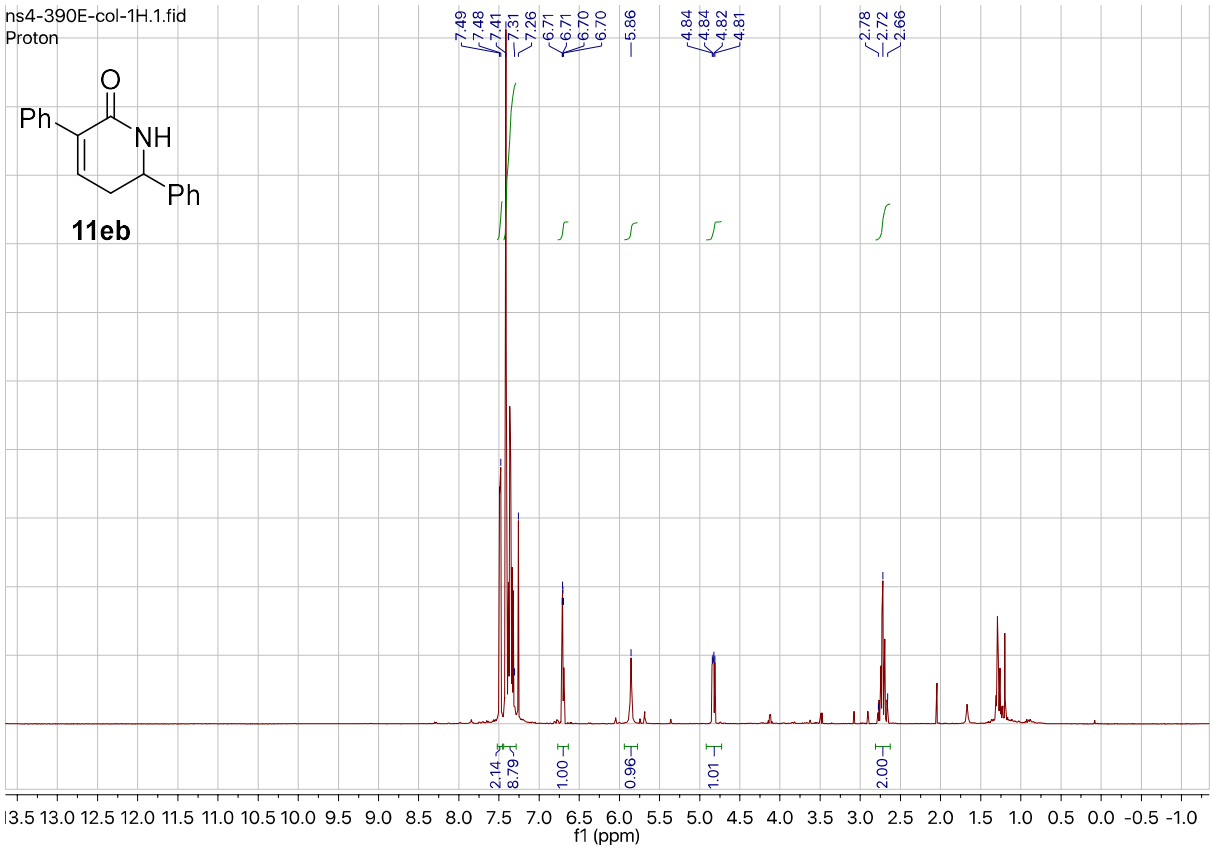
ns4-390E-col-1H.1.fid
Proton
O
Ph
NH
Ph
11eb
7.49
7.48
7.41
7.31
7.26
6.71
6.71
6.70
6.70
5.86
4.84
4.84
4.82
4.81
2.78
2.72
2.66
2.14
8.79
1.00
0.96
1.01
2.00
f1 (ppm)

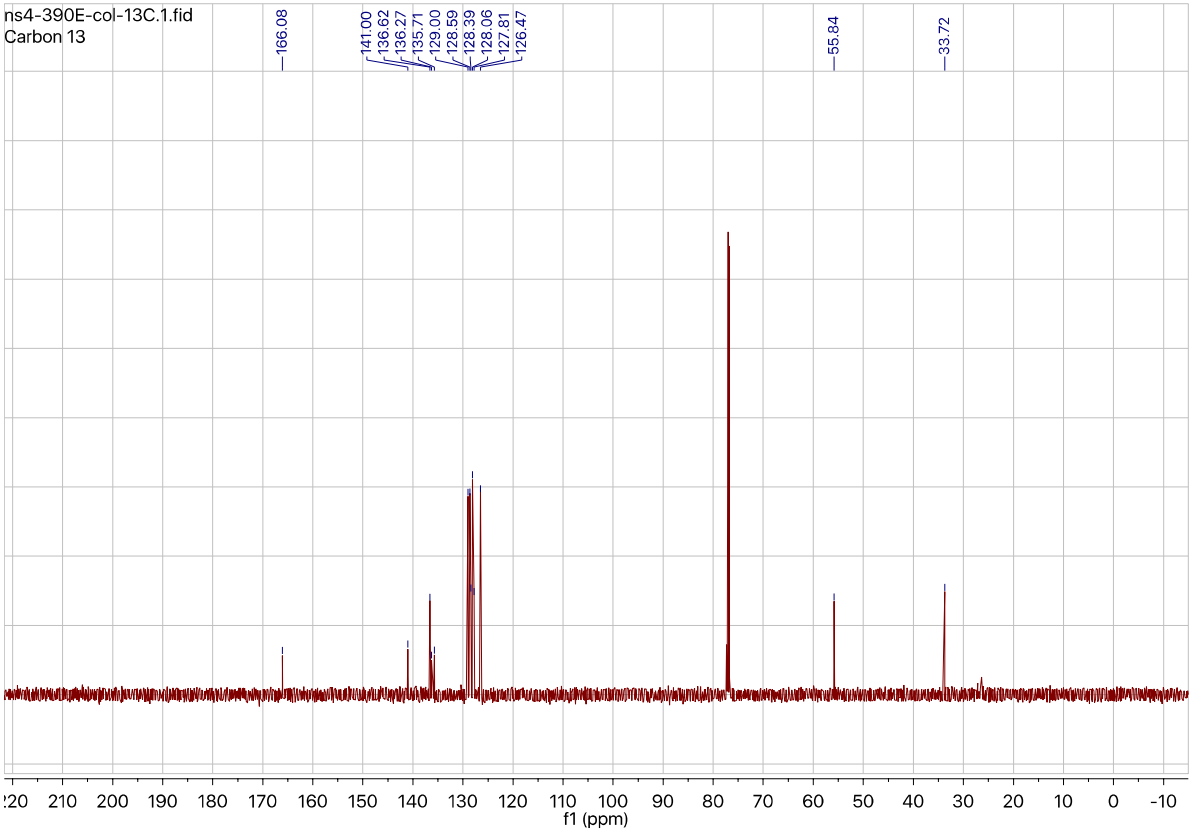
ns4-390E-col-13C.1.fid
Carbon 13
166.08
141.00
136.62
136.27
135.71
129.00
128.59
128.39
128.06
127.81
126.47
55.84
33.72
f1 (ppm)

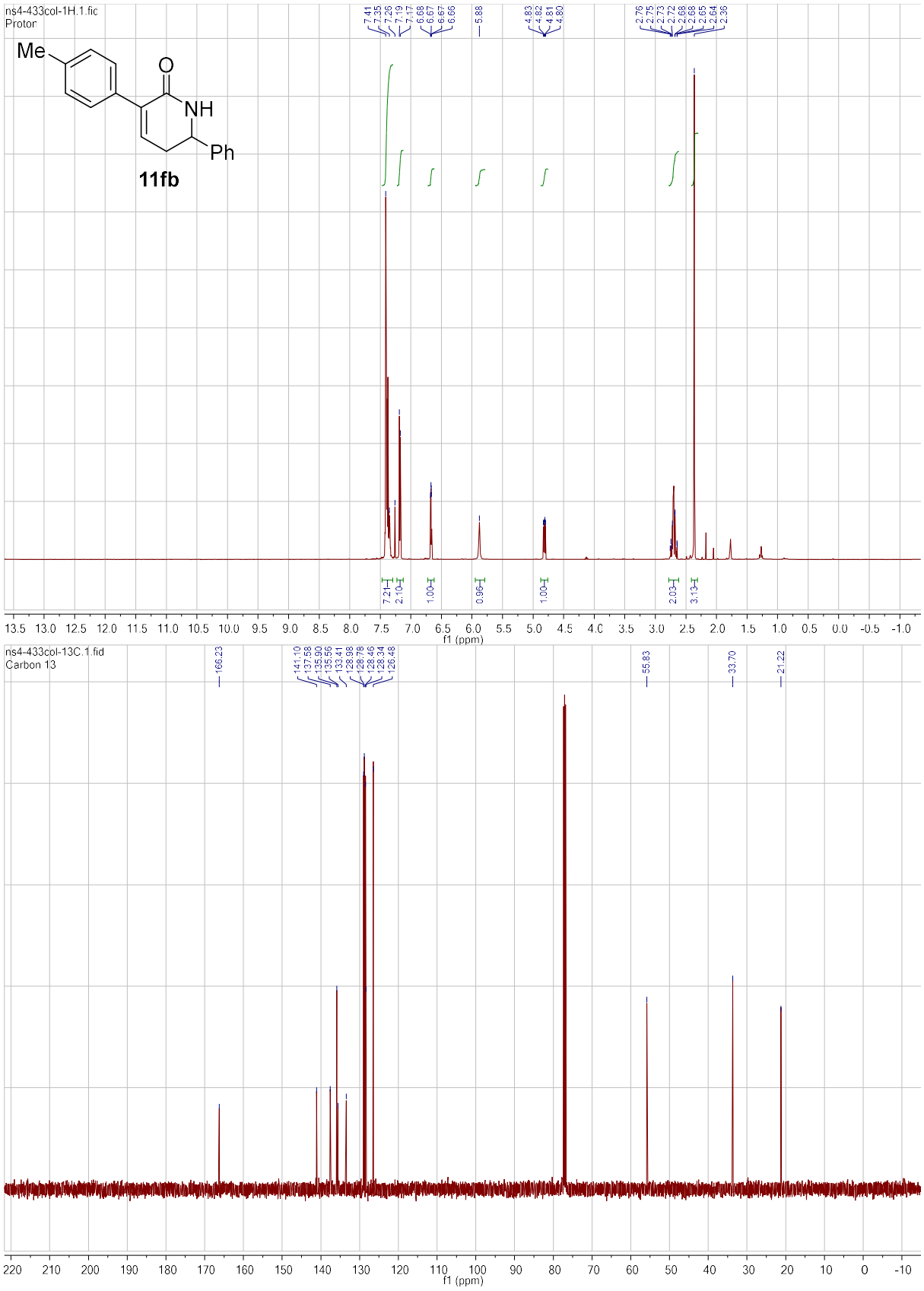
ns4-433col-1H.1.fic
Protor
Me
O
NH
Ph
11fb
7.41
7.35
7.26
7.19
7.17
6.68
6.67
6.67
6.66
5.88
4.83
4.82
4.81
4.80
2.76
2.75
2.73
2.72
2.68
2.68
2.65
2.64
2.36
7.21
2.10
1.00
0.96
1.00
2.03
3.13
f1 (ppm)
ns4-433col-13C.1.fid
Carbon 13
166.23
141.10
137.58
135.90
135.56
133.41
128.98
128.78
128.46
128.34
126.48
55.83
33.70
21.22
f1 (ppm)

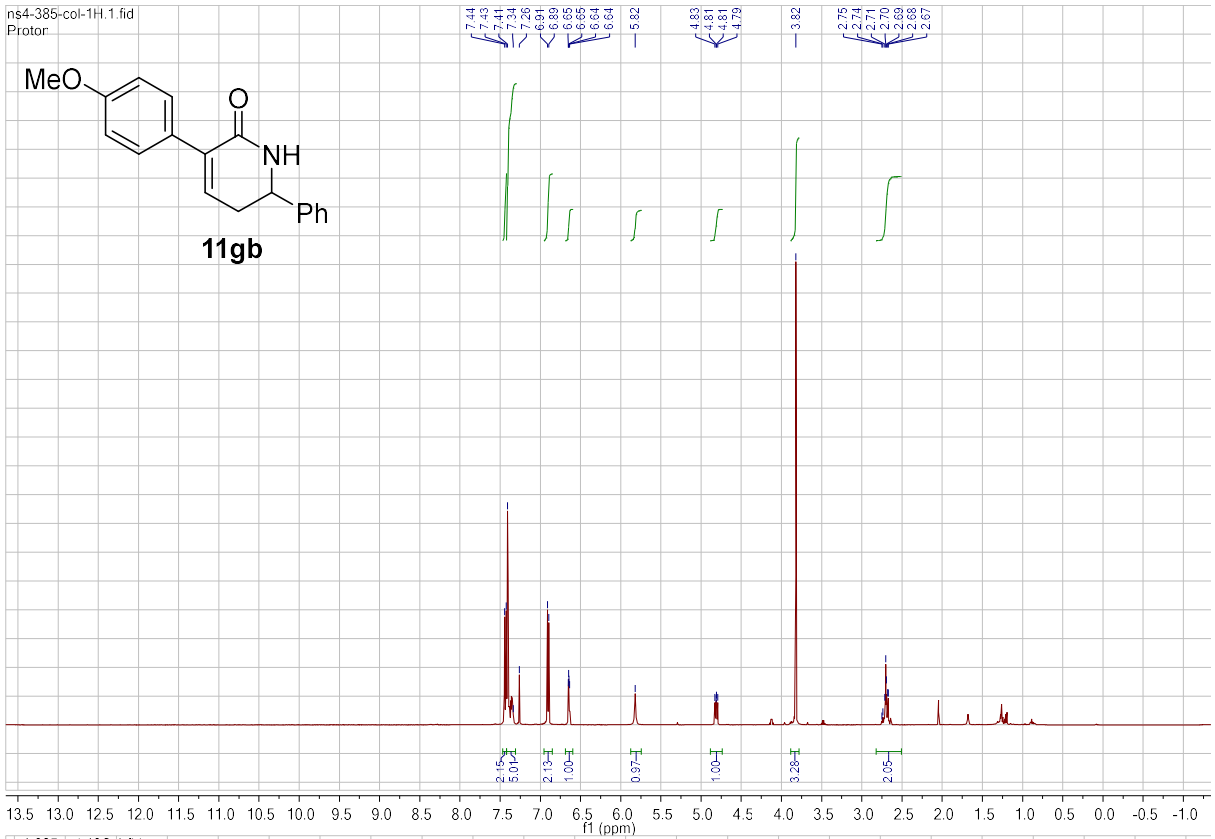
ns4-385-col-1H.1.fid
Proton
MeO
O
NH
Ph
11gb
7.44
7.43
7.41
7.34
7.26
6.91
6.89
6.65
6.65
6.64
6.64
5.82
4.83
4.81
4.81
4.79
3.82
2.75
2.74
2.71
2.70
2.69
2.68
2.67
2.15
5.01
2.13
1.00
0.97
1.00
3.28
2.05
f1 (ppm)

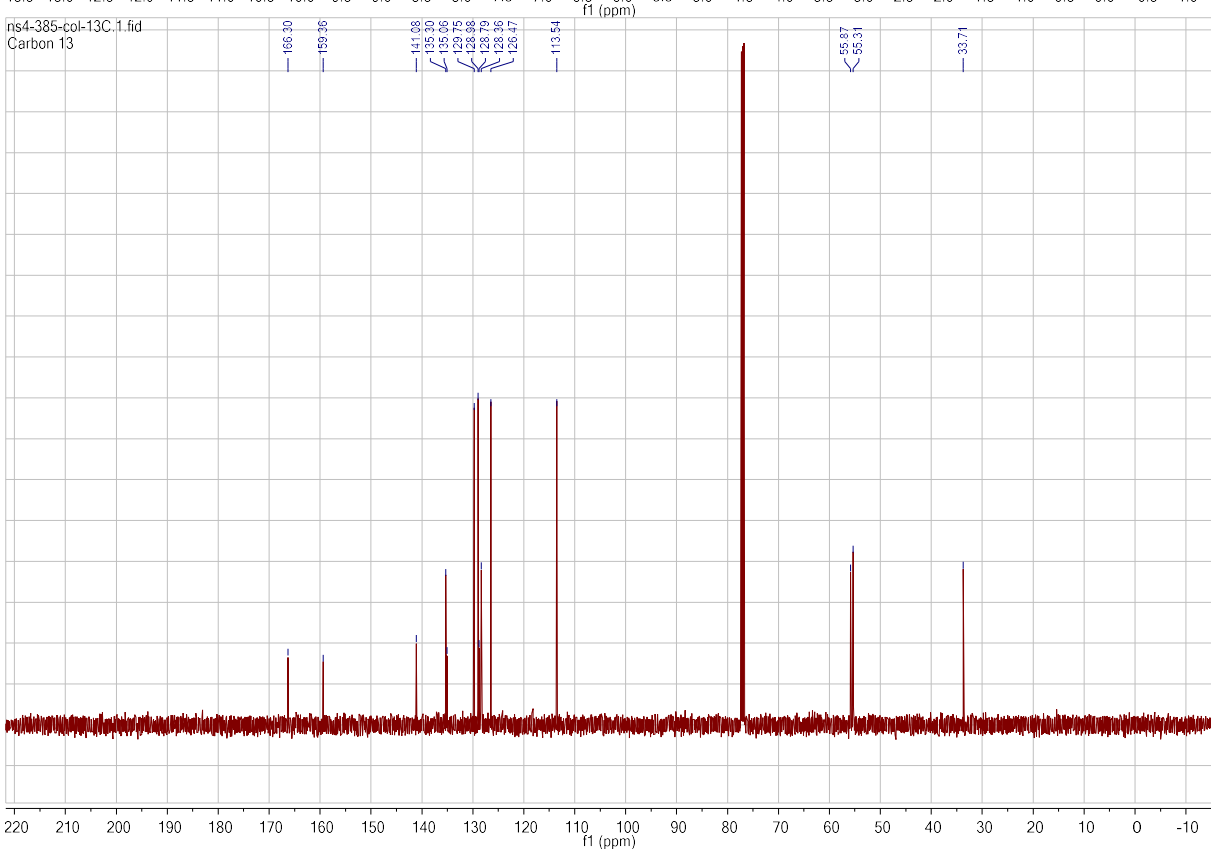
ns4-385-col-13C.1.fid
Carbon 13
166.30
159.36
141.08
135.30
135.06
129.75
128.98
128.79
128.36
126.47
113.54
55.87
55.31
33.71
f1 (ppm)

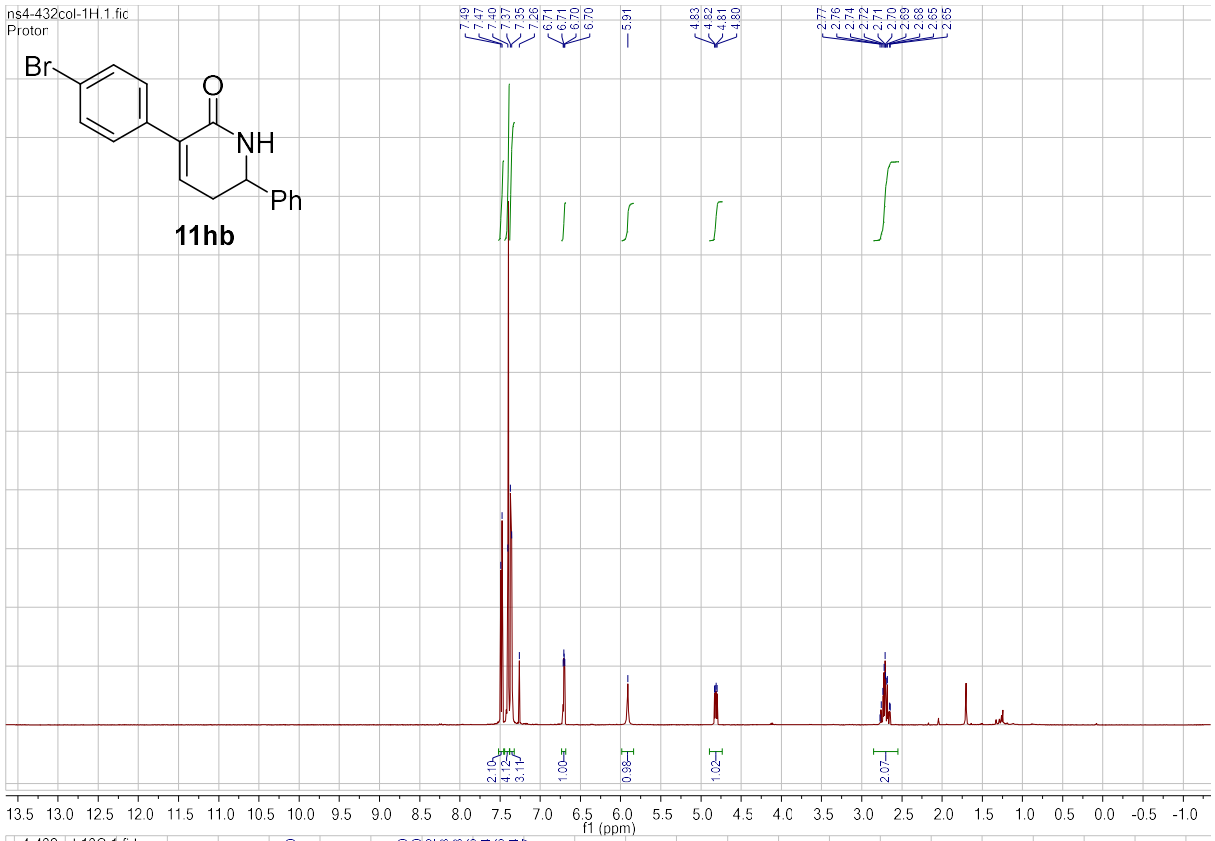
ns4-432col-1H.1.fic
Protor
Br
O
NH
Ph
11hb
7.49
7.47
7.40
7.37
7.35
7.26
6.71
6.71
6.70
6.70
5.91
4.83
4.82
4.81
4.80
2.77
2.76
2.74
2.72
2.71
2.70
2.69
2.68
2.65
2.65
2.19
4.13
3.11
1.00
0.98
1.02
2.07
f1 (ppm)

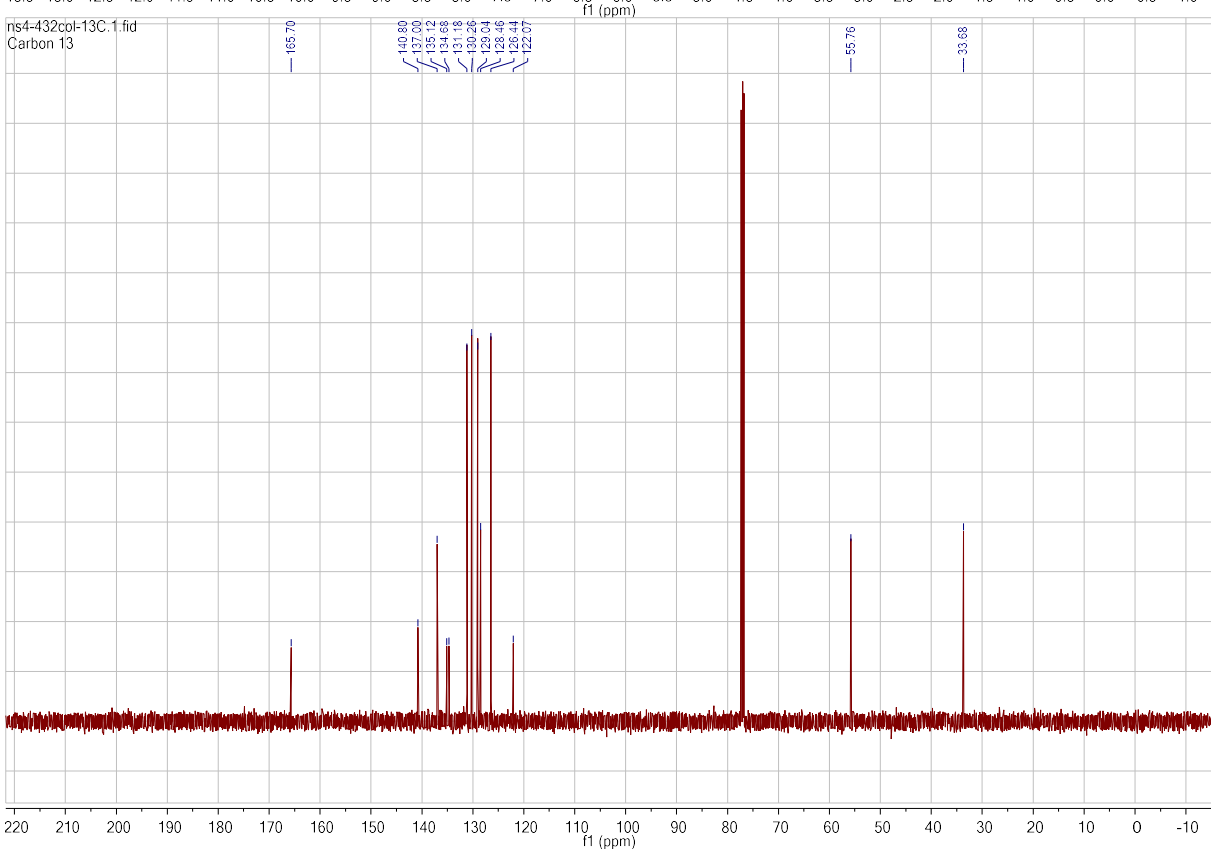
ns4-432col-13C.1.fid
Carbon 13
165.70
140.80
137.00
135.12
134.68
131.18
130.26
129.04
128.46
126.44
122.07
55.76
33.68
f1 (ppm)

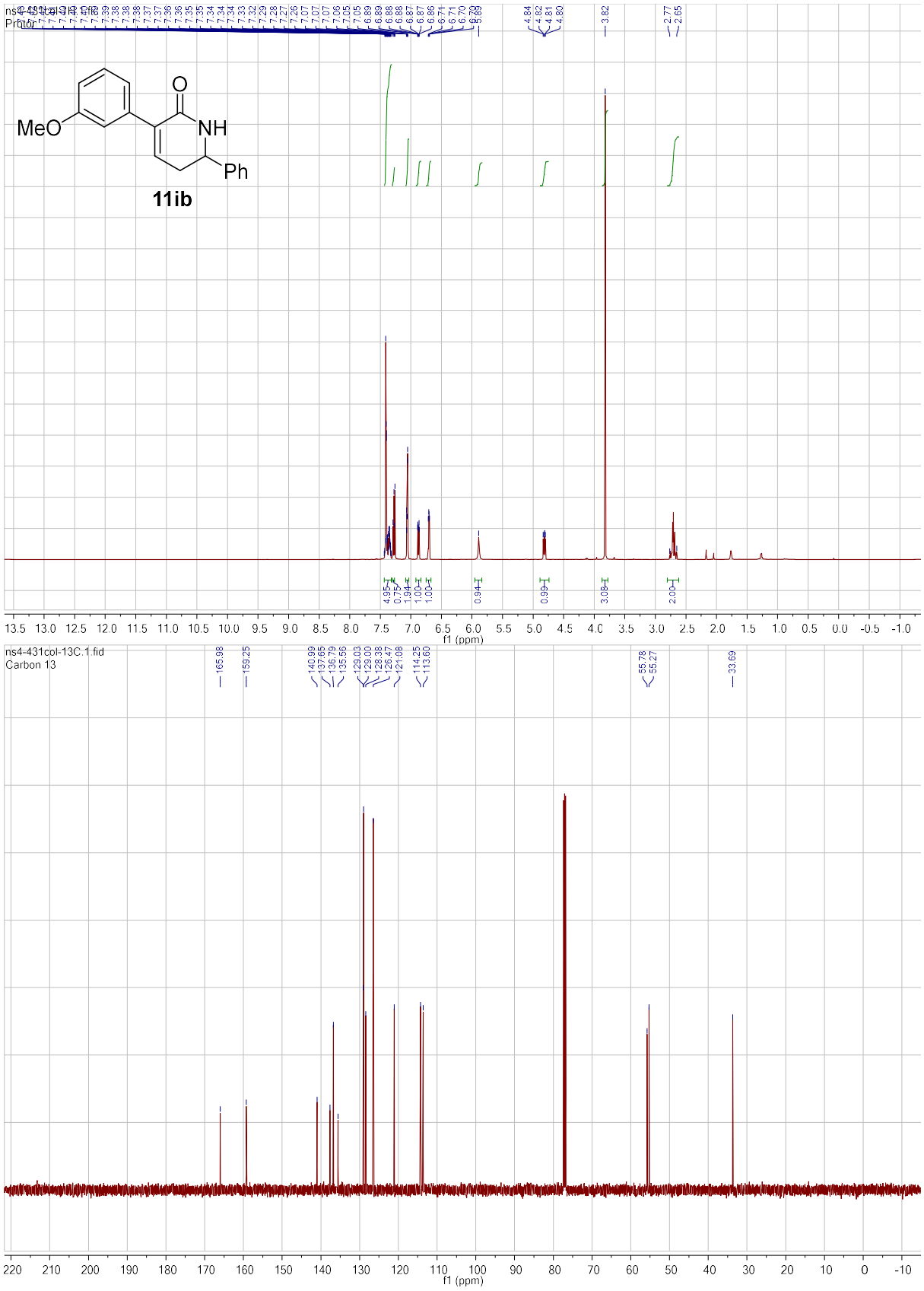
MeO
O
NH
Ph
11ib
ns4-431col-13C.1.fid
Carbon 13
f1 (ppm)

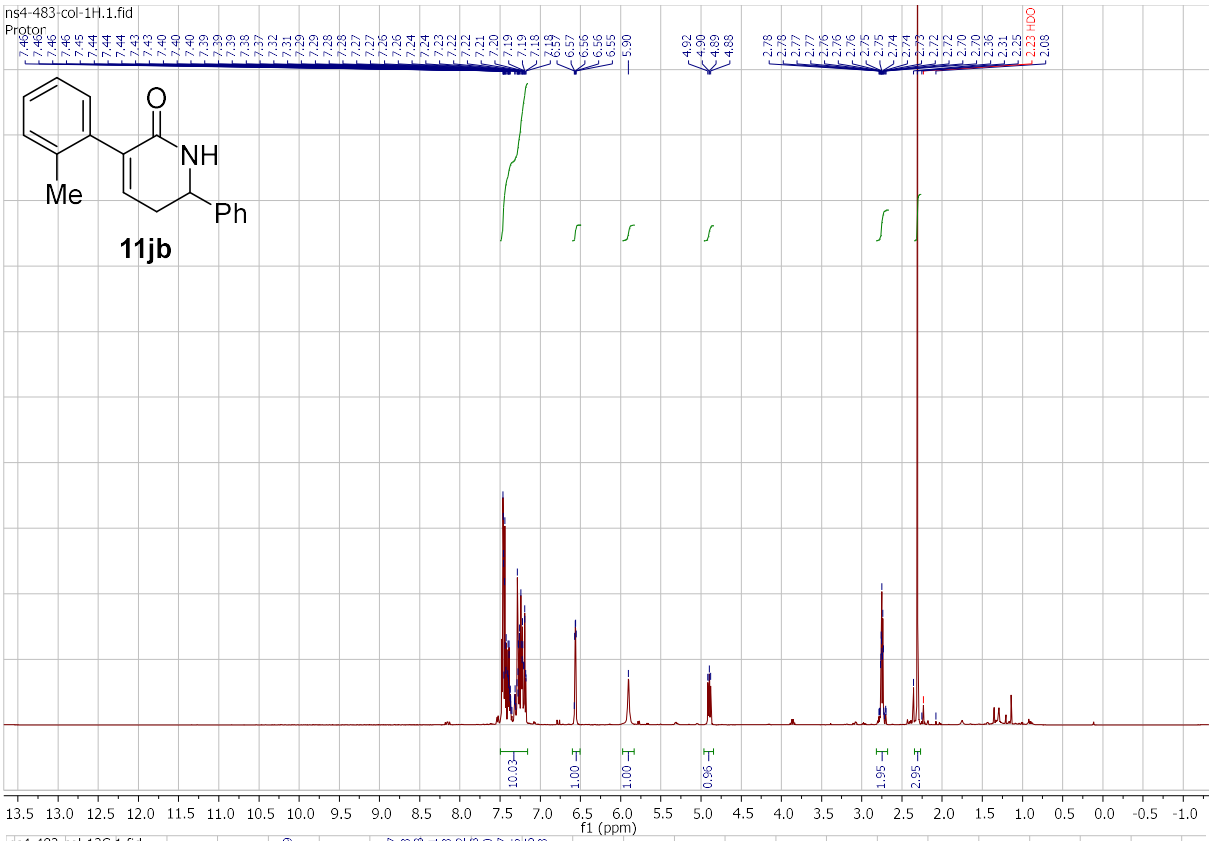
ns4-483-col-1H.1.fid
Proton
O
NH
Me
Ph
11jb
f1 (ppm)

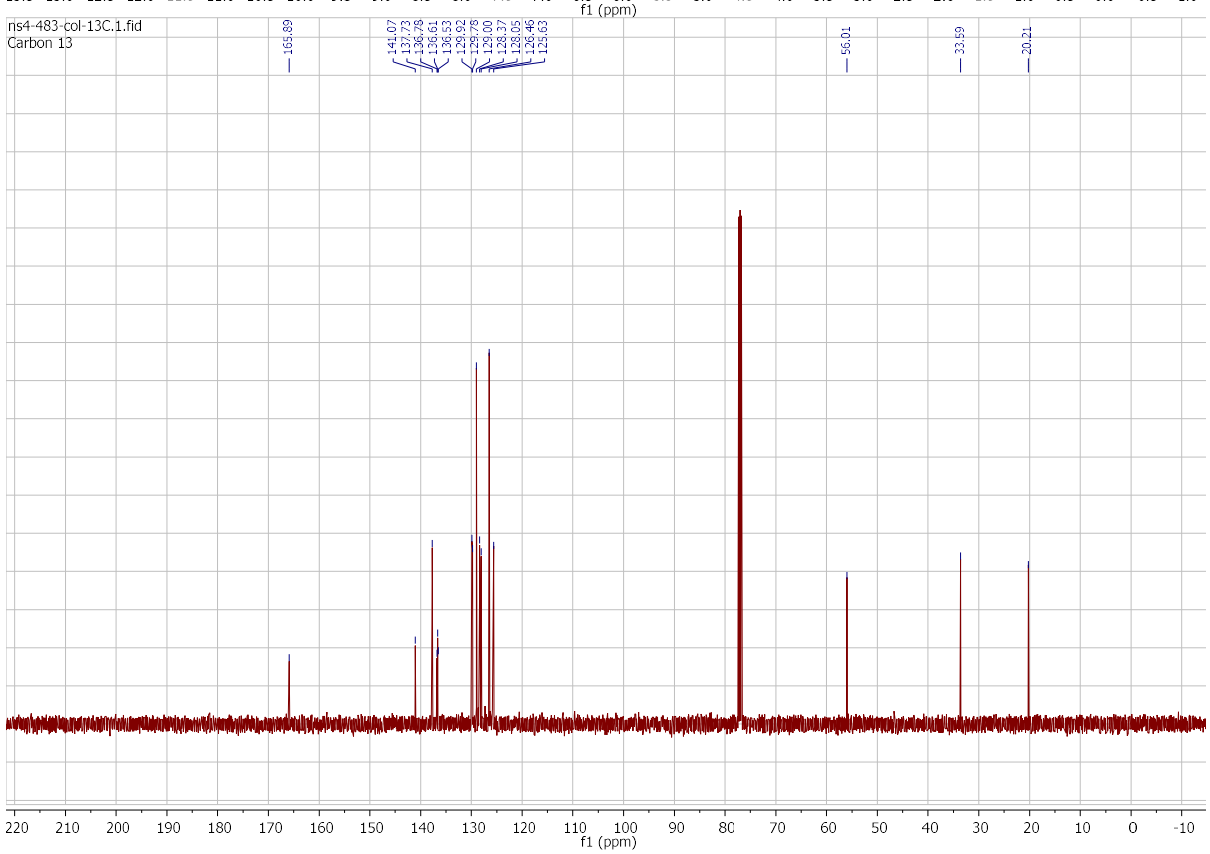
ns4-483-col-13C.1.fid
Carbon 13
165.89
141.07
137.73
136.78
136.61
136.53
129.82
129.78
129.00
128.37
128.05
126.46
125.63
56.01
33.59
20.21
f1 (ppm)

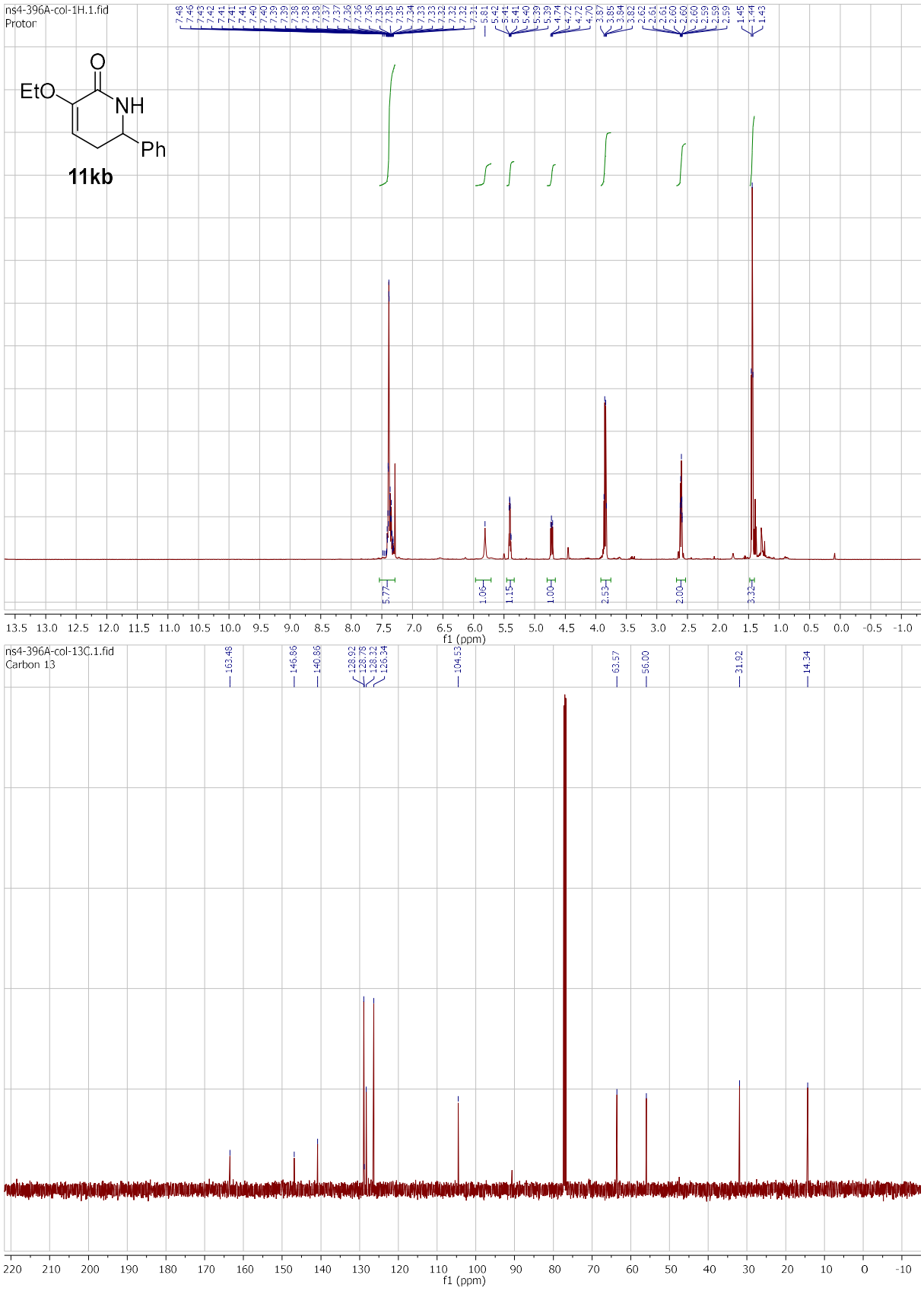
ns4-396A-col-1H.1.fid
Protor
EtO
O
NH
Ph
11kb
f1 (ppm)
ns4-396A-col-13C.1.fid
Carbon 13
f1 (ppm)

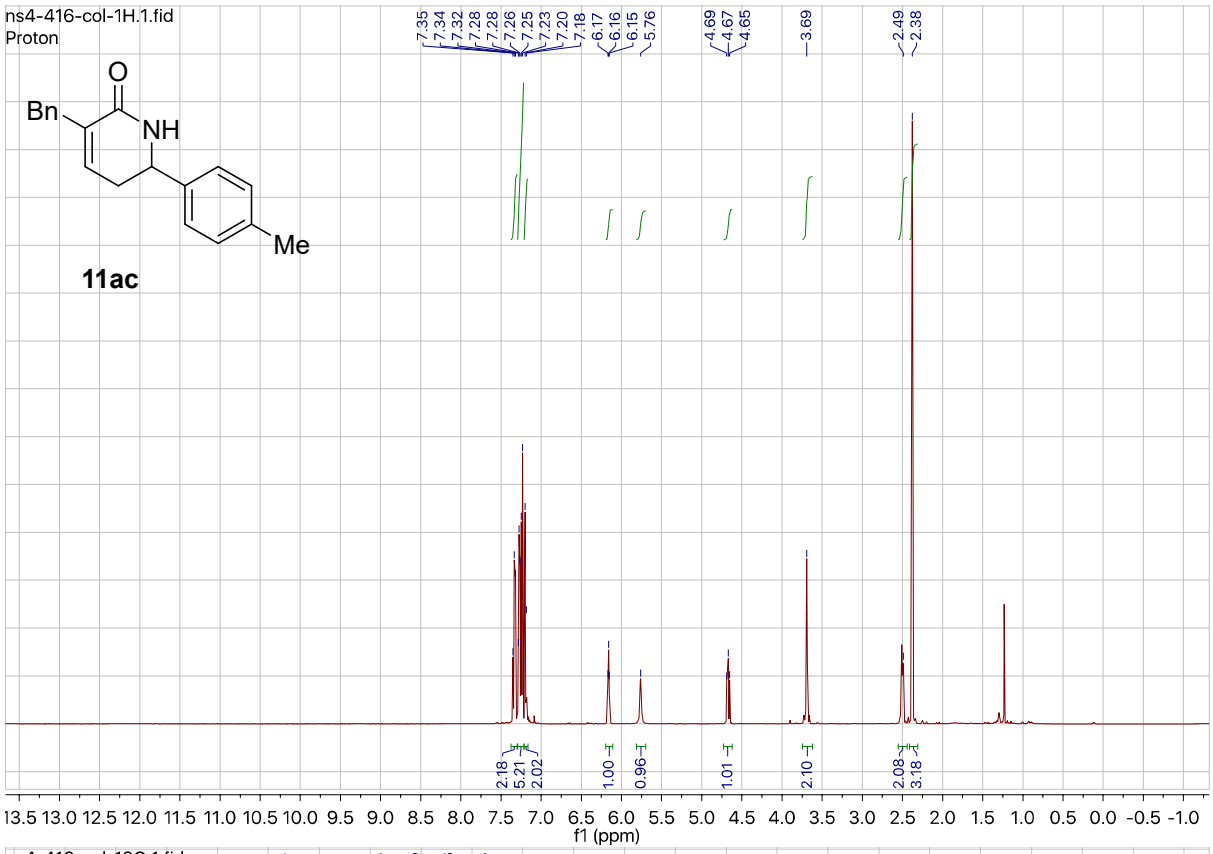
ns4-416-col-1H.1.fid
Proton
O
Bn
NH
Me
11ac
7.35
7.34
7.32
7.28
7.28
7.26
7.25
7.23
7.20
7.18
6.17
6.16
6.15
5.76
4.69
4.67
4.65
3.69
2.49
2.38
2.18
5.21
2.02
1.00
0.96
1.01
2.10
2.08
3.18
f1 (ppm)

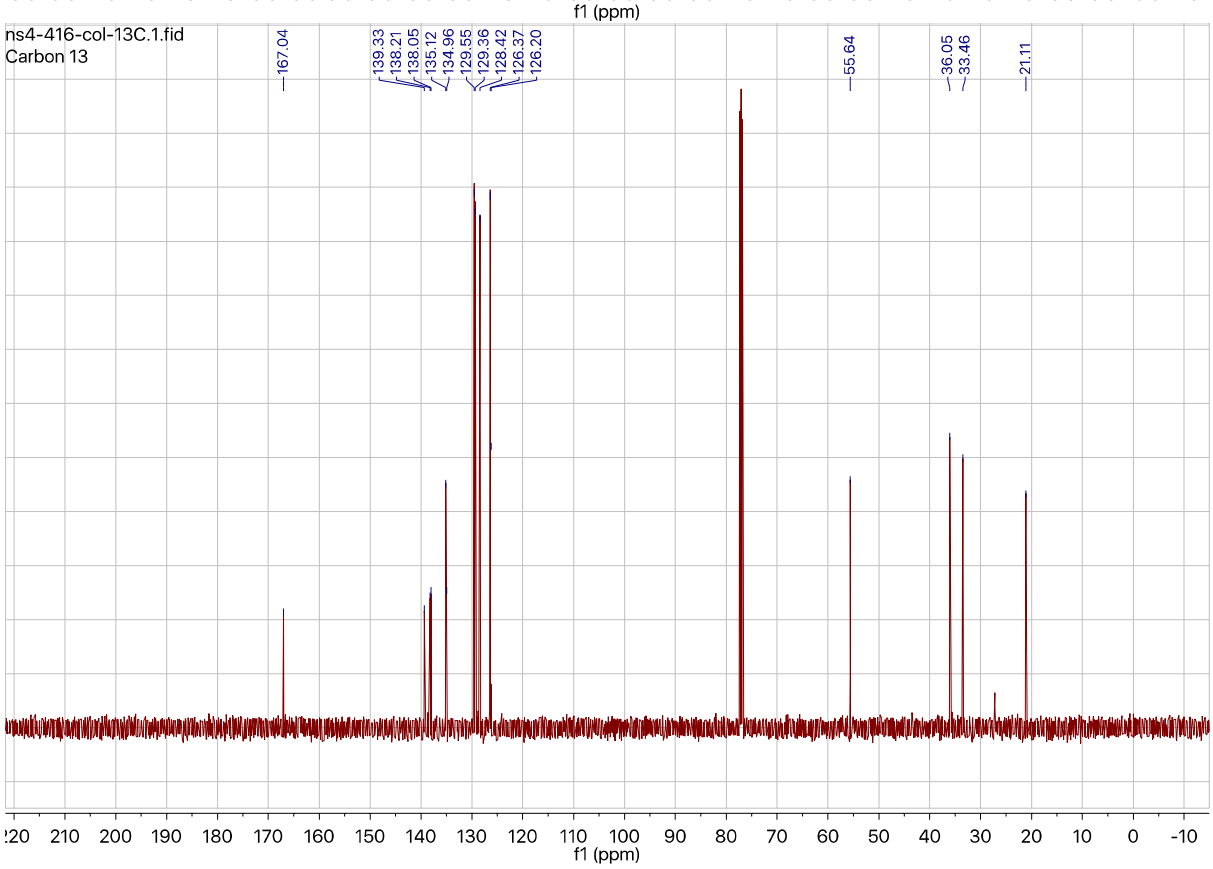
ns4-416-col-13C.1.fid
Carbon 13
167.04
139.33
138.21
138.05
135.12
134.96
129.55
129.36
128.42
126.37
126.20
55.64
36.05
33.46
21.11
f1 (ppm)

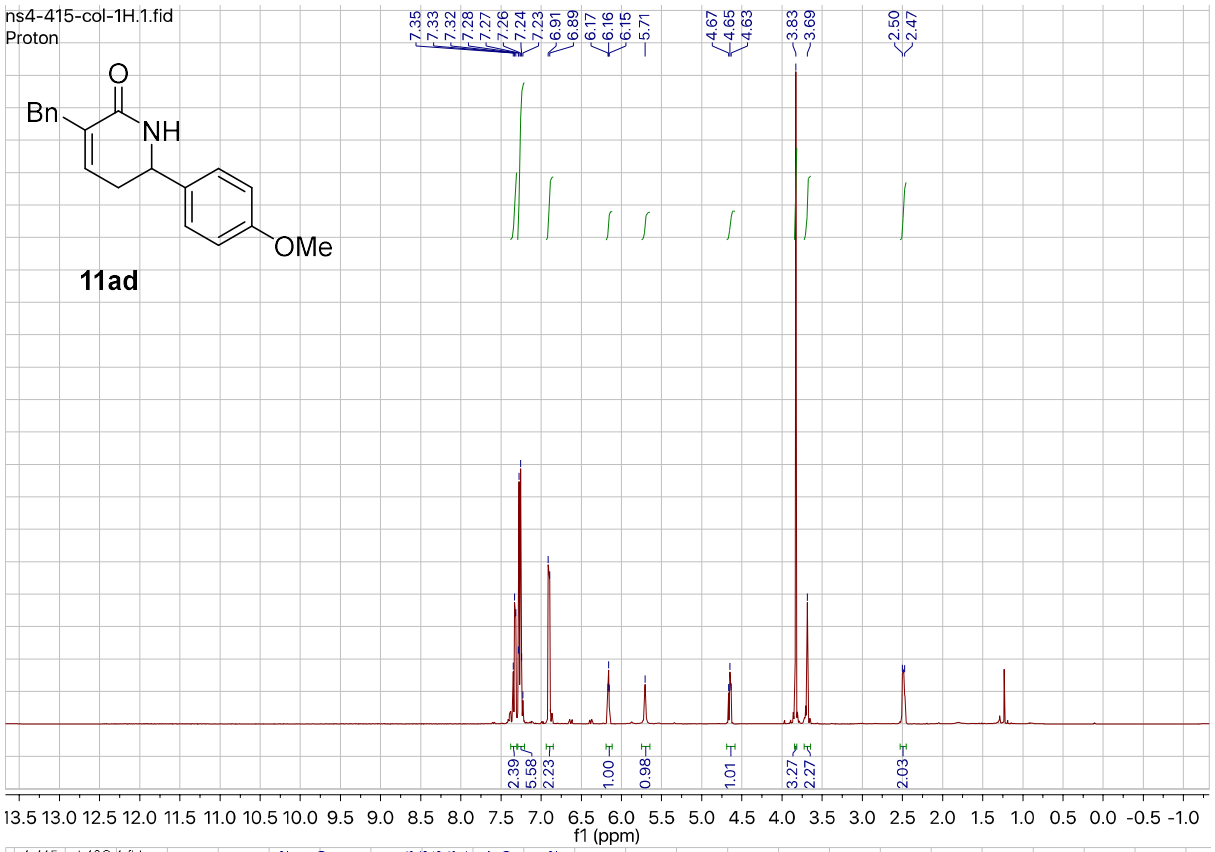
ns4-415-col-1H.1.fid
Proton
O
Bn
NH
OMe
11ad
7.35
7.33
7.32
7.28
7.27
7.26
7.24
7.23
6.91
6.89
6.17
6.16
6.15
5.71
4.67
4.65
4.63
3.83
3.69
2.50
2.47
2.39
5.58
2.23
1.00
0.98
1.01
3.27
2.27
2.03
f1 (ppm)

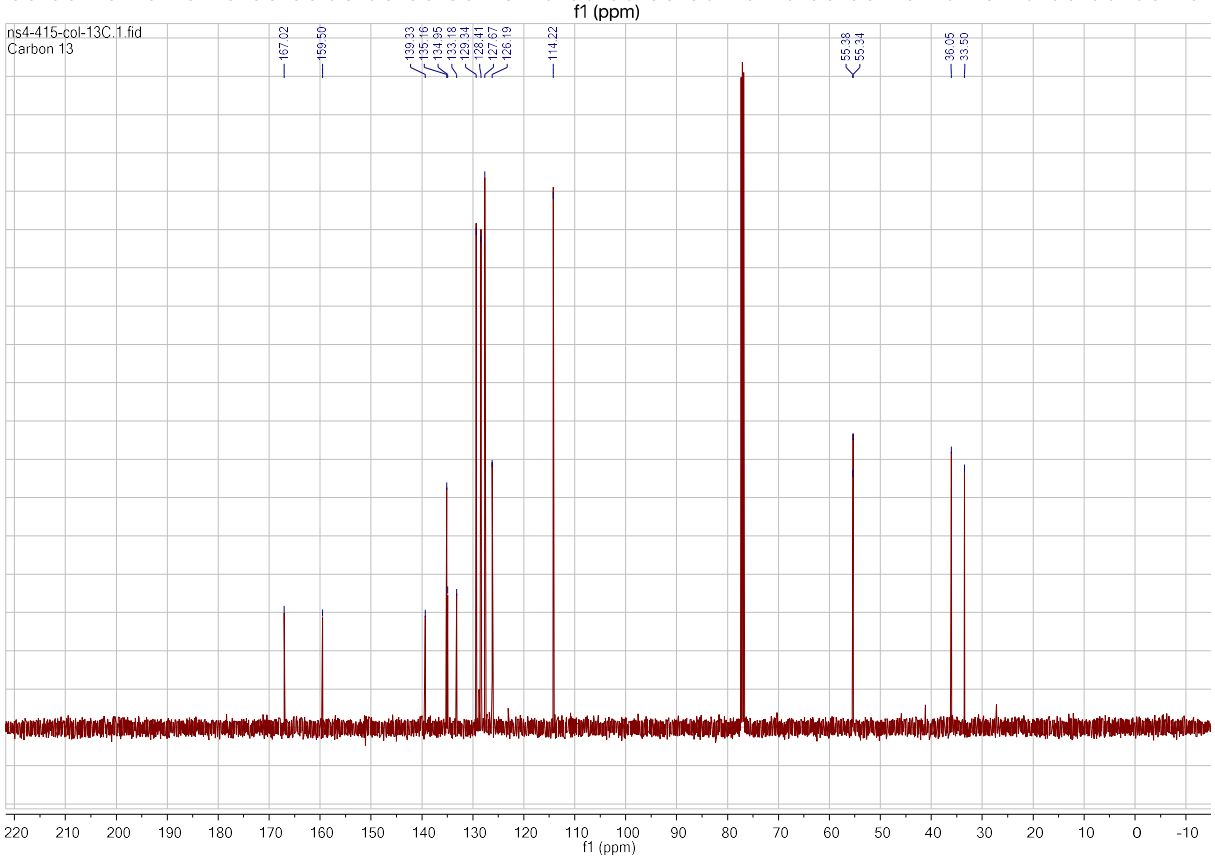
ns4-415-col-13C.1.fid
Carbon 13
167.02
159.50
139.33
135.16
134.95
133.18
129.34
128.41
127.67
126.19
114.22
55.38
55.34
36.05
33.50
f1 (ppm)

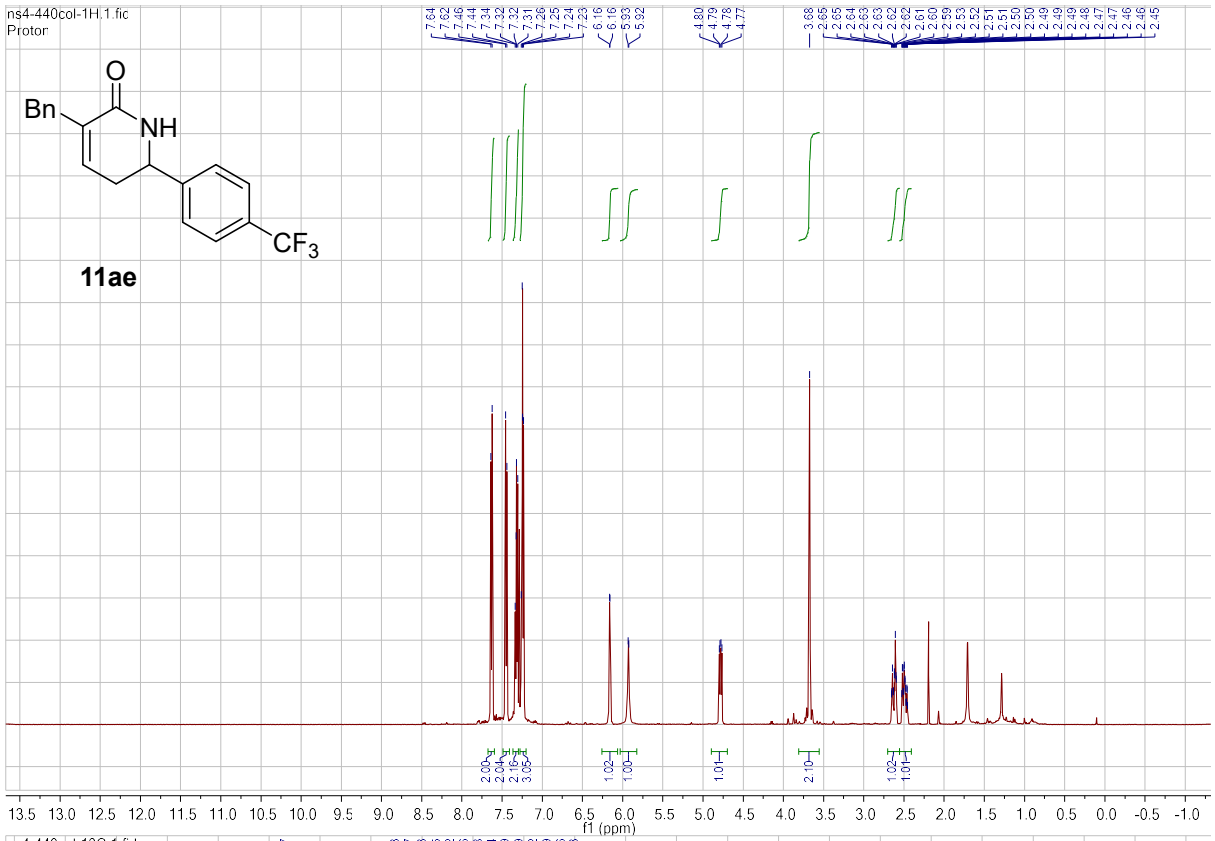
ns4-440col-1H.1.fic
Protor
O
Bn
NH
CF3
11ae
f1 (ppm)

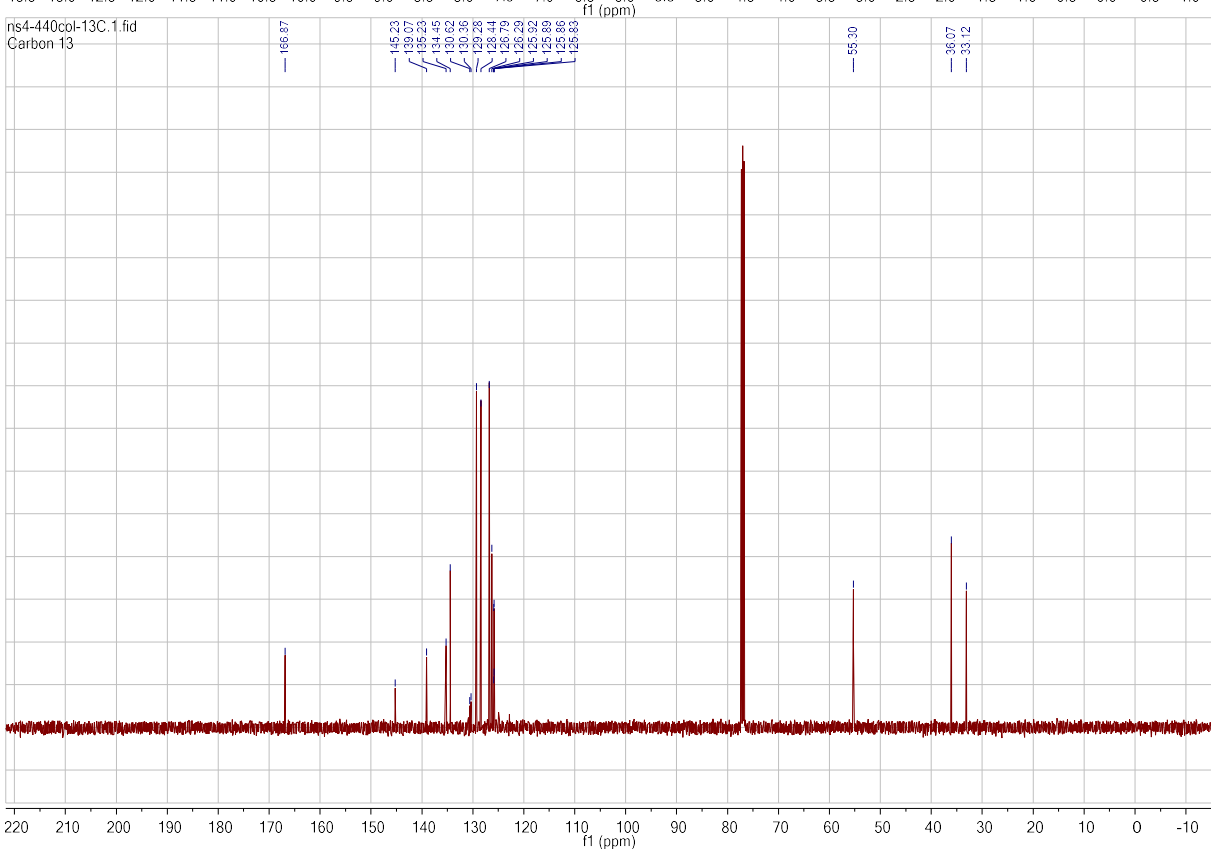
ns4-440col-13C.1.fid
Carbon 13
f1 (ppm)

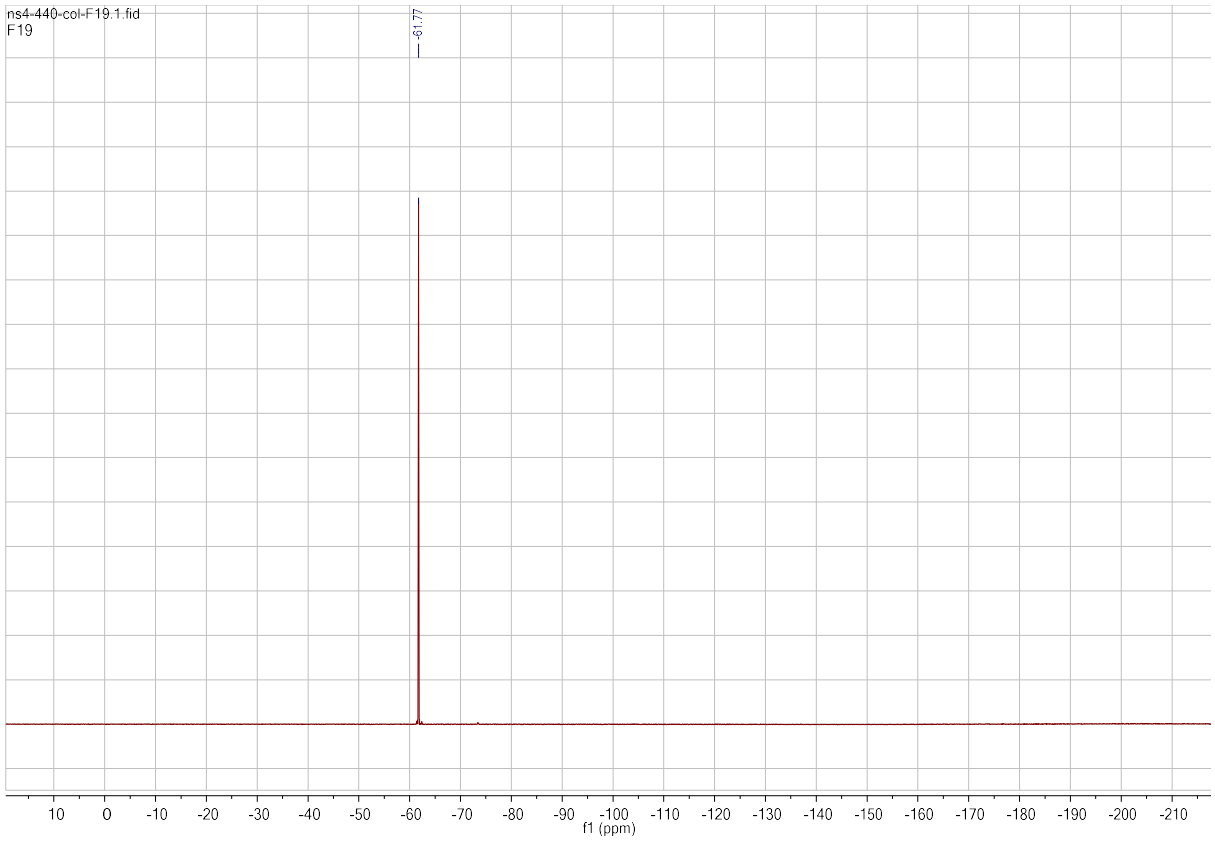
ns4-440-col-F19.1.fid
F19
-61.77
10 0 -10 -20 -30 -40 -50 -60 -70 -80 -90 -100 -110 -120 -130 -140 -150 -160 -170 -180 -190 -200 -210
f1 (ppm)

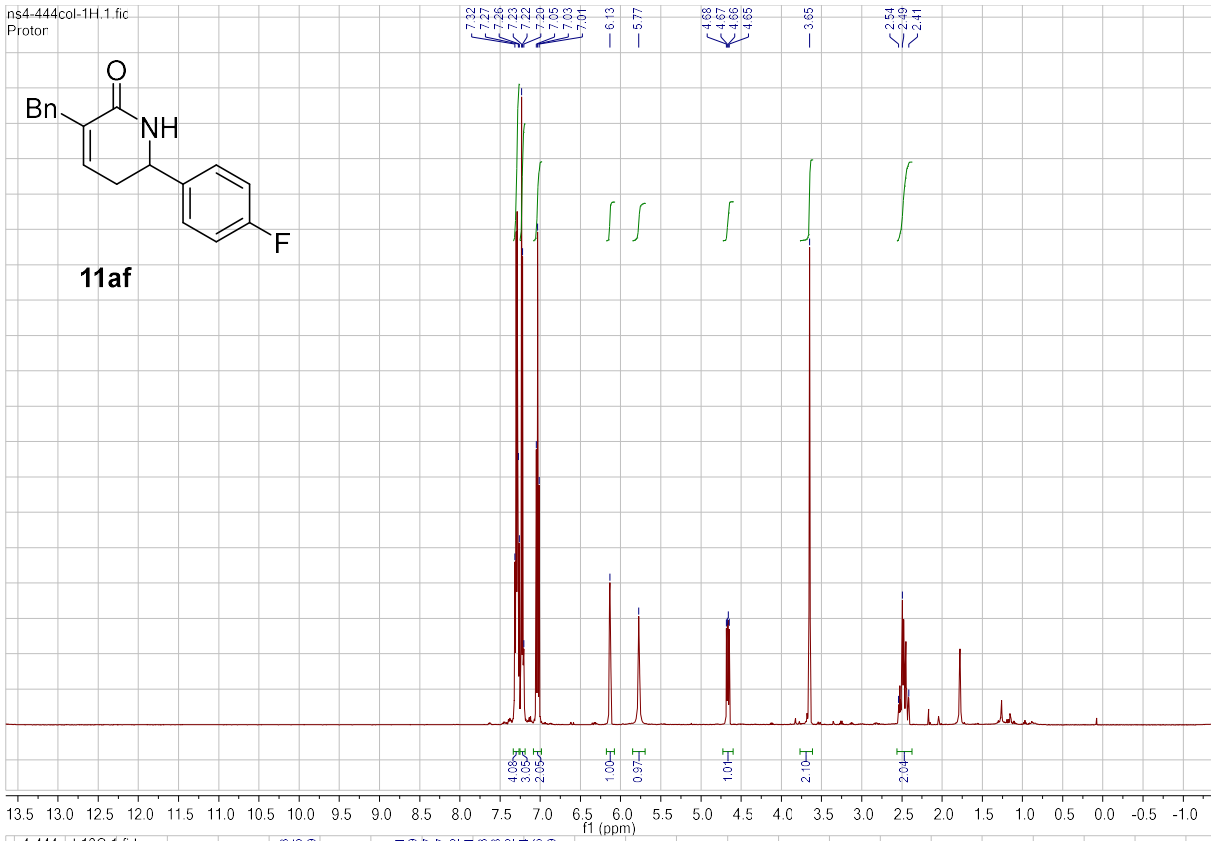
ns4-444col-1H.1.fic
Protor
O
Bn
NH
F
11af
7.32
7.27
7.26
7.23
7.22
7.20
7.05
7.03
7.01
6.13
5.77
4.68
4.67
4.66
4.65
3.65
2.54
2.49
2.41
4.08
3.05
2.05
1.00
0.97
1.01
2.10
2.04
f1 (ppm)

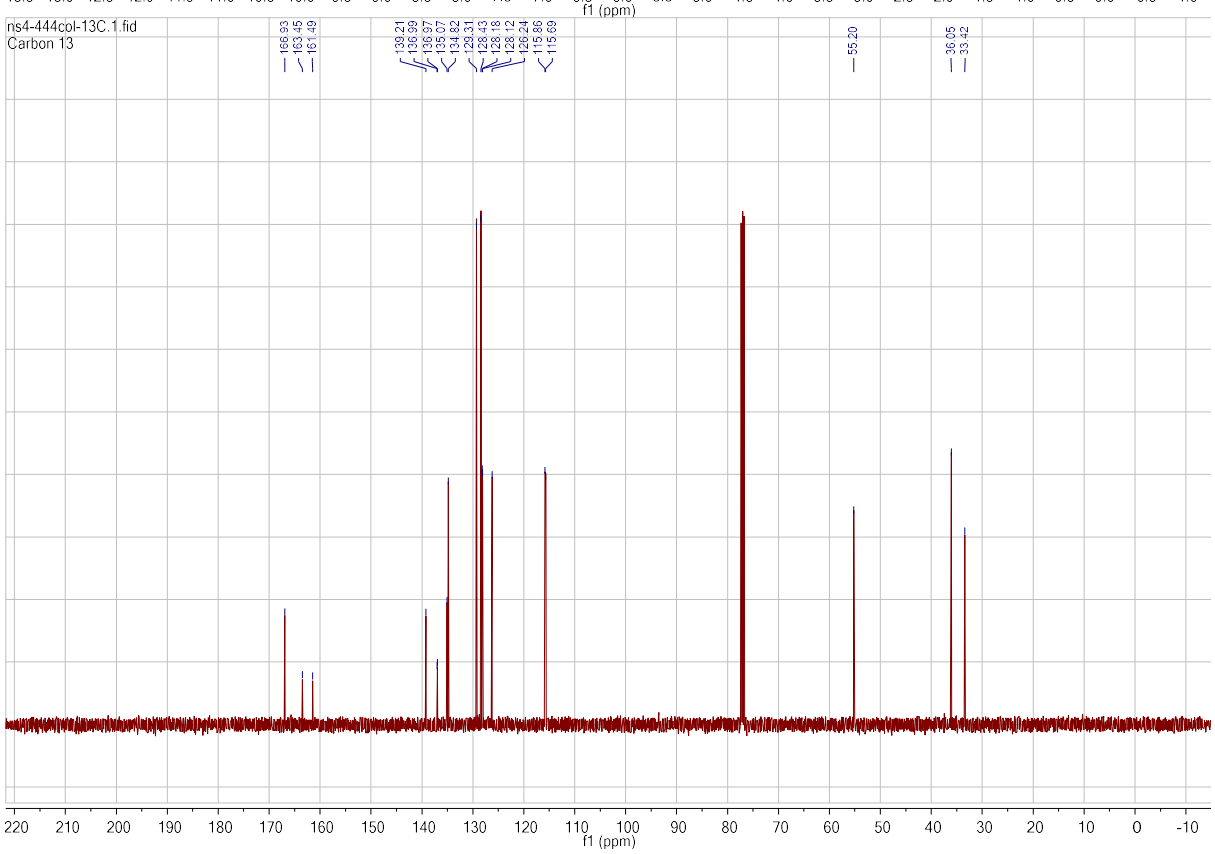
ns4-444col-13C.1.fid
Carbon 13
166.93
163.45
161.49
139.21
136.99
136.97
135.07
134.82
129.31
128.43
128.18
128.12
126.24
115.86
115.69
55.20
36.05
33.42
f1 (ppm)

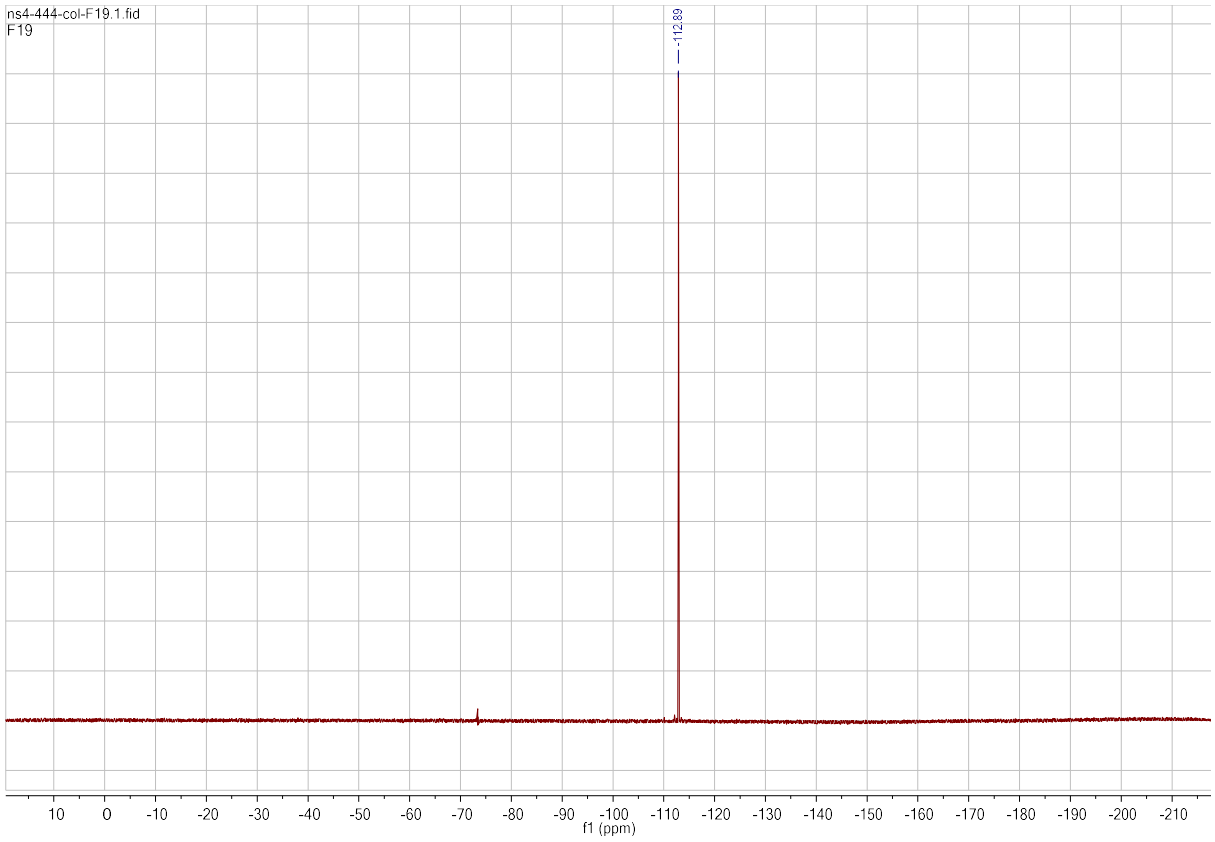
ns4-444-col-F19.1.fid
F19
-112.89
10 0 -10 -20 -30 -40 -50 -60 -70 -80 -90 -100 -110 -120 -130 -140 -150 -160 -170 -180 -190 -200 -210
f1 (ppm)

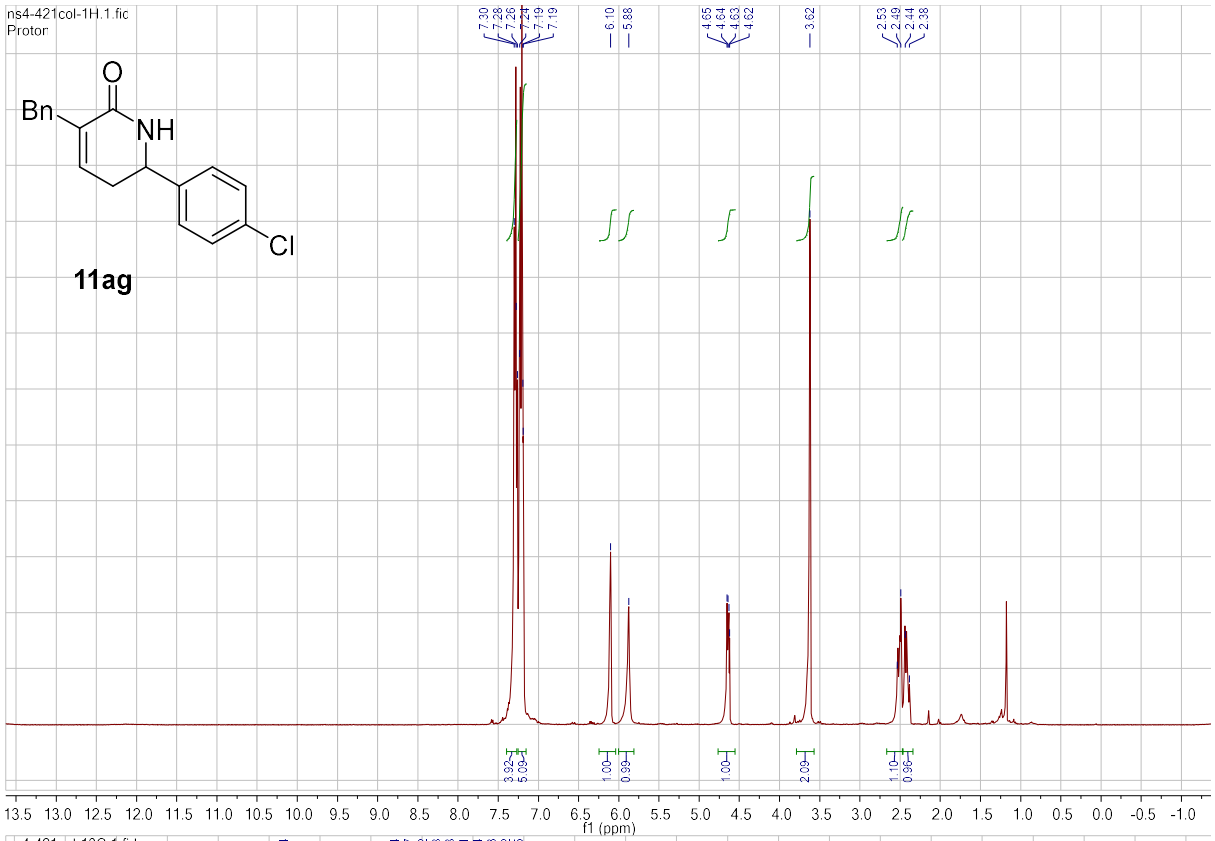
ns4-421col-1H.1.fic
Protor
O
Bn
NH
Cl
11ag
7.30
7.28
7.26
7.24
7.19
7.19
6.10
5.88
4.65
4.64
4.63
4.62
3.62
2.53
2.49
2.44
2.38
3.92
5.09
1.00
0.99
1.00
2.09
1.10
0.96
f1 (ppm)

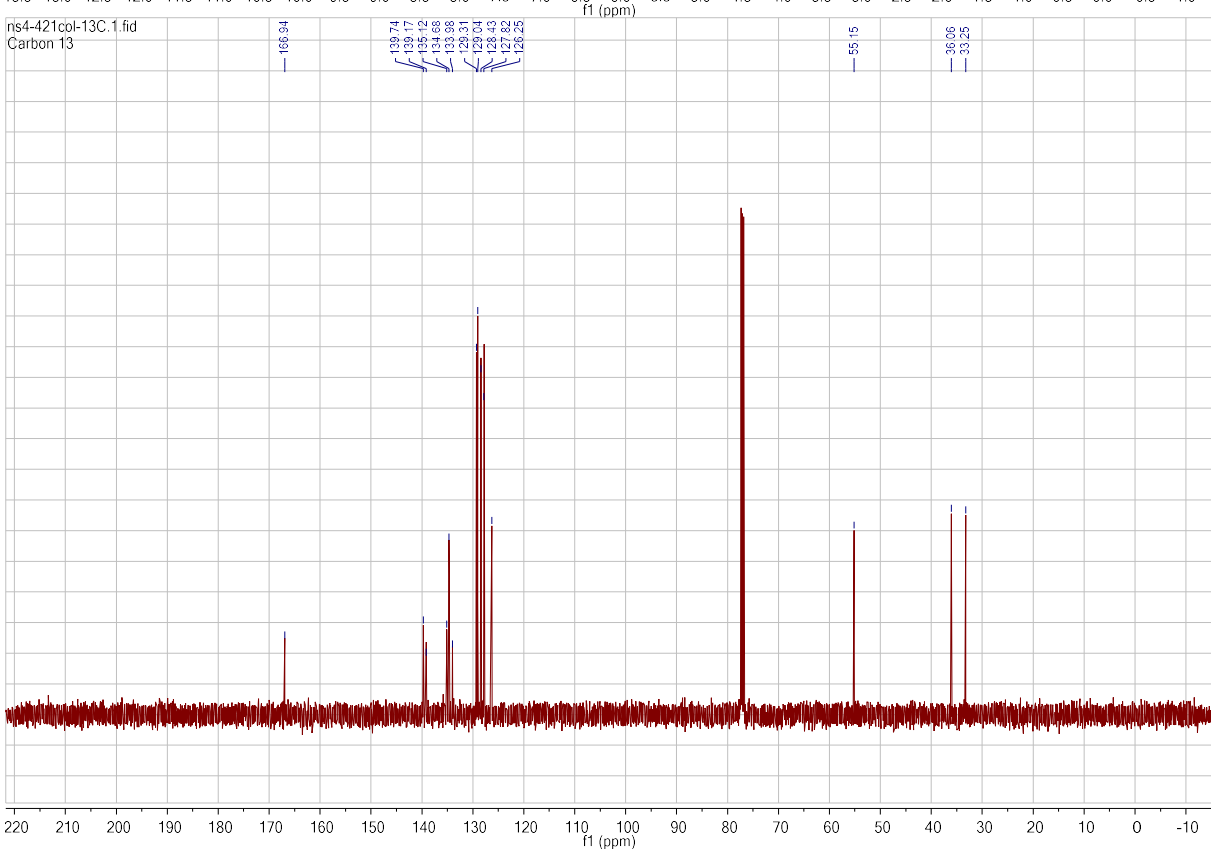
ns4-421col-13C.1.fid
Carbon 13
166.94
139.74
139.17
135.12
134.68
133.88
129.31
129.04
128.43
127.82
126.23
55.15
36.06
33.25
f1 (ppm)

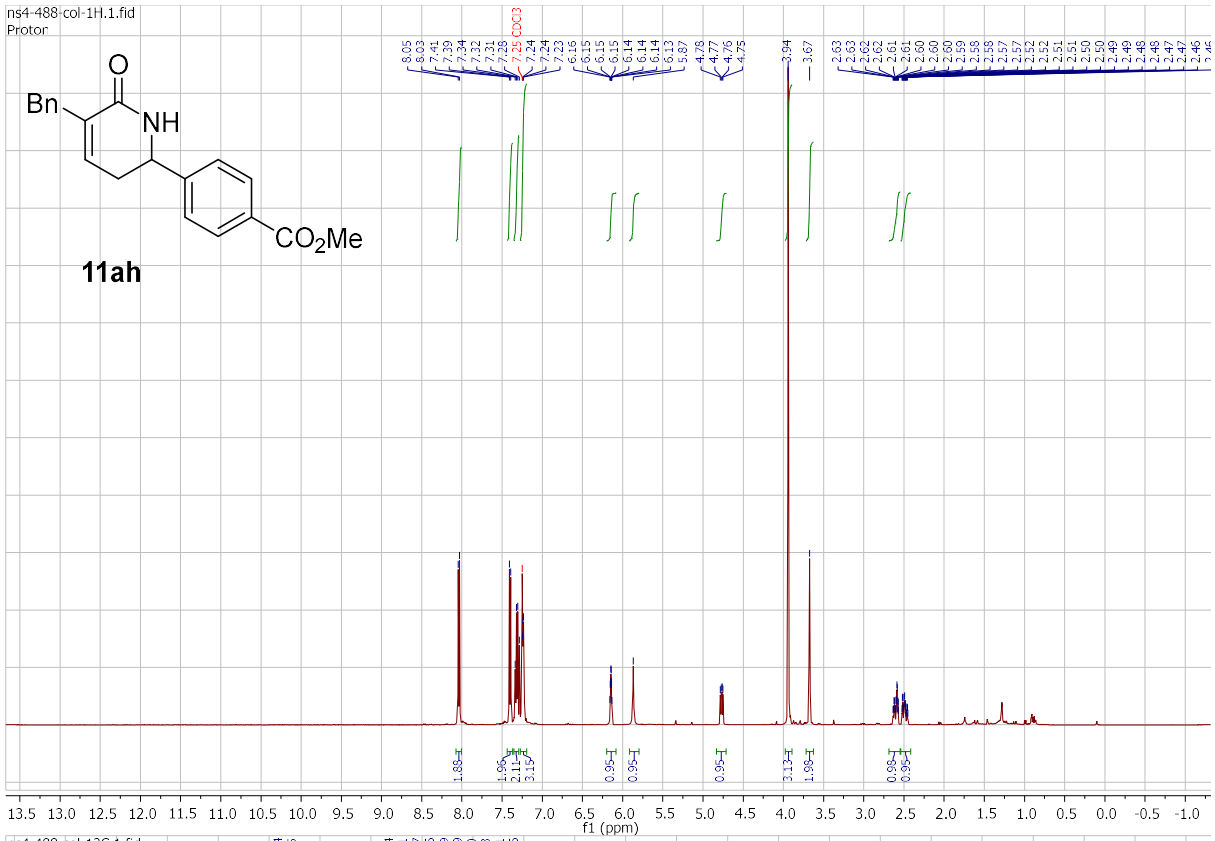
ns4-488-col-1H.1.fid
Proton
Bn
NH
O
CO2Me
11ah
f1 (ppm)

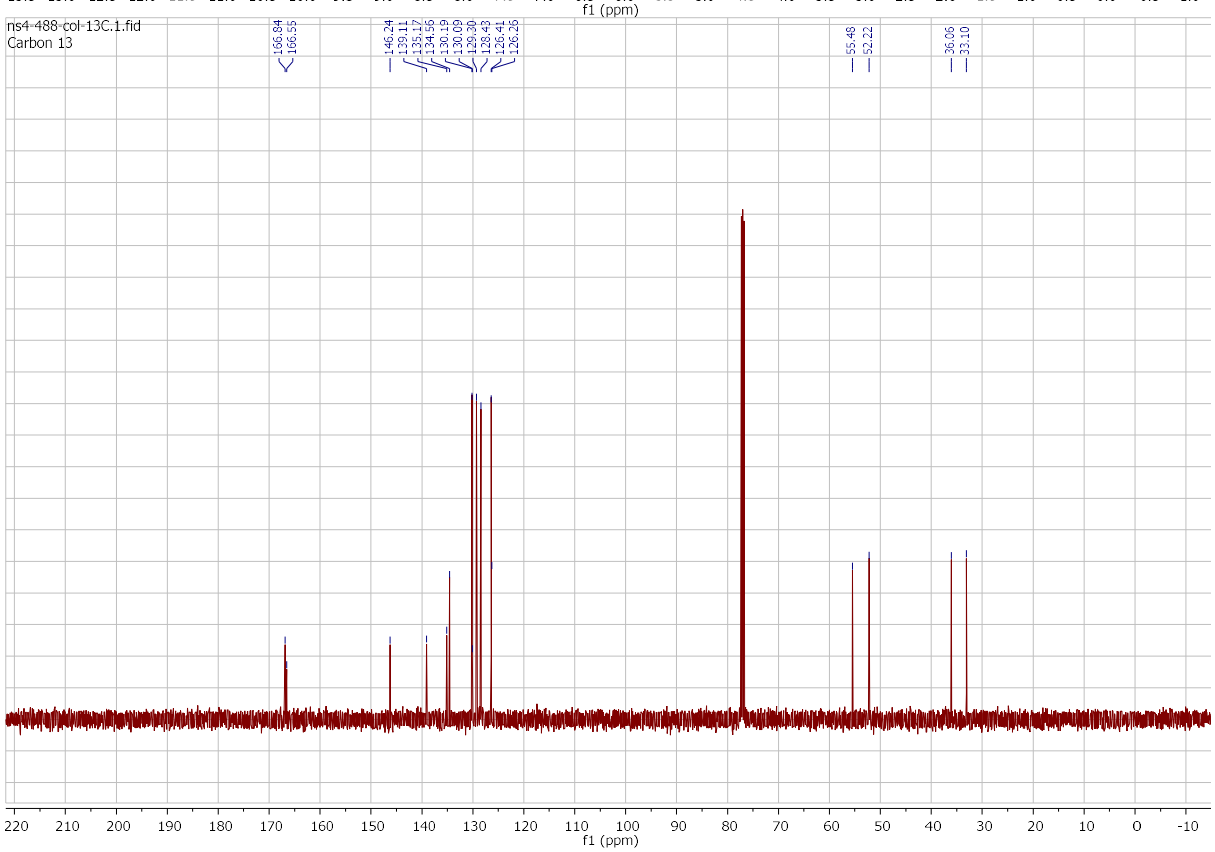
ns4-488-col-13C.1.fid
Carbon 13
f1 (ppm)

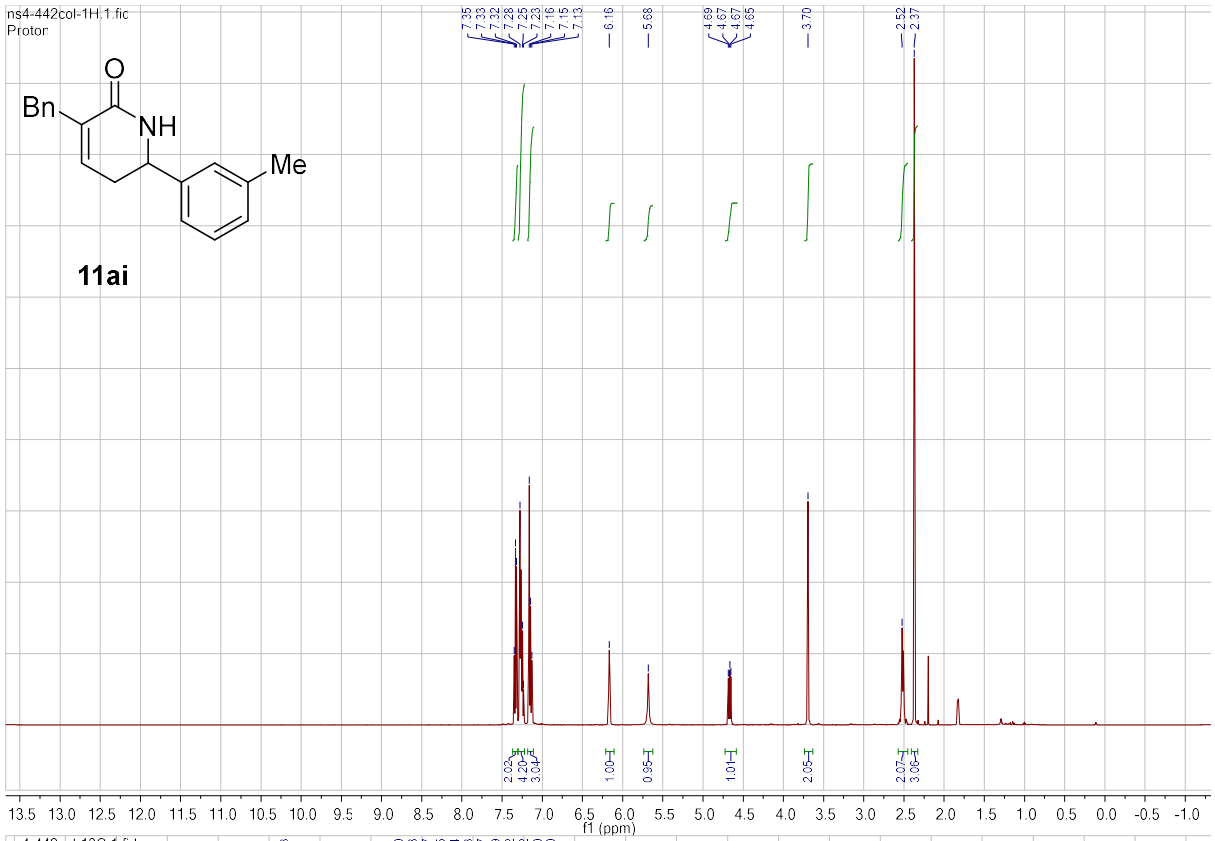
ns4-442col-1H.1.fic
Protor
O
Bn
NH
Me
11ai
7.35
7.33
7.32
7.28
7.25
7.23
7.16
7.15
7.13
6.16
5.88
4.69
4.67
4.67
4.65
3.70
2.52
2.37
2.02
4.20
3.04
1.00
0.95
1.01
2.05
2.07
3.06
f1 (ppm)

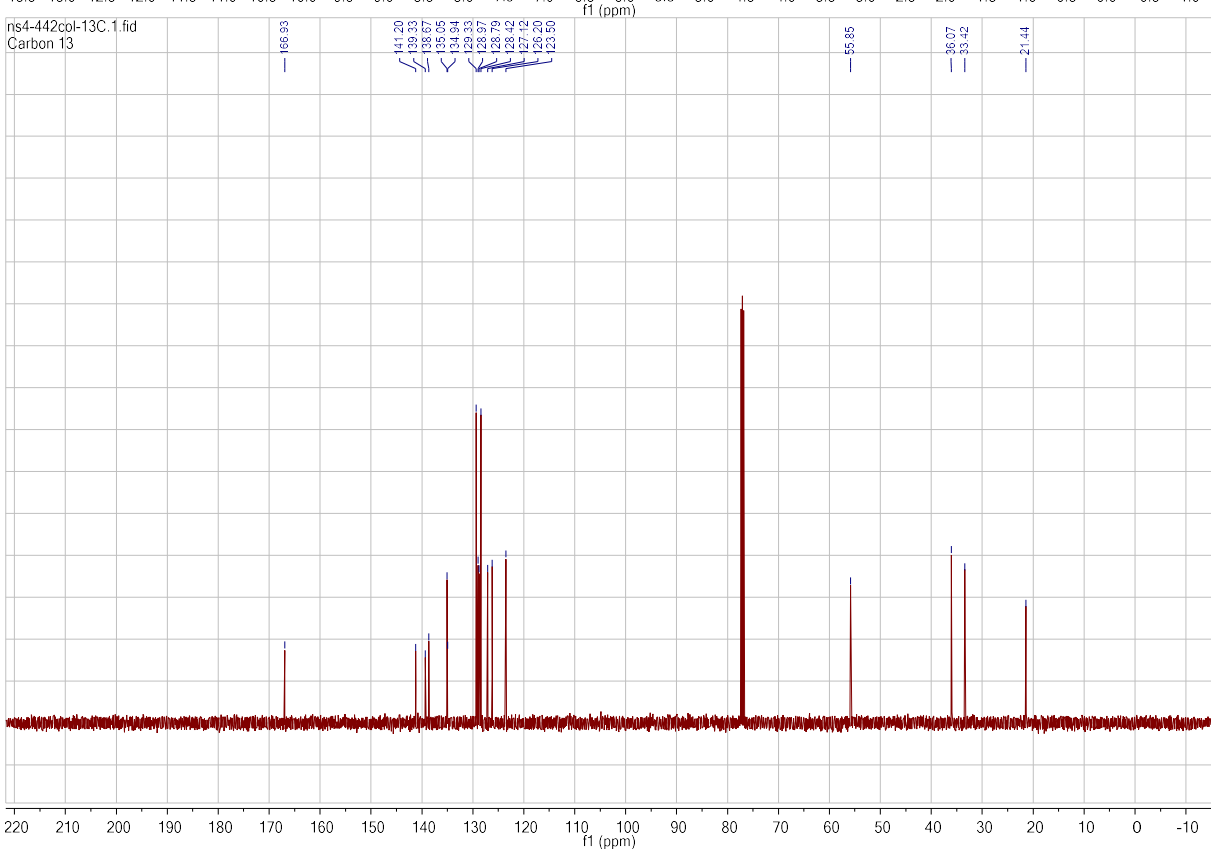
ns4-442col-13C.1.fid
Carbon 13
166.93
141.20
139.33
138.67
135.05
134.94
129.33
128.97
128.79
128.42
127.12
126.20
123.50
55.85
36.07
33.42
21.44
f1 (ppm)

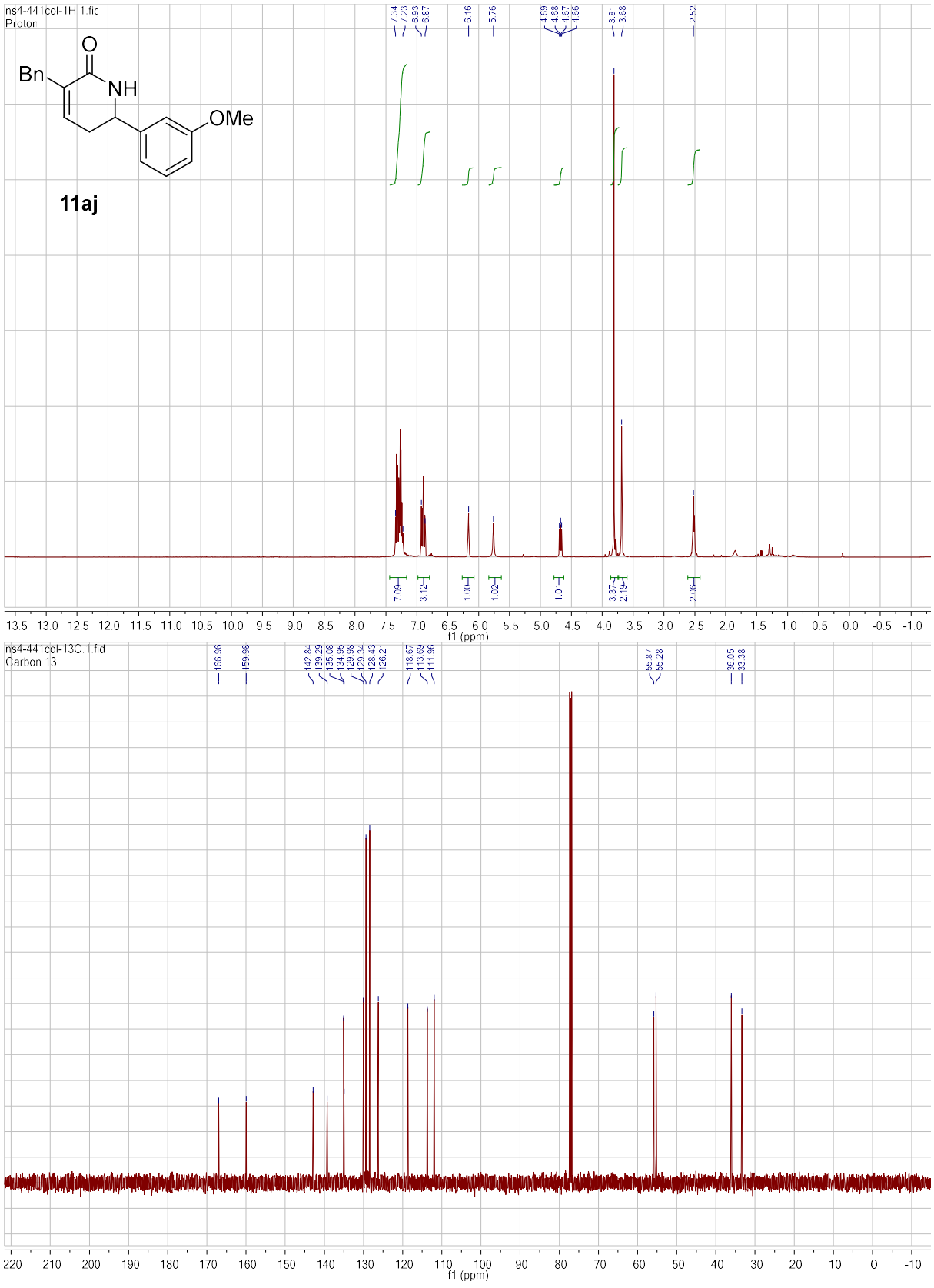
ns4-441col-1H.1.fic
Protor
O
Bn
NH
OMe
11aj
7.34
7.23
6.93
6.87
6.16
5.76
4.69
4.68
4.67
4.66
3.81
3.68
2.52
7.09
3.12
1.00
1.02
1.01
3.37
2.19
2.06
f1 (ppm)
ns4-441col-13C.1.fid
Carbon 13
166.96
159.98
142.84
139.29
135.08
134.95
129.98
129.34
128.43
126.21
118.67
113.69
111.96
55.87
55.28
36.05
33.38
f1 (ppm)

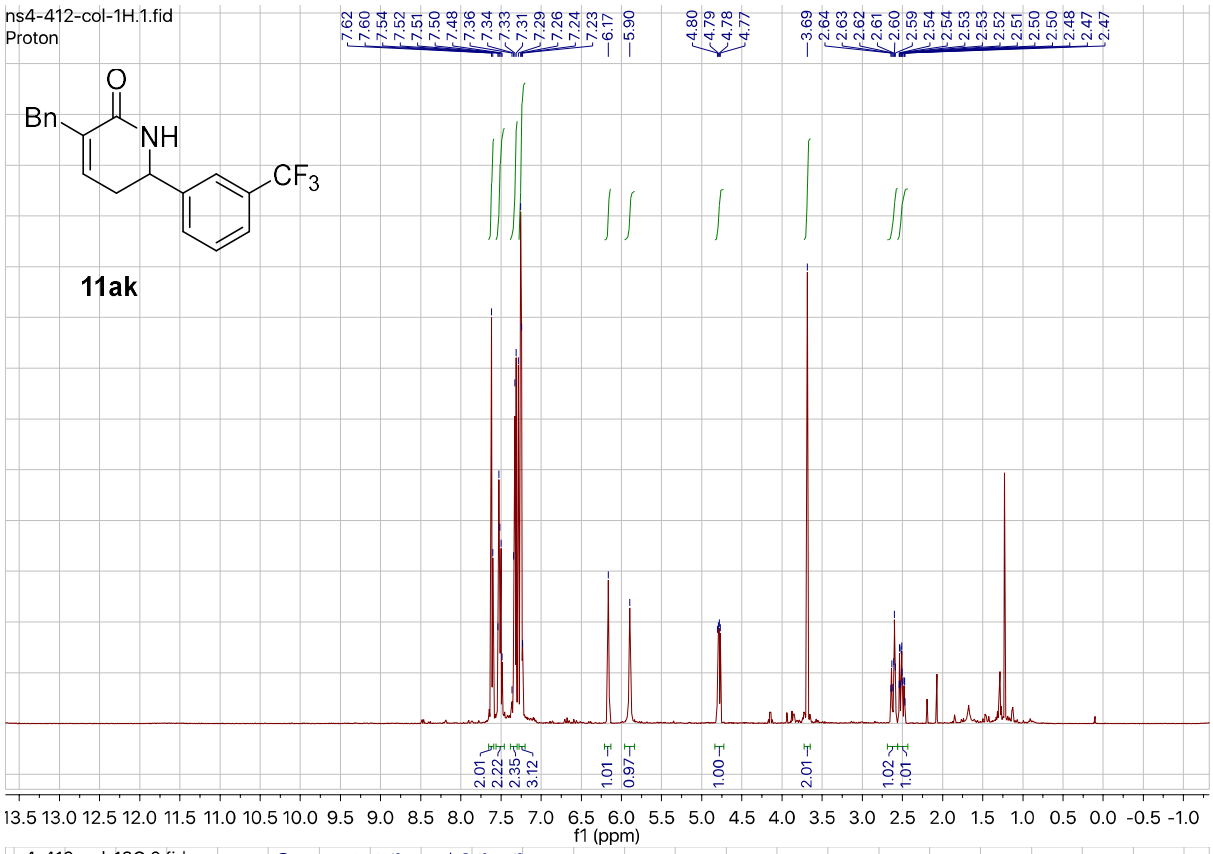
ns4-412-col-1H.1.fid
Proton
Bn
NH
CF3
O
11ak
f1 (ppm)

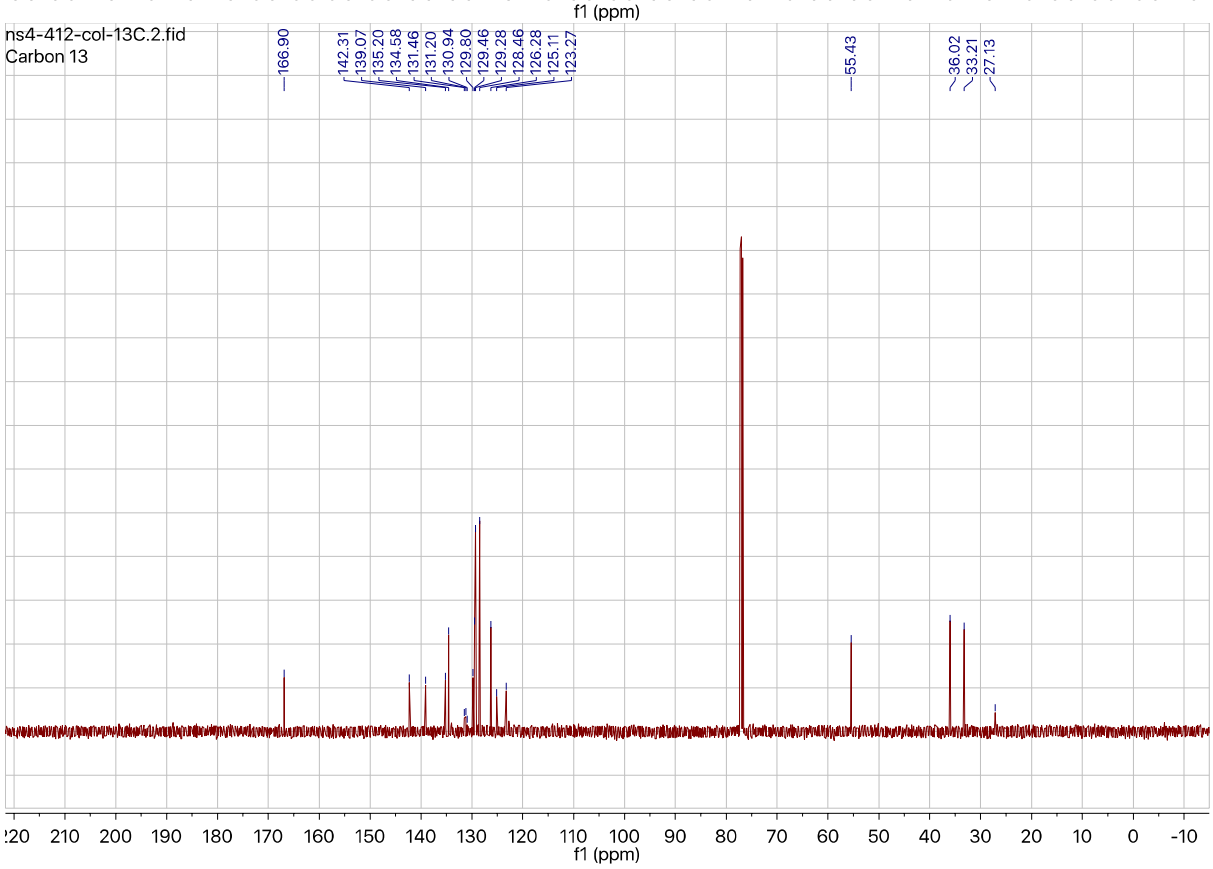
ns4-412-col-13C.2.fid
Carbon 13
f1 (ppm)

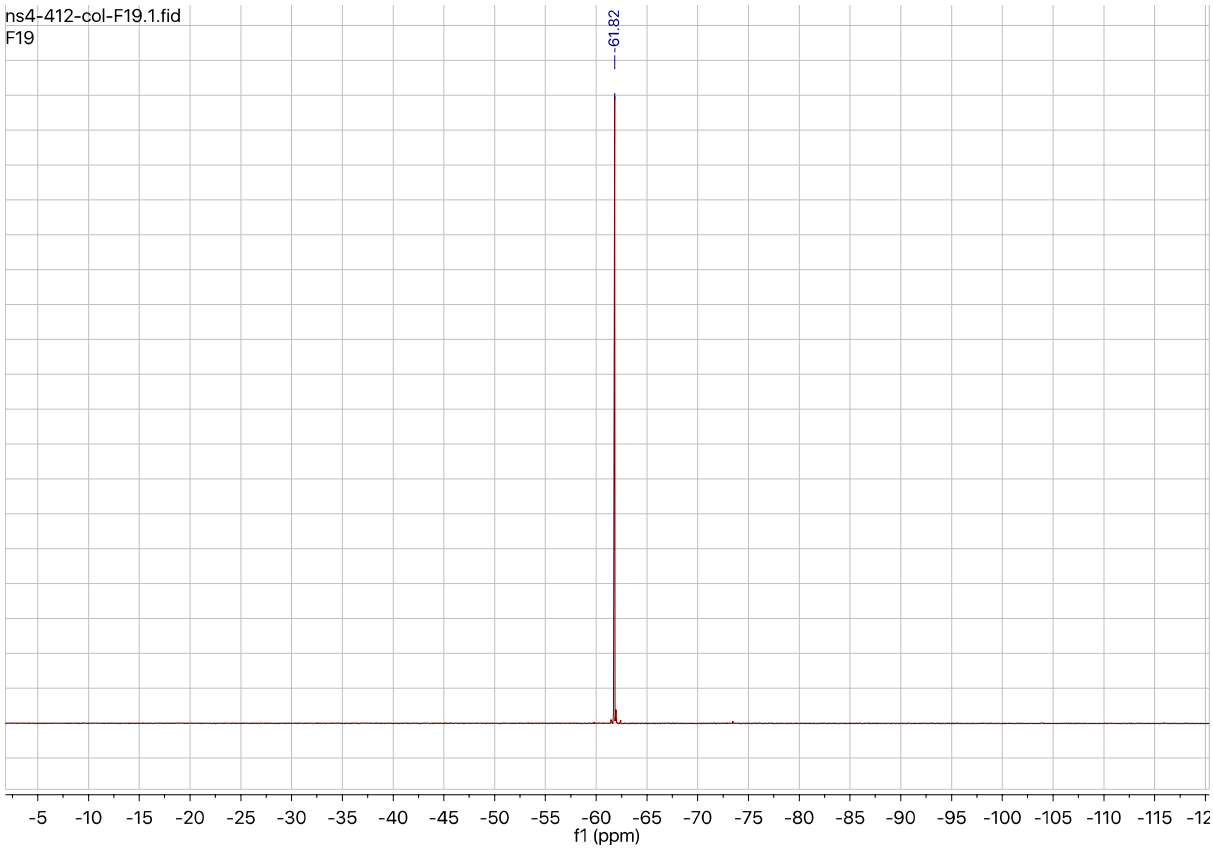
ns4-412-col-F19.1.fid
F19
-61.82
-5 -10 -15 -20 -25 -30 -35 -40 -45 -50 -55 -60 -65 -70 -75 -80 -85 -90 -95 -100 -105 -110 -115 -12
f1 (ppm)

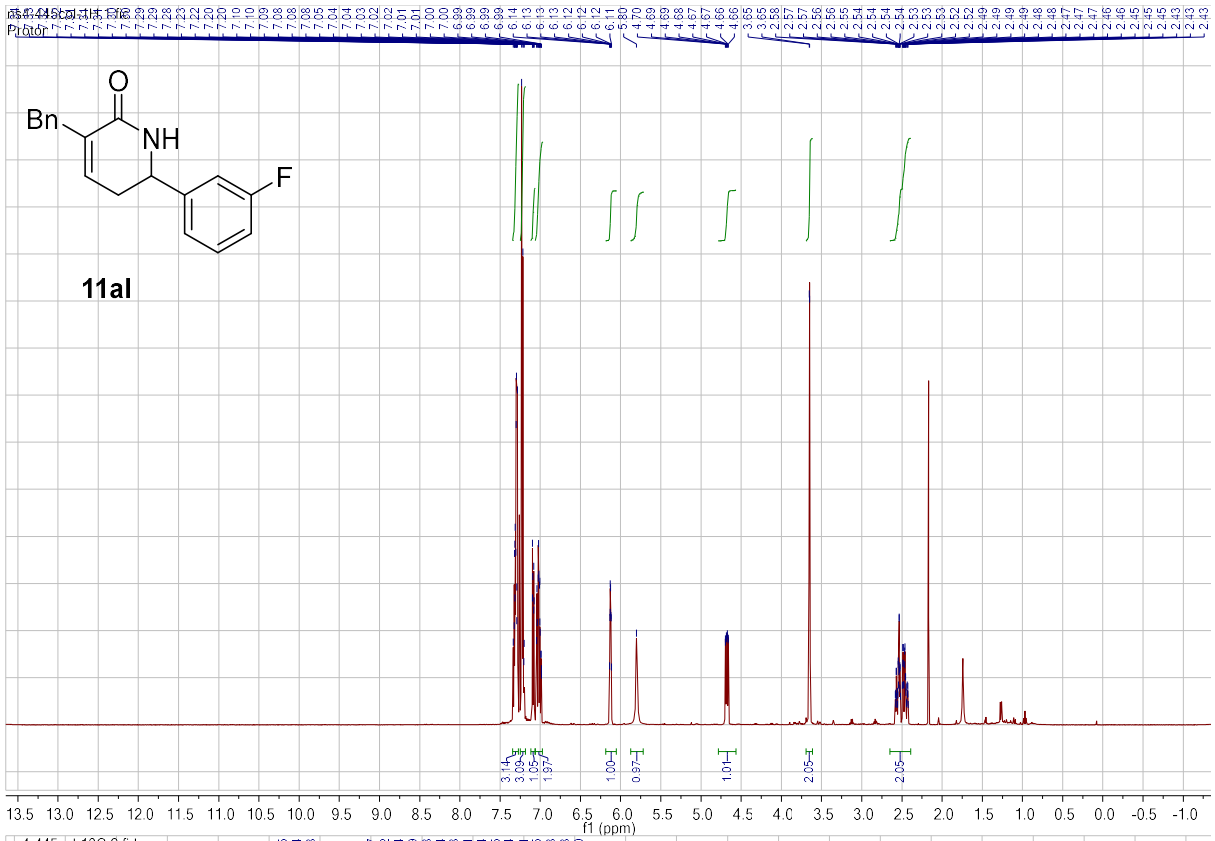
Bn
O
NH
F
11al
f1 (ppm)

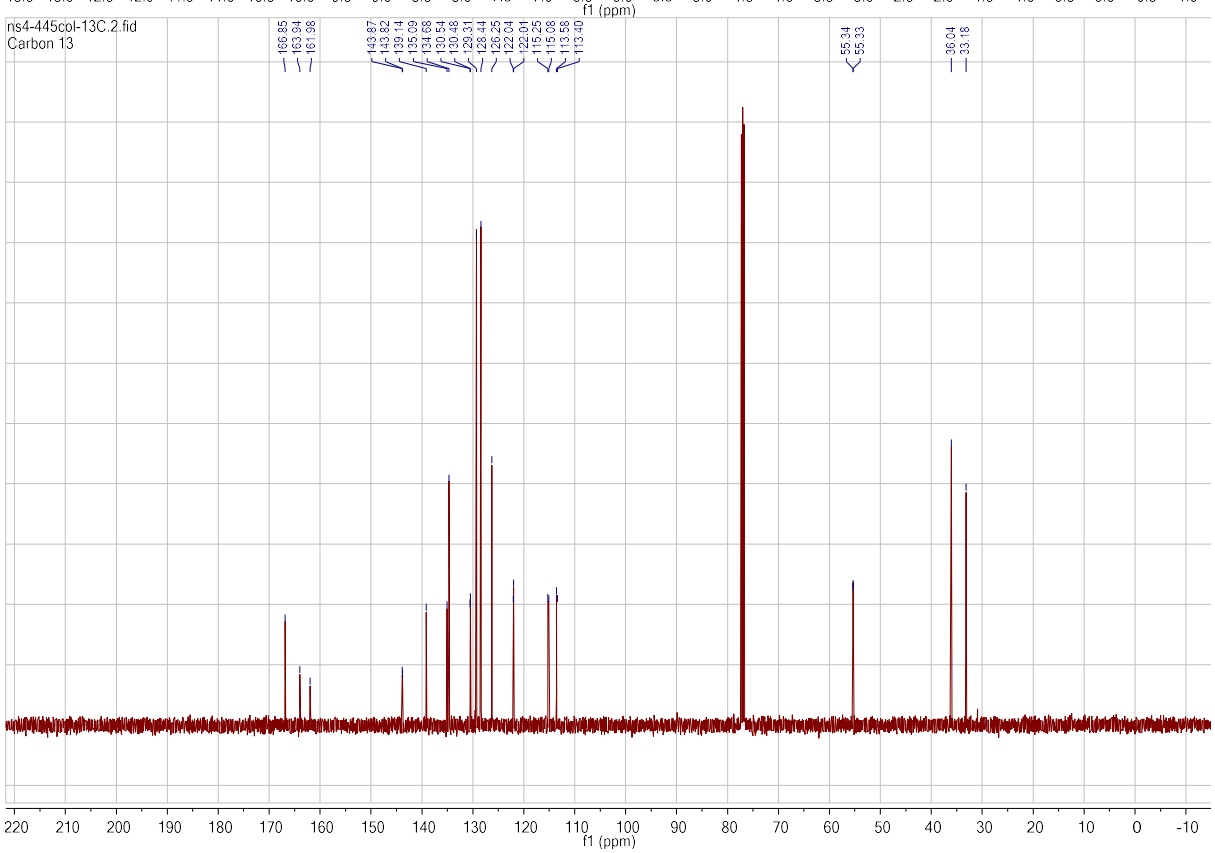
ns4-445col-13C.2.fid
Carbon 13
f1 (ppm)

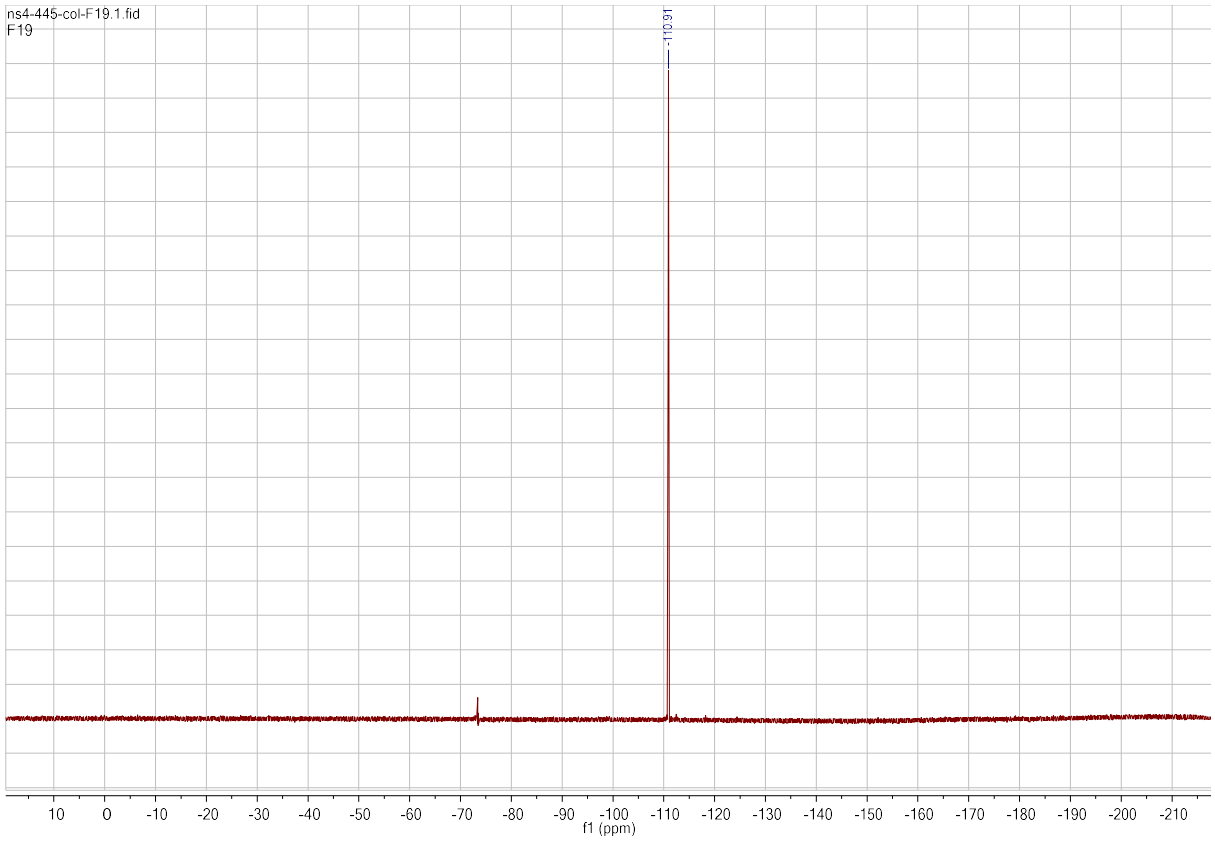
ns4-445-col-F19.1.fid
F19
-110.91
10 0 -10 -20 -30 -40 -50 -60 -70 -80 -90 -100 -110 -120 -130 -140 -150 -160 -170 -180 -190 -200 -210
f1 (ppm)

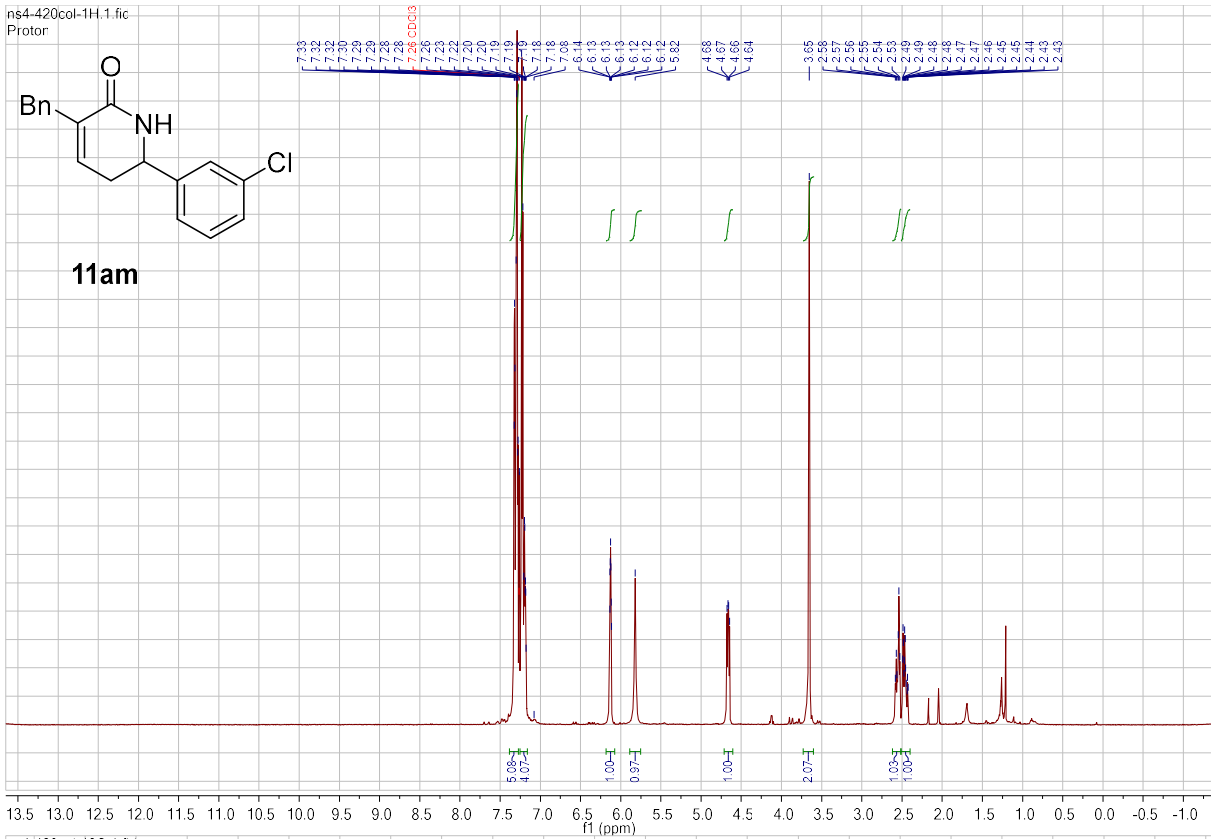
ns4-420col-1H.1.fic
Protor
O
Bn
NH
Cl
11am
f1 (ppm)

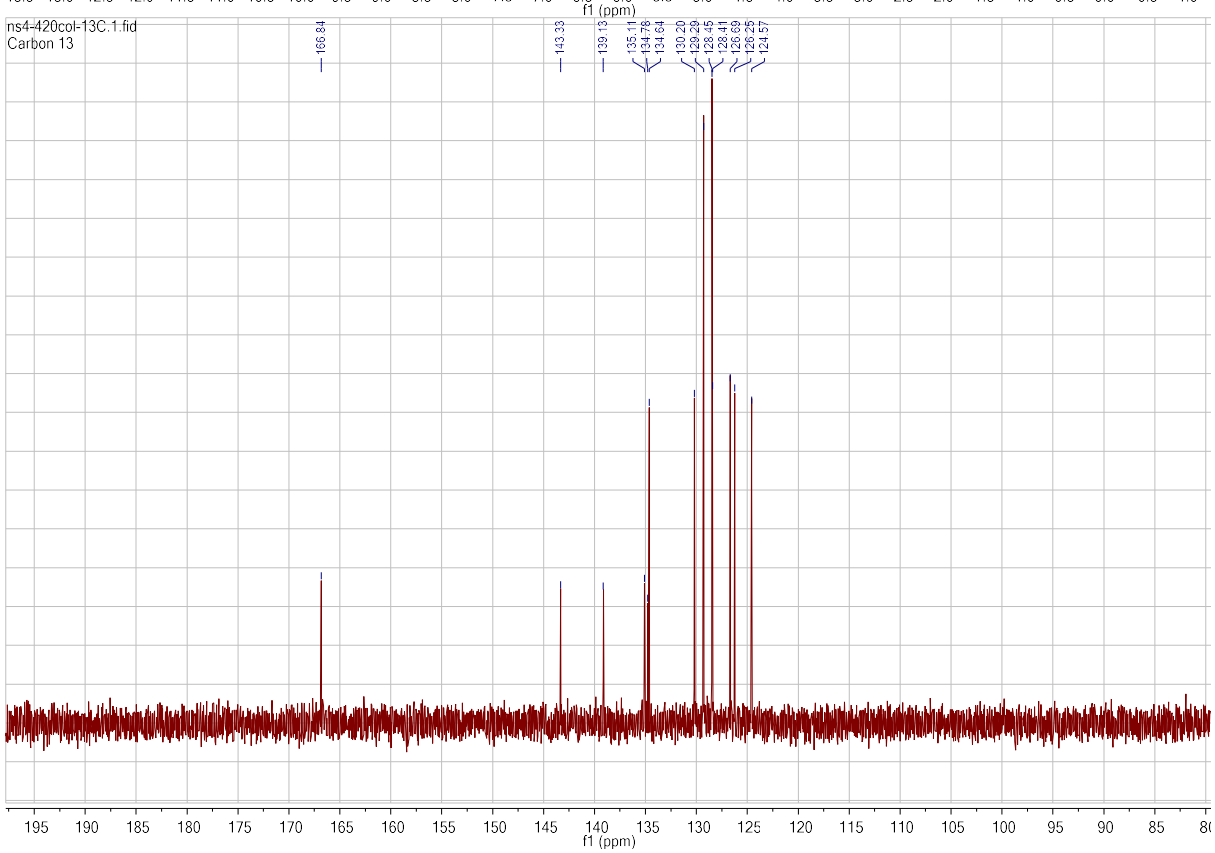
ns4-420col-13C.1.fid
Carbon 13
f1 (ppm)

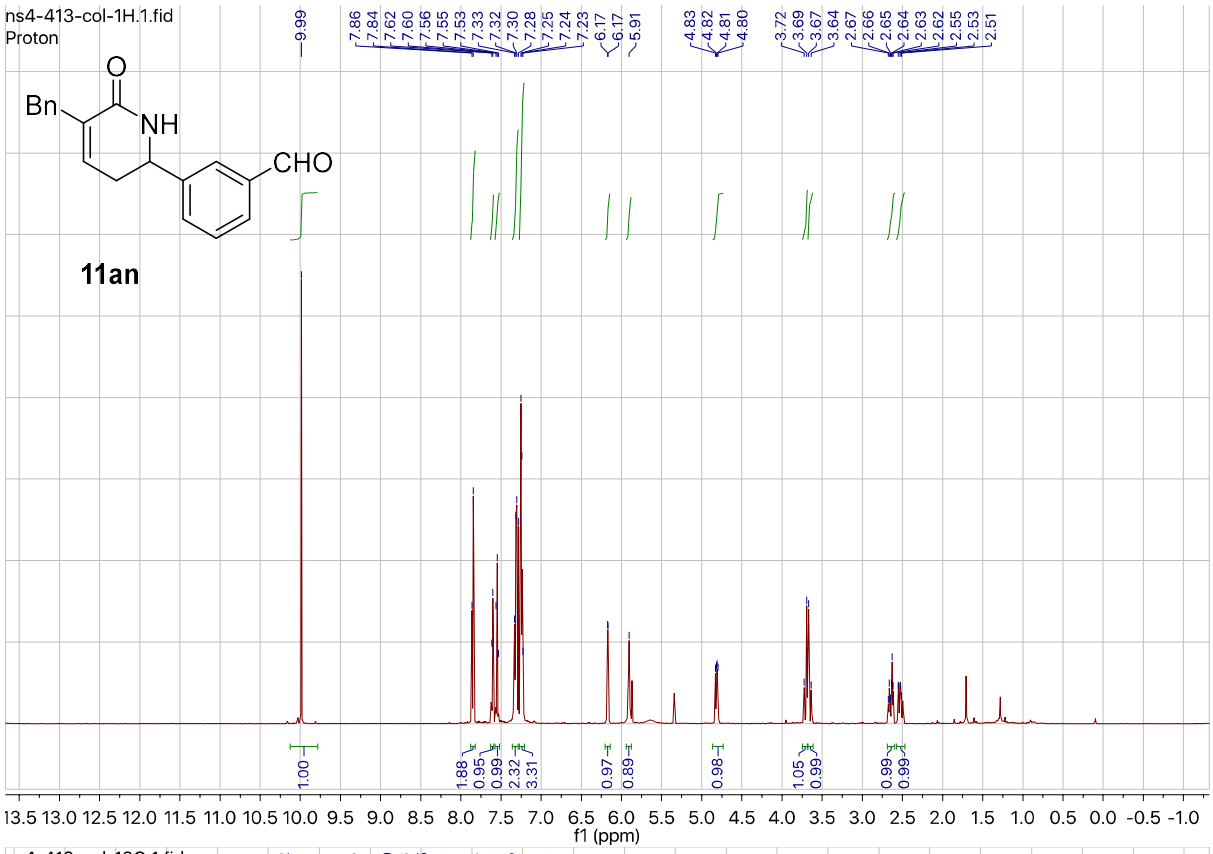
ns4-413-col-1H.1.fid
Proton
Bn
NH
O
CHO
11an
f1 (ppm)

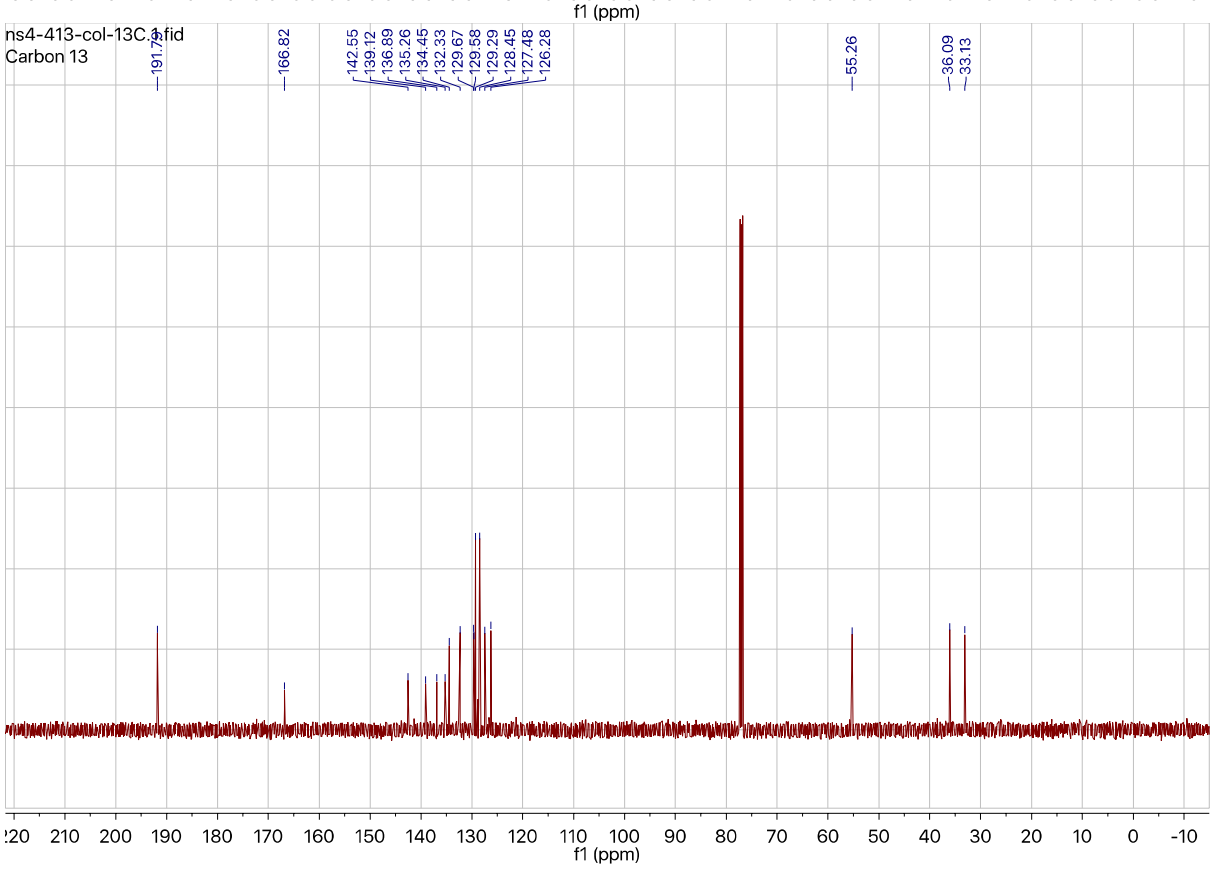
ns4-413-col-13C.1.fid
Carbon 13
f1 (ppm)

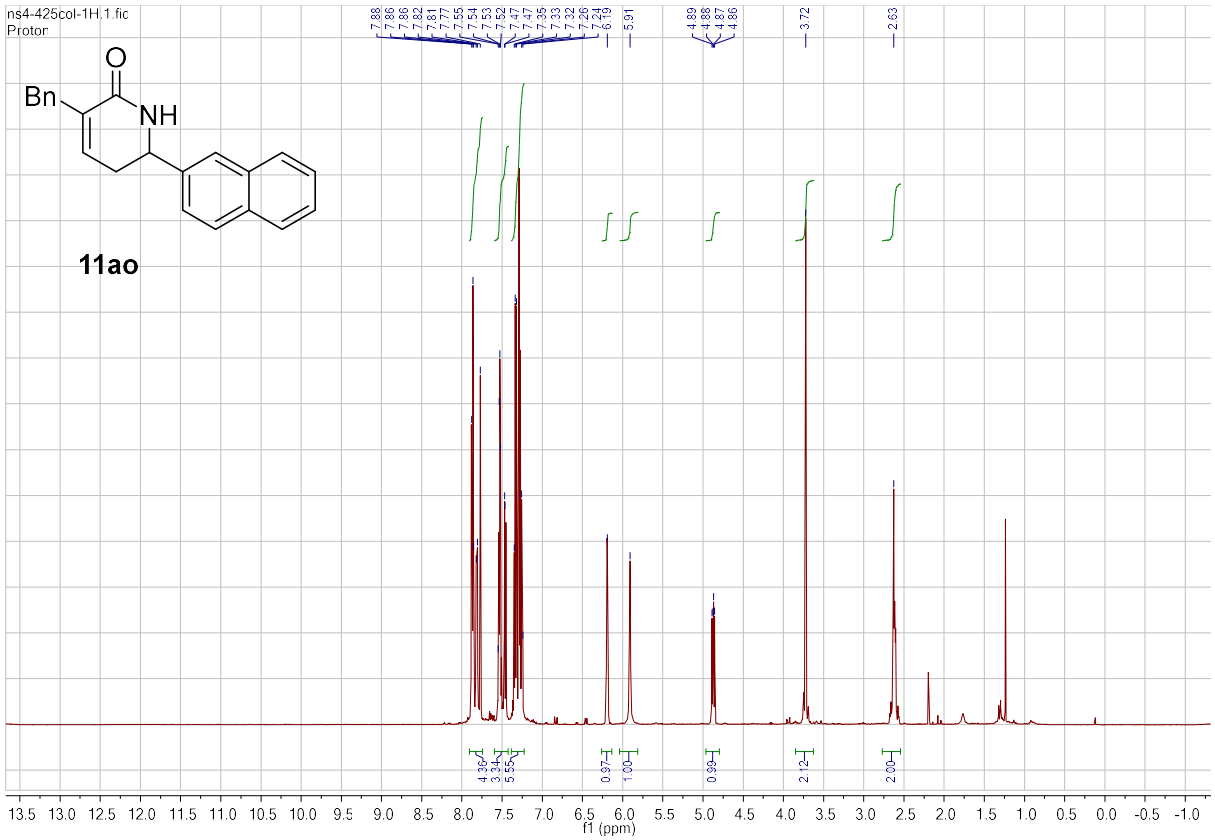
ns4-425col-1H.1.fic
Protor
Bn
NH
O
11ao
7.88
7.86
7.86
7.82
7.81
7.77
7.55
7.54
7.53
7.52
7.47
7.47
7.36
7.33
7.32
7.26
7.24
6.19
5.91
4.89
4.88
4.87
4.86
3.72
2.63
4.36
3.34
5.55
0.97
1.00
0.99
2.12
2.00
13.5 13.0 12.5 12.0 11.5 11.0 10.5 10.0 9.5 9.0 8.5 8.0 7.5 7.0 6.5 6.0 5.5 5.0 4.5 4.0 3.5 3.0 2.5 2.0 1.5 1.0 0.5 0.0 -0.5 -1.0
f1 (ppm)

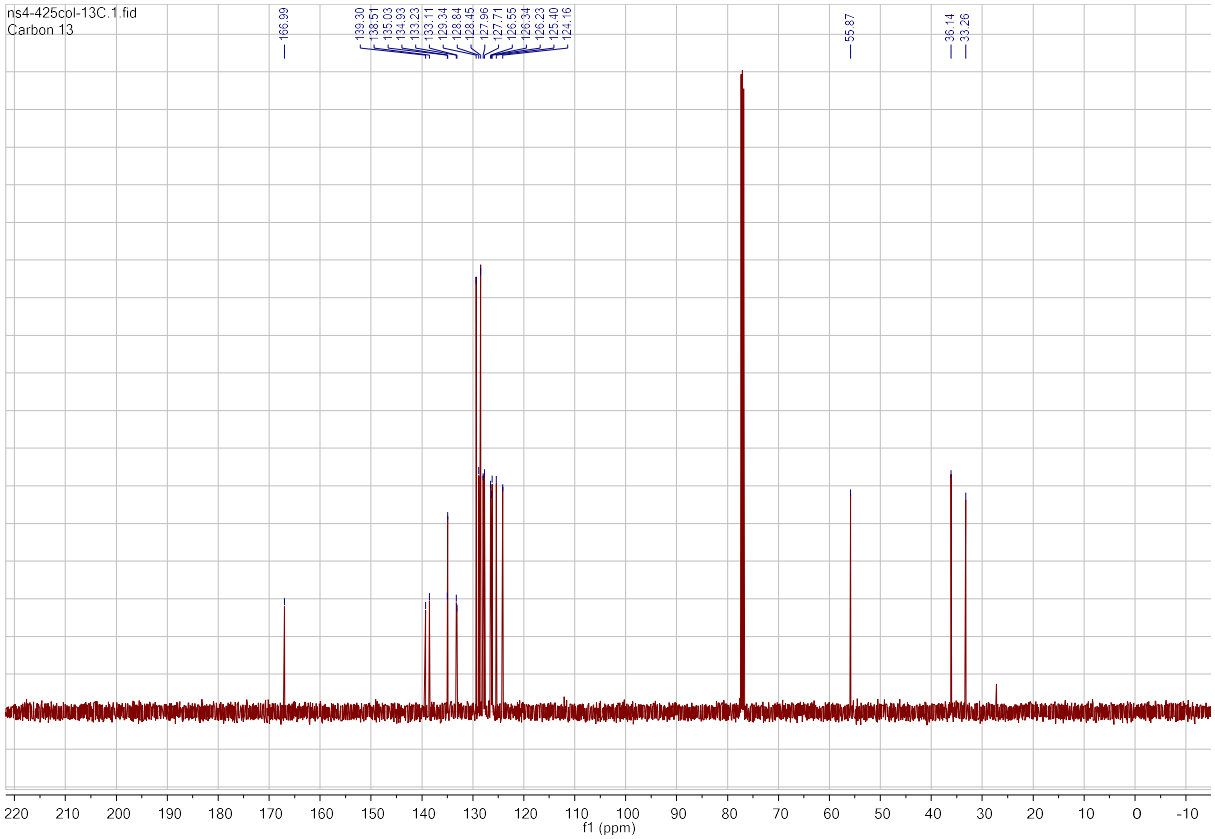
ns4-425col-13C.1.fid
Carbon.13
168.99
139.30
138.51
135.03
134.93
133.23
133.11
129.34
128.84
128.45
127.96
127.71
126.55
126.34
126.23
125.40
124.16
55.87
36.14
33.26
220 210 200 190 180 170 160 150 140 130 120 110 100 90 80 70 60 50 40 30 20 10 0 -10
f1 (ppm)

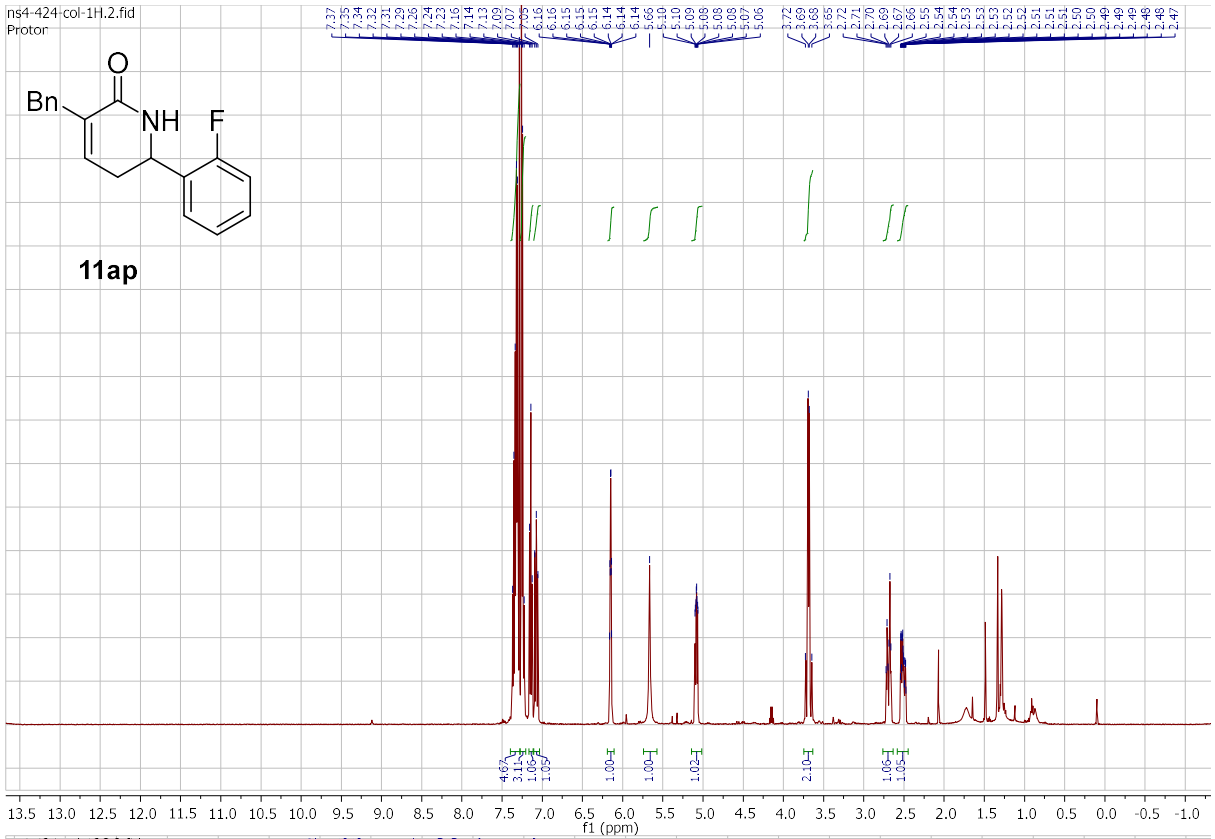
ns4-424-col-1H.2.fid
Proton
O
Bn
NH
F
11ap
f1 (ppm)

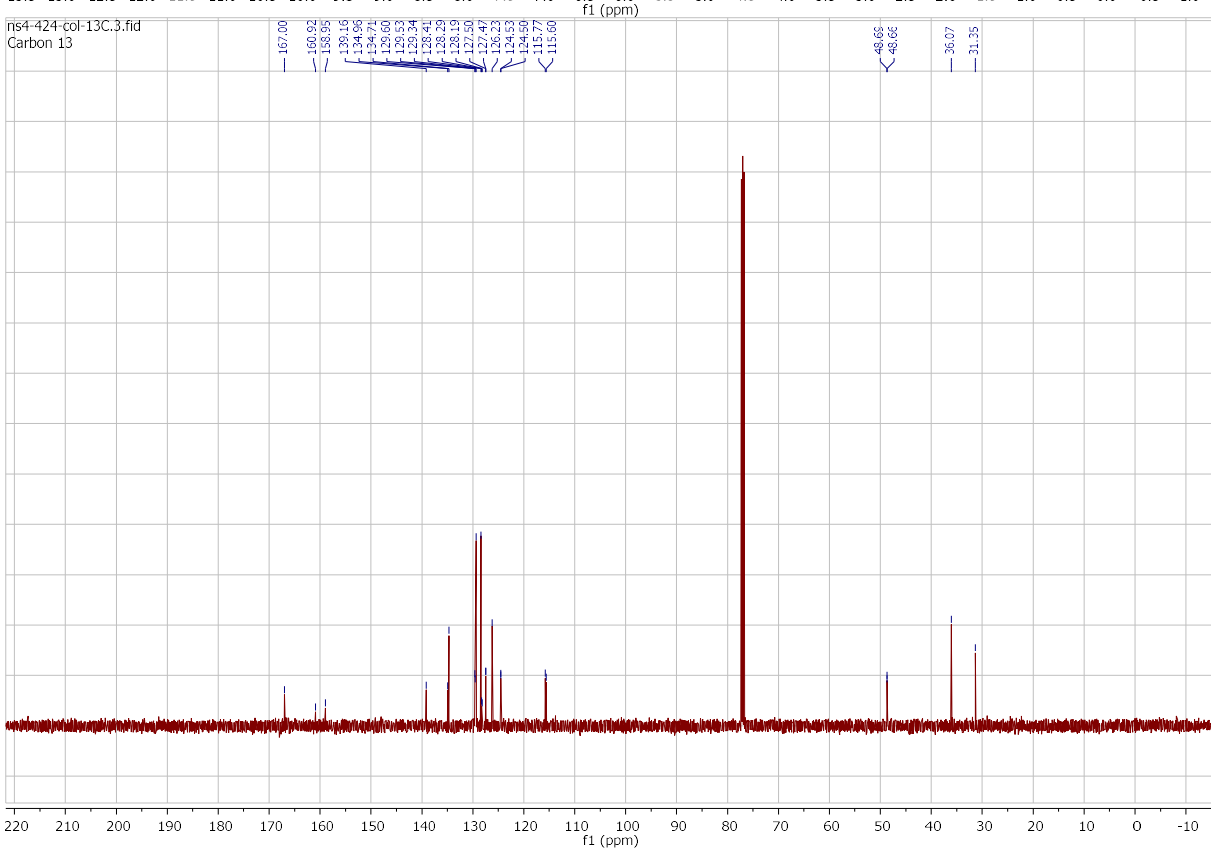
ns4-424-col-13C.3.fid
Carbon 13
f1 (ppm)

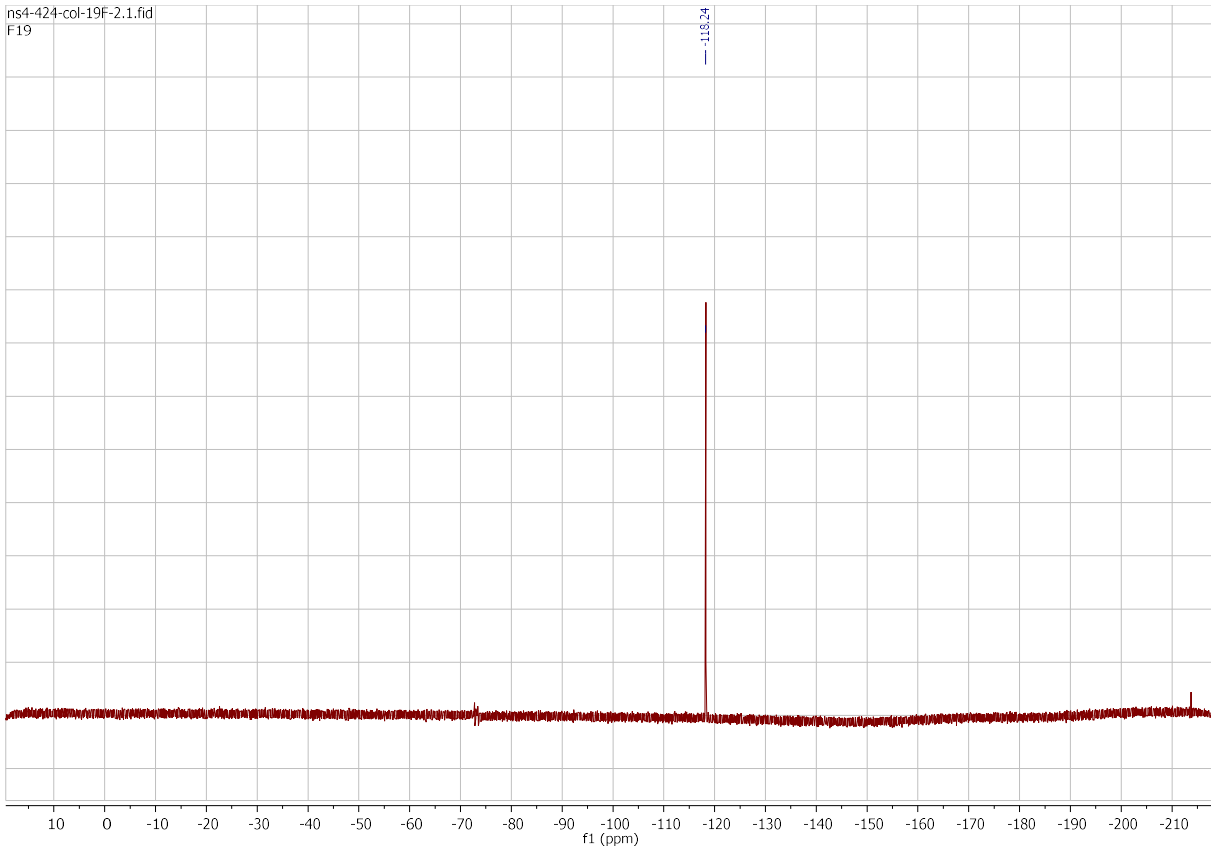
ns4-424-col-19F-2.1.fid
F19
-118.24
10
0
-10
-20
-30
-40
-50
-60
-70
-80
-90
-100
-110
-120
-130
-140
-150
-160
-170
-180
-190
-200
-210
f1 (ppm)

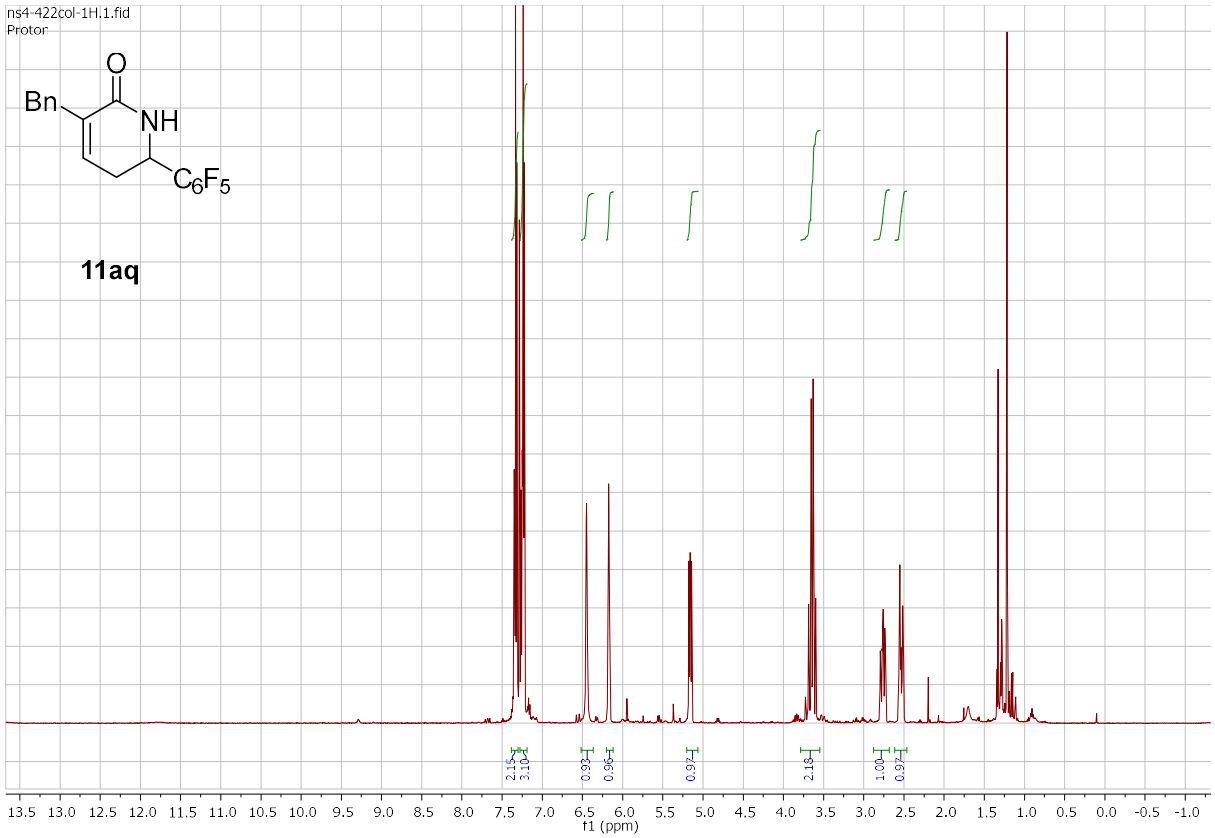
ns4-422col-1H.1.fid
Protor
O
Bn
NH
C6F5
11aq
2.15
3.10
0.93
0.96
0.97
2.16
1.00
0.97
13.5 13.0 12.5 12.0 11.5 11.0 10.5 10.0 9.5 9.0 8.5 8.0 7.5 7.0 6.5 6.0 5.5 5.0 4.5 4.0 3.5 3.0 2.5 2.0 1.5 1.0 0.5 0.0 -0.5 -1.0
f1 (ppm)

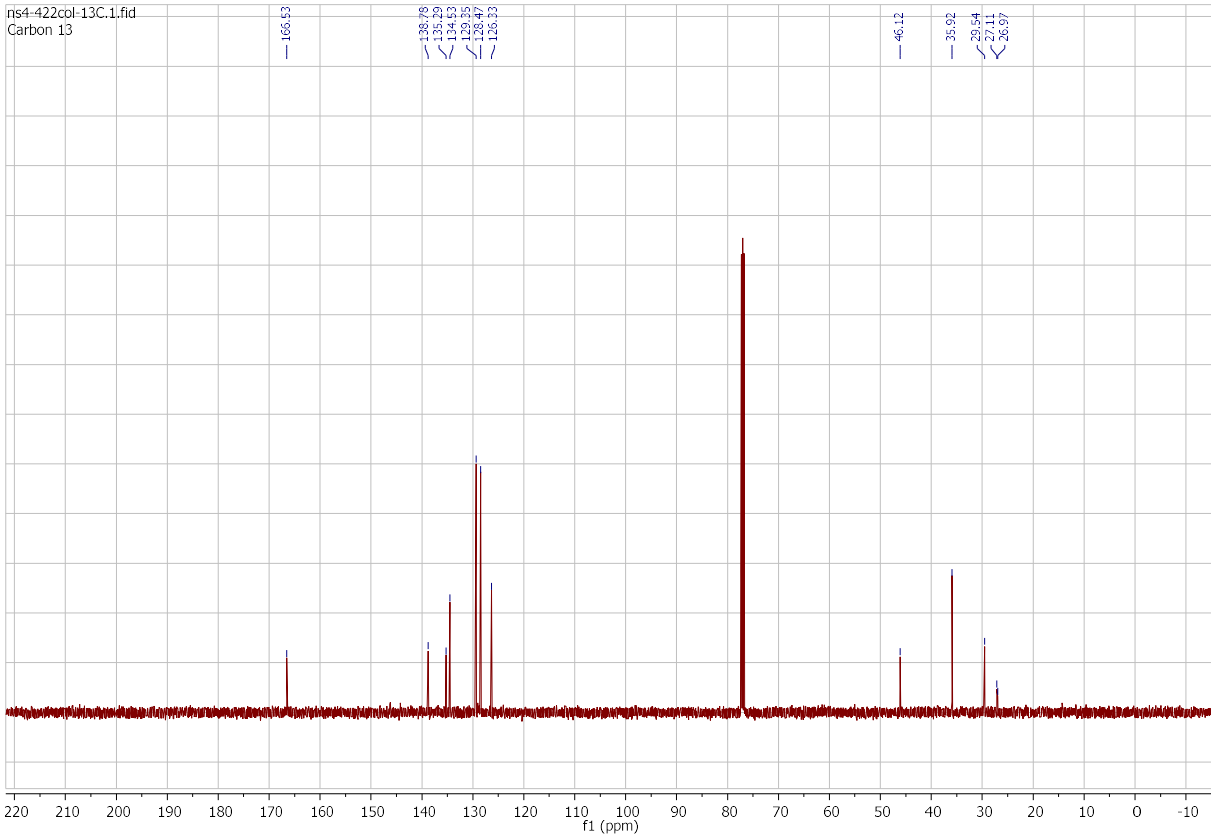
ns4-422col-13C.1.fid
Carbon 13
166.53
138.78
135.29
134.53
129.35
128.47
126.33
46.12
35.92
29.54
27.11
26.97
220 210 200 190 180 170 160 150 140 130 120 110 100 90 80 70 60 50 40 30 20 10 0 -10
f1 (ppm)

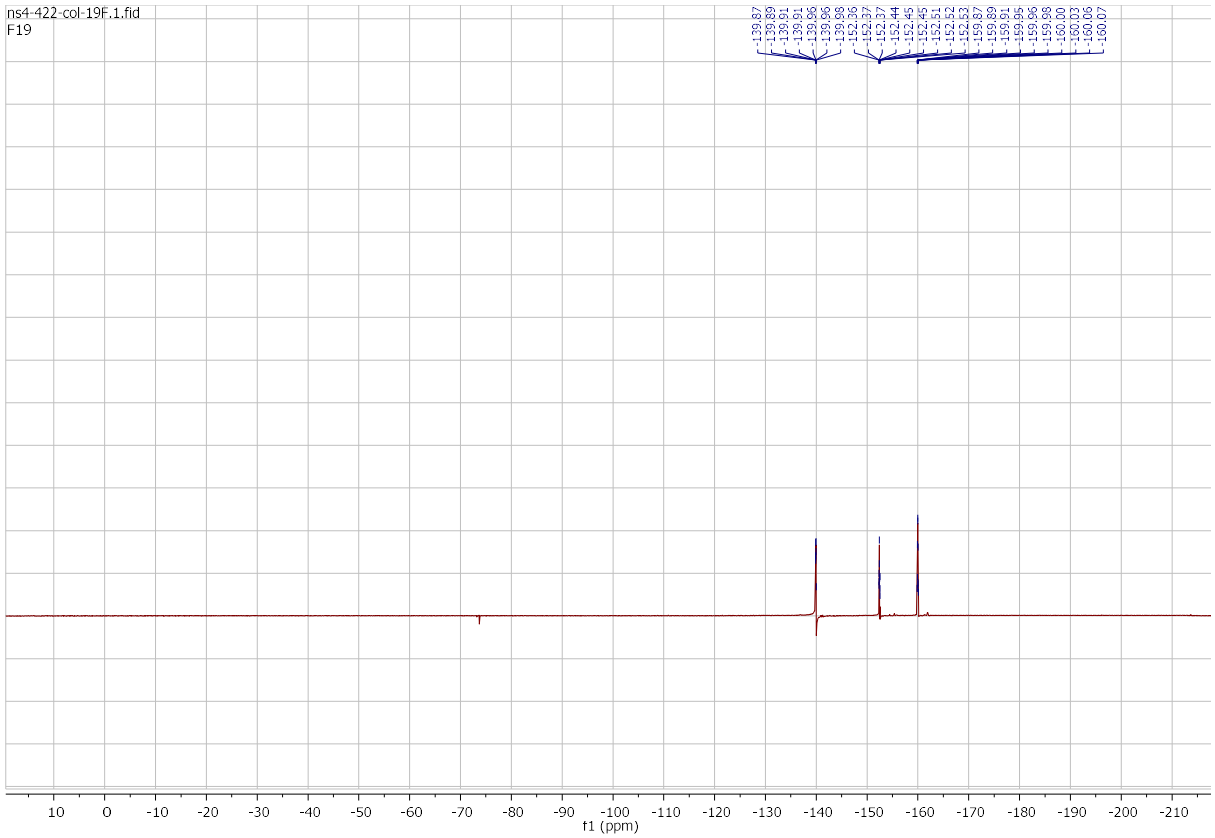
ns4-422-col-19F.1.fid
F19
-139.87
-139.89
-139.91
-139.91
-139.96
-139.96
-139.98
-152.36
-152.37
-152.37
-152.44
-152.45
-152.45
-152.51
-152.52
-152.53
-159.87
-159.89
-159.91
-159.95
-159.96
-159.98
-160.00
-160.03
-160.06
-160.07
10 0 -10 -20 -30 -40 -50 -60 -70 -80 -90 -100 -110 -120 -130 -140 -150 -160 -170 -180 -190 -200 -210
f1 (ppm)

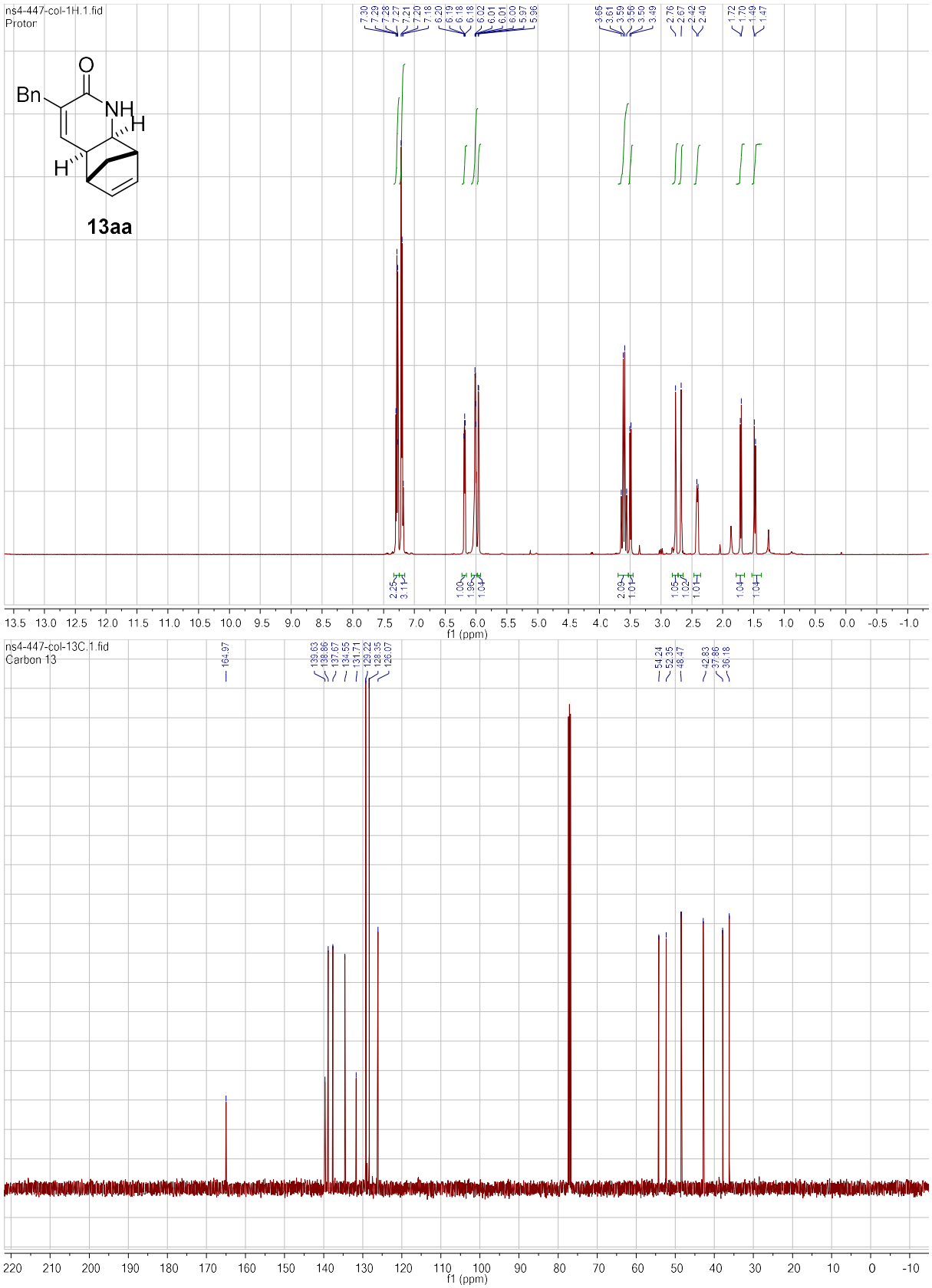
ns4-447-col-1H.1.fid
Protor
Bn
NH
H
H
O
13aa
f1 (ppm)
ns4-447-col-13C.1.fid
Carbon 13
f1 (ppm)

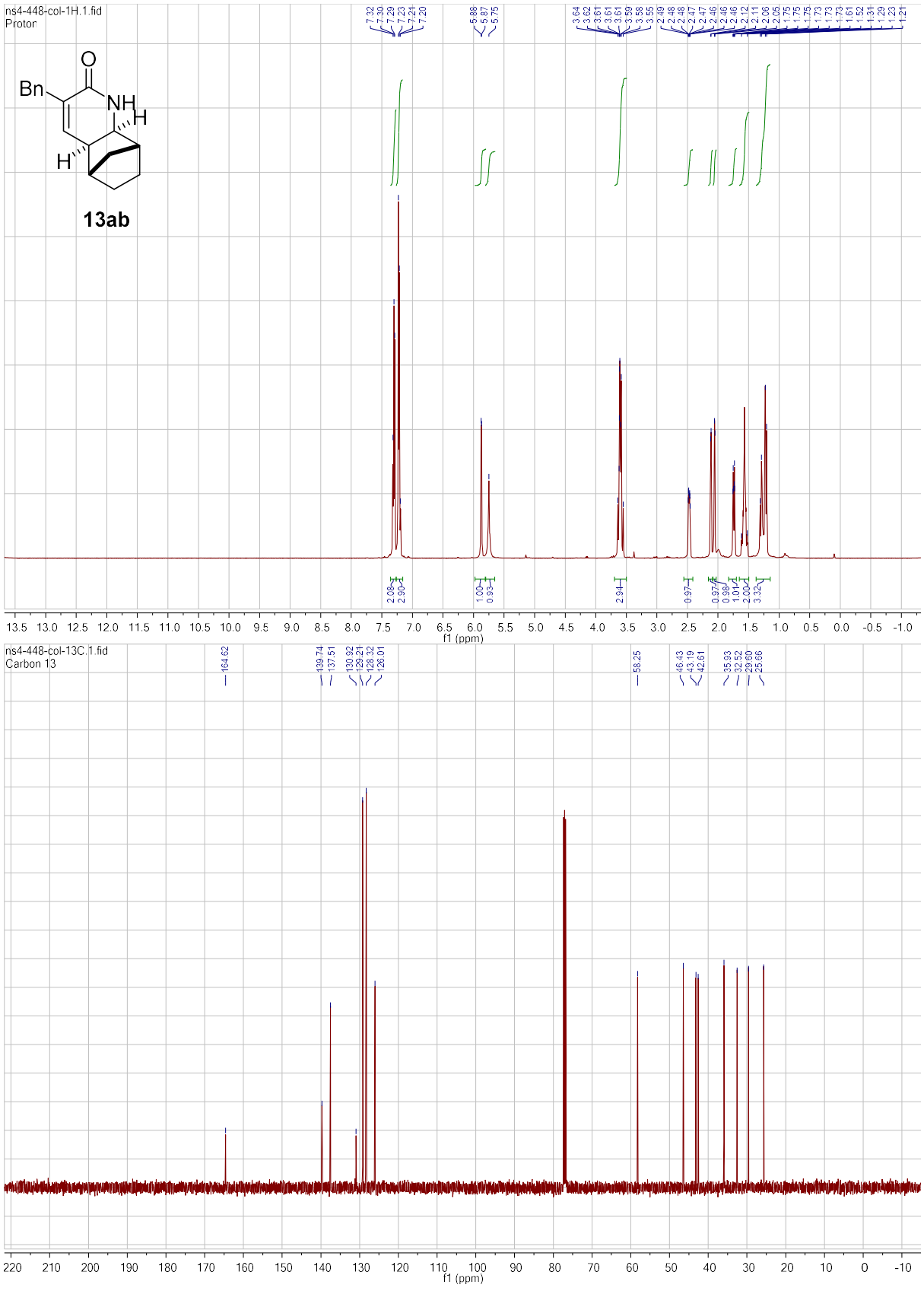
ns4-448-col-1H.1.fid
Protor
Bn
NH
H
H
O
13ab
f1 (ppm)
ns4-448-col-13C.1.fid
Carbon 13
f1 (ppm)

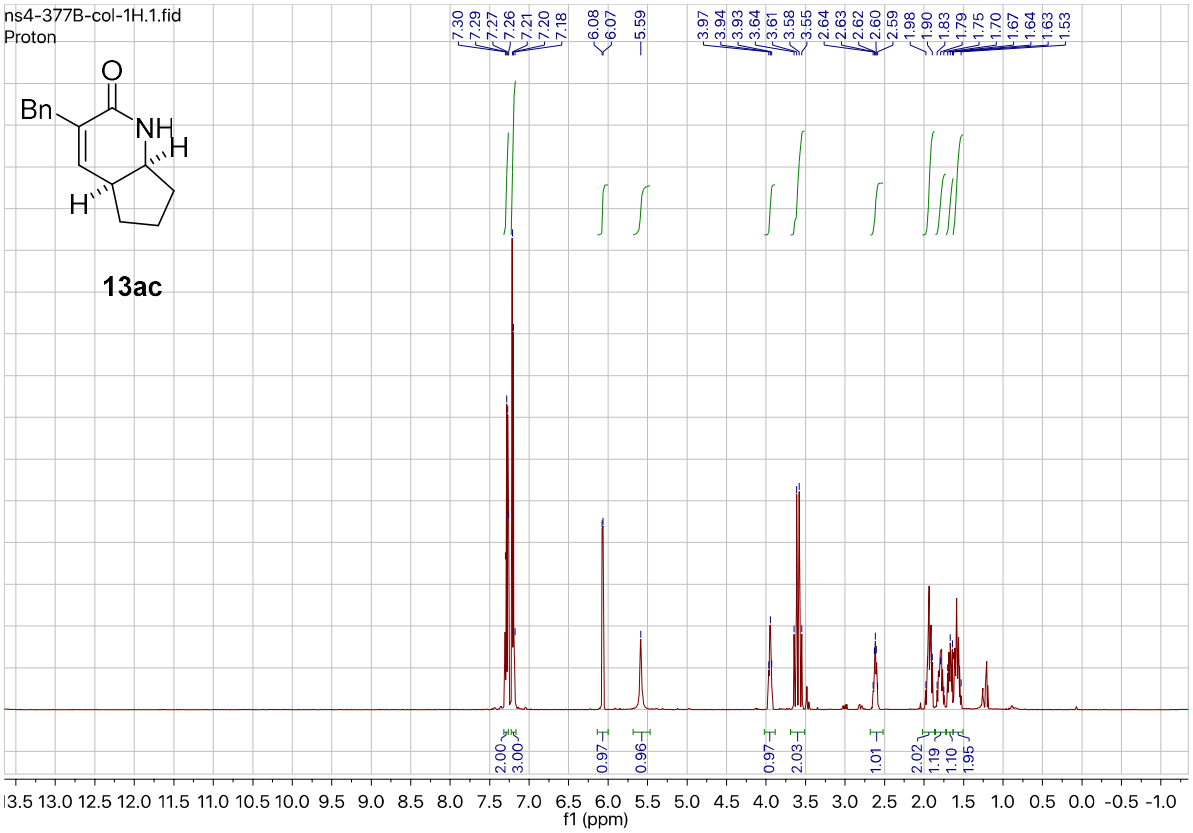
ns4-377B-col-1H.1.fid
Proton
Bn
O
NH
H
H
13ac
7.30 7.29 7.27 7.26 7.21 7.20 7.18
6.08 6.07
5.59
3.97 3.94 3.93 3.64 3.61 3.58 3.55
2.64 2.63 2.62 2.60 2.59
1.98 1.90 1.83 1.79 1.75 1.70 1.67 1.64 1.63 1.53
2.00 3.00 0.97 0.96 0.97 2.03 1.01 2.02 1.19 1.10 1.95
f1 (ppm)

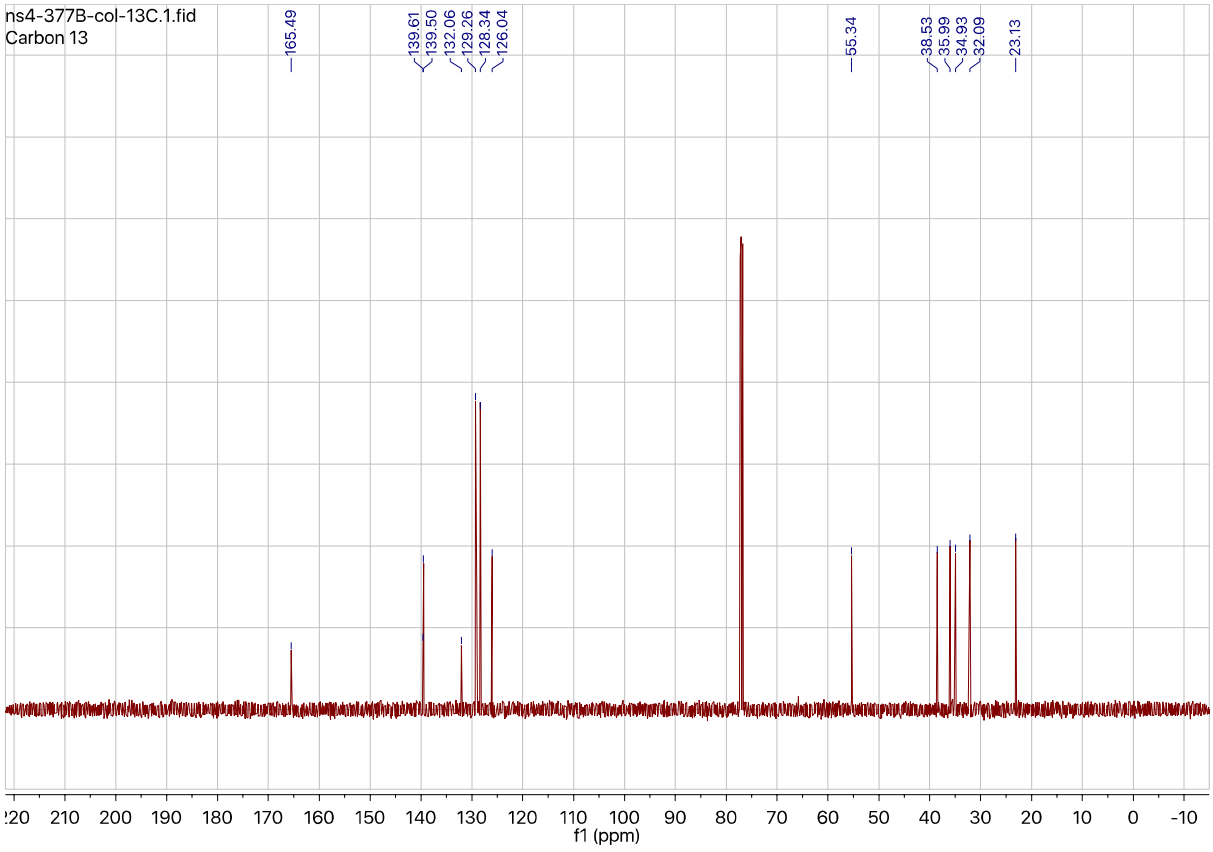
ns4-377B-col-13C.1.fid
Carbon 13
165.49
139.61 139.50 132.06 129.26 128.34 126.04
55.34
38.53 35.99 34.93 32.09
23.13
f1 (ppm)

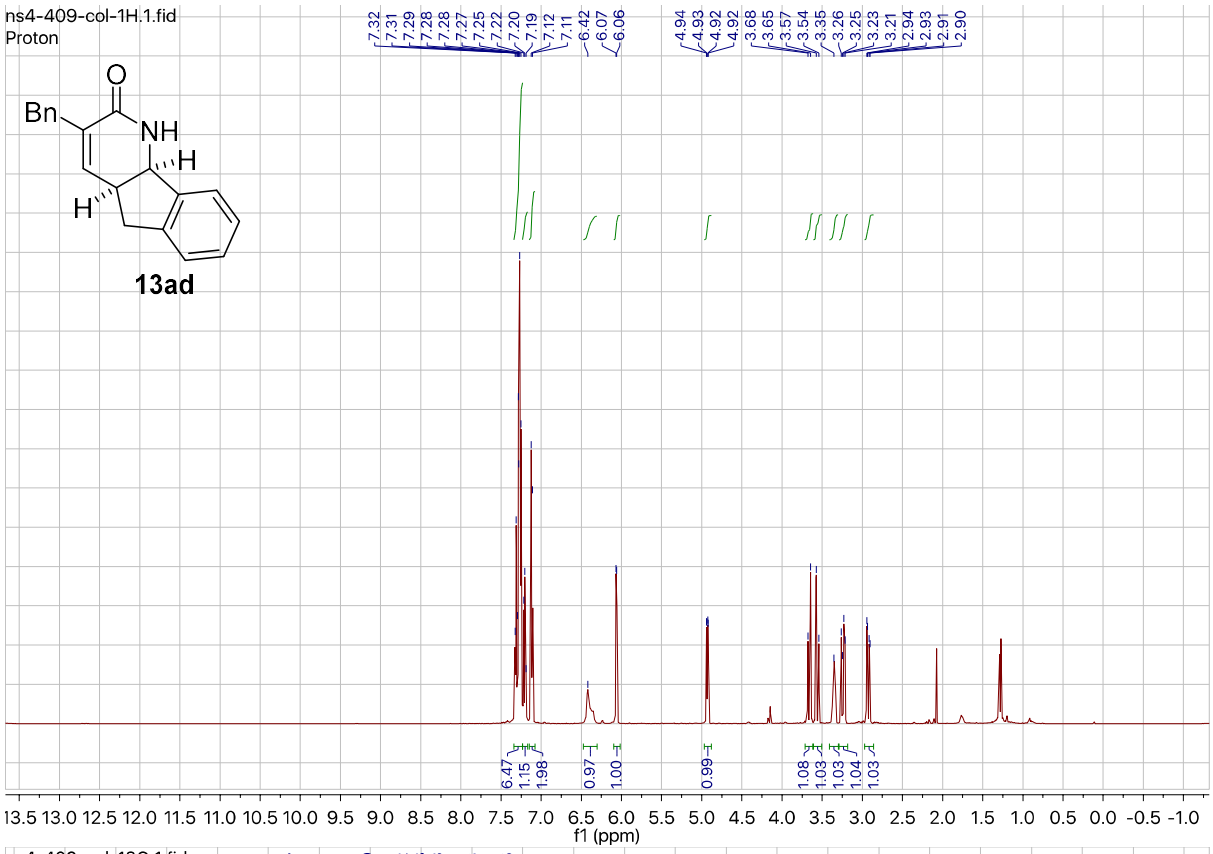
ns4-409-col-1H.1.fid
Proton
Bn
NH
H
H
O
13ad
7.32
7.31
7.29
7.28
7.28
7.27
7.25
7.22
7.20
7.19
7.12
7.11
6.42
6.07
6.06
4.94
4.93
4.92
4.92
3.68
3.65
3.57
3.54
3.35
3.26
3.25
3.23
3.21
2.94
2.93
2.91
2.90
6.47
1.15
1.98
0.97
1.00
0.99
1.08
1.03
1.03
1.04
1.03
f1 (ppm)

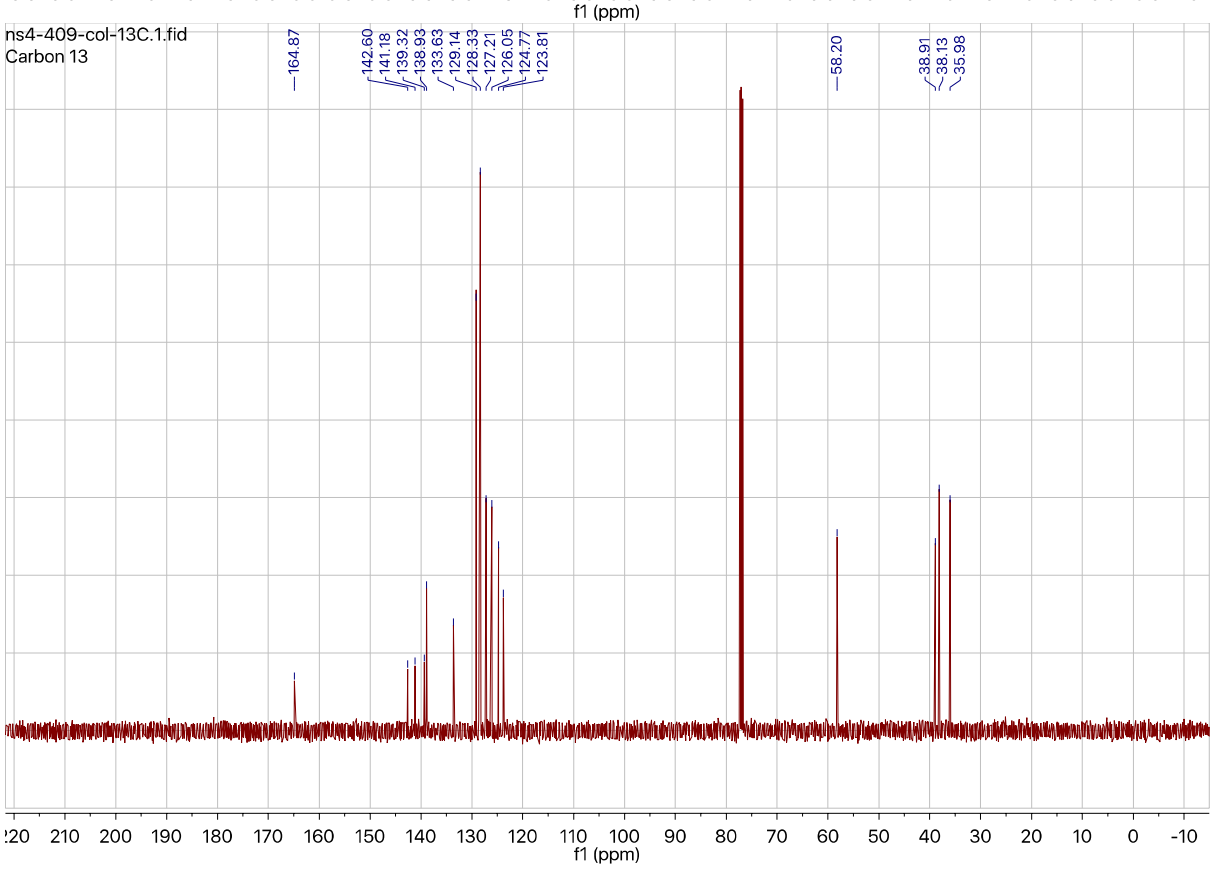
ns4-409-col-13C.1.fid
Carbon 13
164.87
142.60
141.18
139.32
138.93
133.63
129.14
128.33
127.21
126.05
124.77
123.81
58.20
38.91
38.13
35.98
f1 (ppm)

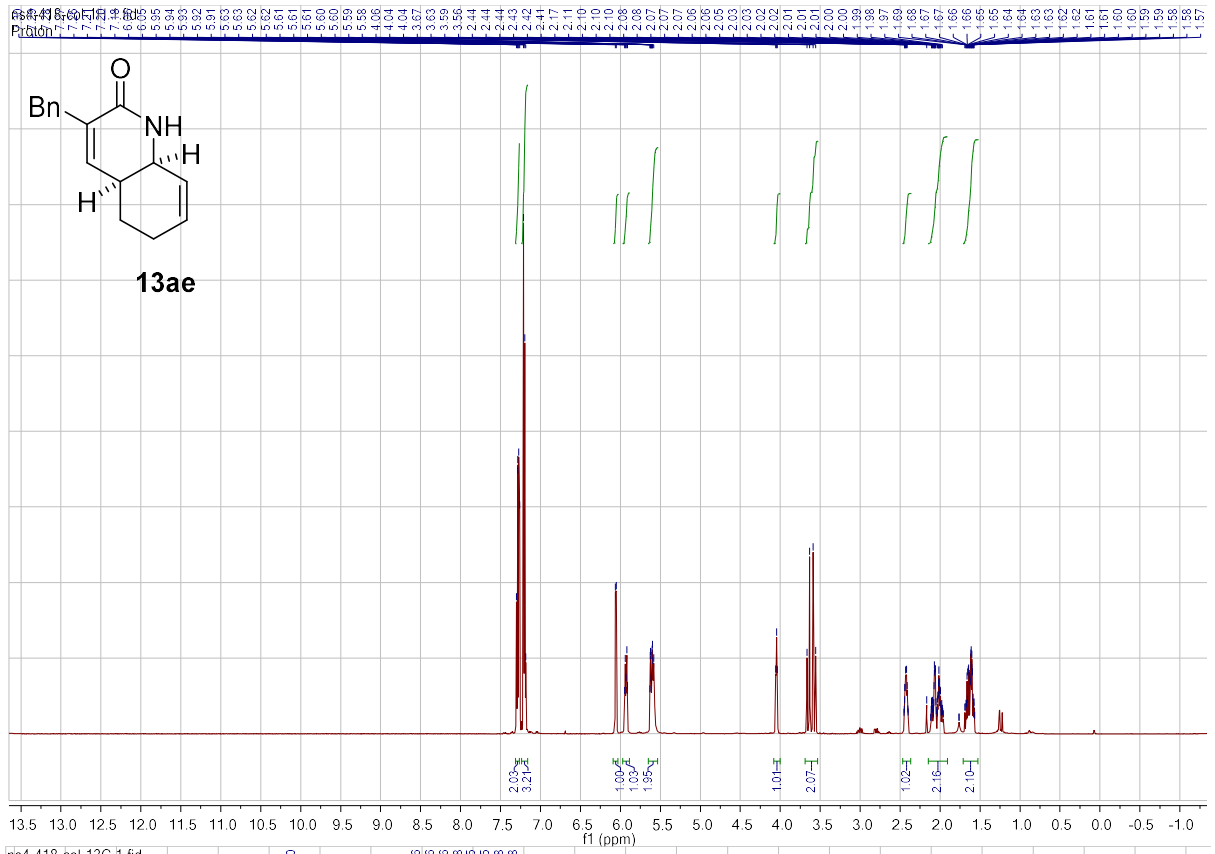
Bn
NH
H
H
O
13ae
f1 (ppm)

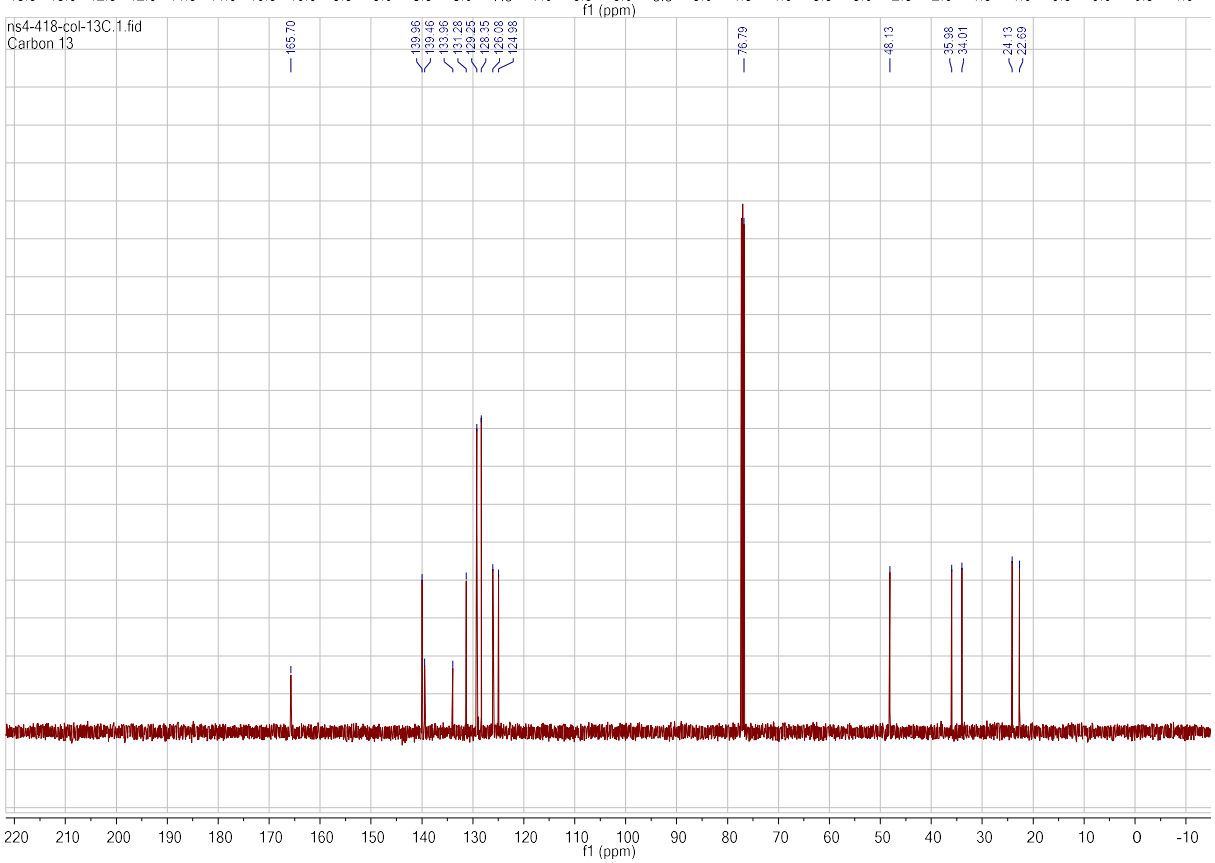
ns4-418-col-13C.1.fid
Carbon 13
165.70
139.96
139.46
133.96
131.28
129.25
128.35
126.08
124.98
76.79
48.13
35.98
34.01
24.13
22.69
f1 (ppm)

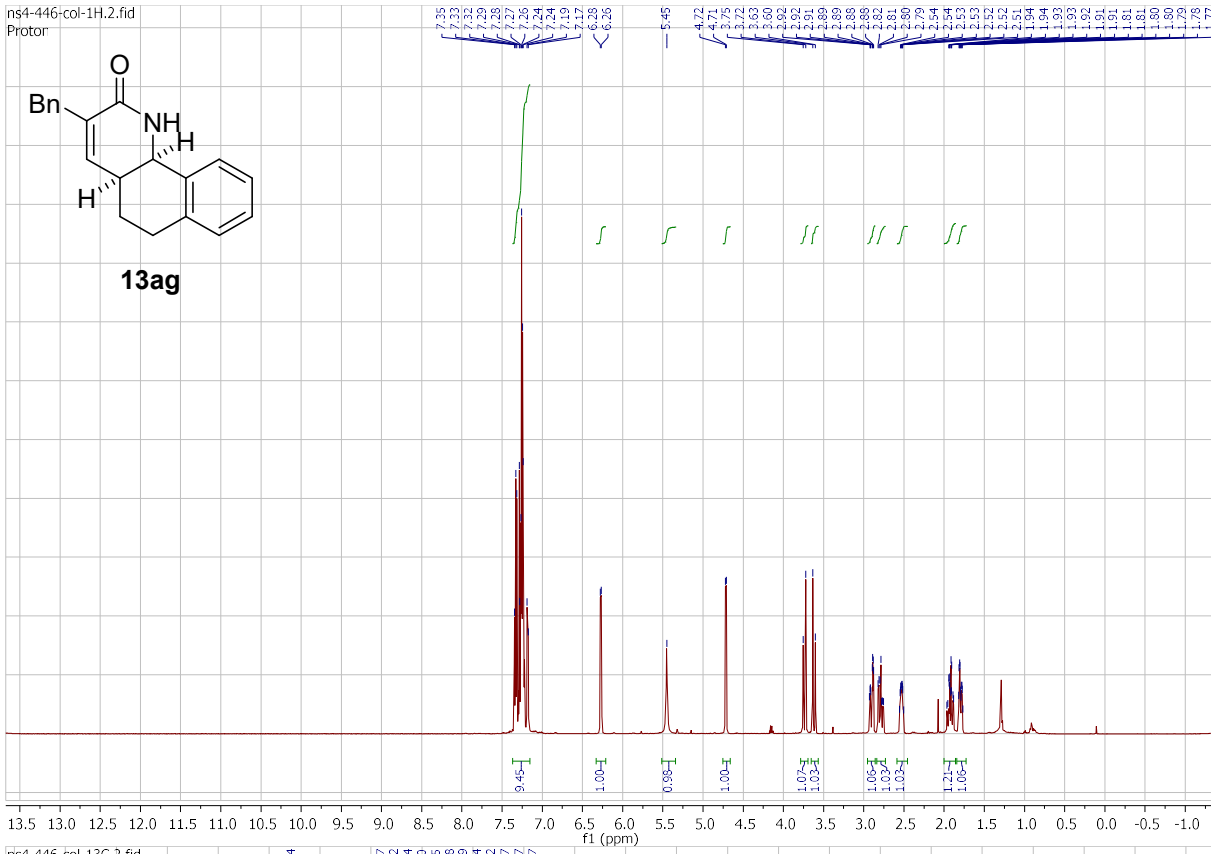
ns4-446-col-1H.2.fid
Protor
O
Bn
NH
H
H
13ag
f1 (ppm)

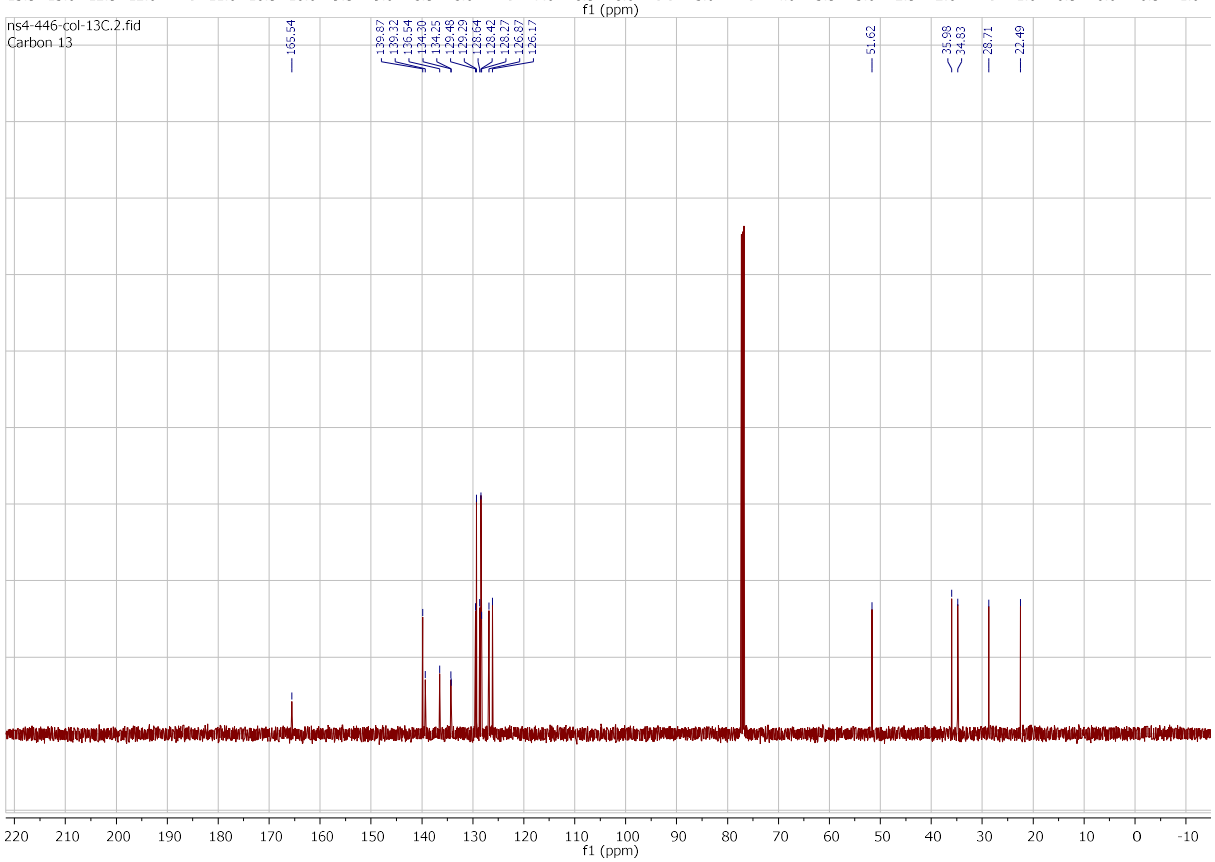
ns4-446-col-13C.2.fid
Carbon 13
f1 (ppm)

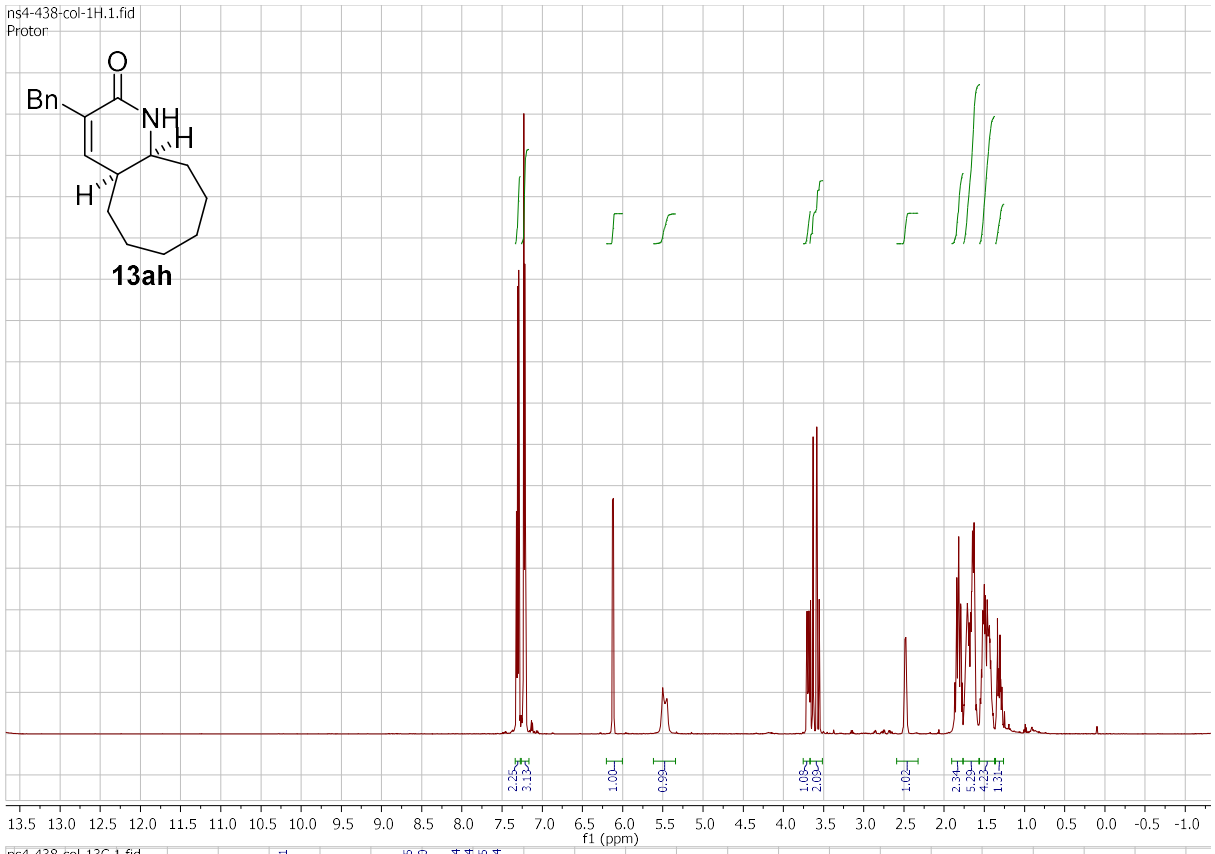
ns4-438-col-1H.1.fid
Proton
Bn
O
NH
H
H
13ah
2.25
3.13
1.00
0.99
1.08
2.09
1.02
2.34
5.29
4.22
1.31
13.5 13.0 12.5 12.0 11.5 11.0 10.5 10.0 9.5 9.0 8.5 8.0 7.5 7.0 6.5 6.0 5.5 5.0 4.5 4.0 3.5 3.0 2.5 2.0 1.5 1.0 0.5 0.0 -0.5 -1.0
f1 (ppm)

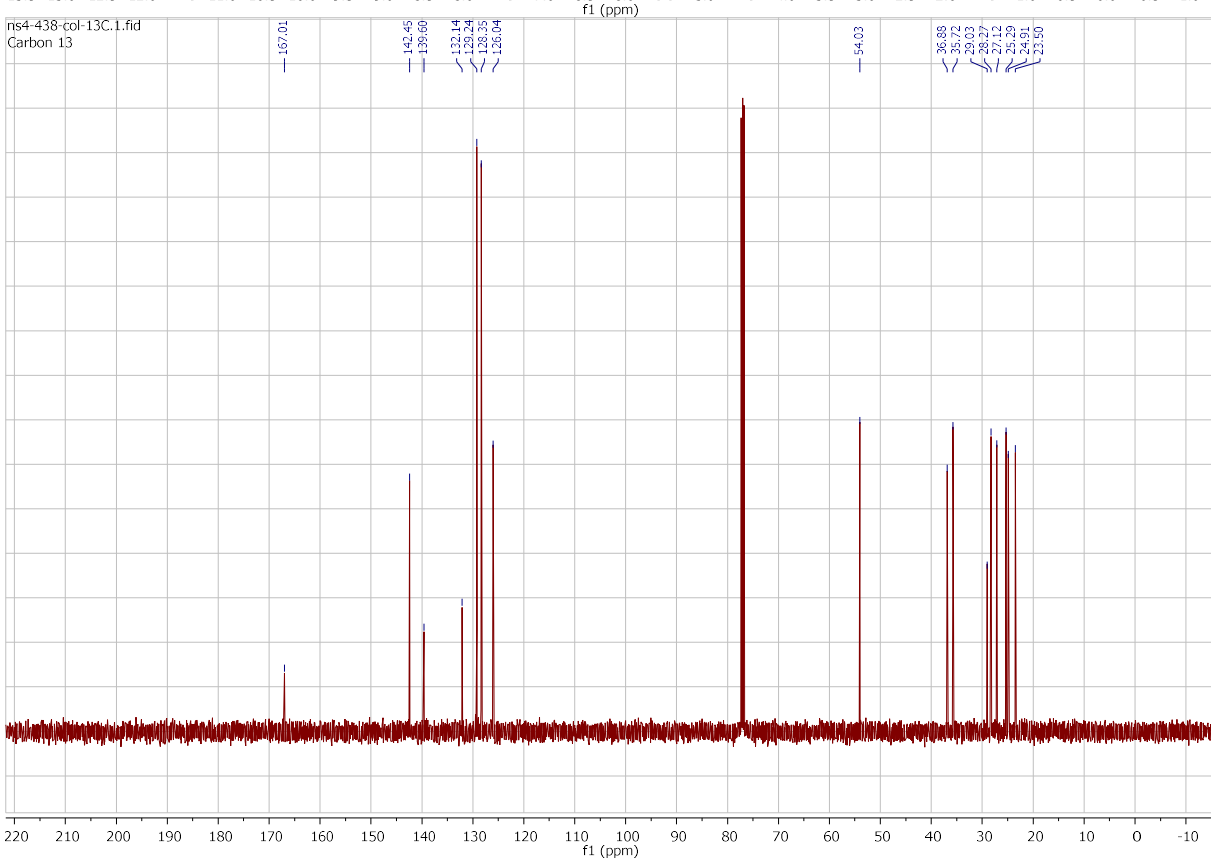
ns4-438-col-13C.1.fid
Carbon 13
167.01
142.45
139.66
132.14
129.24
128.35
126.04
54.03
36.88
35.72
29.03
28.27
27.12
25.29
24.91
23.50
220 210 200 190 180 170 160 150 140 130 120 110 100 90 80 70 60 50 40 30 20 10 0 -10
f1 (ppm)

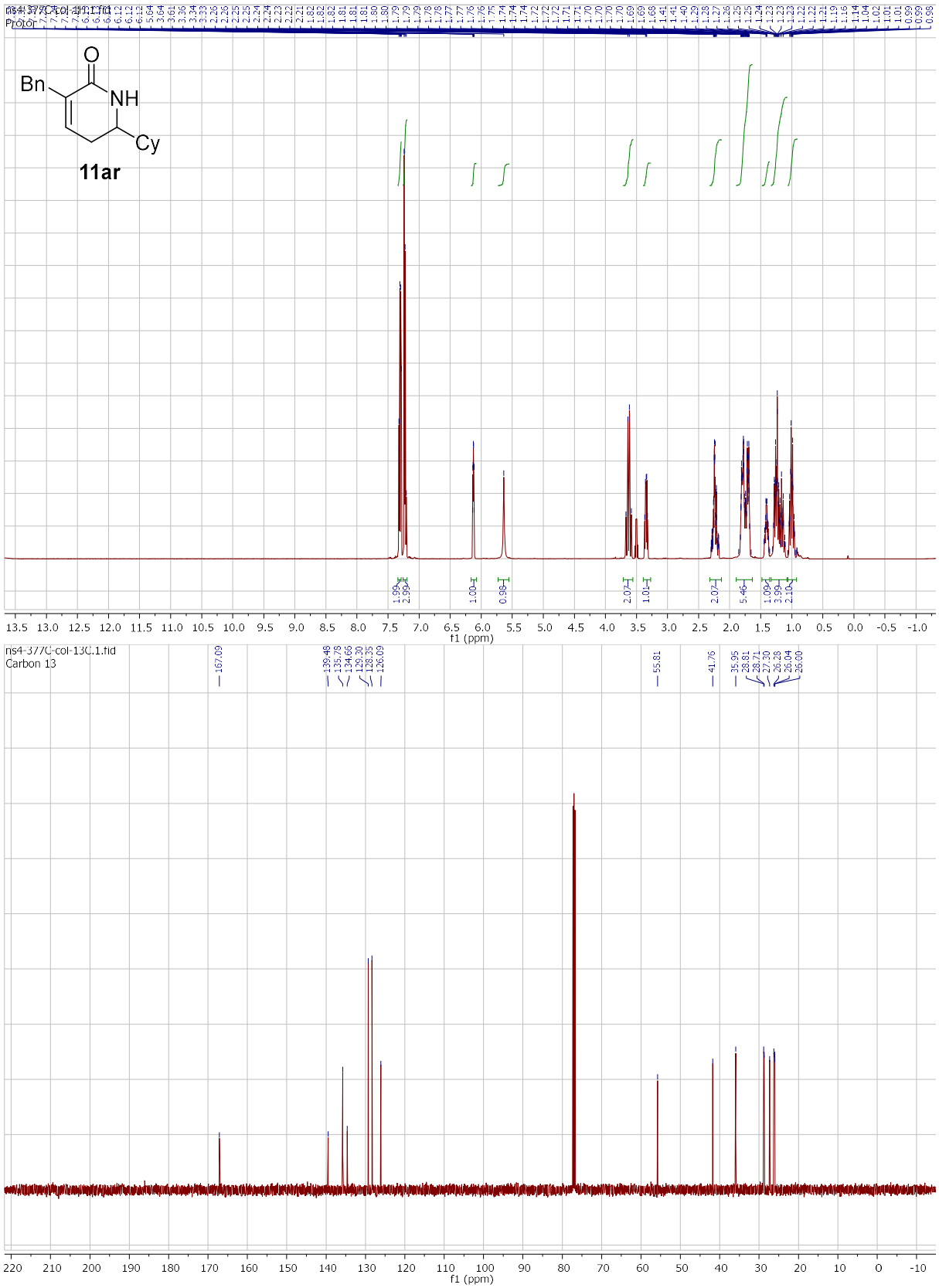
Bn
O
NH
Cy
11ar
f1 (ppm)
Carbon 13
f1 (ppm)

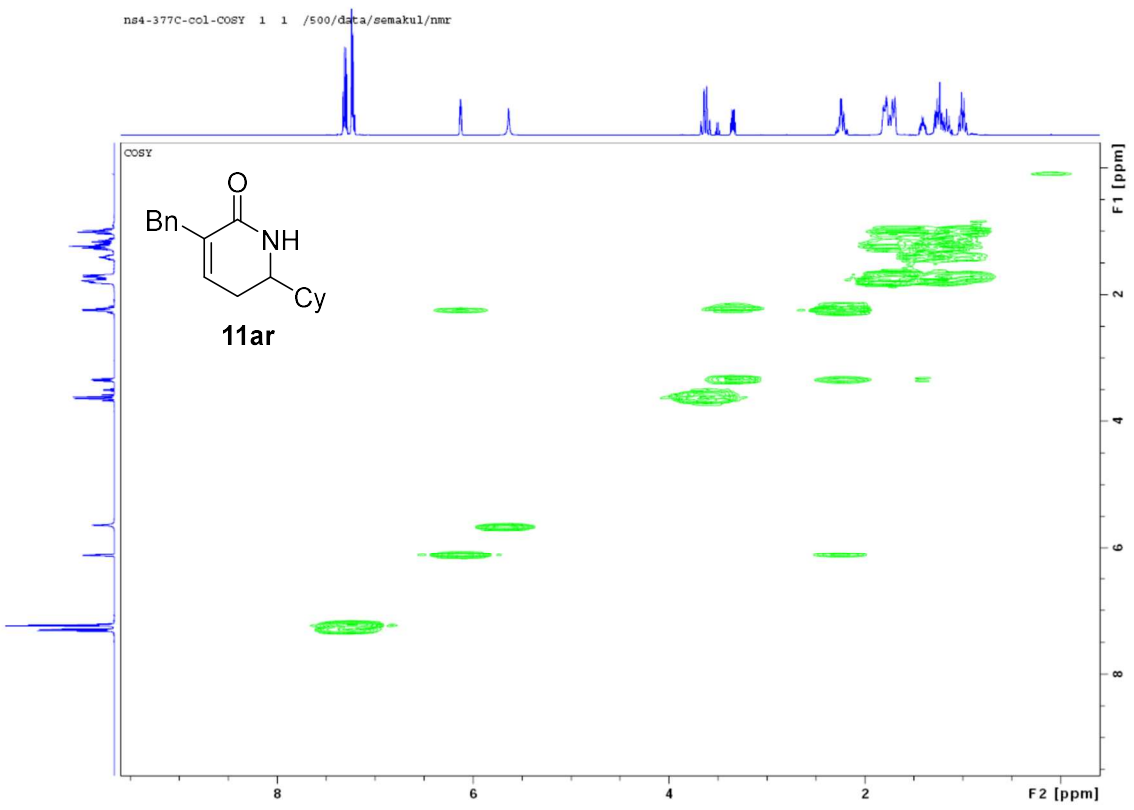
ns4-377C-col-COSY 1 1 /500/data/semakul/nmr
COSY
Bn
NH
Cy
11ar
F1 [ppm]
F2 [ppm]
2
4
6
8

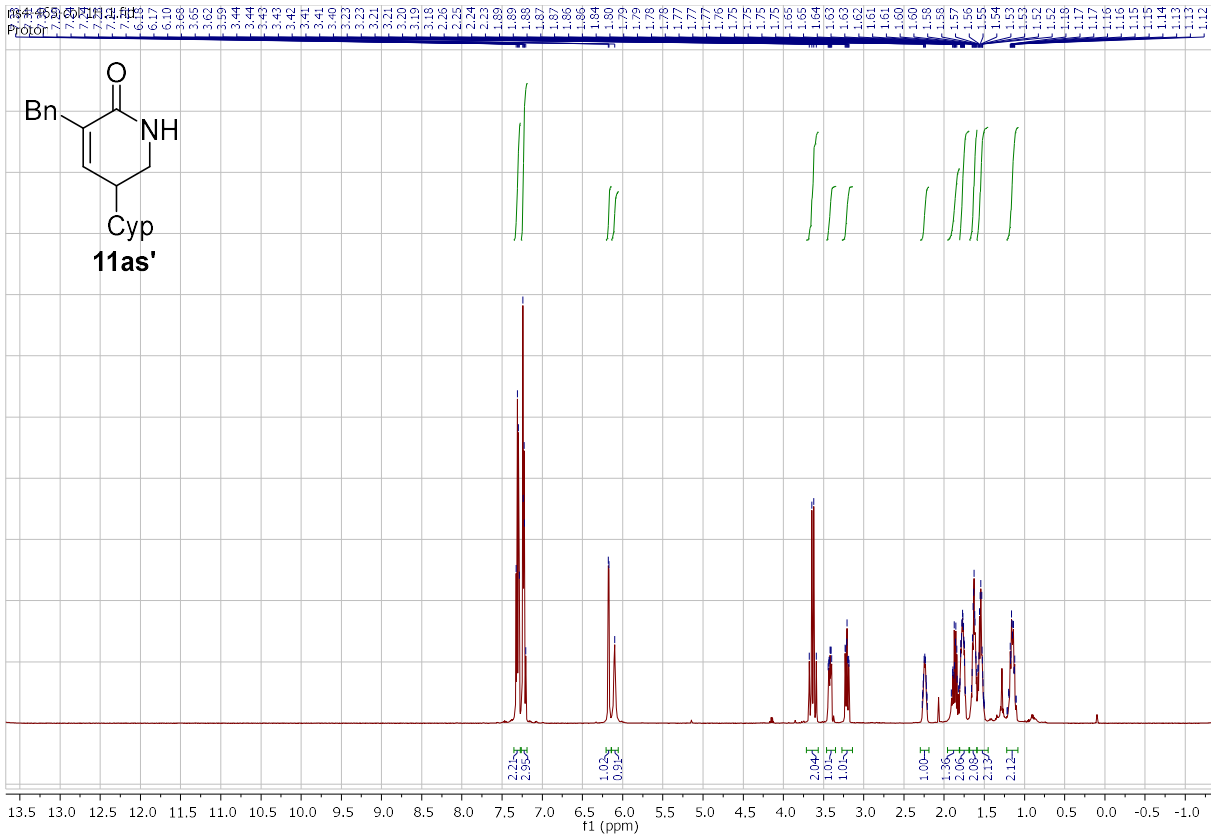
Bn
O
NH
Cyp
11as'
f1 (ppm)

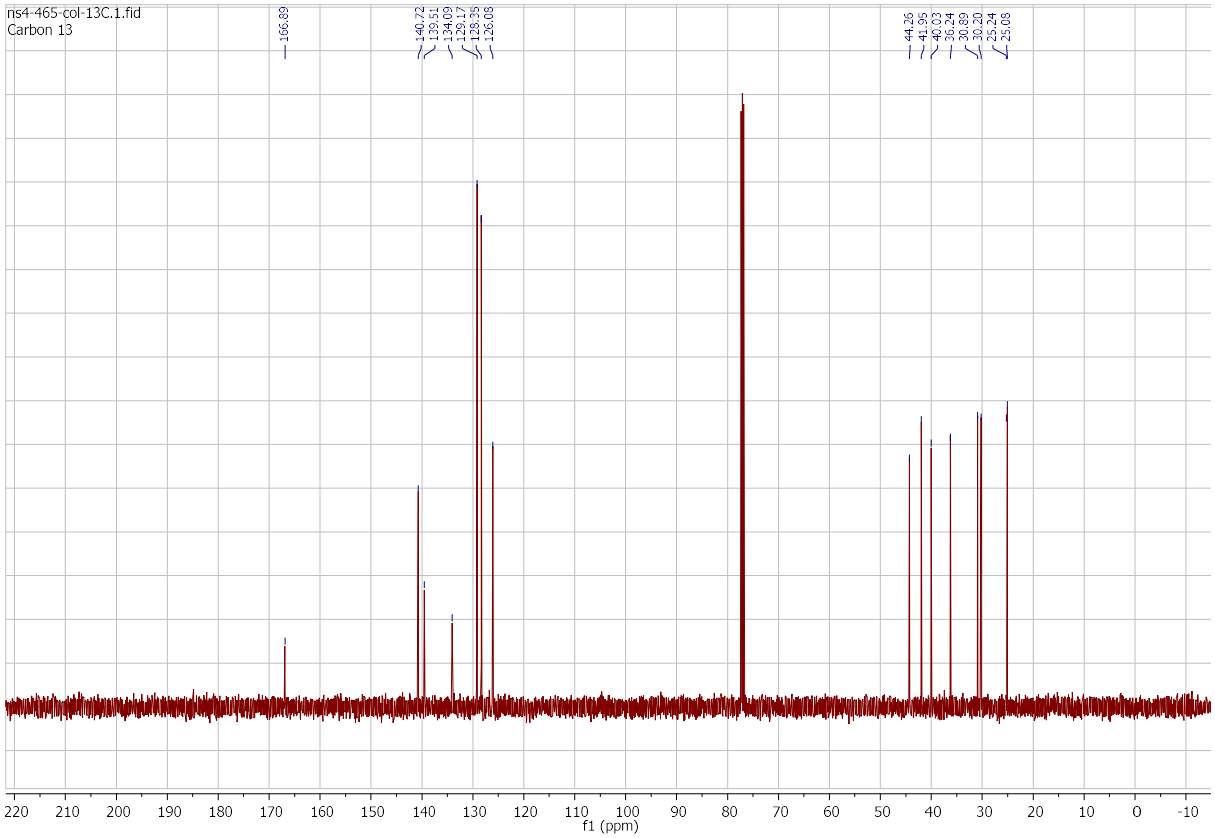
ns4-465-col-13C.1.fid
Carbon 13
f1 (ppm)

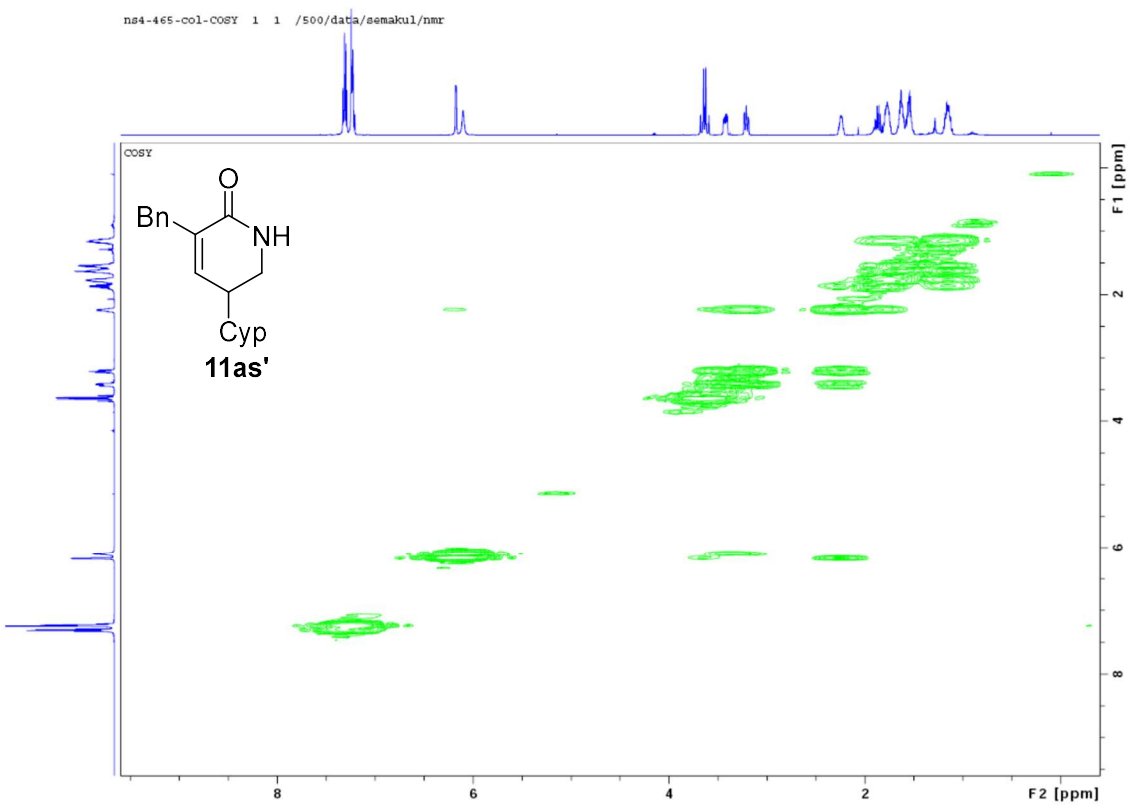
ns4-465-col-COSY 1 1 /500/data/semakul/nmr
COSY
O
Bn
NH
Cyp
11as'
F1 [ppm]
F2 [ppm]
2
4
6
8

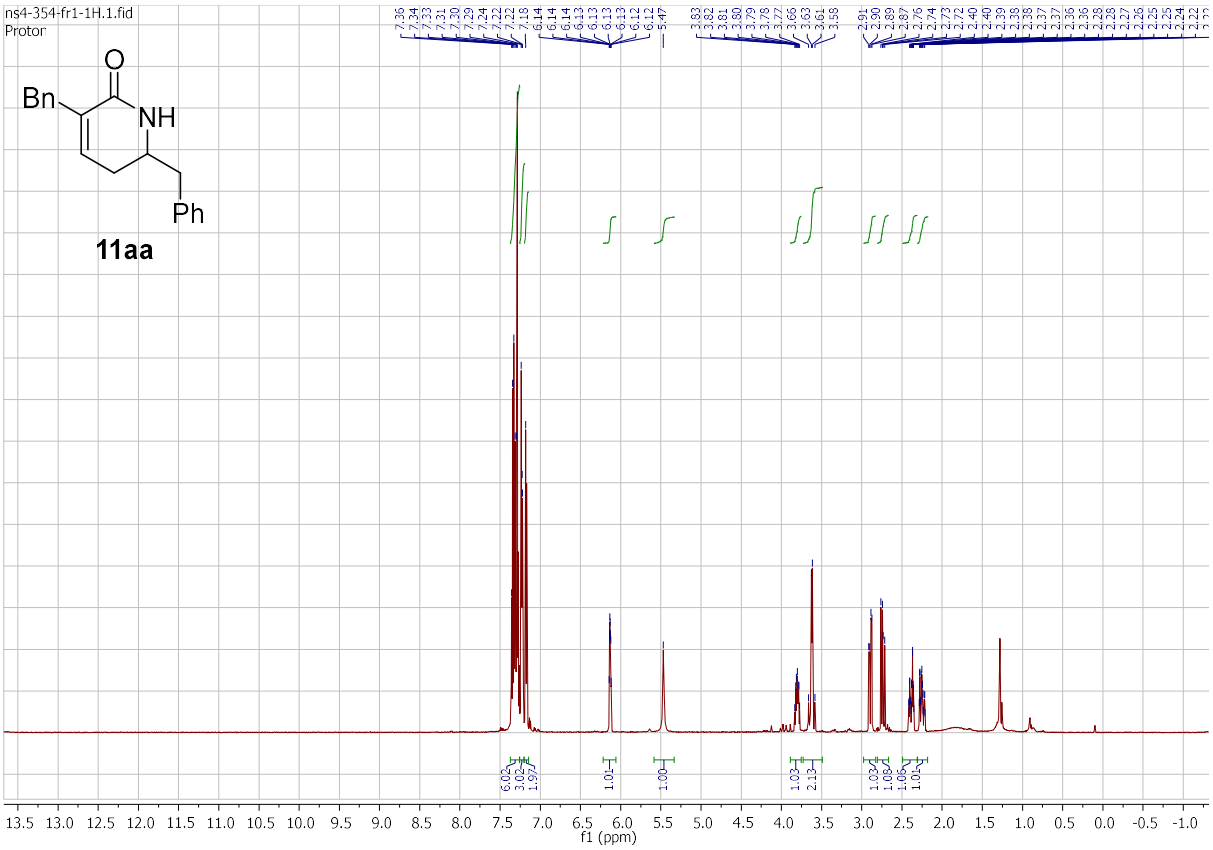
ns4-354-fr1-1H.1.fid
Protor
O
Bn
NH
Ph
11aa
f1 (ppm)

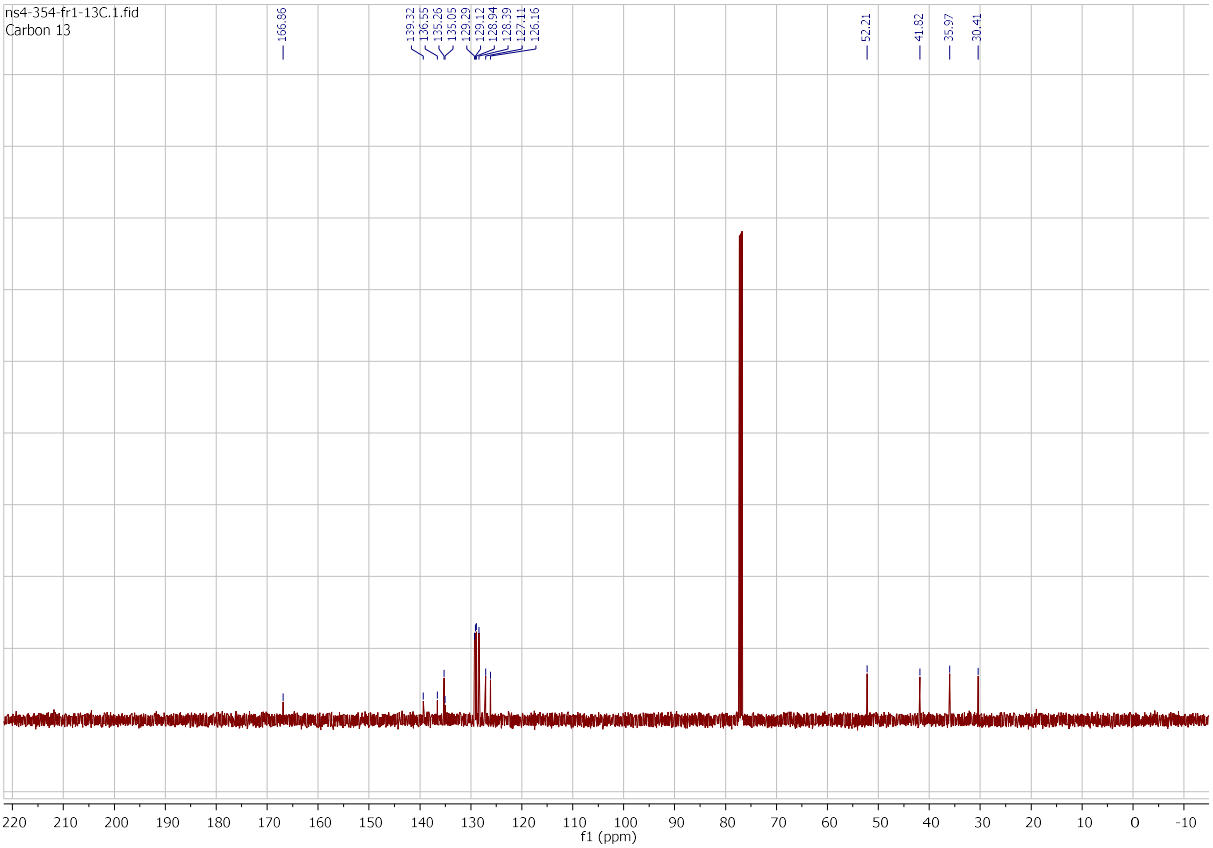
ns4-354-fr1-13C.1.fid
Carbon 13
f1 (ppm)

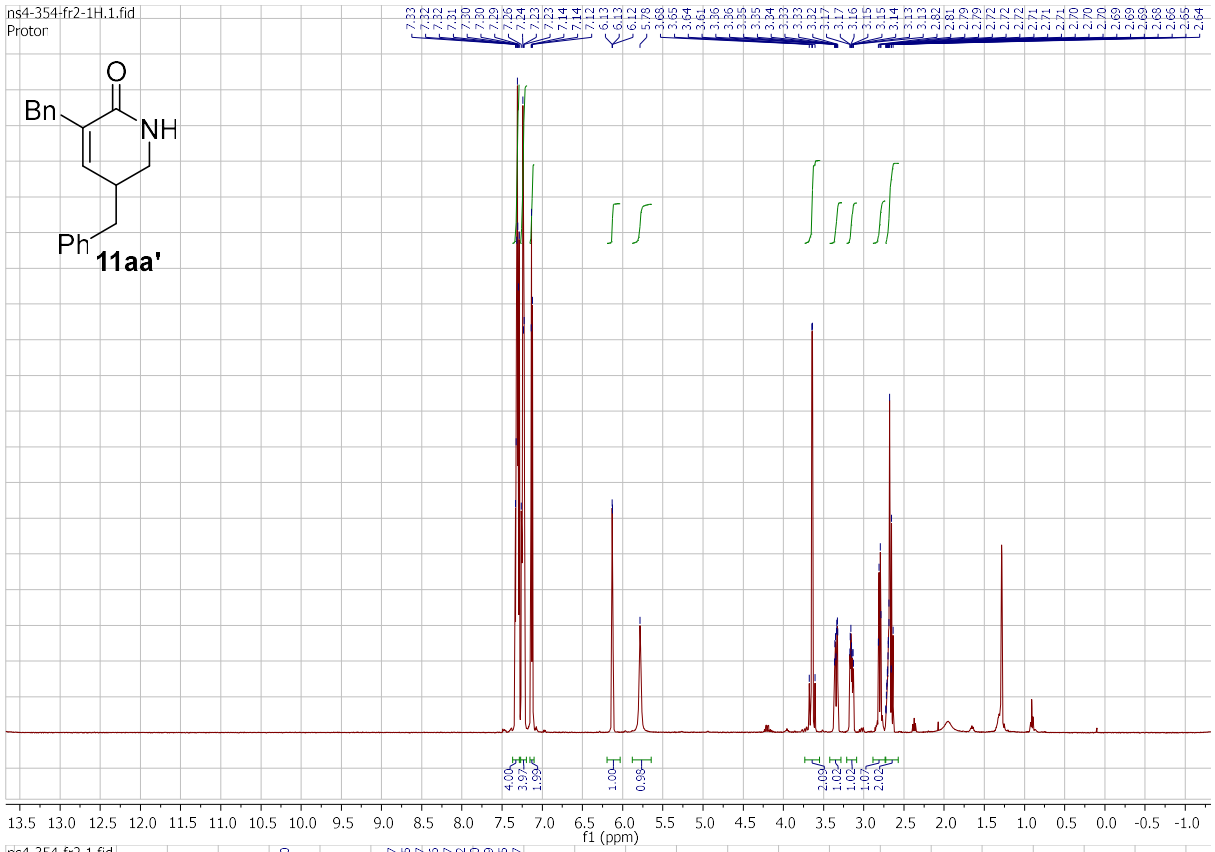
ns4-354-fr2-1H.1.fid
Protor
O
Bn
NH
Ph
11aa'
f1 (ppm)

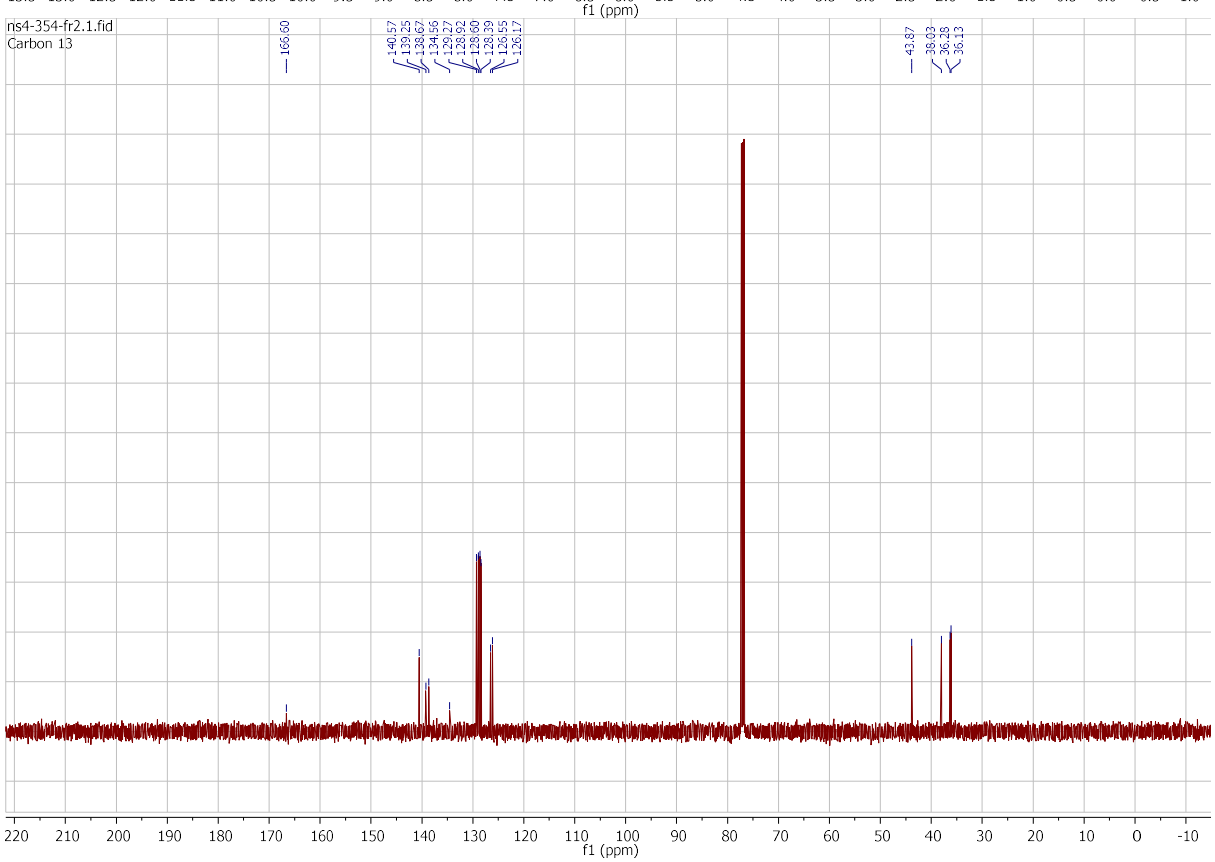
ns4-354-fr2.1.fid
Carbon 13
f1 (ppm)

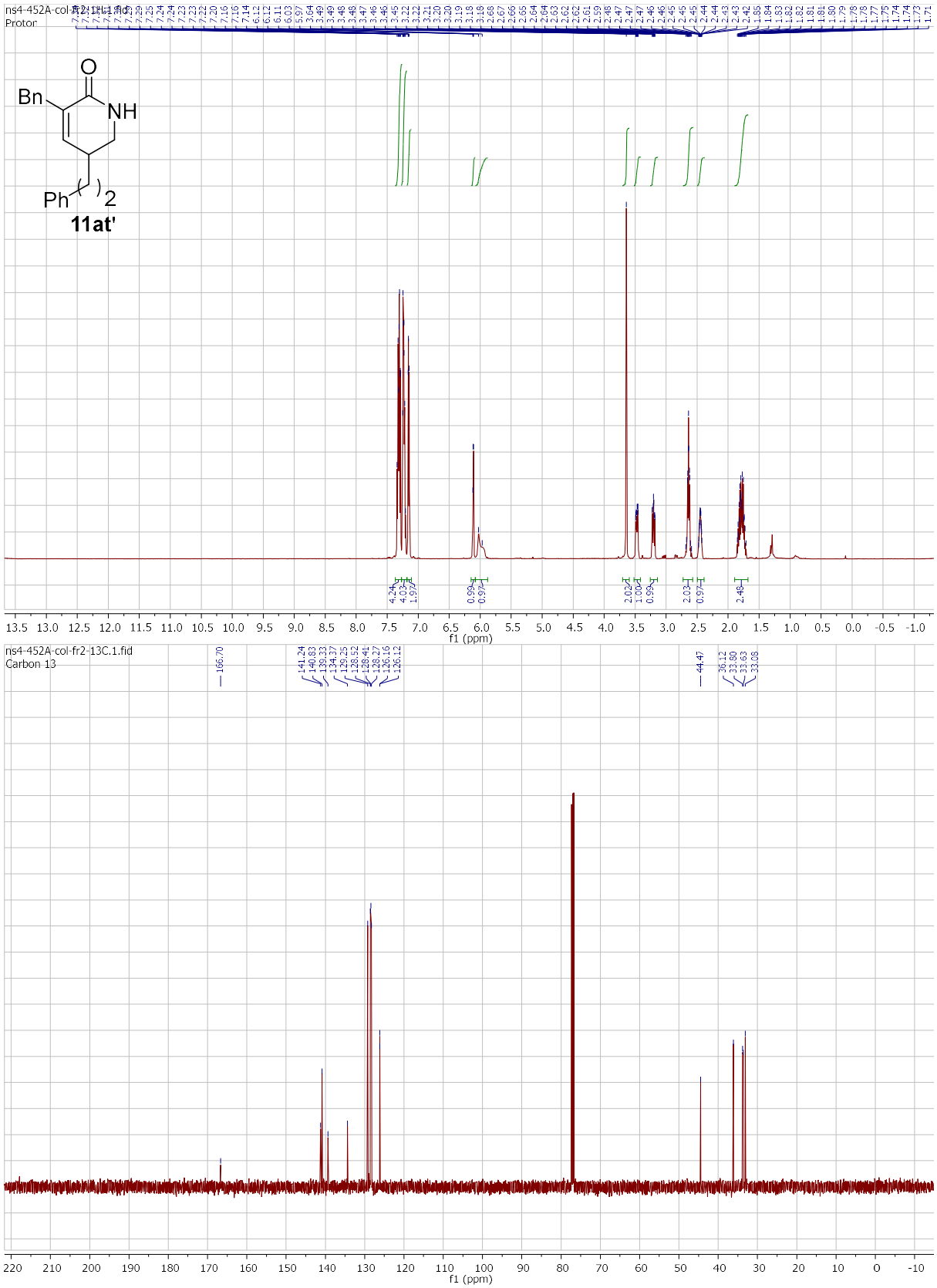
Proton
Bn
NH
Ph
2
11at'
f1 (ppm)
Carbon 13
f1 (ppm)


Bn
O
NH
n-pent
11au'
f1 (ppm)

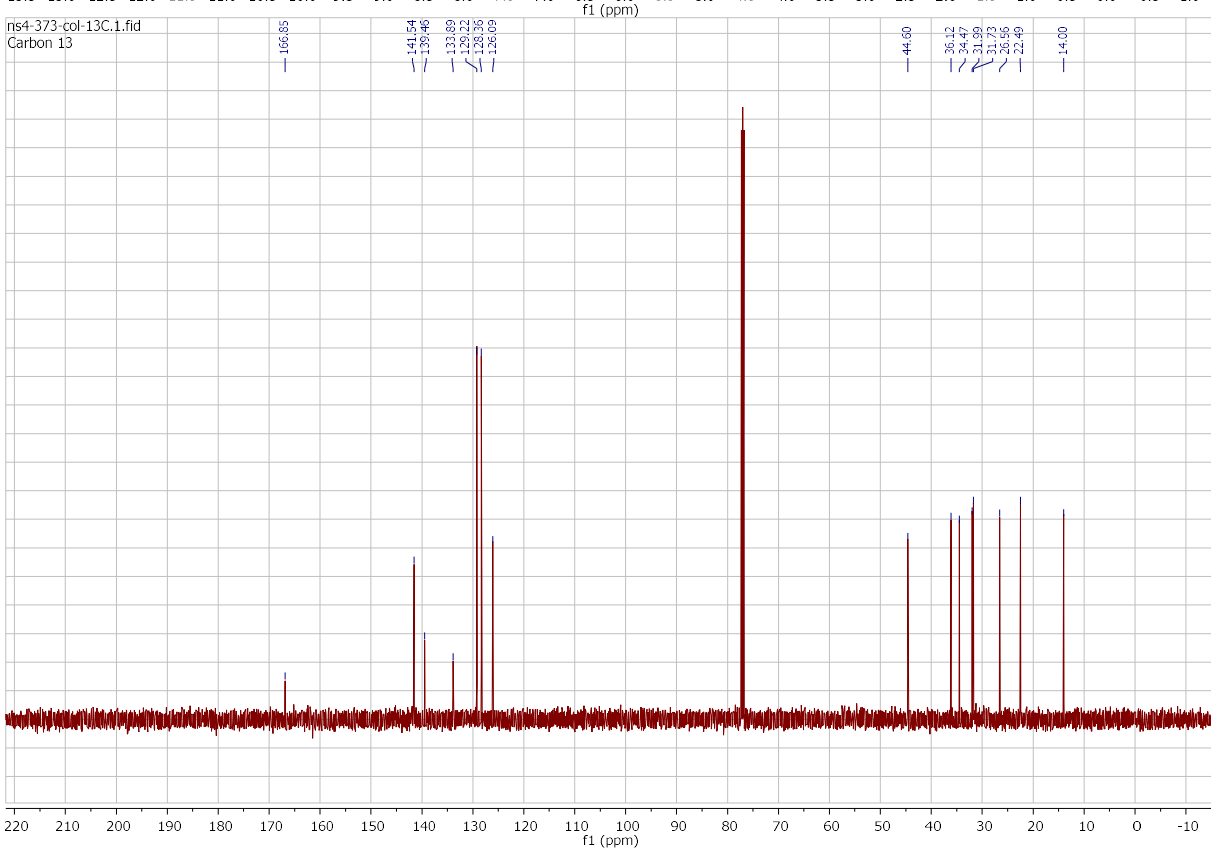
ns4-373-col-13C.1.fid
Carbon 13
166.85
141.54
139.46
133.89
129.22
128.35
126.09
44.60
36.12
34.47
31.99
31.73
26.56
22.49
14.00
f1 (ppm)

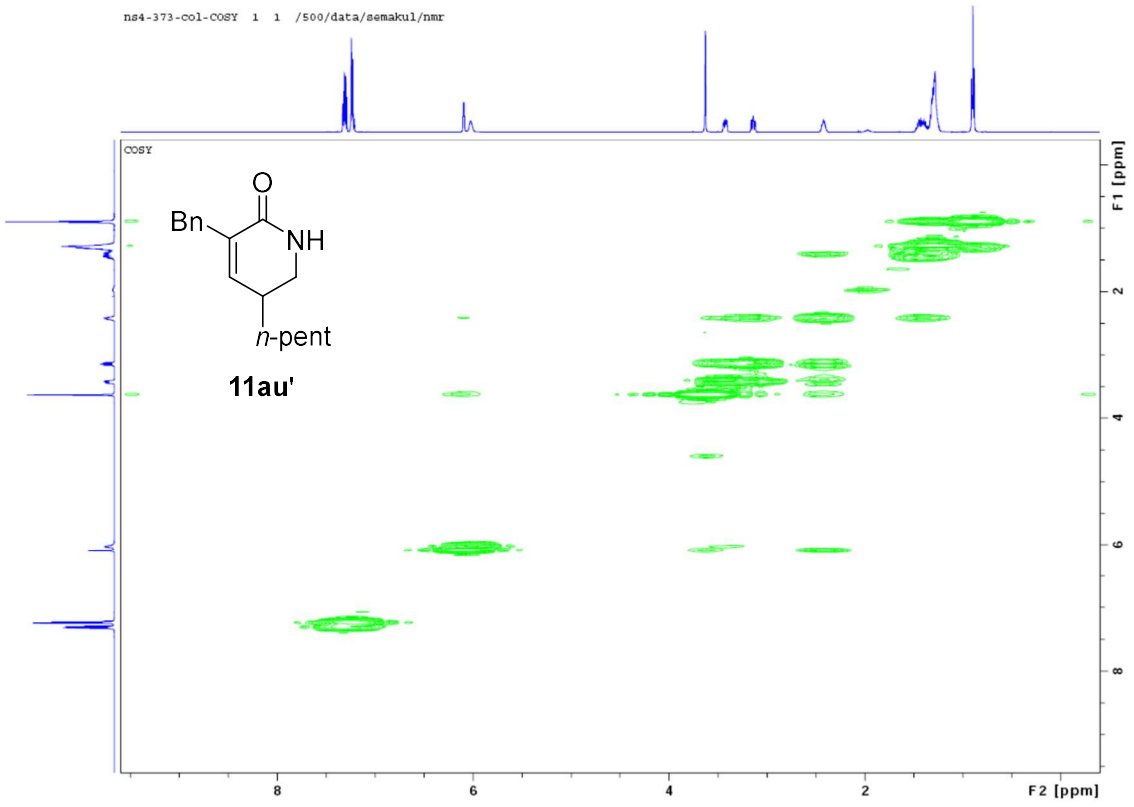
ns4-373-col-COSY 1 1 /500/data/semakul/nmr
COSY
Bn
NH
n-pent
11au'
F1 [ppm]
F2 [ppm]
2
4
6
8
2
4
6
8

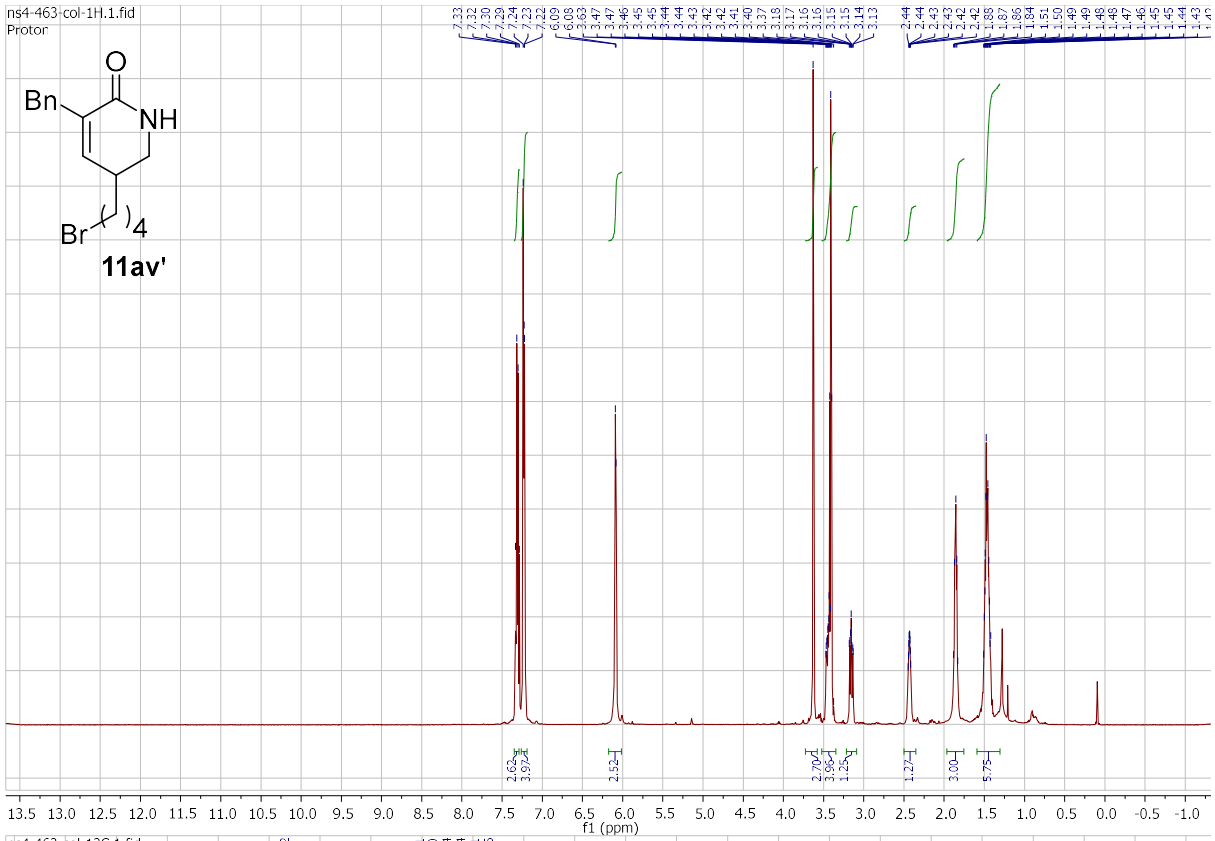
ns4-463-col-1H.1.fid
Protor
O
Bn
NH
Br
4
11av'
f1 (ppm)

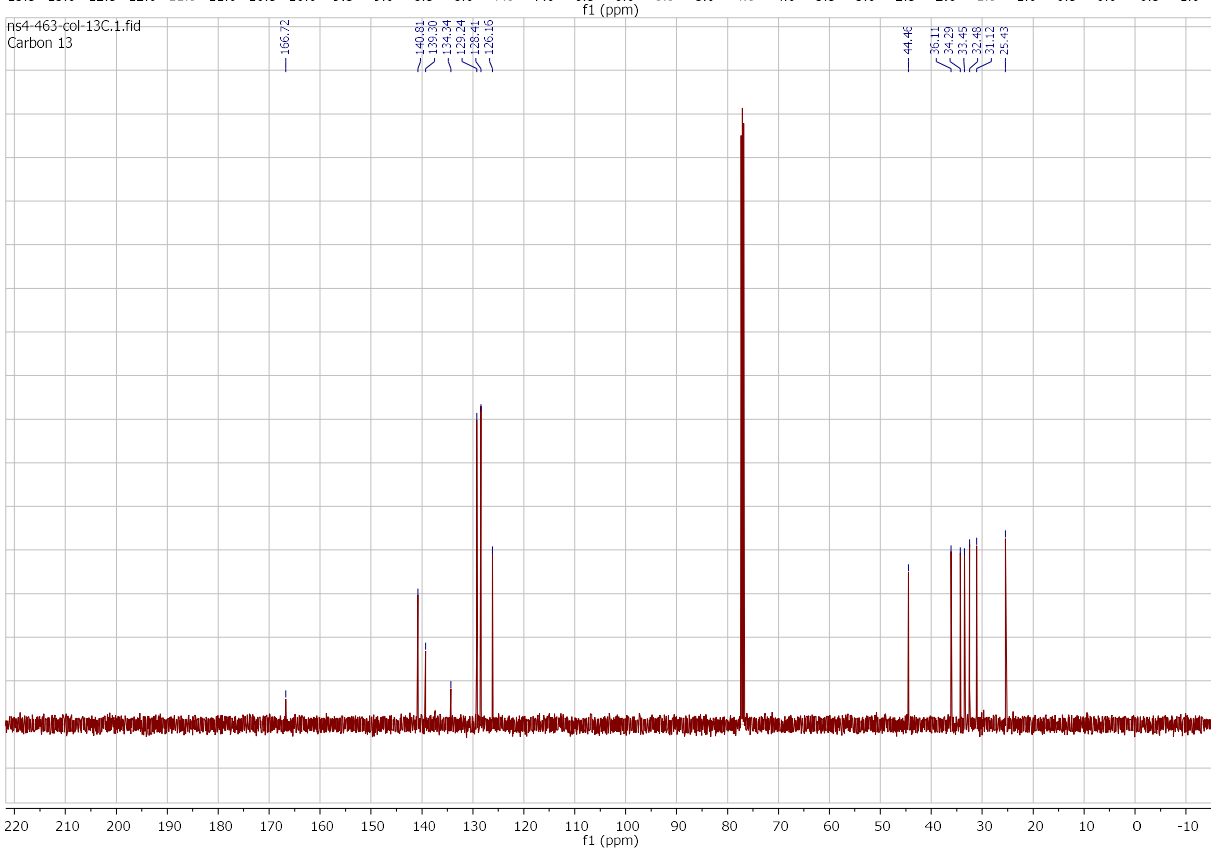
ns4-463-col-13C.1.fid
Carbon 13
f1 (ppm)

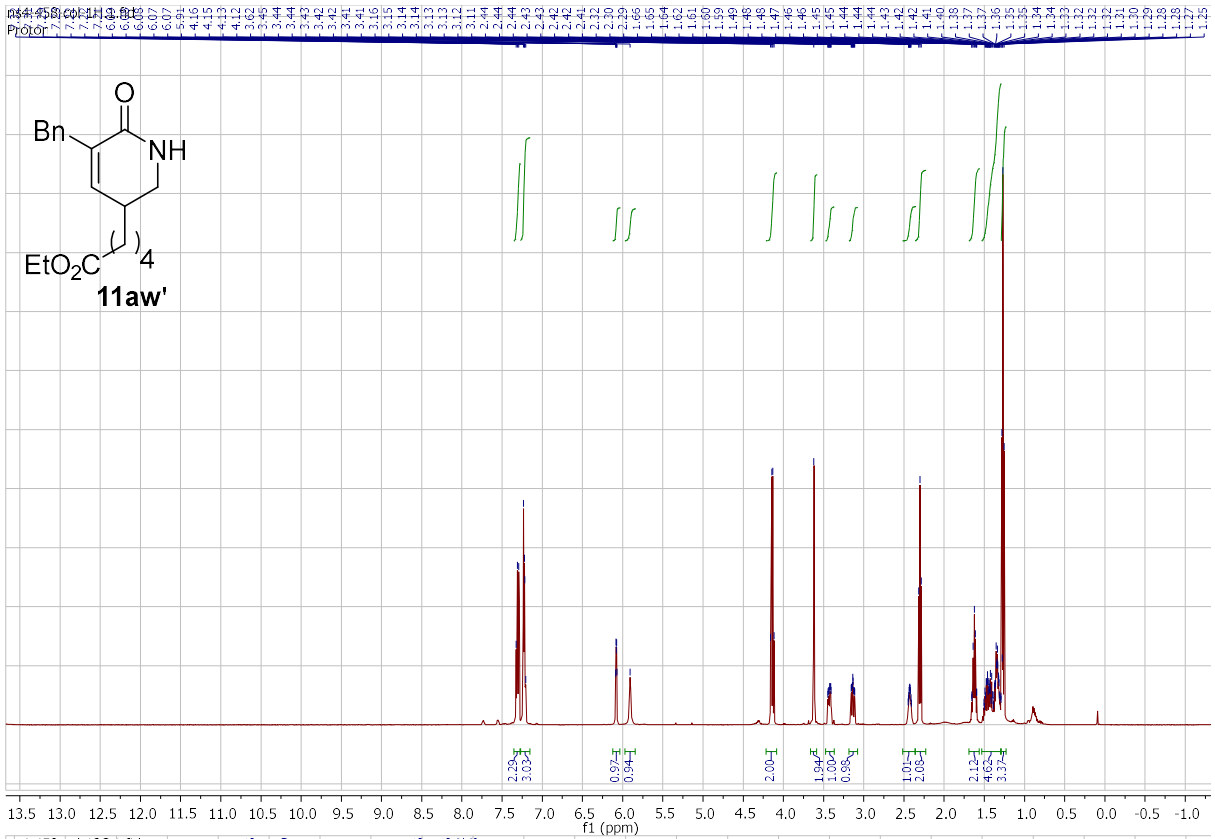
Bn
O
NH
EtO2C
4
11aw'
f1 (ppm)

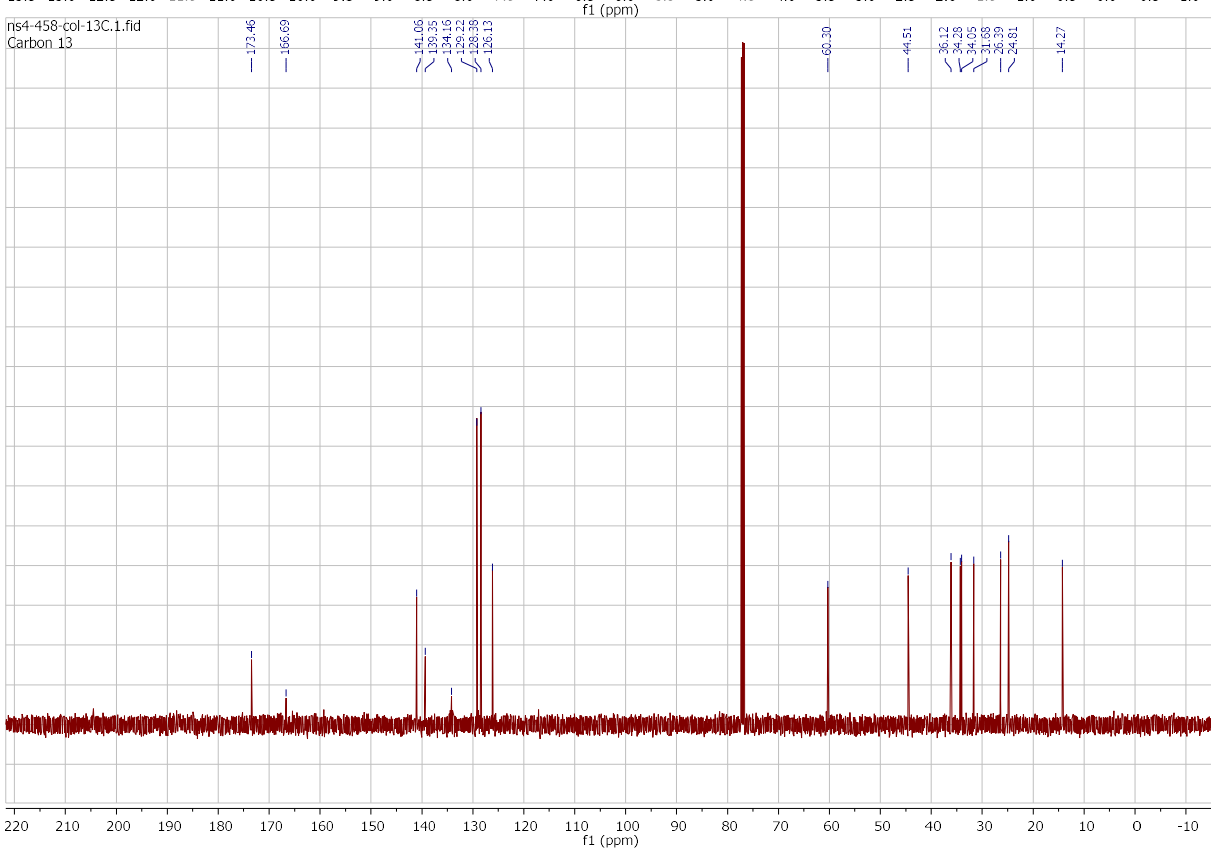
ns4-458-col-13C.1.fid
Carbon 13
f1 (ppm)

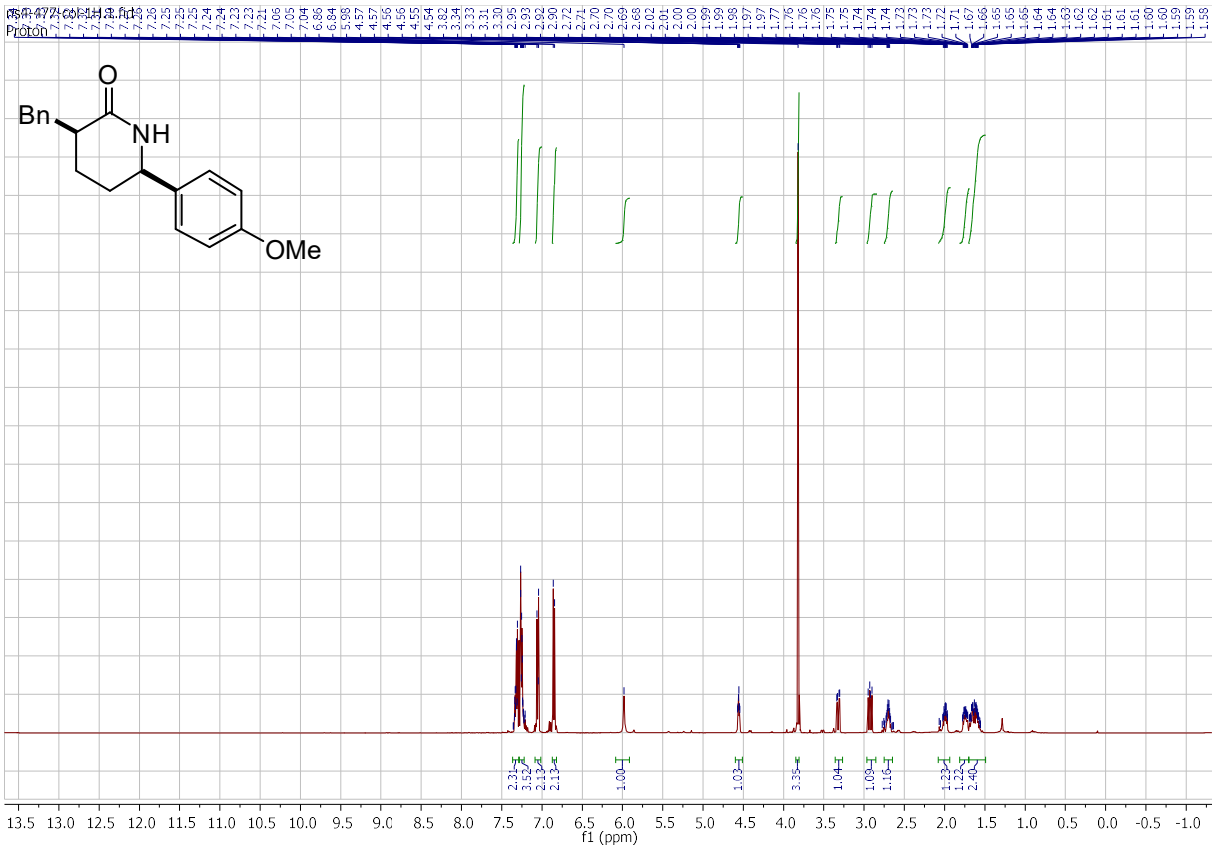
ns4-477-col-1H 2.1.fid
Proton
O
Bn
NH
OMe
2.31
3.52
2.13
2.13
1.00
1.03
3.35
1.04
1.09
1.16
1.23
1.22
2.40
13.5 13.0 12.5 12.0 11.5 11.0 10.5 10.0 9.5 9.0 8.5 8.0 7.5 7.0 6.5 6.0 5.5 5.0 4.5 4.0 3.5 3.0 2.5 2.0 1.5 1.0 0.5 0.0 -0.5 -1.0
f1 (ppm)

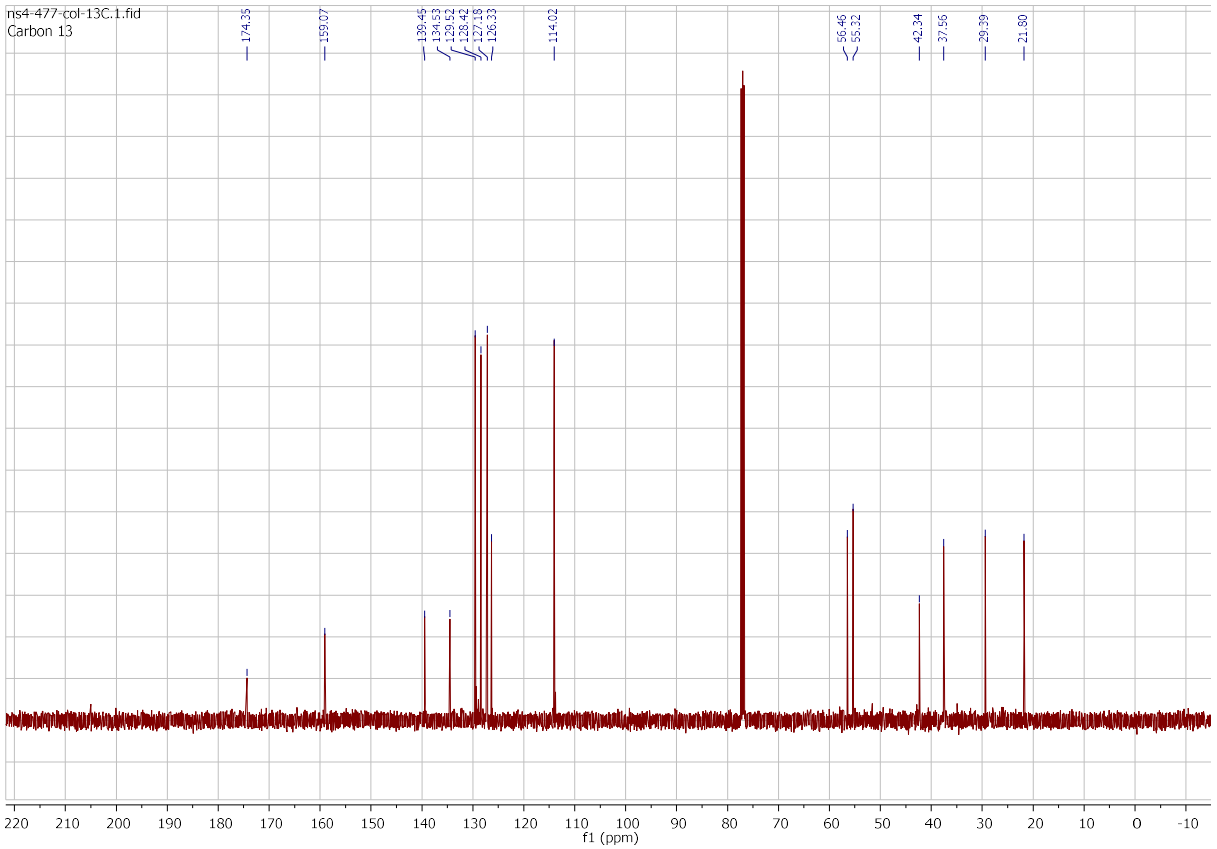
ns4-477-col-13C.1.fid
Carbon 13
174.35
159.07
130.45
130.53
129.51
128.42
127.38
126.33
114.02
56.46
55.32
42.34
37.56
29.39
21.80
220 210 200 190 180 170 160 150 140 130 120 110 100 90 80 70 60 50 40 30 20 10 0 -10
f1 (ppm)

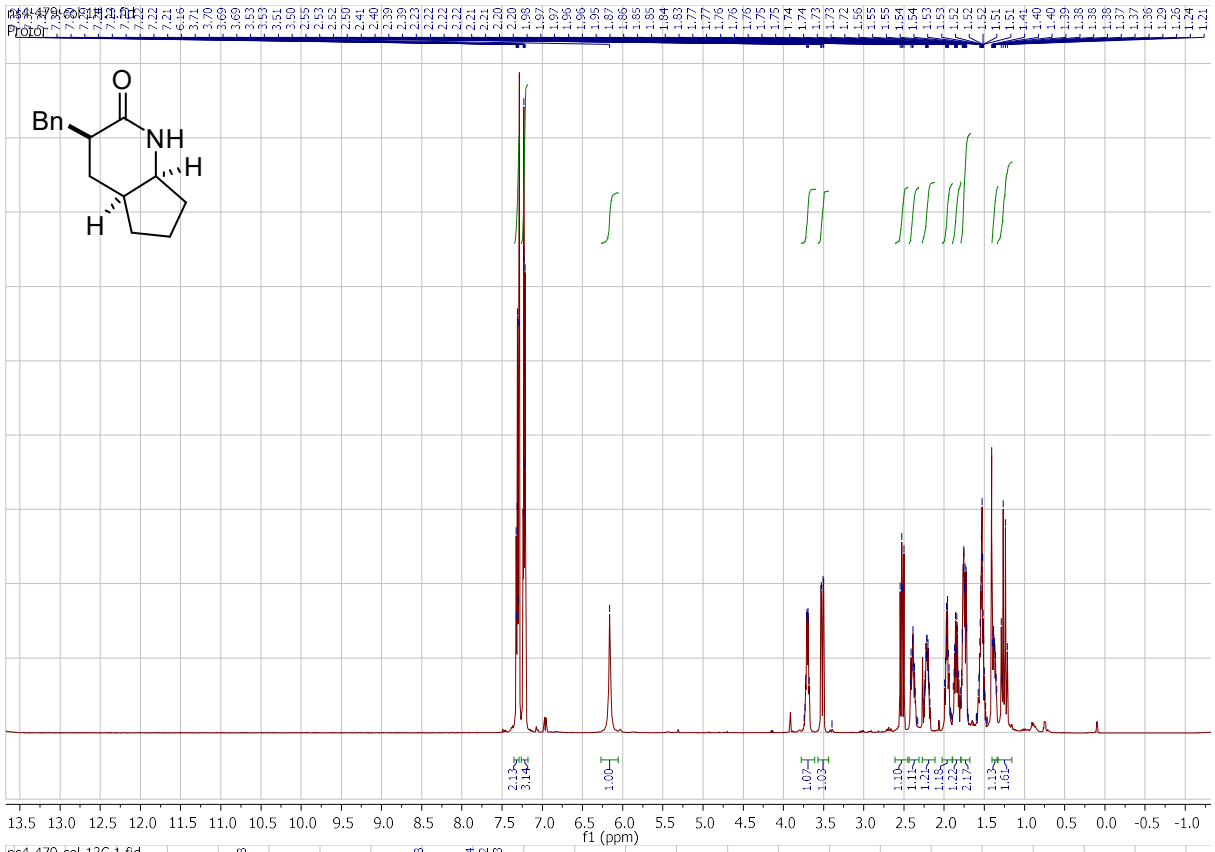
Bn
O
NH
H
H
f1 (ppm)

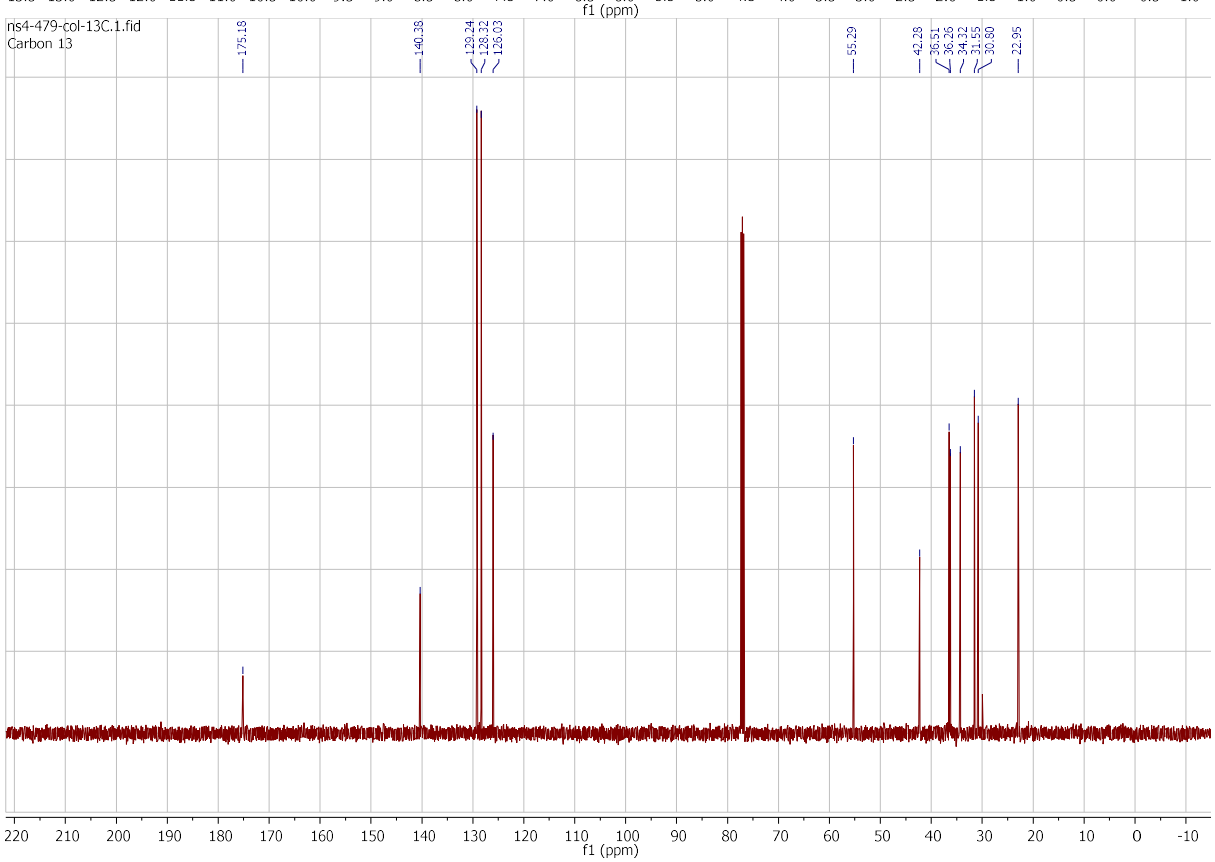
ns4-479-col-13C.1.fid
Carbon 13
175.18
140.38
129.24
128.32
126.03
55.29
42.28
36.61
36.26
34.32
31.55
30.80
22.95
f1 (ppm)